Proceedings of the 27th Workshop on General Relativity and Gravitation in Japan

November 27th–December 1st 2017
Higashi Hiroshima Arts & Culture Hall Kurara, Saijo, Higashi-hiroshima, Japan

Volume 2

Oral Presentations: Day 3, 4, 5

http://www-tap.scphys.kyoto-u.ac.jp/jgrg/index.html

Contents

Wednesday 29th

Invited lecture 9:30–10:30

[Chair: Masaaki Takahashi]

Nicola Bartolo (Padova Univ, INFN),

“Inflaon: current status and future prospects”
(50+10)

[JGRG27 (2017) 112901]

Inflation: current status and future prospects

Nicola Bartolo
Department of Physics and Astronomy, ``G. Galilei'', University of Padova
INFN-Padova, INAF-OAPD

UNIVERSITÀ DEGLI STUDI DI PADOVA

Outline

- *Inflation: a short introduction*
- *Current status*
- *Prospects for the future:*
  looking for new signatures and new observational tests
  (primordial non-Gaussianity, gravitational waves, CMB spectral distortions)
- *Conclusions*

Based on
N.B., M. Liguori, M. Shiraishi, JCAP 1603, 29 (2016)
N.B., C. Caprini, V. Domcke, D. Figueroa, J. Garcia-Bellido, M. C. Guzzetti. et al. JCAP 1612, 026 (2016)
N.B., S. Matarrese, M. Peloso, A. Ricciardone, Phys.Rev. D87, 023504 (2013)
N.B., D. Cannone, A. Ricciardone, G. Tasinato, JCAP 1603, 044 (2016)
A. Ravenni, M. Liguori, N.B., M. Shiraishi, arXiv:1707.04759
F. Oppizzi, M. Liguori, A. Renzi, F. Arroja, N.B., arXiv:1711.08286
N.B., G. Orlando, JCAP 1707, 034 (2017)
N.B., A. Keaghias, M.Liguori, A. Riotto, M. Shiraishi, V. Tansella, arXiv:1711.08286

Inflation: a short recap

Fitting into the Big Picture

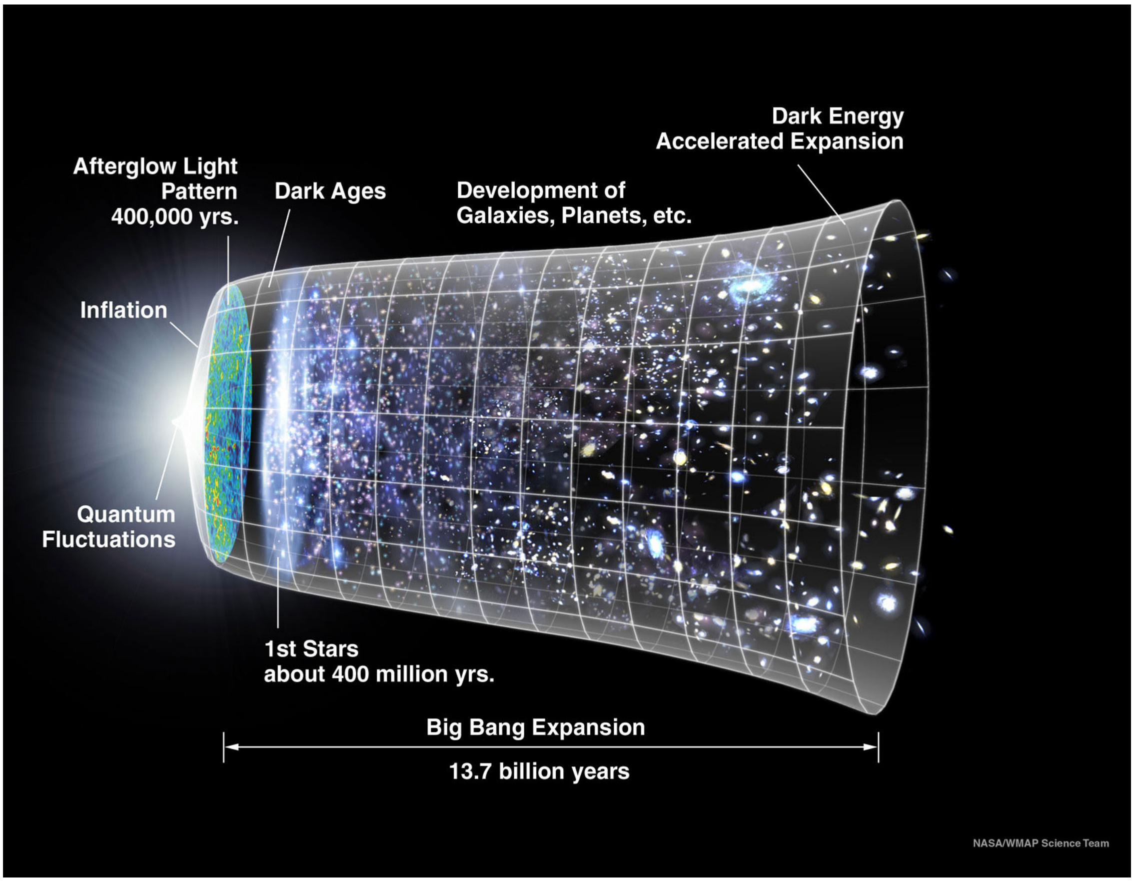

Precision cosmology in the *Planck* era

ΛCDM: The standard cosmological model

just 6 numbers…….
describe the Universe composition and evolution

Homogeneous background

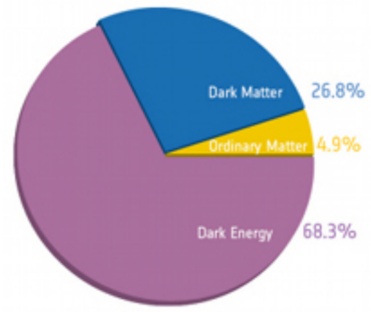

$\Omega_{b}, \Omega_{c}, \Omega_{\Lambda}, H_{0}, \tau$

- atoms 4%
- cold dark matter 23%
- dark energy 73%

Λ?? CDM??

Perturbations

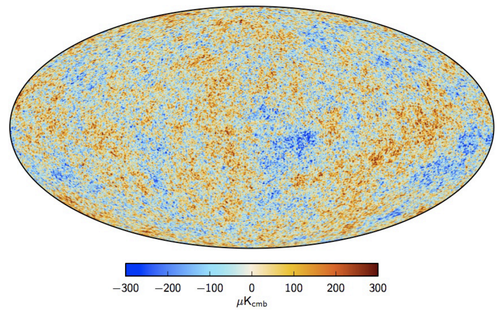

A_{s}, n_{s}, r

- nearly scale-invariant
- adiabatic
- Gaussian

ORIGIN???

Credit: L. Verde

Initial conditions

INFLATION

accelerated expansion in the early universe

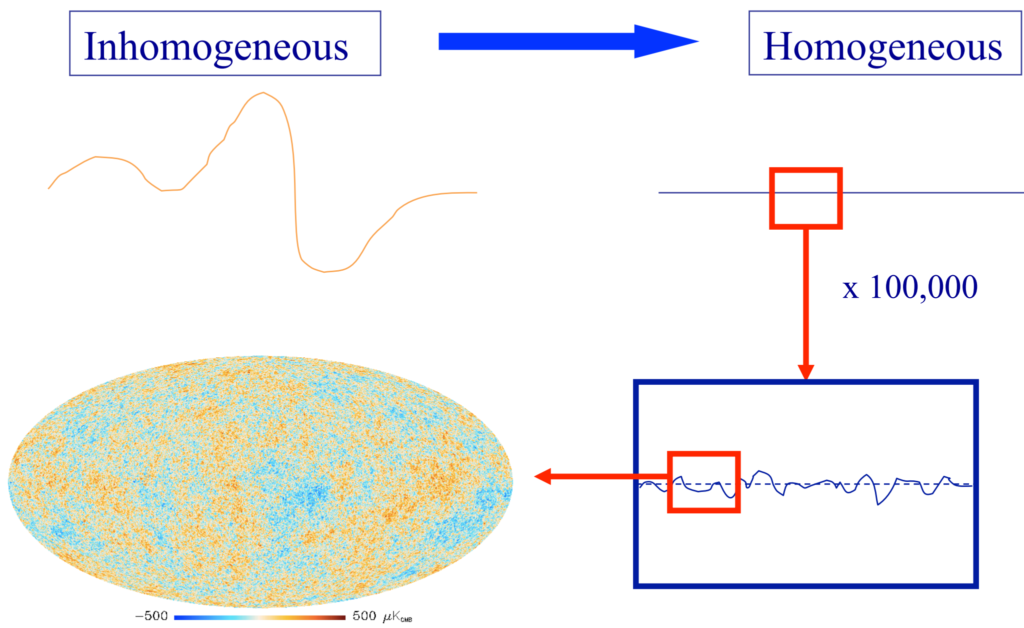

Quantum fluctuations of a scalar field, the inflaton, set the ***initial conditions*** for CMB anisotropies and Large-Scale Structure formation

Inflation

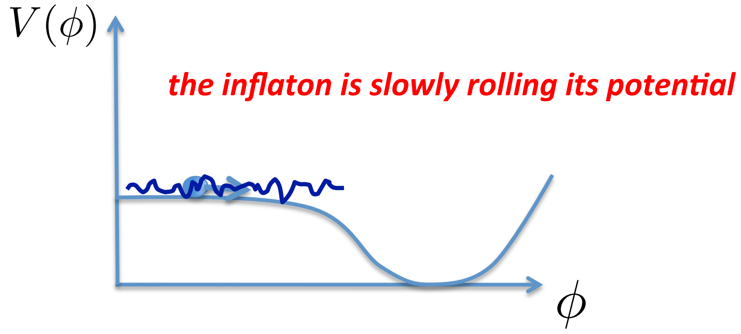

$$V(\phi) >> \frac{1}{2}\dot{\phi}^2 \rightarrow H^2 = \frac{8\pi G}{3}V(\phi) \simeq const \rightarrow a(t) \propto e^{Ht} \left(H(t) = \frac{\dot{a}}{a}\right)$$

✓ Fluctuations in the inflaton produce fluctuations in the universe expansion from place to place, so that each region in the universe goes through the same expansion history but at slightly different times:

accelerated expansion in the early universe

✓ To induce acceleration the potential must be flat

$$\zeta \sim \frac{\Delta T}{T} \sim \frac{\delta\rho}{\rho} \qquad \zeta \simeq \frac{H\delta\phi}{\dot{\phi}}$$

$$\boxed{\varepsilon = \frac{M_{Pl}^2}{2}\left(\frac{V_\phi}{V}\right)^2 << 1}$$

✓ To have long enough inflation, V(ϕ) must be flat for long enough

$$\boxed{\eta = M_{Pl}^2 \frac{V_{\phi\phi}}{V} << 1}$$

Observational predictions

- **Primordial density (scalar) perturbations**

$$\mathcal{P}_\zeta(k) = \frac{16}{9}\frac{V^2}{M_{\rm Pl}^4\dot{\phi}^2}\left(\frac{k}{k_0}\right)^{n-1}$$

amplitude

spectral index: $n - 1 = 2\eta - 6\epsilon$
(or ``tilt'')

$$\epsilon = \frac{M_{\rm Pl}^2}{16\pi}\left(\frac{V'}{V}\right)^2 \ll 1; \;\; \eta = \frac{M_{\rm Pl}^2}{8\pi}\left(\frac{V''}{V}\right) \ll 1$$

- **Primordial (tensor) gravitational waves:** *a smoking gun for inflation*

$$\mathcal{P}_{\rm T}(k) = \frac{128}{3}\frac{V}{M_{\rm Pl}^4}\left(\frac{k}{k_0}\right)^{n_{\rm T}}$$

Energy scale of inflation

Tensor spectral index: $n_{\rm T} = -2\epsilon$

- **Tensor-to-scalar perturbation ratio**

$$r = \frac{\mathcal{P}_{\rm T}}{\mathcal{P}_\zeta} = 16\epsilon$$

- **Consistency relation** (valid for *all* single field models of slow-roll inflation):

$$r = -8n_T$$

Current observational status

Planck parameters measurements

Parameter	TT+lowP 68 % limits	TT+lowP+lensing 68 % limits	TT+lowP+lensing+ext 68 % limits	TT,TE,EE+lowP 68 % limits	TT,TE,EE+lowP+lensing 68 % limits	TT,TE,EE+lowP+lensing+ext 68 % limits
$\Omega_b h^2$	0.02222 ± 0.00023	0.02226 ± 0.00023	0.02227 ± 0.00020	0.02225 ± 0.00016	0.02226 ± 0.00016	0.02230 ± 0.00014
$\Omega_c h^2$	0.1197 ± 0.0022	0.1186 ± 0.0020	0.1184 ± 0.0012	0.1198 ± 0.0015	0.1193 ± 0.0014	0.1188 ± 0.0010
$100\theta_{MC}$	1.04085 ± 0.00047	1.04103 ± 0.00046	1.04106 ± 0.00041	1.04077 ± 0.00032	1.04087 ± 0.00032	1.04093 ± 0.00030
τ	0.078 ± 0.019	0.066 ± 0.016	0.067 ± 0.013	0.079 ± 0.017	0.063 ± 0.014	0.066 ± 0.012
$\ln(10^{10} A_s)$	3.089 ± 0.036	3.062 ± 0.029	3.064 ± 0.024	3.094 ± 0.034	3.059 ± 0.025	3.064 ± 0.023
n_s	0.9655 ± 0.0062	0.9677 ± 0.0060	0.9681 ± 0.0044	0.9645 ± 0.0049	0.9653 ± 0.0048	0.9667 ± 0.0040
H_0	67.31 ± 0.96	67.81 ± 0.92	67.90 ± 0.55	67.27 ± 0.66	67.51 ± 0.64	67.74 ± 0.46
Ω_Λ	0.685 ± 0.013	0.692 ± 0.012	0.6935 ± 0.0072	0.6844 ± 0.0091	0.6879 ± 0.0087	0.6911 ± 0.0062
Ω_m	0.315 ± 0.013	0.308 ± 0.012	[illegible]	[illegible]	[illegible]	0.3089 ± 0.0062
$\Omega_m h^2$	0.1426 ± 0.0020	0.1415 ± 0.0019	[illegible]	[illegible]	[illegible]	0.14170 ± 0.00097
$\Omega_m h^3$	0.09597 ± 0.00045	0.09591 ± 0.00045	0.09593 ± 0.00045	0.09601 ± 0.00029	0.09596 ± 0.00030	0.09598 ± 0.00029
σ_8	0.829 ± 0.014	0.8149 ± 0.0093	0.8154 ± 0.0090	0.831 ± 0.013	0.8150 ± 0.0087	0.8159 ± 0.0086
$\sigma_8 \Omega_m^{0.5}$	0.466 ± 0.013	0.4521 ± 0.0088	0.4514 ± 0.0066	0.4668 ± 0.0098	0.4553 ± 0.0068	0.4535 ± 0.0059
$\sigma_8 \Omega_m^{0.25}$	0.621 ± 0.013	0.6069 ± 0.0076	0.6066 ± 0.0070	0.623 ± 0.011	0.6091 ± 0.0067	0.6083 ± 0.0066
z_{re}	$9.9^{+1.8}_{-1.6}$	$8.8^{+1.7}_{-1.4}$	$8.9^{+1.3}_{-1.2}$	$10.0^{+1.7}_{-1.5}$	$8.5^{+1.4}_{-1.2}$	$8.8^{+1.2}_{-1.1}$
$10^9 A_s$	$2.198^{+0.076}_{-0.085}$	2.139 ± 0.063	2.143 ± 0.051	2.207 ± 0.074	2.130 ± 0.053	2.142 ± 0.049
$10^9 A_s e^{-2\tau}$	1.880 ± 0.014	1.874 ± 0.013	1.873 ± 0.011	1.882 ± 0.012	1.878 ± 0.011	1.876 ± 0.011
Age/Gyr	13.813 ± 0.038	13.799 ± 0.038	13.796 ± 0.029	13.813 ± 0.026	13.807 ± 0.026	13.799 ± 0.021
z_*	1090.09 ± 0.42	1089.94 ± 0.42	1089.90 ± 0.30	1090.06 ± 0.30	1090.00 ± 0.29	1089.90 ± 0.23
r_*	144.61 ± 0.49	144.89 ± 0.44	144.93 ± 0.30	144.57 ± 0.32	144.71 ± 0.31	144.81 ± 0.24
$100\theta_*$	1.04105 ± 0.00046	1.04122 ± 0.00045	1.04126 ± 0.00041	1.04096 ± 0.00032	1.04106 ± 0.00031	1.04112 ± 0.00029
z_{drag}	1059.57 ± 0.46	1059.57 ± 0.47	1059.60 ± 0.44	1059.65 ± 0.31	1059.62 ± 0.31	1059.68 ± 0.29
r_{drag}	147.33 ± 0.49	147.60 ± 0.43	147.63 ± 0.32	147.27 ± 0.31	147.41 ± 0.30	147.50 ± 0.24
k_D	0.14050 ± 0.00052	0.14024 ± 0.00047	0.14022 ± 0.00042	0.14059 ± 0.00032	0.14044 ± 0.00032	0.14038 ± 0.00029
z_{eq}	3393 ± 49	3365 ± 44	3361 ± 27	3395 ± 33	3382 ± 32	3371 ± 23
k_{eq}	0.01035 ± 0.00015	0.01027 ± 0.00014	0.010258 ± 0.000083	0.01036 ± 0.00010	0.010322 ± 0.000096	0.010288 ± 0.000071
$100\theta_{s,eq}$	0.4502 ± 0.0047	0.4529 ± 0.0044	0.4533 ± 0.0026	0.4499 ± 0.0032	0.4512 ± 0.0031	0.4523 ± 0.0023

n=1 excluded at 5.6 sigma!!

Observational constraints: *Planck*

Amplitude of primordial density (scalar) perturbations

$$\ln(10^{10} A_s) = 3.062 \pm 0.029 \quad (68\%\ \mathrm{CL})$$

Spectral index of primordial density (scalar) perturbations

$$n_s = 0.9677 \pm 0.0060 \quad (68\%\ \mathrm{CL})$$

n=1 (Harrison Zeld' ovich spectrum) excluded at than 5.6 sigmas!

Two fundamental observational constants of cosmology in addition to three very well known (Ω_b, Ω_{cdm}, Ω_Λ).

Constraints on tensor modes

Model	Parameter	*Planck* TT+lowP	*Planck* TT+lowP+lensing	*Planck* TT+lowP+BAO	*Planck* TT,TE,EE+lowP
ΛCDM+r	n_s	0.9666 ± 0.0062	0.9688 ± 0.0061	0.9680 ± 0.0045	0.9652 ± 0.0047
	$r_{0.002}$	< 0.103	$\boxed{< 0.114}$	< 0.113	< 0.099
	$-2\Delta \ln \mathcal{L}_{max}$	0	0	0	0
ΛCDM+r +$dn_s/d\ln k$	n_s	0.9667 ± 0.0066	0.9690 ± 0.0063	0.9673 ± 0.0043	0.9644 ± 0.0049
	$r_{0.002}$	< 0.180	< 0.186	< 0.176	< 0.152
	r	< 0.168	< 0.176	< 0.166	< 0.149
	$dn_s/d\ln k$	$-0.0126^{+0.0098}_{-0.0087}$	$-0.0076^{+0.0092}_{-0.0080}$	-0.0125 ± 0.0091	-0.0085 ± 0.0076
	$-2\Delta \ln \mathcal{L}_{max}$	-0.81	-0.08	-0.87	-0.38

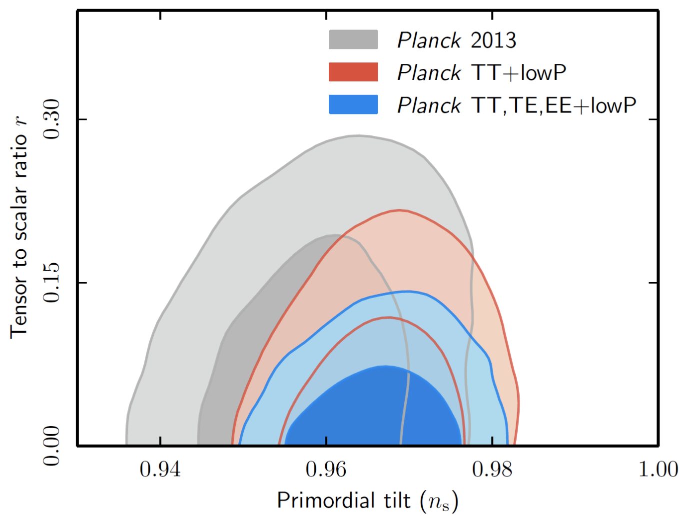

Energy scale of inflation

$$V^{1/4} < 1.9 \times 10^{16} \quad \mathrm{GeV}$$

From the BICEP2/Keck Array/Planck+ Keck Array 95 GHz
r<0.07 (95 @95% CL)

A new era of B-mode polarization has started

What are the implications for inflationary models ?**

** I am talking here about single-field slow roll models of inflation

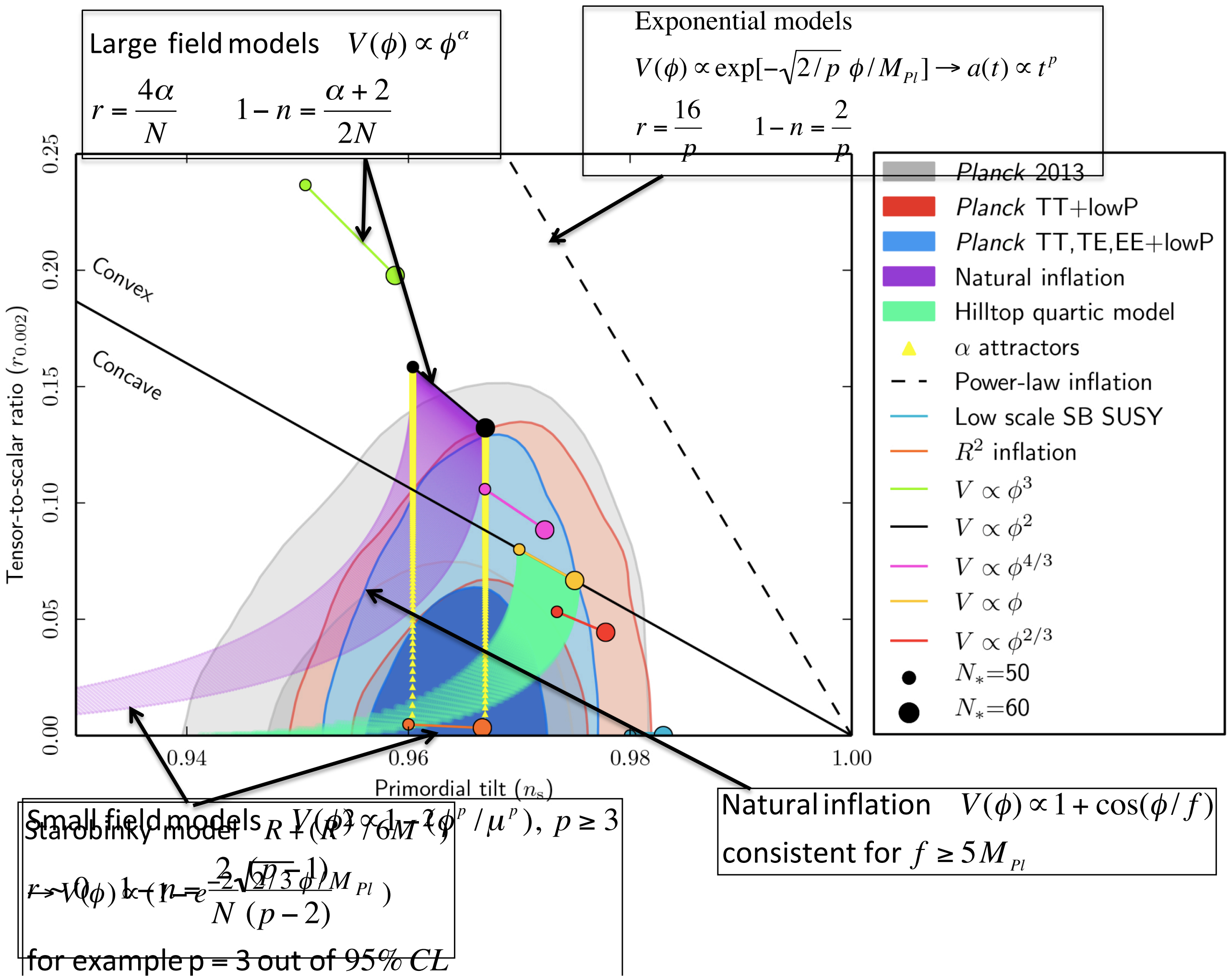

ANGULAR POWER SPECTRUM OF TEMPERATURE CMB ANISOTROPIES MEASURED BY *PLANCK*

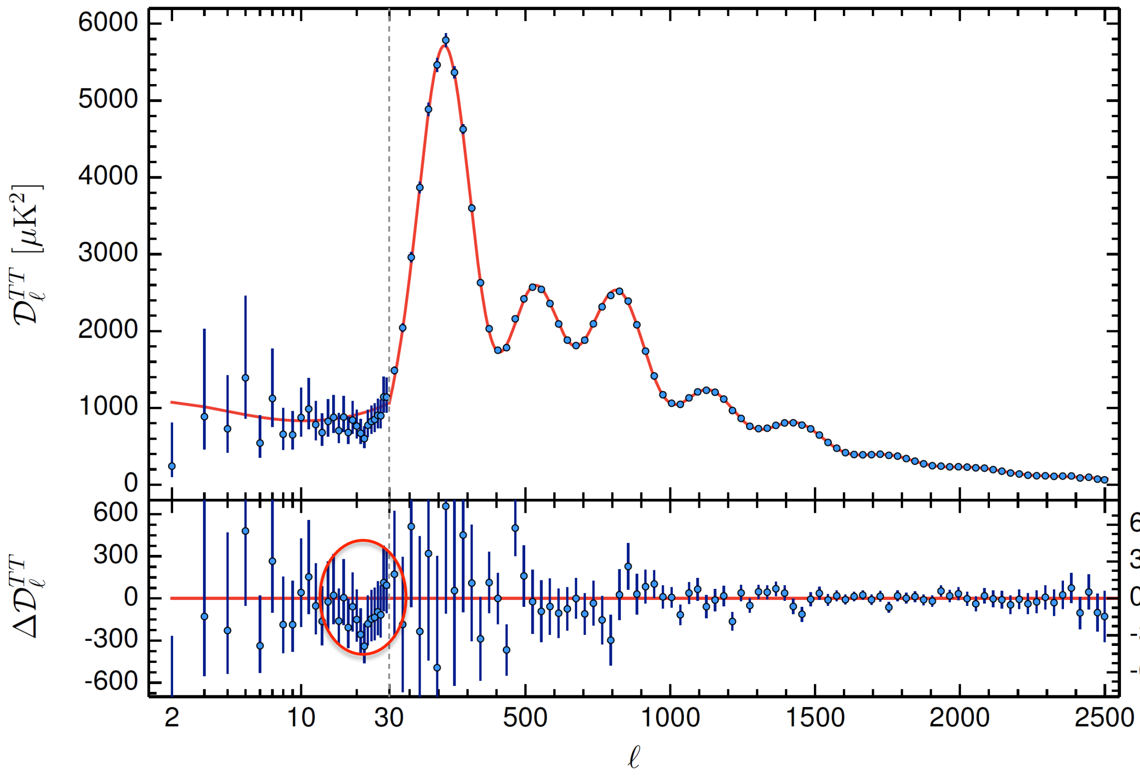

Beyond-slow roll: Reconstructing the inflationary potential

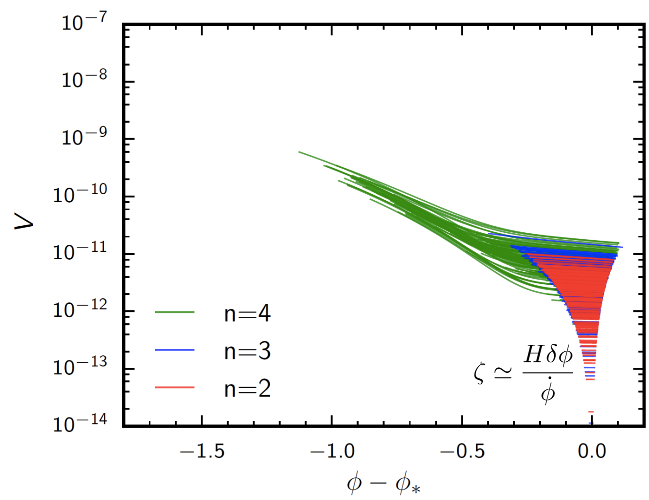

$$\zeta \simeq \frac{H\delta\phi}{\dot\phi}$$

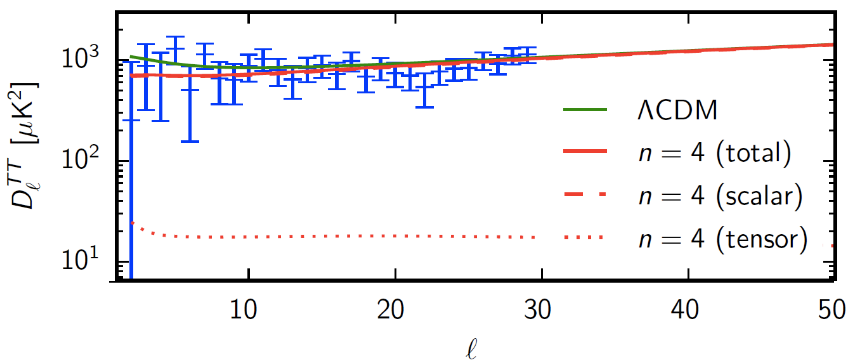

No significant evidence of deviations from a featureless power-spectrum

Why Inflation is sensitive to high-energy fundamental physics?

Sensitivity of Inflation to fundamental physics and symmetries

A worked example
take $V(\phi)_{slow\text{-}roll}$

operators like $\phi^2 V(\phi)_{slow\text{-}roll} / \Lambda^2$

induce $\eta = M^2_{PL}\,(V''/V) = (M_{Pl}/\Lambda) \sim 1$!!

whatever physics there is around the Planck scale, it must ensure these terms are not induced (largely suppresses them)
→ Ultraviolet sensitivity

At least two (main) avenues:

- ***gravitational waves***
- ***primordial non-Gaussianity***

Primordial non-Gaussianity

(aka: going beyond the (r-n_s) plane)

Primordial NG

ζ(**x**): primordial perturbations

If the fluctuations are Gaussian distributed then their statistical properties are completely characterized by the two-point correlation function, $\langle \zeta(\mathbf{x}_1)\zeta(\mathbf{x}_2)\rangle$ or its Fourier transform, the power-spectrum.

Thus a non-vanishing ***three point function***, or its Fourier transform, the ***bispectrum is an indicator of non-Gaussianity***

$$\left\langle \zeta(\vec{k}_1)\zeta(\vec{k}_2)\zeta(\vec{k}_3)\right\rangle = (2\pi)^3\delta^{(3)}(\vec{k}_1+\vec{k}_2+\vec{k}_3)\underbrace{f_{NL}}_{\text{Amplitude}}\underbrace{F(k_1,k_2,k_3)}_{\text{Shape}}$$

$$\rightarrow \left\langle \frac{\Delta T}{T}(n_1)\frac{\Delta T}{T}(n_2)\frac{\Delta T}{T}(n_3)\right\rangle$$

Primordial NG

Gaussian ⟺ free (i.e. non-interacting) field, linear theory

Collection of independent harmonic oscillators
(no mode-mode coupling)

Physical origin of primordial NG:
self-interactions of the inflaton field, e.g. $\lambda\,\phi^3$,
interactions between different fields,
non-linear evolution of the fields during inflation,
gravity itself is non linear…..

Why primordial NG is important?

Bispectrum vs power spectrum information

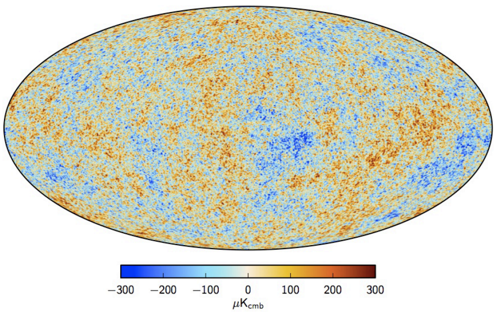

Planck 2015 Results. I. Overview of products and scientific results

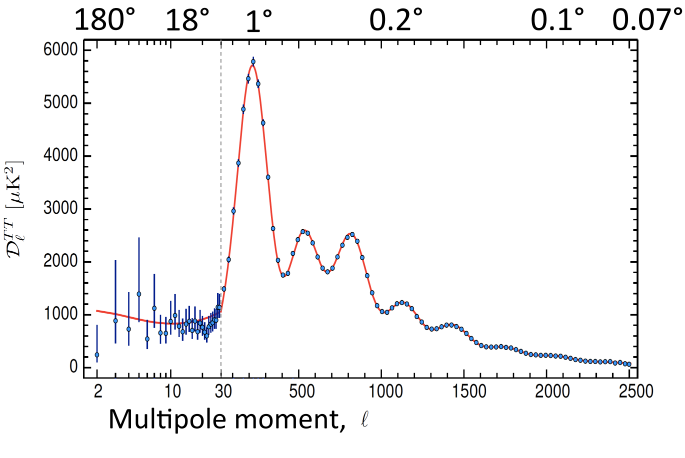

5×10^6 pixels compressed into ~2500 numbers: O.K. only if gaussian

If not we could miss precious information

Measure 3 point-function and higher-order

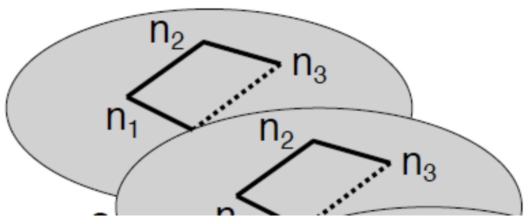

Another (among many) good reason:

f_{NL} and shape are model dependent:
e.g.: standard single-field models of slow-roll inflation predict

$$f_{NL} \sim O(\varepsilon,\eta) \ll 1$$

(Acquaviva, Bartolo, Riotto, Matarrese 2002; Maldacena 2002)

A detection of a primordial $|f_{NL}|\sim 1$ would rule out *all* standard single-field models of slow-roll inflation

Shapes of NG: local NG

Bispectrum peaks for squeezed triangles $k_3 \ll k_1 \sim k_2$

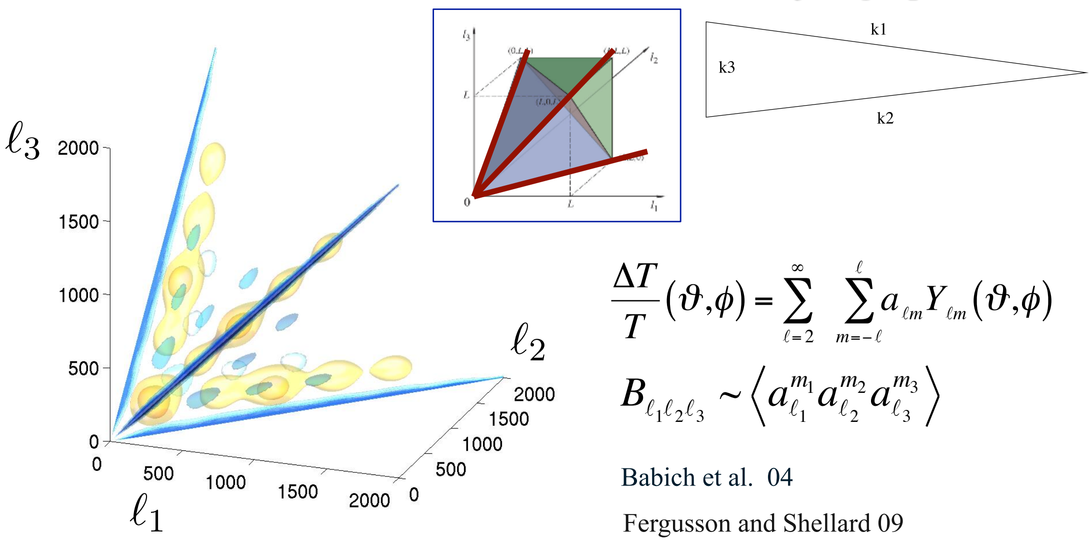

$$\frac{\Delta T}{T}(\vartheta,\phi) = \sum_{\ell=2}^{\infty} \sum_{m=-\ell}^{\ell} a_{\ell m} Y_{\ell m}(\vartheta,\phi)$$

$$B_{\ell_1\ell_2\ell_3} \sim \left\langle a_{\ell_1}^{m_1} a_{\ell_2}^{m_2} a_{\ell_3}^{m_3} \right\rangle$$

Babich et al. 04

Fergusson and Shellard 09

$$\zeta(\mathbf{x}) = \zeta_g(\mathbf{x}) + \frac{3}{5} f_{\rm NL} \zeta_g^2(\mathbf{x})$$

Non-linearities develop outside the horizon during or immediately after inflation (e.g. ***multifield models of inflation***)

Equilaterl NG

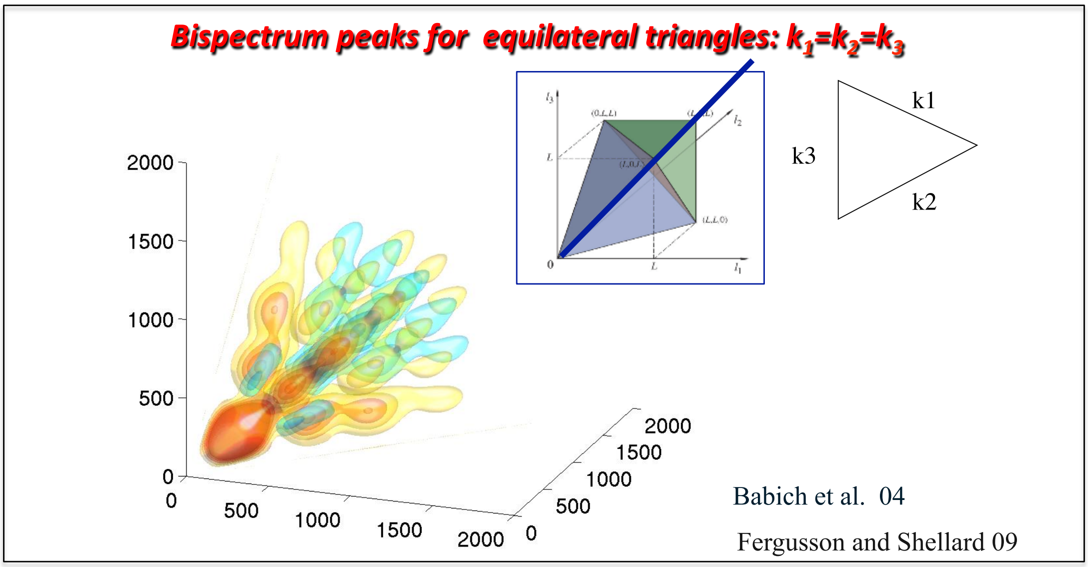

Single field models of inflation with non-canonical kinetic term L=P(φ, X) where X=(∂ φ)² (DBI or K-inflation) where NG comes from higher derivative interactions of the inflaton field

Example: $\delta\dot{\phi}(\nabla\delta\phi)^2$

The CMB bispectrum as seen by Planck

$$\frac{\Delta T}{T}(\vartheta,\phi) = \sum_{\ell=2}^{\infty}\sum_{m=-\ell}^{\ell} a_{\ell m} Y_{\ell m}(\vartheta,\phi)$$

$$B_{\ell_1\ell_2\ell_3} = \sum_m \begin{pmatrix} \ell_1 & \ell_2 & \ell_3 \\ m_1 & m_2 & m_3 \end{pmatrix} \left\langle a_{\ell_1}^{m_1} a_{\ell_2}^{m_2} a_{\ell_3}^{m_3} \right\rangle;$$

$$B_{\ell_1\ell_2\ell_3} = h_{\ell_1\ell_2\ell_3} b_{\ell_1\ell_2\ell_3}$$

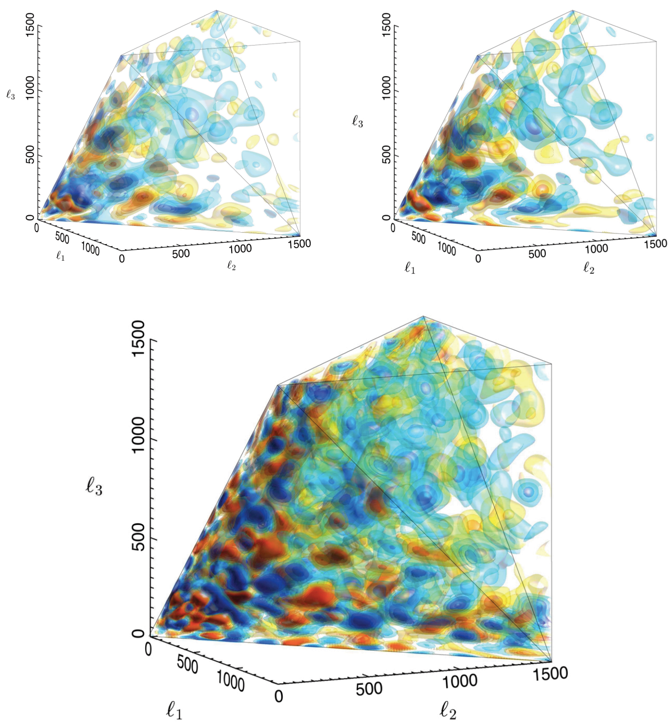

Limits set by Planck

See Planck 2015 results. XVII. Constraints on primordial non-Gaussianity

Observational limits set by Planck

Shape and method	f_{NL}(KSW) Independent	f_{NL}(KSW) ISW-lensing subtracted
SMICA (T)		
Local	10.2 ± 5.7	**2.5 ± 5.7**
Equilateral	−13 ± 70	**−16 ± 70**
Orthogonal	−56 ± 33	**−34 ± 33**
SMICA (T+E)		
Local	6.5 ± 5.0	**0.8 ± 5.0**
Equilateral	3 ± 43	**−4 ± 43**
Orthogonal	−36 ± 21	**−26 ± 21**

e.g. models with non-standard kinetic terms

e.g. multi-field models of inflation

Planck 2015 results. XVII. Constraints on primordial non-Gaussianity.

Implications for inflation models

- The standard models of single-field slow-roll inflation has survived the most stringent tests of Gaussianity to-date:
  deviations from primordial Gaussianity are less than 0.01% level. This is a fantastic achievement, one of the most precise measurements in cosmology!

$$\Phi(\mathbf{x}) = \underbrace{\Phi^{(1)}(\mathbf{x})}_{\sim 10^{-5}} + \underbrace{f_{\rm NL}}_{\sim\text{few}} \underbrace{\left(\Phi^{(1)}(\mathbf{x})\right)^2}_{\sim 10^{-10}} + \ldots\ldots$$

- ***The NG constraints*** on different primordial bispectrum shapes ***severly limit/rule out specific key (inflationary) mechanisms alternative to the standard models of inflation***

General single-field models of inflation:
Implications for Effective Field Theory of Inflation

$$S = \int d^4x\,\sqrt{-g}\left[-\frac{M_{\rm Pl}^2\dot{H}}{c_s^2}\left(\dot{\pi}^2 - c_s^2\frac{(\partial_i\pi)^2}{a^2}\right) - M_{\rm Pl}^2\dot{H}(1-c_s^{-2})\dot{\pi}\frac{(\partial_i\pi)^2}{a^2} + \left(M_{\rm Pl}^2\dot{H}(1-c_s^{-2}) - \frac{4}{3}M_3^4\right)\dot{\pi}^3\right]$$

$$f_{\rm NL} \propto \frac{1}{c_s^2}$$

(Cheung et al. 08; Weinberg 08)
for extensions see also N.B., Fasiello, Matarrese, Riotto 10)

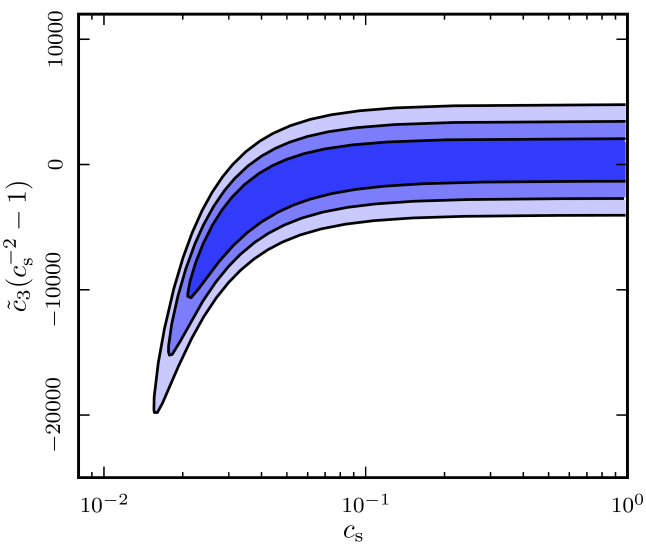

Constraints obtained from

$$f_{\rm NL}^{\rm equil} = -16 \pm 70 \quad (68\%\,\mathrm{CL})$$

$$f_{\rm NL}^{\rm ortho} = -34 \pm 33 \quad (68\%\,\mathrm{CL})$$

$$\boxed{c_s \geq 0.02 \ \text{ at } 95\%\ \mathrm{CL}}$$

What can we expect in the future?

CMB B-modes a smoking gun of inflation

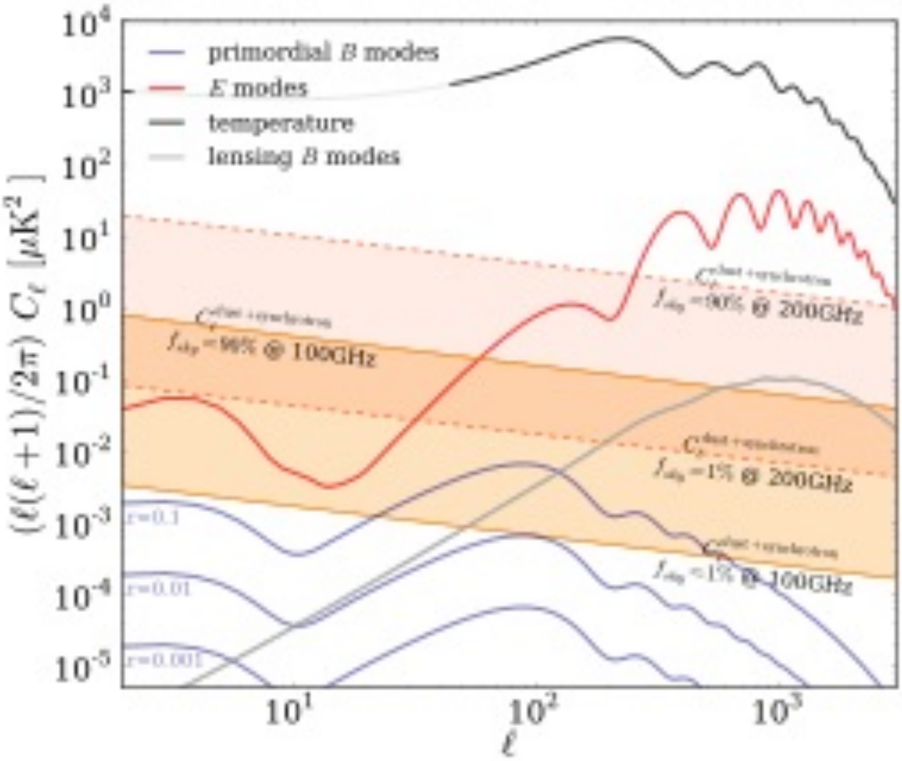

Forecasts for tensor-to-scalar ratio r

- **For future space CMB missions.**

Future constraints on inflationary models

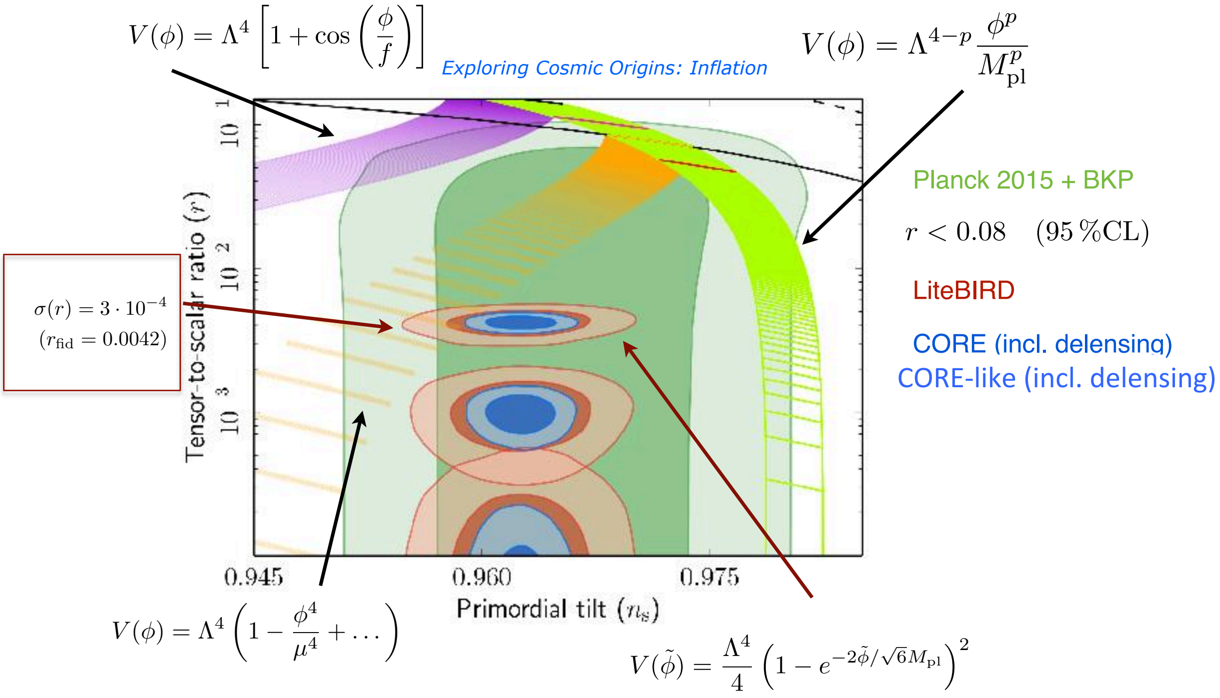

Bispectrum forecasts

$$\left\langle \zeta(\vec{k}_1)\zeta(\vec{k}_2)\zeta(\vec{k}_3)\right\rangle = (2\pi)^3\delta^{(3)}(\vec{k}_1+\vec{k}_2+\vec{k}_3)f_{NL}F(k_1,k_2,k_3)$$

	LiteCORE 80	LiteCORE 120	**CORE M5**	COrE+	Planck 2015	LiteBIRD	ideal 3000
T local	4.5	3.7	**3.6**	3.4	(5.7)	9.4	2.7
T equilat	65	59	**58**	56	(70)	92	46
T orthog	31	27	**26**	25	(33)	58	20
T lens-isw	0.15	0.11	**0.10**	0.09	(0.28)	0.44	0.07
E local	5.4	4.5	**4.2**	3.9	(32)	11	2.4
E equilat	51	46	**45**	43	(141)	76	31
E orthog	24	21	**20**	19	(72)	42	13
E lens-isw	0.37	0.29	**0.27**	0.24		1.1	0.14
T+E local	2.7	2.2	**2.1**	1.9	(5.0)	5.6	1.4
T+E equilat	25	22	**21**	20	(43)	40	15
T+E orthog	12	10.0	**9.6**	9.1	(21)	23	6.7
T+E lens-isw	0.062	0.048	**0.045**	0.041		0.18	0.027

Running non-Gaussianity constraints

$$B(k_1,k_2,k_3) \propto f_{\rm NL}\left(\frac{k_1+k_2+k_3}{3\mathbf{k}_{piv}}\right)^{n_{\rm NG}} F(k_1,k_2,k_3)$$

where F is of the local or equilateral type

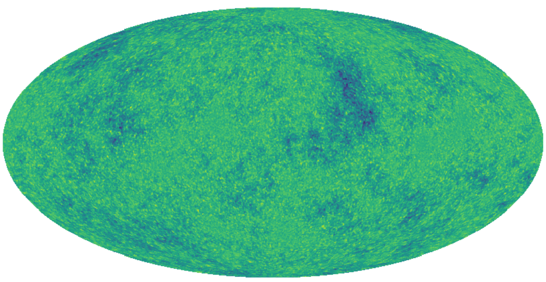

$n_{\rm NG} = -0.6$

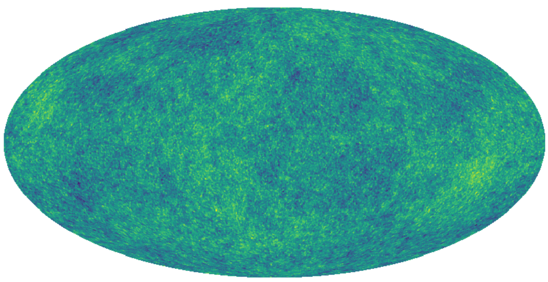

$n_{\rm NG} = 0.6$

Oppizzi, Liguori, Renzi, Arroja, N.B., *arXiv:1711.08286*

Running non-Gaussianity constraints

$B(k_1,k_2,k_3) \propto f_{\rm NL}\left[(k_1k_2)^{n_\varsigma-4}k_3^{n_{\rm NG}}+2\text{ perms.}\right]$

(e.g., curvaton models)

model	$n_{\rm NG}$	$\mathbf{k}_{piv}$
one-field (local)	$0.2^{+1.5}_{-0.5}$	$0.035\,{\rm Mpc}^{-1}$
two-field (local)	$0.4^{+0.9}_{-0.7}$	$0.01\,{\rm Mpc}^{-1}$
geometric mean (equil.)	$-0.4^{+1.4}_{-0.5}$	$0.01\,{\rm Mpc}^{-1}$

$B(k_1,k_2,k_3) \propto f_{\rm NL}\left[(k_1k_2)^{n_\varsigma+(n_{\rm NG}/2)-4}+2\text{ perms.}\right]$

(e.g., two-field models)

$$B(k_1,k_2,k_3) \propto f_{\rm NL}\left(\frac{k_1k_2k_3}{\mathbf{k}_{piv}}\right)^{n_{\rm NG}/3} F(k_1,k_2,k_3)$$

(general single-field, with non-standard kinetic term, e.g. DBI inflation).

Oppizzi, Liguori, Renzi, Arroja, N.B., *arXiv:1711.08286*

Running non-Gaussianity forecasts

Experiment	(ℓ_{max})	$f^{loc}_{\rm NL}=5$	$f^{loc}_{\rm NL}=10$	$f^{loc}_{\rm NL}=25$
Planck	(2400)	1.7	0.8	0.3
LiteBIRD	(1350)	1.6	0.8	0.3
LiteCOrE 120	(3000)	0.7	0.4	0.1
COrE	(3000)	0.7	0.3	0.1

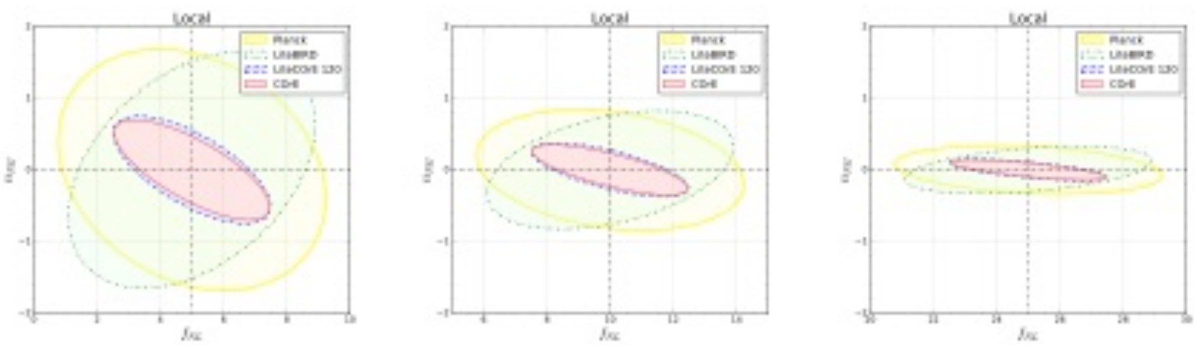

For values of f_NL which do not correspond to the current best-fit value but are well within the current scale-independent 95% C.L. intervals, significant n_{NG} improvements are expected with future surveys.

Oppizzi, Liguori, Renzi, Arroja, N.B., *arXiv:1711.08286*

What can be new inflationary signatures?

Tensor non-Gaussianities

Motivations: the nature of gravitational waves (I)

- ✓ A detection of GW would not by itself determine the precise mechanism generating the the tensor modes: ***alternative and new observational probes***

- ✓ ***<u>Go beyond the power spectrum and look for the statistical properties of GW:</u>***

$$\langle \gamma_{\mathbf{k}_1} \gamma_{\mathbf{k}_2} \gamma_{\mathbf{k}_3} \rangle \qquad \langle \gamma\zeta\zeta \rangle \qquad \langle \zeta\gamma\gamma \rangle$$

Full-sky	$\sum_n \ell_n = \text{even}$	$\sum_n \ell_n = \text{odd}$
Flat-sky	left-handed = right-handed	left-handed = (−) right-handed
Non-vanishing in parity-conserving universe	$\langle TTT \rangle$, $\langle TEE \rangle$, $\langle TTE \rangle$, $\langle EEE \rangle$, $\langle BBE \rangle$, $\langle BBT \rangle$	$\langle BTT \rangle$, $\langle BEE \rangle$, $\langle BET \rangle$, $\langle BBB \rangle$

$$a^T_{\ell m} \to (-1)^\ell a^T_{\ell m}\,,$$
$$a^E_{\ell m} \to (-1)^\ell a^E_{\ell m}\,,$$
$$a^B_{\ell m} \to (-1)^{\ell+1} a^B_{\ell m}$$

N.B.: single-field models do predcit these signals

M. Shiraishi, D. Nitta, and S. Yokoyama, `11; J.Maldacena, G. Pimenthel `11; X. Gao, T. Kobayashi, M. Shiraishi, M. Yamaguchi, J. Yokoyama, and S. Yokoyama, '13; M. Shiraishi, M.Liguori, J. Fergusson `15; Meerburg et al. `16; L. Dai, D. Jeong, M. Kamionkowski `13 and many more Refs.

The nature of gravitational waves (II)

- ✓ ***These observables can be signatures of <u>new physics.</u>***
  e.g.:
  - these correlators obey specific consistency relations in standard single-field
    If violated could signal
    * ***anisotropic evolution during inflation***
      (see, e.g., N.B., Matarrese, Peloso, Ricciardone, '13; Akhshik, Emami,Firouzjahi, Wang '14; Endlich, Horn, Nicolis, Wang, '14; Bordin, Creminelli et al. '16)
    * ***extra light spin-2 or higher spin particles***
      (Harkani-Hamed, Maldacena '16).
    * ***symmetry breaking patterns different w.r.t single-field models (solid-like models of inflation)***
      (Endlich, Nicolis, Wang, '13; N.B, Cannone, Ricciardone, Tasinato 16; Akhshik 15
  - also ***parity breaking signatures*** (see specific example later)

- ✓ Analyses of this type have already been carried out within *Planck:*
  we have all the tools and expertise to build a full pipeline to fully characterize tensor non-Gaussianities.

Present constraints on tensor NG $\langle \gamma_{\mathbf{k}_1} \gamma_{\mathbf{k}_2} \gamma_{\mathbf{k}_3} \rangle$

Parity-odd

Planck

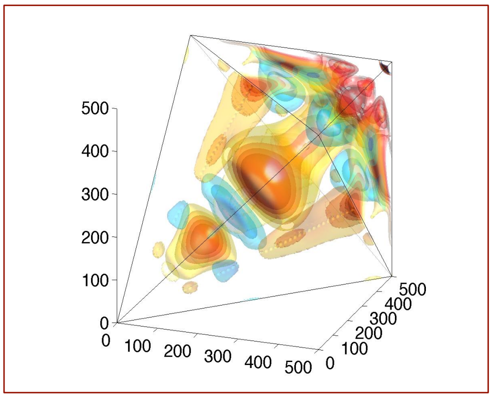

WMAP

M. Shiraishi, M. Liguori, J. Fergusson 2014

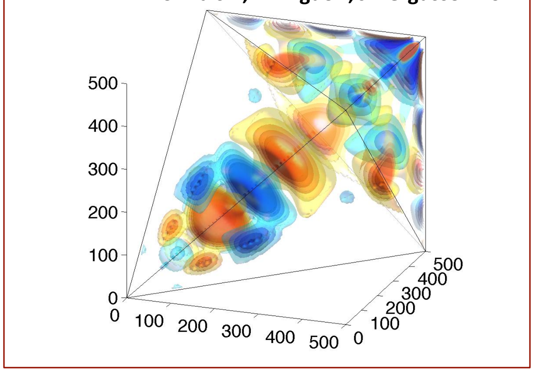

	Even	Odd	All
SMICA			
T	2 ± 15	120 ± 110	4 ± 15
T+E	0 ± 13		
SEVEM			
T	2 ± 15	120 ± 110	5 ± 15
T+E	4 ± 13		
NILC			
T	3 ± 15	110 ± 100	5 ± 15
T+E	1 ± 13		

- We fit parity-odd and parity-even pseudo-scalar bispectra to *Planck* data.
- Constraints and reconstruction consistent with WMAP.

Present constraints on tensor NG and forecasts

$$\langle \gamma \zeta \zeta \rangle$$

From <TTT>

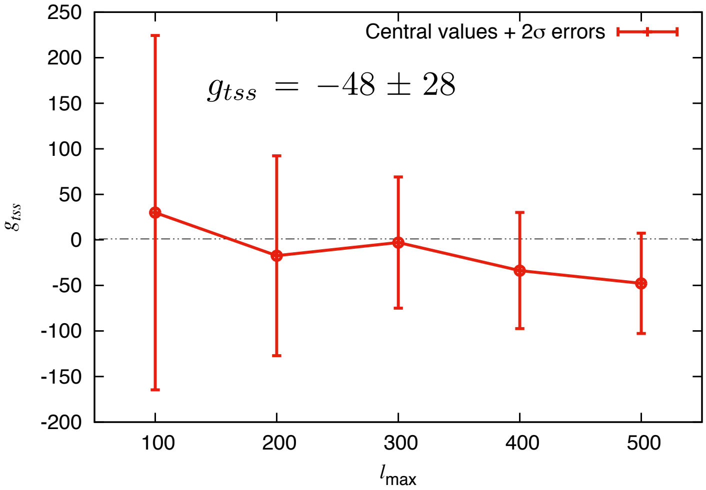

Shiraishi, Liguori, Fergusson, arXiv:1710.06778

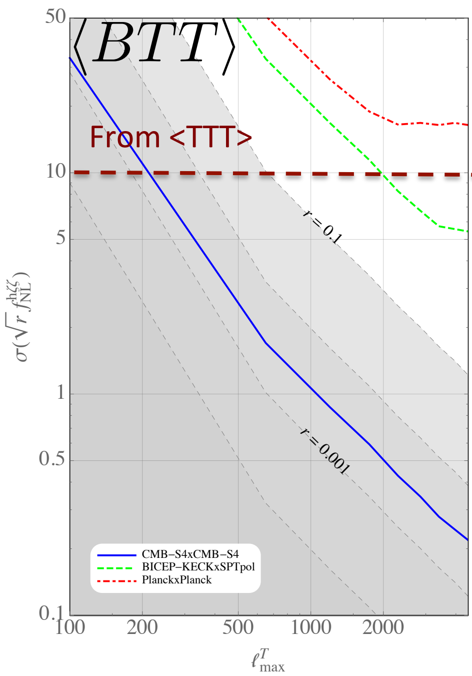

Meerburg et al. 2016

S4-like experiment ***can improve by two orders of magnitude w.r.t to <TTT> bispectra.***

- Notice that for an experiment like LiteBird looking for tensor non-Gaussianities could be particularly relevant:

  * high sensitivity to B-mode polarization

  * limited to relatively low l, where typically the tensor modes are most significant

Modifying gravity during inflation and non-Gaussianity

- Example: ***graviton non-Gaussianities beyond ordinary Einstein gravity*** considered in Madacena & Pimentel (2011); Soda, Kodama, Nozawa (2011); Shiraishi, Nitta, Yokoyama (2011)

$\langle\gamma\gamma\gamma\rangle$ from higher derivative corrections

$$S = \int d\tau d^3x \lambda^{-2} \left(\sqrt{-g}C^3 + \tilde{C}C^2\right)$$

$$C^3 = C^{\alpha\beta}{}_{\gamma\delta} C^{\gamma\delta}{}_{\sigma\rho} C^{\sigma\rho}{}_{\alpha\beta}$$

$$\widetilde{C}C^2 = \epsilon^{\alpha\beta\mu\nu} C_{\mu\nu\gamma\delta} C^{\gamma\delta}{}_{\sigma\rho} C^{\sigma\rho}{}_{\alpha\beta}$$

however such primordial NG is unobservably small.

Testing parity breaking signatures via GWs

Slow-roll inflation with a Chern-Simons term

$$S = \frac{1}{2}\int d^4x\,\sqrt{g}\,\left[M_{pl}^2 R - g_{\mu\nu}D^\mu\phi D^\nu\phi - 2V(\phi)\right] + f(\phi)\epsilon^{\mu\nu\rho\sigma}C_{\mu\nu}{}^{\kappa\lambda}C_{\rho\sigma\kappa\lambda}$$

parity-breaking term

$C_{\mu\nu\rho\sigma}$: Weyl tensor, traceless component of the Riemann tensor
$\epsilon_{\mu\nu\rho\sigma}$: Levi-Civita pseudotensor

- Left (L) and Right(R) polarized gravitational waves are generated

Asymmetry in the power spectrum of the primordial gravitational waves

$$\Theta_{R-L} = \frac{P_T^R - P_T^L}{P_T^R + P_T^L} = \frac{\pi}{2}\frac{H}{M_{C-S}}$$

***see N.B., Giorgio Orlando. JCAP 2017* (arXiv:1706.04627)**

Constraints and forecasts for future experiments

arXiv:1605.09357v1 [astro-ph.CO] 30 May 2016

Testing chirality of primordial gravitational waves with Planck and future CMB data: no hope from angular power spectra

Martina Gerbino,[a,b] Alessandro Gruppuso,[c,d] Paolo Natoli,[e] Maresuke Shiraishi,[f] Alessandro Melchiorri[g]

[a]The Oskar Klein Centre for Cosmoparticle Physics, Department of Physics, Stockholm University, AlbaNova, SE-106 91 Stockholm, Sweden
[b]The Nordic Institute for Theoretical Physics (NORDITA), Roslagstullsbacken 23, SE-106 91 Stockholm, Sweden
[c]INAF, Istituto di Astrofisica Spaziale e Fisica Cosmica di Bologna, via P. Gobetti 101, I-40129 Bologna, Italy
[d]INFN, Sezione di Bologna, Via Irnerio 46, I-40126 Bologna, Italy
[e]Dipartimento di Fisica e Scienze della Terra and INFN, Università degli Studi di Ferrara, Via Saragat 1, I-44100 Ferrara, Italy
[f]Kavli Institute for the Physics and Mathematics of the Universe (Kavli IPMU, WPI), UTIAS, The University of Tokyo, Chiba, 277-8583, Japan
[g]Physics Department and INFN, Università di Roma "La Sapienza", P.le Aldo Moro 2, 00185, Rome, Italy
E-mail: martina.gerbino@fysik.su.se, gruppuso@iasfbo.inaf.it, paolo.natoli@gmail.com, maresuke.shiraishi@ipmu.jp, alessandro.melchiorri@roma1.infn.it

Abstract. We use the 2015 Planck likelihood in combination with the Bicep2/Keck likelihood (BKP and BK14) to constrain the chirality, χ, of primordial gravitational waves in a scale-invariant scenario. In this framework, the parameter χ enters theory always coupled to the tensor-to-scalar ratio, r, e.g. in combination of the form $\chi \cdot r$. Thus, the capability to detect χ critically depends on the value of r. We find that with present data set χ is *de facto* unconstrained. We also provide forecasts for χ from future CMB experiments, as COrE+, exploring several fiducial values of r. We find that the current limit on r is tight enough to disfavor a neat detection of χ. For example in the unlikely case in which $r \sim 0.1(0.05)$, then the maximal chirality case, i.e. $\chi = \pm 1$, could be detected with a significance of $\sim 2.5(1.5)\sigma$ at best. We conclude that the two-point statistics at the basis of CMB likelihood functions is currently unable to constrain chirality and may only provide weak limits on χ in the most optimistic scenarios. Hence, it is crucial to investigate the use of other observables, e.g. provided by higher order statistics, to constrain these kind of parity violating theories with the CMB.

Non-Gaussianities from the Chern-Simons term

$$\langle \gamma_R(\vec{k}_1)\gamma_R(\vec{k}_2)\zeta(\vec{k}_3)\rangle_{C-S} = -\left(H^2 \frac{\partial^2}{\partial^2\phi} f(\phi)\right)^* \left(\sum_{i<j} P_T(k_i)P_T(k_j)\right) F'(k_i)$$

$$F'(k_i) = 8 \; \frac{(k_1+k_2)(k_3^2-k_2^2-k_1^2)\left(1-\frac{k_3^2-k_2^2-k_1^2}{2k_1k_2}\right)^2}{\left(\sum_i k_i^3\right)}$$

Shape of the bispectrum: peaks for squeezed configurations $k_3 << k_1 \sim k_2$

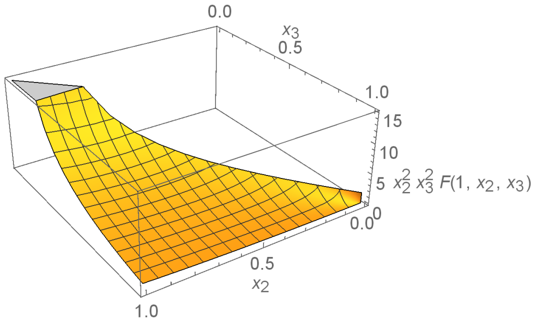

coefficent of parity violation in the bispectrum $\langle\gamma\gamma\zeta\rangle$

$$B^{\gamma\gamma\zeta}_{R-L} = \frac{\langle\gamma_R\gamma_R\zeta\rangle_{TOT} - \langle\gamma_L\gamma_L\zeta\rangle_{TOT}}{\langle\gamma_R\gamma_R\zeta\rangle_{TOT} + \langle\gamma_L\gamma_L\zeta\rangle_{TOT}} \sim 2\left(H^2 \frac{\partial^2}{\partial^2\phi} f(\phi)\right)^*$$

$$\langle a^B_{\ell_1 m_1} a^B_{\ell_2 m_2} a^T_{\ell_3 m_3}\rangle \sim [\langle\gamma_R\gamma_R\zeta\rangle - \langle\gamma_L\gamma_L\zeta\rangle] \propto \; B^{\gamma\gamma\zeta}_{L-R}$$

for $\ell_1+\ell_2+\ell_3 = \mathrm{odd}$

N.B., Giorgio Orlando, '17

Gravitational waves from inflation
&
(future) interferometric measurements

Complementarity between CMB and interferometers

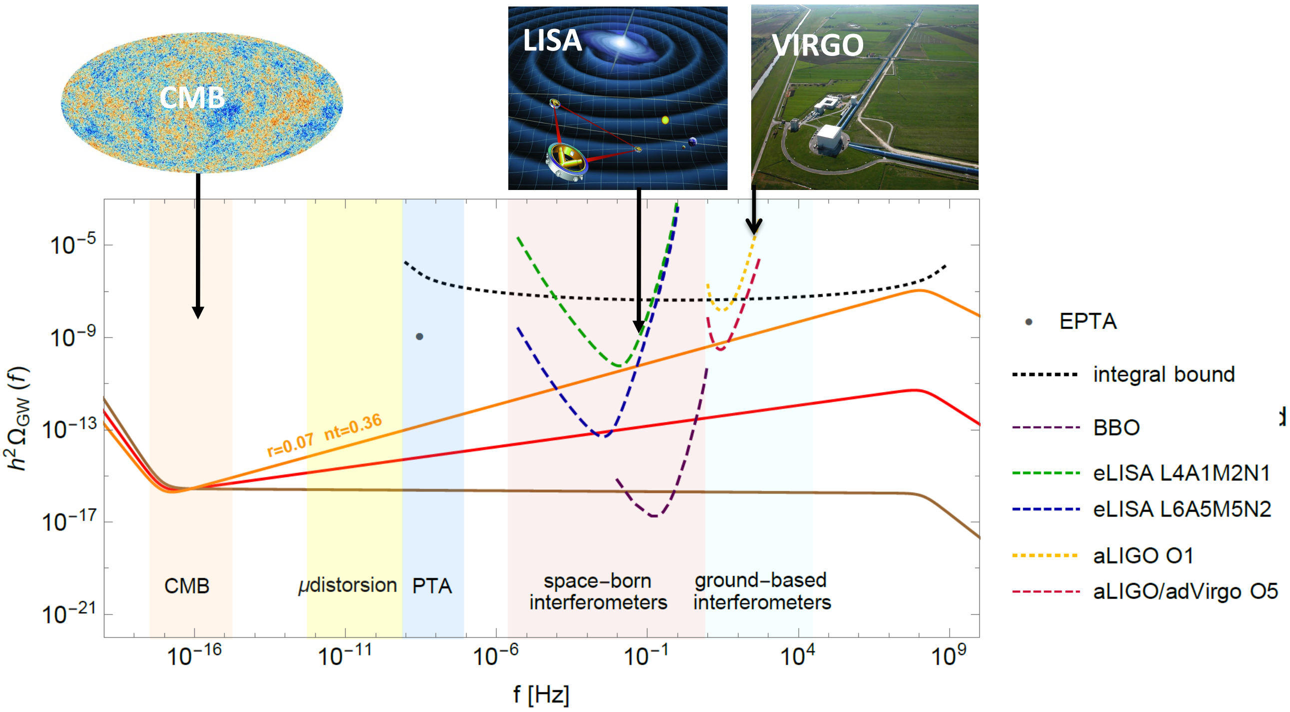

From M.C. Guzzetti, N.B., M. Liguori, S. Matarrese, ``Gravitational waves from Inflation'', arXiv:1605.01615

Complementarity between CMB and interferometers

➢ Data from interferometers have already provided useful constraints.

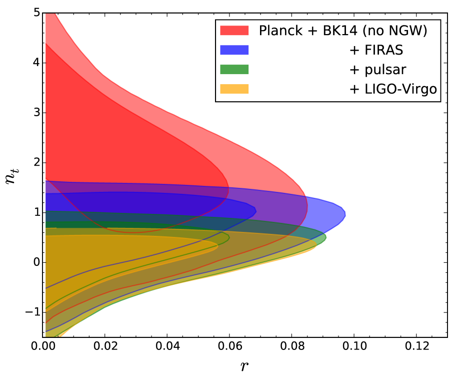

$$r < 0.085 \quad n_T = 0.04^{+0.61}_{-0.85} \quad (95\%\ \text{C.L.})$$

G. Cabass, L. Pagano et al. 2015

➢ One can test for
- additional degrees of freedom besides the inflaton
- new symmetry patterns in the inflationary sector (see, e.g., N.B., Cannone, Ricciardone, Tasinato `15).

<u>Case studies have been proposed in ``Science with the space-based interferometer LISA. IV: Probing inflation with gravitational waves''</u>, N.B., C. Caprini, V. Domcke, D. Figueroa, J. Garcia-Bellido, M. C. Guzzetti. et al. (including M.Liguori & S. Matarrese), arxiv 1610.06481, accepted for publication in JCAP

The nature of gravitational waves

GW PRODUCTION	Discriminant	Specific discriminant	Examples of specific models	Produced GW
Vacuum oscillations quantum fluctuations of the gravitational field stretched by the accelerated expansion	**theory of gravity**	General Relativity	*single-field slow-roll*	*broad spectrum*
			all other models in GR	broad spectrum
		MG/EFT approach	G-Inflation	broad spectrum
			Potential-driven G-Inflation	broad spectrum
			EFT approach	broad spectrum
Classical production second-order GW generated by the presence of a source term in GW equation of motion	**source term**	vacuum inflaton fluctuations	*all models*	*broad spectrum*
		fluctuations of extra scalar fields	inflaton+spectator fields	broad spectrum
			curvaton	broad spectrum
		gauge particle production	pseudoscalar inflaton+gauge field	broad spectrum
			scalar infl.+pseudoscalar+gauge	broad spectrum
		scalar particle production	scalar inflaton+ scalar field	peaked
		particle production during preheating	chaotic inflation	peaked
			hybrid inflation	peaked

From M.C Guzzetti, N.B., M. Liguori, S. Matarrese, ``Gravitational waves from Inflation'', arXiv:1605.01615

- ✓ A detection of GW would not by itself determine the precise mechanism generating the the tensor modes
- ✓ In addition to the standard quantum vacuum amplification of tensor perturbations on cosmological scales various mechanisms exist that produce during inflation (or immediately after inflation) a ***classical background of gravitational waves.***
- ✓ This *might* lead to the breaking of the one-to-one correspondence between amplitude of gravitational waves and energy scale of inflation → crucial to study and constrain these scenarios

The nature of gravitational waves

ANY inflationary model → quantum fluctuations of the gravitational field

POSSIBLE EXTRA PRODUCTION

due to further fields besides the gravitational one

CLASSICAL gw production

$$h''_{ij} + 2\mathcal{H}h'_{ij} - \nabla^2 h_{ij} = \frac{2}{M_{\rm pl}^2}\hat{\Pi}_{ij}^{lm}T_{lm}$$

SOURCE TERM

$$\Rightarrow \quad \Omega_{\rm gw} = \Omega_{\rm gw}^{vacuum} + \Omega_{\rm gw}^{sourced}$$

This and the next 2 slides courtesy of Maria Chiara Guzzetti.

The nature of gravitational waves: test specific models combining different observables

INFLATION WITH SPECTATOR FIELD

inflaton + spectator field σ

$$\Rightarrow \quad \Omega_{\rm gw} = \Omega_{\rm gw}^{vacuum} + \Omega_{\rm gw}^{sourced}$$

curvature and tensor power spectra

T. Fujita, J. Yokoyama and S. Yokoyama, PTEP 2015 (2015) 043E01, 1411.3658.

$$\begin{cases} P_S(k) \simeq \dfrac{H^2}{4\epsilon M_{pl}^2}\left(\dfrac{k}{k_*}\right)^{n_s^{(v)}-1} + \dfrac{1}{32\pi c_s^7}\dfrac{H^4}{M_{pl}^4}\left(\dfrac{k}{k_*}\right)^{-4\epsilon-7s} \\ P_T(k) \simeq \underbrace{\dfrac{2H^2}{M_{pl}^2}\left(\dfrac{k}{k_*}\right)^{n_T^{(v)}}}_{\text{VACUUM FLUCTUATIONS}} + \underbrace{\dfrac{8}{15\pi c_s^3}\dfrac{H^4}{M_{pl}^4}\left(\dfrac{k}{k_*}\right)^{-4\epsilon-3s}}_{\text{CLASSICAL PRODUCTION}} \end{cases}$$

N. B., C. Caprini, V. Domcke, D. Figueroa, et al. (including M.C. Guzzetti, M. Liguori & S. Matarrese), *arxiv 1610.06481, accepted in JCAP*

The nature of gravitational waves: test specific models combining different observables

INFLATION WITH SPECTATOR FIELD

inflaton + spectator field σ

$$\Rightarrow \quad \Omega_{\rm gw} = \Omega_{\rm gw}^{vacuum} + \Omega_{\rm gw}^{sourced}$$

c_s $\longrightarrow$ gw **amplitude**

σ speed of sound

$s = \dot{c}_s / H c_s$ $\longrightarrow$ gw **spectral index**

speed of sound evolution

at CMB scales

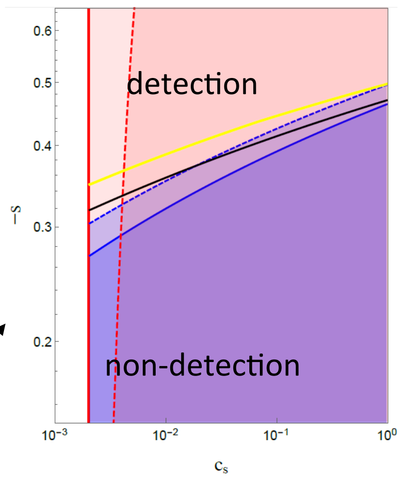

- **CMB data**
- **LISA**
- **aLIGO**
- **indirect bounds**

***non-Gaussianity**

<u>Notice that here primordial non-Gaussianity constraints on f_{NL} and the running of f_{NL} can play a crucial role</u>

N. B., C. Caprini, V. Domcke, D. Figueroa, et al. (including M.C. Guzzetti, M. Liguori & S. Matarrese), *arxiv 1610.06481, accepted in JCAP*

Blue tensor tilt from new symmetry patterns in the infationary sector

- ***Blue tensor tilt*** can also arise in models with a non-standard spacetime symmetry breaking pattern, such as ***solid*** (Endlich, Nicolis, Wang, 2013) or ***supersolid inflation***
  (Bartolo, D. Cannone, A. Ricciardone and G. Tasinato, 2016; Cannone, Tasinato and Wands, 2015)

- In these scenarios, space reparameterization invariance is spontaneously broken during inflation, by means of background fields with space-dependent vacuum expectation values leading to a mass for the graviton and consequently to a blue tensor tilt.

$$\phi^0 = t + \pi \, , \qquad \phi^i = \alpha\, x^i + \alpha\, \sigma^i$$

Blue tensor tilt from new symmetry patterns in the infationary sector

$$S_{(2)} \;=\; \frac{M_{\rm Pl}^2}{8} \int dt\, d^3x\, a^3(t)\, n(t) \left[\dot{h}_{ij}^2 - \frac{c_T^2(t)}{a^2}\, (\partial_l h_{ij})^2 - m_h^2(t)\, h_{ij}^2 \right]$$

$$\mathcal{P}_h \;=\; \frac{H^2}{2\pi^2\, M_{\rm Pl}^2\, c_T^3} \left(\frac{k}{k_*} \right)^{n_T} \qquad n_T \;=\; \frac{2}{3}\, \frac{m_h^2}{H^2}$$

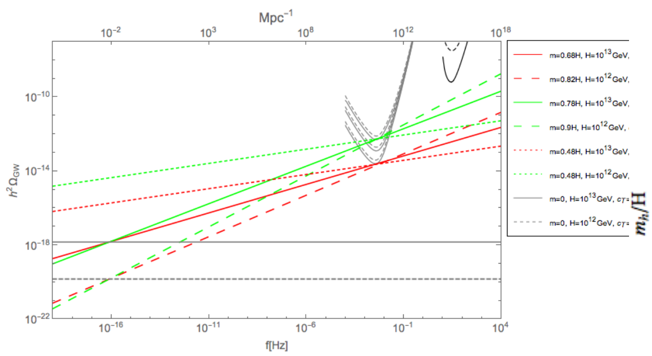

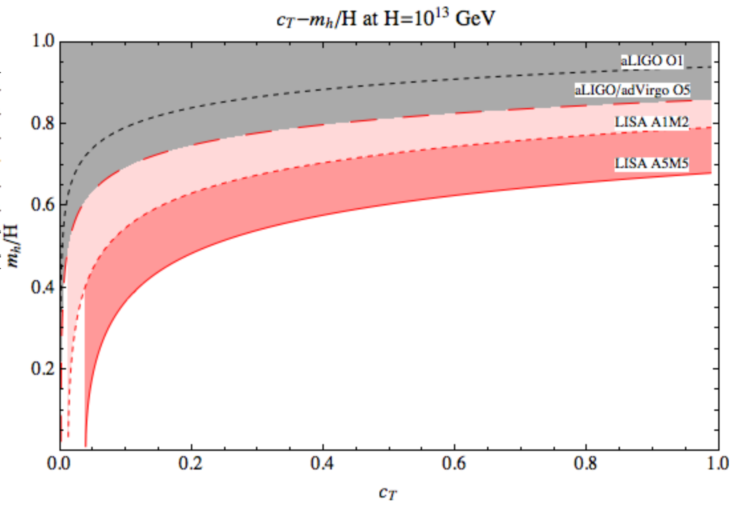

N. B., C. Caprini, V. Domcke, D. Figueroa, et al. (including M.C. Guzzetti, M. Liguori & S. Matarrese), *arxiv 1610.06481, accepted in JCAP*

New oscillatory primordial bispectra

- Specific non-Gaussianities which are signatures of ***new higher-spin particles during inflation***

- one can ask about ***new light-massless*** degrees of freedom during inflation

- one can ask about ***new massive*** particles

New oscillatory primordial bispectra

- Specific non-Gaussianities which are signatures of ***new massive higher-spin particles during inflation***

$$\frac{\langle\zeta\zeta\zeta\rangle}{\langle\zeta\zeta\rangle_{\rm short}\langle\zeta\zeta\rangle_{\rm long}} \sim \left(\sum_{s=0,1,2,\ldots}\frac{C_s}{k_1^3k_3^3}\left(\frac{k_1}{k_3}\right)^{3/2}\mathcal{P}_s(\hat{\mathbf{k}}_1.\hat{\mathbf{k}}_3)\,\cos\left[\mu_s\ln\left(\frac{k_1}{k_3}\right)+\phi_s\right]+(k_3\leftrightarrow k_2)\right)$$

Angular dependence which depends o the ***spin***
(already shown for spin-1 see, e.g.,
Barnaby, Namba, Peloso 2012,
N. B. , Matarrese, Peloso, Ricciardone 2013
Shiraishi, Komatsu, Peloso, Barnaby 2013)

$$\boxed{\mu_s = \sqrt{(m_s/H)^2-(s-1/2)^2}}$$

Oscillations that depend on the ***mass*** of the new particles

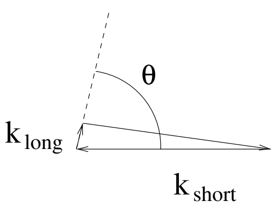

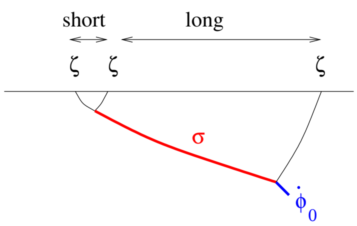

See Maldacena & Arkani-Hamed, '15
also, e.g.,
T. Noumi, M. Yamaguchi and D. Yokoyama '13
Lee, Baumann, Pimentel, '16

Massless new degrees of freedom

- ***Lesson from vector fields***: spinning degrees of freedom can be long-lived on super-Hubble scales if suitably coupled to the inflaton field.

- Consider the case of a U(1) vector field coupled to the inflaton fied **

$$\mathcal{L} = -\frac{I^2(\varphi)}{4} F_{\mu\nu} F^{\mu\nu}$$

** Among others: Ratra 1992; Himmetoglu 2010; Dulaney & Gresham 2010l; Gumrukcuoglu, Himmetoglu, Peloso; 2010;
Watanabe, Kanno, Soda, 2010; Hervik, Mota, Thorsurd, 2011; Barnaby, Namba, Peloso 2012;
Bonvin, Caprini, Durrer 2012; N. B. , Matarrese, Peloso, Ricciardone 2013;
Biagetti, Kehagias et al 2013; ; Naruko, Komatsu, Yamaguchi 2014

Detecting higher spin fields through statistical anisotropy

- One can generalize these arguments to higher spin fields

<u>**Vector fields:**</u> $$\left\langle \zeta_{\vec{k}_1} \zeta_{\vec{k}_2} \right\rangle = (2\pi)^3 \delta^{(3)}(\vec{k}_1 + \vec{k}_2) \bar{P}_\zeta(k_1) \left(1 + c_1 \sin^2\theta_k\right)$$

Spin dependence

<u>**Generic spin s:**</u> $$\left\langle \zeta_{\vec{k}_1} \zeta_{\vec{k}_2} \right\rangle = (2\pi)^3 \delta^{(3)}(\vec{k}_1 + \vec{k}_2) \bar{P}_\zeta(k_1) \left(1 + c_s \sin^{2s}\theta_k\right)$$

$$\left\langle \zeta_{\vec{k}_1} \zeta_{\vec{k}_2} \right\rangle = (2\pi)^3 \delta^{(3)}(\vec{k}_1 + \vec{k}_2) P_\zeta(k_1) \times \left[1 + \sum_{L\geq 1} \sum_{M} g_{LM} Y_{LM}(\hat{k}_1)\right]$$

- If particle of spin s then g_{LM} runs up to g_{2s,m}

N.B., A. Keaghias, M.Liguori, A. Riotto, M. Shiraishi, V. Tansella, arXiv:1711.08286
N. B. , Matarrese, Peloso, Ricciardone Phys.Rev. D87, 023504 (2013)

Detecting higher spin fields through statistical anisotropy

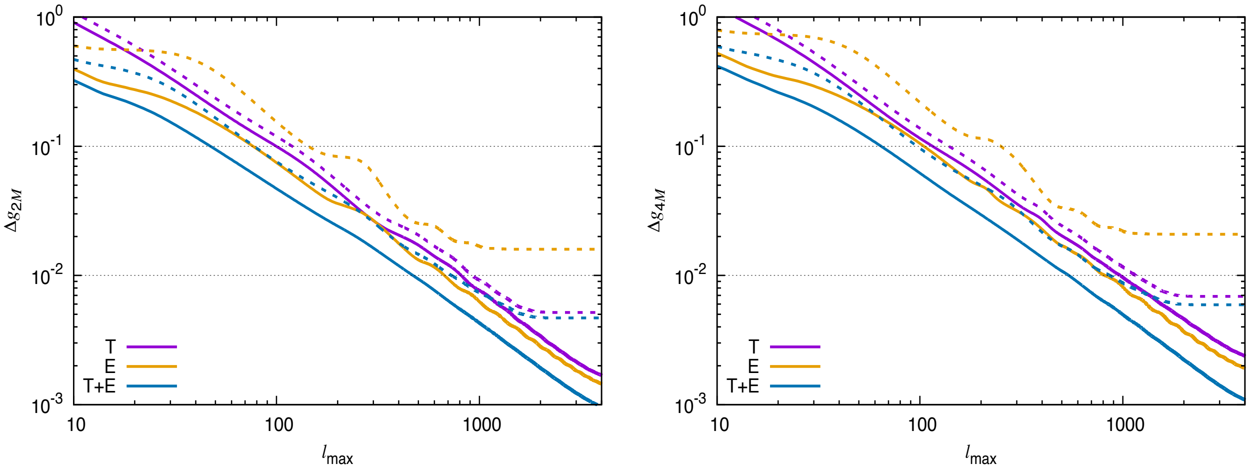

N.B., A. Keaghias, M.Liguori, A. Riotto, M. Shiraishi, V. Tansella, arXiv:1711.08286

- g_{LM} can be probed down to O(10^{-3}) through CMB; similar conclusions for LSS surveys

- independence of forecasted constraints from L.

What can be furhter new observational avenues?

New observational strategies

CMB is a priviliged laboratory for cosmic inflation. However different observables can be competitive, and in the future, have a better sensitivity to, e.g., primordial non-Gaussianity

- Large-Scale-Structure Surveys
- CMB spectral distortions
- Future high-redshift large radio surveys
- High-redshift 21cm fluctuations

New observational strategies

CMB is a priviliged laboratory for cosmic inflation. However different observables can be competitive, and in the future, have a better sensitivity to, e.g., primordial non-Gaussianity

- Large-Scale-Structure Surveys
- **CMB spectral distortions**
- Future high-redshift large radio surveys
- High-redshift 21cm fluctuations

CMB spectral distortions

- We know there must be tiny deviations from a perfect black body of the CMB spectrum in the frequency domain

- Not detected yet (apart y-distortions from Sunyaev-Zel'dovich effect)

- $\frac{\Delta I_\nu}{I_\nu} < 10^{-4}$ $\qquad \mu < 9\times 10^{-5}$ $\qquad y < 1.5\times 10^{-5}$ $\quad$ (95% C.L)

FROM COBE/FIRAS

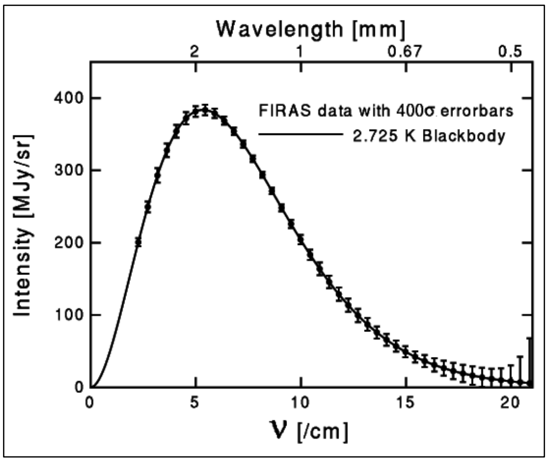

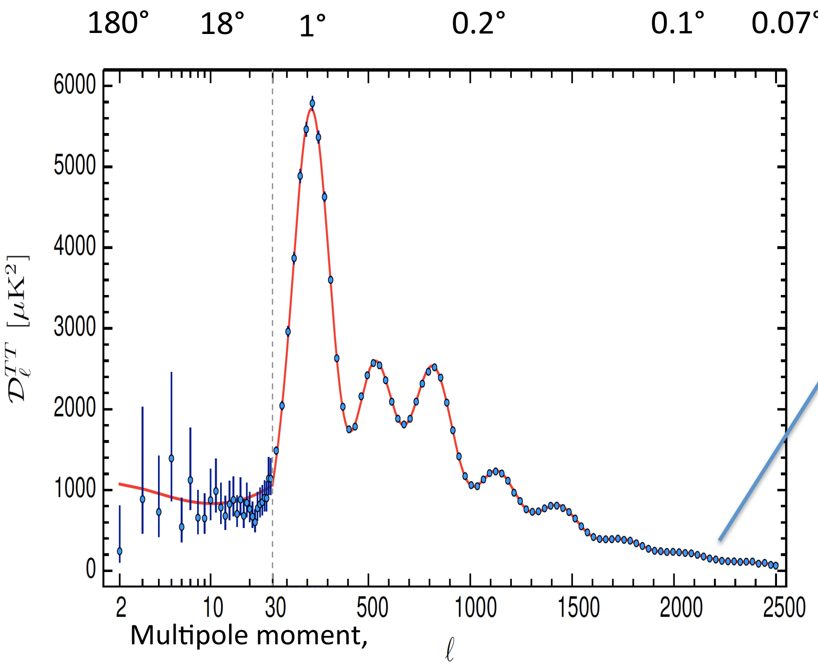

$$f = \frac{1}{e^{\frac{h\nu}{K_B T}} e^{\frac{\mu}{k_B T}}} - 1$$

$$\mu \approx \frac{1.4}{4} \left[\langle \delta_\gamma^2(x)\rangle_p\right]_{z_f}^{z_i}$$

- Energy injection from ***dissipation of acoustic waves due to Silk damping***
  The relevant redshit range is $\mathbf{5\times 10^4 = z_f < z < z_i = 2\times 10^6}$

  → relevant scales are $k_D(z_i)$ = 12000 Mpc^{-1} and $k_D(z_f)$ = 46 Mpc^{-1}

CMB spectral distortions

- Various planned and proposed satellite missions can achieve the required sensitivity to measure the (monopole) primordial μ and y spectral distortions: these are predicted to be $\langle\mu\rangle \approx 1.9\times10^{-9}$ and $\langle y\rangle \approx 4.2\times10^{-8}$

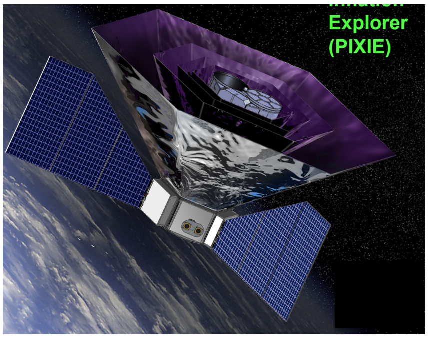

Sensitive to a minimum $\langle\mu\rangle_{min} \approx 10^{-9}$

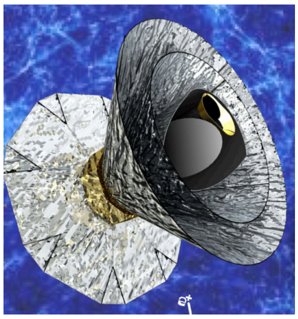

PRISM

Sensitive to a minimum $\langle\mu\rangle_{min} \approx 10^{-8}$

- Besides being a probe of the standard ΛCDM model (including inflation) it can unveil new physics, e.g. about
  - decaying and annihilating dark matter particles
  - black holes and cosmic strings

  and it can allow to measure a whole series of signals like y-distortions from re-ionized gas

A powerful source of information

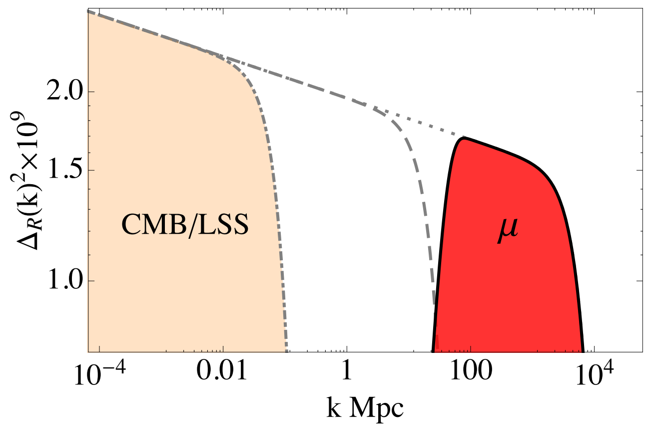

(From Pajer & Zaldarriaga 2012)

- CMB spectral distortions expected in the standard ΛCDM modeL: AN ALMOST UNEXPLOITED OBSERVATIONAL WINDOW (see, e.g., Kathri and Sunyaev 2013, arXiv: 1303.7212; Chluba 2016, arXiv: 1603.02496)

- **In particular can probe very small scales 10^{-4} - 0.02 Mpc!**

CMB spectral distortions and NG

- Pajer & Zaldarriaga (2012) and Ganc & Komatsu (2012) pointed out that the cross-correlation between CMB μ-distortion and CMB temperature fluctuations can be a diagnostic very sensitive to local-type bispectra peaking in the squeezed configuration: a cosmic variance limited experiment can achieve f_{NL}~0.001

Local primordial non-Gaussianity correlates short- with long-mode perturbations, so it induces a correlation between the dissipation process on small scales

$$\mu \sim \delta_\gamma^2 \sim \zeta_{\mathbf{k_1}}\zeta_{\mathbf{k_2}}$$

and the long-mode fluctuations in the CMB

$$\delta T/T \sim \zeta_{\mathbf{k}}$$

$$\downarrow$$

$$C_\ell^{\mu T} \sim \langle \zeta_{\mathbf{k_1}}\zeta_{\mathbf{k_2}}\zeta_{\mathbf{k_3}} \rangle$$

A simple argument in real space

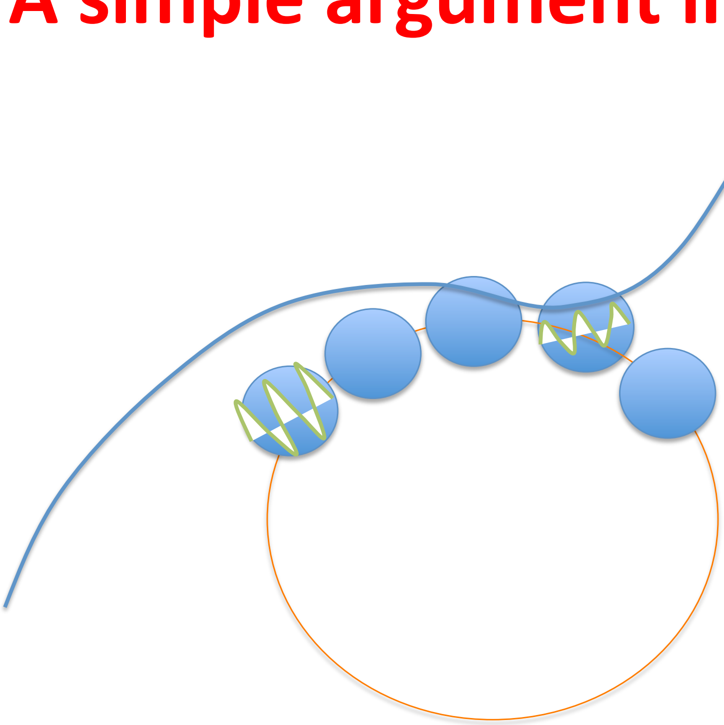

If there is a local model of non-Gaussianity, then the small scale power spectrum of curvature perturbation $\Delta^2_\zeta(k,x)$ will be modulated from patch to patch, by the long-wavelength curvature fluctuation and correlated to it

Looking at the inflationary trispectra (4-point correlation functions)

Looking at the inflationary trispectra

$$\langle \hat{\zeta}_{\vec{k}_1} \hat{\zeta}_{\vec{k}_2} \hat{\zeta}_{\vec{k}_3} \hat{\zeta}_{\vec{k}_4} \rangle = (2\pi)^3 \delta^{(3)}(\vec{k}_1 + \vec{k}_2 + \vec{k}_3 + \vec{k}_4) T_\zeta(\vec{k}_1, \vec{k}_2, \vec{k}_3, \vec{k}_4)$$

Scalar exchange:
comes from terms in the 3-oder action, e.g. $(\delta\phi)^3$

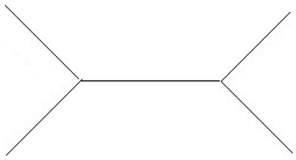

$\tau_{NL} \propto f^2_{NL}$

Contact interaction: e.g. $\lambda\,(\delta\phi)^4$ (intrinsic contributions from the 4-th order action)

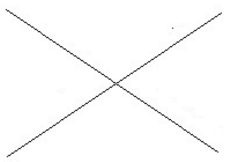

g_{NL}

Local trispectra

Possible models

$$\zeta(\mathbf{x}) = \zeta^{\mathrm{G}}(\mathbf{x}) + \frac{3}{5} f_{\mathrm{NL}} \left(\zeta^{\mathrm{G}}(\mathbf{x})\right)^2 + \frac{9}{25} g_{\mathrm{NL}} \left(\zeta^{\mathrm{G}}(\mathbf{x})\right)^3$$

or

$$\zeta(\mathbf{x}) = \zeta^{\mathrm{G}}(\mathbf{x}) + \sqrt{\tau_{\mathrm{NL}}}\,\sigma(\mathbf{x})\zeta^{\mathrm{G}}(\mathbf{x})$$

Typically arising in multi-field models of inflation

Looking at the inflationary trispectra

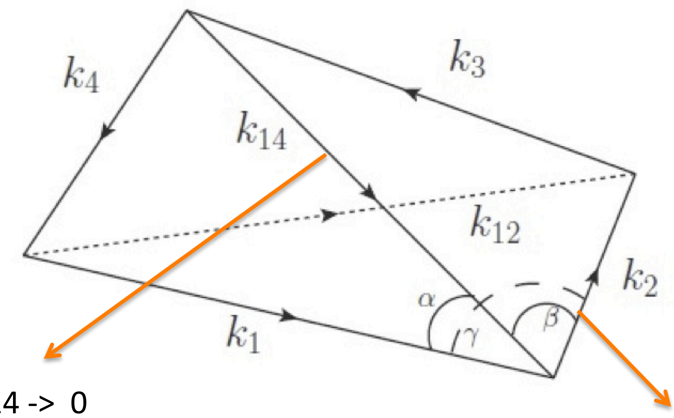

e.g. k_14 -> 0
corresponds to τ_NL:
a modulation of power spectra

e.g. k_2 -> 0
corresponds to g_NL:
a modulation of the bispectrum

Observational limits set by Planck

$$\tau_{\rm NL}^{\rm loc} < 2800 \quad (95\%\,{\rm CL})$$

$$\begin{aligned} g_{\rm NL}^{\rm local} &= (-9.0 \pm 7.7) \times 10^4; \\ g_{\rm NL}^{\dot\sigma^4} &= (-0.2 \pm 1.7) \times 10^6; \\ g_{\rm NL}^{(\partial\sigma)^4} &= (-0.1 \pm 3.8) \times 10^5. \quad (68\%\,{\rm CL}) \end{aligned}$$

Also From LSS

$-4.5 \times 10^5 < g_{\rm NL} < 1.6 \times 10^5 \;\; 95\%{\rm CL}$ *(Giannantonio et al. 2013)*

A simple guide argument

Why TTμ is sensitive to trispectrum (g_NL)?

Tμ is a bispectrum and T(Tμ) is a modulation of a bispectrum (exactly what g_{NL} does).

Forecasts for g_{NL}

Cosmic variance dominated case

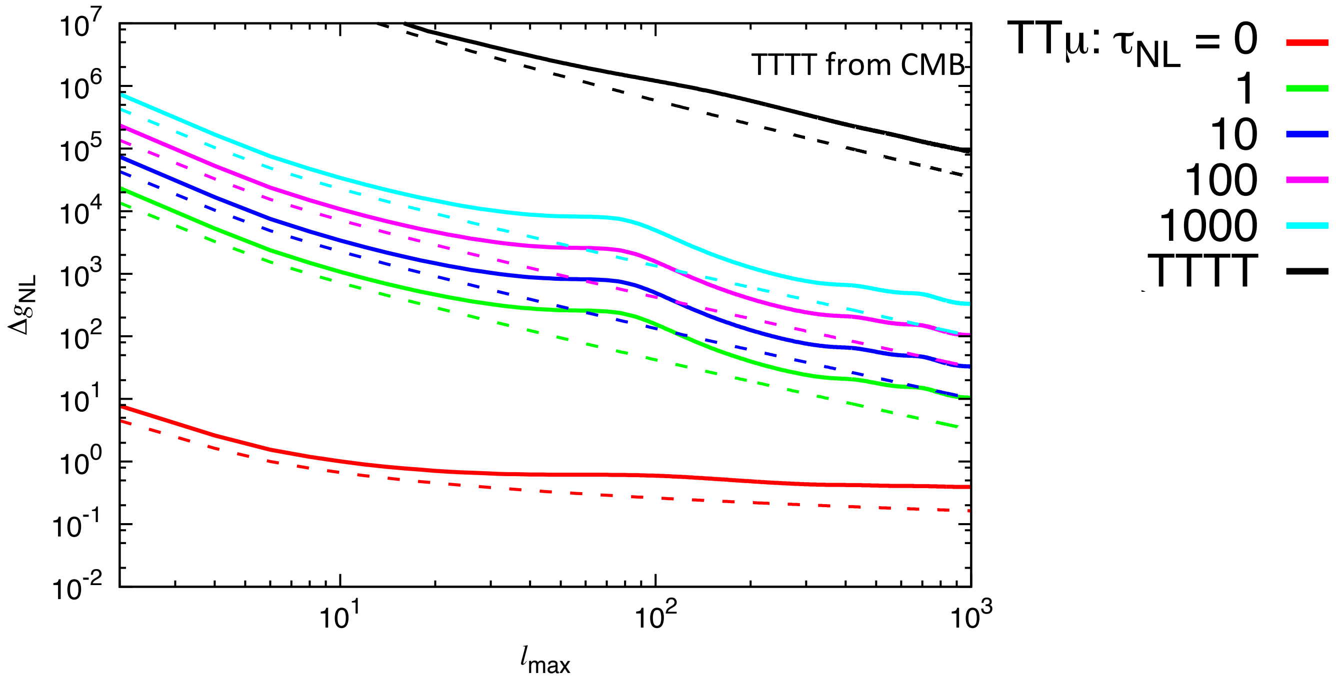

You can reach Δg_{NL}~0.4:
5 orders of magnitude improvement w.r.t to current constraints

g_{NL} forecasts for experiments

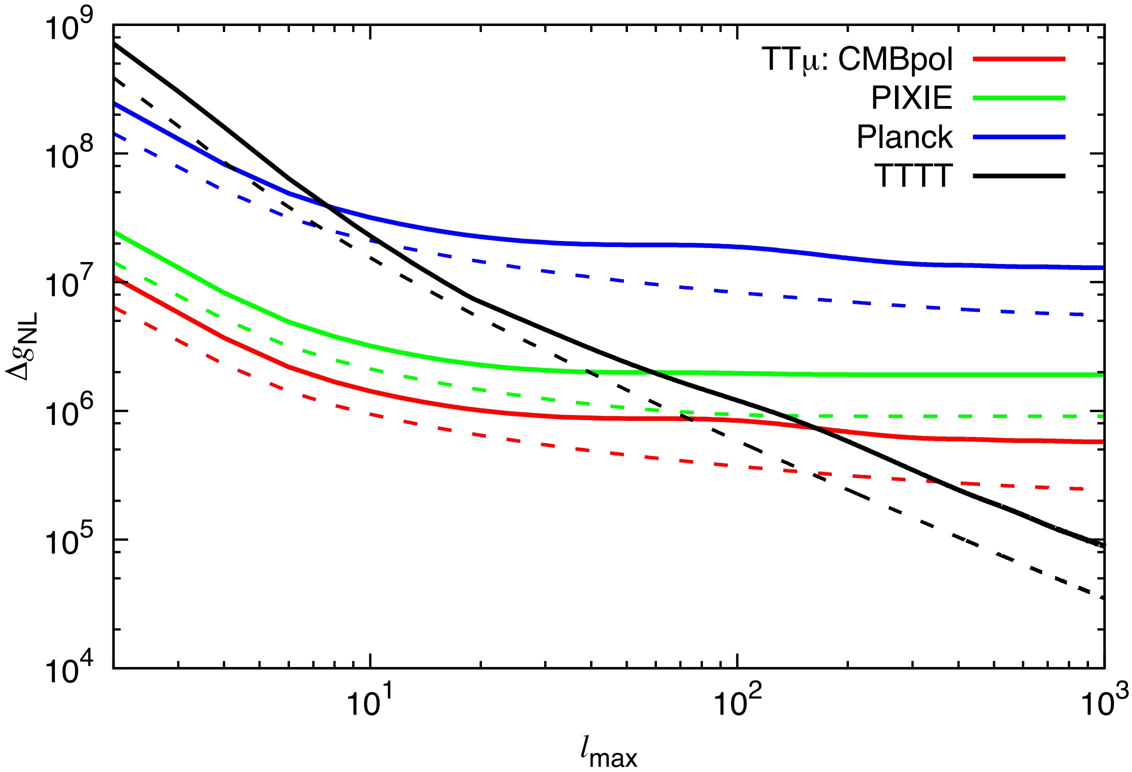

So why CMB spectral distortions are interesting in this context?

Among many reasons:

- **1**. Although CMB spectral distortion constraints on primordial NG might seem futuristic, the amount of information is so high that it is worth investigating the various issues

2. We are testing the predictions of the standard cosmological model: ΛCDM+standard models of inflation

3. Statistical estimators of primordial NG built from spectral distortions can present some advantages: e.g., our TTμ provides an *unbiased estimator* for the local trispectrum g_{NL}

4. The specific signal in Tμ, TTμ depends on the specific inflationary models considered (e.g. imprints from primordial vector fields, non-Bunch Davies vacuum states).
Also: can test alternative models of inflation, like ekpyrotic models which predict g_{NL} <-1700 a or -1000 < g_{NL} <-100.

4. CMB spectral distortions and constraints on inflationary models

arXiv:1612.08270

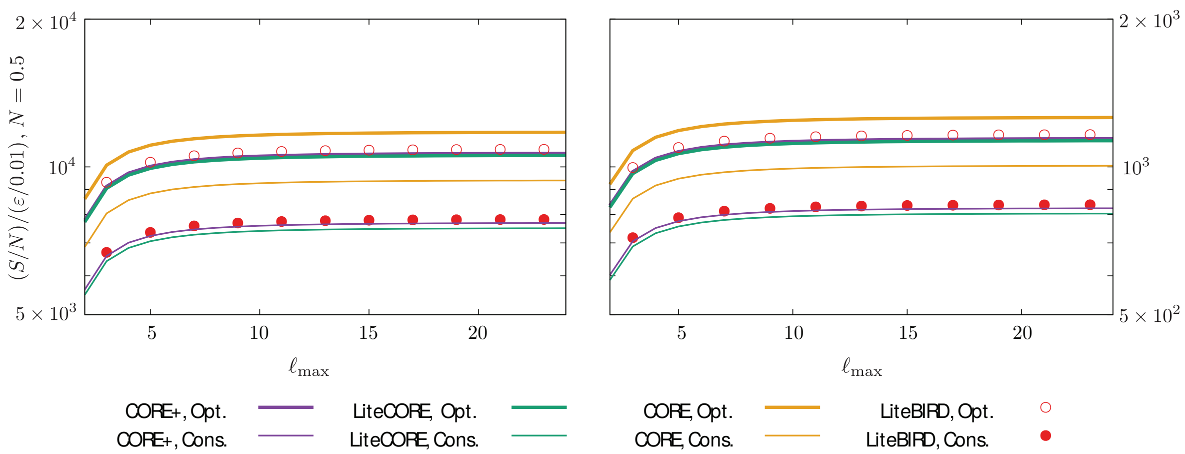

Deviations from a Bunch-Davies vacuum state during inflation could be already detected by Planck via CMB μ-spectral distortions;
for sure at reach of a PIXIE like experiment

Conclusions

- Simplest models of inflation are successful, completely in agreement with data.
- However, we do not know the precise mechanism behind inflation.
- Look for new signatures from inflation and alternative observations to probe the nature of inflation.
- Some examples that have been focused some attention recently: tensor non-Gaussianity, signatures from extra higher spin particles during inflation.
- Look for synergies between CMB and interferometric measurements.
- A potentially very rewarding avenue: CMB spectral distortions (some models can be already tested with present data)

Session4a 11:00–12:30

[Chair: Takeshi Chiba]

4a1. Yuki Sakakihara (Osaka City U.), "Dynamics in f(R) gravity with bounded curvature" (10+5)

[JGRG27 (2017) 112902]

29th Nov. 2017

Dynamics in f(R) gravity with bounded curvature

Yuki Sakakihara (Osaka City University)

ref. Stefano Ansoldi(University of Udine),
Eduardo Guendelman(Ben Gurion University of the Negev), Hideki Ishihara(OCU), YS. in prep.

MOTIVATION

- How could field strength and coupling constant be related?

e.g. Pure Yang-Mills Theory

Ref. Ryttov and Sannino, 2008

By integrating β function, we have

$$\mu = \Lambda_1 \exp\left(\frac{8\pi^2}{g^2\beta_0}\right)(g^2\beta_0)^{\beta_1/(2\beta_0^2)}$$

μ: energy scale
g: coupling constant
β_0, β_1: (positive) constants
Λ_1: invariant mass scale depending on field strength

It would be natural that the gravitational constant has running.

If we "mimic" this relation in gravity case,

$$\left(\frac{\mu}{R^{1/2}}\right)^{1/p} = \exp\left(\frac{\bar{c}}{G}\right)\frac{G}{\bar{c}}$$

G: gravitational constant
R: Ricci scalar
p: positive constant
$\bar{c}$: dimensional constant or function of R

MOTIVATION

$$\left(\frac{\mu}{R^{1/2}}\right)^{1/p} = \exp\left(\frac{\bar{c}}{G}\right)\frac{G}{\bar{c}}$$

$$S_{\mathrm{G}} = \frac{1}{8\pi}\int d^4x\sqrt{-g}\,\frac{R}{G(R)}$$

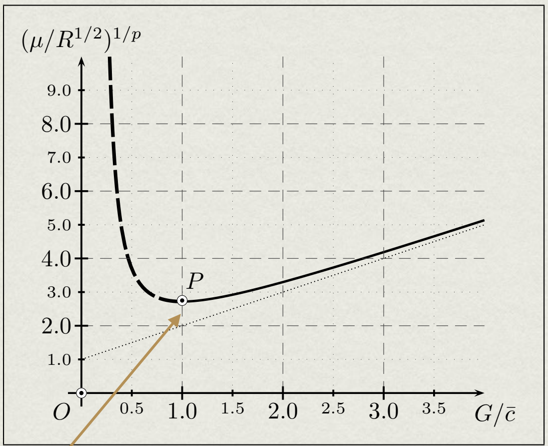

Maximum curvature

y-axis: left-hand side

x-axis: $\frac{G}{\bar{c}}$

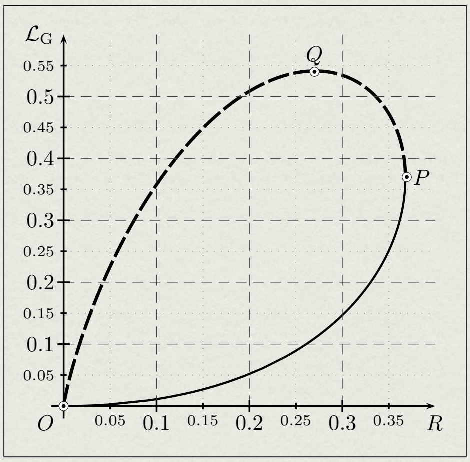

y-axis: Lagrangian density

x-axis: Ricci scalar

Petal-like shape

MOTIVATION

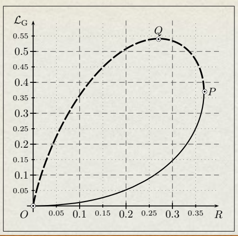

Petal-like shape

$$S_{\mathrm{G}} = \frac{1}{8\pi}\int d^4x\sqrt{-g}\,\frac{R}{G(R)}$$

Features

- Curvature is bounded.
- Lagrangian density is also bounded.
- The derivative diverges at maximum curvature
- This model would be discussed in the context of f(R) gravity

There are already many discussions on f(R) gravity, including cosmological solutions.

We focus on f(R) where the derivatives (f_R, …) are divergent.

- We are not so interested in the precise functional form of f(R)
- To examine the features of such models, we assume f(R) has circular shape.

CIRCULAR MODEL SETUP

- Radius: normalized to 1
- Center of the circle: (X, Y)
- Positive R
  - R_l: minimum curvature
  - R_r: maximum curvature

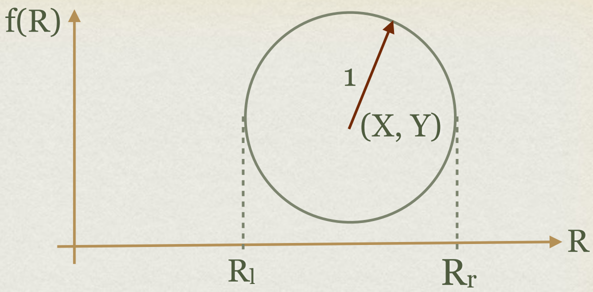

- Flat FLRW solutions ... two first order differential equations for (R, H)

$$\dot{R} = \frac{1}{f_{RR}H}\left[\frac{1}{6}\left(f_R R - f\right) - f_R H^2\right] \qquad \dot{H} = \frac{R}{6} - 2H^2$$

  - Infinite time is needed to reach minimum/maximum curvature. The upper and the lower half of the circle can be analyzed separately.
  - The equations of the upper half is the same as that of the lower half with (X, -Y)

IMPORTANT POINTS ON PHASE SPACE

- Stationary points
  - R_l: minimum curvature $f_R/f_{RR} \to 0$
  - R_r: maximum curvature $f_R/f_{RR} \to 0$
  - R_e, which satisfies $f_R(R_e)\, R_e - 2f(R_e) = 0$

- Throat on H=0 line
  - $\bar{R}$: which satisfies

$$f_R(\bar{R})\bar{R} - f(\bar{R}) = 0$$

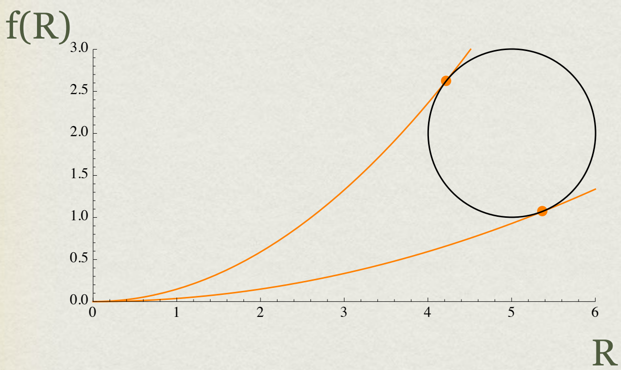

finding a where a R^2 is tangent to the circle

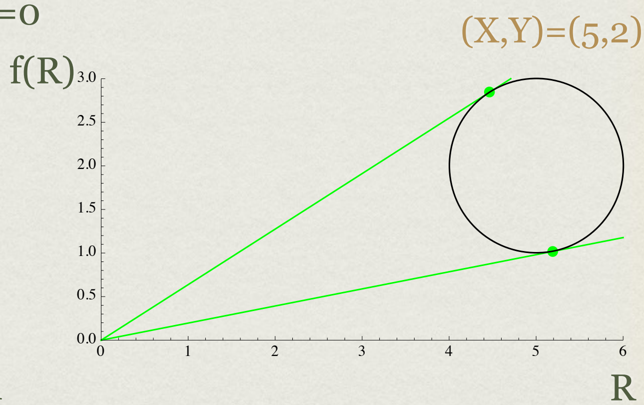

finding b where b R is tangent to the circle

STABILITY OF STATIONARY POINTS

$$J = \begin{pmatrix} \partial\dot{R}/\partial R & \partial\dot{R}/\partial H \\ \partial\dot{H}/\partial R & \partial\dot{H}/\partial H \end{pmatrix}$$

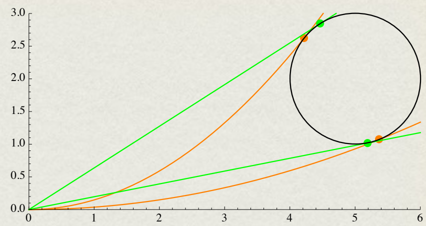

- R_l, R_r
  det $J= (R/3)[f_{RRR}f_R/f_{RR}^2-1]=2R/3>0$
  tr $J=(-H)[f_{RRR}f_R/f_{RR}^2+3]$
  Reality: $(R/12)(f_{RRR}f_R/f_{RR}^2-5)^2>0$
  Both are stable nodes for $H(R_{l,r})>0$
  and unstable nodes for $H(R_{l,r})<0$

  - $f_{RRR}f_R/f_{RR}^2=3(R_{l,r}-X)^2=3$
  - $f_R/f_{RR}=(R-X)[1-(R-X)^2]$
  - $|R-X|<1$

- R_e
  det $J=(1/6)f_R/f_{RR}-R/3 =-R/6-(1/6)[X+(R-X)^3] <0$
  tr $J=-3H$
  Reality: $(25/12)R-(2/3)f_R/f_{RR}=(17/12)R+(2/3)[X+(R-X)^3]>0$
  Saddle point

  - They do not depend on Y

PHASE SPACE

cf. upper half, (X,Y)=(5,2)

H>0 region

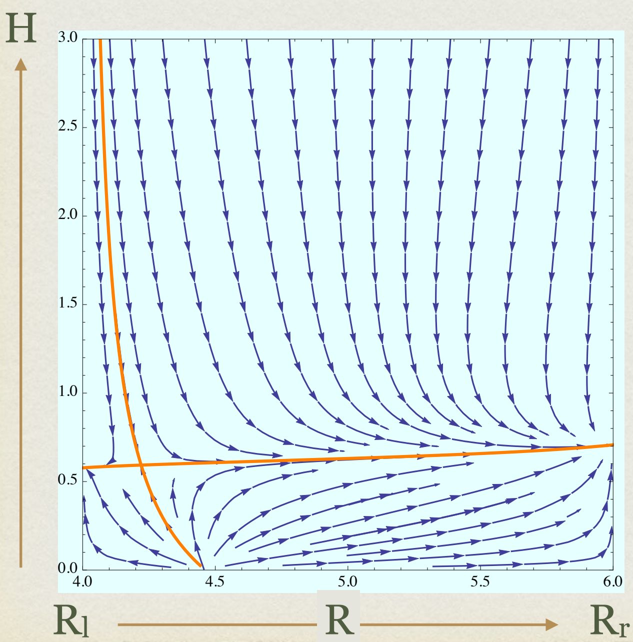

H<0 region

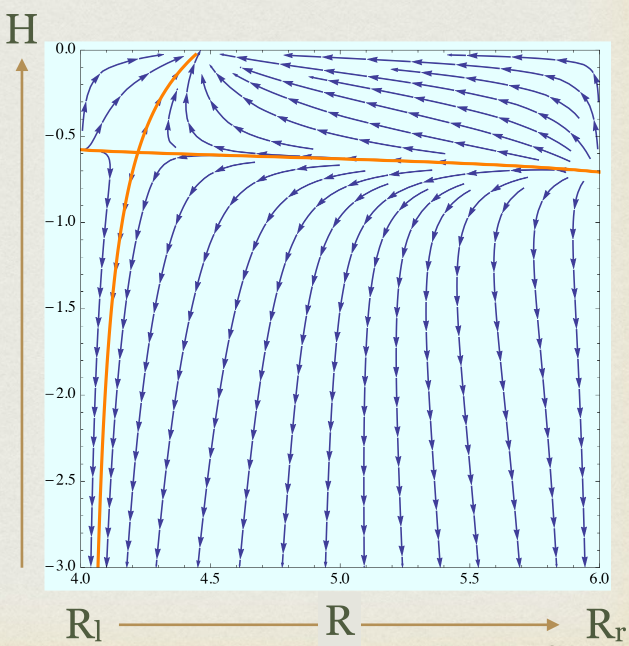

PHASE SPACE

cf. upper half, (X,Y)=(5,2)

H>0 region

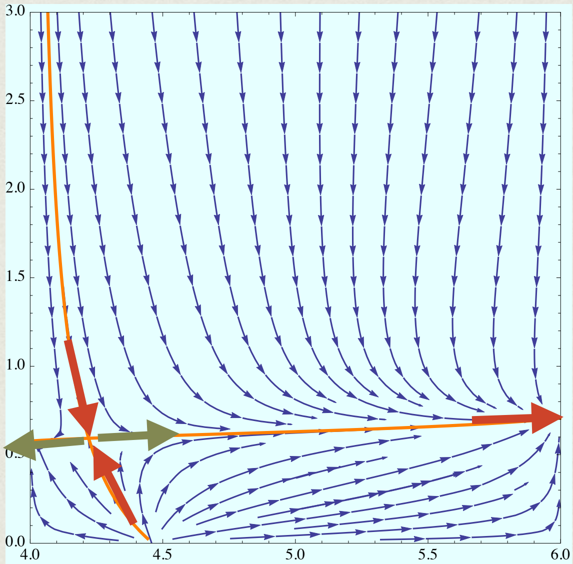

R_l R_r

H<0 region

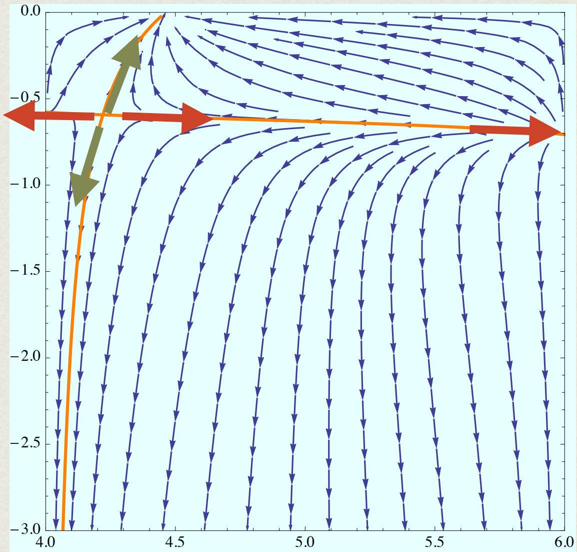

R_l R_r

PHASE SPACE

cf. upper half, (X,Y)=(5,2)

H>0 region

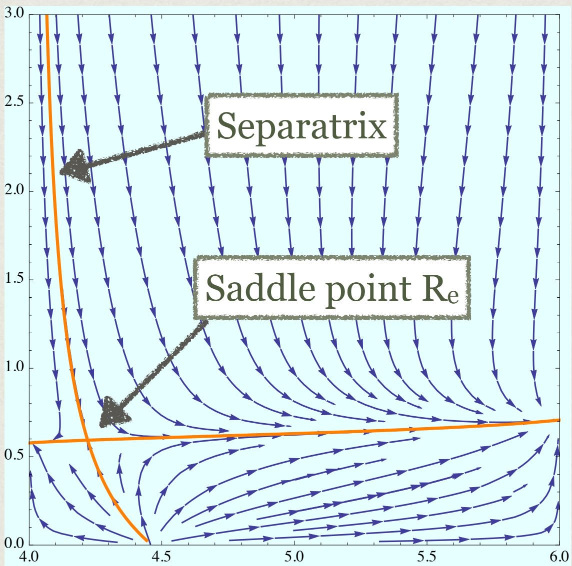

R_l R_r

H<0 region

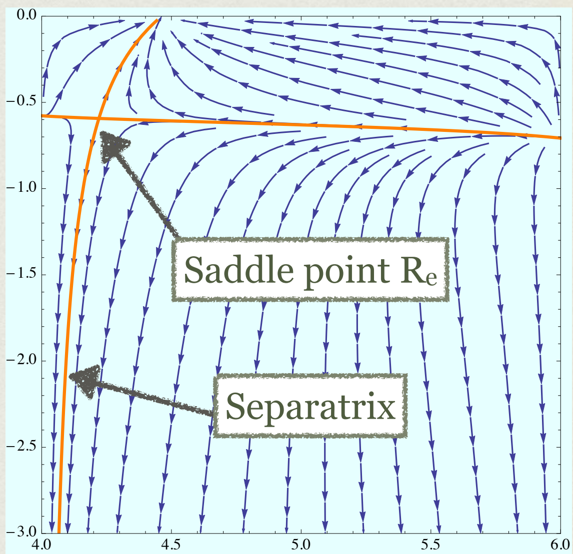

R_l R_r

PHASE SPACE

cf. upper half, (X,Y)=(5,2)

H>0 region

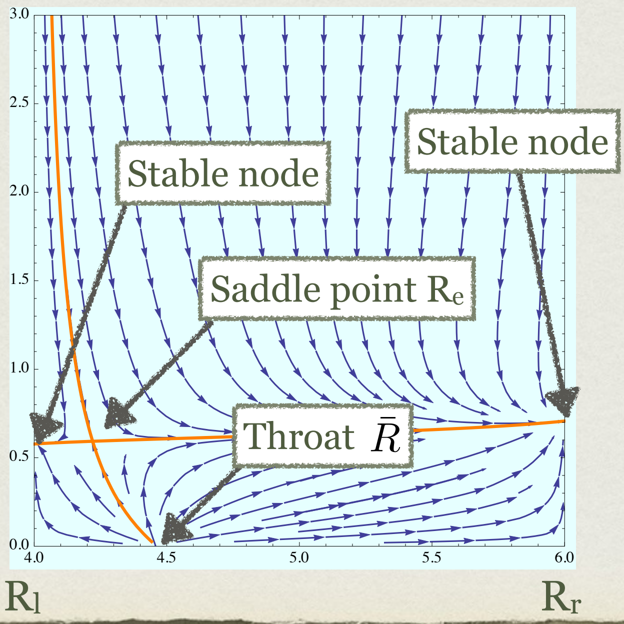

H<0 region

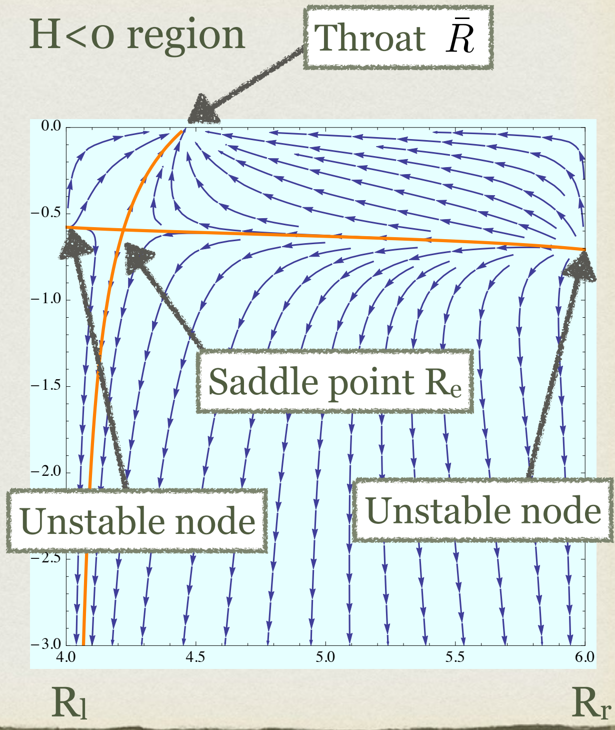

FATE OF THE SOLUTIONS

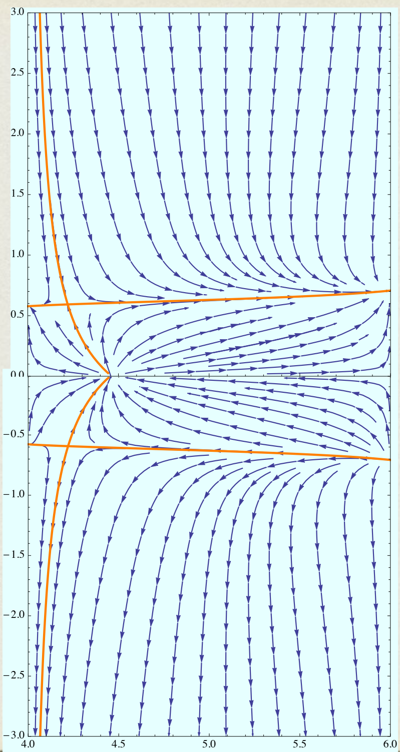

- Reach R_l (min. curv.) or R_r (max. curv.)
- Large negative H

CHANGING PARAMETERS

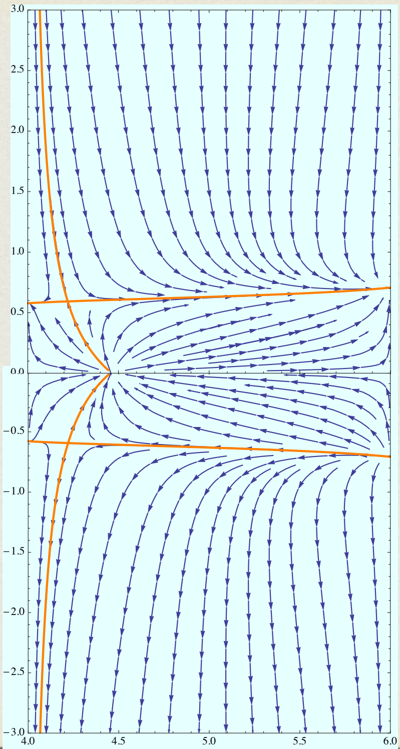

- When we change the center of the circle
  - The exact position of R_l, R_r, R_e and $\bar{R}$ changes
  - The existence and the stability never change as long as the circle is placed in R>0 region
  - X=1 (the circle is tangent to y-axis) case, should be treated independently.
    R_l, R_e and $\bar{R}$ coincide with each other.

SUMMARY

- We motivated bounded curvature models with divergence in f_R at the boundary of f(R) by referring to the renormalization of the gravitational constant.
- As a simple model, we proposed a circular-type f(R).
- We examined flat-FLRW solutions in it. We showed the stability of stationary points and the structure of phase space (R, H).
- The qualitative features would apply to other bounded curvature models.

Future Plan

- We discussed flat FLRW case. If we move the circle to the left and consider negative R region, we should take into account spatial curvature.
- Perturbative stability
- Timescales of each step:
  if the system could be applied to cosmological scenario.

4a4. Tomohiro Fujita (Kyoto U.),
"Statistically Anisotropic Primordial Gravitational Waves from Gauge Field" (10+5)
[JGRG27 (2017) 112905]

PRESENTATION

Statistically Anisotropic Primordial Gravitational Waves from Gauge Field

Tomohiro Fujita (Kyoto U)

Based on collaboration w/
I.Obata, T.Tanaka, S.Yokoyama

29th/Nov/2017 @JGRG27

京都大学 KYOTO UNIVERSITY

Main Message

PRESENTATION

① Original anisotropic inflation is challenging.

It's excluded with 99.999%.

Comments welcome!

② Spectator version is viable and interesting.

It has a new observational signature.

Statistical Anisotropy of GW

1 page review on anisotropic inflation

PRESENTATION

[Watanabe, Kanno, Soda (2009)]

- $$S = \int dx^4 \sqrt{-g}\left[\frac{1}{2}M_{\rm Pl}^2 R - \frac{1}{2}(\partial_\mu\varphi)^2 - V(\varphi) - \frac{1}{4}f(\varphi)^2 F_{\mu\nu}F^{\mu\nu}\right]$$

  Inflaton is coupled to U(1) gauge field

- This model has slow-roll solution when the coupling function is

  $$f(\varphi) = \exp\left[\frac{2c}{M_{\rm Pl}^2}\int \frac{V}{\partial_\varphi V}\mathrm{d}\varphi\right], \qquad (c>1)$$

- The attractor solution of Background $\boldsymbol{E} = -f\dot{\boldsymbol{A}}/a$

  $$\rho_E(t) = \frac{\rho_E^{\rm att}}{1+\Omega\, a^{-4(c-1)}} \qquad \rho_E^{\rm att} \equiv \frac{3}{2}\frac{c-1}{c^2}\epsilon_V M_{\rm Pl}^2 H^2,$$

- Statistical anisotropy of $\mathcal{P}_\zeta$ is predicted.

  $$\mathcal{P}_\zeta(\boldsymbol{k}) = \mathcal{P}_\zeta^{(0)}(k)\left(1+g_*\sin^2\theta\right) \qquad \cos\theta \equiv \hat{\boldsymbol{k}}\cdot\hat{\boldsymbol{E}}$$

Prediction and Observation

PRESENTATION

Model prediction is

$$g_* = \frac{16c\,N_k^2}{\epsilon_H M_{\rm Pl}^2 H^2}\rho_E$$

$$\xrightarrow{\rho_E \to \rho_E^{\rm att}} 24(c-1)N_k^2,$$

$$\approx 0.01\left(\frac{c-1}{10^{-7}}\right)\left(\frac{N_k}{60}\right)^2$$

Model parameter c has to be

$$c-1 \lesssim 10^{-7}$$

Non-detection of g_* by Planck constrains

$$g_* \lesssim 0.01$$

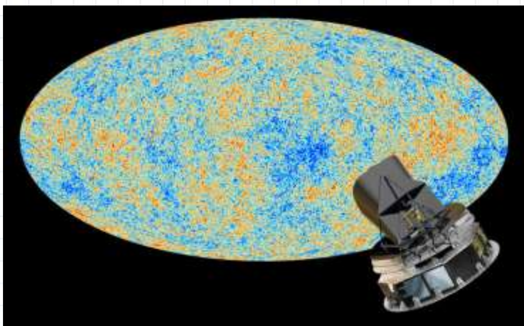

Really Attracted?

PRESENTATION

- Attractor solution was assumed $\rho_E \to \rho_E^{\text{att}}$
- We found $\rho_E \not\to \rho_E^{\text{att}}$ due to Stochastic Effect
- With stochastic effect, we expect

$$\langle \rho_E \rangle \simeq 10^3 \rho_E^{\text{att}} \Longrightarrow \langle g_* \rangle \simeq 10$$

Scalar Field Analogy

PRESENTATION

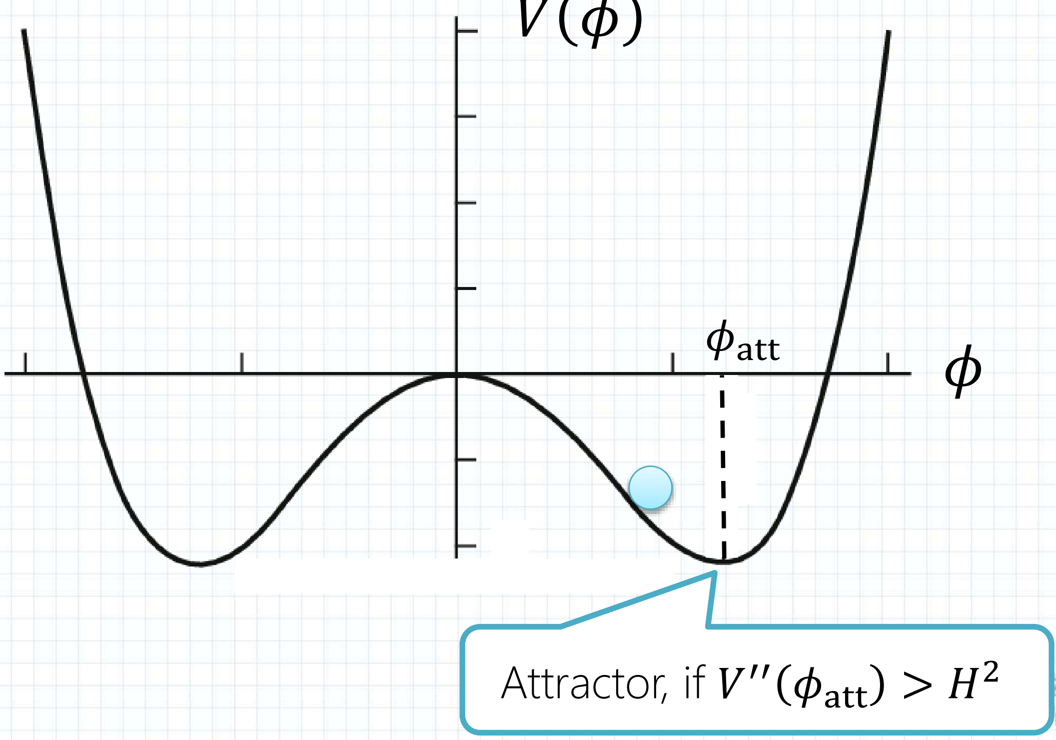

Scalar Field Analogy

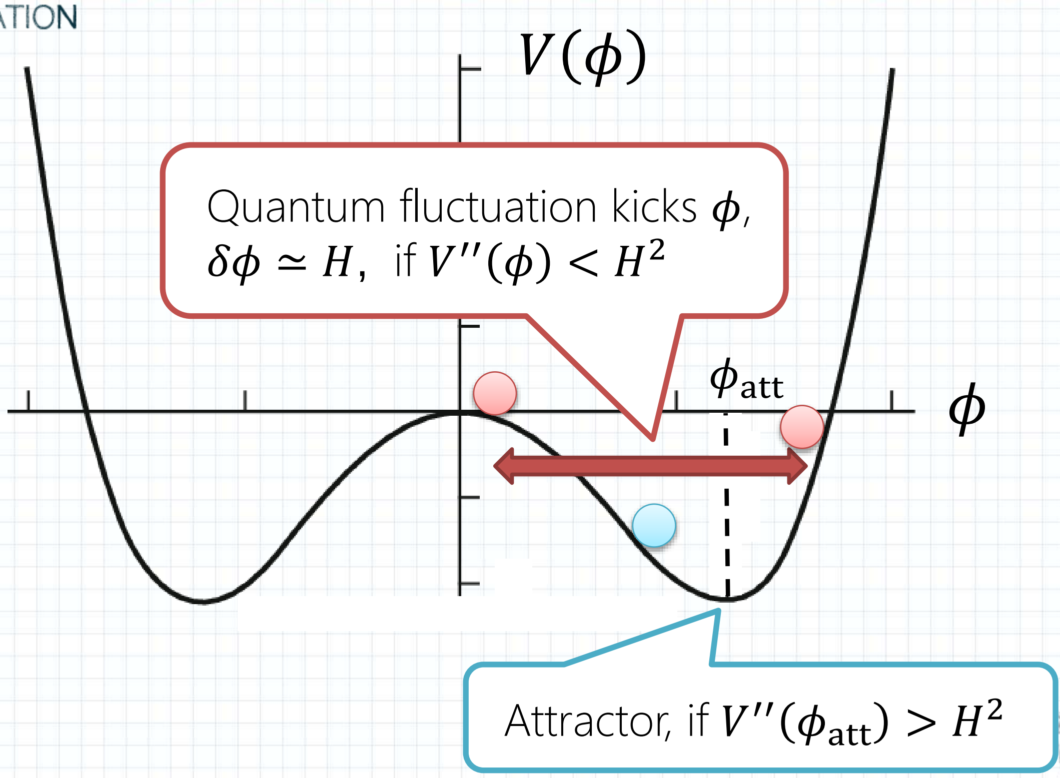

Electric field in Anisotropic inflation

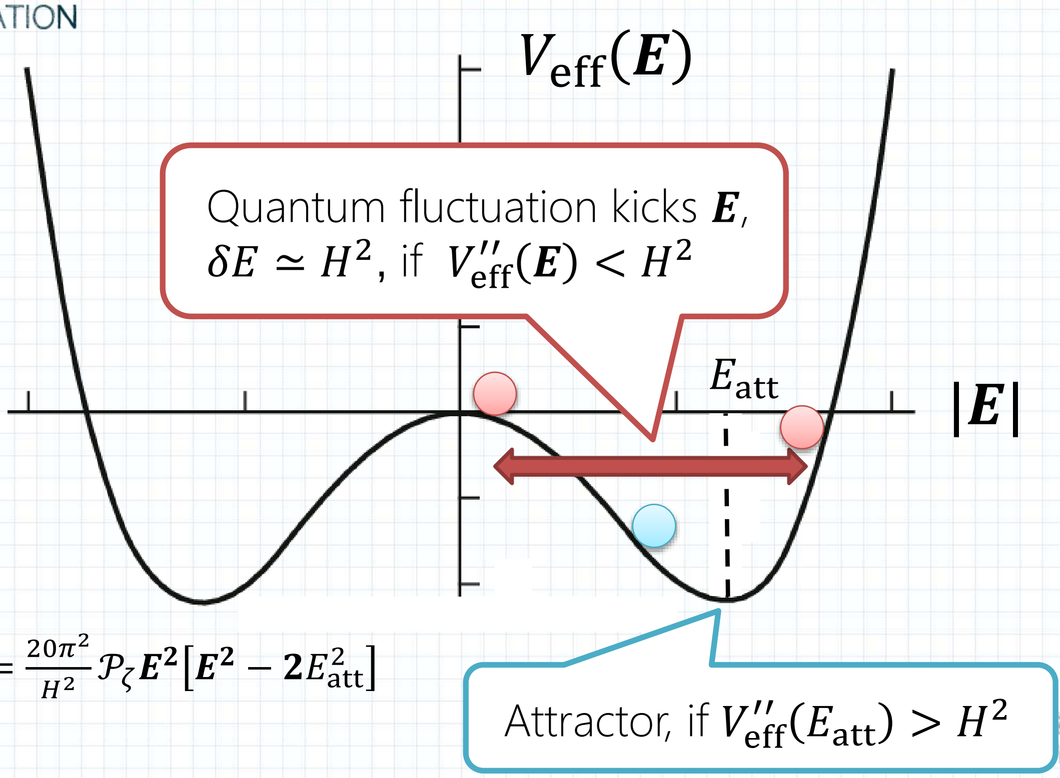

$$V_{\rm eff}(\boldsymbol{E}) = \frac{20\pi^2}{H^2}\mathcal{P}_\zeta \boldsymbol{E}^2\left[\boldsymbol{E}^2 - 2E_{\rm att}^2\right]$$

Electric field in Anisotropic inflation

PRESENTATION

$V_{\rm eff}(\boldsymbol{E})$

Quantum fluctuation kicks $\boldsymbol{E}$,

$$V''_{\rm eff}(E_{\rm att}) = 20(c-1)H^2 \approx 10^{-6}H^2$$

***E* does not go to the Attractor**

Attractor, if $V''_{\rm eff}(E_{\rm att}) > H^2$

Stochastic Formalism of scalar field

PRESENTATION

[Starobinsky&Yokoyama (1994)]

- Fluctuations affecting background ⇨ Stochastic Formalism
- EoM with random noise term (Langevin eq.)

$$3H\dot{\phi} + V'(\phi) = \xi_\phi$$

- ξ_ϕ is a Gaussian noise

$$\langle \xi_\phi(t) \rangle = 0, \qquad \langle \xi_\phi(t)\xi_\phi(t') \rangle = \frac{H^3}{(2\pi)^2}\delta(t-t'),$$

Stochastic Formalism of vector field

PRESENTATION

- Fluctuations affecting background $\Rightarrow$ Stochastic Formalism
- EoM with random noise term (Langevin eq.)

$$5H\dot{\boldsymbol{E}} + V'_{\rm eff}(\boldsymbol{E}) = \boldsymbol{\xi}_E$$

- $\boldsymbol{\xi}_E$ is a Gaussian noise only with diagonal part

$$\langle \boldsymbol{\xi}_E(t) \rangle = 0, \quad \left\langle \xi_i^E(t)\xi_j^E(t') \right\rangle = \frac{H^5}{2\pi^2}\delta_{ij}\delta(t-t'),$$

Numerical sol of Langevin eq.

PRESENTATION

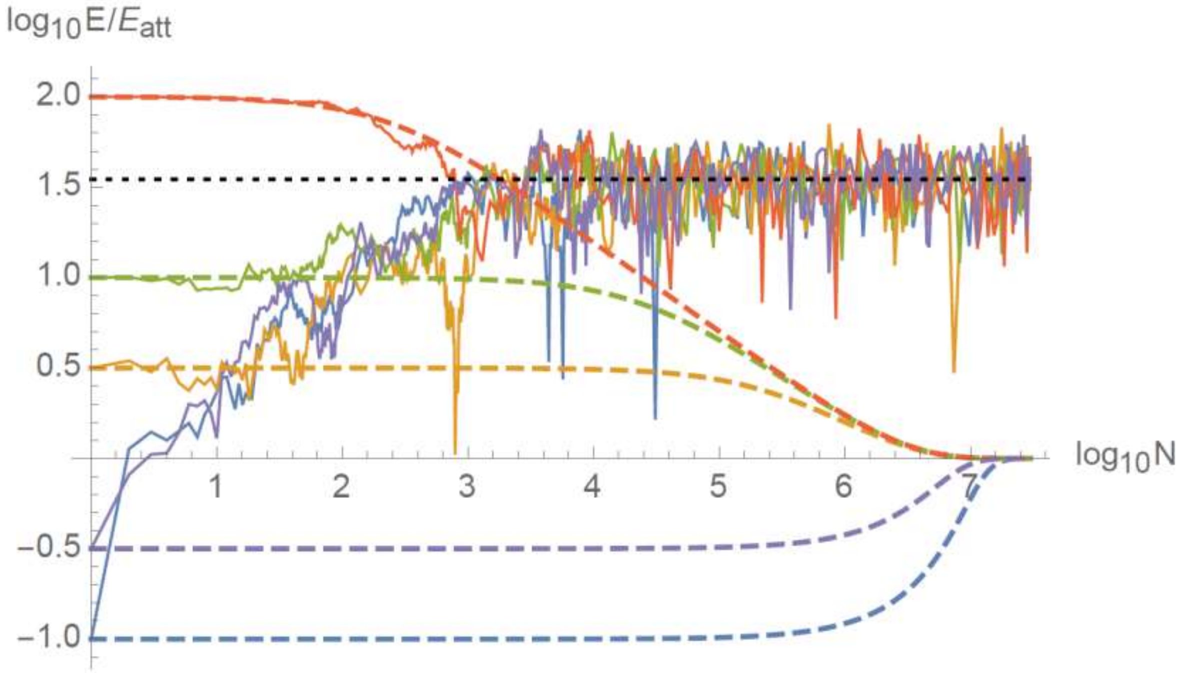

$$\langle |\boldsymbol{E}| \rangle \simeq 30E_{\rm att}, \quad \Rightarrow \quad \langle g_* \rangle \simeq 10,$$

Probability Distribution Function

PRESENTATION

- Evolution of $\boldsymbol{E}$ is now probabilistic

- We obtain the PDF of $|\boldsymbol{E}|$ by solving FP eq.

$$\boxed{\frac{\partial P(\mathcal{E},\mathcal{N})}{\partial \mathcal{N}} = \frac{\partial}{\partial \mathcal{E}}\left[\frac{\partial U}{\partial \mathcal{E}} P(\mathcal{E},\mathcal{N})\right] + \frac{\partial^2}{\partial \mathcal{E}^2} P(\mathcal{E},\mathcal{N}),}$$

$$U(\mathcal{E}) = -(c-1)\mathcal{E}^2 + 4\mathcal{P}_\zeta^{(0)}\mathcal{E}^4 - 2\ln\mathcal{E}.$$

$$\mathcal{E} \equiv \sqrt{\frac{c-1}{8\mathcal{P}_\zeta^{(0)}}\frac{E_{\rm IR}}{E_{\rm att}}} \approx 2.5\frac{E_{\rm IR}}{E_{\rm att}}\left(\frac{c-1}{10^{-7}}\right)^{\frac{1}{2}}, \qquad {\rm d}\mathcal{N} \equiv H{\rm d}t.$$

Probability Distribution Function

PRESENTATION

- We obtain the PDF of $|\boldsymbol{E}|$ by solving FP eq.

$$\frac{\partial P(\mathcal{E},\mathcal{N})}{\partial \mathcal{N}} = \frac{\partial}{\partial \mathcal{E}}\left[\frac{\partial U}{\partial \mathcal{E}} P(\mathcal{E},\mathcal{N})\right] + \frac{\partial^2}{\partial \mathcal{E}^2} P(\mathcal{E},\mathcal{N}),$$

- The static equilibrium solution is

$$P_{\rm eq}(\mathcal{E}) = {\rm N}^{-1}\exp\left[-U(\mathcal{E})\right],$$

$$U(\mathcal{E}) = -(c-1)\mathcal{E}^2 + 4\mathcal{P}_\zeta^{(0)}\mathcal{E}^4 - 2\ln\mathcal{E}.$$

Expected Values

PRESENTATION

- The expected values in the equilibrium are

$$\frac{\langle E_{\rm IR}\rangle}{E_{\rm att}} = \sqrt{\frac{8\mathcal{P}_\zeta^{(0)}}{c-1}}\langle\mathcal{E}\rangle = \sqrt{\frac{8\mathcal{P}_\zeta^{(0)}}{c-1}}\int_0^\infty \mathrm{d}\mathcal{E}\,\mathcal{E}P_{\rm eq}(\mathcal{E}) \approx 35,$$

consistent with numerical sol. of Langevin eq.

Numerical sol of Langevin eq.

PRESENTATION

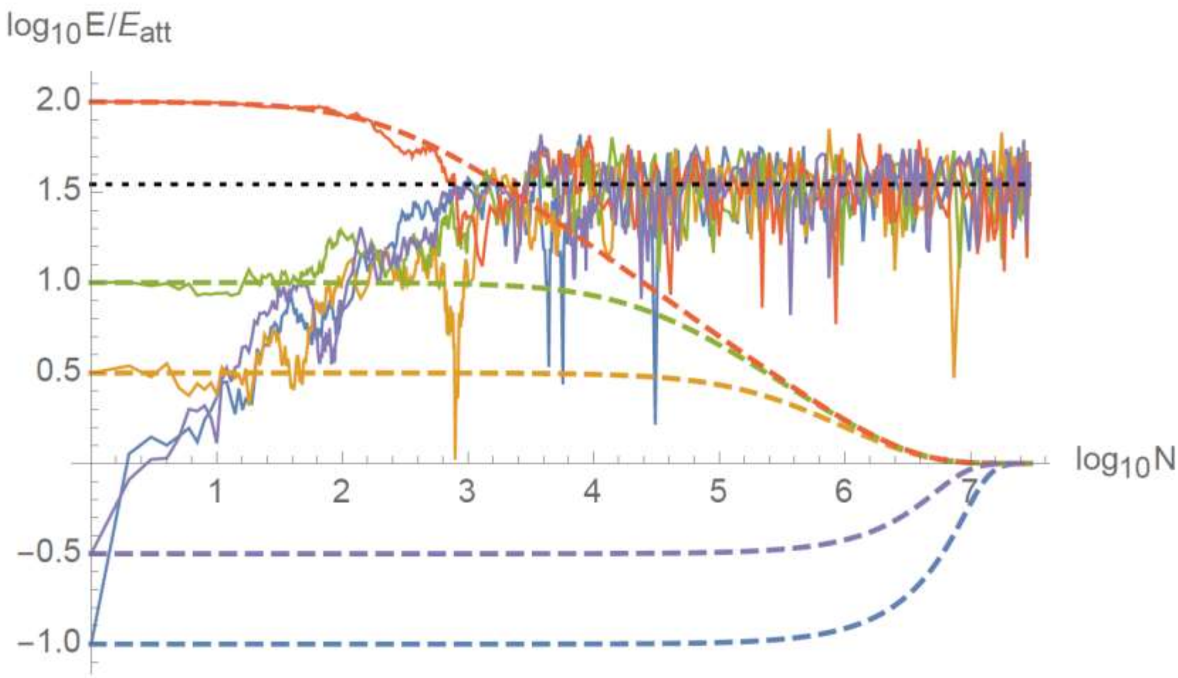

$$\langle|\boldsymbol{E}|\rangle \simeq 30E_{\rm att}, \quad \Rightarrow \quad \langle g_*\rangle \simeq 10,$$

Expected Values

PRESENTATION

- The expected values in the equilibrium are

$$\frac{\langle E_{\rm IR}\rangle}{E_{\rm att}} = \sqrt{\frac{8\mathcal{P}_\zeta^{(0)}}{c-1}}\langle\mathcal{E}\rangle = \sqrt{\frac{8\mathcal{P}_\zeta^{(0)}}{c-1}}\int_0^\infty d\mathcal{E}\,\mathcal{E}P_{\rm eq}(\mathcal{E}) \approx 35,$$

consistent with numerical sol. of Langevin eq.

$$\frac{\langle\rho_E^{\rm IR}\rangle}{\rho_E^{\rm att}} = \frac{\langle E_{\rm IR}^2\rangle}{E_{\rm att}^2} = \frac{8\mathcal{P}_\zeta^{(0)}}{c-1}\int_0^\infty d\mathcal{E}\,\mathcal{E}^2 P_{\rm eq}(\mathcal{E}) \approx 1400.$$

It implies $\langle g_*\rangle \simeq 10$

The PDF of g_*

PRESENTATION

Prob $\approx 1.3\times 10^{-5}$ at best

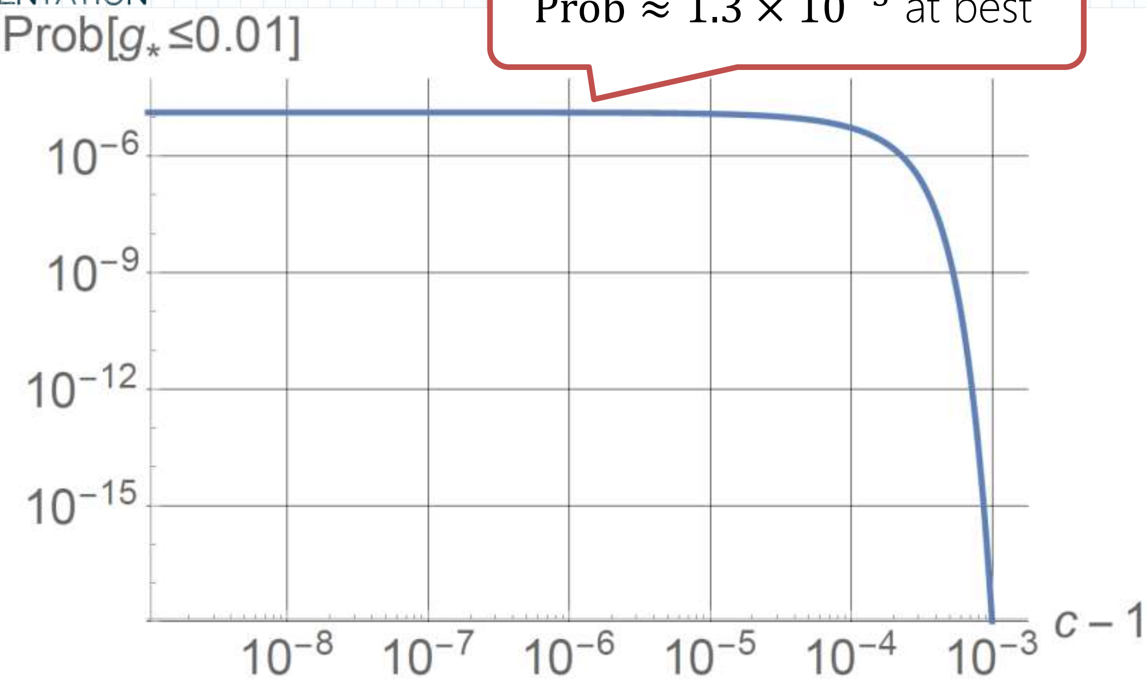

The electric field is assumed to be in the equilibrium

Summary of original Anisotropic Inf.

PRESENTATION

- $g_* \approx 0.01 \left(\frac{c-1}{10^{-7}}\right)\left(\frac{N_k}{60}\right)^2$, if $|\boldsymbol{E}| = E_{\text{att}}$.
- But, $V''_{\text{eff}}(E_{\text{att}}) = 20(c-1)H^2$. Attractor is not attractive...
- One should take into account stochastic effect
- $\mathbf{Prob}[g_* \leq 0.01] \leq 0.0013\%$, irrespective of c
- End of story??

Main Message

PRESENTATION

① Original anisotropic inflation is challenging.

It's excluded with 99.999%.

② Spectator version is viable and interesting.

It has a new observational signature.

Statistical Anisotropy of GW

THE THEME
OF CHAPTER IS...

Thank you !

4a5. Daiske Yoshida (Kobe U.),
"Exploring the string axiverse and parity violation in gravity with gravitational waves" (10+5)
[JGRG27 (2017) 112906]

4a5: JGRG27 2017 @ Kurara, Saijo, Higashi-hiroshima

Exploring the string axiverse and parity violation in gravity with gravitational waves

Speaker : Daiske Yoshida
Jiro Soda
Kobe Univ.

Related articles

"Exploring the string axiverse and parity violation in gravity with gravitational waves"
Daiske Yoshida and Jiro Soda
arXiv: 1708.09592

"Electromagnetic waves propagating in the string axiverse"
Daiske Yoshida and Jiro Soda
arXiv: 1710.09198

String axiverse and Axion dark matter

- String theory gives the massive pseudo-scalar fields (Axion).
  A. Arvanitaki, et al (2010),
  P. Svrcek and E. Witten (2006)
- Their mass is $10^{-33} \sim 10^{-10}\,\mathrm{eV}$. Its range is the very wide.

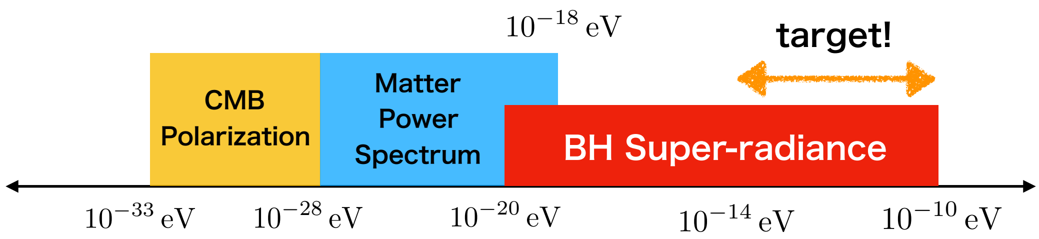

- Compactification of the extra dimensions $\rightarrow$ $\Phi\tilde{F}F$, $\Phi\tilde{R}R$
- It is indicated that the axion can behave as the cold dark matter.
  W. Hu, R. Barkana, and A. Gruzinov (2000)

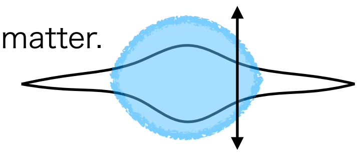

- To challenge the ultimate theory, we must detect them.

Dynamical Chern-Simons gravity

- This theory contains the coupling of the gravitational field and the scalar field.
  R. Jackiw and S. Y. Pi (2003)
- If we believe the string axiverse, this theory suggests the coupling with the gravitational field and axion.
- Its interaction is given by

$$\alpha = \sqrt{\frac{\kappa}{2}}\ell^2 \qquad l \sim 10^8\mathrm{km}$$

$$S_{\mathrm{CS}} = \frac{1}{4}\alpha \int_{\mathcal{V}} dx^4 \sqrt{-g}\,\Phi\tilde{R}R$$

$$\tilde{R}R \equiv \underbrace{\frac{1}{2}\epsilon^{\gamma\delta\rho\sigma} R^{\alpha}{}_{\beta\rho\sigma}}_{\equiv \tilde{R}^{\alpha}{}_{\beta}{}^{\gamma\delta}} R^{\beta}{}_{\alpha\gamma\delta}$$

- This theory generates the parity-violated GW for circular polarization, h_{R}, h_{L} .

System

- Action

$$S = \kappa \int_{\mathcal{V}} dx^4 \sqrt{-g}\, R + \frac{1}{4}\alpha \int_{\mathcal{V}} dx^4\, \sqrt{-g}\, \Phi \tilde{R} R$$
$$-\frac{1}{2}\int_{\mathcal{V}} dx^4 \sqrt{-g}\, \left[g^{\mu\nu}(\nabla_\mu \Phi)(\nabla_\nu \Phi) + 2V(\Phi)\right]$$

- Equations of motion

→ Gravitational field : $G_{\mu\nu} + \frac{\alpha}{\kappa} C_{\mu\nu} = \frac{1}{2\kappa} T_{\mu\nu}$

$$C^{\mu\nu} \equiv (\nabla_\alpha \Phi)\epsilon^{\alpha\beta\gamma(\mu}\nabla_\gamma R^{\nu)}{}_\beta + (\nabla_\alpha \nabla_\beta \Phi)\tilde{R}^{\beta(\mu\nu)\alpha}$$

→ Axion : $\nabla_\mu \nabla^\mu \Phi - \frac{dV(\Phi)}{d\Phi} = -\frac{\alpha}{4}\tilde{R}R$

Settings

- We set the spacetime as follows,

$$ds^2 \simeq a(\eta)^2(-d\eta^2 + \delta_{ij}dx^i dx^j + h_{ij}dx^i dx^j).$$

- We give some assumptions to solve this system.
  → The axion has the time-dependence only. $\Phi(x^\mu) = \Phi(\eta)$

  → Its potential is given by $V(\Phi) = \frac{1}{2}m^2\Phi^2$.

  → The expansion of Universe can be neglected in the scale of the time when the GWs through the core of Galaxy for 1 pc.

$$a(\eta) \simeq 1 \quad \rightarrow \quad \Phi(\eta) \simeq \Phi_0 \cos(m\eta)$$

- The EoM of GW

$$h''_A + \frac{\epsilon_A \delta \cos(m\eta)}{1 + \epsilon_A \frac{k}{m}\delta \sin(m\eta)} k\, h'_A + k^2 h_A = 0$$

$$\delta \equiv \frac{\alpha}{\kappa} m^2 \Phi_0$$

$$\epsilon_A \equiv \begin{cases} 1 & : \quad A = \mathrm{R} \\ -1 & : \quad A = \mathrm{L} \end{cases}$$

Parametric resonance

- The Swings

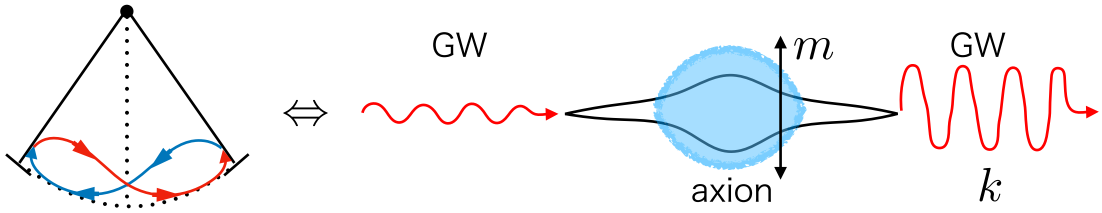

- The EoM of parametric resonance $\frac{d^2x}{dt^2} + \beta(t)\frac{dx}{dt} + \omega^2(t)x = 0$

  The condition of parametric resonance
  → $\beta(t)$ and $\omega^2(t)$ can have the dependence of time only.
  → $\beta(t)$ and\or $\omega^2(t)$ are assumed to vary periodically, with the same period T.

- The features of resonance frequency of parametric resonance

→ Resonance frequency has the width.
→ When GW satisfy the relation, $k = m/2$, the resonance frequency has the widest band at the frequency.

Estimation of the Growth rate

- Estimation of the resonance frequency

  → Resonance frequency $k_{\mathrm{r}} = \frac{m}{2} \Rightarrow f_{\mathrm{r}} = \frac{k_{\mathrm{r}}}{2\pi} \simeq 1.2 \times 10^4\,\mathrm{Hz}\left(\frac{m}{10^{-10}\,\mathrm{eV}}\right)$

  → Band of the resonance frequency $\frac{m}{2} - \frac{m}{8}\delta \lesssim k_{\mathrm{r}} \lesssim \frac{m}{2} + \frac{m}{8}\delta$

- Growth rate of the amplitude of GW

$$\Gamma_{\max} = \frac{m}{2}\delta$$
$$= 2.8 \times 10^{-24}\,\mathrm{eV} \times \left(\frac{m}{10^{-10}\,\mathrm{eV}}\right)^2 \left(\frac{l}{10^4\,\mathrm{km}}\right)^2 \sqrt{\frac{\rho}{0.3\,\mathrm{GeV/cm^3}}}$$

$$\Rightarrow t_{\times 10} = 8.1 \times 10^{23}\,\mathrm{eV}^{-1} \times \left(\frac{10^{-10}\,\mathrm{eV}}{m}\right)^2 \left(\frac{10^4\,\mathrm{km}}{l}\right)^2 \sqrt{\frac{0.3\,\mathrm{GeV/cm^3}}{\rho}}$$

Numerical results: 1/2

- Plots of the growth of the amplitude of GW

$$\ell = 10^8\,\mathrm{km},\ \ m = 10^{-10}\,\mathrm{eV},\ \ \rho = 0.3\times 10^6\,\mathrm{GeV/cm^3}$$
$$\delta \simeq 0.02$$

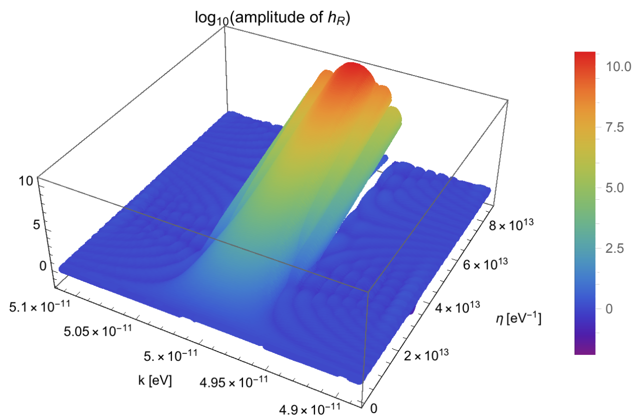

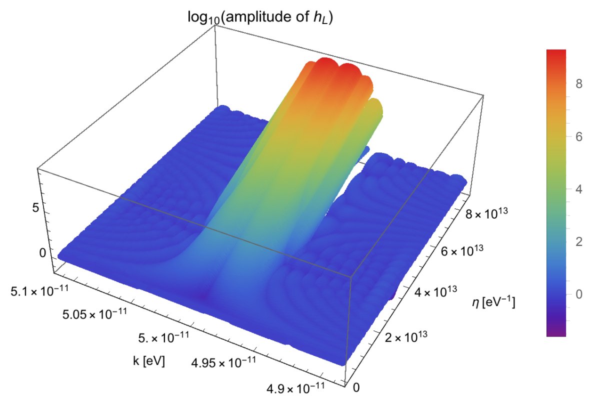

→ In the circular polarization basis, each of the amplitudes grows asymmetrically.
→ In this situation, h_R becomes 10^4 times as large as h_L .

Numerical results: 2/2

- The plot of the parity violation is below.

$$\mathrm{parity}(\eta) = \frac{|h_R|^2 - |h_L|^2}{|h_R|^2 + |h_L|^2}$$

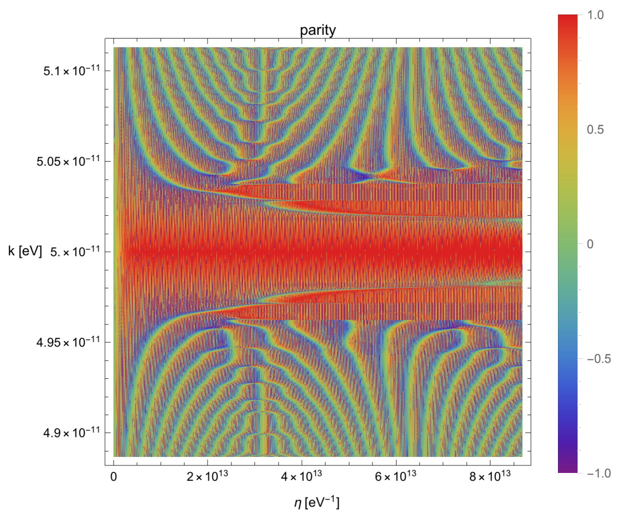

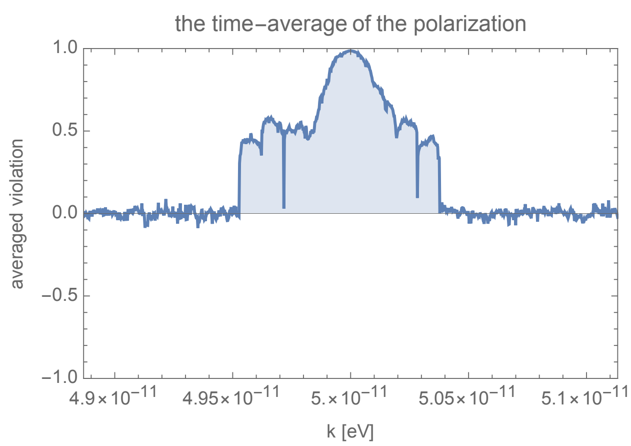

- The color indicates the level of the polarization.
  → The strong polarization near the resonance frequency.

Conclusion

- String axiverse generates the axions which have the light mass, and they behave as the cold dark matter well.

- The dCS gravity have the interaction of the gravitational field and the axion dark matter.

- This effect may use to detect the counterpart of the GR.
  → They might give the new constraint to the abundance of the axion dark matter or the CS-coupling.

4a6. Takashi Hiramatsu (Rikkyo U.), "Reconstruction of primordial tensor power spectrum from B-mode observations" (10+5) [JGRG27 (2017) 112907]

Reconstruction of primordial tensor power spectrum from B-mode observations

Takashi Hiramatsu

Rikkyo University

Collaboration with Eiichiro Komatsu (MPA)
Masashi Hazumi (KEK)
Misao Sasaki (YITP)

Introduction : CMB B-mode observation

- A polarisation mode of photons $(Q,U) \to (E_{\ell m}, B_{\ell m})$
- Generated by gravitational waves (tensor perturbations)
- No detections so far, but possibly to be done in the (near) future (e.g. LiteBIRD)

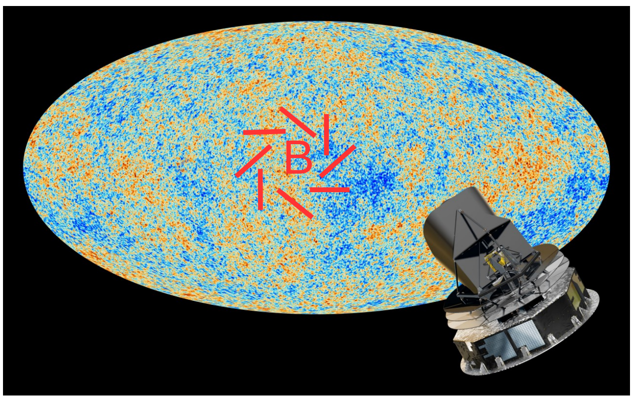

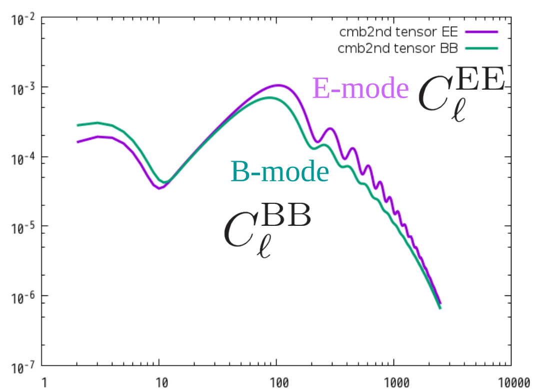

Gives fruitful information on inflation and the early Universe.

Introduction : Reconstruction

How well can we distinguish primordial power spectra predicted in various models from the fiducial one (inflation) ?

$$||$$

How well can we measure the primordial spectra under some observational noises ?

$$P^{(T)}(k) + \delta P^{(T)}(k) \qquad\qquad C_\ell^{(T)BB} + \mathcal{N}_\ell$$

Fisher matrix

Fisher Information Matrix for CMB

$$F_{ij} = \frac{1}{2}\sum_{\ell=2}^{\ell_{\max}}(2\ell+1)\frac{1}{\mathcal{N}_\ell^2}\left(\frac{\partial C_\ell^{(T)BB}}{\partial\theta_i}\right)\left(\frac{\partial C_\ell^{(T)BB}}{\partial\theta_j}\right)$$

$$\mathcal{N}_\ell = C_\ell^{(T)BB} + C_\ell^{(S)\mathrm{lens}} + N_\ell$$ “noise”

θ_i : characterising the primordial spectrum $P^{(T)}(k)$

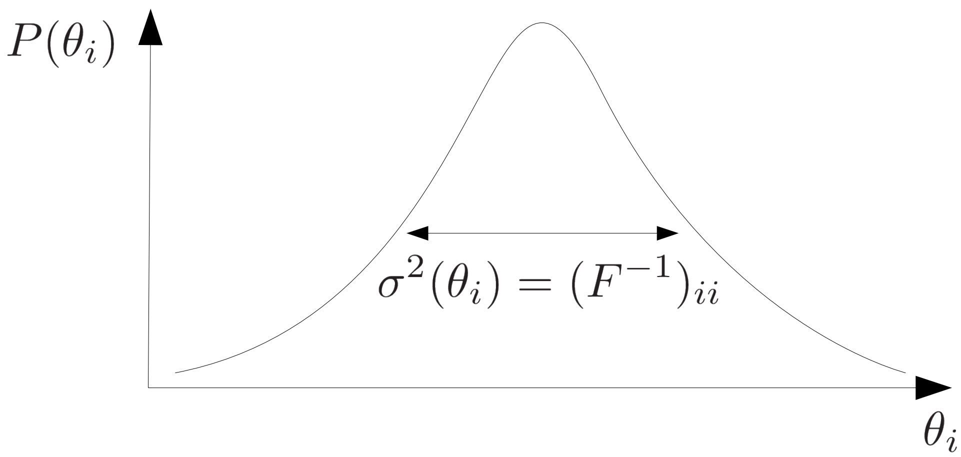

Building block 1/3 : Tensor B-mode

Angular power spectrum of B-mode fluctuations

$$C_\ell^{(T)BB} = 4\pi \int T_{B\ell}^{(T)2}(k)\mathcal{P}_h(k)\frac{dk}{k}$$

(ℓ is an index of $Y_{\ell m}$)

$$\mathcal{P}_h(k) = \frac{k^3}{2\pi^2}P_h(k)$$

Transfer function given by solving Boltzmann equations with parameters from Planck 2015 results :

$$\begin{aligned} h &= 0.6774 & T_{\gamma,0} &= 2.7255\ \mathrm{K} \\ h^2\Omega_{\mathrm{CDM}} &= 0.1188 & \tau &= 0.066 \\ h^2\Omega_{\mathrm{b}} &= 0.02230 & Y_p &= 0.24667 \\ N_{\mathrm{eff}} &= 3.046 \end{aligned}$$

Building block 2/3 : Lensing B-mode

B-mode induced by E→ B conversion of lensing

Smith et al., JCAP 1206 (2012) 014, arXiv:1010.0048

$E_\ell^{(S)}$ $\phi^{(S)}$ $B_\ell^{(S)}$

Lensing potential

$$C_\ell^{(S)\mathrm{lens}} \approx \frac{1}{2\ell+1}\sum_{\ell' L}^{\ell'_{\max}} \mathcal{S}_{\ell\ell' L}^2 C_{\ell'}^{(S)EE} C_L^{(S)\phi\phi}$$

2000

$$\begin{cases} C_\ell^{(S)\phi\phi} \approx 16\pi \displaystyle\int \frac{dk}{k}\mathcal{P}_{\mathcal{R}}(k)\left[\int_0^{\chi_{\mathrm{LSS}}} d\chi\, T_\Psi(k,\eta_0-\chi)j_\ell(k\chi)\left(\frac{\chi_{\mathrm{LSS}}-\chi}{\chi_{\mathrm{LSS}}\chi}\right)\right]^2 \\ C_\ell^{(S)EE} = 4\pi \displaystyle\int \frac{dk}{k}\mathcal{P}_{\mathcal{R}}(k)T_{E\ell}^{(S)2}(k) \end{cases}$$

Building block 3/3 : Detector noise

For simplicity, here we consider a white noise (independent to ℓ)

Katayama & Komatsu, APJ 737 (2011) 78, arXiv:1101.5210

$$N_\ell = \left(\frac{\pi}{10800} \frac{w_p^{-1/2}}{\mu\mathrm{K} \cdot \mathrm{arcmin}} \right)^2 \mu K^2 \cdot \mathrm{str}$$

$$w_p^{-1/2} = 63.1\ \mu K \cdot \mathrm{arcmin}$$ (Planck, averaged over 3 bands)

Zaldarriaga et al. arXiv:0811.3918

$$\downarrow$$

$$w_p^{-1/2} = \mathcal{O}(1) \mu\mathrm{K} \cdot \mathrm{arcmin}$$ (Future experiments)

Modelling tensor power spectrum

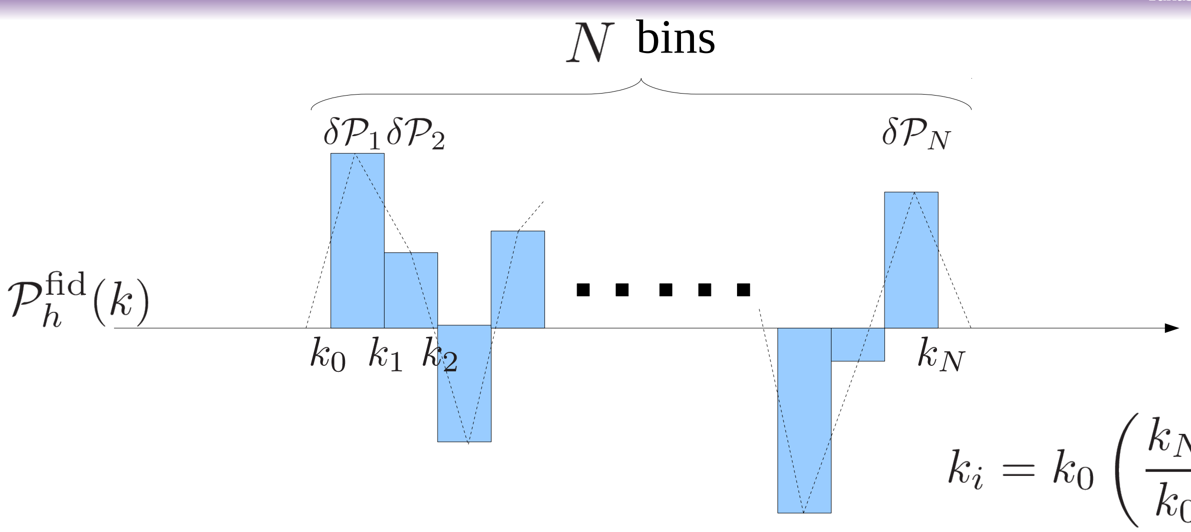

$$k_i = k_0 \left(\frac{k_N}{k_0} \right)^{i/N}$$

$$\mathcal{P}_h(k) = \begin{cases} \mathcal{P}_h^{\rm fid}(k) + \delta\mathcal{P}_i & \text{for } k_{i-1} \le k \le k_i \text{ with } 1 \le i \le N \\ \mathcal{P}_h^{\rm fid}(k) & \text{for } k \le k_0 \text{ and } k_N < k \end{cases}$$

e.g. Hlozek et al., APJ 749 (2012) 90 , arXiv:1105.4887

$$\mathcal{P}_h^{\rm fid}(k) = r\mathcal{P}_{\mathcal{R}0} \left(\frac{k}{k_{\rm pivot}} \right)^{n_T}$$ following the Planck 2015 results

Fisher Information Matrix for CMB

$$F_{ij} = \frac{1}{2}\sum_{\ell=2}^{\ell_{\max}}(2\ell+1)\frac{1}{\mathcal{N}_\ell^2}\left(\frac{\partial C_\ell^{(T)BB}}{\partial\theta_i}\right)\left(\frac{\partial C_\ell^{(T)BB}}{\partial\theta_j}\right)$$

$\ell_{\max}$ ← 500

Katayama & Komatsu, APJ 737 (2011) 78, arXiv:1101.5210

Model parameter : $\theta_i = \delta\mathcal{P}_i$

Numerator : $\dfrac{\partial}{\partial\theta_i}C_\ell^{(T)BB} = 4\pi\displaystyle\int_{k_{i-1}}^{k_i} T_{B\ell}^{(T)2}(k)\frac{dk}{k}$

Denominator : $\mathcal{N}_\ell = C_\ell^{(T)BB} + C_\ell^{\rm lens} + N_\ell$

Uncertainty to measure $\delta\mathcal{P}_i$: $\sigma_{\delta\mathcal{P}_i}^2 = (F^{-1})_{ii}$

Results : 1-σ error of binned spectrum

Contributions from the noise sources

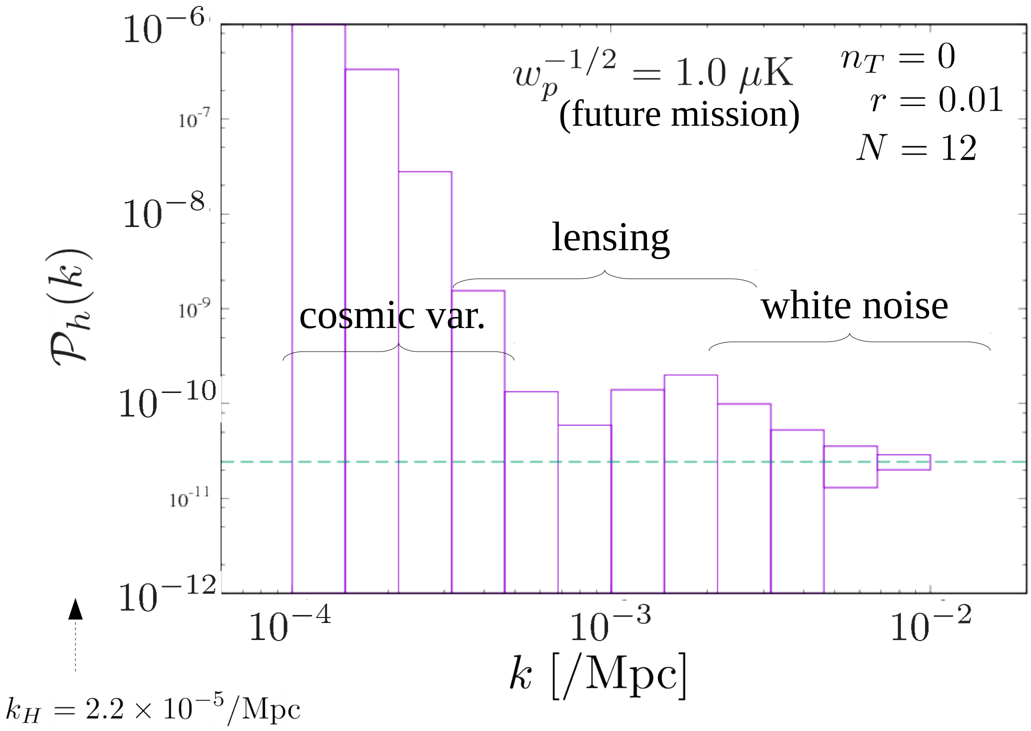

Results : demonstration

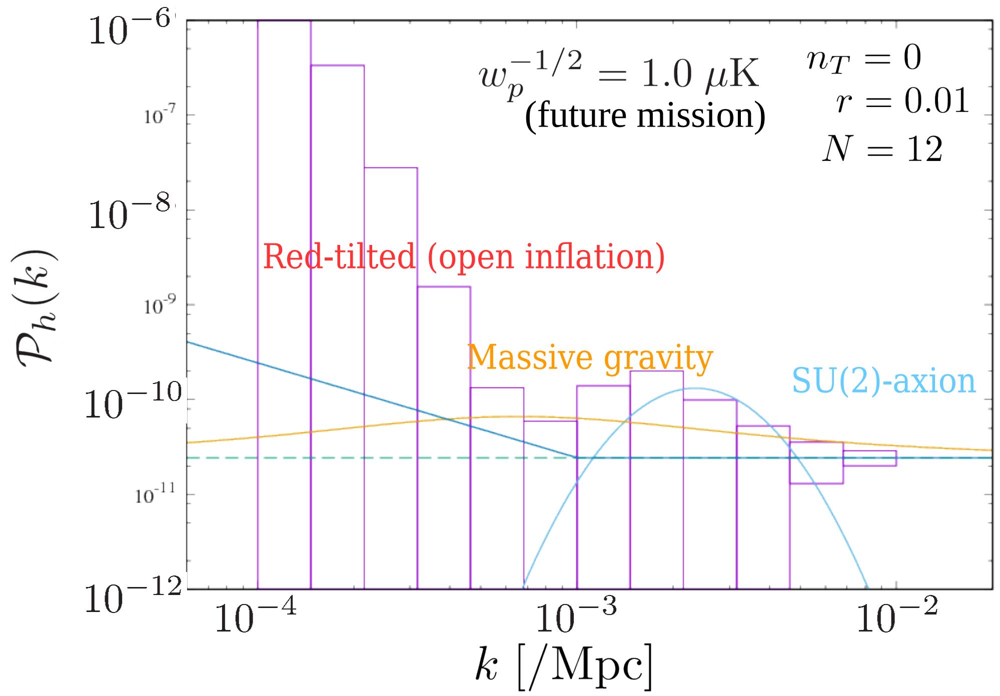

Red-tilted — Yamauchi et al., PRD 84 (2011) 043513

SU(2)-axion — Thorne et al., arXiv:1707.03240; Dimastrogiovanni et al., JCAP 01 (2017) 019

Massive gravity — Sasaki, private communication; Domenech et al., JCAP 1705 (2017) 034

Results : demonstration

Takashi Hiramatsu

More quantitatively, we should estimate χ^2.

$$\chi^2 = \sum_{ij} \Delta\mathcal{P}_i(k) F_{ij} \Delta\mathcal{P}_j(k)$$

$$\Delta\mathcal{P}_i(k) = \mathcal{P}_i^{\mathrm{model}}(k) - \mathcal{P}_i^{\mathrm{fid}}(k)$$

Probability to exceed (PTE) = Probability to confuse a model spectrum with the fiducial one.

$$P(\chi^2 > a) = \int_a^\infty f(\chi^2)\, d\chi^2$$

$$f(\chi^2) = \frac{x^{k/2-1} e^{-x/2}}{2^{k/2}\Gamma(k/2)}$$

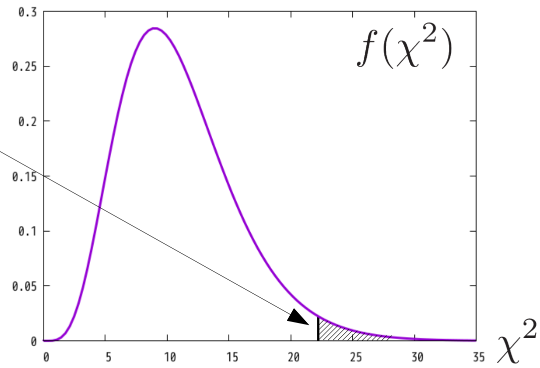

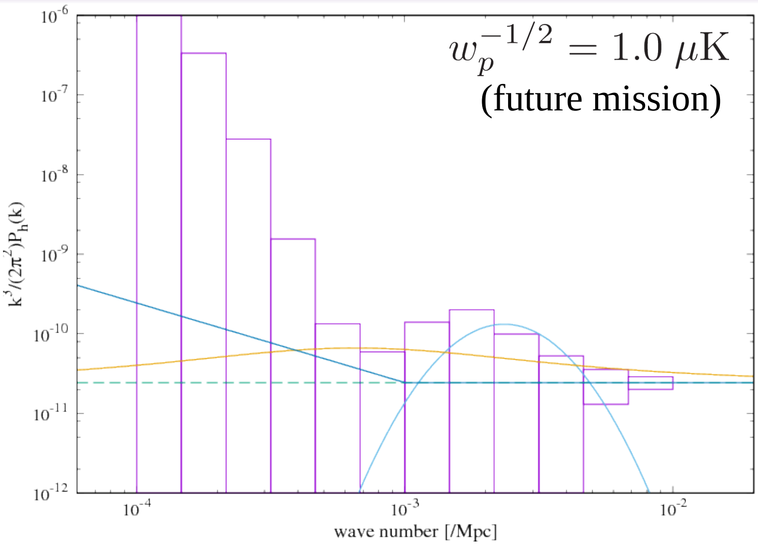

	χ^2	PTE
SU(2)	1.20×10^2	1.75×10^{-20}
Massive	1.47×10^2	7.74×10^{-26}
Red	2.17×10^1	2.68×10^{-2}

Distinguishable from fiducial spectrum with a high significance !

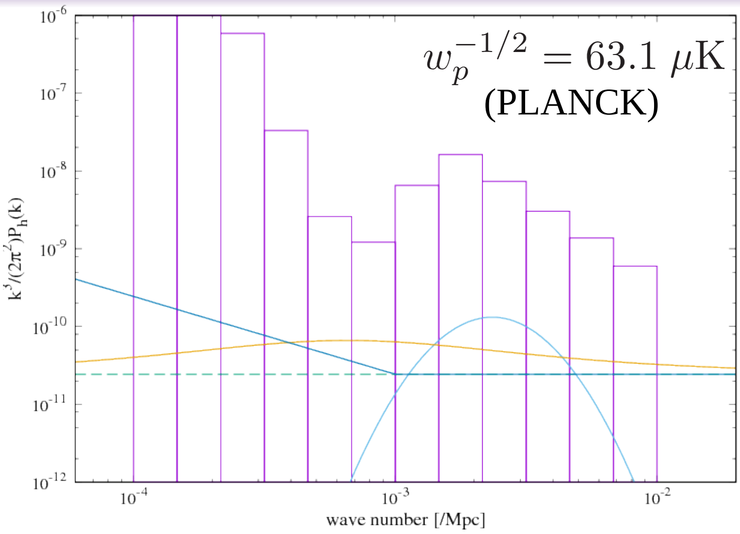

	χ^2	PTE
SU(2)	6.48×10^{-1}	1.00
Massive	1.74	9.99×10^{-1}
Red	1.86	9.99×10^{-1}

All models cannot be distinguished from the fiducial one.

Simulator is to be in public

- To be available on your web browser
- Compute from numerical data of spectrum as well as in built-in models

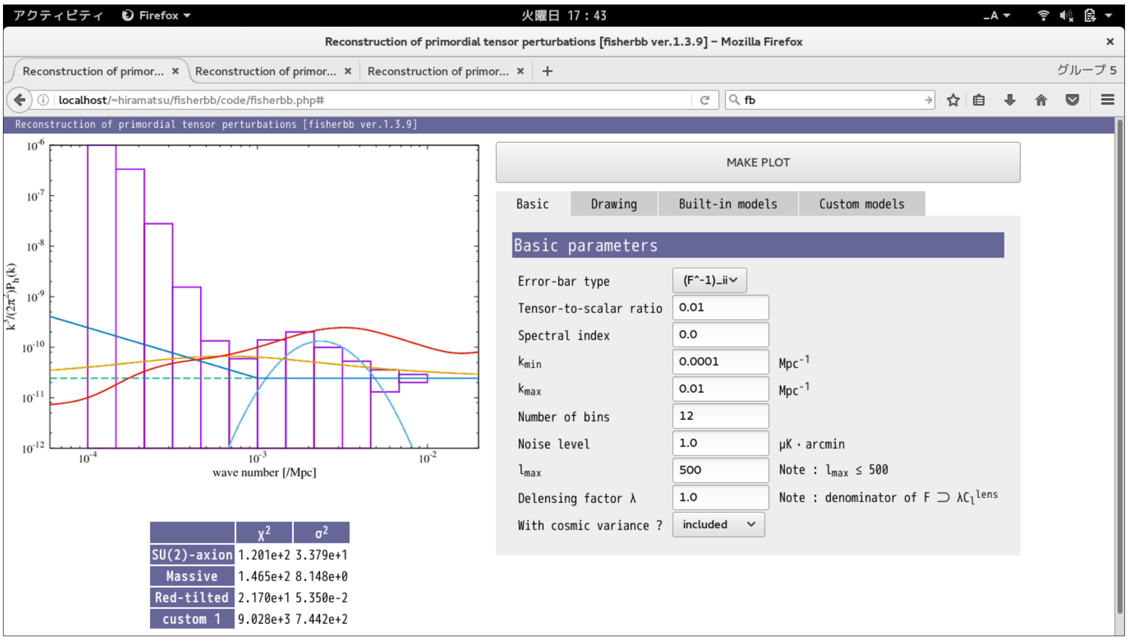

Summary

How significantly can we distinguish theoretical models from the fiducial power spectrum ?

Computed the Fisher matrix for a primordial tensor power spectrum parametrised as bandpowers within bins.
(but, with a simple detector noise model + no other foreground noises)

If only a theoretical prediction of GW spectrum is prepared, we can instantly know its detectability without running a Boltzmann solver. (+ simulator is to be appeared)

Session4b 11:00–12:30

[Chair: Hideki Ishihara]

4b1. Kentaro Tomoda (Kobe U.), "Curvature obstructions to the existence of isometries" (10+5) [JGRG27 (2017) 112908]

Curvature obstructions to the existence of isometries

Kentaro Tomoda (Kobe Univ.)

with

B. Kruglikov (Univ. of Tromso)
V. Matveev (Univ. of Jena)

2017/11/29 JGRG

Killing equation

$$\nabla_{(a}K_{b)} = 0$$

QUESTIONS:

- Are there any solutions for given metrics?
- If yes, how many solutions are there?
- How to determine the number of solutions?

I will give partial answers the above Qs

Some history

- In 2 dim. the questions were completely solved by G. Darboux (1887)

$$\begin{tikzcd}
dR=0 \arrow[r, "\text{yes}"] \arrow[d, "\text{no}"] & \boxed{\text{3 KVs}} \\
dR\wedge d[(\nabla_a R)(\nabla^a R)]=0 \arrow[r, "\text{no}"] \arrow[d, "\text{yes}"] & \boxed{\text{no KV}} \\
dR\wedge d\Box R=0 \arrow[r, "\text{yes}"] \arrow[ur, "\text{no}"] & \boxed{\text{1 KV}}
\end{tikzcd}$$

$$R_{abcd} = \frac{1}{2} R g_{a[c} g_{d]b}$$

Some history

- In 2 dim. the questions were completely solved by G. Darboux (1887)

- In 4 dim. R. Kerr (1963) showed that the algorithm exists for Einstein spaces (Any concrete algorithms are not known)

- I show the algorithm for 3 dim. concretely as a first step towards higher dimensions

Our result

$$I_1 = R$$
$$I_2 = R_{ab}R^{ab}$$
$$I_3 = R_{ab}R^{bc}R^{a}{}_{c}$$

$$\begin{array}{l}
R_{ab} \propto g_{ab} \xrightarrow{\text{yes}} \boxed{\text{6 KVs}} \\
\quad \downarrow \text{no} \\
\nabla_a R_{bc} = 0 \xrightarrow{\text{yes}} \boxed{\text{4 KVs}} \\
\quad \downarrow \text{no} \\
dI_1 \wedge dI_2 \wedge dI_3 = 0 \xrightarrow{\text{no}} \boxed{\text{no KV}} \\
\quad \downarrow \text{yes} \\
dI_i \wedge dI_j = 0 \xrightarrow{\text{no}} \boxed{\text{case 2}} \\
\quad \downarrow \text{yes} \\
dI_i = 0 \xrightarrow{\text{no}} \boxed{\text{case 1}} \\
\quad \searrow \text{yes} \\
\qquad \boxed{\text{case 0}}
\end{array}$$

$$R_{abcd} = 4g_{[a|[c}R_{d]|b]} - \frac{1}{2}Rg_{a[c}g_{d]b}$$

Case 2 ($dI_i \wedge dI_j = 0 \xrightarrow{\text{no}} \boxed{\text{case 2}}$)

$$\begin{array}{l}
\kappa_{ab} = \nabla_{[a}A_{b]} = 0 \xrightarrow{\text{no}} \boxed{\text{no KV}} \\
\qquad \downarrow \text{yes} \\
\qquad \boxed{\text{1 KV}}
\end{array}$$

where

$$\begin{aligned}
U^a &\propto \epsilon^{abc}(\nabla_b I_i)(\nabla_c I_j) \\
h_{ab} &= g_{ab} - U_a U_b \\
\kappa_{ab} &= \frac{1}{2}\mathcal{L}_U h_{ab} \\
A_a &= U^b \nabla_b U_a
\end{aligned}$$

Case 1 ($dI_i = 0 \xrightarrow{\text{no}} \boxed{\text{case 1}}$)

Is $\nabla_a R$ a geodesic? $\xrightarrow{\text{no}}$ $\boxed{\text{case 2}}$

$\downarrow$ yes

Is $\nabla_a R$ an eigenvecor of R_{ab}? $\xrightarrow{\text{no}}$ $\boxed{\cdots}$ SKIP

$\downarrow$ yes

$\tau_r = \kappa_g = \hat{\kappa}_g = 0 \xrightarrow{\text{no}} \boxed{\cdots} \longrightarrow \boxed{\text{2 KVs}}$ SKIP

$\downarrow$ yes

$\mathcal{L}_N \lambda = \mathcal{L}_B \lambda = 0 \xrightarrow{\text{no}} \boxed{\text{case 2}}$

$\downarrow$ yes

$\boxed{\text{3 KVs}}$

Case 1 ($dI_i = 0 \xrightarrow{\text{no}} \boxed{\text{case 1}}$)

Branch where $\nabla_a R$ is NOT a geodesic

the Frenet-Serret frame:

$$T^a \propto \nabla^a R$$

$$N^a \propto T^b \nabla_b T^a$$

$$B^a = \epsilon^{abc} T_b N_c$$

after some algebra

→ Our analysis reduces to the case 2

with the identification $\underline{B^a \to U^a}$ at most 1KV

Case 1 ($dI_i = 0 \xrightarrow{\text{no}} \boxed{\text{case 1}}$)

Branch where $\nabla_a R$ is a geodesic and an eigenvec. of R_{ab}

$\{T^a \propto \nabla^a R, N^a, B^a\}$: the eigensystem of R_{ab}

Curve theoretic parameters:

$$T^b \nabla_b \begin{pmatrix} T^a \\ N^a \\ B^a \end{pmatrix} = \begin{pmatrix} 0 & 0 & 0 \\ 0 & 0 & \tau \\ 0 & -\tau & 0 \end{pmatrix} \begin{pmatrix} T^a \\ N^a \\ B^a \end{pmatrix}$$

Case 1 ($dI_i = 0 \xrightarrow{\text{no}} \boxed{\text{case 1}}$)

Branch where $\nabla_a R$ is a geodesic and an eigenvec. of R_{ab}

$\{T^a \propto \nabla^a R, N^a, B^a\}$: the eigensystem of R_{ab}

$$N^b \nabla_b \begin{pmatrix} T^a \\ N^a \\ B^a \end{pmatrix} = \begin{pmatrix} 0 & -\kappa_g & \tau_r \\ \kappa_g & 0 & \kappa_n \\ -\tau_r & -\kappa_n & 0 \end{pmatrix} \begin{pmatrix} T^a \\ N^a \\ B^a \end{pmatrix}$$

$$B^b \nabla_b \begin{pmatrix} T^a \\ N^a \\ B^a \end{pmatrix} = \begin{pmatrix} 0 & \tau_r & -\hat{\kappa}_g \\ -\tau_r & 0 & -\hat{\kappa}_n \\ \hat{\kappa}_g & \hat{\kappa}_n & 0 \end{pmatrix} \begin{pmatrix} T^a \\ N^a \\ B^a \end{pmatrix}$$

Case 1 ($dI_i = 0 \xrightarrow{\text{no}} \boxed{\text{case 1}}$)

Branch where $\nabla_a R$ is a geodesic and an eigenvec. of R_{ab}

$\{T^a \propto \nabla^a R, N^a, B^a\}$: the eigensystem of R_{ab}

If $\tau_r = \kappa_g = \hat{\kappa}_g = 0$

then R_{ab} has Segre type {21} with eigenvalues

$$\{0, \lambda, \lambda\}$$

Case 1 ($dI_i = 0 \xrightarrow{\text{no}} \boxed{\text{case 1}}$) again

Is $\nabla_a R$ a geodesic? $\xrightarrow{\text{no}} \boxed{\text{case 2}}$

$\downarrow$ yes

Is $\nabla_a R$ an eigenvecor of R_{ab}? $\xrightarrow{\text{no}} \boxed{\cdots}$ SKIP

$\downarrow$ yes

$\tau_r = \kappa_g = \hat{\kappa}_g = 0 \xrightarrow{\text{no}} \boxed{\cdots}$ SKIP $\longrightarrow \boxed{\text{2 KVs}}$

$\downarrow$ yes

$\mathcal{L}_N \lambda = \mathcal{L}_B \lambda = 0 \xrightarrow{\text{no}} \boxed{\text{case 2}}$

$\downarrow$ yes

$\boxed{\text{3 KVs}}$

Curve theoretic parameters regulate the number of KVs

Case 0 ($dI_i = 0 \xrightarrow{\text{yes}} \boxed{\text{case } 0}$)

All eigenvalues of R_{ab} are constants

Possible Segre types: $\{111\}$, $\{21\}$, $\{\cancel{3}\}$

$$\text{Segre type of } R_{ab} \text{ is } \{21\} \xrightarrow{\text{yes}} \boxed{\cdots}$$

at most 4KVs

$$\downarrow \text{no}$$

$$\boxed{\cdots}$$

at most 3KVs

under construction

Summary

$$\nabla_{(a}K_{b)} = 0$$

PARTIAL ANSWERS:

- Local curvature obstructions prevent the existence of Killing vector fields
- The obstructions are given by the curve (or surface) theoretic parameters
- Using our algorithm, we can determine the number of KVs without solving the Killing Eq. if dim. = 3

APPENDIX

4 dim. case

$$
\begin{array}{ccc}
R_{abcd} \propto g_{c[a}g_{b]d} & \xrightarrow{\text{yes}} & \boxed{\text{10 KVs}} \\
\downarrow \text{no} & & \\
\nabla_a R_{bcde} = 0 & \xrightarrow{\text{yes}} & \boxed{\text{8 KVs}} \\
\downarrow \text{yes} & & \\
dI_i \wedge dI_j \wedge dI_k \wedge dI_l = 0 & \xrightarrow{\text{no}} & \boxed{\text{no KV}} \\
\downarrow \text{yes} & & \\
dI_i \wedge dI_j \wedge dI_k = 0 & \xrightarrow{\text{no}} & \boxed{\text{case 3}} \\
\downarrow \text{yes} & & \\
dI_i \wedge dI_j = 0 & \xrightarrow{\text{no}} & \boxed{\text{case 2}} \\
\downarrow \text{yes} & & \\
dI_i = 0 & \xrightarrow{\text{no}} & \boxed{\text{case 1}} \\
\downarrow \text{yes} & & \\
\boxed{\text{case 0}} & &
\end{array}
$$

$$
\begin{aligned}
I_1 &= R \\
I_2 &= R_{ab}R^{ab} \\
I_3 &= R_{ab}R^{bc}R^{a}{}_{c} \\
I_4 &= R_{ab}R^{bc}R_{cd}R^{ad} \\
I_5 &= C_{abcd}C^{abcd} \\
I_6 &= C_{abcd}C^{cdef}C^{ab}{}_{ef} \\
I_7 &= C_{abcd}C^{cdef}C_{efgh}C^{abgh} \\
I_8 &= C_{abcd}C^{cdef}C_{efgh}C^{ghij}C^{ab}{}_{ij} \\
I_9 &= C_{abcd}C^{cdef}C_{efgh}C^{ghij}C_{ijkl}C^{abel}
\end{aligned}
$$

Example

$$ds^2 \;=\; 2dxdy + z^\alpha dy^2 + e^{\beta y + x^\gamma} dz^2$$

The existence of KVs depends on (α, β, γ)

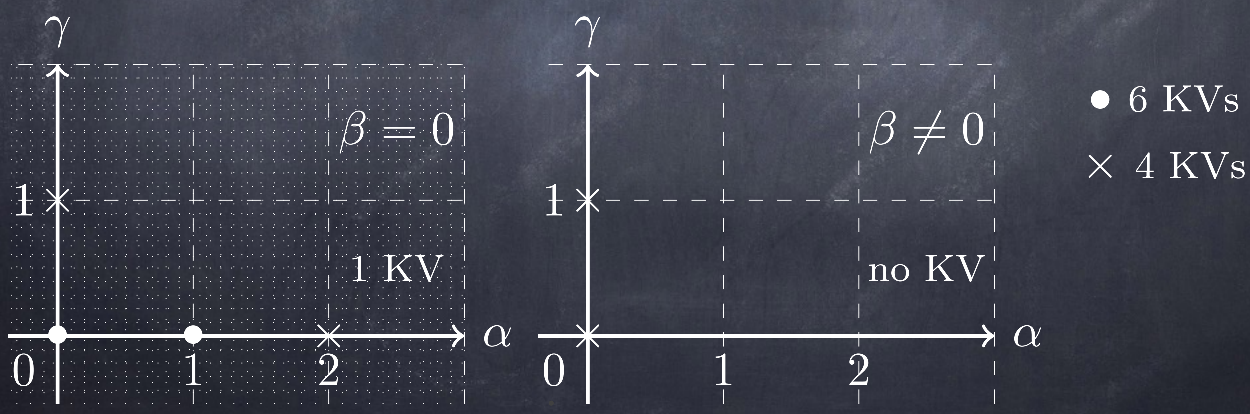

4b2. Masashi Kimura (Instituto Superior Tecnico, U.of Lisbon),

“A simple test for stability of black hole by S-deformation” (10+5)

[JGRG27 (2017) 112909]

A simple test for stability of BH by S-deformation

Class.Quant.Grav. 34 (2017) 235007
[arXiv:1706.01447]

Masashi Kimura
(IST, University of Lisbon)

29th Nov 2017

Linear gravitational perturbation

Linear gravitational perturbation on a highly symmetric BH usually reduces to

$$\left[-\frac{\partial^2}{\partial t^2}+\frac{\partial^2}{\partial x^2}-V(x)\right]\tilde{\Phi}=0$$

$\tilde{\Phi}(t,x)=e^{-i\omega t}\Phi(x)$

$$\left[-\frac{d^2}{dx^2}+V\right]\Phi=\omega^2\Phi$$

unstable mode → $\omega^2<0$ mode
(negative energy bound state)

$$\left[-\frac{d^2}{dx^2}+V\right]\Phi=\omega^2\Phi$$

$$\Longrightarrow \left[\bar{\Phi}\frac{d\Phi}{dx}\right]_{-\infty}^{\infty}+\int dx\left[\left|\frac{d\Phi}{dx}\right|^2+V|\Phi|^2\right]=\omega^2\int dx|\Phi|^2$$

$V\geq 0$ implies non-existence of $\omega^2<0$ mode

Sometimes, V contains negative regions

S-deformation [Kodama and Ishibashi 2003]

$$-\frac{d}{dx}\left[\bar{\Phi}\frac{d\Phi}{dx}+S|\Phi|^2\right]+\left|\frac{d\Phi}{dx}+S\Phi\right|^2+\left(V+\frac{dS}{dx}-S^2\right)|\Phi|^2=\omega^2|\Phi|^2$$

For continuous and bounded S

$$-\left[\bar{\Phi}\frac{d\Phi}{dx}+S|\Phi|^2\right]_{-\infty}^{\infty}+\int dx\left[\left|\frac{d\Phi}{dx}+S\Phi\right|^2+\left(V+\frac{dS}{dx}-S^2\right)|\Phi|^2\right]=\omega^2\int dx\,|\Phi|^2$$

We can say $\omega^2\geq 0$ if $V+\frac{dS}{dx}-S^2\geq 0$

In general, it is hard to find an appropriate S analytically

In that case, numerical approach (solving PDE) was used so far

Today's talk

I want to propose a simple method for finding an appropriate S-deformation

My personal motivation:

There is an unsolved problem in our paper 10 years ago

Very easy new method

[Kimura 2017]

Just solve $\boldsymbol{V + \frac{dS}{dx} - S^2 = 0}$ numerically

As far as I checked, we can easily find continuous and bounded $\boldsymbol{S}$
if spacetime is stable

Toy model

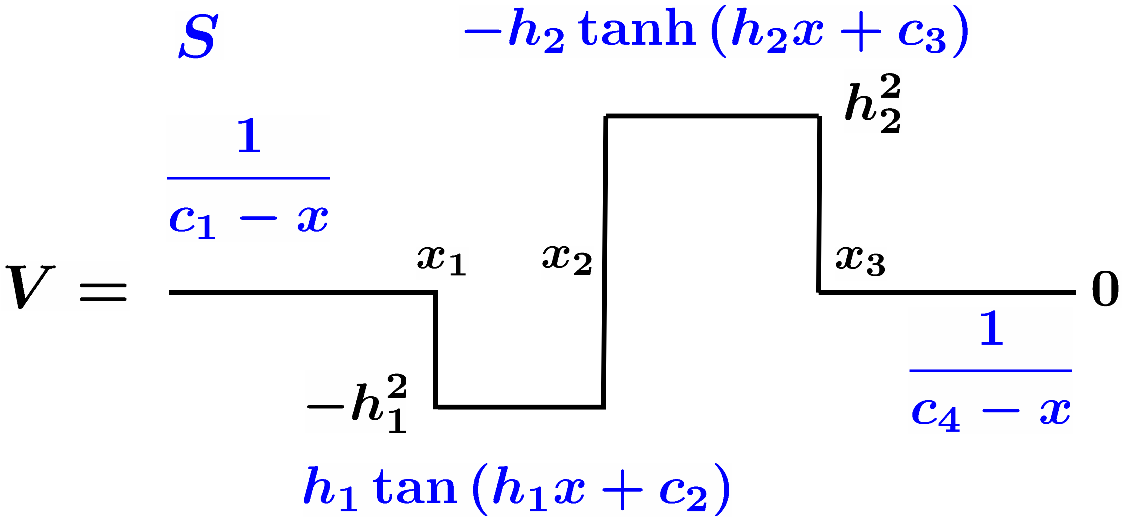

- continuity at $x = x_1, x_2, x_3$
- $S|_{x \to \pm\infty} \sim \mp$
- $S|_{x_1} > 0, S|_{x_2} > 0, S|_{x_3} < 0$

typical case

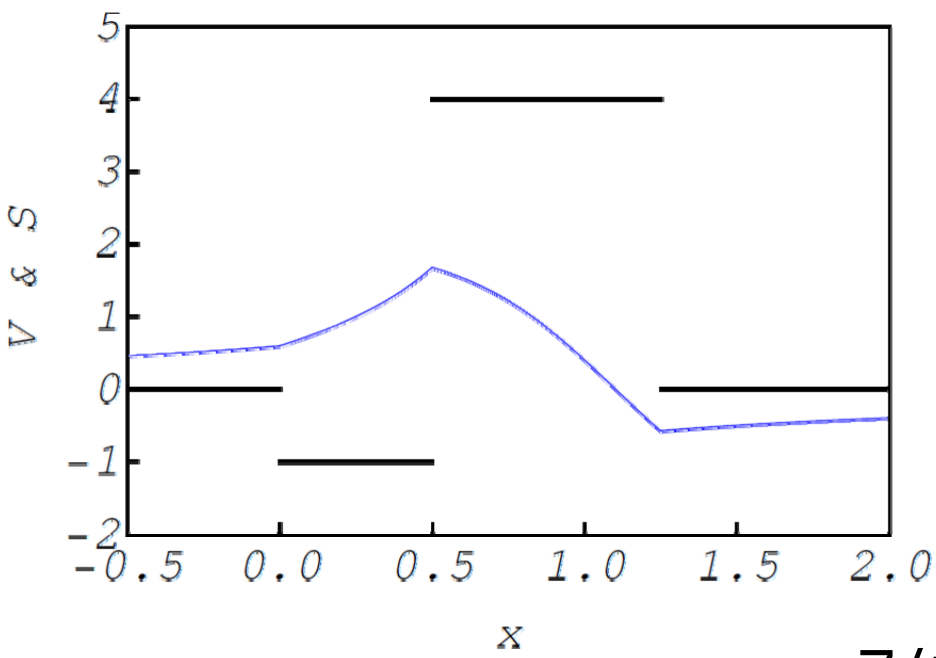

Existence condition

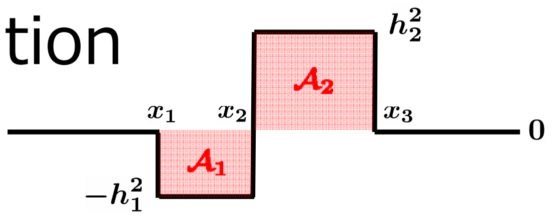

$$\Gamma := \frac{\mathcal{A}_2}{\mathcal{A}_1}$$

Condition for existence of regular S

$$\Gamma > \Gamma_{\rm cr}$$

$$\frac{\sqrt{x_3 - x_2}}{\sqrt{x_2 - x_1}} \tan\left(h_1 (x_2 - x_1)\right) = \sqrt{\Gamma_{\rm cr}} \tanh\left(h_1 \sqrt{\Gamma_{\rm cr}} \sqrt{x_2 - x_1} \sqrt{x_3 - x_2}\right)$$

Condition for non-existence of bound state

$$\Gamma > \Gamma_{\rm cr}$$

Regular S exists if and only if spacetime is stable (i.e., no $\omega^2 < 0$ mode case)

Finite size box case

$$V = \begin{cases} \infty & (\ |x| \geq L\ ) \\ \text{function of } x & (\ |x| < L\ ) \end{cases}$$

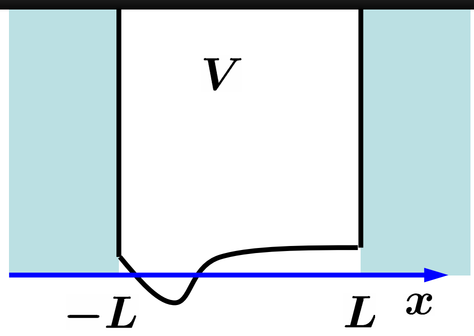

Proposition. *If the potential is in a finite size box, there exists an appropriate S-deformation for stable case*

Numerical calculation $V + \frac{dS}{dx} - S^2 = 0$

We need to find a boundary condition so that

S is continuous in $-\infty < x < \infty$

Appropriate boundary conditions can be found by setting $S = 0$ in $V > 0$ region

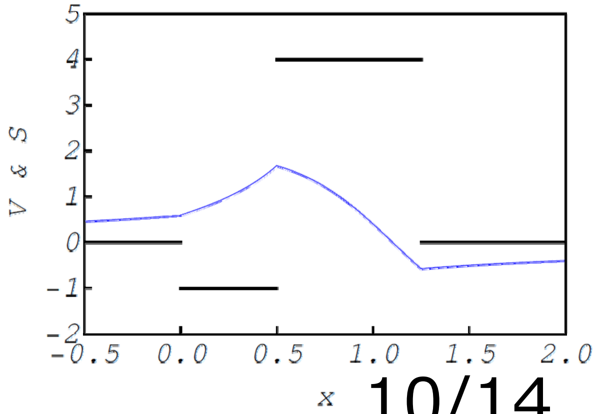

10 Dim Schwarzschild BH

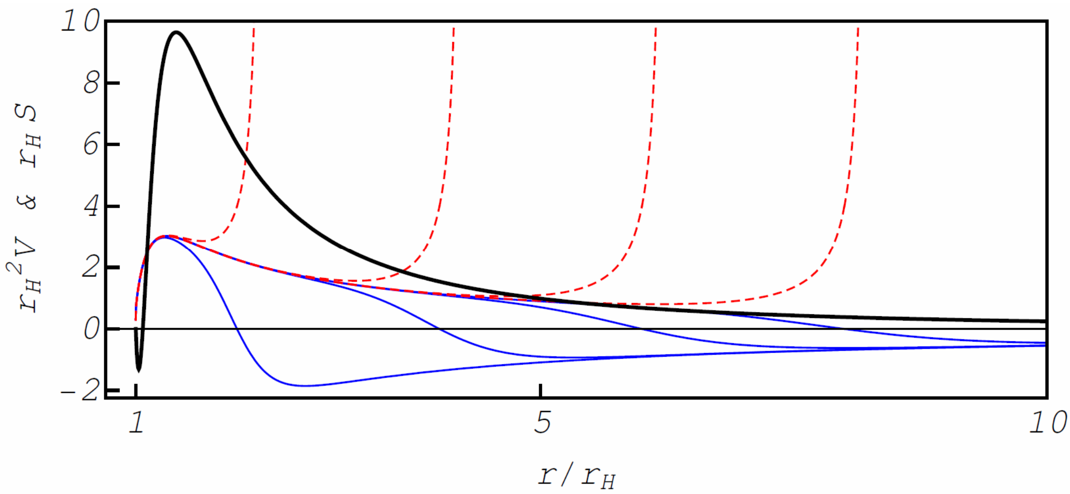

If we set S=0 in V>0 region, we obtain appropriate S-deformations

Squashed Kaluza-Klein BH (K=1)

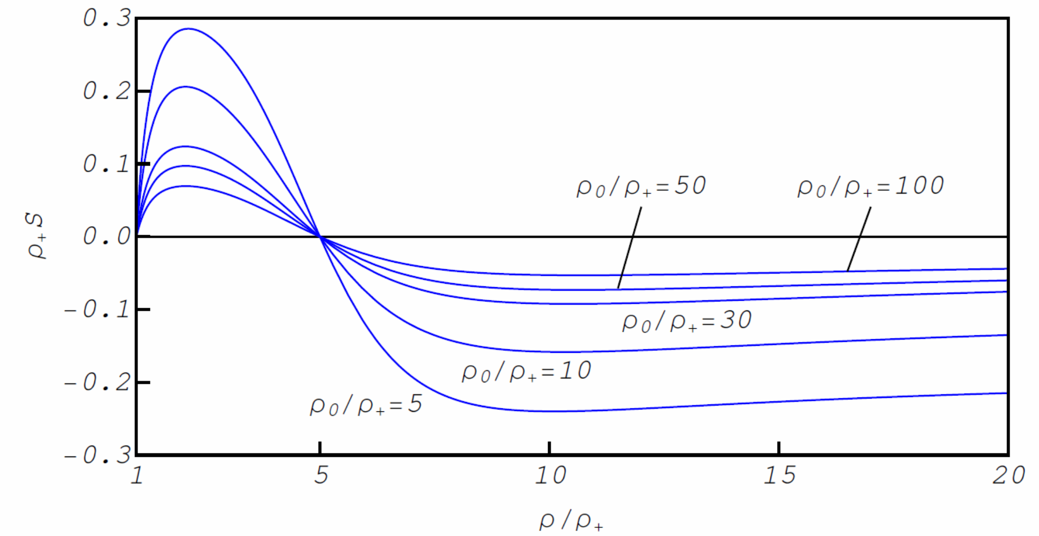

Ansolved problem in 10 years ago is solved

Black string

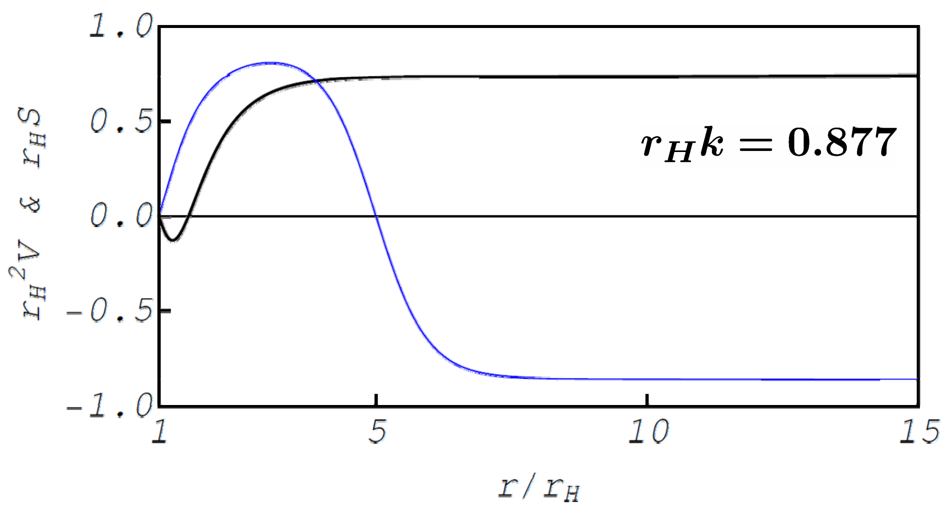

If $r_H k < r_H k_{\rm cr} \simeq 0.876$ there exists an unstable mode [Gregory and Laflamme, 1993]

Summary and discussion

We discussed a new method for finding S-deformation by solving $V + \frac{dS}{dx} - S^2 = 0$

Surprisingly, this method works well

This is a good test for stability of BH

4b3. Yoshimune Tomikawa (Matsuyama U.),
“On uniqueness of static spacetimes with non-trivial conformal scalar field” (10+5)
[JGRG27 (2017) 112910]

JGRG27 11/27-12/1（2017）

On uniqueness of static spacetimes with non-trivial conformal scalar field

Yoshimune Tomikawa
Faculty of Economics, Matsuyama University

based on
Y. Tomikawa, T. Shiromizu, K. Izumi, CQG 34, 155004 (2017)

Contents

1. Introduction
2. Set up and BBMB solution
3. Uniqueness of BBMB spacetime
4. Summary and Future issues

1. Introduction

Uniqueness of black hole

Israel (1967), Bunting, Masood-ul-Alam (1987)

- Static and asymptotically flat black hole solution of vacuum Einstein equation is unique to the Schwarzschild black hole.

Carter (1971, 1973), et al.

- Stationary and asymptotically flat black hole solution of vacuum Einstein equation is unique to the Kerr black hole.

How does it change if there is the scalar field?

No-hair theorem

Bekenstein (1972), Saa (1996), et al.

- There is a no-hair theorem that static and asymptotically flat black holes do not have regular scalar hair with non-negative potential.

→They are unique to the Schwarzschild black hole.

But, there is the Bocharova-Bronnikov-Melnikov-Bekenstein (BBMB) solution in the Einstein-conformal scalar field system.

Bocharova, Bronnikov, Melnikov (1970), Bekenstein (1974, 1975)

BBMB black hole

Bocharova, Bronnikov, Melnikov (1970),
Bekenstein (1974, 1975)

The BBMB black hole is static, spherically symmetric and asymptotically flat solution with conformal scalar field.

The metric is the same as that of the extreme Reissner-Nordström solution.

The scalar field is singular at the event horizon.

Question

Uniqueness of BBMB black hole holds?

Result

We will prove that the region outside "photon sphere" of static and asymptotically flat spacetime in the Einstein-conformal scalar field system is unique to the BBMB solution.

2. Set up and BBMB solution

Asymptotically flat, static spacetime

$$ds^2 = -V^2(x^k)dt^2 + g_{ij}(x^k)dx^i dx^j$$

event horizon $V = 0$

asymptotic boundary conditions :

$$\begin{cases} V = 1 - m/r + O(1/r^2) \\ g_{ij} = (1 + 2m/r)\delta_{ij} + O(1/r^2) \\ \phi = O(1/r) \end{cases}$$

Field equations

- Einstein equation

$\left(1 - \frac{\kappa}{6}\phi^2\right) R_{\mu\nu} = \kappa S_{\mu\nu}$ → The surface S_p where $\phi = \phi_p := \pm\sqrt{6/\kappa}$ holds is singular.

$$\begin{cases} (0,0) \quad \left(1 - \frac{\kappa}{6}\phi^2\right) V D^2 V = \frac{\kappa}{6}[V^2 (D\phi)^2 + 2\phi V D^i V D_i \phi] \\ (i,j) \quad \left(1 - \frac{\kappa}{6}\phi^2\right) ({}^{(3)}R_{ij} - V^{-1} D_i D_j V) = \frac{\kappa}{6}[4 D_i\phi D_j \phi - g_{ij}(D\phi)^2 - 2\phi D_i D_j \phi] \end{cases}$$

$$\begin{cases} D_i \text{ : covariant derivative on } \Omega \\ {}^{(3)}R_{ij} \text{ : Ricci tensor on } \Omega \end{cases}$$

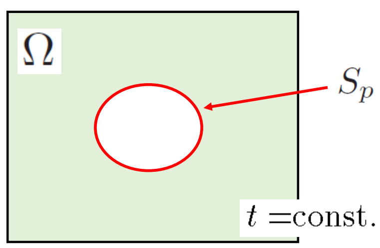

- scalar field equation

$\nabla^2 \phi = 0$ → $D_i(V D^i \phi) = 0$

BBMB solution

Bocharova, Bronnikov, Melnikov (1970),
Bekenstein (1974, 1975)

metric : $ds^2 = -\left(1-\frac{m}{r}\right)^2 dt^2 + \left(1-\frac{m}{r}\right)^{-2} dr^2 + r^2 d\Omega_2^2$

scalar field : $\phi = \pm\sqrt{\frac{6}{\kappa}}\frac{m}{r-m}$

event horizon : $r = m$ scalar field diverges at event horizon

BBMB black hole has photon sphere at $r = 2m$.

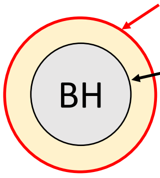

photon sphere $r = 2m \rightarrow 1 - \frac{\kappa}{6}\phi^2 = 0 \rightarrow S_p$

event horizon $r = m$

S_p : surface satisfying $\phi = \phi_p := \pm\sqrt{6/\kappa}$

3. Uniqueness of BBMB spacetime

Uniqueness theorem outside S_p

Theorem

The outside region of S_p of the static and asymptotically flat spacetime in the Einstein-conformal scalar field system is unique to the BBMB solution.

S_p : surface satisfying $\phi = \phi_p := \pm\sqrt{6/\kappa}$

Step of proof

1. We show the relation between ϕ and V. $\varphi = V^{-1} - 1$ $\left(\varphi := \pm\sqrt{\kappa/6}\phi\right)$
2. Using the surgery and positive mass theorem, we show that static time slice Ω is conformally flat and V^{-1} is the harmonic function.
3. Electrostatic potential problem with spherical boundary tells us that Ω is spherically symmetric.

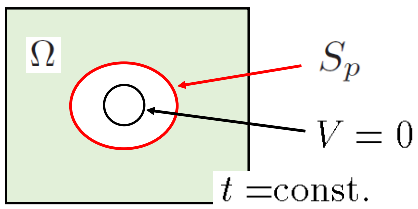

Relation between ϕ and V

(0,0)-component of Einstein eq. and scalar field eq.

$\rightarrow D_i[(1-\varphi)D^i\Phi]=0$

$$\begin{cases}\Phi := (1+\varphi)V \\ \varphi := \pm\sqrt{\kappa/6}\phi\end{cases}$$

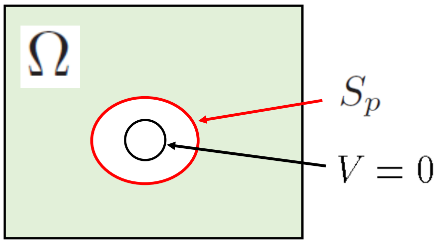

integration over Ω

$\Phi = 1$

$\varphi = V^{-1}-1 \longrightarrow V=\frac{1}{2}$ at S_p

Regularity at S_p

$$\begin{aligned}R_{\mu\nu\sigma\rho}R^{\mu\nu\sigma\rho} &= -\frac{4}{\rho^4}+\frac{4}{\rho^2}\left[k_{ij}k^{ij}+\frac{2}{\rho^2}(\mathcal{D}\rho)^2+\left(k-\frac{1}{\rho}\right)^2\right] \\ &\quad+\frac{4}{(2V-1)^2\rho^2}\left[\left(k_{ij}-\frac{1}{\rho}h_{ij}\right)^2+\frac{2}{\rho^2}(\mathcal{D}\rho)^2+\left(k-\frac{4V}{\rho}\right)^2\right]\end{aligned}$$

$\mathcal{D}_i\rho|_{S_p}=0$, $k_{ij}|_{S_p}=\frac{1}{\rho_p}h_{ij}|_{S_p}$

(totally umbilic)

- h_{ij} : induced metric of S_p
- $\rho := |D\log V|^{-1}$: lapse function
- k_{ij} : extrinsic curvature of S_p
- $\mathcal{D}_i$: covariant derivative w.r.t. h_{ij}

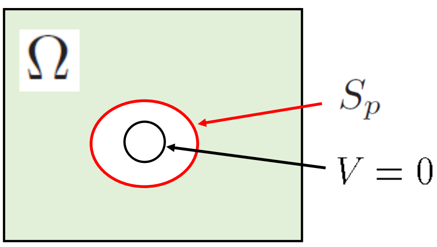

Step of proof

1. We show the relation between ϕ and V. $\varphi = V^{-1} - 1$ $\left(\varphi := \pm\sqrt{\kappa/6}\phi\right)$
2. Using the surgery and positive mass theorem, we show that static time slice Ω is conformally flat and V^{-1} is the harmonic function.
3. Electrostatic potential problem with spherical boundary tells us that Ω is spherically symmetric.

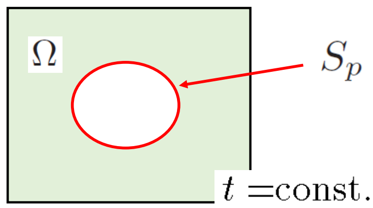

Conformally flat

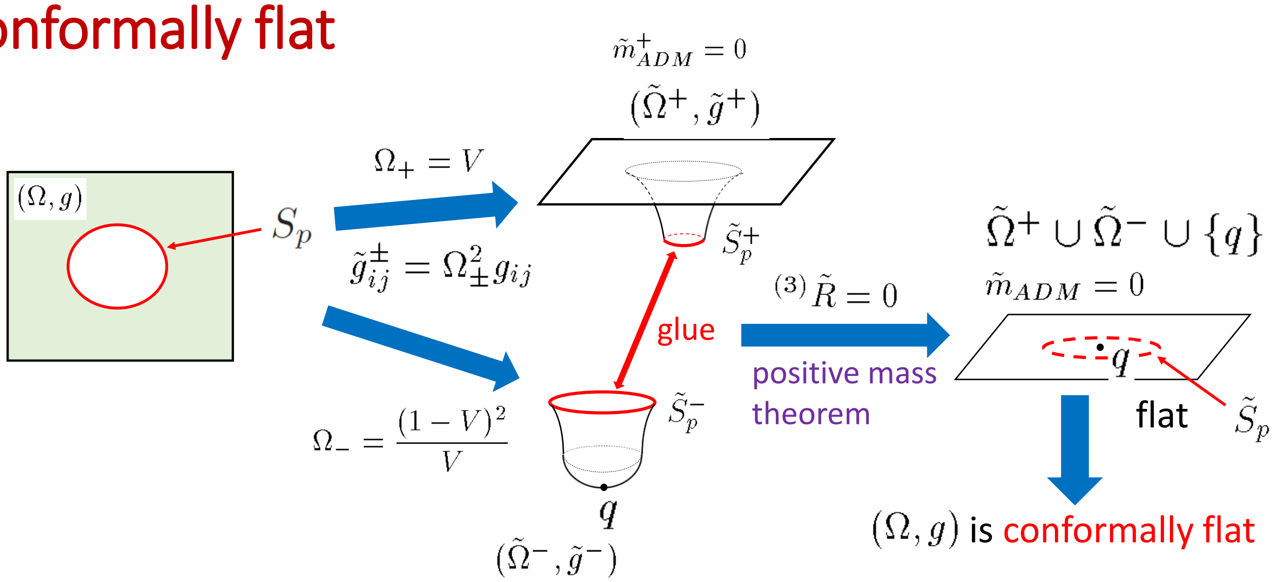

($\tilde{S}_p$ is totally umbilic surface in the flat space)

Step of proof

1. We show the relation between ϕ and V. $\varphi = V^{-1} - 1$ $\left(\varphi := \pm\sqrt{\kappa/6}\phi\right)$

2. Using the surgery and positive mass theorem, we show that static time slice Ω is conformally flat and V^{-1} is the harmonic function.

3. Electrostatic potential problem with spherical boundary tells us that Ω is spherically symmetric.

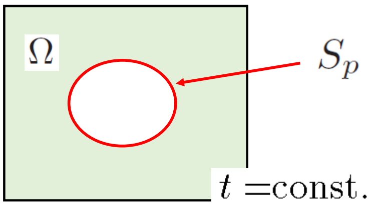

Spherically symmetric

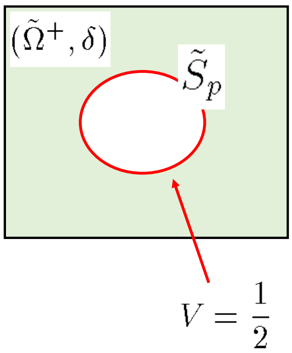

We can see that $\Delta_\delta V^{-1} = 0$ holds in the flat space $(\tilde{\Omega}^+, \delta)$, where Δ_δ is the flat Laplacian.

$\tilde{S}_p$ is the totally umbilic surface in the flat space.

➡ $\tilde{S}_p$ is the spherically symmetric surface in the Euclid space.

➡ The electrostatic potential problem tells us that (Ω, g) is spherically symmetric.

➡ Regular spherically symmetric solutions with conformal scalar field is unique to the BBMB solution.

Xanthopoulos, Zannias (1991)

4. Summary and Future issues

Summary

We proved that the region outside S_p of static and asymptotically flat spacetime in the Einstein-conformal scalar field system is unique to the BBMB solution.

Future issues

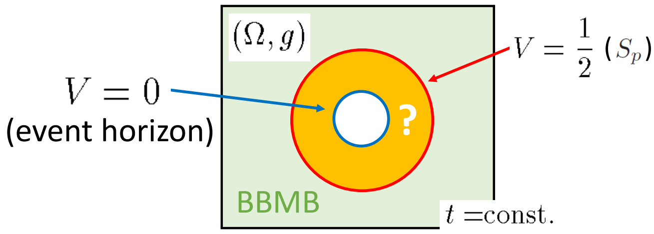

- The uniqueness of the whole region (including the region between the event horizon and S_p)?

- Penrose-like inequality for photon sphere?

  partially addressed in the another context
  ⇒ loosely trapped surface, transversely trapping surface

  Shiromizu, Tomikawa, Izumi, Yoshino (2017),
  Yoshino, Izumi, Shiromizu, Tomikawa (2017)

…

4b4. Makoto Nakamura (Yamagata U.),

"On the Cauchy problem for semi-linear Klein-Gordon equations in de Sitter spacetime"

(10+5)

[JGRG27 (2017) 112911]

On the Cauchy problem for semi-linear
Klein-Gordon equations in de Sitter spacetime

Makoto NAKAMURA (Yamagata University)

1 Introduction

Let $n \geq 1$, $M > 0$, $H > 0$, $c > 0$. Consider the Cauchy problem

$$(P) \quad \begin{cases} (\partial_t^2 - c^2 e^{-2Ht}\Delta + M^2)u(t,x) + c^2 e^{nHt/2} f(e^{-nHt/2}u(t,x)) = 0 \\ \qquad\qquad\qquad\qquad\qquad\qquad \text{for} \quad (t,x) \in [0,T) \times \mathbb{R}^n \\ u(0,\cdot) = u_0(\cdot) \in H^1(\mathbb{R}^n), \quad \partial_t u(0,\cdot) = u_1(\cdot) \in L^2(\mathbb{R}^n) \end{cases}$$

Known results:

1. D'Ancona (1995), D'Ancona-Giuseppe (2001): Global classical solutions for $(\partial_t^2 - a(t)\Delta)u + |u|^{p-1}u = 0$, $a(t) \geq 0$, $n = 1, 2, 3$.

2. Yagdjian-Galstian (2009): Fundamental solutions, $L^p - L^q$ estimates.

3. Yagdjian (2012): Small global solutions for $f(u) = \pm|u|^{p-1}u$, $1 < p < \infty$, $(u_0, u_1) \in H^s(\mathbb{R}^n) \oplus H^s(\mathbb{R}^n)$, $s > n/2 \geq 1$.

Derivation of equations: Put $x^0 := t$, $x := (x^1, \cdots, x^n)$.

$ds^2 = -c^2 dt^2 + e^{2ct/R} dx^2$: line element in de Sitter spacetime

$c > 0$: speed of light, $R > 0$: radius of the universe

$H := c/R$: Hubble constant, $(g_{\alpha\beta})_{0\le\alpha,\beta\le n} := \mathrm{diag}(-c^2, e^{2Ht}, \cdots, e^{2Ht})$

$ds^2 = \sum_{0\le\alpha,\beta\le n} g_{\alpha\beta} dx^\alpha dx^\beta$, $g := \det(g_{\alpha\beta})$, $(g^{\alpha\beta}) := (g_{\alpha\beta})^{-1}$.

Then the equation of motion of the scalar field v with mass m and the potential V must satisfy

$$(\sqrt{|g|})^{-1}\partial_\alpha(\sqrt{|g|} g^{\alpha\beta}\partial_\beta v) = m^2 v + V'(v),$$

$$\text{i.e. } (\partial_t^2 + nH\partial_t - c^2 e^{-2Ht}\Delta + m^2c^2)v + c^2 V'(v) = 0.$$

By $u = e^{\mu t} v$ for $\mu \in \mathbb{R}$,

$$\left\{\partial_t^2 + (nH - 2\mu)\partial_t - c^2 e^{-2Ht}\Delta + m^2c^2 + \mu(\mu - nH)\right\} u + c^2 e^{\mu t} V'(e^{-\mu t} u) = 0.$$

Putting $\mu = nH/2$, $M^2 := mc^2 - (nH/2)^2$ and $f := V'$, we obtain

$$(\partial_t^2 - c^2 e^{-2Ht}\Delta + M^2)u + c^2 e^{nHt/2} f(e^{-nHt/2}u) = 0.$$

Remark 1.1 $\mu \le nH/2$ for energy estimates, $\mu \ge nH/2$ for contraction argument.

Example : $f(u) = \lambda|u|^{p-1}u$ or $f(u) = \lambda|u|^p$ for $\lambda \in \mathbb{R}$.

For $T > 0$, let $X(T) := \{u : \|u\|_{X(T)} < \infty\}$, where

$$\|u\|_{X(T)} := \max\{M\|u\|_{L^\infty((0,T),L^2(\mathbb{R}^n))}, \|\partial_t u\|_{L^\infty((0,T),L^2(\mathbb{R}^n))},$$
$$c\|e^{-Ht}\nabla u\|_{L^\infty((0,T),L^2(\mathbb{R}^n))}, c\sqrt{H}\|e^{-Ht}\nabla u\|_{L^2((0,T)\times\mathbb{R}^n))}\}.$$

Theorem 1.2 Let p satisfy

$$1 \le p \begin{cases} < \infty & \text{if } n = 1, 2 \\ \le 1 + \frac{2}{n-2} & \text{if } n \ge 3. \end{cases}$$

Then

(1) $\forall u_0$ and $\forall u_1$, $\exists T = T(\|u_0\|_{H^1(\mathbb{R}^n)} + \|u_1\|_{L^2(\mathbb{R}^n)}) > 0$ and $\exists! u \in C([0,T), H^1(\mathbb{R}^n)) \cap C^1([0,T), L^2(\mathbb{R}^n)) \cap X(T)$ of (P).

(2) If $\|u_0\|_{H^1(\mathbb{R}^n)} + \|u_1\|_{L^2(\mathbb{R}^n)} \ll 1$ and $1 + 4/n \le p$, then u is global.

Lemma 1.3 [see Strichartz '77] Let $\beta > (8\pi e)^{-1/2}$. Then

$$\|u\|_{L^q(\mathbb{R}^2)} \leq \beta q^{1/2} \|\nabla u\|_{L^2(\mathbb{R}^2)}^{1-2/q} \|u\|_{L^2(\mathbb{R}^2)}^{2/q} \quad \text{for } 2 \leq \exists q_0 \leq \forall q < \infty.$$

Theorem 1.4 Let $n = 2$, $\lambda \in \mathbb{R}$, $\alpha > 0$, $0 < \nu \leq 2$, $j_0 \geq 2/\nu$. Let

$$f(u) = \lambda u \left(e^{\alpha |u|^\nu} - \sum_{0 \leq j < j_0} \frac{\alpha^j}{j!} |u|^{\nu j} \right).$$

Let $D := \|u_0\|_{H^1(\mathbb{R}^n)} + \|u_1\|_{L^2(\mathbb{R}^n)} \ll 1$.
Then $\exists! u \in C([0,\infty), H^1(\mathbb{R}^2)) \cap C^1([0,\infty), L^2(\mathbb{R}^2)) \cap X(\infty)$: sol. of (P).

Remark 1.5
· $\nu \leq 2$ seems to be optimal.
· $f(u) = \lambda u(e^{\alpha|u|^2} - 1) = \lambda\alpha|u|^2 u + \cdots$ when $\nu = 2$. Note $1 + 4/n = 3$.

Remark 1.6 N.-Ozawa (1998, 1999, 2001), N. (2011) for Schrödinger equations, wave equations, Klein-Gordon equations, complex Ginzburg-Landau equations and dissipative wave equations.

Theorem 1.7 (Continuous dependence and asymptotic)
(1) Let v be the solution of (P) for $v_0 \in H^1(\mathbb{R}^n)$ and $v_1 \in L^2(\mathbb{R}^n)$. Then

$$\|u - v\|_{X(T)} \longrightarrow 0 \quad \text{if } \|u_0 - v_0\|_{H^1} + \|u_1 - v_1\|_{L^2} \to 0.$$

(2) If u is global, then there exists a free solution v s.t.

$$\lim_{t\to\infty} \{e^{-Ht}\|u(t) - v(t)\|_{L^2(\mathbb{R}^n)} + \|\partial_t u(t) - \partial_t v(t)\|_{H^{-1}(\mathbb{R}^n)}\} = 0.$$

Theorem 1.8 (Large global solutions) Let $\lambda \geq 0$. Assume (1) or (2).
(1) $f(u) = \lambda |u|^{p-1} u$ with

$$1 \leq p \begin{cases} < \infty & \text{if } n = 1, 2 \\ \leq 1 + \frac{2}{n-2} & \text{if } n \geq 3. \end{cases}$$

(2) $n = 2$, $0 < \alpha < \infty$, $0 < \nu \leq 2$, $0 \leq j_0 < \infty$.
$f(u) = \lambda u(e^{\alpha|u|^\nu} - \sum_{0 \leq j < j_0} \frac{\alpha^j}{j!} |u|^{\nu j})$. When $\nu = 2$, we assume

$$\int_{\mathbb{R}^2} c^2 |\nabla u_0|^2 + M^2 u_0^2 + |u_1|^2 + c^2 \lambda \sum_{j \geq j_0} \frac{\alpha^j}{j!(\nu j + 2)} |u_0|^{\nu j + 2} dx \leq \frac{2c^2\pi}{\alpha}.$$

Then $\exists! u \in C([0,\infty), H^1(\mathbb{R}^n)) \cap C^1([0,\infty), L^2(\mathbb{R}^n)) \cap X(\infty)$: sol. of (P).

2 Estimates for linear terms

$$\begin{cases} (\partial_t^2 - c^2 e^{-2Ht}\Delta + M^2)u(t,x) + h(t,x) = 0 & \text{for } (t,x) \in [0,T) \times \mathbb{R}^n \\ u(0,\cdot) = u_0(\cdot), \quad \partial_t u(0,\cdot) = u_1(\cdot). \end{cases}$$

We put the energy density

$$e(u) := \{(\partial_t u)^2 + M^2 u^2 + c^2 e^{-2Ht}|\nabla u|^2\}/2.$$

Multiplying $\partial_t u$ to the equation,

$$\int_{\mathbb{R}^n} e(u)(t)dx + Hc^2\|e^{-Ht}\nabla u\|^2_{L^2((0,t)\times\mathbb{R}^n)} + \iint_{(0,t)\times\mathbb{R}^n} \partial_t u(s,x)h(s,x)dxds = \int_{\mathbb{R}^n} e(u)(0)dx$$

for $t \geq 0$. For $T > 0$,

$$\begin{aligned} &\|\partial_t u\|_{L^\infty((0,T),L^2(\mathbb{R}^n))} + M\|u\|_{L^\infty((0,T),L^2(\mathbb{R}^n))} \\ &\quad + c\|e^{-Ht}\nabla u\|_{L^\infty((0,T),L^2(\mathbb{R}^n))} + \sqrt{H}c\|e^{-Ht}\nabla u\|_{L^2((0,T)\times\mathbb{R}^n)} \\ &\quad \lesssim \|u_1\|_{L^2(\mathbb{R}^n)} + M\|u_1\|_{L^2(\mathbb{R}^n)} + c\|\nabla u_0\|_{L^2(\mathbb{R}^n)} + \|h\|_{L^1((0,T),L^2(\mathbb{R}^n))}. \end{aligned}$$

Remark

(1) For the heat equation

$$\begin{cases} (\partial_t - \Delta)u(t,x) + h(t,x) = 0 & \text{for } (t,x) \in [0,T) \times \mathbb{R}^n \\ u(0,\cdot) = u_0(\cdot), \end{cases}$$

the energy estimates show

$$\|u\|_{L^\infty((0,T),L^2(\mathbb{R}^n))} + \|\nabla_x u\|_{L^2((0,T)\times\mathbb{R}^n)} \leq C\|u_0\|_{L^2(\mathbb{R}^n)} + \|h\|_{L^1((0,T),L^2(\mathbb{R}^n))}. \tag{2.1}$$

(2) For the dissipative wave equation

$$\begin{cases} (\partial_t^2 - \Delta + \partial_t)u(t,x) + h(t,x) = 0 & \text{for } (t,x) \in [0,T) \times \mathbb{R}^n \\ u(0,\cdot) = u_0(\cdot), \quad \partial_t u(0,\cdot) = u_1(\cdot), \end{cases}$$

the energy estimates show

$$\|u\|_{L^\infty((0,T),H^1(\mathbb{R}^n))} + \|\partial_t u\|_{L^\infty((0,T),L^2(\mathbb{R}^n))} + \|\nabla_{t,x} u\|_{L^2((0,T)\times\mathbb{R}^n)} \leq C\|u_0\|_{H^1(\mathbb{R}^n)} + C\|u_1\|_{L^2(\mathbb{R}^n)} + C\|h\|_{L^1((0,T),L^2(\mathbb{R}^n))}. \tag{2.2}$$

Integral equation :

$$(\partial_t^2 + a(t))Fu + Fh = 0, \quad \text{where} \ \ a(t) := c^2 e^{-2Ht}\xi^2 + M^2.$$

Let $\{\rho_j\}_{j=0,1}$ be the solution of

$$\begin{array}{l} (\frac{d^2}{dt^2} + a(t))\rho_0(t) = 0, \quad \rho_0(0) = 1, \quad \partial_t \rho_0(0) = 0 \\ (\frac{d^2}{dt^2} + a(t))\rho_1(t) = 0, \quad \rho_1(0) = 0, \quad \partial_t \rho_1(0) = 1. \end{array}$$

Put $K_j(t) := F^{-1}\rho_j(t)F$ for $j = 0,1$, $K(t,s) := K_1(t)K_0(s) - K_0(t)K_1(s)$. Then

$$u(t) = \Phi(u)(t) := K_0(t)u_0 + K_1(t)u_1 + \int_0^t K(t,s)h(s)ds.$$

It is easy to show

$$\|K_0(t)u_0\|_{H^1(\mathbb{R}^n)} \lesssim e^{Ht}\|u_0\|_{H^1(\mathbb{R}^n)}, \quad \|K_1(t)u_1\|_{H^1(\mathbb{R}^n)} \lesssim e^{Ht}\|u_1\|_{L^2(\mathbb{R}^n)}$$
$$\|\int_0^t K(t,s)h(s)ds\|_{H^1(\mathbb{R}^n)} \lesssim e^{2Ht}\|h\|_{L^1((0,t),L^2(\mathbb{R}^n))}$$

and $\Phi(u) \in C([0,T),H^1) \cap C^1([0,T),L^2)$ if $u_0 \in H^1$, $u_1 \in L^2$, $h \in L^1((0,T),L^2)$.

3 Estimates for nonlinear terms

Lemma 3.1 Let p_0 satisfy $1 \le p_0 \le \min\{p, 1+4/n\}$. Then
(1) For $f(u) = \lambda|u|^{p-1}u$,

$$\begin{aligned} \left\| e^{nHt/2} f(e^{-nHt/2}u) \right\|_{L^1((0,T),L^2(\mathbb{R}^n))} &\le CT^{1-n(p_0-1)/4} \|e^{-Ht}\nabla u\|_{L^\infty((0,T),L^2(\mathbb{R}^n))}^{n(p-p_0)/2} \\ &\cdot \|e^{-Ht}\nabla u\|_{L^2((0,T),L^2(\mathbb{R}^n))}^{n(p_0-1)/2} \|u\|_{L^\infty((0,T),L^2(\mathbb{R}^n))}^{p-n(p-1)/2} \\ &\le CT^{1-n(p_0-1)/4}\|u\|_X^p \end{aligned}$$

(2) For $f(u) = \lambda u(e^{\alpha|u|^\nu} - \sum_{0\le j<j_0} \frac{\alpha^j}{j!}|u|^{\nu j})$,

$$\begin{aligned} \left\| e^{nHt/2} f(e^{-nHt/2}u) \right\|_{L^1((0,T),L^2(\mathbb{R}^2))} &\le CT^{1-n(p_0-1)/4} \sum_{j\ge j_0} a(j) \\ \cdot \|e^{-Ht}\nabla u\|_{L^\infty((0,T),L^2(\mathbb{R}^n))}^{n(p(j)-p_0)/2} &\|e^{-Ht}\nabla u\|_{L^2((0,T),L^2(\mathbb{R}^n))}^{n(p_0-1)/2} \|u\|_{L^\infty((0,T),L^2(\mathbb{R}^n))}^{p(j)-n(p(j)-1)/2} \\ &\le CT^{1-n(p_0-1)/4} \sum_{j\ge j_0} a(j)\|u\|_X^{p(j)} \end{aligned}$$

Proof. (1) Due to $\||u|^p\|_{L^2} \le C\|\nabla u\|_{L^2}^{ap}\|u\|_{L^2}^{(1-a)p}$ by $0 \le a := n(p-1)/2p \le 1$.
(2) Due to Moser-Trudinger inequality. □

3.1 Proof of Theorem 1.8

Let $n=2$, $f(u)=\lambda u(e^{\alpha|u|^{\nu}}-\sum_{0\le j<j_0}\frac{\alpha^j}{j!}|u|^{\nu j})$. Put $V(u):=\int_0^u f(v)dv$. Then $V'(u)=f(u)$. Multiplying $\partial_t u$ to

$$(\partial_t^2-c^2e^{-2Ht}\Delta+M^2)u+c^2e^{nHt/2}V'(e^{-nHt/2}u)=0,$$

we have

$$\begin{aligned}&E(u)(t)+c^2H\|e^{-H\cdot}\nabla u\|^2_{L^2((0,t)\times\mathbb{R}^n)}\\ &+c^2nH\int_0^t\int_{\mathbb{R}^n}e^{nHs}\left\{e^{-nHs/2}uV'(e^{-nHs/2}u)/2-V(e^{-nHs/2}u)\right\}dxds=E(u)(0),\end{aligned}$$

where

$$\begin{aligned}E(u)(t):=\Big\{&\|\partial_t u(t,\cdot)\|^2_{L^2(\mathbb{R}^n)}+M^2\|u(t,\cdot)\|^2_{L^2(\mathbb{R}^n)}+c^2\|e^{-Ht}\nabla u(t,\cdot)\|^2_{L^2(\mathbb{R}^n)}\\ &+c^2e^{nHt}\int_{\mathbb{R}^n}V(e^{-nHt/2}u(t,x))dx\Big\}/2.\end{aligned}$$

Since V satisfies $vV'(v)/2-V(v)\ge 0$ for $v\in\mathbb{R}$, we have

$$E(u)(t)+c^2H\|e^{-H\cdot}\nabla u\|^2_{L^2((0,t)\times\mathbb{R}^n)}\le E(u)(0).$$

Lemma 3.2 Let $n=\nu=2$. Let u_L be the free solution of

$$(\partial_t^2-c^2e^{-2Ht}\Delta+M^2)u_L=0,\quad u_L(0,\cdot)=u_0(\cdot),\quad \partial_t u_L(0,\cdot)=u_1(\cdot).$$

If $\|e^{-Ht}\nabla u_L\|^2_{L^\infty((0,T_0),L^2(\mathbb{R}^2))}<2\pi/\alpha$ for some $T_0>0$, then
$0<\exists T=T(\|u_0\|_{H^1},\|u_1\|_{L^2},\|e^{-Ht}\nabla u_L\|_{L^\infty((0,T_0),L^2(\mathbb{R}^2))})\ll 1$
$\exists! u_N\in X(T)$ with $\|u_N\|_{X(T)}\ll 1$ and

$$\begin{cases}(\partial_t^2-c^2e^{-2Ht}\Delta+M^2)u_N+c^2e^{nHt/2}V'(e^{-nHt/2}(u_L+u_N))=0\\ u_N(0,\cdot)=0,\quad \partial_t u_N(0,\cdot)=0.\end{cases}$$

Remark 3.3 $u=u_L+u_N$.

$$\begin{aligned}&\|e^{-Ht}\nabla u_L\|^2_{L^\infty L^2}<2\pi/\alpha,\quad \|u_N\|_{X(T)}\ll 1\\ \Longrightarrow\ &\|e^{-Ht}\nabla(u_L+u_N)\|^2_{L^\infty L^2}<2\pi/\alpha\\ \Longrightarrow\ &\sum_{j\ge j_0}a(j)\|e^{-Ht}\nabla(u_L+u_N)\|^{2j+1}_{L^\infty L^2}<\infty\\ \Longrightarrow\ &\|e^{nHt/2}V'(e^{-nHt/2}(u_L+u_N))\|_{L^1L^2}<\infty,\end{aligned}$$

where $p(j):=\nu j+1$, $a(j):=\alpha^j\beta^{p(j)}(2p(j))^{p(j)/2}/j!$.

Proof of the theorem. Note $u = u_L + u_N$. Let $T^* := \sup\{T : \ u \in X(T)\} < \infty$. For $0 < \varepsilon \ll 1$, let u_L^* be the solution of

$$\begin{cases} (\partial_t^2 - c^2 e^{-2Ht}\Delta + M^2)u_L^* = 0 \ \text{ for } \ (t,x) \in [T^* - \varepsilon, \infty) \times \mathbb{R}^2 \\ u_L^*(T^* - \varepsilon, \cdot) = u(T^* - \varepsilon, \cdot), \ \partial_t u_L^*(T^* - \varepsilon, \cdot) = \partial_t u(T^* - \varepsilon, \cdot). \end{cases}$$

The energy estimate shows

$$E(u_L^*)(t) + c^2 H \|e^{-Hs}\nabla u_L^*\|^2_{L^2((T^*-\varepsilon,t)\times\mathbb{R}^2)} \le E(u_L^*)(T^* - \varepsilon) \quad \text{for } \ t \in [T^* - \varepsilon, T^*)$$

$$E(u_L^*)(t) \ge c^2 \|e^{-Ht}\nabla u_L^*(t,\cdot)\|^2_{L^2}/2 \quad \text{by Def. of } E$$

$$E(u_L^*)(T^* - \varepsilon) \le E(u)(T^* - \varepsilon) \le E(u)(0) - c^2 H \|e^{-Hs}\nabla u\|^2_{L^2((0,T^*-\varepsilon)\times\mathbb{R}^2)}.$$

Since $\|e^{-Hs}\nabla u\|^2_{L^2((0,T^*/2)\times\mathbb{R}^2)} \ne 0$, we have

$$\begin{aligned} c^2 \|e^{-Hs}\nabla u_L^*\|^2_{L^\infty((T^*-\varepsilon,T^*),L^2)}/2 \le E(u)(0) - c^2 H \|e^{-Hs}\nabla u\|^2_{L^2((0,T^*/2)\times\mathbb{R}^2)} \\ < c^2\pi/\alpha. \end{aligned}$$

Therefore, the lemma shows time local solutions beyond T^*, a contraction.

4b5. Taishi Ikeda (Nagoya U.),
"Dyson bound of energy flux in gravitational collapse" (10+5)
[JGRG27 (2017) 112912]

Gravitational collapse of massless scalar field and Maximal Power Hypothesis

Taishi Ikeda
(Nagoya Univ.)

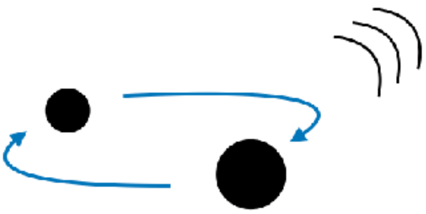

? $< \dfrac{c^5}{2G}$

Collaborator
Vitor Cardoso (IST)
Chul-Moon Yoo (Nagoya Univ.)
Christopher Moore (IST)

Energy source in the universe

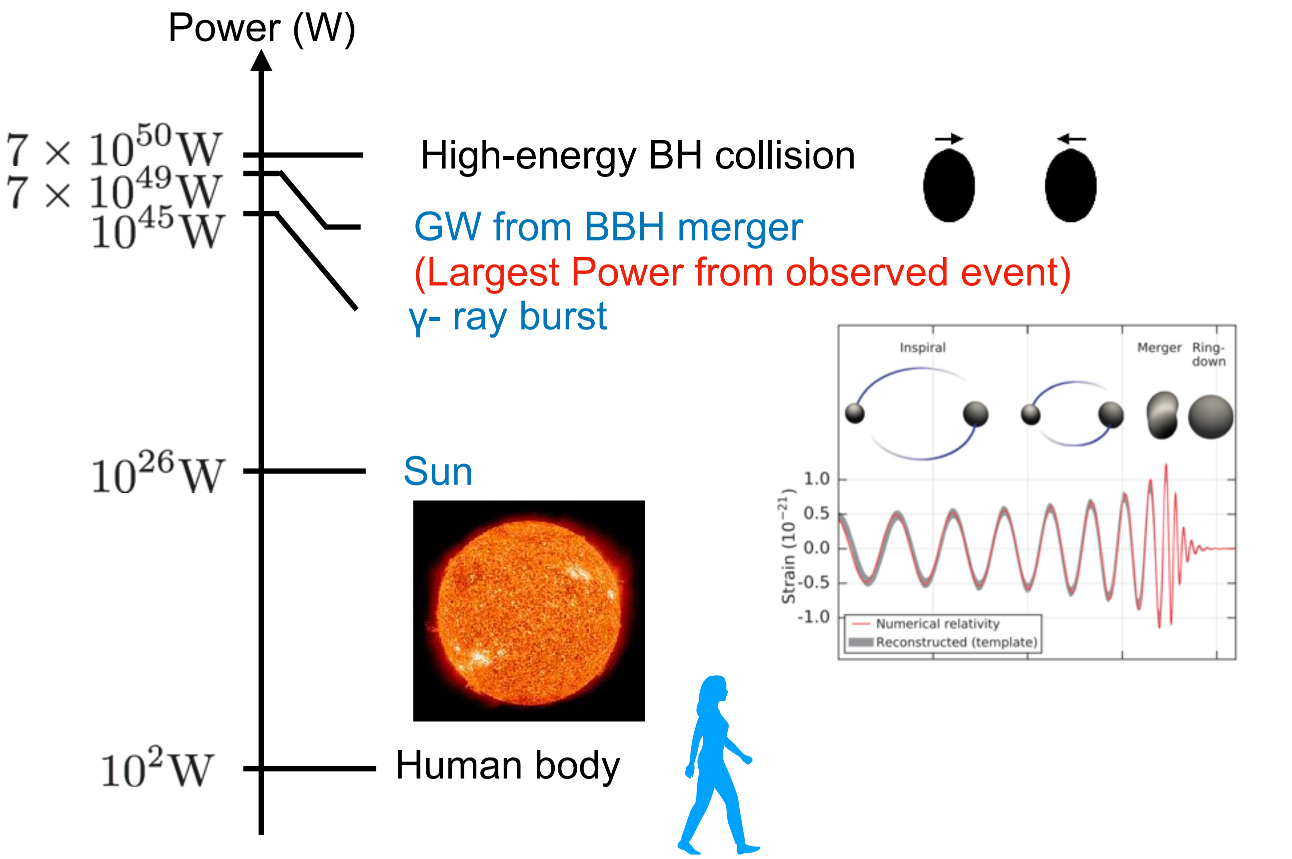

Fundamental Question

- Question
  - How large power can be emitted from one isolated system ?
  - Is there upper bound of power from one isolated system ?

- Planck Power

$$\mathcal{P}_{\mathrm{P}} = \frac{c^5}{G} \simeq 4.0 \times 10^{52}\mathrm{W}$$

  - Planck power does not contain $\hbar$.

    ➡ $\mathcal{P}_{\mathrm{P}}$ characterizes the power from the classical gravity-dominated process (not quantum).

Energy source in the universe

Power (W)

$4 \times 10^{52}\mathrm{W}$ — Planck Power: $\mathcal{P}_{\mathrm{P}}$

$7 \times 10^{50}\mathrm{W}$ — High-energy BH collision

$7 \times 10^{49}\mathrm{W}$ — GW from BBH merger (Largest Power from observed event)

$10^{45}\mathrm{W}$ — γ- ray burst

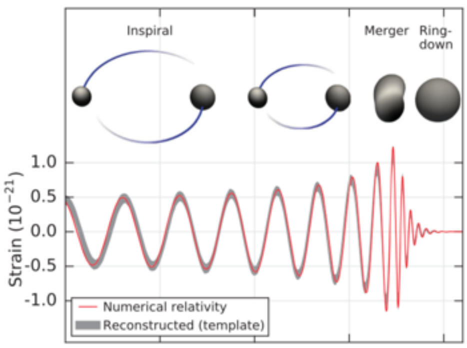

$10^{26}\mathrm{W}$ — Sun

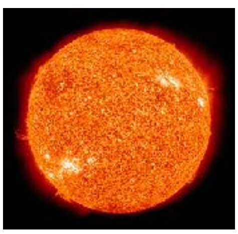

$10^{2}\mathrm{W}$ — Human body

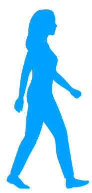

Talk Plan

- **Part 1**
  - Power from the gravitational collapse in massless scalar field.
- **Part 2**
  - Is there upper bound of power from a one-isolated system ?

Talk Plan

- **Part 1**
  - Power from the gravitational collapse in massless scalar field.
- **Part 2**
  - Is there upper bound of power from a one-isolated system ?

What we want to do.

- What we want to do.
  - How large power can be emitted from gravitational collapse of massless scalar field in spherically symmetric spacetime.

$$S[g_{\mu\nu},\Phi]=\int d^4x\sqrt{-g}\left\{\frac{R}{8\pi}-g^{\mu\nu}\partial_\mu\Phi\partial_\nu\Phi\right\}$$

- When does power become large ?
  - The system needs to have sufficient energy.
  - The large power is emitted from a visible large curvature region.
  - ➡ It is expected that power becomes large in no BH spacetime round the threshold of BH formation.

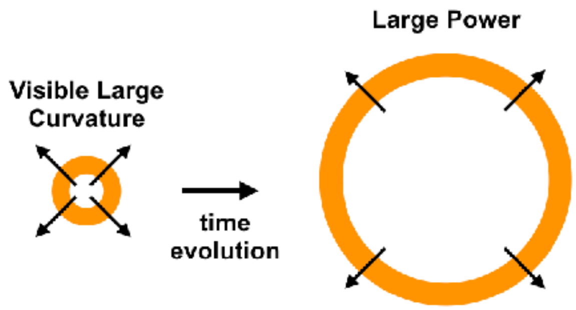

What we want to do.

- We performed numerical simulations.
  - Initial data : pure ingoing pulse of scalar field

$$\Phi(t=0,r)=Ar^7e^{-(r-r_0)^2/w^2}$$

  - Initial parameter : A
  - Time evolution : G-BSSN formulation
  - Power is defined by using Kodama flux at far region.

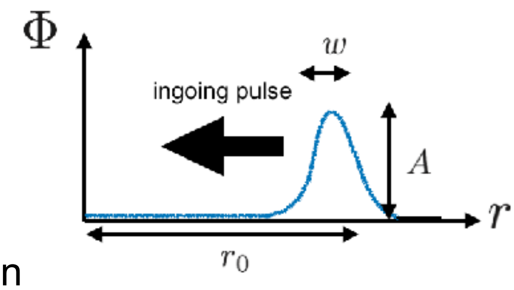

Numerical Result

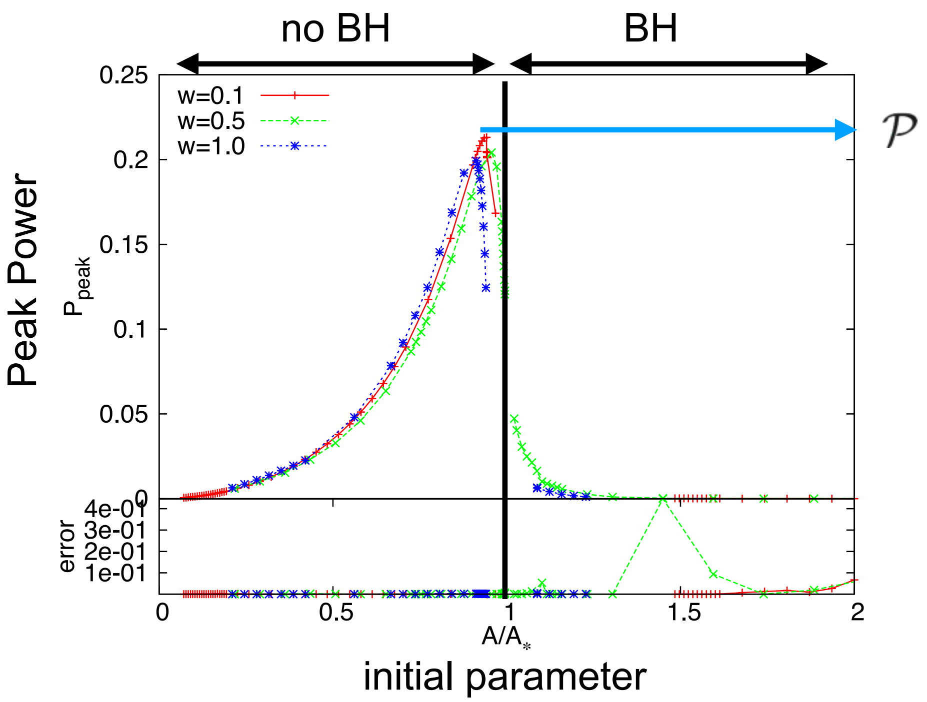

$$\mathcal{P} \simeq 0.2\mathcal{P}_{\rm P} \simeq 7 \times 10^{51}\,{\rm W}$$

Energy source in the universe

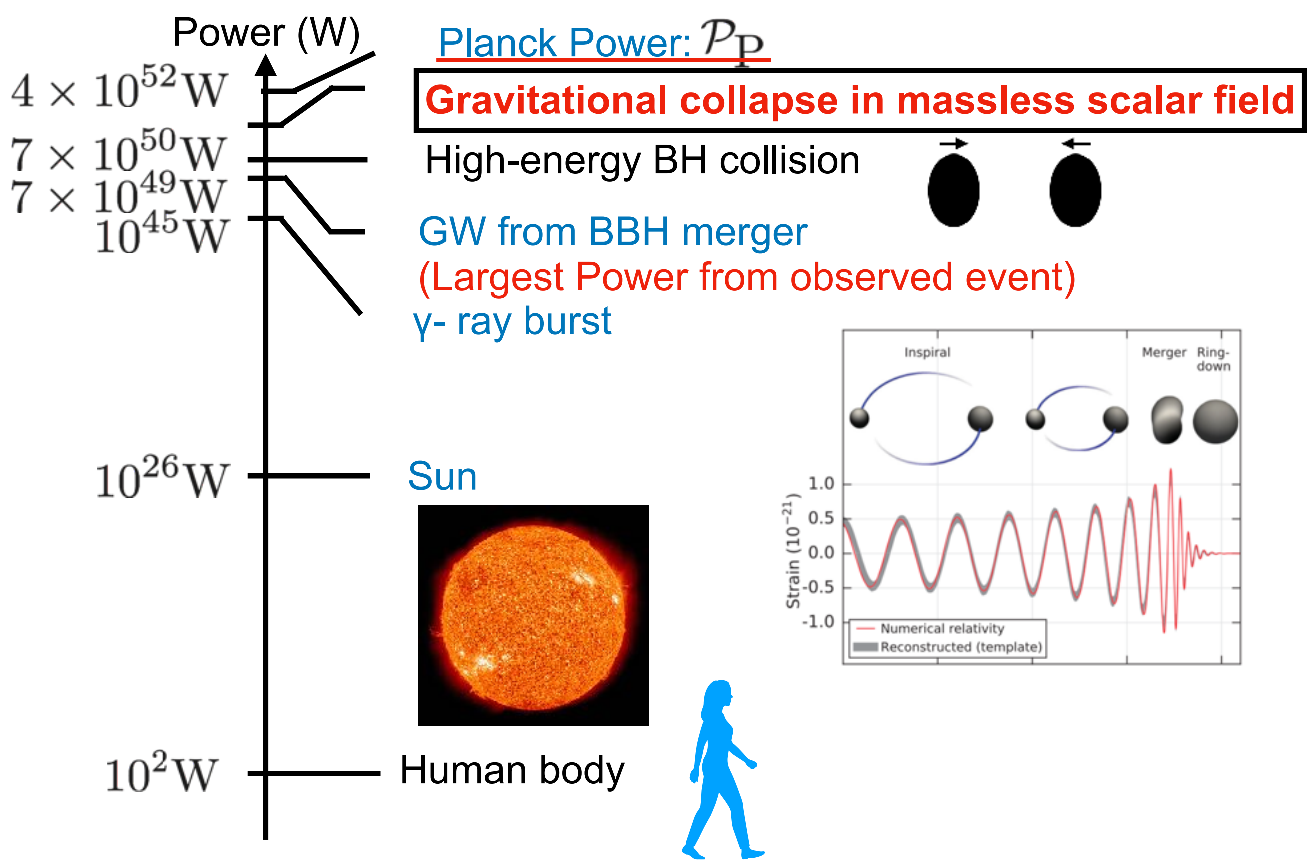

Energy source in the universe

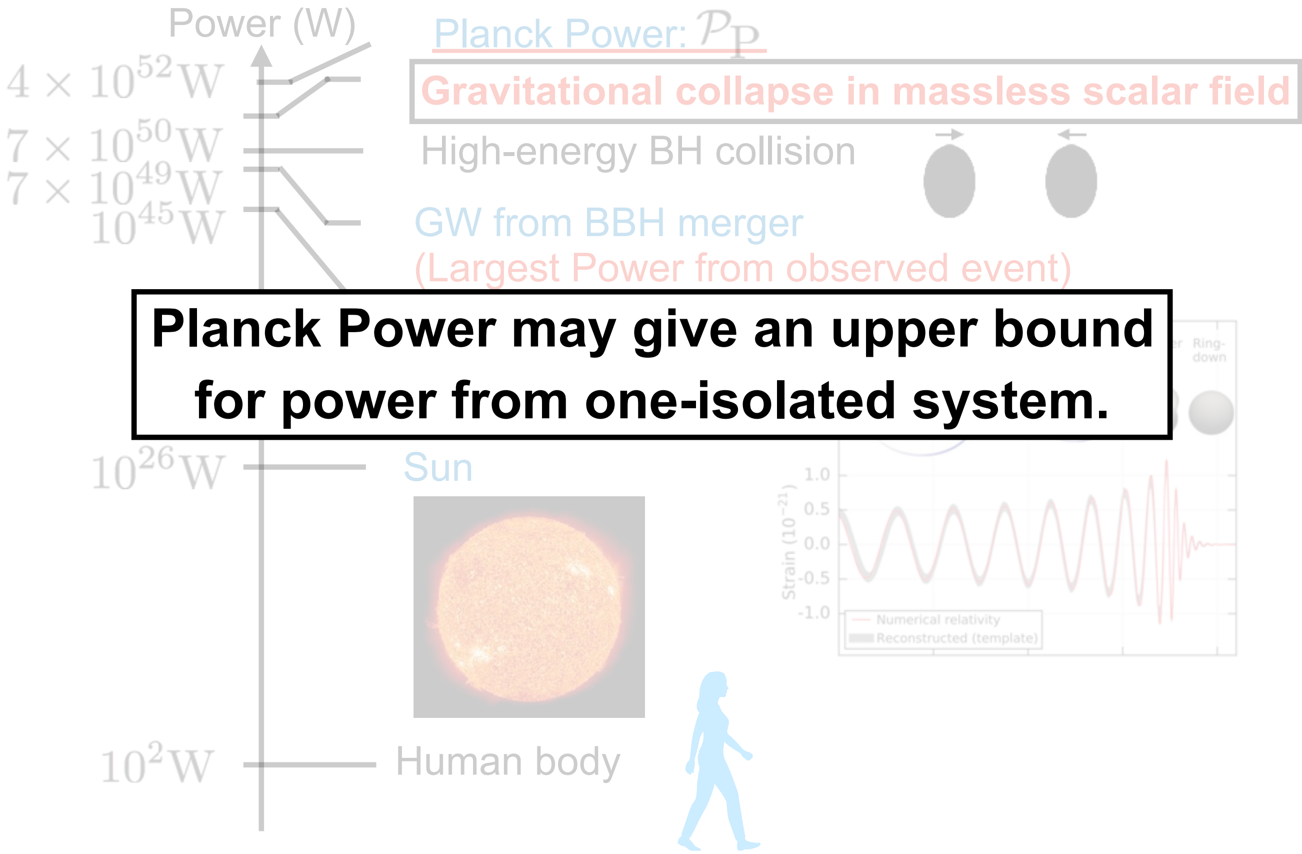

Talk Plan

- **Part 1**
  - Power from the gravitational collapse in massless scalar field.
- **Part 2**
  - Is there upper bound for power from a one-isolated system ?

Maximal Power Hypothesis

- Maximal Power Hypothesis (MPH) (K.Thorne, G.Gibbons et al)

$0.5\mathcal{P}_{\mathrm{P}}$ is an upper bound for the power of any gravity dominated process ($\mathcal{P}_{\mathrm{P}}$: Planck Power)

$$\mathcal{P} < \frac{1}{2}\mathcal{P}_{\mathrm{P}} = 2.0 \times 10^{52}\mathrm{W} \quad \text{(Dyson bound)}$$

- Intuitive understanding
  - spherically symmetric system
    - Assume that the flux propagates at speed of light.
    - To emit the flux, BH must not appear.

$$1 > \frac{2G\Delta E}{c^4 \Delta r}$$

$$\Rightarrow \mathcal{P} = \frac{\Delta E}{\Delta t} = c\frac{\Delta E}{\Delta r} \leq \frac{c^5}{2G}$$

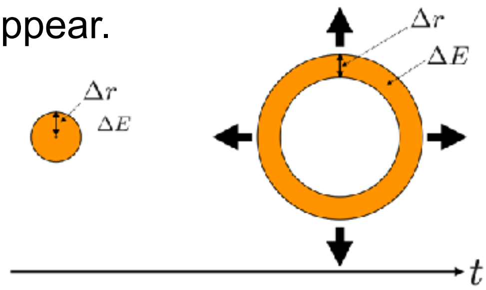

Maximal Power Hypothesis

- Maximal Power Hypothesis (MPH) (K.Thorne, G.Gibbons et al)

$0.5\mathcal{P}_{\mathrm{P}}$ is an upper bound for the power of any process in the universe. ($\mathcal{P}_{\mathrm{P}}$: Planck Power)

$$\mathcal{P} < \frac{1}{2}\mathcal{P}_{\mathrm{P}} = 2.0 \times 10^{52}\mathrm{W} \quad \text{(Dyson bound)}$$

However, is this Hypothesis really correct ?

- Intuitive understanding
  - spherically symmetric system
    - Assume that the flux propagates at speed of light.
    - To emit the flux, BH must not appear.

$$1 > \frac{2G\Delta E}{c^4 \Delta r}$$

$$\Rightarrow \mathcal{P} = \frac{\Delta E}{\Delta t} = c\frac{\Delta E}{\Delta r} \leq \frac{c^5}{2G}$$

Counter examples

- Counter example 1
  - We can construct the outgoing initial data whose power is larger than $0.5\mathcal{P}_\mathrm{P}$,artificially.

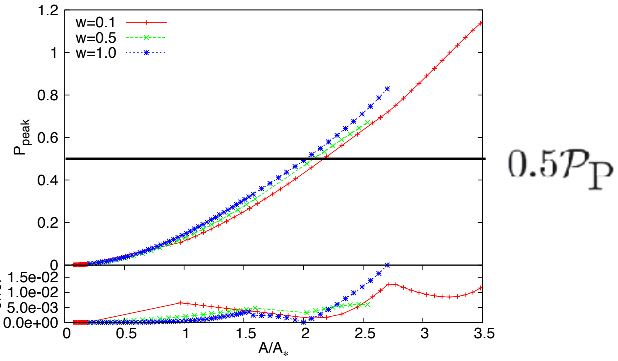

- Counter example 2
  - We can construct the solutions which have an arbitrary large power by cut and paste two spacetimes.

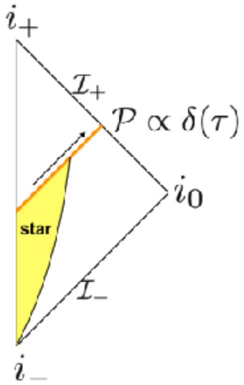

Counter examples

- Counter example 1
  - We can construct the outgoing initial data whose power is

larger than Planck power

It is necessary to add some conditions to the MPH.

- Counter example 2
  - We can construct the solutions which have an arbitrary large power by cut and paste two spacetimes.

Candidate of Additional Condition (?)

- Additional condition1
  - In order that MPH is correct, the spacetime must not have visible singularity at past.
  - This condition excludes the counter example 1.

$$\mathcal{P} = c\frac{\Delta E}{\Delta r} > \frac{c^5}{2G}$$

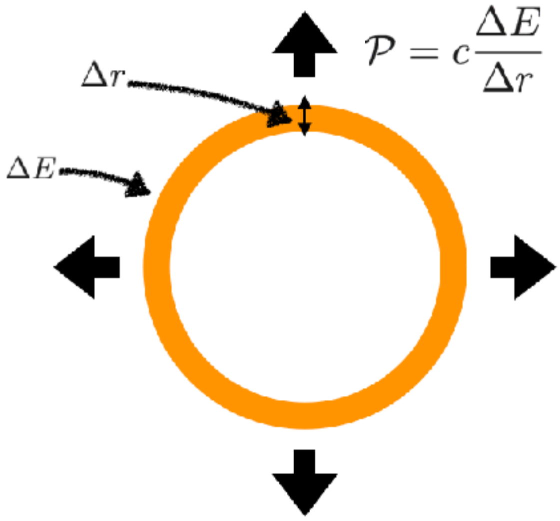

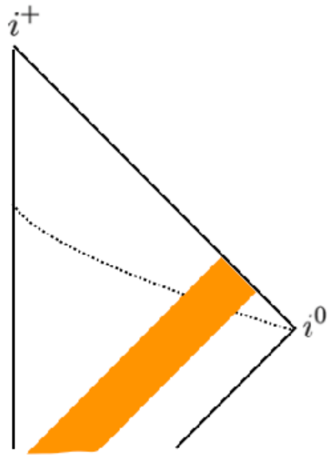

Candidate of Additional Condition (?)

- Additional condition1
  - In order that MPH is correct, the spacetime must not have visible singularity at past.
  - This condition excludes the counter example 1.

$$\mathcal{P} = c\frac{\Delta E}{\Delta r} > \frac{c^5}{2G}$$

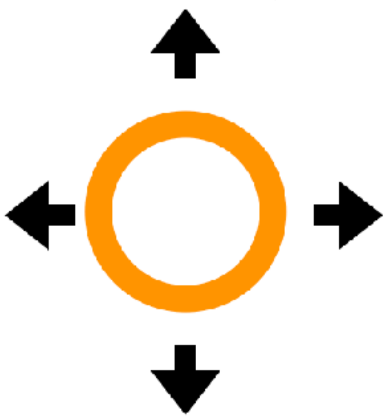

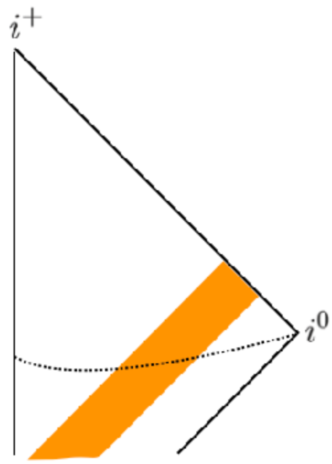

Candidate of Additional Condition (?)

- Additional condition1
  - In order that MPH is correct, the spacetime must not have visible singularity at past.
  - This condition excludes the counter example 1.

$$\mathcal{P} = c\frac{\Delta E}{\Delta r} > \frac{c^5}{2G}$$

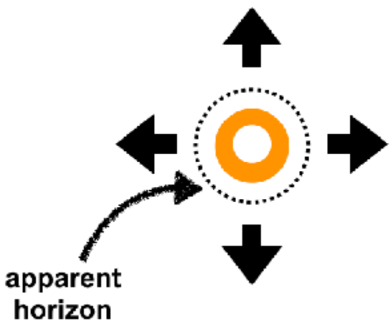

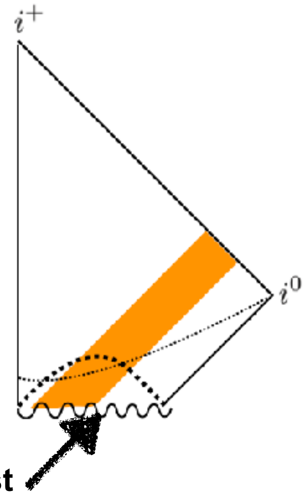

Candidate of Additional Condition (?)

- Additional condition 2
  - In order that MPH is correct, the length scale L of source must be smaller than the time scale Δt of the pulse.
  - This condition excludes the counter example 2.

If : $\Delta t < L$,
MPH can be incorrect.

If : $\Delta t > L$,
MPH is correct.

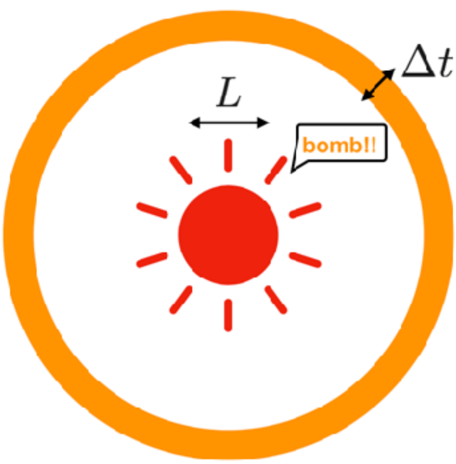

Candidate of Additional Condition (?)

- Additional condition 2
  - In order that MPH is correct, the length scale L of source must be smaller than the time scale Δt of the pulse.
  - This condition excludes the counter example 2.

Anyway, further discussion of MPH is needed.

the power can become arbitrary large.

If : $\Delta t > L$,
the power has an upper bound $0.5\mathcal{P}_{\mathrm{P}}$.

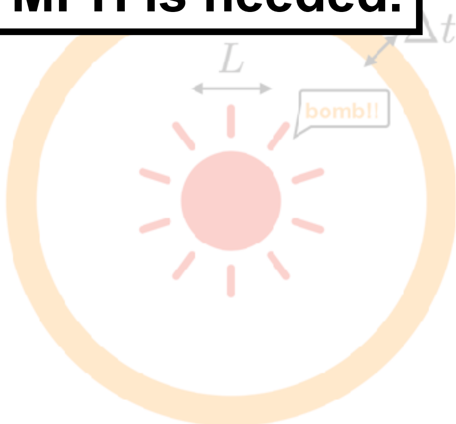

Summary

- Our questions
  - How large power can be emitted from one isolated system ?
  - Is there upper bound of power from one isolated system ?

- In Part I
  - I showed that the power which can be emitted from the gravitational collapse of massless scalar field is

$$\mathcal{P} \simeq 0.2\mathcal{P}_{\mathrm{P}} \simeq 7 \times 10^{51}\mathrm{W}$$

  - This value is larger than the case of BBH merger.
- In Part II
  - I discussed the validity of Maximal Power Hypothesis (MPH).
  - The further discussion of MPH is needed.

4b6. Pedro Cunha (Aveiro U. & IST Lisbon), "Light ring stability in ultra-compact objects" (10+5) [JGRG27 (2017) 112913]

Light ring stability in ultra-compact objects

Pedro Cunha

Physics Department of the University of Aveiro and CIDMA
IST - University of Lisbon, Portugal

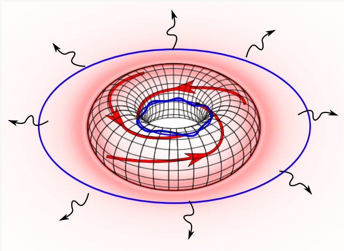

arXiv:1708.04211, P. Cunha, E. Berti and C. Herdeiro,

accepted in *Physical Review Letters*

Could the LIGO events be sourced by BH-mimickers?

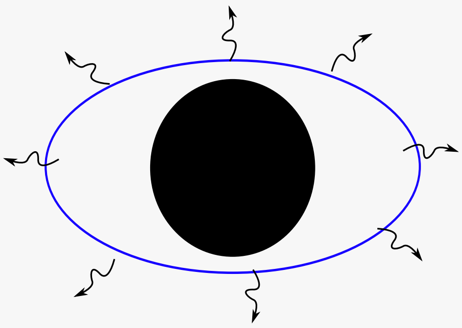

First LIGO detections:

- consistent with a Black Hole (BH) merger.
- signature of a perturbed Light Ring (LR) .

Alternative LIGO candidates:

- *Horizonless* objects with a LR $\rightarrow$ vibrate like a BH (initially).
- Are these objects viable BH-mimickers?

Outline of the argument

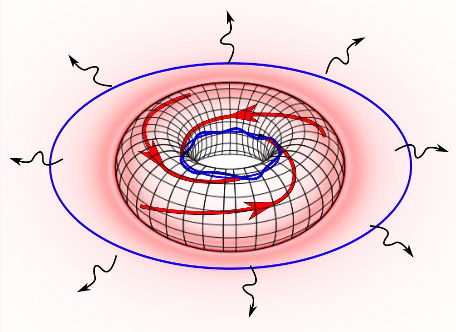

$\Longrightarrow$ horizonless UCOs are *not viable*, within reasonable conditions.

- Reasonable assumptions, *e.g.* smoothness, causality and axial symmetry.
- LRs come in pairs $\to$ one is *stable* (unless NEC is violated).
- Stable LR traps radiation $\to$ destabilizes object.

Assumptions for the spacetime

$\simeq$ flat spacetime

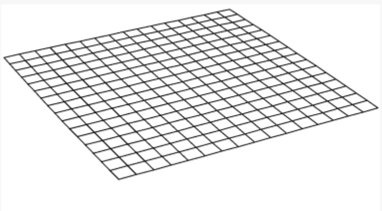

$\longrightarrow$

UCO

We assume:

- dynamical formation from gravitational collapse.
- initial flat spacetime and causality $\Longrightarrow$ topological triviality (Geroch).

- UCO is stationary, axially-symmetric and asymptotically flat.
- *no* event horizon; $\mathbb{Z}_2$ reflection symmetry *not* needed.
- The metric is *smooth*.

Spacetime metric

We consider a metric:

- 4D, in quasi-isotropic coord. (t, r, θ, φ).
- with Killing vectors ∂_t (stationarity) and ∂_φ (axial-symmetry).

- with $g_{r\theta} = 0,\ \ g_{rr} > 0,\ \ g_{\theta\theta} > 0$ (gauge freedom).
- with $g_{\varphi\varphi} > 0$ (preserve causality).
- until otherwise specified $\rightarrow$ no assumptions on field equations.

Geodesic motion

The null geodesic flow:

- determined by the Hamiltonian $\mathcal{H} = \frac{1}{2} g^{\mu\nu} p_\mu\, p_\nu = 0$.
- $$\begin{aligned} 2\mathcal{H} &= (g^{ij} p_i\, p_j) \ + \ (g^{ab} p_a\, p_b), \qquad i \in \{r, \theta\},\ a \in \{t, \varphi\}. \\ &= \quad K \quad\ + \quad V\,. \end{aligned}$$

- Killing vectors $\partial_t, \partial_\varphi \implies E = -p_t, \quad L = p_\varphi \quad$ (constants).
- $p_r = p_\theta = 0 \iff K = 0 \iff V = 0\,.$

Light rings

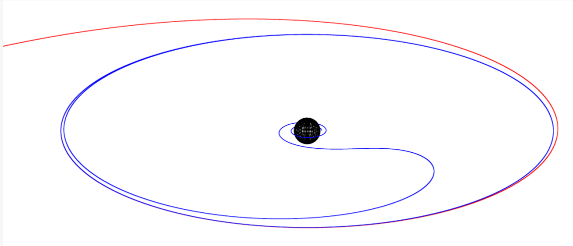

- *Light ring* (LR) $\iff$ circular photon orbit.
- Tangent vector field is a linear combination of (only) $\partial_t, \partial_\varphi$.
- Along trajectory $p_r = p_\theta = V = 0$ and $\dot{p}_\mu = 0$.
- $\dot{p}_\mu = -\left(\partial_\mu g^{rr} p_r^2 + \partial_\mu g^{\theta\theta} p_\theta^2 + \partial_\mu V\right)/2.$

At a LR: $\implies$ $\boxed{V = \nabla V = 0}$

Effective potentials

- Shortcoming of $V \to$ depending on parameters E, L.
- Can be factorized as $V = (L^2 g^{tt})(\sigma - H_+)(\sigma - H_-)$, $\sigma \equiv E/L$.
- Explicitly $H_\pm = \left(-g_{t\varphi} \pm \sqrt{D}\right)/g_{\varphi\varphi}$, $D \equiv g_{t\varphi}^2 - g_{tt}g_{\varphi\varphi}$.
- $V = 0 \iff (\sigma = H_+ \quad \vee \quad \sigma = H_-)$

At a LR: $\implies$ $\boxed{\nabla H_\pm = 0}$ (critical point of $H_\pm$)

$\nabla H_\pm$ as a map

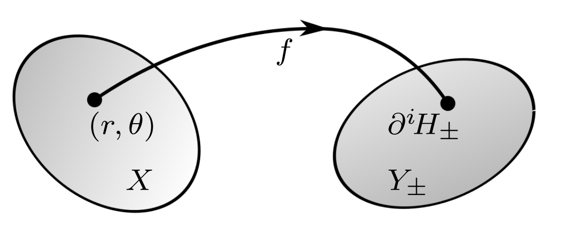

Consider $\nabla H_\pm$ as a *map* $f : X \to Y_\pm$:

- X is a compact, simply connected 2D region parametrized by (r, θ).
- $Y_\pm$ is a 2D space parametrized by the components $\partial^i H_\pm, \quad i \in \{r, \theta\}$.
- LR $\to$ origin of $Y_\pm$.

Brouwer degree (topology)

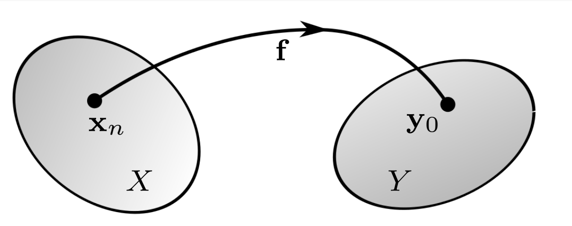

Consider a smooth map $\mathbf{f} : X \to Y$

- take a regular value $\mathbf{y}_0 \in Y$ with finite solutions to $\mathbf{f}(\mathbf{x}_n) = \mathbf{y}_0$.
- the Jacobian $J_n = \det(\partial \mathbf{f} / \partial \mathbf{x}_n) \neq 0$ is computed at each $\mathbf{x}_n$.

The Brouwer degree of $\mathbf{f}$ is: $\quad w = \sum_n \text{sign}(J_n)$.

- It is independent on the choice $\mathbf{y}_0$.
- It is invariant under homotopies (continuous deformations of the map).

Brouwer degree (topology)

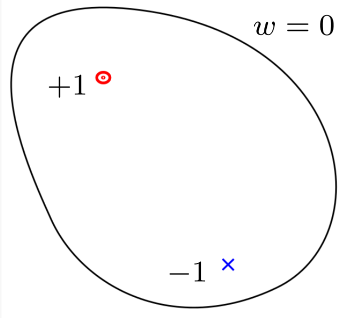

Each critical point $\nabla H_\pm = 0$:

- is assigned a *topological* charge w.
- sign w depends on the Jacobian $J_n = |\partial^2 H_\pm / \partial^2 \mathbf{x}_n|$.

Charge of a critical point:

- maximum/minimum $\implies$ $w = +1$.
- saddle point $\implies$ $w = -1$.

Illustration Brouwer degree w

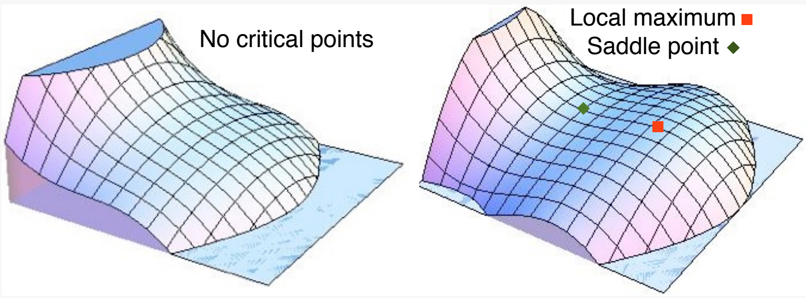

- Illustrative potential $H(x, y) = x(x^2 - a) - (1 + x^2)y^2$.
- Conservation of w under a *smooth* deformation of $(x, y) \to \nabla H$.

- $a = -2 \to$ no critical points $\to w = 0$ (Left).
- $a = 1 \to$ two critical points, $w = +1 - 1 = 0$ (Right).

Light Ring existence

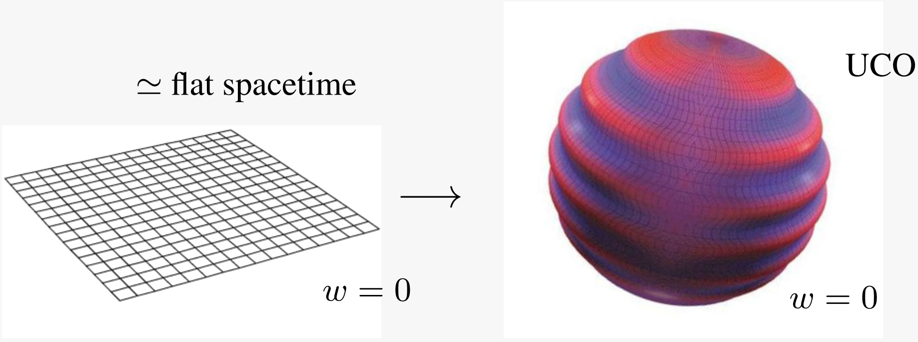

Flat spacetime (start):

- no LRs $\implies$ $\nabla H_{\pm} \neq 0$ $\implies$ total $w = 0$.

UCO (final):

- UCO can be smoothly deformed into flat spacetime.
- total w still zero.
- LRs must be formed in pairs.

Light Ring types

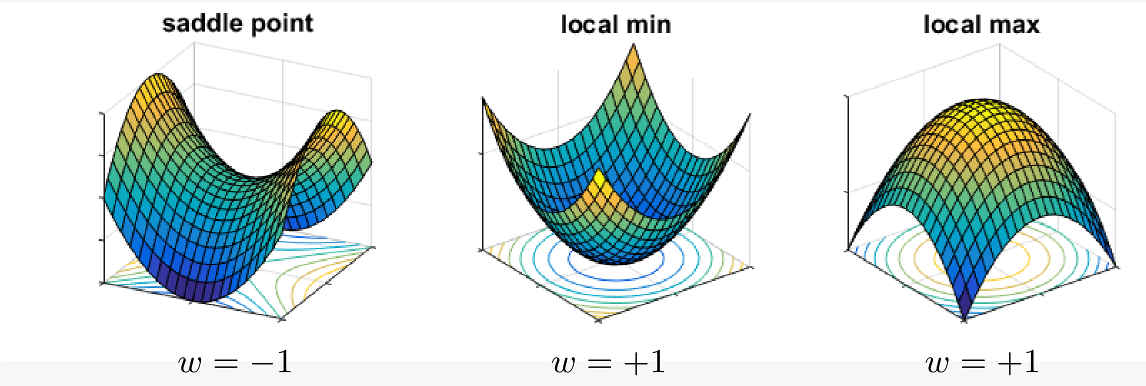

Different types of LRs:

- Saddle point of V $\rightarrow$ unstable LR $(w = -1)$ $\rightarrow$ GW signal.
- Local minimum of V $\rightarrow$ stable LR $(w = +1)$ $\rightarrow$ spacetime instability.
- Local maximum of V $\rightarrow$ unstable LR $(w = +1)$ $\rightarrow$ *exotic* LR.

Relation to NEC

Consider Einstein's field equations:

$$G^{\mu\nu} = 8\pi\, T^{\mu\nu}.$$

At a LR:

$$\boxed{T^{\mu\nu}\, p_\mu\, p_\nu = \frac{1}{16\pi}\partial_i\partial^i V.}$$

If the LR is exotic (local maximum of V):

- $\partial_i\partial^i V < 0 \implies T^{\mu\nu}p_\mu p_\nu < 0.$
- Null Energy Condition (NEC) is violated for an exotic LR!
- Enforcing NEC $\implies$ UCO has a stable LR.

Conclusions

Under generic and reasonable physical conditions:

- Light Rings are created in pairs.
- If the Null Energy Condition is preserved, one of the LRs is stable.
- BH mimickers are potentially unstable.
- The first observations from LIGO should be really from BHs.

Acknowledgements

- Work is supported by the FCT IDPASC Portugal Ph.D. Grant No. PD/BD/114071/2015 and by CIDMA Strategic Project No. UID/MAT/04106/2013.

Session5a 14:00–15:15

[Chair: Takahiro Tanaka]

5a4. Soichiro Morisaki (RESCEU U. Tokyo), "Search for non-minimally coupled scalar field dark matter with gravitational-wave observations" (10+5) [JGRG27 (2017) 112917]

SCHOOL OF SCIENCE
THE UNIVERSITY OF TOKYO

Search for non-minimally coupled scalar field dark matter with gravitational-wave observations

Soichiro Morisaki
RESCEU

Collaborate with Teruaki Suyama.

Ultralight scalar field dark matter

- Dark matter may be **ultralight scalar field**.
  - ➢ Motivated by string theory
  - ➢ As a resolution to small-scale problem [1]

[1] W. Hu, R. Barkana, and A. Gruzinov, Phys. Rev. Lett. 85, 1158 (2000).

- The scalar-wave background in the Galaxy?

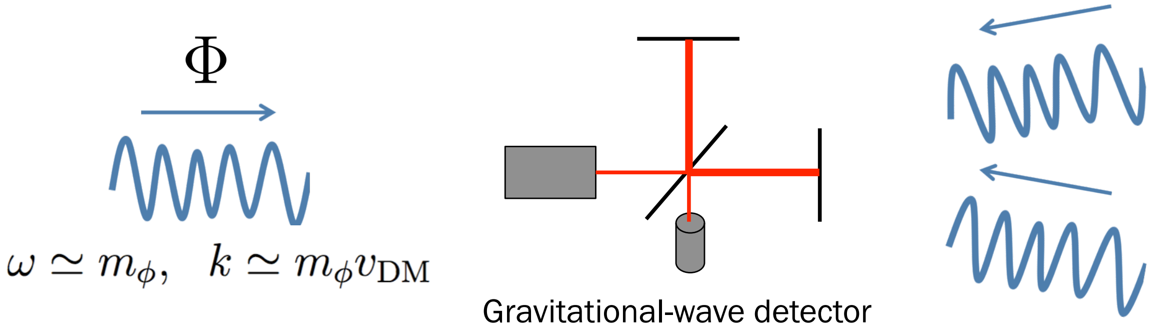

- Too weak to be detected except for PTA [2].

[2] A. Aoki and J. Soda, Int. J. Mod. Phys. **D**26 (2016).

Non-minimal coupling

- Scalar field can have **non-minimal coupling** with Ricci scalar.
- Some consistent cosmological scenarios with this type of dark matter [1] [2].

[1] P. J. Steinhardt and C. M. Will, Phys. Rev. D **52**, 628 (1995).
[2] P. Chen, T. Suyama, and J. Yokoyama, Phys. Rev. D **92**, 124016 (2015).

How can we probe non-minimally coupled scalar field dark matter with gravitational-wave observations?

Model

$$S = \int d^4x \sqrt{-\tilde{g}} \left(\underbrace{\frac{M_{\rm pl}^2}{2} f(\Phi) \tilde{R}}_{\text{Non-minimal coupling}} - \frac{1}{2} \tilde{g}^{\mu\nu} \partial_\mu \Phi \partial_\nu \Phi - \tilde{V}(\Phi) \right) + S_{\rm m}(\tilde{g}_{\mu\nu}, \Psi_m)$$

Φ : scalar field $\tilde{g}_{\mu\nu}$: metric matter feels (Jordan metric)

Model

$$S=\int d^4x\sqrt{-\tilde{g}}\left(\frac{M_{\rm pl}^2}{2}f(\Phi)\tilde{R}-\frac{1}{2}\tilde{g}^{\mu\nu}\partial_\mu\Phi\partial_\nu\Phi-\tilde{V}(\Phi)\right)+S_{\rm m}(\tilde{g}_{\mu\nu},\Psi_m)$$

Φ : scalar field $\tilde{g}_{\mu\nu}$: metric matter feels (Jordan metric)

$$\Big\downarrow \quad g_{\mu\nu}\equiv f(\Phi)\tilde{g}_{\mu\nu},\quad \phi\equiv\int f^{-1}\sqrt{f+\frac{3}{2}M_{\rm pl}^2f'^2}d\Phi$$

$$S=\int d^4x\sqrt{-g}\left(\frac{M_{\rm pl}^2}{2}R-\frac{1}{2}g^{\mu\nu}\partial_\mu\phi\partial_\nu\phi-V(\phi)\right)+S(\tilde{g}_{\mu\nu},\Psi_m)$$

$g_{\mu\nu}$: Einstein metric

- $g_{\mu\nu}$ and ϕ decouple.
- $\tilde{g}_{\mu\nu}=f(\Phi)g_{\mu\nu}\equiv A^2(\phi)g_{\mu\nu}.$

Model

$$S=\int d^4x\sqrt{-g}\left(\frac{M_{\rm pl}^2}{2}R-\frac{1}{2}g^{\mu\nu}\partial_\mu\phi\partial_\nu\phi-V(\phi)\right)+S(A^2(\phi)g_{\mu\nu},\Psi_m)$$

<u>$V(\phi)$</u>

$$V(\phi)=\frac{m_\phi^2}{2}\phi^2+\mathcal{O}(\phi^3)$$

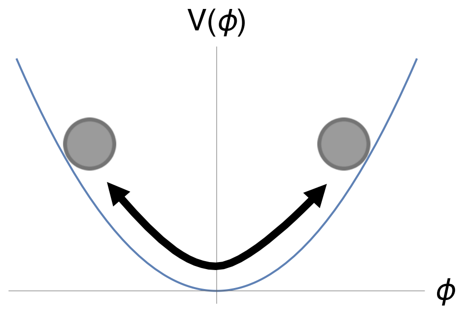

In the Solar system,

$$\tilde{g}_{\mu\nu}\simeq A^2(\phi)\eta_{\mu\nu}=[1+\underline{(\text{oscillate with }\omega\sim m_\phi)}]\,\eta_{\mu\nu}.$$

can be detected by gravitational-wave detectors

<u>$A^2(\phi)$</u>

$$A^2(\phi)=\begin{cases}1+\frac{\phi}{M} & \text{(Linear case)}\\ 1+\left(\frac{\phi}{M}\right)^2 & \text{(Quadratic case)}\end{cases}$$

Current constraints

We studied current constraints on this model.

- The fifth-force experiments
- Shapiro delay measurement by Cassini.

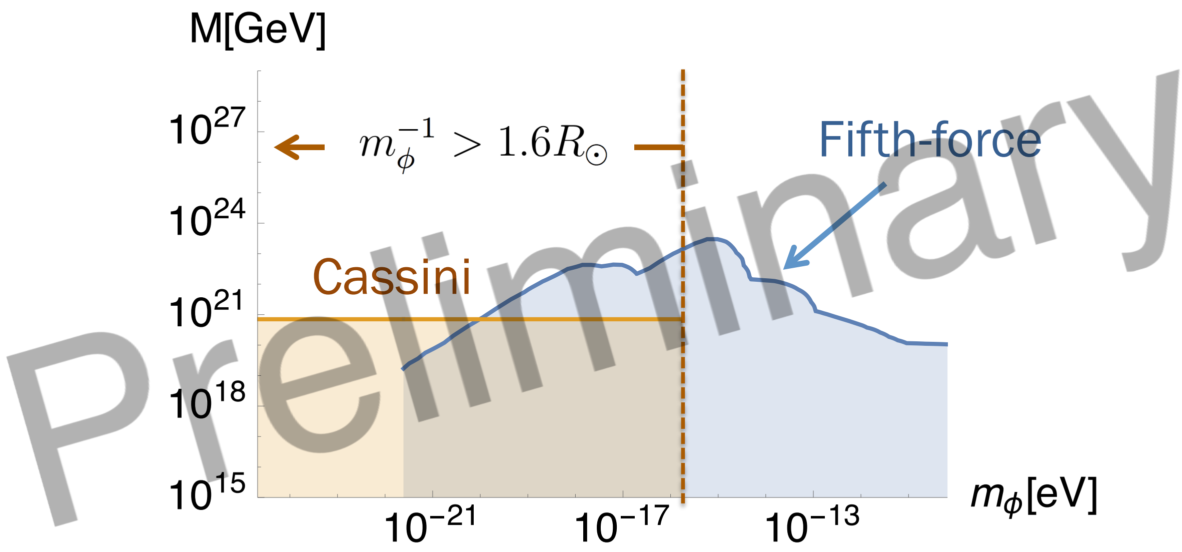

For linear case

Current constraints

We studied current constraints on this model.

- The fifth-force experiments
- Shapiro delay measurement by Cassini.

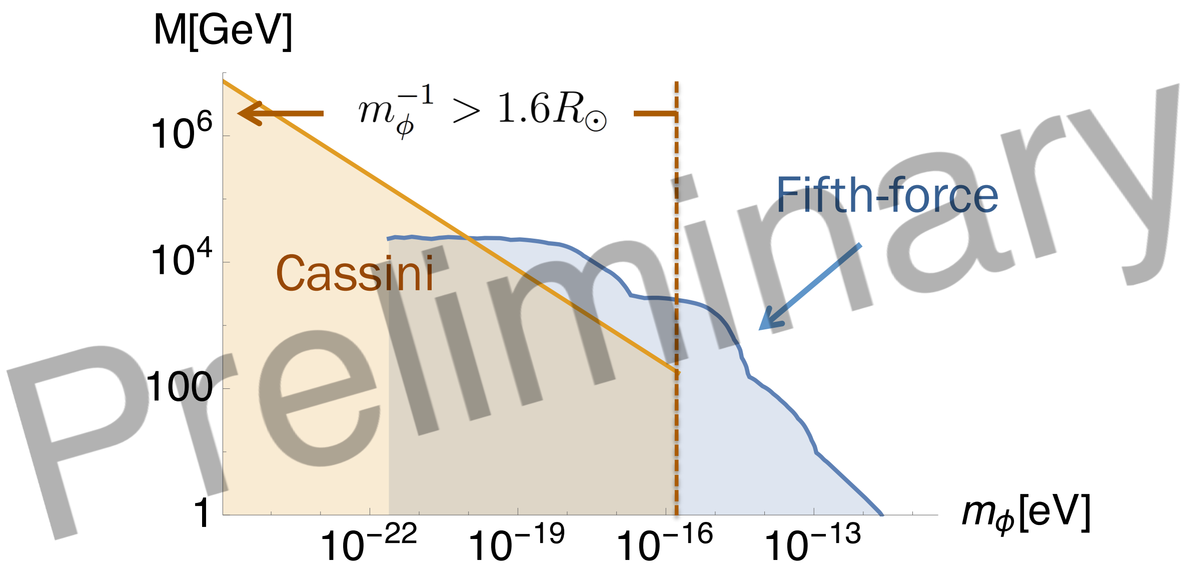

For quadratic case

How is the signal

Nearly monochromatic.

$$h(t) = A(t)\cos(\omega t + \psi(t)),$$

$$\omega = \begin{cases} m_\phi & \text{(Linear case)} \\ 2m_\phi & \text{(Quadratic case)} \end{cases}$$

The amplitude and the phase modulates due to

1. the velocity dispersion of dark matter
2. the motion of the detector

$\rightarrow$ $\dfrac{\Delta\omega}{\omega} \sim \max\left[v_{\rm DM}^2, \dfrac{1}{\omega T_{\rm d}}\right]$ $\quad T_{\rm d}$: time scale of the detector's motion

How to analyze data

Apply incoherent method [1] for continuous-wave search

Decompose the data into small chunks, where the signal looks monochromatic.

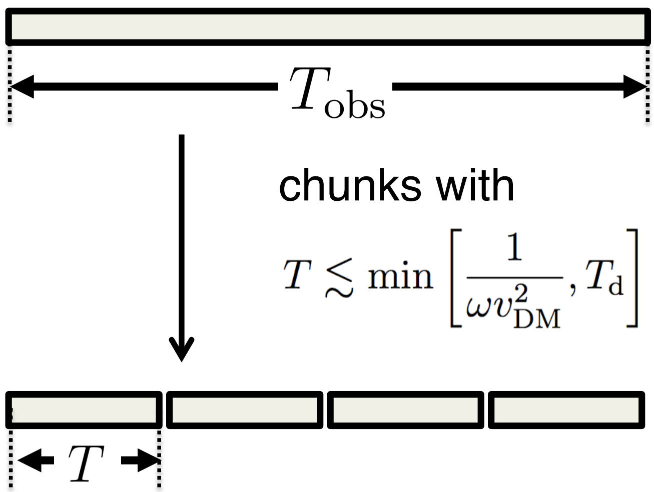

$$\hat{\rho} \equiv \sum_{i=1}^{N} P_i(f), \quad P_i(f)\text{: spectrum of the i-th chunk}$$

$$\rightarrow \quad h_{\rm th} \propto T^{-\frac{1}{2}} N^{-\frac{1}{4}}, \quad N\text{: the number of chunks}$$

[1] P. R. Brady and T. Creighton, Phys. Rev. D 61, 082001 (2000).

Setup

- Maxwell-Boltzmann distribution for ϕ with $v_{\mathrm{DM}} = 10^{-3}, \quad \rho_{\mathrm{DM}} = 0.3\ \mathrm{GeV/cm^3}$.

- Assume the scalar waves can be detected if

$$E[\hat{\rho}] > \underline{\rho_{\mathrm{c}}}$$

Threshold with F. A. P. = 0.05

- Take into account
  - ➢ The motion of the Solar system
  - ➢ The variation of the detectors' orientation

Result (Linear case)

Improved by a factor of 10 ~ 10^6

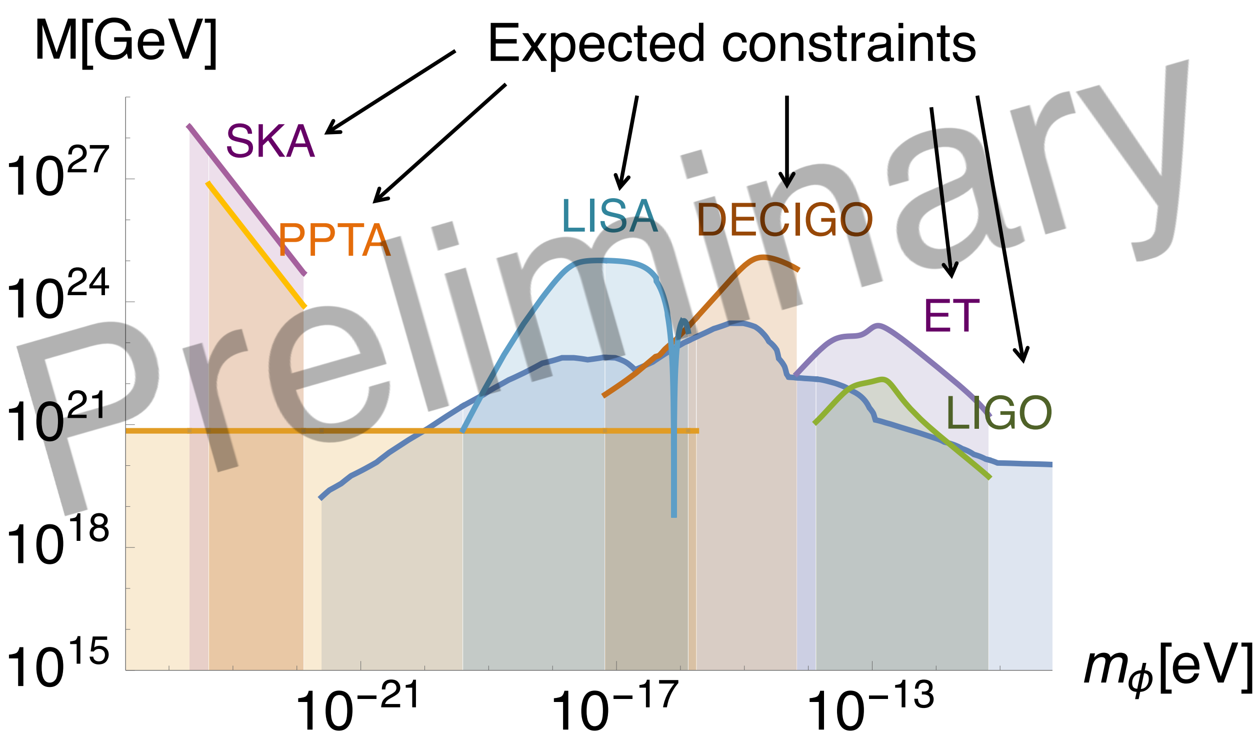

Result (Quadratic case)

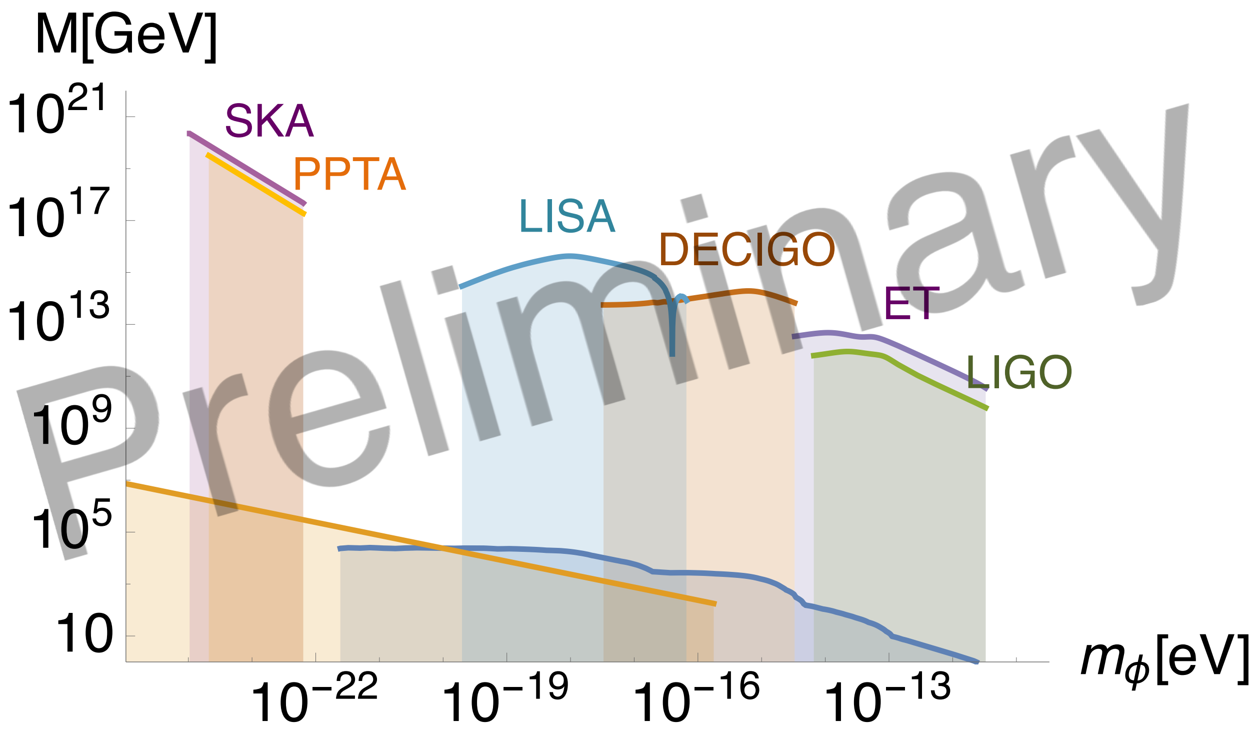

Conclusion

- We studied how we can probe non-minimally coupled scalar field dark matter with gravitational-wave observations

- We proposed a suitable method to detect the scalar field dark matter.

- The constraints will be improved.

5a5. Osamu Seto (Hokkaido U.),
"Non-minimally coupled Coleman-Weinberg inflation" (10+5)
[JGRG27 (2017) 112918]

Non-minimally coupled Coleman-Weinberg inflation

Osamu Seto (Hokkaido Univ.)

With

Kunio Kaneta (IBS → Minnesota)

Ryo Takahashi (Tohoku)

Ref: 1708.06455 [hep-ph]

§ Introduction

Inflation solves [Guth, Sato … (1981)]

- the flatness problem
- the horizon problem
- …

provides

- seeds of the density perturbation $\delta\phi$

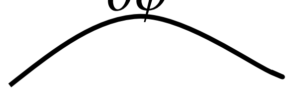

  [Hawking, Starobinsky, Guth and Pi (1982)]

- gravitational wave background $\delta g_{\mu\nu}$

  [Starobinsky (1979), Rubakov et al (1982)]

§ Slow roll inflation

- Energy scale of inflation is not clear yet…

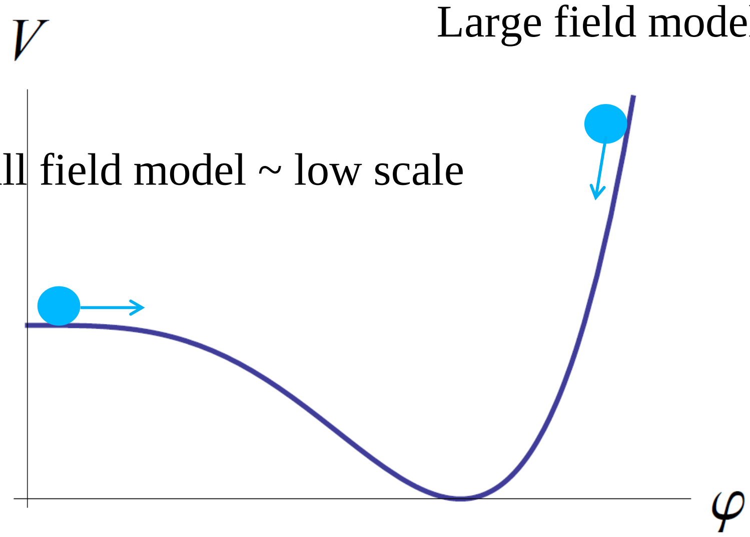

Slow roll param.

$$\eta = \frac{V_{\varphi\varphi}}{V},$$

$$\epsilon = \frac{1}{2}\left(\frac{V_\varphi}{V}\right)^2,$$

Amplitude

$$\mathcal{P}_\zeta = \left(\frac{H^2}{2\pi|\dot{\varphi}|}\right)^2 = \frac{V}{24\pi^2\varepsilon}$$

§ Low scale inflation is attractive

For instance,

- To supress axion isocurvature perturbation

  $H_{inf} < 10^7$ GeV [Planck Coll. (2017)]

- Baryon DM generation through Q-ball [Enqvist and McDonald (1999)]

  $T_R \sim 100$ GeV

- Gravitino overproduction

  $T_R < 10^5$ GeV [Kawasaki et al (2008), Cybrut et al (2009)]

- Relaxion [Graham et al (2015)]

  $H_{inf} < \Lambda_{QCD}$

Q: What is the lowest scale with a specific potential (model)?

§ Inflation by Coleman-Weinberg potential

- Number of *e*-folds

$$N_* \simeq 62 - \ln \frac{10^{16}\mathrm{GeV}}{V_*^{1/4}} - \frac{1}{3} \ln \frac{V_*^{1/4}}{\rho_R^{1/4}}$$

- Too red spectral index, $0.94 < n_s < 0.95$
  [Barenboim et al (2014)]
- Linear term by e.g., fermion condensation
  [Iso et al (2015)]

$$V(\phi) = \frac{A}{4}\phi^4 \left(\ln \frac{\phi^2}{M^2} - \frac{1}{2} \right) - C\phi + V_0, \quad V_0 = \frac{AM^4}{8}.$$

$$\tilde{C} \equiv C(M_{\rm pl}/M)^3/(AM^3)$$

§ Inflation by Coleman-Weinberg potential

- With Linear term

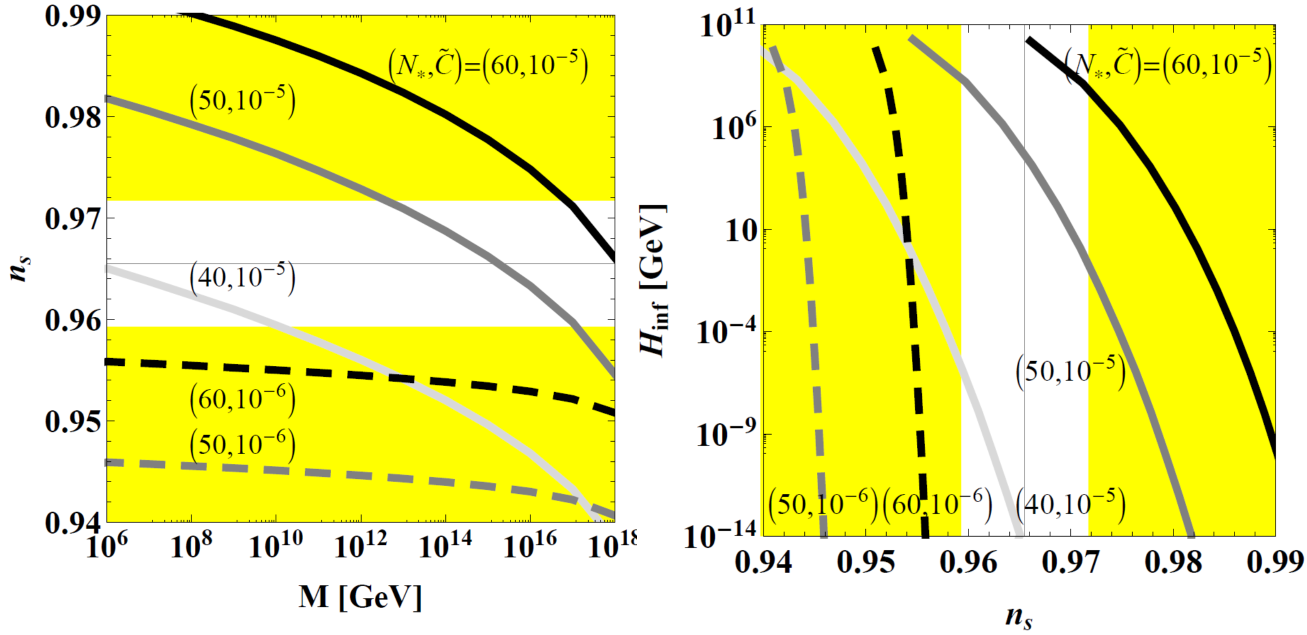

§ Non-minimally Coleman-Weinberg inflation

- A simple non-minimally coupled to gravity

$$\mathcal{L}_\xi = -\xi \bar{\phi}^2 \mathcal{R}/2$$

does not work [Iso et al (2015)]

- Another form

$$\mathcal{L} = -\xi M \bar{\phi} \mathcal{R} \left(\ln \frac{\bar{\phi}}{M} - c \right)$$

$$\tilde{C} \equiv \left(\frac{M_{\rm pl}}{M} \right)^3 \frac{C}{AM^3},$$

$$C \equiv \frac{cA\xi M^5}{4M_{\rm pl}^2},$$

with logarithmic correction [De Simone et al (2008)]

§ Non-minimally Coleman-Weinberg inflation

- Resultant scalar potential

$$V_E(\bar\phi(\phi)) = \frac{V(\bar\phi(\phi))}{\Omega^4(\bar\phi(\phi))} \simeq \frac{A}{4}\bar\phi^4\left(\ln\frac{\bar\phi^2}{M^2}-\frac{1}{2}\right)+V_0\left(1+\frac{2\xi M\bar\phi}{M_{\rm pl}^2}\left(\ln\frac{\bar\phi}{M}-c\right)\right)$$

- Slow roll parameters

$$V_E'(\bar\phi(\phi)) = \frac{dV_E}{d\bar\phi}\frac{1}{\frac{d\phi}{d\bar\phi}} \simeq A\bar\phi^3\ln\frac{\bar\phi^2}{M^2}+\frac{A\xi M^5}{4M_{\rm pl}^2}\left(\ln\frac{\bar\phi}{M}-c+1\right),$$

$$V_E''(\bar\phi(\phi)) \simeq A\bar\phi^2\left(2+3\ln\frac{\bar\phi^2}{M^2}\right)+\frac{A\xi M^5}{4M_{\rm pl}^2\bar\phi}.$$

§ Non-minimally Coleman-Weinberg inflation

- Scale of VEV

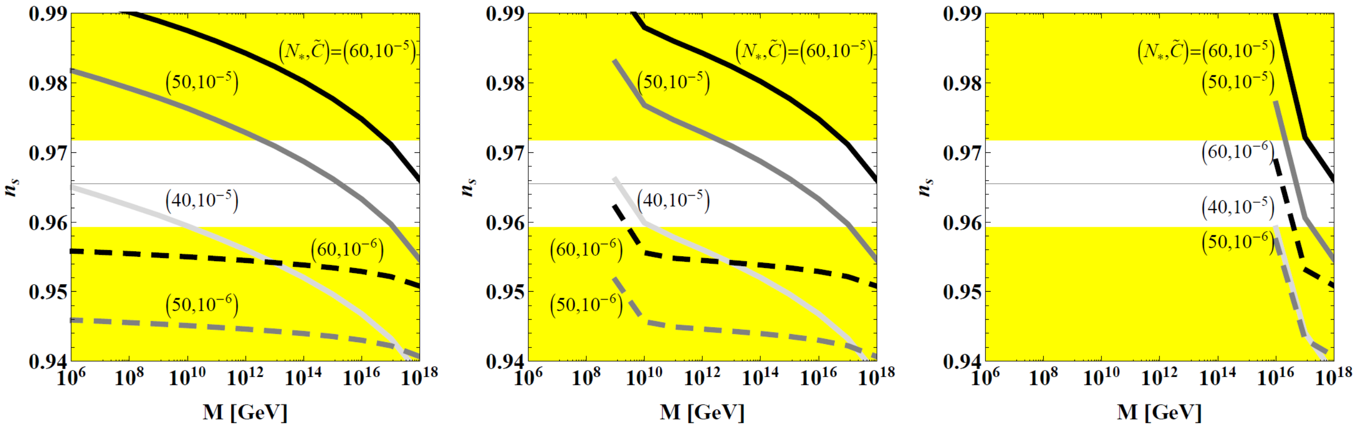

'igure 3: n_s in the CW model with a logarithmic form of non-minimal coupling to gravity. Left enter, and right figures correspond to $\xi = 10^{-24}$, 10^{-16}, and 10^{-8} cases, respectively. Curve

§ Non-minimally Coleman-Weinberg inflation

- Scale of Hubble parameter

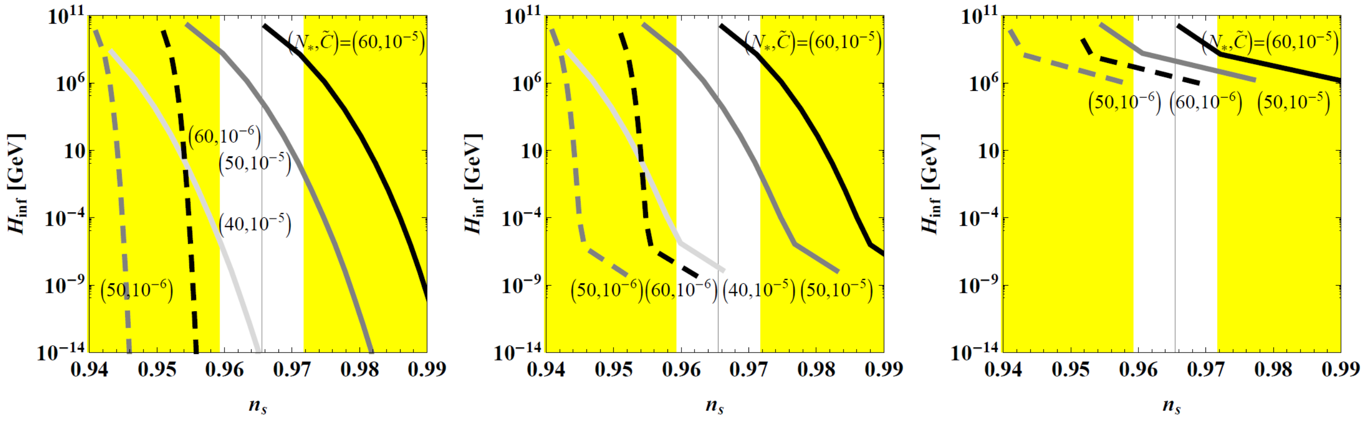

igure 4: $H_{\rm inf}$ in the CW model with a logarithmic form of non-minimal coupling to gravit
eft, center, and right figures correspond to $\xi = 10^{-24}$, 10^{-16}, and 10^{-8} cases, respectivel

§ Non-minimally Coleman-Weinberg inflation

- Maximal *e*-folds

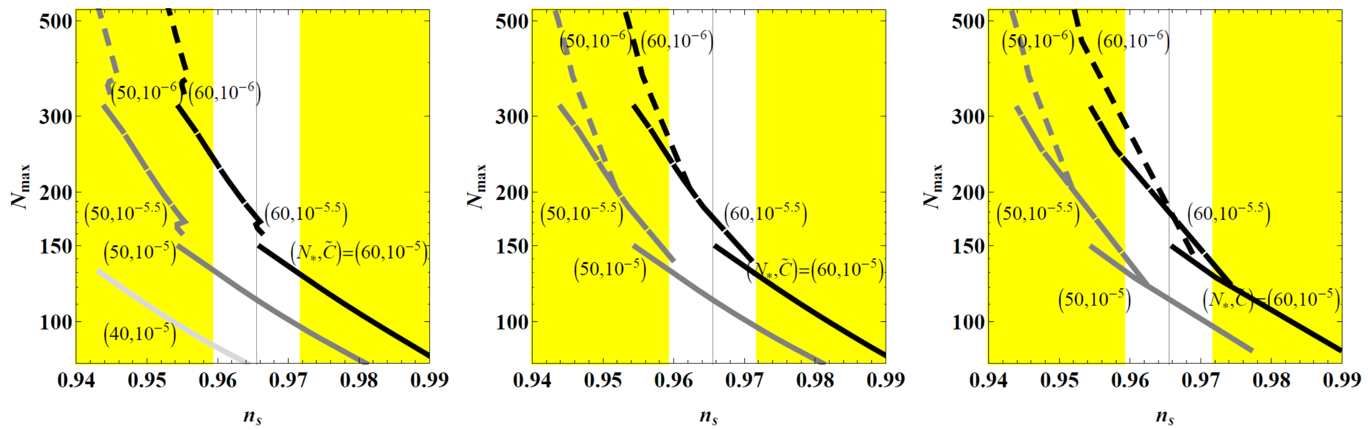

igure 5: $N_{\rm max}$ in the CW model with a logarithmic form of non-minimal coupling to gravity
eft, center, and right figures correspond to $\xi = 10^{-24}$, 10^{-16}, and 10^{-8} cases, respectively

§ Summary

- Logarithmic non-miminal coupling to gravity
- Reduce the nergy scale of inflation significantly
- *Nmax* cannot be enormous.

Session5b 14:00–15:15

[Chair: Tomohiro Harada]

5b1. Masato Minamitsuji (CENTRA, IST, U. of Lisbon),
“Boson stars in a generalized Proca theory” (10+5)
[JGRG27 (2017) 112919]

centra
multidisciplinary centre for astrophysics

FCT
Fundação para a Ciência e a Tecnologia
MINISTÉRIO DA CIÊNCIA, TECNOLOGIA E ENSINO SUPERIOR

Boson Stars in a Generalized Proca Theory

Masato Minamitsuji

Phys. Rev. D96, 044017 (2017)

See also
Heisenberg, Kase, Minamitsuji, and Tsujikawa
JCAP 1708, 08 (2017), PRD 96, 084049 (2017)

Compact Objects in Modified Gravity

$$G_{\mu\nu}(g) + H_{\mu\nu}\left(g_{\mu\nu}, \phi, A_\mu, f_{\mu\nu} \cdots\right) = 8\pi G T_{\mu\nu}$$

Black holes

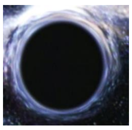

Hairy solutions

Neutron stars

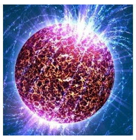

EOS-independent relations

Observationally verified $\Longleftarrow$

Boson stars

Kaup (68)
Ruffini & Bonazzola (69)
Jetzer (92)

Gravitationally bound solitonic objects

$\mu^2|\phi|^2$

$\mu = 10^{-10} eV \Longrightarrow M \sim M_\odot$

$\Longrightarrow$Not observationally verified

Generalized Proca Theories

Tasinato (14) Heisenberg (14)
Allys, Peter, & Rodriguez (16)
Beltran Jimenez, & Heisenberg (16)

Most general vector-tensor theories with 2[nd] order EOMs

$$S = \int d^4x\sqrt{-g}\left(F + \sum_{i=2}^{6} L_i\right) \qquad X := -\frac{1}{2}g^{\mu\nu}A_\mu A_\nu \qquad F := -\frac{1}{4}F^{\mu\nu}F_{\mu\nu}$$

$$Y := A^\mu A^\nu F_{\mu\alpha}F_\nu{}^\alpha \qquad L^{\mu\nu\alpha\beta} := \frac{1}{4}\varepsilon^{\mu\nu\rho\sigma}\varepsilon^{\alpha\beta\gamma\delta}R_{\rho\sigma\gamma\delta}$$

$$L_2 = G_2\,(X, F, Y) \qquad L_3 = -G_3\,(X)\nabla_\mu A^\mu$$

$$L_4 = G_4\,(X)R + G_{4X}(X)\left[\left(\nabla_\mu A^\mu\right)^2 - \nabla_\mu A_\nu \nabla^\nu A^\mu\right]$$

$$L_5 = G_5\,(X)G_{\mu\nu}\nabla^\mu A^\nu - \frac{G_{5X}(X)}{6}\left[\left(\nabla_\mu A^\mu\right)^3 - 3\nabla_\mu A^\mu \nabla_\rho A_\sigma \nabla^\sigma A^\rho + 2\nabla_\rho A_\sigma \nabla^\gamma A^\rho \nabla^\sigma A_\gamma\right]$$
$$-g_5(X)\tilde{F}^{\alpha\mu}\tilde{F}^\beta{}_\mu \nabla_\alpha A_\beta$$

$$L_6 = \frac{1}{4}G_6\,(X)L^{\mu\nu\alpha\beta}F_{\mu\nu}F_{\alpha\beta} + \frac{1}{2}G_{6X}(X)\tilde{F}^{\alpha\beta}\tilde{F}^{\mu\nu}\nabla_\alpha A_\mu \nabla_\beta A_\nu$$

Hairy Static Black Holes

$$ds^2 = -f(r)dt^2 + \frac{dr^2}{h(r)} + r^2 d\Omega^2 \qquad A_\mu dx^\mu = A_0(r)dt + A_1(r)dr$$

- Analytic solutions for $X = const$

Charged stealth Schwarzschild solution ($X = P^2/2$)

Chagoya, Niz, & Tasinato (16)

$$L = \frac{M_{pl}^2}{2}R - \frac{1}{4}F^{\mu\nu}F_{\mu\nu} + \beta G^{\mu\nu}A_\mu A_\nu \;\leftrightarrow\; G_4(X) = \frac{1}{2}M_p^2 + \beta X$$

$\beta = \frac{1}{4}$:

$$f(r) = h(r) = 1 - \frac{2M}{r} \qquad A_0(r) = P + \frac{Q}{r} \;\Rightarrow\; F_{tr} = \frac{Q}{r^2}$$

$$A_1(r) = \pm\frac{\sqrt{Q^2 + 2PQr + 2MP^2 r}}{r}\frac{1}{f(r)}$$

Heisenberg, Kase, Minamitsuji, & Tsujikawa (17)

$$L = \frac{M_{pl}^2}{2} R - \frac{1}{4} F^{\mu\nu} F_{\mu\nu} + L_i \qquad G_i(X), g_i(X) \propto X^n$$

1. Cubic vector Galileon coupling: $G_3 = \beta_3 X$

$$f = 1 - \frac{2M}{r} - \frac{P^2 M^3}{6M_{\rm pl}^2 r^3} + \frac{M^4 P^2 (P^2 - 2M_{\rm pl}^2) + 3M_{\rm pl}^2 \tilde{b}_2^2}{3M_{\rm pl}^2 (2M_{\rm pl}^2 - P^2) r^4} \qquad h = 1 - \frac{2M}{r} - \frac{P^2 M^2}{2M_{\rm pl}^2 r^2} - \frac{P^2 M^3}{2M_{\rm pl}^2 r^3} + \frac{2M^4 P^2 (P^2 - 2M_{\rm pl}^2) + 12 M_{\rm pl}^2 \tilde{b}_2^2}{3M_{\rm pl}^2 (2M_{\rm pl}^2 - P^2) r^4}$$

$$A_0 = P - \frac{PM}{r} - \frac{PM^2}{2r^2} - \frac{PM^3 (P^2 + 6M_{\rm pl}^2)}{12 M_{\rm pl}^2 r^3} - \frac{P^2 M^4 (2P^2 + 5M_{\rm pl}^2)(P^2 - 2M_{\rm pl}^2) + 8M_{\rm pl}^4 \tilde{b}_2^2}{8PM_{\rm pl}^2 (P^2 - 2M_{\rm pl}^2) r^4}$$

$$A_1 = \frac{\tilde{b}_2}{r^2} + \frac{M(M + 2\tilde{b}_2 \beta_3)}{\beta_3 r^3} + \frac{12 M^3 M_{\rm pl}^2 + \tilde{b}_2 M^2 (P^2 + 16 M_{\rm pl}^2) \beta_3}{4\beta_3 M_{\rm pl}^2 r^4}$$

$M, \tilde{b}_2, P$ are independent

$G_3(X), G_4(X)$

○ Constraints from GW170817 and GRB170817A

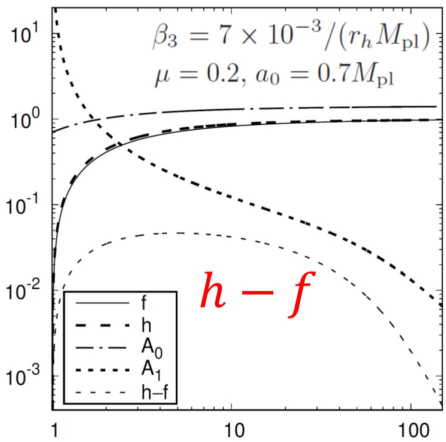

2. Intrinsic vector-mode coupling: $G_6 = \frac{\beta_6}{M_{\rm pl}^2} \left(\frac{X}{M_{\rm pl}^2} \right)^n \qquad A_1 = 0$

$$f = 1 - \frac{2M}{r} + \frac{Q^2}{2M_{\rm pl}^2 r^2} - \frac{\beta_6 P^{2n} Q^2}{2^{1+n} M_{\rm pl}^{4+2n} r^4} - \frac{2^{-n} \beta_6 P^{2n-1} Q^2 [MP(6n-5) + 8Qn]}{10 M_{\rm pl}^{4+2n} r^5}$$

$$h = 1 - \frac{2M}{r} + \frac{Q^2}{2M_{\rm pl}^2 r^2} + \frac{\beta_6 M P^{2n} Q^2 (2n-1)}{2^{1+n} M_{\rm pl}^{4+2n} r^5}$$

$$A_0 = P + \frac{Q}{r} - \frac{2^{-n} \beta_6 M P^{2n} Q}{M_{\rm pl}^{2+2n} r^4} - \frac{2^{-n} \beta_6 P^{2n-1} Q (32 M^2 M_{\rm pl}^2 P n + 28 M M_{\rm pl}^2 Q n - 3PQ^2)}{20 M_{\rm pl}^{4+2n} r^5}$$

$P = P(M, Q) \quad G_2 = -g_4(X) F, g_5(X), G_6(X)$

○ Constraints from GW170817 and GRB170817A

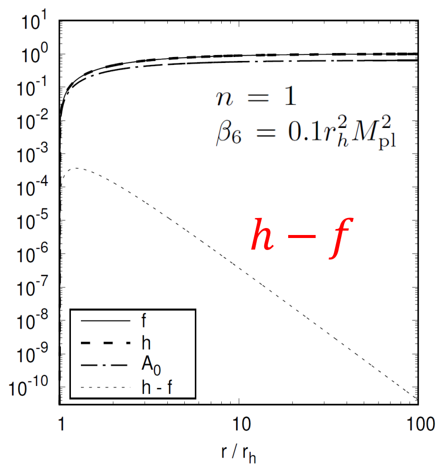

3. No regular black hole for G_5

× Constraints from GW170817 and GRB170817A

Boson Stars

- Gravitationally bound solitonic objects constituted by bosons

$$V = \mu^2|\phi|^2: \quad M \sim M_p^2/\mu \quad (\ll M_{ch} \sim M_p^3/\mu^2)$$

Kaup (68), Ruffini, & Bonazzola (69) , Friedberg, Lee, & Pang (87)

"mini" boson stars $\quad \mu = 10^{-10} eV \Longrightarrow M \sim M_\odot$

$$V = \mu^2|\phi|^2 + \lambda|\phi|^4: \quad M \sim \sqrt{\lambda}\, M_p^3/\mu^2 \; (\sim M_{ch})$$

Colpi, Shapiro, & Wasserman (86)

- Massive complex vector bosons can form a "mini" boson star

Brito, Cardoso, Herdeiro, & Radu (16)

$$L = M_p^2 R - F^{\mu\nu}\bar{F}_{\mu\nu} - \mu^2 A^\mu \bar{A}_\mu: \quad M \sim M_p^2/\mu$$

- Boson stars in the presence of (healthy) higher-derivative interactions.

$|\phi|^2 R_{GB}$ — Baibhav & Maity (17)

$G^{\mu\nu}\partial_\mu\phi\partial_\nu\bar{\phi}$ — Brihaye, Cisterna, & Erices (16)

Boson Stars in a Generalized Proca Theory

$$S = \int d^4x\sqrt{-g}\left[\frac{1}{2\kappa^2}R - \frac{1}{4}F^{\mu\nu}\bar{F}_{\mu\nu} - \frac{1}{2}\left(\mu^2 g^{\mu\nu} - \underline{\beta G^{\mu\nu}}\right)A_\mu\bar{A}_\nu\right]$$

Noether current $\quad j^\mu = \frac{i}{2}\left(\bar{F}^{\mu\nu}A_\nu - F^{\mu\nu}\bar{A}_\nu\right)$ **:** $\nabla_\mu j^\mu = 0$

Ansatz $\quad g_{\mu\nu}dx^\mu dx^\nu = -\sigma(r)^2\left(1 - \frac{2m(r)}{r}\right)d\hat{t}^2 + \left(1 - \frac{2m(r)}{r}\right)^{-1}dr^2 + r^2 d\Omega_2^2,$

$$A_\mu dx^\mu = e^{-i\hat{\omega}\hat{t}}\left(a_0(r)d\hat{t} + i a_1(r)dr\right)$$

$$a_0(r) = f_0 + \frac{f_0}{6}\left\{\left(\mu^2 - \frac{\hat{\omega}^2}{\sigma_0^2}\right) + \frac{f_0^2\kappa^2}{2\sigma_0^2}\left(\mu^2 - \frac{2\hat{\omega}^2}{\sigma_0^2}\right)\beta + \frac{f_0^2\kappa^2}{36\mu^2\sigma_0^6}\left(3f_0^2\mu^2\kappa^2\left(3\mu^2\sigma_0^2 - 14\hat{\omega}^2\right) + 4\hat{\omega}^2\left(9\mu^2\sigma_0^2 - 8\hat{\omega}^2\right)\right)\beta^2 + O\left(\beta^3\right)\right\}r^2 + O\left(r^4\right),$$

$$a_1(r) = -\frac{f_0\hat{\omega}}{3\sigma_0^2}\left\{1 + \frac{f_0^2\kappa^2}{\sigma_0^2}\beta + \frac{f_0^2\kappa^2}{18\mu^2\sigma_0^4}\left(21f_0^2\mu^2\kappa^2 - 12\mu^2\sigma_0^2 + 16\hat{\omega}^2\right)\beta^2 + O\left(\beta^3\right)\right\}r + O\left(r^3\right),$$

$$m(r) = \frac{f_0^2\kappa^2}{12\sigma_0^2}\left\{\mu^2 + \frac{3f_0^2\mu^2\kappa^2 + 4\hat{\omega}^2}{6\sigma_0^2}\beta + \frac{3f_0^4\mu^2\kappa^4 + 20f_0^2\kappa^2\hat{\omega}^2}{12\sigma_0^4}\beta^2 + O\left(\beta^3\right)\right\}r^3 + O\left(r^5\right),$$

$$\sigma(r) = \sigma_0 + \frac{f_0^2\kappa^2}{\sigma_0}\left\{\frac{\mu^2}{4} + \frac{3f_0^2\mu^2\kappa^2 - 3\mu^2\sigma_0^2 + 4\hat{\omega}^2}{18\sigma_0^2}\beta + \frac{f_0^2\kappa^2}{48\sigma_0^4}\left(5f_0^2\mu^2\kappa^2 - 8\mu^2\sigma_0^2 + 20\hat{\omega}^2\right)\beta^2 + O(\beta^3)\right\}r^2 + O\left(r^4\right).$$

$$ds^2 \to -\sigma_\infty^2 \left(1 - \frac{2m_\infty}{r}\right) d\hat{t}^2 + \left(1 - \frac{2m_\infty}{r}\right)^{-1} dr^2 + r^2 d\Omega_2^2 \quad : \omega = \frac{\hat{\omega}}{\sigma_\infty} \implies \omega \leq \mu$$

ADM mass

$$M := \frac{m_\infty}{G} = M_p^2 m_\infty$$

Noether charge

$$Q = \int_\Sigma d^3x \sqrt{-g} j^{\hat{t}} = 4\pi \int_0^\infty dr \frac{r^2 a_1(r)\left(\hat{\omega} a_1(r) - a_0'(r)\right)}{\sigma(r)}$$

Binding energy $B := M - \mu Q$ gravitationally bound if $B < 0$

$\mu = \kappa = \sigma_0 = 1$
$\implies (f_0, \beta)$

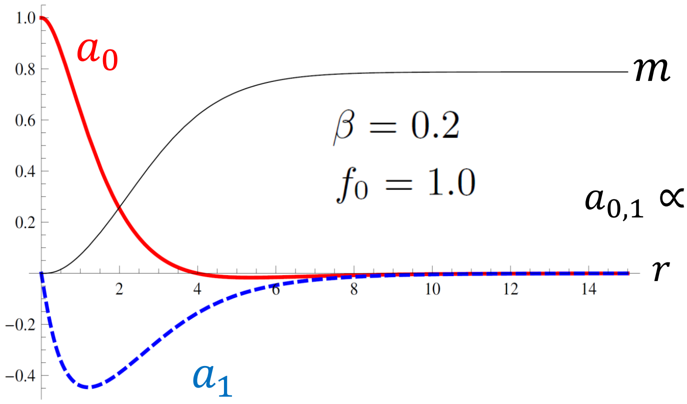

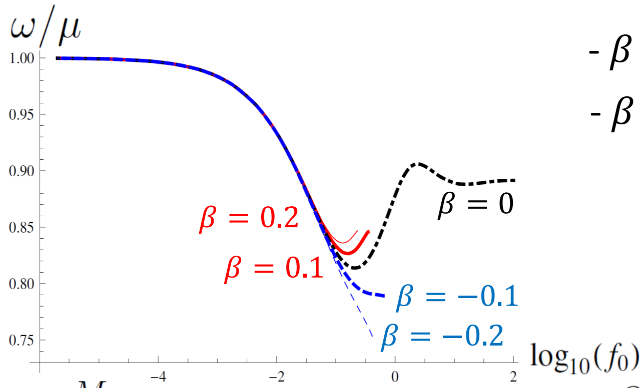

- $\beta < 0$: a single-valued function of ω
- $\beta > 0$: no solution above $f_0 > f_{0,max}$

$f_{0,max} = 0.231 M_p$ for $\beta = 0.2$

A universal feature in higher-derivative theories

Baibhav & Maity (17) Brihaye, Cisterna, & Erices (16)

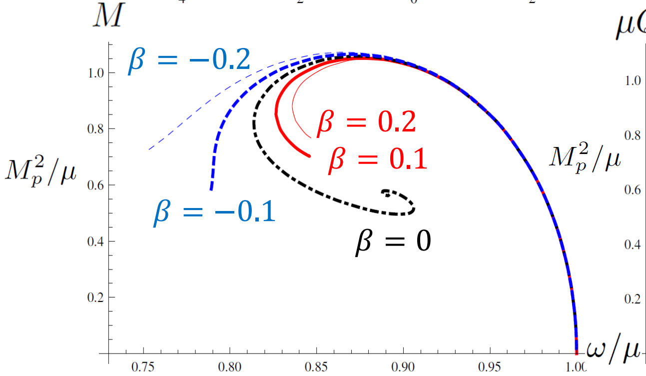

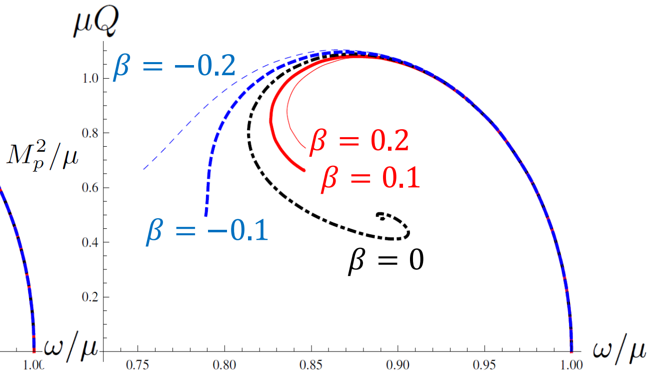

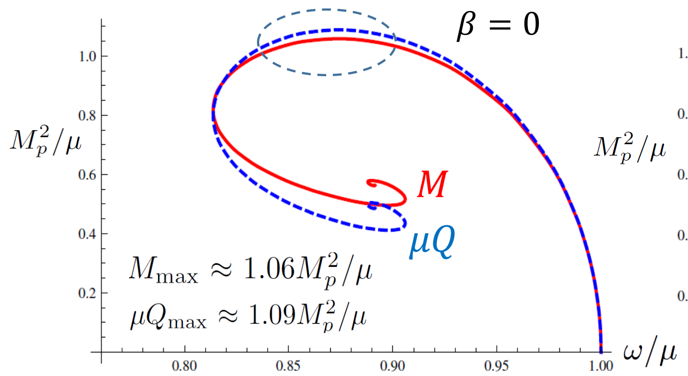

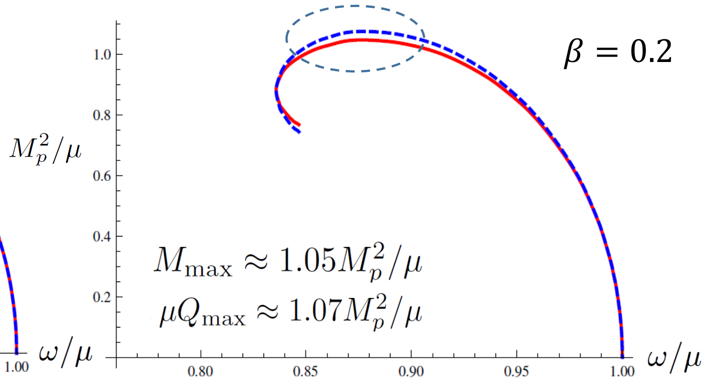

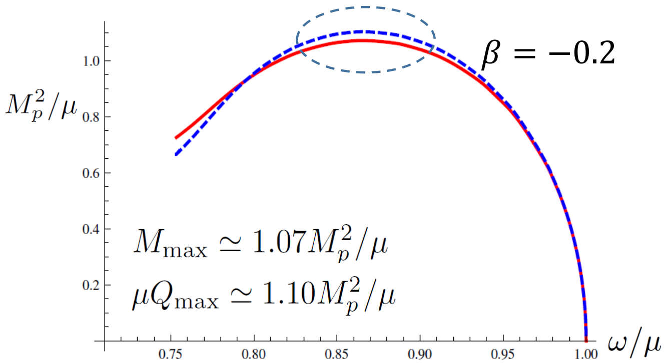

- $f_0 = 0 \Longrightarrow \omega/\mu = 1$:
  Minkowski solution $M = Q = 0$
- $M, \mu Q \sim M_p^2/\mu$
- Maximal mass and charge with $B < 0$.

Compactness $\mathcal{C} := \dfrac{GM}{\mathcal{R}} = \dfrac{M}{M_p^2 \mathcal{R}} = \dfrac{m_\infty}{\mathcal{R}}$ $\qquad \mathcal{R} := \dfrac{1}{Q} \displaystyle\int_\Sigma d^3x \sqrt{-g} \left(r j^{\hat{t}} \right)$

Jeter & van der Bij (89)

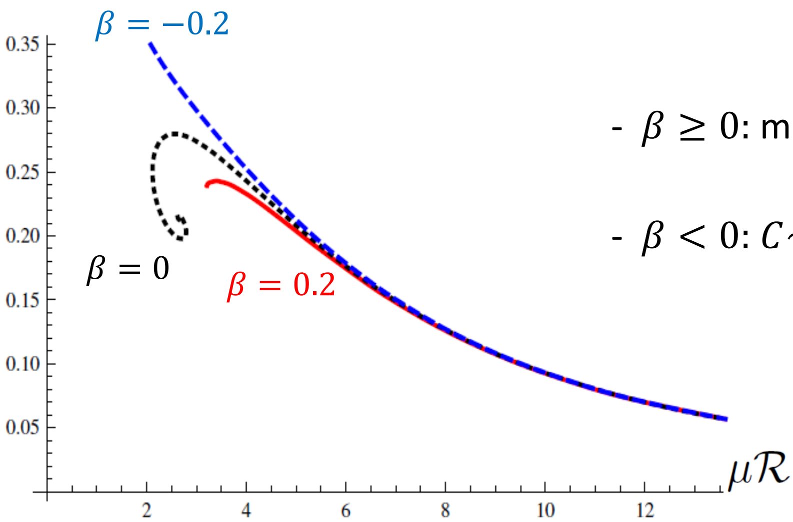

- $\beta \geq 0$: multivalued function of R.
- $\beta < 0$: $C \sim 0.35 \Longrightarrow$ Photospheres ?
  Unstable?

Summary

- Black holes and boson stars in generalized Proca theories.

  A bunch of hairy black hole solutions

  Sensitivity of boson stars to nonminimal couplings

- Neutron stars in generalized Proca theories Kase, Minamitsuji, & Tsujikawa 1711.08713

  $M \geq 2M_{\odot}$ for vector galileons

  No-hair properties for intrinsic vector mode couplings

- For further constraints

  Stability of black holes and neutron stars

  Constraints from the speed of GWs in light of GW170817.

Thank you.

5b4. Takayuki Ohgami (Yamaguchi U.),
"Optical Images of Wormhole Surrounded by dust"
(10+5)
[JGRG27 (2017) 112922]

Optical Images of Gravastar Surrounded by Dust

Takayuki OHGAMI and Nobuyuki SAKAI (Yamaguchi Univ.)

(5b4) *29 Nov. 2017*

Outline

- What's Gravastar?
- Purpose.
- Motion of interstellar medium.
- Optical images of gravastar.
- Summary.

What's Gravastar?

- One of the super compact objects as final state of gravitational collapse of stars (proposed by Mazur & Mottola, 2004).
- In this model, an interior de Sitter region and an exterior Schwarzschild background are connected by a shell.

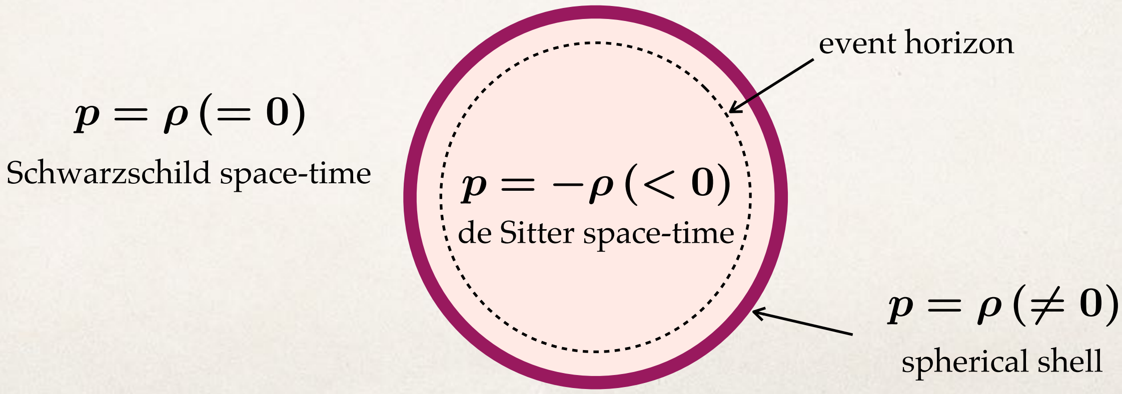

- Metric of outside shell and inside shell

$$ds^2 = -A(r)dt^2 + A^{-1}(r)dr^2 + r^2(d\theta^2 + \sin^2\theta\, d\varphi^2)$$

  - **Outside** : Schwarzschild space-time

$$A(r) = 1 - \frac{2GM}{r}$$

  - **Inside** : de Sitter space-time

$$A(r) = 1 - H^2 r^2$$

- This idea does not have two fundamental problems of black holes.
  - Singularity problem
  - Information loss problem

- Thin shell model (Visser & Wiltshire, 2004)
- Sakai, Saida, Tamaki found parameters when gravastars are stable for radial perturbation (2004).
- Our model
  - $2GMH = 0.4$
  - Radius of shell ; $R/2GM \sim 1.3$
  - This gravastar has an unstable circular orbit.

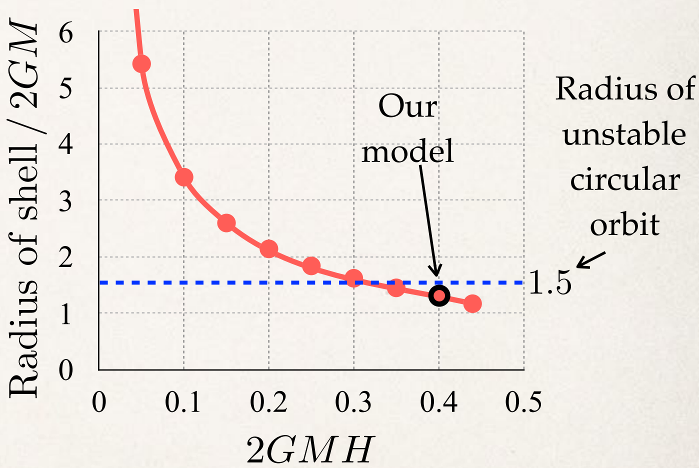

Relationship of parameters of stable gravastar.

Purpose.

- We propose a new method of detecting gravastar by electro-magnetic observations.
- We want to confirm whether it is possible to distinguish black holes from gravastars by optical images.

Motion of interstellar medium.

- Hydrodynamics equations in GR.
  - **Continuity equation**

    $(nu^{\mu})_{;\mu} = 0$

  - **Euler equations**

    $(\rho + P)u_{\mu;\nu}u^{\nu} = -P_{,\mu} - u_{\mu}P_{,\nu}u^{\nu}$

u^{μ} :	four vector
n :	number density
ρ :	energy density
P :	pressure
m :	mass of dust

- Assumption
  - Interstellar medium is dust ($\rho = nm,\ P = 0$).
  - Stationary and spherical symmetry.

- Hydrodynamics solution
  - **Inside of shell** (de Sitter space-time)
    - Because of expanding space-time solution, dust sticks to shell.
  - **Outside of shell** (Schwarzschild space-time)
    - Dust falls into shell.
    - Density distribution

      $$\rho \propto r^{-\frac{3}{2}}$$

    - Radial component of four vector

      $$u^{r} \propto r^{-\frac{1}{2}}$$

- Dust piles up shell.
  - We consider some cases of density on shell $\rho_{\rm shell}$.

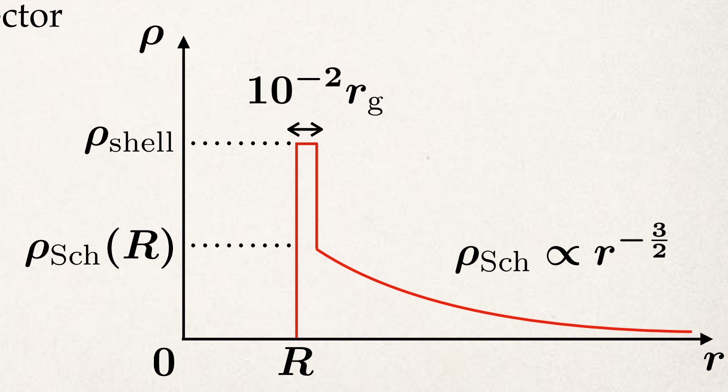

density distribution

Optical images of gravastar.

- How to calculate
  - **Ray tracing**
    - Compute null geodesic equations and radiative transfer equation.
    - Trace path of light as pixels in an image plane.

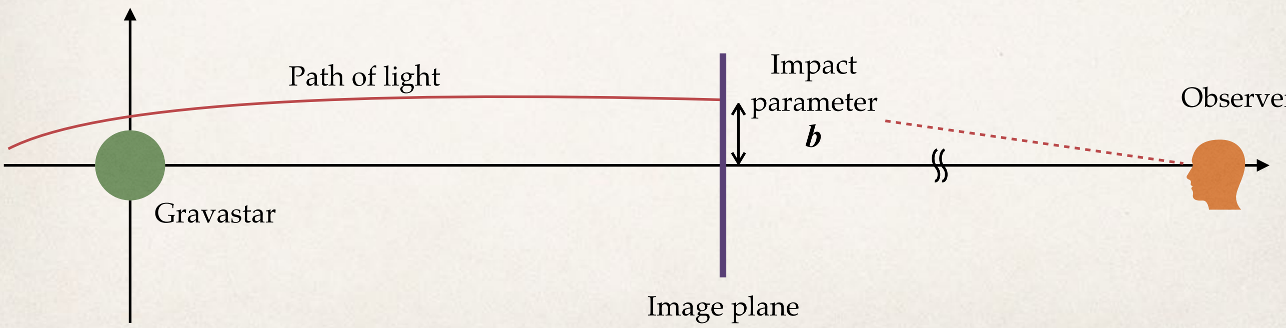

- Models
  - **Model 1** : Matter of shell does not interact with photons.
    - Light rays pass through gravastar interior.
  - **Model 2** : Matter of shell interacts with photons.
    - Light rays don't pass through gravastar interior.

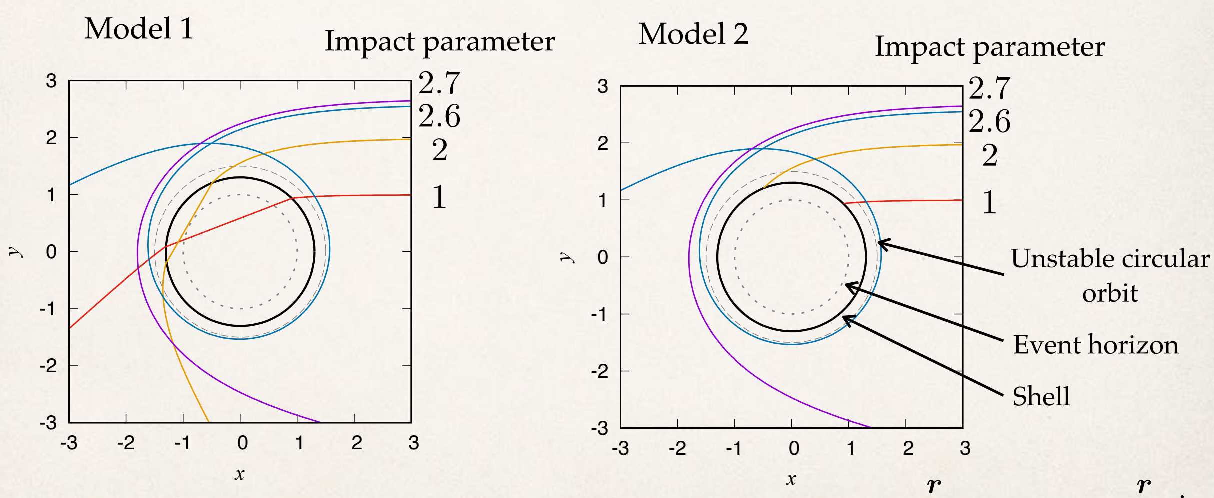

Null geodesics on gravastar space-time

$$x \equiv \frac{r}{r_g} \cos\varphi, \quad y \equiv \frac{r}{r_g} \sin\varphi$$

Results : Low density case

$$\frac{\rho_{\rm shell}}{\rho_{\rm Sch}(R)} = 10, 100$$

Model 1

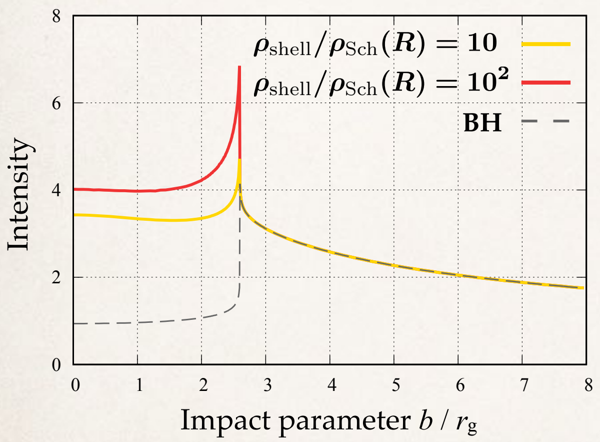

Model 2

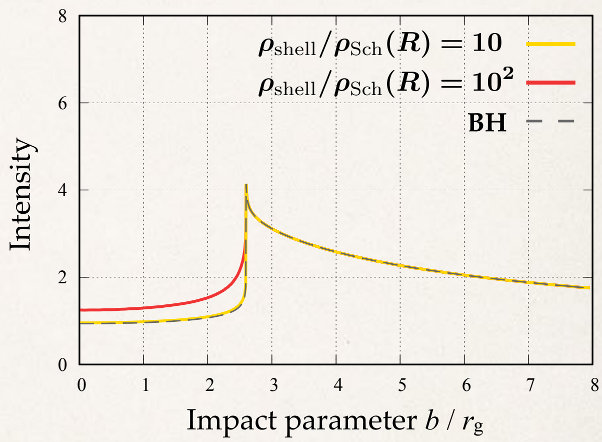

- When density on shell is **low**, model dependence is large.
  - In model 2, we probably can't distinguish gravastar from BHs.

Results : High density case

$$\frac{\rho_{\rm shell}}{\rho_{\rm Sch}(R)} = 1000$$

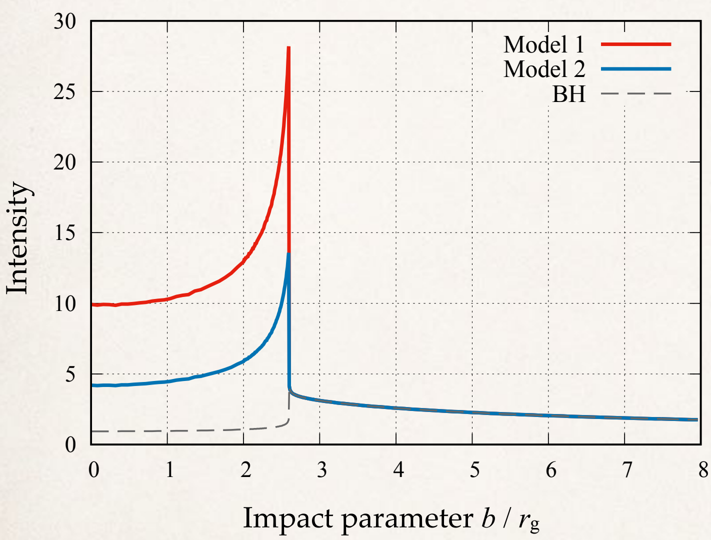

Optical images

Model 1

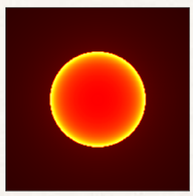

Model 2

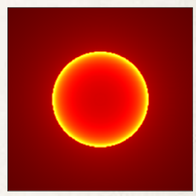

BH

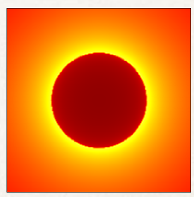

- When density on shell is **high**, intensity distributions are independent of models.
  - Optical images isn't dark and look like a bright sphere with a brighter ring.

Summary.

- Set a situation that dust falls into shell and piles up stationary.
- Obtained optical images of thin shell gravastar model surrounded by optically thin dust by computing null geodesic eqs. and radiative transfer eq.
- If density on shell is high, we would observe gravastar as a extremely compact bright sphere with a brighter ring.

5b5. Tetu Makino (Yamaguchi U.),
"Mathematical study of rotating gaseous stars"
(10+5)
[JGRG27 (2017) 112923]

Mathematical Theory of Rotating Gaseous Stars

Tetu Makino (Prof Emer at Yamaguchi Univ.)

November 29, 2017 //
The 27th Workshop on Genaral Relativity and Gravitation in Japan

Financially supprted by

the Yamaguchi University Foundation, Research Grant A1-2 (2017)

Einstein-Euler equations

$$R_{\mu\nu} - \frac{1}{2}g_{\mu\nu} = \frac{8\pi \mathsf{G}}{\mathsf{c}^4}T_{\mu\nu}, \tag{1}$$
$$T^{\mu\nu} = (\mathsf{c}^2\rho + P)U^\mu U^\nu - Pg^{\mu\nu} \tag{2}$$

for the metric $ds^2 = g_{\mu\nu}dx^\mu dx^\nu$

Assumption (A):

P is a given function of $\rho > 0$ such that $0 < P, 0 < dP/d\rho < \mathsf{c}^2$ for $\rho > 0$;

there exists a smooth function Λ which is analytic near 0, $\Lambda(0) = 0$, and

$$P = \mathsf{A}\rho^\gamma(1 + \Lambda(\mathsf{A}\rho^{\gamma-1}/\mathsf{c}^2)) \tag{3}$$

Here A, γ are positive cnstants, and

$$6/5 < \gamma < 3/2.$$

Result of [1]: Newtonian problem governed by **the Euler-Poisson equations**: ($\mathsf{c} = +\infty$) admits axially and equatorialy symmetric slowly rotating solutions with the density distribution

$$\rho_{\mathsf{N}}(r,\zeta) = \Big(\frac{\gamma-1}{\mathsf{A}\gamma}\Big)^{\frac{1}{\gamma-1}} \max(u_{\mathsf{N}}(r,\zeta),0)^{\frac{1}{\gamma-1}}$$

with compact support, where $r = \sqrt{(x_1)^2+(x_2)^2+(x_3)^2}, \zeta = x_3/r$ for $x = (x_1,x_2,x_3) \in \mathbb{R}^3$, and the velocity field

$$\vec{v}_{\mathsf{N}} = -\Omega x_2 \frac{\partial}{\partial x_1} + \Omega x_1 \frac{\partial}{\partial x_2}$$

with sufficiently small constant angular velosity Ω.

5

Problem: Find a solution of the Einstein-Euler equations, which tends to the solution $\rho_{\mathsf{N}}, \vec{v}_{\mathsf{N}}$ as $\mathsf{c} \to \infty$ of the form:

$$ds^2 = e^{2F}(\mathsf{c}dt + Ad\phi)^2 - e^{-2F}[e^{2K}(d\varpi^2+dz^2)+\Pi^2 d\phi^2] \qquad (4)$$

Here $x_1 = \varpi\cos\phi, x_2 = \varpi\sin\phi, x_3 = z$.

Main Result:

When $u_{\mathsf{O}}/\mathsf{c}^2$ is sufficiently small, we have a solution

$$F = \frac{1}{\mathsf{c}^2}\Big(\Phi_{\mathsf{N}} - \frac{\Omega^2}{2}\varpi^2\Big) + O(1/\mathsf{c}^4), \quad K = -\frac{\Omega^2}{2\mathsf{c}^2}\varpi^2 + O(1/\mathsf{c}^4),$$

$$A = -\varpi^2\frac{\Omega}{\mathsf{c}}(1+O(1/\mathsf{c}^2)), \quad \Pi = \varpi(1+O(1/\mathsf{c}^4)),$$

$$\rho = \Big(\frac{\gamma-1}{\mathsf{A}\gamma}\Big)^{\frac{1}{\gamma-1}}\max(u,0)^{\frac{1}{\gamma-1}}(1+O(1/\mathsf{c}^2)), \quad u = u_{\mathsf{N}} + O(1/\mathsf{c}^2) \quad (5)$$

Here Φ_{N} is the ρ_{N} is the Newton potential generated by ρ_{N}, and $u_{\mathsf{O}} = u_{\mathsf{N}}(0,0)$.

The equations to be solved reduce to

$$\frac{\partial^2 F}{\partial\varpi^2} + \frac{\partial^2 F}{\partial z^2} + \frac{1}{\Pi}\Big(\frac{\partial F}{\partial\varpi}\frac{\partial\Pi}{\partial\varpi} + \frac{\partial F}{\partial z}\frac{\partial\Pi}{\partial z}\Big) + \frac{e^{4F}}{2\Pi^2}\Big[\Big(\frac{\partial A}{\partial\varpi}\Big)^2 + \Big(\frac{\partial A}{\partial z}\Big)^2\Big]$$
$$= \frac{4\pi\mathsf{G}}{\mathsf{c}^4}e^{-2F+2K}(\epsilon + 3P), \tag{6a}$$

$$\frac{\partial}{\partial\varpi}\Big(\frac{e^{4F}}{\Pi}\frac{\partial A}{\partial\varpi}\Big) + \frac{\partial}{\partial z}\Big(\frac{e^{4F}}{\Pi}\frac{\partial A}{\partial z}\Big) = 0, \tag{6b}$$

$$\frac{\partial^2\Pi}{\partial\varpi^2} + \frac{\partial^2\Pi}{\partial z^2} = \frac{16\pi\mathsf{G}}{\mathsf{c}^4}e^{-2F+2K}P\Pi, \tag{6c}$$

$$\frac{\partial\Pi}{\partial\varpi}\frac{\partial K}{\partial\varpi} - \frac{\partial\Pi}{\partial z}\frac{\partial K}{\partial z} = \frac{1}{2}\Big(\frac{\partial^2\Pi}{\partial\varpi^2} - \frac{\partial^2\Pi}{\partial z^2}\Big) + \Pi\Big[\Big(\frac{\partial F}{\partial\varpi}\Big)^2 - \Big(\frac{\partial F}{\partial z}\Big)^2\Big] +$$
$$-\frac{e^{4F}}{4\Pi}\Big[\Big(\frac{\partial A}{\partial\varpi}\Big)^2 - \Big(\frac{\partial A}{\partial z}\Big)^2\Big], \tag{6d}$$

$$\frac{\partial\Pi}{\partial z}\frac{\partial K}{\partial\varpi} + \frac{\partial\Pi}{\partial\varpi}\frac{\partial K}{\partial z} = \frac{\partial^2\Pi}{\partial\varpi\partial z} + 2\Pi\frac{\partial F}{\partial\varpi}\frac{\partial F}{\partial z} - \frac{e^{4F}}{2\Pi}\frac{\partial A}{\partial\varpi}\frac{\partial A}{\partial z}, \tag{6e}$$

$$F = -\frac{u}{\mathsf{c}^2} + \text{Const.}. \tag{6f}$$

(6a),(6b),(6c) are elliptic equations on F, A, Π when K is given, and (6d),(6e) are a first order system on K when F, A, Π are given.

[Point 1]: When $P = 0$, the integrability condition of (6d)(6e) is guaranteed a priori, but when $P \neq 0$, it is not the case and a divice is needed.

Anyway we apply the fixed point theorem for contraction mappings by setting appropriate functional sapces.

[Point 2]: Through this process, we need the crucial lemma of [1] in order to prove the solvability of the elliptic equation on F.

[Point 1]:

$$\text{(6d),(6e)} \qquad \Leftrightarrow \qquad \frac{\partial K}{\partial \varpi} = \tilde{K}_1, \quad \frac{\partial K}{\partial z} = \tilde{K}_3,$$

where

$$\tilde{K}_1 = \Big[\Big(\frac{\partial \Pi}{\partial \varpi}\Big)^2 + \Big(\frac{\partial \Pi}{\partial z}\Big)^2\Big]^{-1}\Big(\frac{\partial \Pi}{\partial \varpi}\cdot \mathrm{RH(6d)} + \frac{\partial \Pi}{\partial z}\cdot \mathrm{RH(6e)}\Big), \tag{7a}$$

$$\tilde{K}_3 = \Big[\Big(\frac{\partial \Pi}{\partial \varpi}\Big)^2 + \Big(\frac{\partial \Pi}{\partial z}\Big)^2\Big]^{-1}\Big(-\frac{\partial \Pi}{\partial z}\cdot \mathrm{RH(6d)} + \frac{\partial \Pi}{\partial \varpi}\cdot \mathrm{RH(6e)}\Big). \tag{7b}$$

But

$$\begin{aligned}\frac{\partial \tilde{K}_1}{\partial z} - \frac{\partial \tilde{K}_3}{\partial \varpi} = \frac{8\pi \mathsf{G}}{\mathsf{c}^4} e^{-2F+2K} P\Pi \Big[\Big(\frac{\partial \Pi}{\partial \varpi}\Big)^2 + \Big(\frac{\partial \Pi}{\partial z}\Big)^2\Big]^{-1} \times \\ \times \Big[\Big(\frac{\partial K}{\partial \varpi} - \tilde{K}_1\Big)\frac{\partial \Pi}{\partial z} - \Big(\frac{\partial K}{\partial z} - \tilde{K}_3\Big)\frac{\partial \Pi}{\partial \varpi}\Big].\end{aligned} \tag{8}$$

Lemma 1 : *Even if $P \neq 0$, we have*

$$\tilde{K} = K \quad \Rightarrow \quad \frac{\partial K}{\partial \varpi} = \tilde{K}_1, \quad \frac{\partial K}{\partial z} = \tilde{K}_3 \quad \Rightarrow (6\mathrm{d}),\ (6\mathrm{e}),$$

where

$$\tilde{K}(\varpi, z) := \int_0^z \tilde{K}_3(0, z')dz' + \int_0^{\varpi} \tilde{K}_1(\varpi', z)d\varpi' \tag{9}$$

[Point 2]

Post-Newtonian approximation:

$$F = \frac{1}{\mathsf{c}^2}\Big(\Phi_{\mathsf{N}} - \frac{\Omega^2}{2}\varpi^2\Big) - \frac{w}{\mathsf{c}^4}, \tag{10a}$$

$$A = \Big(-\frac{\Omega}{\mathsf{c}} + \frac{Y}{\mathsf{c}^3}\Big)\varpi^2, \tag{10b}$$

$$\Pi = \varpi\Big(1 + \frac{X}{\mathsf{c}^4}\Big), \tag{10c}$$

$$K = -\frac{\Omega^2}{2\mathsf{c}^2}\varpi^2 + \frac{V}{\mathsf{c}^4} \tag{10d}$$

$$u = u_{\mathsf{N}} + \frac{w}{\mathsf{c}^2} \tag{10e}$$

$$\Rightarrow \quad \rho = \Big(\frac{\gamma - 1}{\mathsf{A}\gamma}\Big)^{\frac{1}{\gamma-1}} \max(u, 0)^{\frac{1}{\gamma-1}}(1 + [u/\mathsf{c}^2]_1)$$

$$\Big[\frac{\partial^2}{\partial\varpi^2}+\frac{1}{\varpi}\frac{\partial}{\partial\varpi}+\frac{\partial^2}{\partial z^2}+\frac{1}{(\gamma-1)\mathsf{a}^2}\max\Big(\frac{u_{\mathsf{N}}}{u_{\mathsf{O}}},0\Big)^{\frac{1}{\gamma-1}-1}\Big]w=$$
$$=8\Big(\Phi_{\mathsf{N}}-\frac{\Omega^2}{2}\varpi^2\Big)\Omega^2-2\Omega\Big(2Y+\varpi\frac{\partial Y}{\partial\varpi}\Big)+$$
$$-4\pi\mathsf{G}\Big(-2\Phi_{\mathsf{N}}\rho_{\mathsf{N}}+\Big(\frac{\gamma}{\gamma-1}\Lambda_1+3\Big)P_{\mathsf{N}}\Big)+R_a, \tag{11a}$$
$$\Big[\frac{\partial^2}{\partial\varpi^2}+\frac{3}{\varpi}\frac{\partial}{\partial\varpi}+\frac{\partial^2}{\partial z^2}\Big]Y=\frac{8}{\varpi}\frac{\partial}{\partial\varpi}\Big[\Phi_{\mathsf{N}}-\frac{\Omega^2}{2}\varpi^2\Big]\Omega+R_b, \tag{11b}$$
$$\Big[\frac{\partial^2}{\partial\varpi^2}+\frac{2}{\varpi}\frac{\partial}{\partial\varpi}+\frac{\partial^2}{\partial z^2}\Big]X=16\pi\mathsf{G}P_{\mathsf{N}}+R_c, \tag{11c}$$

Lemma 2: *Given axially and equatorially symmetric, compactly supporeted function g, the integral equation*

$$Q=\mathcal{K}\Big[\frac{1}{(\gamma-1)}\max\Big(\frac{u_{\mathsf{N}}}{u_{\mathsf{O}}},0\Big)^{\frac{1}{\gamma-1}-1}Q+g\Big]$$

admits a unique axially and equatorially symmetric solution Q. Here

$$\mathcal{K}f(x)=\frac{1}{4\pi}\int\frac{f(x')}{|x-x'|}dx'-\frac{1}{4\pi}\int\frac{f(x')}{|x'|}dx'.$$

Note that then

$$\Big[\frac{\partial^2}{\partial\varpi^2}+\frac{1}{\varpi}\frac{\partial}{\partial\varpi}+\frac{\partial^2}{\partial z^2}+\frac{1}{(\gamma-1)}\max\Big(\frac{u_{\mathsf{N}}}{u_{\mathsf{O}}},0\Big)^{\frac{1}{\gamma-1}-1}\Big]Q+g=0,$$
$$Q(0,0)=0$$

Open problem :

The solution is constructed on a bounded domain which contains the support of ρ. The mathching problem to the exterior vacuum metric which is defind on the whole space and asymptotically flat at the space infinity.

The preprint is available at arXiv [2].

参考文献

[1] Juhi Jang and T. Makino, ARMA, 225(2017), 873-900.

[2] T. Makino, On slowly rotating axisymmetric solutions of the Einstein-Euler equations, arXiv:1705.07392.

THANK YOU

FOR YOUR ATTENTION!

***

Please visit my Homepage:

“Arkivo de Tetu Makino”

(http://hc3.seikyou.ne.jp/home/Tetu.Makino)

Invited lecture 16:15–17:45

[Chair: Takashi Nakamura]

Hideyuki Tagoshi (ICRR Univ. of Tokyo),
"Status and prospect of KAGRA " (35+10)
[JGRG27 (2017) 112924]

Status and prospect of KAGRA

Hideyuki Tagoshi (ICRR, Univ. Tokyo)

on behalf of the KAGRA collaboration

2017/11/29 JGRG27@Higashi Hiroshima

6.8 GW events observed by LIGO and Virgo

GW150914

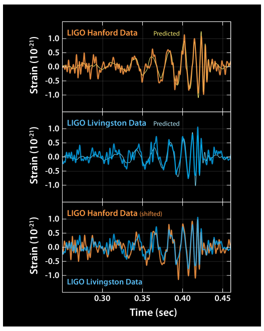

GW151226

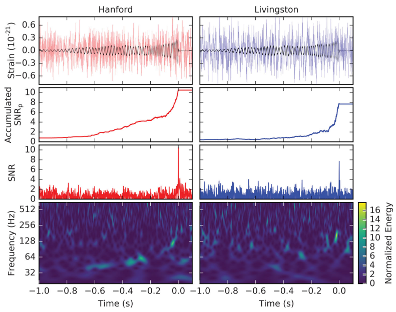

GW170104

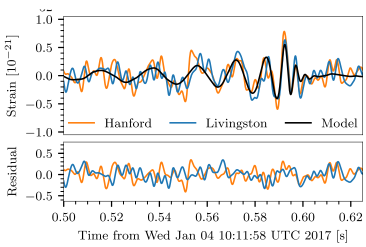

(+ LVT151012)

GW170608

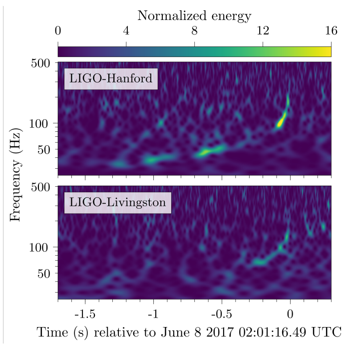

GW170814

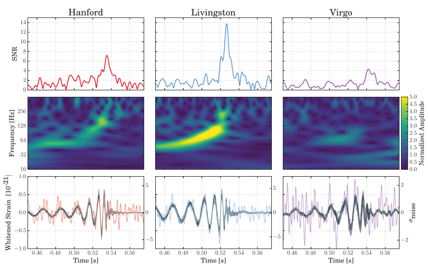

GW170817

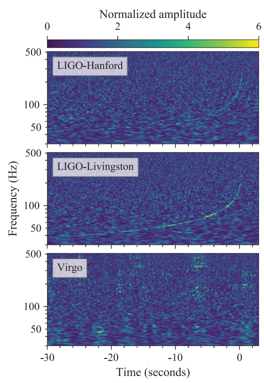

Gravitational Wave Astronomy

GW150914

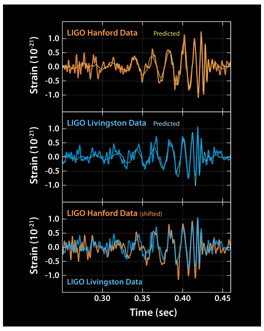

Begining of GW Astronomy

Begining of Multi-messenger GW Astronomy

GW170817

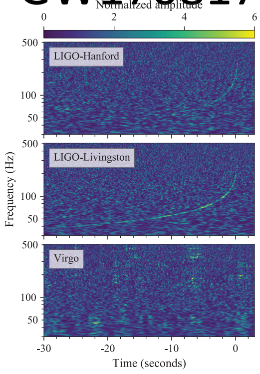

GW170817
GRB170817A
SSS17a / AT2017gfo
Multi-messenger Observations

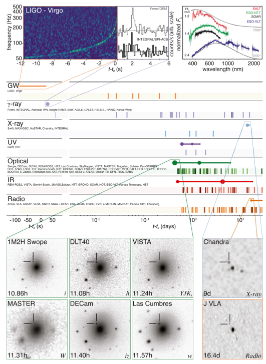

3

How about KAGRA ?

Contents

- Introduction
- KAGRA Construction
- iKAGRA test run, data analysis
- bKAGRA schedule, O3
- Data management, Data analysis
- Prospect of science by KAGRA and LIGO-Virgo

KAGRA

Host Institute: ICRR, U Tokyo
Cooperative institutes: NAOJ, KEK, and many universities.
(～250 people, ～80 institutes)

- Kamioka mine, Hida City, Gifu
- 3km laser interferometer
- Underground site
- Cryogenic mirror

Design sensitivity - aLIGO, aVIRGO, KAGRA -

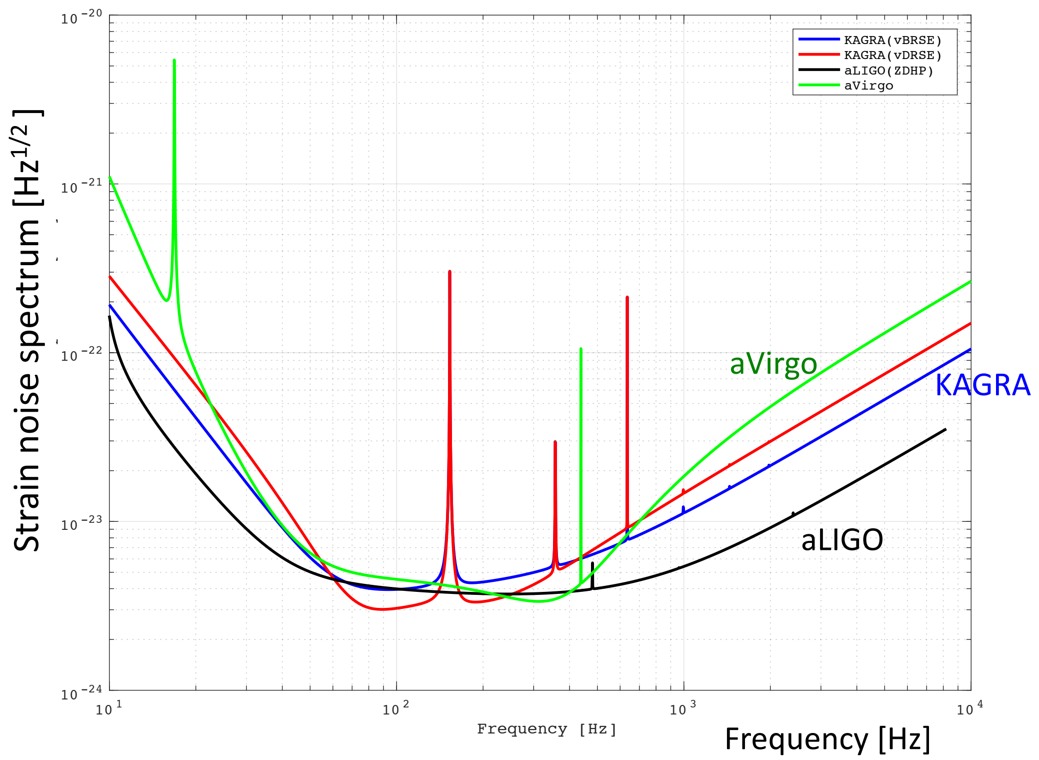

Data for the KAGRA noise spectrum :
http://gwcenter.icrr.u-tokyo.ac.jp/en/researcher/parameter

Schedule

	2010	2011	2012	2013	2014	2015	2016	2017	2018	2019
Project start										
Tunnel excuvation										
iKAGRA										
					iKAGRA run					
bKAGRA				adv. optical sysmtem						
					cryogenic sysmtem					
Operation										

Tunnel excavation

photo by N.Kanda

Photo : KAGRA tunnel, center corner

KAGRA Arm Tunnel and Corner Station

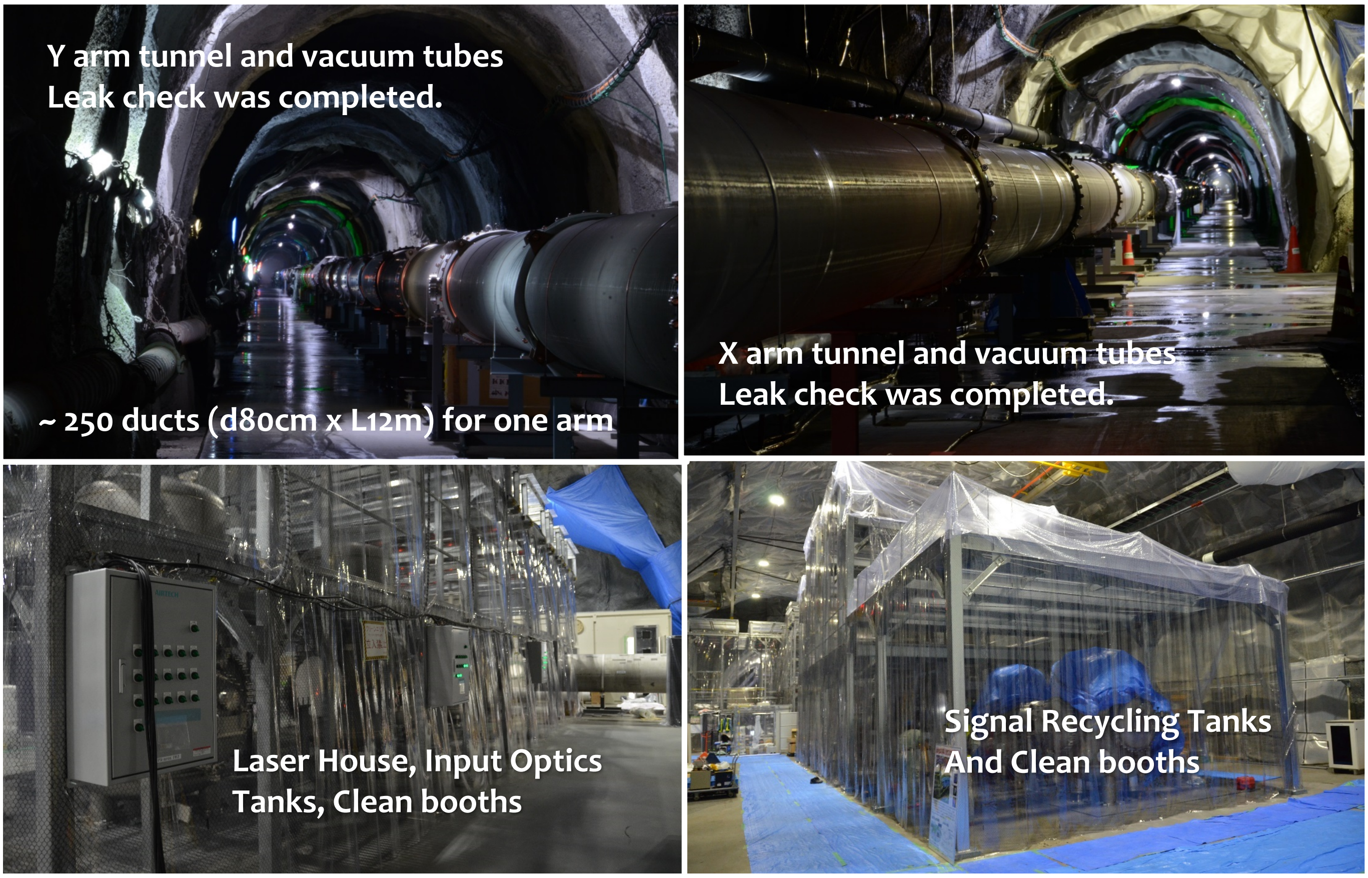

KAGRA observatory: surface buildings

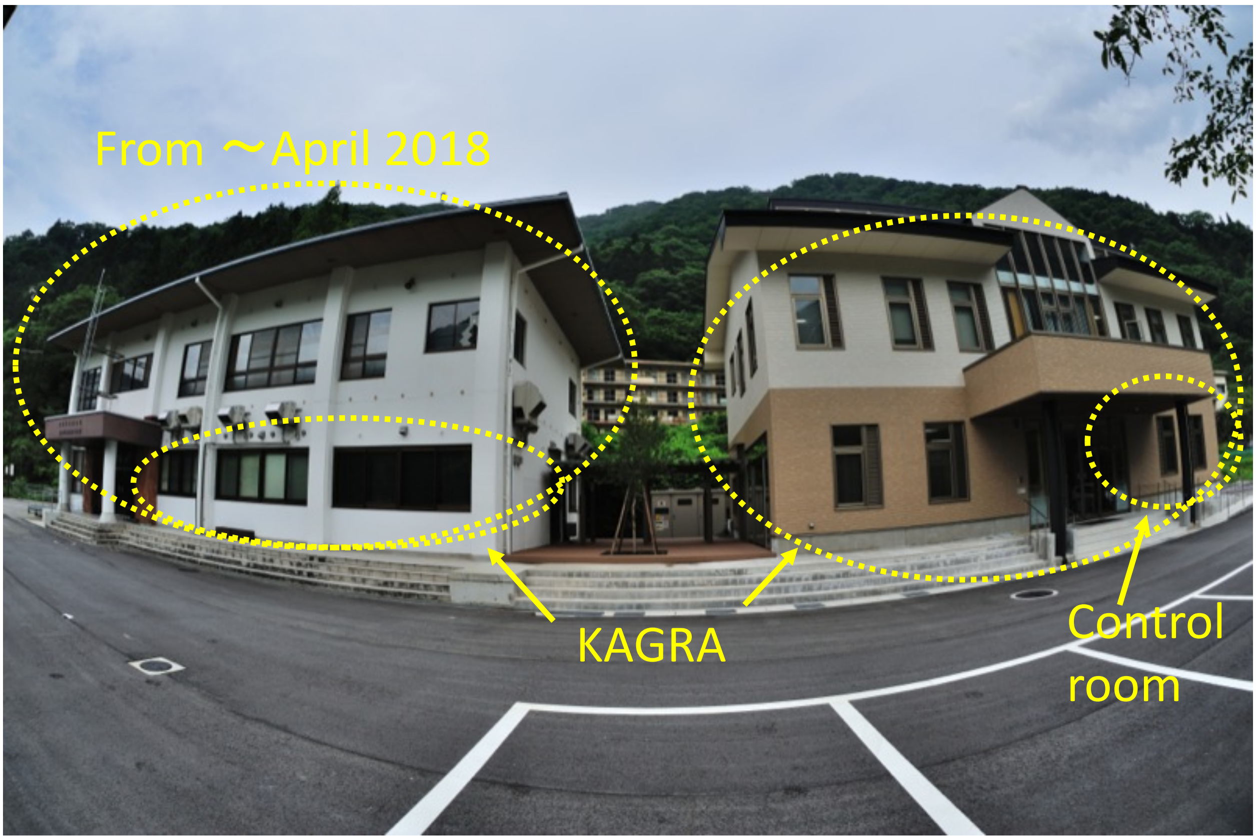

Control room in a surface building

iKAGRA test run

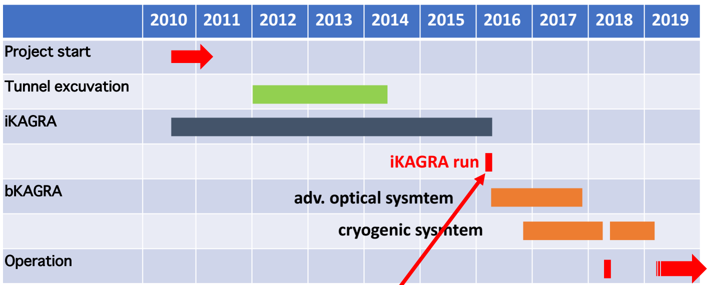

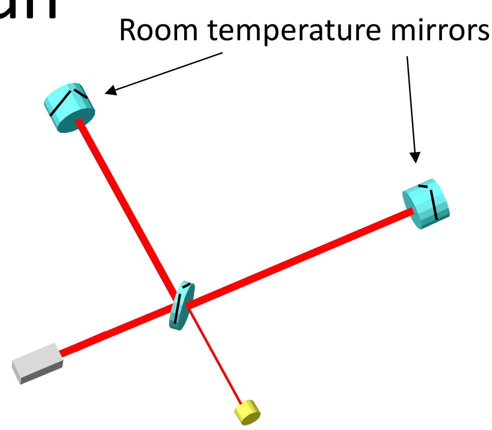

1st run : March 25 - 31, 2016
2nd run : April 12 - 25, 2016

Mail purpose: Demonstration of 3km interferometer operation

- 3km Michelson interferometer (partially in vaccum)
- Typical sensitivity
  - 1st run: 3×10^{-15} Hz$^{-1/2}$ @ 100 Hz
  - 2nd run: 6×10^{-16} Hz$^{-1/2}$ @ 100 Hz
- Duty cycle (= (lock time)/(total time))
  - 1st run: 85.2 %
  - 2nd run: 90.4 %

Start of iKAGRA test run, March 25th 2016

Horizon distance of CBC by iKAGRA

Equal mass, Optimal direction , SNR = 8

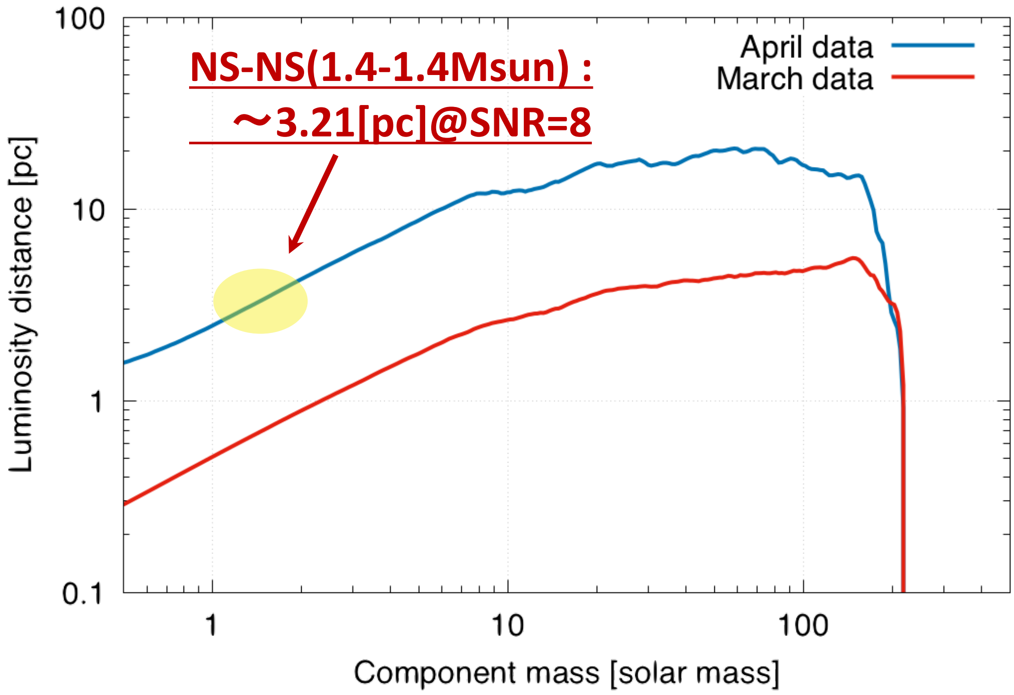

Lock duration of iKAGRA data

The status of the detector controlled well is called “locked”.
In this analysis, we analyze only the data that the lock continues longer than 4096[s].

▪ 1st run (March data)

	total time[s]	total time [day]	percentage [%]
all data	547200	6.33	100
locked data	366976	**4.25**	67.1
Used for CBC	47904	**0.55**	8.76

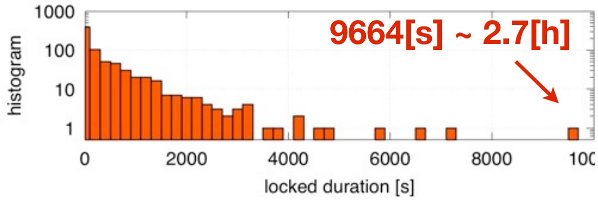

▪ 2st run (April data)

	total time[s]	total time [day]	percentage [%]
all data	1238400	14.33	100
locked data	1066240	**12.34**	86.1
Used for CBC	895552	**10.36**	72.3

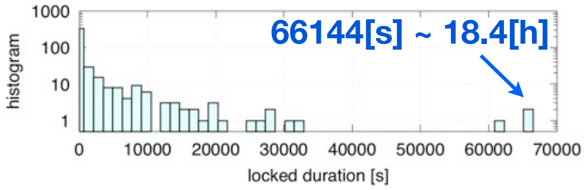

8

Signal Injection test @ iKAGRA

This is often called "Hardware Injection test".
This is done by shaking mirrors.
(The signals injected are not real gravitational wave signals!)

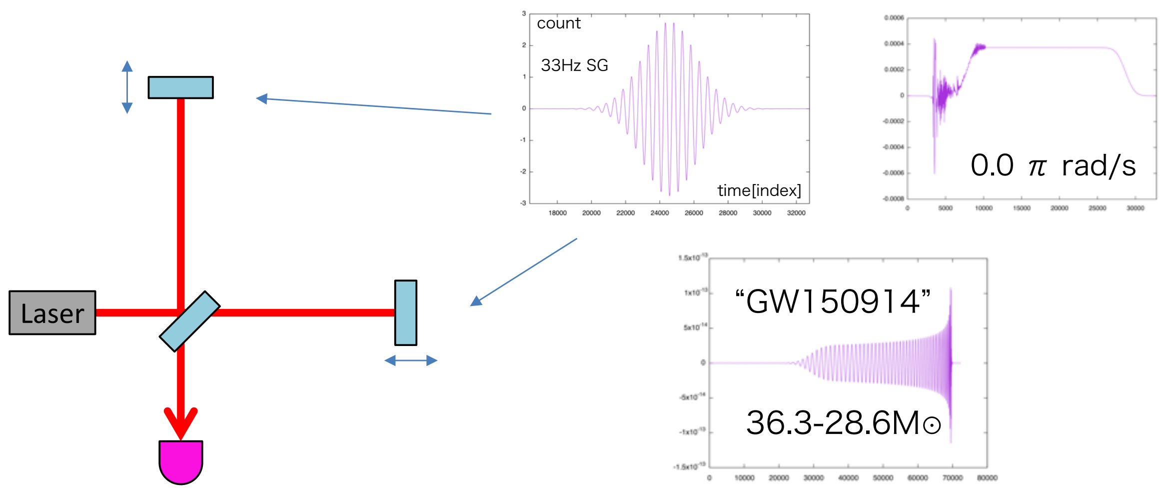

Signal Injection test

by Yokozawa

Run1 : reduced chi square = 1.24 (20262.9/16380)

$$h_{\mathrm{count}} = A \exp\left(-\frac{(t-t_0)^2}{\tau^2}\right)\cos(2\pi f_0(t-t_0))$$

Black : data
Red : Best fit

fit param.	expect	measured
amp.	2.066E-12	2.065e-12±0.002e-12
t_0[s]	1.5	1.5005±small
Q value	20	19.5±0.02
f_0[Hz]	33	32.99±small

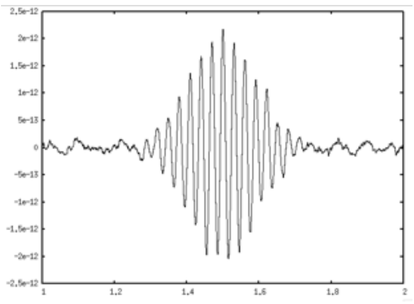

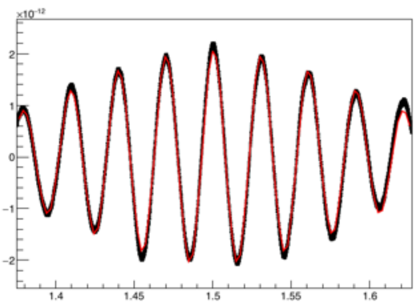

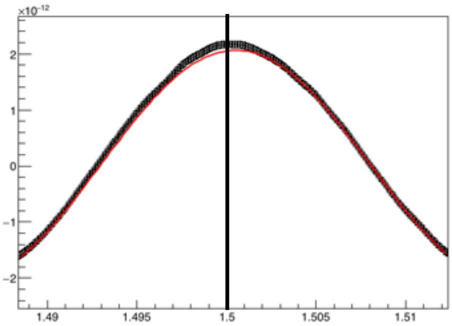

500 μ sec delay was found which was not realized clearly before.
This can be explained by the delay caused during the signal processing in the data aquisition system

HW injection : Parameter estimation study on injected CBC signals

by Narikawa

An example of analysis by lalinference-mcmc

injected signal: EOB waveform, (20,20)Msun, SNR=8
chirp mass=17.4, eta=0.25,
template: IMRPhenom (freq. domain template)

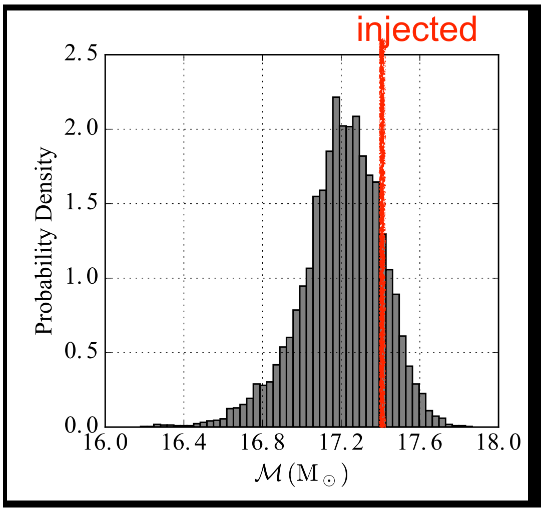

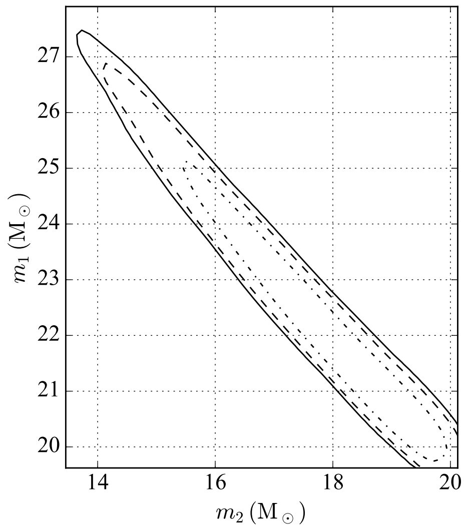

http://gwdoc.icrr.u-tokyo.ac.jp/cgi-bin/private/DocDB/ShowDocument?docid=5882

HW injection : Analysis with Hilbert-Huang transform

by Ueki et al.

- Sine-Gaussian signal:

  Time-Frequency map was recovered with HHT analysis

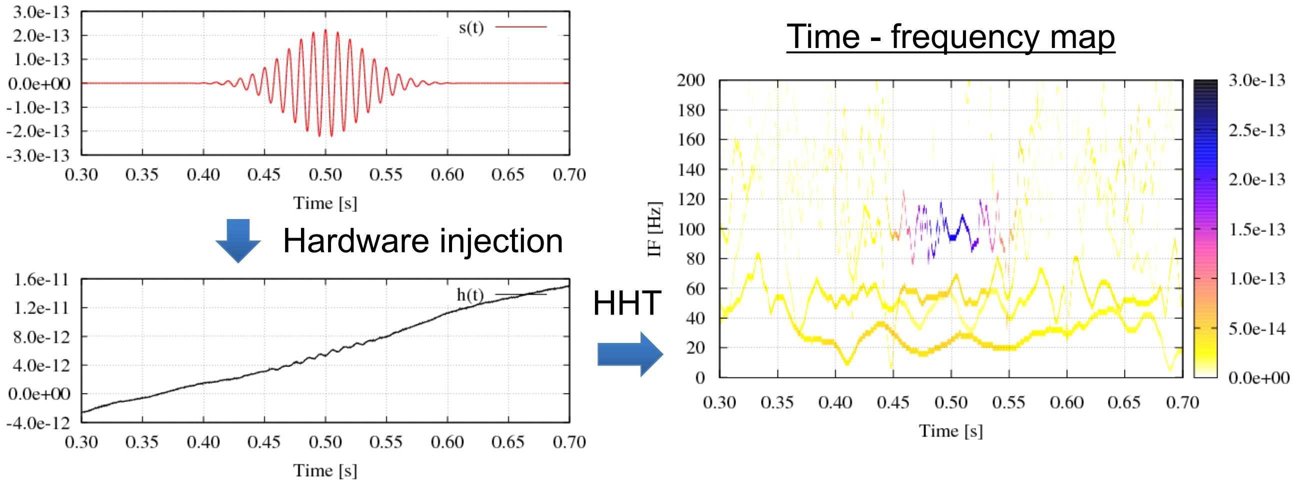

iKAGRA data analysis

- Compact Binary Coalescense (CBC) Search
  - Method: Frequency domain, Matched filter - Chi square analysis
  - Mass range: 1-3Msun
  - Spin: no
  - Template: TaylorF2
  - Template bank: Hexagonal placement method
  - Code: Original code

- Continuous Wave
  - Method: F-statistic
  - Target: 62 known pulsars
  - Frequency: 50 – 1000 Hz

- Burst
  - Method: Excess power
  - Event reconstruction : Clustering based on mathematical morphology
    - All sky search
    - Targeted search for GW associated with GRB events
  - Code: Original Code

bKAGRA

bKAGRA = baseline KAGRA
Final goal : Operation of full configuration KAGRA with good sensitivity

We proceed step-by-step:
We devide bKAGRA commissioning into 3 phases

Phase-1 : Construction of a 3km cryogenic Michelson interferometer, followed by a short operation (no sensitivity goal)

Phase-2 : Construction of KAGRA with full configuration, followed by its operation (Cryogenic RSE, no sensititivity goal)

Phase-3 : Commissioning and observation

bKAGRA Phase-1

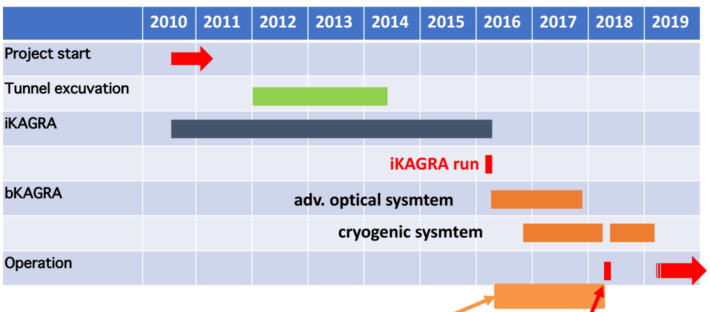

April 2016 – March 2018: Construction
March – April 2018 : test run

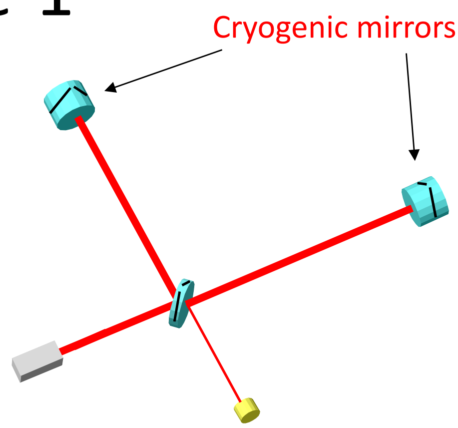

We are now in this phase

- Cryogenic Michelson interferometer
  - No Fabry-Perot cavity
  - No power recycling
  - No signal recycling
  - No target sensitivity

Suspension System Installation

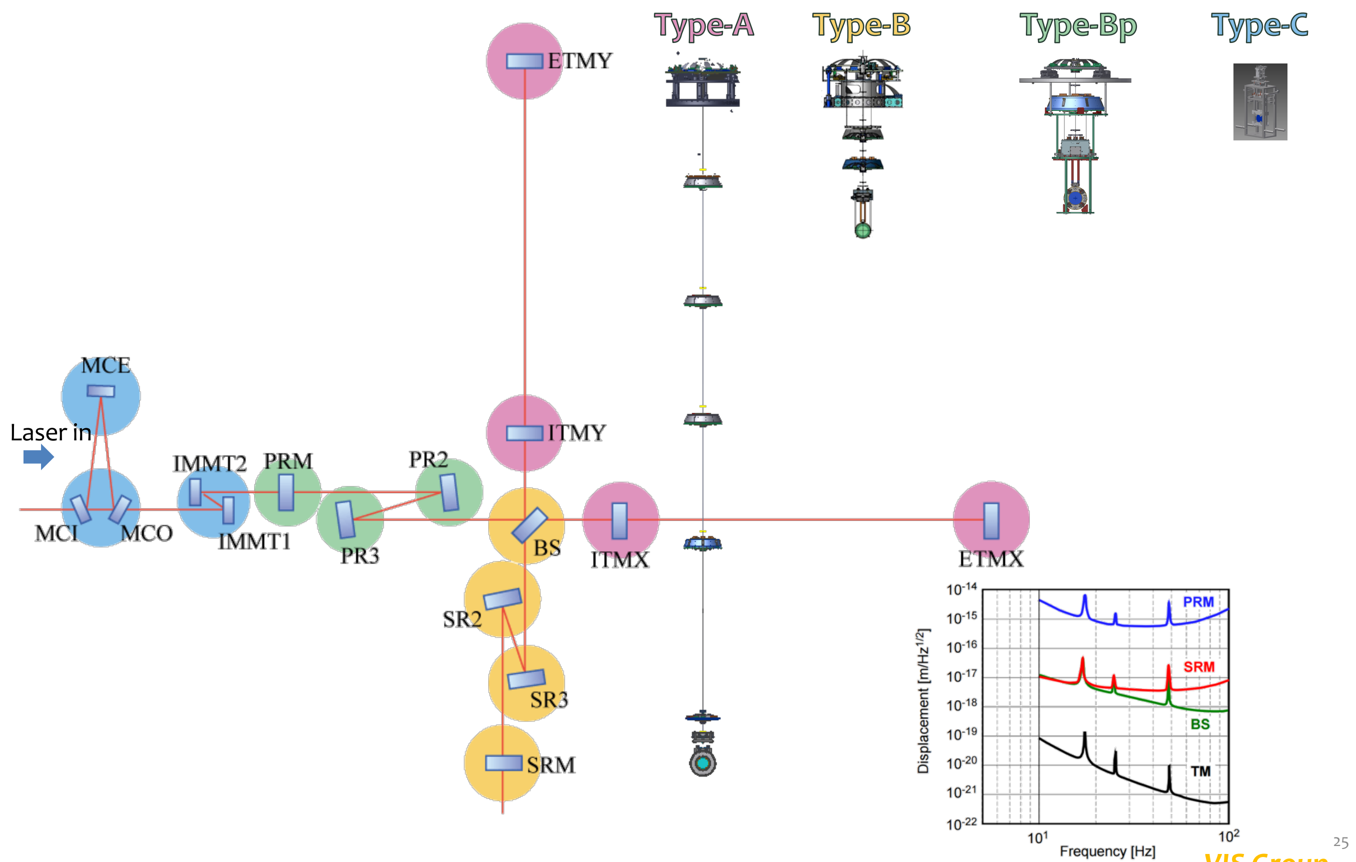

25

VIS Group

Suspension System Installation for phase-1

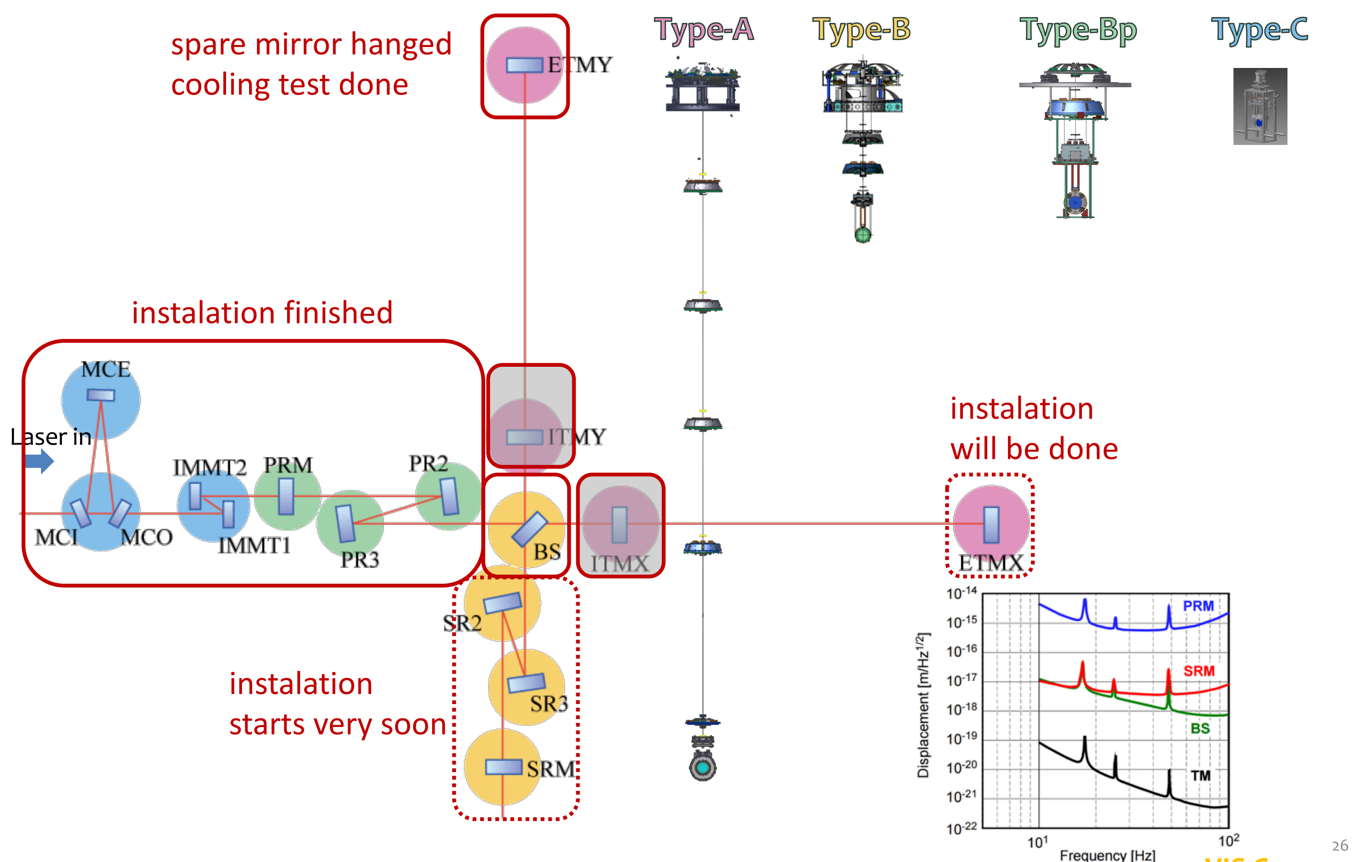

26

VIS Group

bKAGRA Phase-2

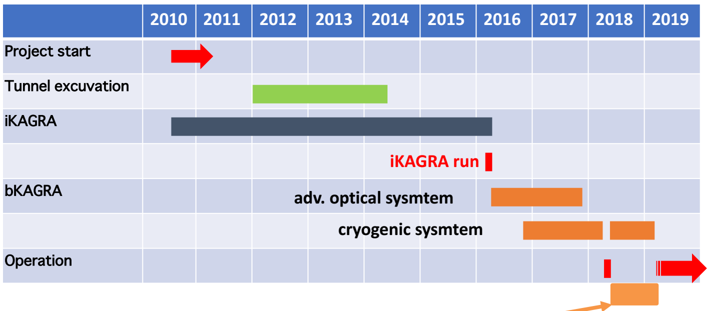

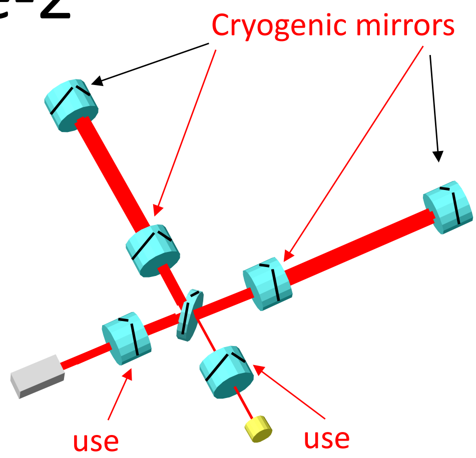

May 2018 – March 2019: Construction
March 2019 ?: test run

- Fabry-Perot, Power recycling, RSE interferometer
    - Full configuration interferometer
    - No target sensitivity

bKAGRA Phase-3

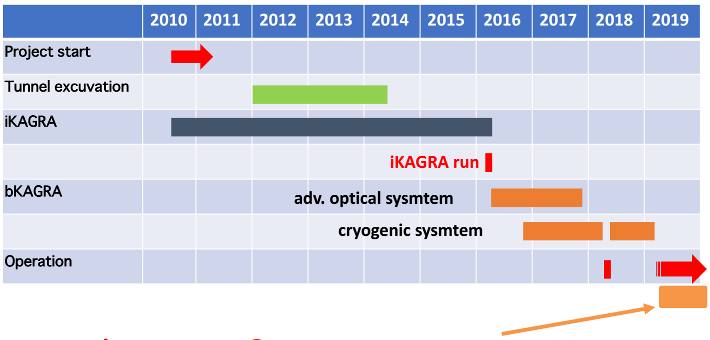

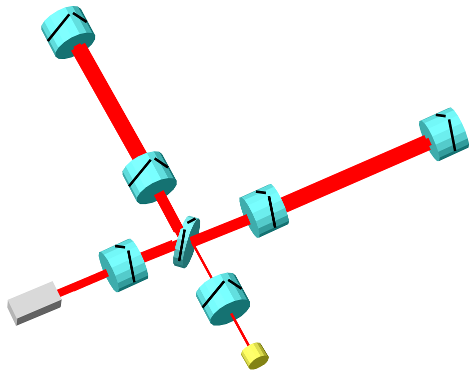

April 2019 - ? : Commissioning
2020- ? : Observation

- Fabry-Perot, Power recycling, RSE interferometer
    - To achieve good sensitivity

Expected schedule of LIGO, Virgo, KAGRA

Observing senario paper by LVK arXiv:1304.0670 (Updated on Sept. 8, 2017)

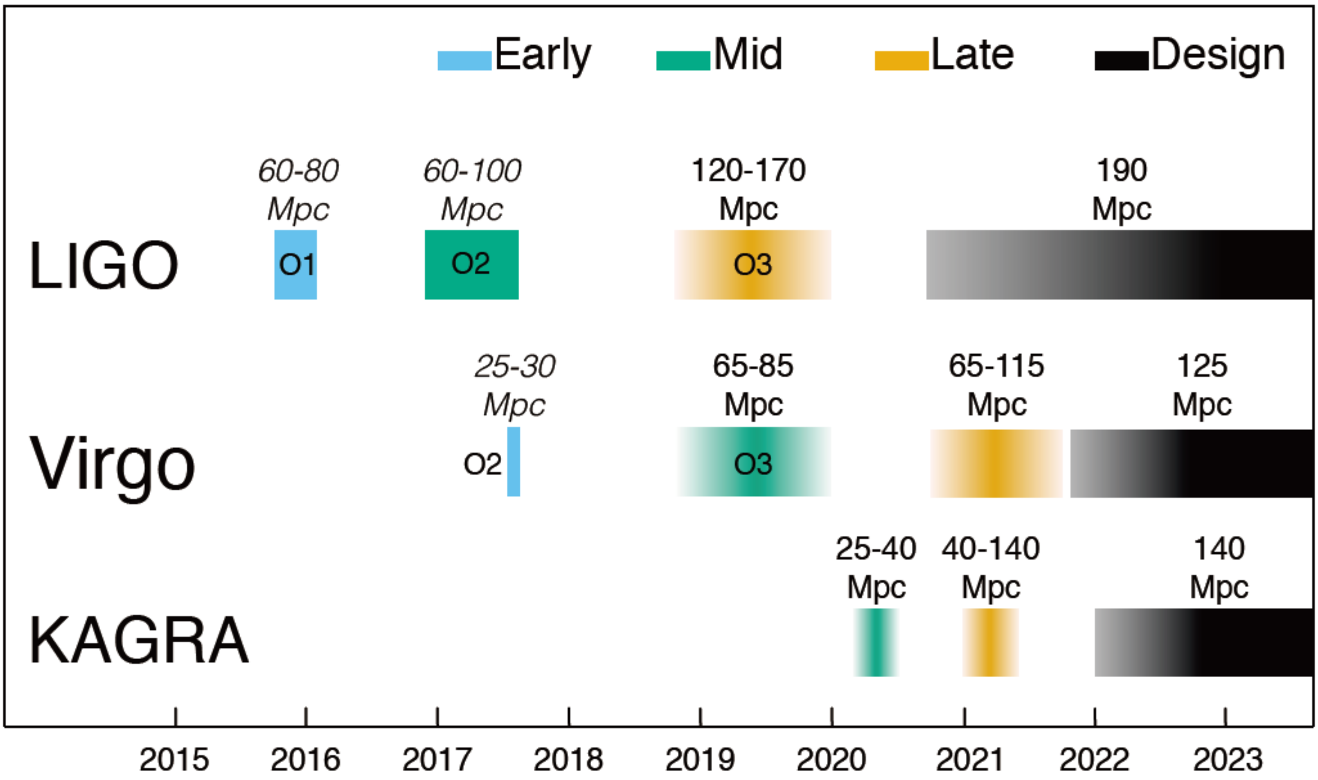

Expected schedule of LIGO, Virgo, KAGRA

arXiv:1304.0670 (Updated on Sept. 8, 2017) (modified)

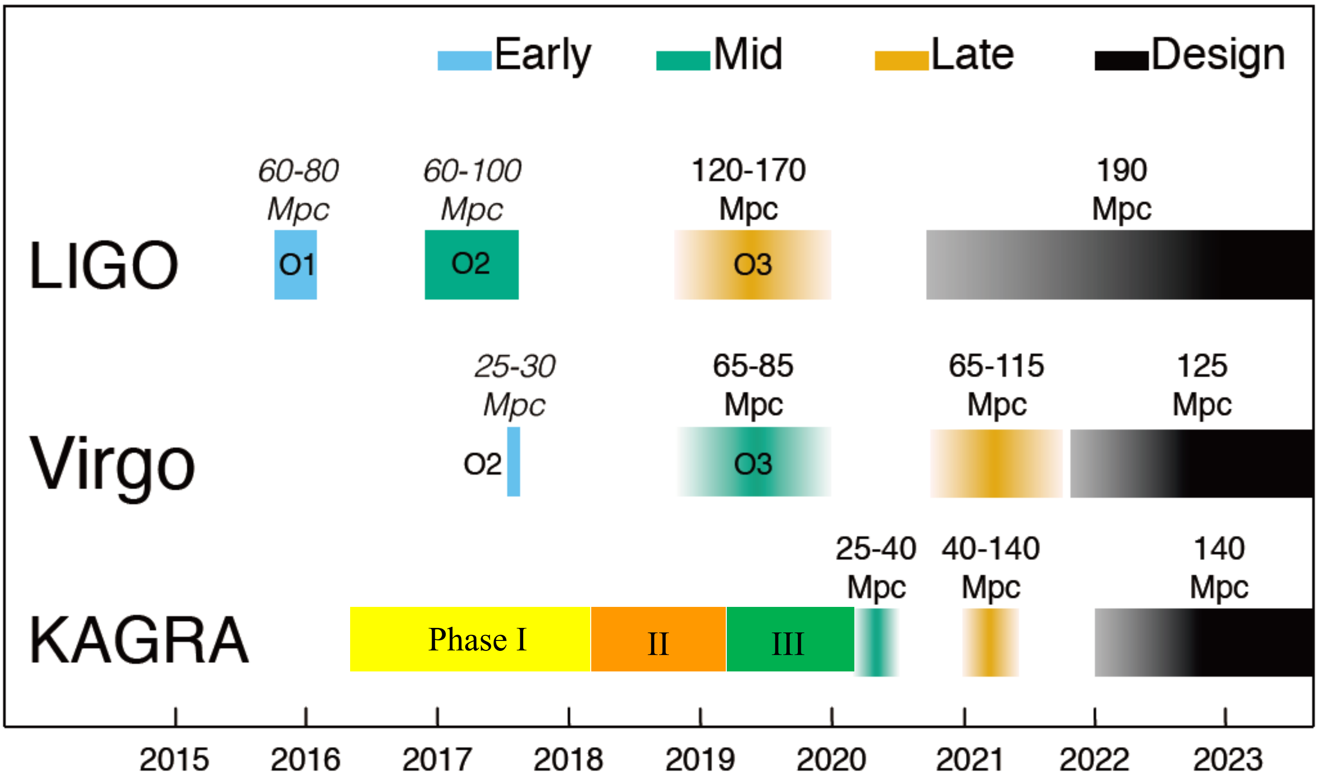

Expected schedule of LIGO, Virgo, KAGRA

arXiv:1304.0670 (Updated on Sept. 8, 2017) (modified)

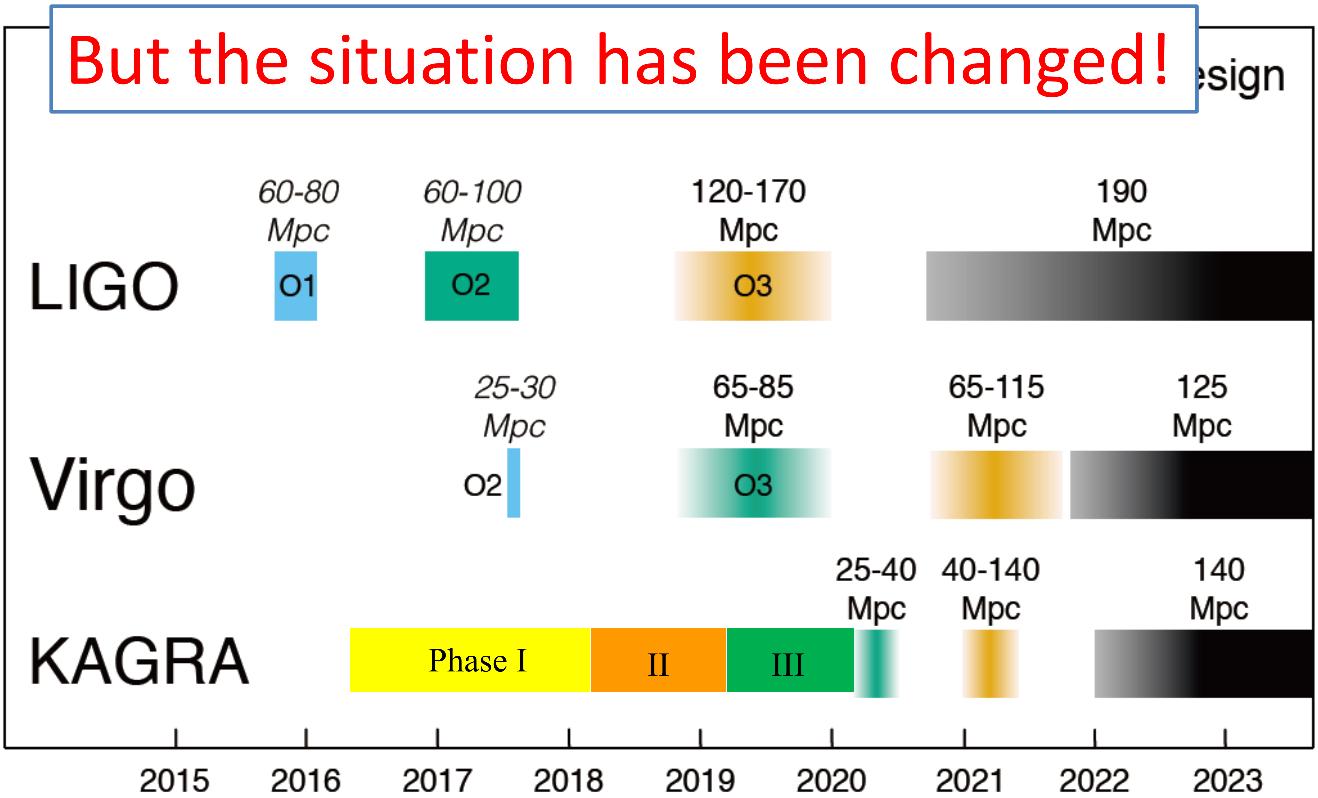

Case of Virgo

http://www.ligo.org/news.php

FIRST TRIPLE LOCK OF LIGO AND VIRGO INTERFEROMETERS

17 June 2017 -- For the first time, all three second generation interferometers---LIGO Hanford, LIGO Livingston, and Virgo---are simultaneously in a locked state. (When an interferometer is "locked" it means that an optical resonance is set up in the arm cavities and is producing a stable interference pattern at the photodetector.) Virgo is joining in an engineering mode, in preparation for the full triple-observing mode planned for later this summer. Congratulations, Virgo!

June 17 2017:
First Triple lock with LIGO

August 1st 2017:
Started observation and joined O2

August 14 2017:
BBH detected!

August 17 2017:
BNS detected!

Image Credit: Virgo Collaboration

We should join O3

International network of ground based gravitational wave detectors

LIGO-Livingston

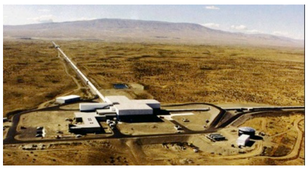

LIGO-Hanford

Virgo

KAGRA

We should join O3

International network of ground based gravitational wave detectors

LIGO-Livingston

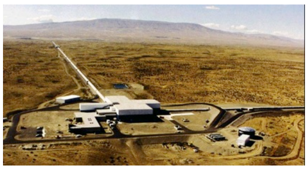

LIGO-Hanford

Virgo

KAGRA

Although the schedule is so tight,
we should definitely join LIGO-Virgo
O3 (Autum of 2018 ～ (1 yr?)) if we can.

Any decision has not been made yet.
Discussion on how we can manage to join
O3 started in the collaboration.

Data Management

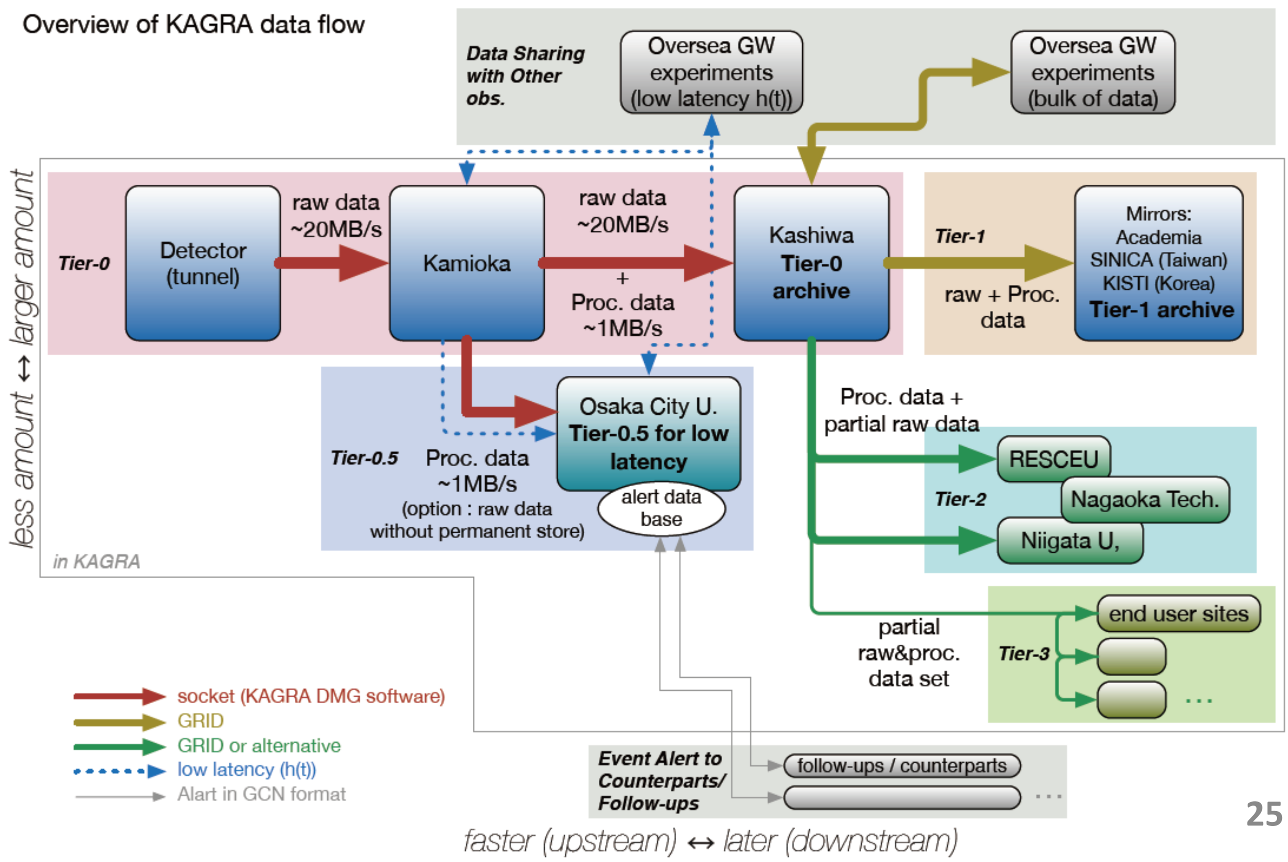

Hardware in Kamioka surface building

@Kamioka surface building

- 200TiB lustre storage system (FEFS), separate MDT and OSS
- 1 data server
- 4 calculation nodes (8cores x 2CPUs) = 64cores
- 2 job management servers

VPN switch

@Kashiwa (ICRR building 6th floor)

- 100 TiB lustre storage system (FEFS), single storage for MDT+OSS
- 2 login server
- VPN switch

placed at computer area beside the control room, 1st floor of analysis build.

200 TiB 'lustre' file system

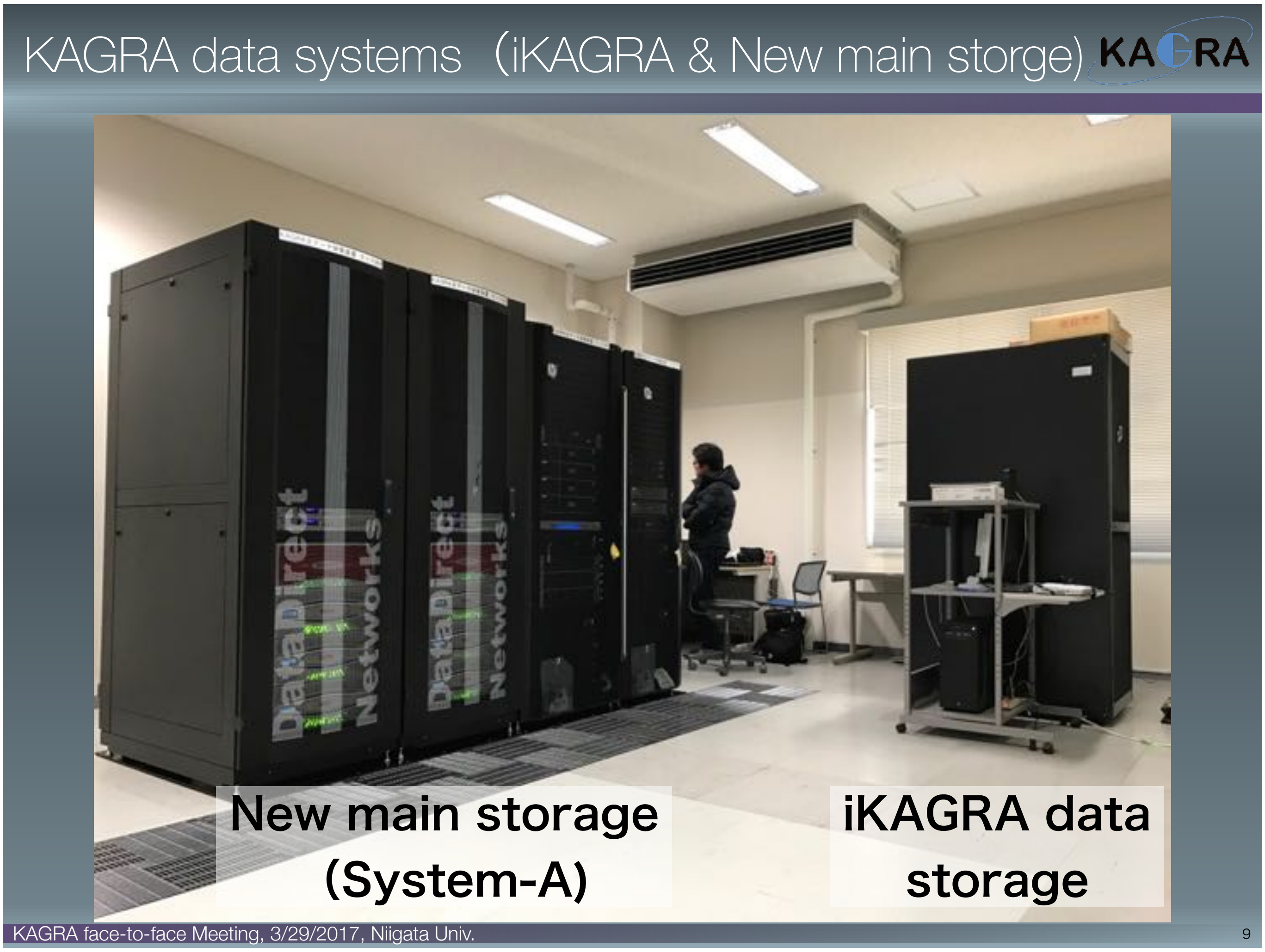

Current data storage

Site	Capacity	Main Usage
Kamioka (surface)	200 TiB	spool, On-site analysis
Kashiwa	100 TiB + 2.4 PiB	iKAGRA data storeage
Osaka City Univ.	304 TiB	CBC, Burst, low latency search
RESCEU	80 TiB	CW
Niigata Univ.	77 TiB	misc. analysis
Academia SINICA (Taiwan Group)	220 TiB	Tier-1 mirroring, etc.
KISTI-GSDC (Korea Group)	150TB (800TB in 2018 and 2019)	Tier-1, Detector characterization
(total)	~ 3.5 PiB	-

summarized by N.Kanda

Computing resources

- Osaka City Univ. (Orion, Gemini)
  28 nodes, 760 cores,
  Memory : 128GB/nodes
  Storage : 290TB

- RESCEU, Univ. Tokyo, (KAMBAI(寒梅))
  540 cores
  Storage: 100TB

- KAGRA Main storage
  336 cores

- KISTI(Korea) 〜 864 core (shared)

- ICRR computing center 〜1000 core (shared)

KAGRA Data Analysis Subsystem

〜43 people

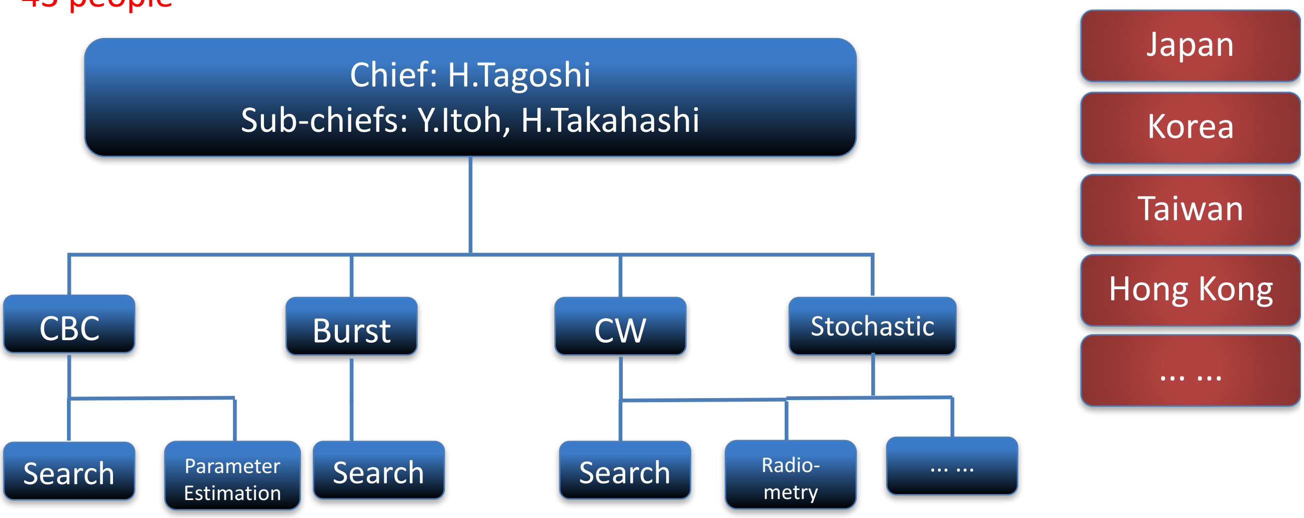

Slide by Narikawa

c.f. arXiv:1705.04008

Signal: BHNS (25,1.4), 100Mpc, i=75deg
Template: TaylorF2

3 detectors including KAGRA

4 detectors including KAGRA

Design-HL	Design-HLV	Design-HLK	Design-HLVK
SNR=27.2	SNR=25.6	SNR=30.0	SNR=30.6
694.6 deg^2	74.4 deg^2	75.2 deg^2	20.4 deg^2

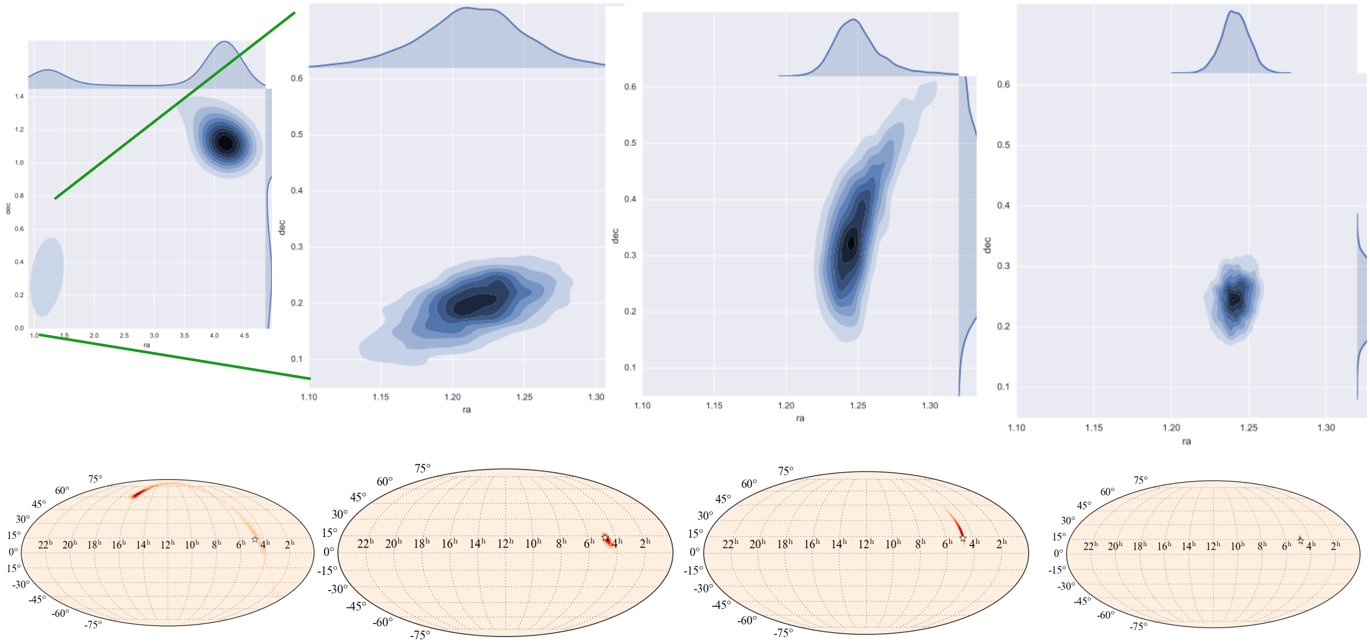

3

Sky localization accuracy

NS-NS @180Mpc (95%CI)

(1.4,1.4)Msun	LHV	LHVK
median of δΩ [Deg^2]	30.25	9.5

J.Veitch et al., PRD85, 104045 (2012)
(Bayesian inference)
See also Rodriguez et al. 1309.3273

L:LIGO-Livingston
H:LIGO-Hanford
V: Virgo
K: KAGRA
I: LIGO-India

direction, inclination, polarization angle are given randomly

BH-NS @200Mpc

(10,1.4)Msun	LHV	LHVK	LHVKI
median of δΩ [Deg^2]	21.5	8.44	4.86

(Tagoshi, Mishra, Arun, Pai, PRD90, 024053 (2014) , Fisher matrix)

CBC and SGRB

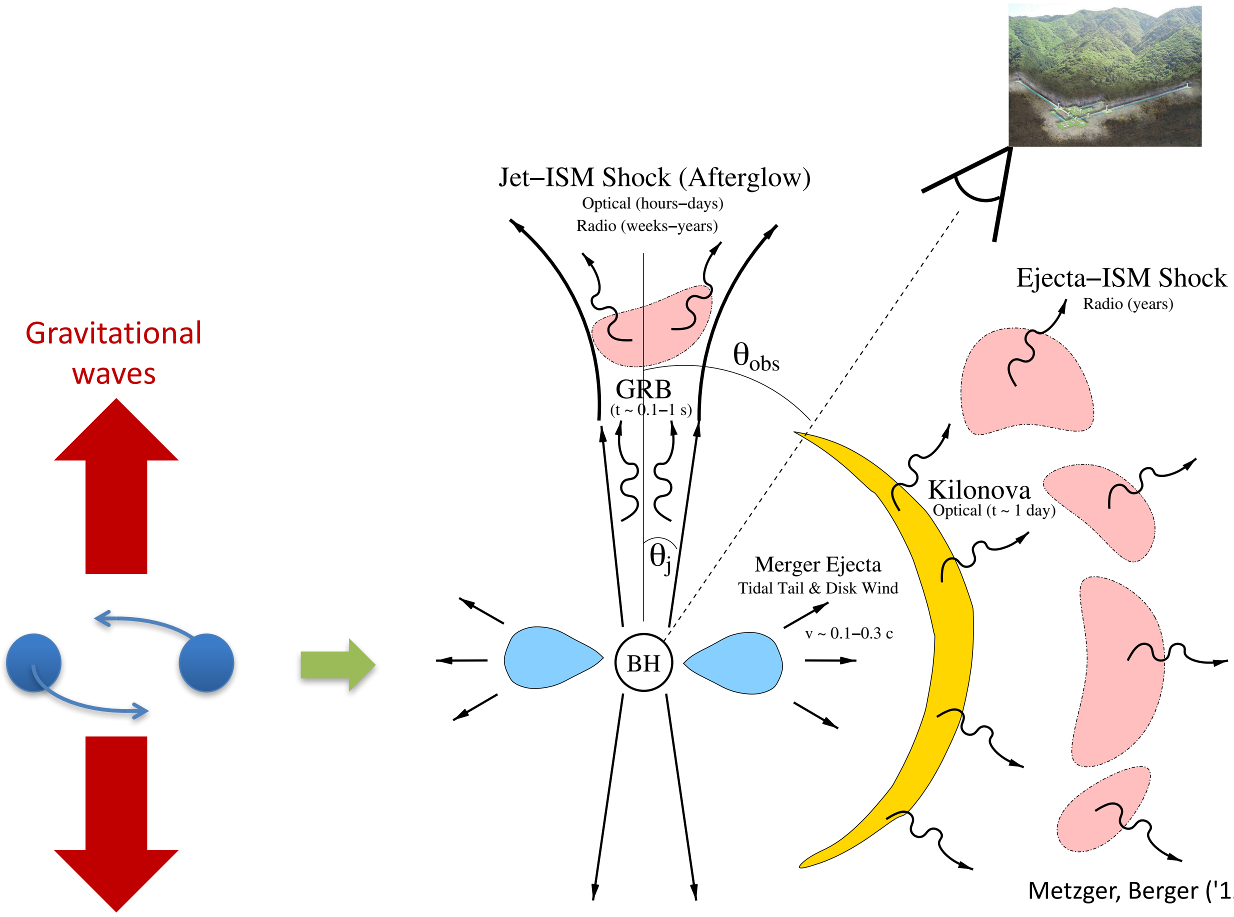

Metzger, Berger ('12)

Inclination angle accuracy

Fisher matrix
Waveform: FWF

Median of $\Delta\iota$ [rad]

(10,1.4) Msun @200Mpc
((1.4,1.4)Msun @200Mpc)

only $SNR_{network}$ >8

	all unknown	direction known	D_L and direction known
LHV	9.3deg (41.5deg)	8.3deg (34.4deg)	3.3deg (8.6deg)
LHVK	7.1deg (24deg)	6.5deg (21.0deg)	2.7deg (6.4deg)
LHVKI	5.8deg (15.5deg)	5.5deg (14.3deg)	2.2deg (5.1deg)

Arun, Tagoshi, Pai, Mishra PRD90, 024060 (2014)
Tagoshi, Mishra, Pai, Arun PRD90, 024053 (2014)

Distance and inclination angle are correlated.
If we know distance, inclination angle can be determined accurately.

c.f. GW170817（1σ）: $\iota \in [144, 180]$ deg
With Planck H0 : $\iota \in [157, 177]$ deg
With distance ladder H0 : $\iota \in [148, 166]$ deg

Expected science from LHVK

- Binary black hole merger
  Testing GR（QNM, No hair theorem, . . . ）
  Testing modified theory of gravity
- BNS, BH-NS mergers
  Relation to Gamma Ray burst
  EOS and internal structure
  Relation to r-process nucleosynthesis
- GW from Supernovae, Rotating neutron stars
- Test of GR (e.g., polarization modes with 4 detectors)

……

Characteristic of Japan

- Collaboration with EM(J-GEM,MAXI,CALET,…), and Neutrino group
- Collaboration with theory people(Numerical Relativity, Supernova explosion, …)

Yasufumi Kojima (Hiroshima Univ.),
“Slow rotation in GR ” (35+10)
[JGRG27 (2017) 112925]

Slow rotation in GR

Yasufumi Kojima/Hiroshima Univ.

JGRG27
Nov 27-Dec 1, 2017 Higashi-Hiroshima

Welcome to Hiroshima(Saijyo)

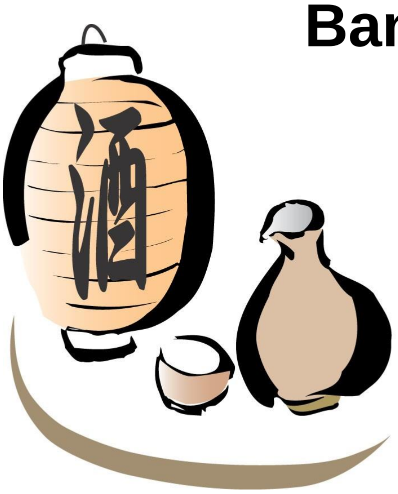

Banquet 6:00 P.M.
2nd floor

A year blessed with many events

The 2017 Nobel Prize in Physics

for decisive contributions to the LIGO detector and the observation of gravitational waves

Rainer Weiss

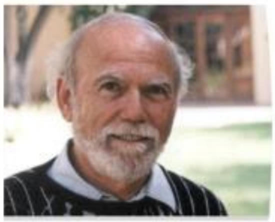

Barry C. Barish

Kip S. Thorne

The first pulsar was observed on November 28, 1967, by Bell Burnel & Hewish

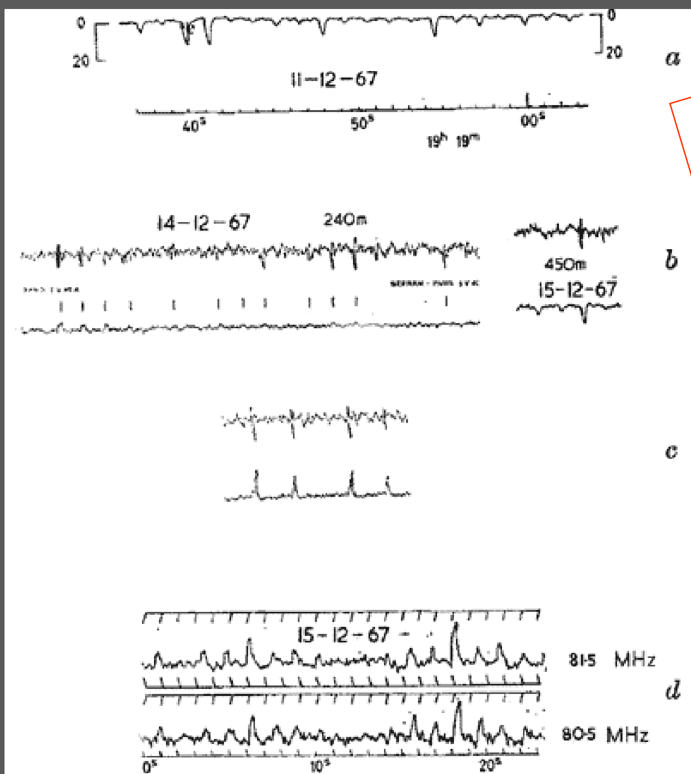

50thAnniversary

SN1987A 30th Anniversary
GW170817/GRB170817A

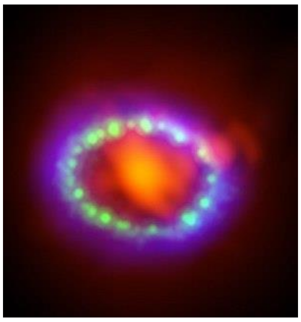

.....

NS

BH

GW

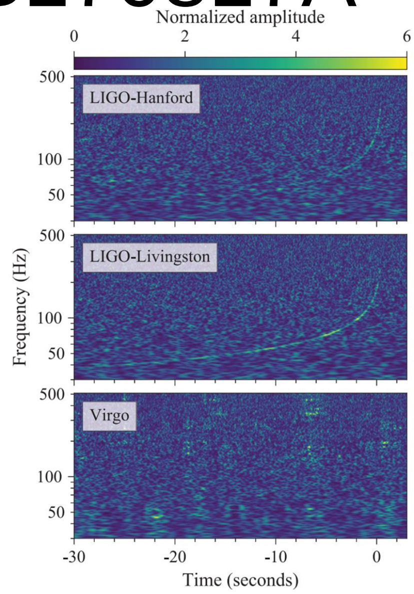

+Rotation

+Magnetic

Lense-Thirring effect

99 yeas ago

Dragging by a spinning object

Week field gravity

$$g_{\mu\nu} = \begin{bmatrix} -1-2\Phi_N + \dots & \vec{A} \\ \vec{A} & 1+\dots \end{bmatrix}$$

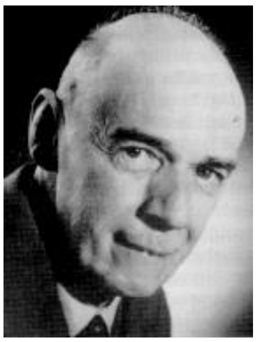

Josef Lense 1890-1985

Hans Thirring (1888 -1976)

Post-Newton

Wikipedia

$$\vec{A} = \vec{r} \times 2I\vec{\omega} / r^3$$

Confirmed by Gravity Probe B (GP-B) Experiment

Everitt et al. 2011

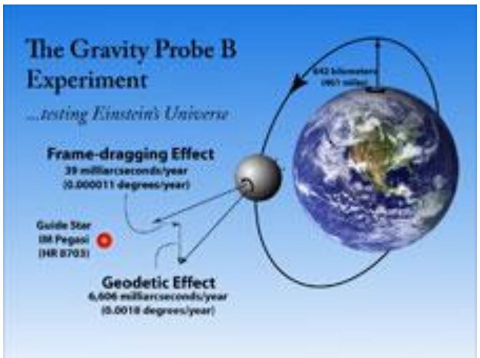

Dragging by Earth rotation

- Geodetic precession <0.5%
- LT precession <15%

in weak gravity and slow spin regime

$M/R \approx 10^{-10}$ $\Omega/\Omega_K \approx 10^{-3}$

Astronomical BH spin

e.g. CygX1

Somewhat controversy

High spin? X-ray spectrum fitting, Line profile

Extreme $a/M \approx 1$ Gou, L+ 2014

$a/M \approx 0.9$ Duro,R + 2016; Basak, R+ 2017

$a/M < 0.8$ Kawano, T+ 2017

Brady's talk

BH spin from GW?

Spin in a probable range

GW151226 14+7.5 Ms (0.25+0.5 → 0.74)

GW170104 31+19 Ms (-0.12+0.5 → 0.64)

GW170814 30+25 Ms (0+0.25 → 0.70)

Cosmological spin evolution of BH

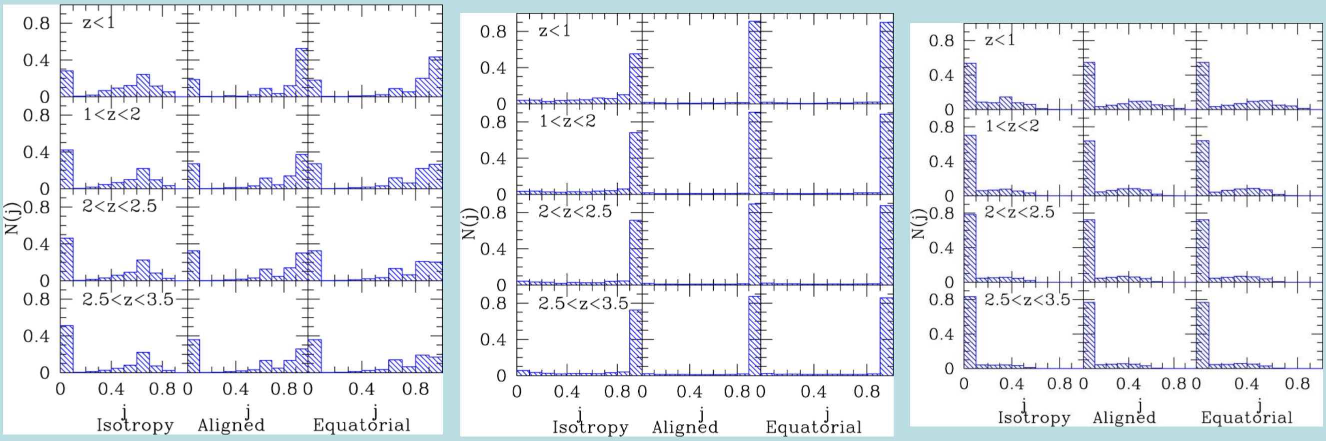

mergers only　　mergers + accretion　　mergers + chaotic accretion

Berti + 2008

Effect of BH spin

- Hydro-dynamical mechanism(accretion disk)

  Material K.E. → Outward radiation
- + magnetic field

MHD case is interesting/complicated

'BZ process'

EM field dominated case considered here

Origin of outward power in EM + GR system
- ✓ Extracting BH Rot. E.
- ✓ Producing EM power from Material K.E.

1 Extracting BH Rot.

Axi-symmetric stationary FF

→ outward flux at horizon when $0 < \Omega_F < \omega_H$

$$P_r = -\tfrac{1}{2}\int d\theta (S\Phi_{,\theta}) = -\tfrac{1}{2}(\Omega_F - \omega_H)\Omega_F \int d\theta G_{,\theta}{}^2 \varpi / \rho$$

$$P \approx B^2 (a/M)^2 M^2$$

$$\approx 10^{45} erg/s (M_9)^2 (B_4)^2$$

Comparison

$$P_{BZ} \approx B^2 (a/M)^2 r_H{}^2 c$$

$$P_{sync} \approx B^2 (\beta\gamma)^2 \sigma_T c$$

Event horizon is passive BC, determined by the exterior (behavior outside BH)

→ Where is the origin?

Ω / Φ problem

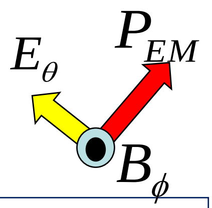

BH spin drags poloidal magnetic field (B_r, B_θ),so that toroidal field B_ϕ and electric field(E_r, E_θ) are induced.

Poynting flux $P_r \propto (E\times B)_r = E_\theta B_\phi$ is generated

$$P = -\oint_r d\theta d\phi (\sqrt{-g} T_t{}^r)$$

$$= -\tfrac{1}{2}\int d\theta (S\Phi_{,\theta}) \propto \int d\theta (E\times B)_r$$

Toroidal B

$$\vec{B} = \tfrac{1}{\varpi}(\vec{\nabla} G \times \vec{e}_\phi) + \tfrac{1}{\alpha\varpi} S \vec{e}_\phi$$

$$\vec{E} = -\tfrac{1}{\alpha}(\vec{\nabla}\Phi - \omega \vec{\nabla} G)$$

Produced by spin

Ideal MHD

$$\boxed{\vec{E}\cdot\vec{B} = 0 \Rightarrow \Phi(G), \vec{\nabla}\Phi = \Omega \vec{\nabla} G}$$

Where is origin of Φ or Ω ?

Toma's talk

2 Producing EM power in two fluids treatment

Radial magnetic field,
split-monopole

In spherically symmetric case,
radial accretion even for
charged fluids

$$\vec{E} = 0, \vec{j} = 0, \rho_e = 0$$

everywhere

$$\boxed{\begin{aligned} \rho_e &= e(n_+ - n_-) \\ j &= e(n_+ v_+ - n_- v_-) \end{aligned}}$$

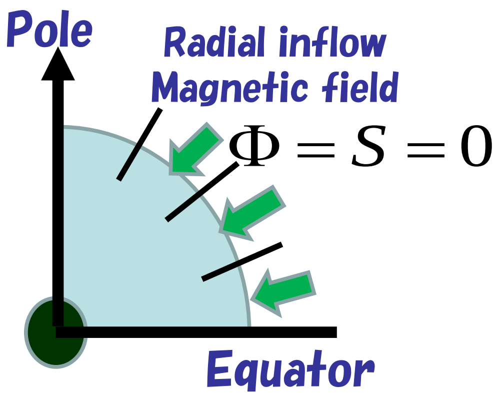

Electromagnetic power induced from pair plasma falling into a rotating black hole I arXiv:1509.04793 MNRAS,454(2015)3902
I II arXiv: 1711.07628

2 Producing EM power in two fluids treatment

Radial magnetic field,
split-monopole

In spherically symmetric case,
radial accretion even for
charged fluids

$$\vec{E} = 0, \vec{j} = 0, \rho_e = 0$$

everywhere

Taking into account B.H. spin (a) up to the first order

EM power is calculated

$$\boxed{P = -\tfrac{1}{2}\int d\theta(\delta S \delta \Phi_{,\theta}) \propto \int d\theta (E \times B)_r}$$

$$\boxed{\begin{aligned} \rho_e &= e(n_+ - n_-) \\ j &= e(n_+ v_+ - n_- v_-) \end{aligned}}$$

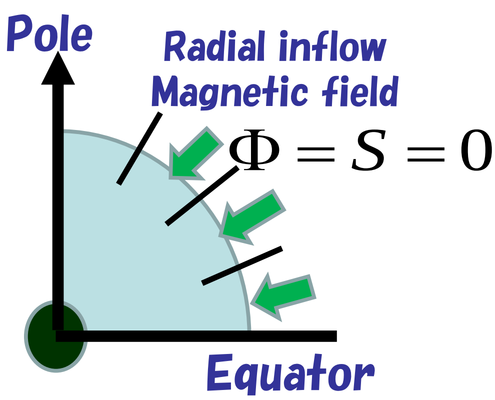

$\delta\Phi, \delta S \neq 0$?

Straightforward calculation

Stationary axially symmetric EM and flows determined by four functions G, Φ, F_+, F_-

- Spherical case as background
  -> Radial flow with no charge and current
- Linear pert. w.r.t. spin parameter a*
- Mode decomposition w.r.t. sym. $\delta G = 0$
  -> a coupled ord. diff. eqs for $\delta\Phi, \delta F (= \delta F_+, -\delta F_-)$
- Large/small number χ, κ involved
  -> WKB approximation $\propto \exp(i\kappa W(r))$
  Many solutions, e.g. Locally oscillating plasma
- Single out radiating mode relevant to EM power
  Results in next page

Micro and Macro scales

Large number between two scales

Two dimensionless number in cold pair plasma

$$\chi = \omega_B (GM/c^3) >> 1, \qquad \omega_B = eB/m$$

$$\kappa = \omega_p (GM/c^3) >> 1, \qquad \omega_p^2 = 4\pi e^2 n/m$$

A ratio χ/κ is moderate, but there is one large number at least.

Direct numerical integration is not easy.

訂正版 Perturbation eqs.

➢ Leading order eqs

$$\left[\kappa^{-2}\frac{d^2}{dx^2}+U_0-\kappa^{-2}U_2\right](xh)-\frac{\sqrt{2}k^{1/2}}{\kappa}\alpha^{-2}x^{-5/4}\left(x^{3/4}p\right)=\frac{4a_*}{\kappa^2\alpha^2x^4}, \quad (73)$$

$$\left[\kappa^{-2}\frac{d^2}{dx^2}-V_0+\kappa^{-2}V_2\right]\left(x^{3/4}p\right)-\frac{1}{k^{1/2}\kappa}\alpha^{-2}x^{-5/4}(xh)=\frac{2a_*}{k^{1/2}\kappa\alpha^2x^{13/4}}, \quad (74)$$

where $x=r/M$, and the potential terms are divided into

$$U_0=(1/\sqrt{2x}), U_2=2/(\alpha^2x^2), \quad (75)$$

$$V_0=\sqrt{2}x^{-3/2}\alpha^{-2}v, \quad v\equiv 1-k^{-1}(2x)^{-3/2}\alpha^2, \quad V_2=3/(16x^2). \quad (76)$$

small small source terms by BH spin

Straightforward calculation

Stationary axially symmetric EM and flows determined by four functions G,Φ,F_+,F_-

◆Spherical case as background

-> Radial flow with no charge and current

◆Linear pert. w.r.t. spin parameter a*

◆Mode decomposition w.r.t. sym. $\delta G=0$

-> a coupled ord. diff. eqs for $\delta\Phi,\delta F(=\delta F_+,-\delta F_-)$

◆Large/small number χ,κ involved

-> WKB approximation $\propto \exp(i\kappa W(r))$

Many solutions, e.g. Locally oscillating plasma

◆ Single out radiating mode relevant to EM power

Results in next page

Result

A coupled 2nd order diff eqs $\propto \exp(i\kappa W(r))$

Two types of solution in leading order
without rotational effect

I oscillatory II exponential

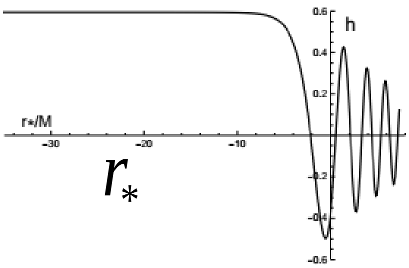

r_*

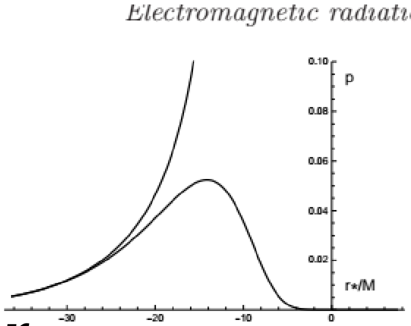

r_*

'Plasma wave' Long wavelength 'EM wave'

Inward Outward

EM power

Solution with source term $\propto a_*$

Outward EM flux through a radius

$$P_r = -\tfrac{1}{2}\int d\theta(\delta S\,\delta\Phi_{,\theta})$$

$P_{EM}(r)$

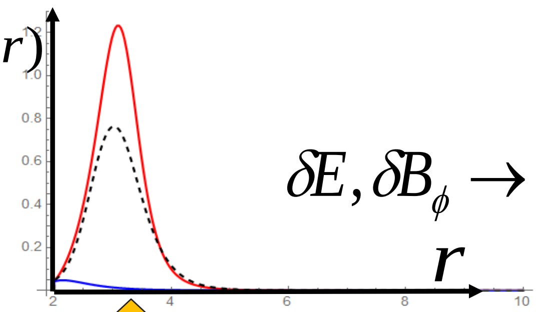

$\delta E, \delta B_\phi \to 0, r \to r_H$

r

Horizon

$r/M \approx 2.5$

EM generation mechanism

$$\delta({}_{Matter}T_t^{\,r}) \Rightarrow \delta({}_{EM}T_t^{\,r})$$

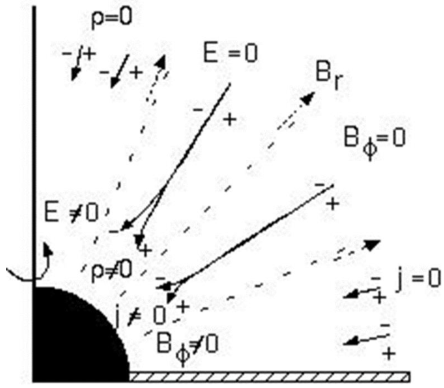

Lorentz force

$$\delta f^{\pm}_{\hat\theta} = \pm e(\delta E_{\hat\theta} + \delta v^{\pm}_{\hat\phi} B_{\hat r} - v_{\hat r}\delta B_{\hat\phi})$$
$$\pm \frac{m\kappa^2}{Mk}\left[\frac{k^{1/2}}{\kappa\alpha x}\left(h+\frac{2a_*}{x^3}\right) - \frac{\alpha}{2x^3}p + \frac{2^{1/2}k}{\alpha x^{3/2}}p\right]\sin\theta,$$

dragging by spin

→ charge separation →growth

$$\delta\rho_e, \delta j_p \neq 0 \Leftrightarrow \delta E, \delta B_\phi \neq 0$$

EM generation mechanism

$$\delta({}_{Matter}T_t^{\,r}) \Rightarrow \delta({}_{EM}T_t^{\,r})$$

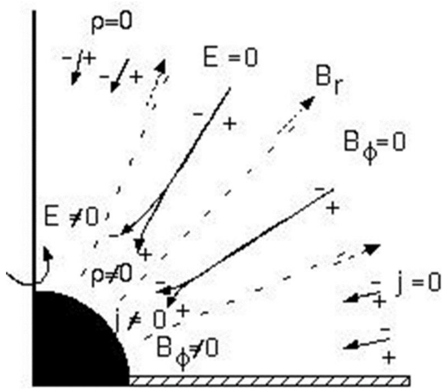

Lorentz force

$$\delta f^{\pm}_{\hat\theta} = \pm e(\delta E_{\hat\theta} + \delta v^{\pm}_{\hat\phi} B_{\hat r} - v_{\hat r}\delta B_{\hat\phi})$$
$$\pm \frac{m\kappa^2}{Mk}\left[\frac{k^{1/2}}{\kappa\alpha x}\left(h+\frac{2a_*}{x^3}\right) - \frac{\alpha}{2x^3}p + \frac{2^{1/2}k}{\alpha x^{3/2}}p\right]\sin\theta,$$

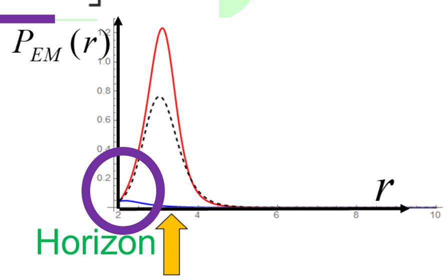

$r/M \approx 25$

→ growth →cancel

$$\delta E, \delta B_\phi \neq 0 \;\Rightarrow\; \delta E, \delta B_\phi \to 0$$

Summary

Canonical value

$$P_{BZ} = \tfrac{1}{6}(a_* B_n GM)^2 c^{-3} \approx 10^{45} erg/s (M_9)^2 (B_4)^2$$

New

$$P_{New} \approx P_{BZ} \times \kappa^{-2} << P_{BZ}$$

$$\boxed{\begin{array}{l} \delta B_\phi \propto \kappa^0 a_*, \delta\Phi \propto \kappa^{-2} a_* \\ \kappa = \omega_p (GM/c^3) >> 1, \omega_p^2 = 4\pi e^2 n/m \end{array}}$$

E field screened by plenty of plasma

Two-fluid effect is not so important in a realistic situation

For efficient Radiation

- Low density region elsewhere

  small $\kappa(\propto n)$

Or

- More complicated configuration

Or

- Rapid rotation

  No ergo-sphere in 1^{st} order BH spin

  EM field may grow inside ergo-sphere

Looking back on JGRG

26 yeas ago

- JGRG1 Dec. 4 - 6, 1991

"Perturbation of Black Space-time and Gravitational Wave"

- JGRG27 Nov. 27-Dec.1, 2017

"Electromagnetic power induced from pair plasma falling into a rotating black hole"

I greatly appreciate this meeting, and pray successful growth.

Party is ready in a moment

Thank you very much

After group photo

Banquet 6:00 P.M.
2nd floor

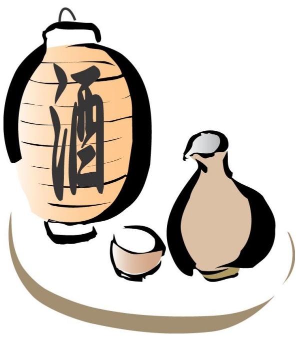

Thursday 30th

Invited lecture 10:00–11:00

[Chair: Misao Sasaki]

Robert R. Caldwell (Dartmouth Univ.),
"A unique and observable prediction in a toy model of axion gauge field inflation" (50+10)
[JGRG27 (2017) 113001]

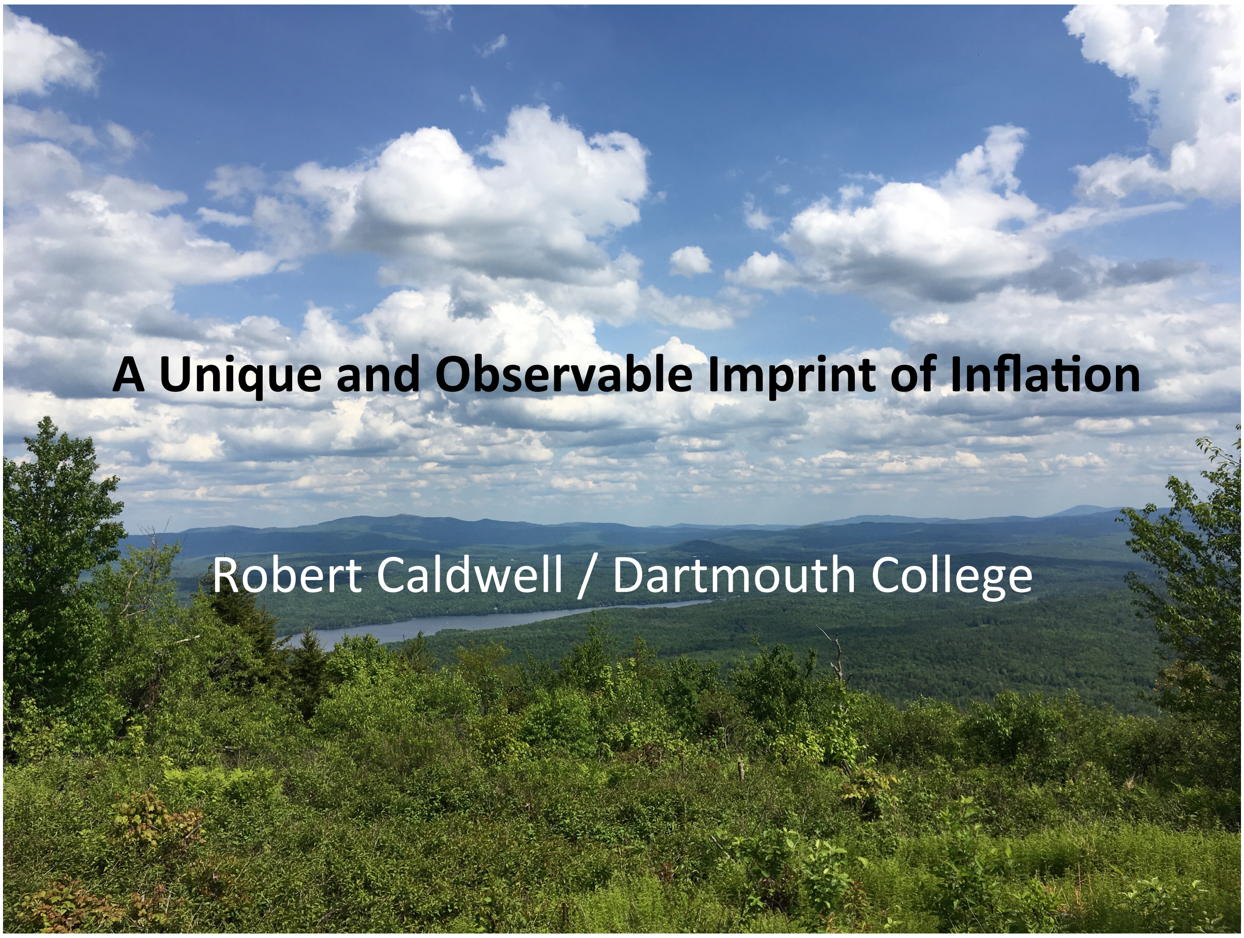

A Unique and Observable Imprint of Inflation

Robert Caldwell / Dartmouth College

Hanover,
New Hampshire

Dartmouth
College

students: Chris Devulder
Nina Maksimova
Jannis Bielefeld

Nordita 2017: "Inflation and the CMB"

Peter Adshead
Evangelos Sfakianakis

Marco Peloso
Ema Dimastrogiovanni

Eiichiro Komatsu
Azadeh Maleknejad

+RC

Cosmic Gauge Fields and Inflation

Novel Gravitational Behavior

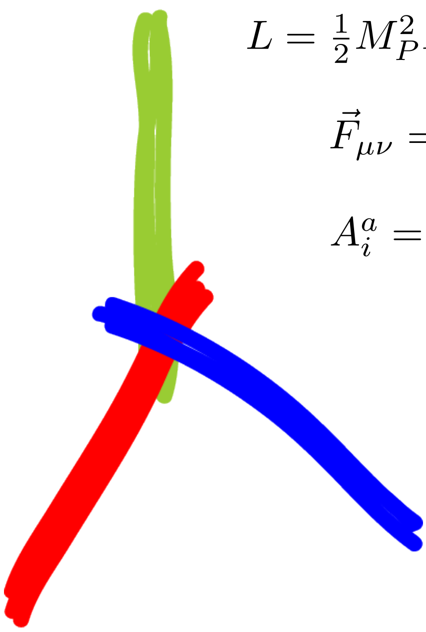

$$L = \frac{1}{2} M_P^2 R - \frac{1}{4} \vec{F}_{\mu\nu} \cdot \vec{F}^{\mu\nu}$$

$$\vec{F}_{\mu\nu} = \partial_\mu \vec{A}_\nu - \partial_\nu \vec{A}_\mu - g \vec{A}_\mu \times \vec{A}_\nu \quad \mathrm{SU(2)}$$

$$A_i^a = \phi(\tau) \delta_i^a \quad \text{flavor} - \text{space locked}$$

$$\delta g_{\mu\nu} = a^2(\tau) h_{\mu\nu}$$
$$\delta \vec{A}_\mu \cdot \vec{e}_\nu = a(\tau) y_{\mu\nu}$$

Devulder, Maksimova, RC 2016, 2017
Bielefeld, RC 2015, 2016
Gertsenshteyn 1961

GW-GF Oscillations

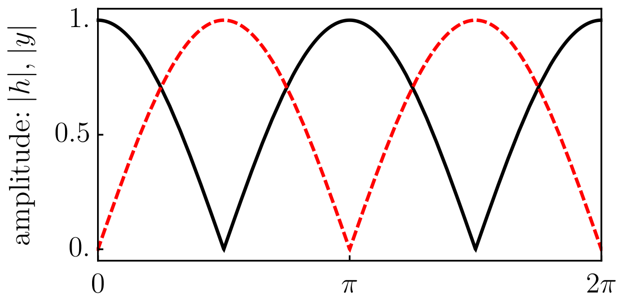

$\mathcal{N}=1$: gravitational wave, gauge field wave

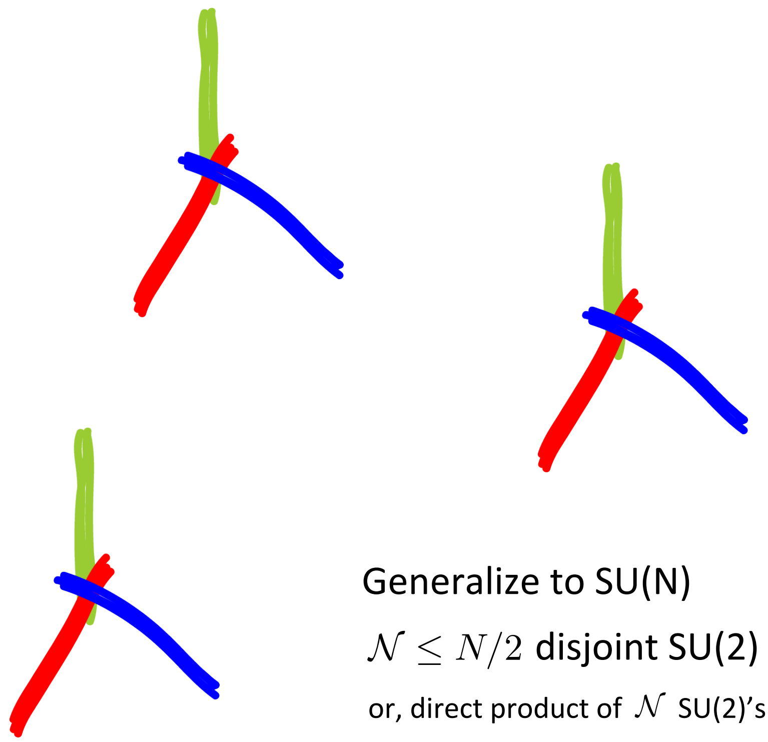

Generalize to SU(N)

$\mathcal{N} \leq N/2$ disjoint SU(2) subgroups

or, direct product of $\mathcal{N}$ SU(2)'s

GW-GF Oscillations

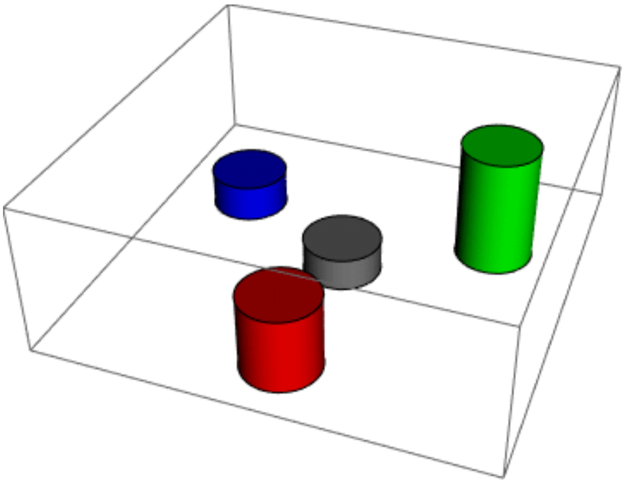

$\mathcal{N}=3$: gravitational wave, gauge field wave

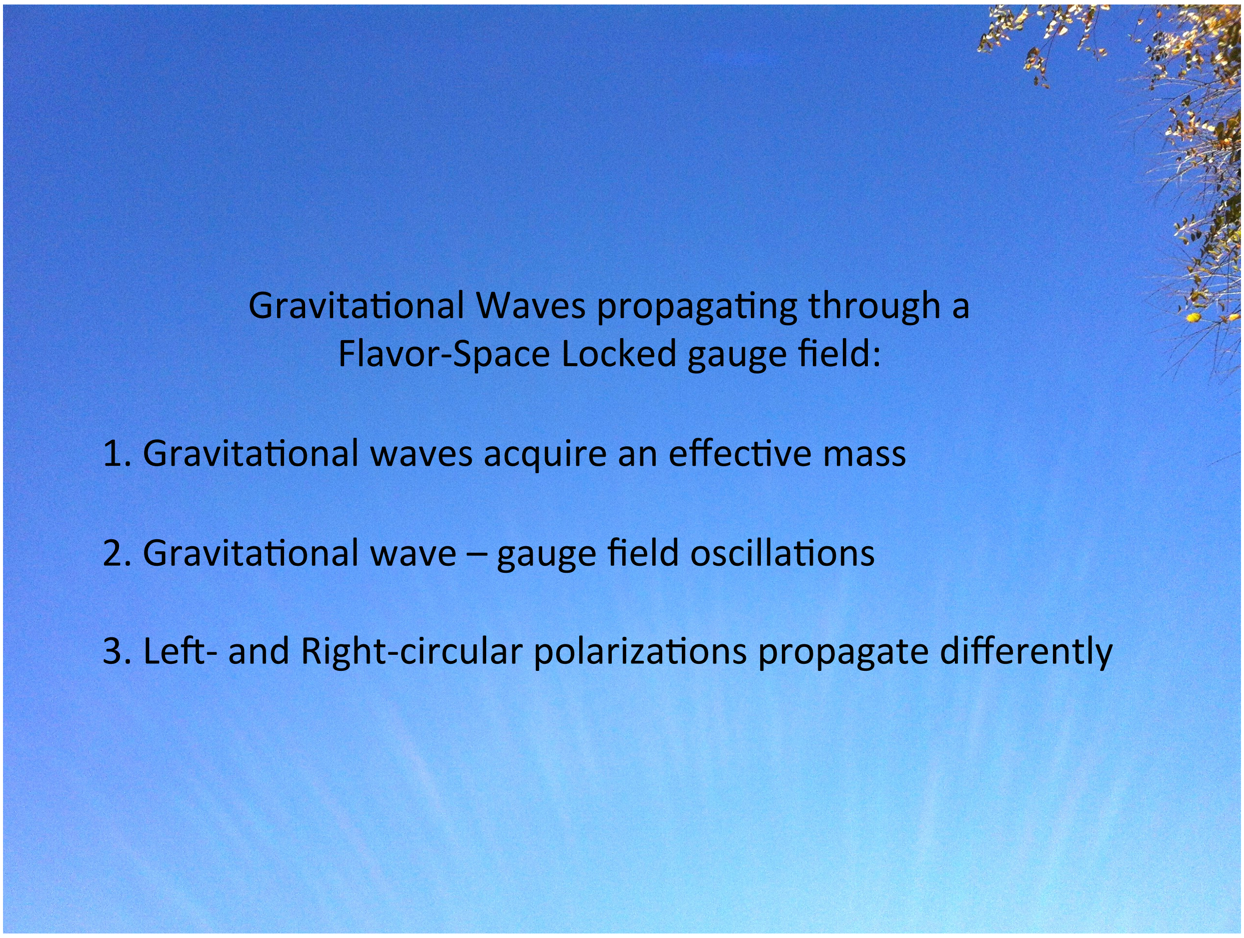

inspiration: Tadashi Tokieda
camera: Ralph Gibson

Models of Inflation

Chromo-Natural Inflation, Gauge-Flation

$$\mathcal{L} = \tfrac{1}{2}M_P^2 R - \tfrac{1}{2}(\partial\chi)^2 - V(\chi) - \tfrac{1}{4}F^a_{\mu\nu}F_a^{\mu\nu} + \tfrac{\chi}{M}F^a_{\mu\nu}\widetilde{F}_a^{\mu\nu}$$

$$V = \mu^4(1-\cos\chi/f) \to \tfrac{1}{2}m^2\chi^2$$

$$\mathcal{L} = \tfrac{1}{2}M_P^2 R - \tfrac{1}{4}F^a_{\mu\nu}F_a^{\mu\nu} + \kappa(F^a_{\mu\nu}\widetilde{F}_a^{\mu\nu})^2$$

Adshead & Wyman 2012;
Maleknejad & Sheikh-Jabbari 2011;
Dimastrogiovanni & Peloso 2013

Models of Inflation

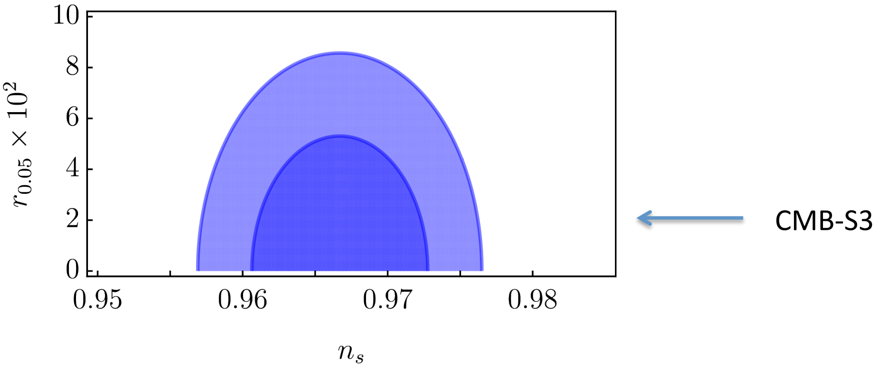

$n_s = 0.9667 \pm 0.0040\,(1\sigma)$ Planck 2016
$r < 0.07\,(95\%\,C.L.)$ BKP 2016

New: Toy Model of Inflation

$$\mathcal{L} = \frac{1}{2} M_P^2 R - \frac{1}{2}(\partial\chi)^2 - V(\chi) - \frac{1}{4} F^a_{\mu\nu} F_a^{\mu\nu} + \frac{\chi}{M} F^a_{\mu\nu} \widetilde{F}_a^{\mu\nu}$$

$$V = \mu^4 (1 - \cos \chi/f)^{n/2}$$

Devulder & RC 2017

$$V = \frac{1}{n} m^4 (\chi/m)^n$$

$$m,\, M \ll M_P$$

$$g \ll 1$$

Also, see: Dimastrogiovanni, Fasiello, Fujita 2017; Adshead, Martinec, Sfakianakis, Wyman 2016; Maleknejad 2016; Agrawal, Fujita, Komatsu 2017

New: Toy Model of Inflation

V is too steep to inflate: $\epsilon_V \gg 1$

But, for a wide range of initial conditions the coupling flattens the effective potential

$$\frac{\partial}{\partial \chi}\left(V - \frac{\chi}{M} F\widetilde{F}\right) \to 0$$

Inflation!

New: Toy Model of Inflation

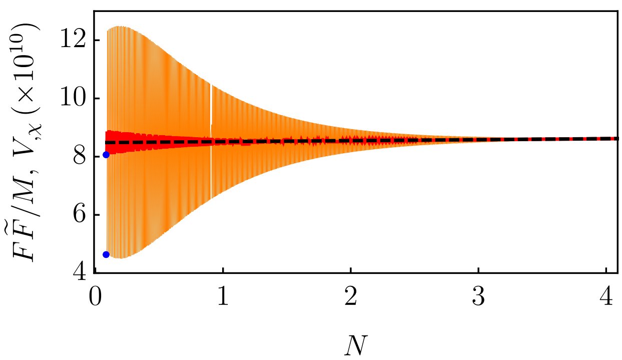

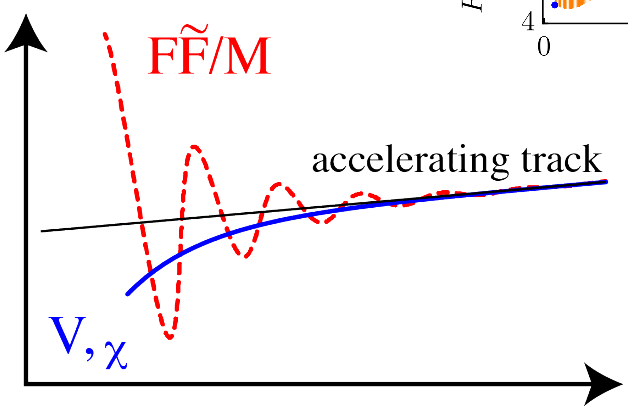

New: Toy Model of Inflation

Scalar Fluctuations: $\delta\chi$, δA

three dynamical modes, three constraints

Dominant mode sound speed: $c_s^2 = 1 - 2/\gamma$

Tensor modes: h, δA

four dynamical modes (2L, 2R)

Dispersion: $\omega_{LR}^2 = k^2 \mp \gamma k \mathcal{H}$

Extra: generalization from SU(2) to SU(N)

New: Toy Model of Inflation

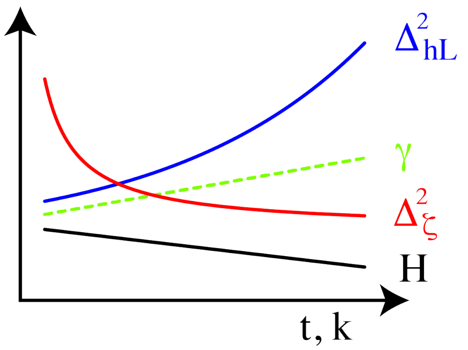

"accelerating track" picture

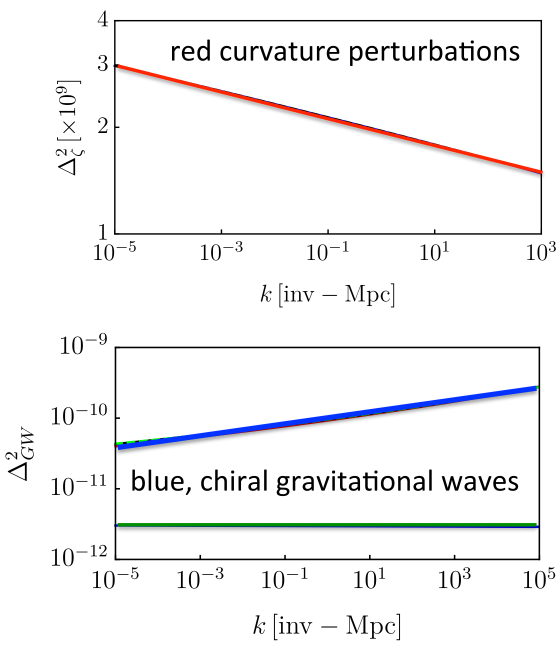

New: Toy Model of Inflation

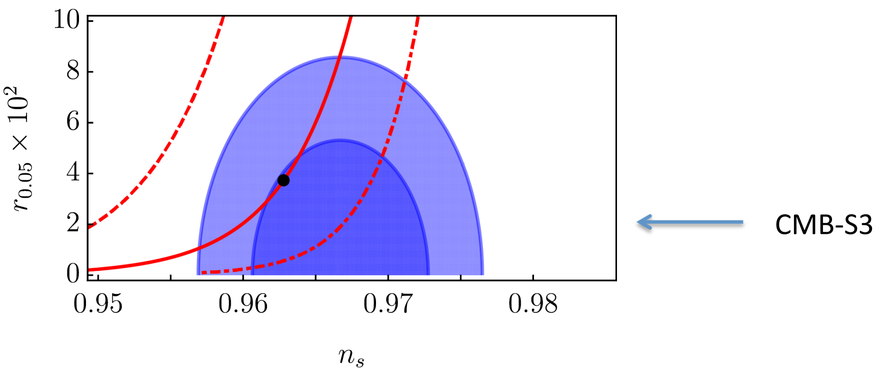

Red curves: family of potential models (n)
Location along curve: vary func(m, M, g) with fixed $\Delta_{\zeta,}$

New: Toy Model of Inflation

- Model does not obey standard slow roll relations
- Scalar spectrum amplitude fixes H_{end}, N-efolds
- Gauge field dominates at end of inflation: w=1/3
- Perturbations under control: $|\delta A| \ll A$
- No instability backreaction: $\Omega_{GW}, \Omega_{\delta A} \ll 1$

Chiral Gravitational Waves

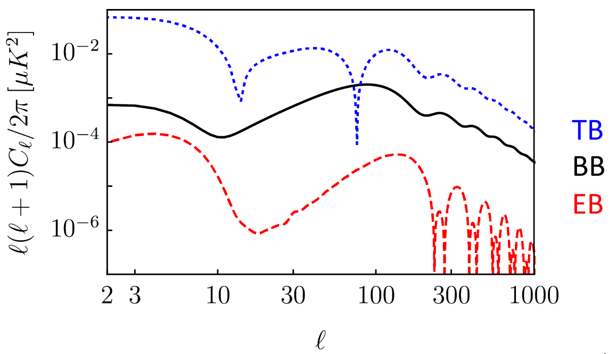

This model predicts

$$\Delta\chi = (P_L - P_R)/(P_L + P_R)$$

$$\Delta\chi \simeq 0.9$$

$$r_{0.05} = 0.035$$

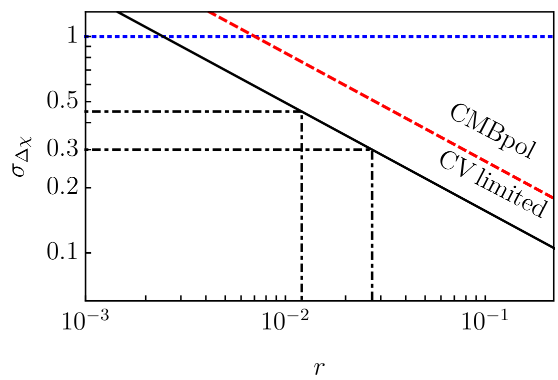

An additional, unique observable!

adapted from
Gluscevic & Kamionkowski 2010

other probes:
Jeong et al 2012, Masui et al 2017

CMB Polarization

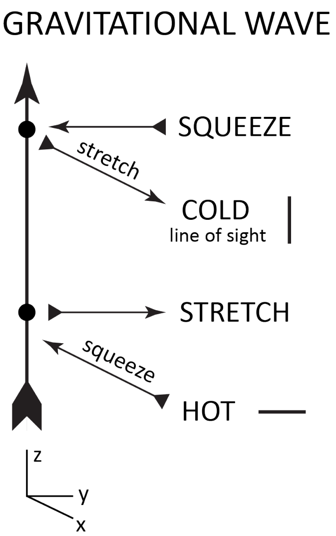

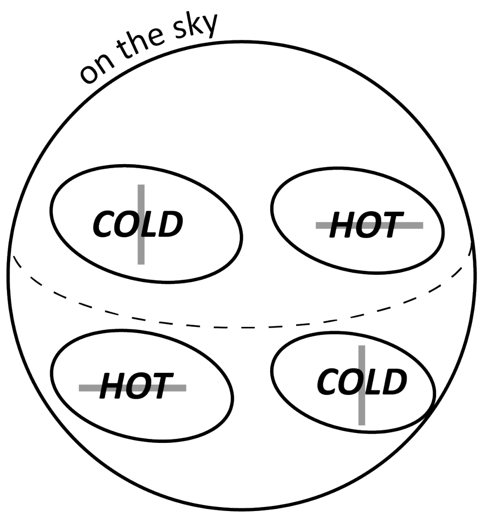

origin of the “B mode” pattern

CMB Polarization

Exactly what are we looking for?

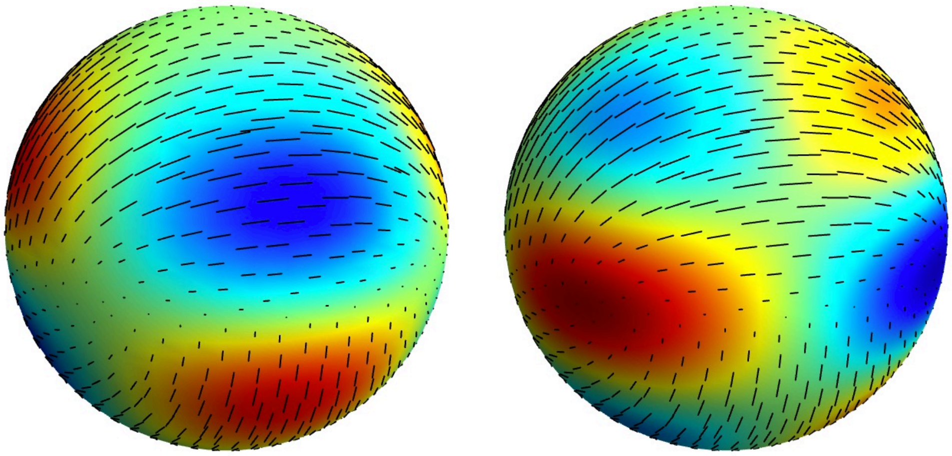

Temperature B Polarization

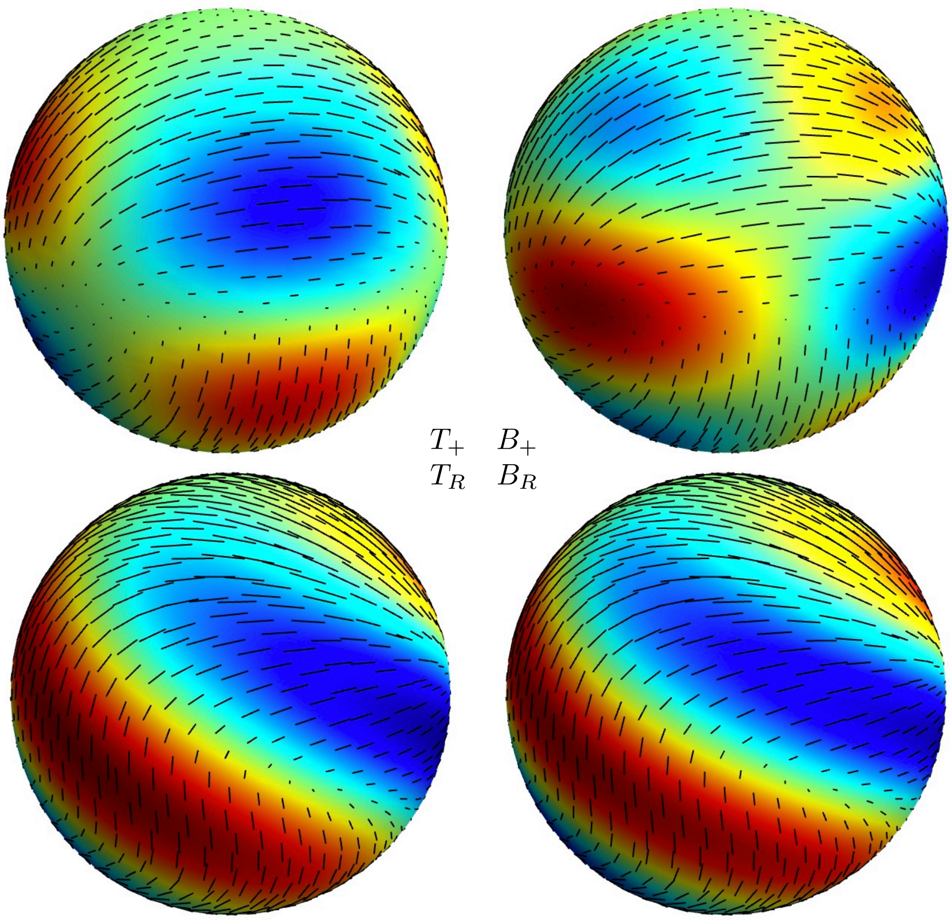

Chiral Gravitational Waves

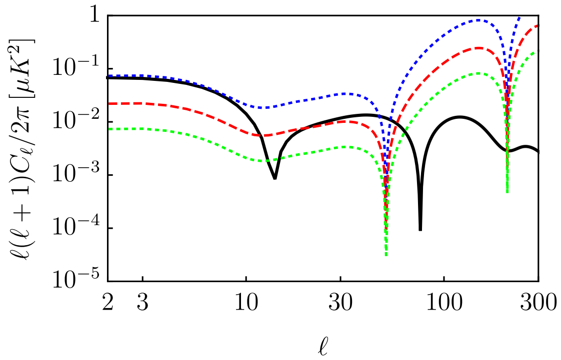

1^o
0.3^o
0.1^o

TB

Contamination from TE due to uncertainty in absolute polarization

TB

BB Lensing

BB

Noise*

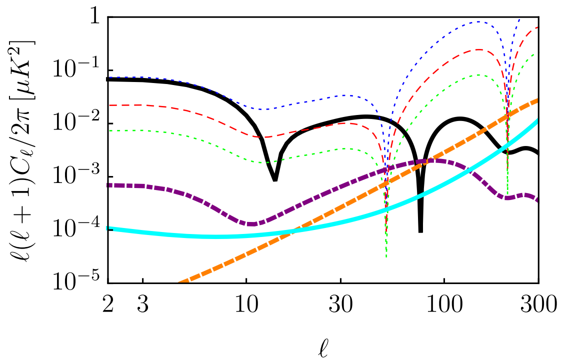

* Instrument noise, residual foregrounds on large scales

See Thorne et al, 2017; Shiraishi et al, 2016.

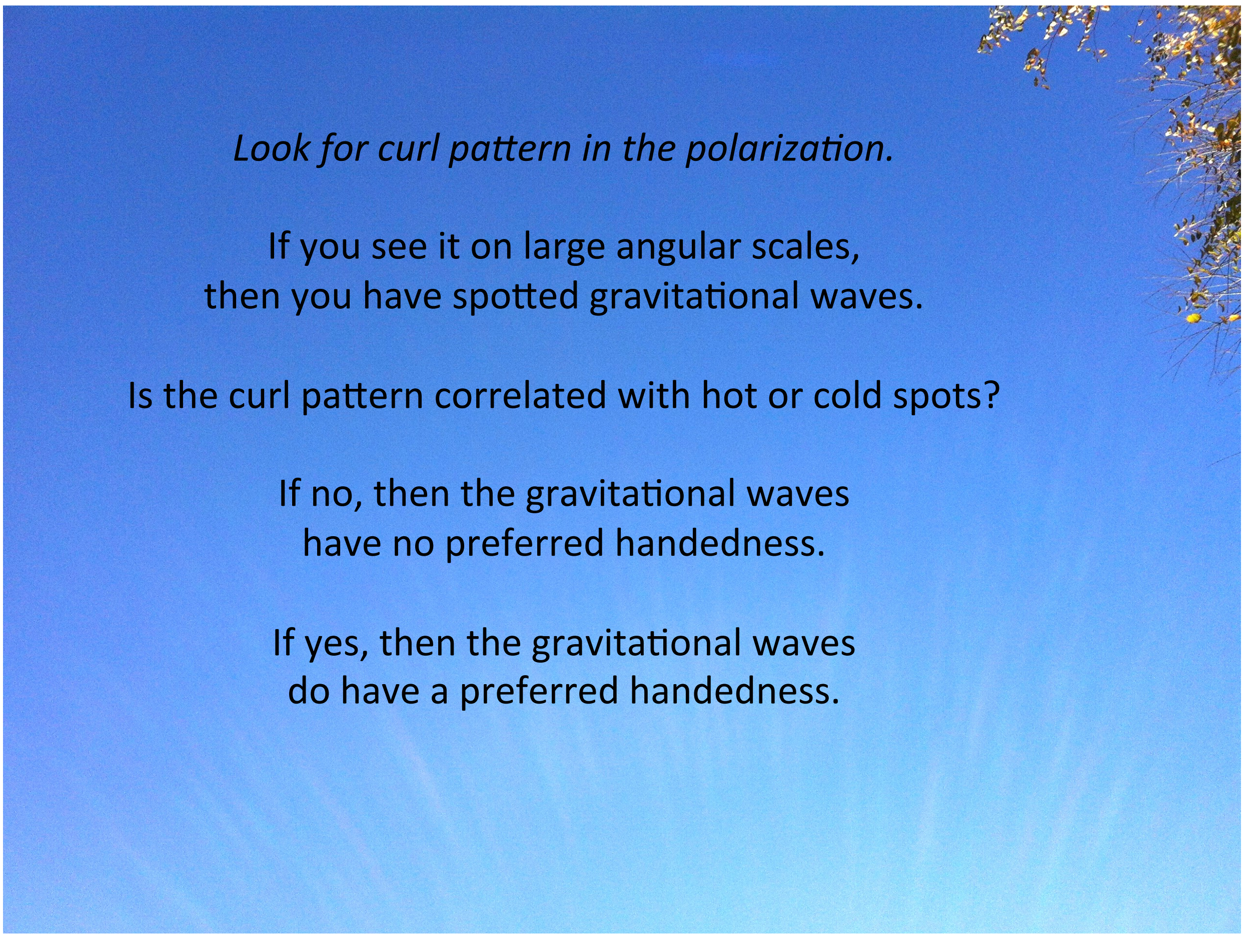

Leptogenesis

$$\nabla_\mu J^\mu_A = \frac{N_{R-L}}{24(16\pi^2)} R\widetilde{R}$$

Axial Current via Gravitational Anomaly

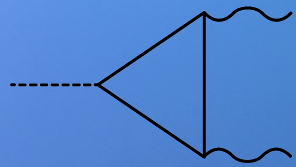

Kimura 1969
Delbourgo & Salam 1972
Eguchi & Freund 1976
Alvarez-Gaume & Witten 1984

Gibbons 1979

$$R\widetilde{R} \propto (\Delta_R^2 - \Delta_L^2)$$

Leptogenesis

$$N_{\ell ep} = \frac{N_{R-L}}{24(16\pi^2)} \int d^4x \sqrt{-g} R\widetilde{R}$$

leptons created,
with asymmetry

$$j_{\ell ep} = \sum_i \left(j_{e^i_L} + j_{\nu^i_L} + j_{e^i_R} \right)$$

Standard Model particles;
chiral biased particle production

Gravitational Leptogenesis: Alexander, Peskin, Sheikh-Jabbari 2006

+ Reheating: Adshead, Long, Sfakianakis 2017

Create the matter-antimatter asymmetry
from chiral gravitational waves

Leptogenesis

Sakharov Conditions

- Violation of baryon number
- CP violation
- Out of equilibrium

… satisfied

- Lepton number violated
- Inflaton/gauge field are parity-odd
- Inflation is far out of equilibrium

Leptogenesis

$$\eta \equiv \frac{n_B}{n_\gamma}$$
$$\simeq \frac{1}{7} \times \frac{28}{79} \times \frac{\langle n_\ell \rangle}{s}$$

Convert to baryon asymmetry by SM electroweak processes

Klebnikov & Shaposhnikov 1988

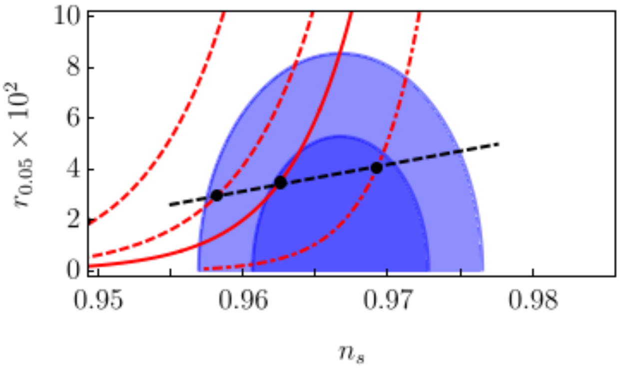

Planck 2016

$$\eta \simeq 6.1(\pm 0.04) \times 10^{-10}$$

CMB-S3 (3σ)

An observable within reach!

Leptogenesis

$$\eta \equiv \frac{n_B}{n_\gamma}$$
$$\simeq \frac{1}{7} \times \frac{28}{79} \times \frac{\langle n_\ell \rangle}{s}$$

Convert to baryon asymmetry
by SM electroweak processes

Klebnikov & Shaposhnikov 1988

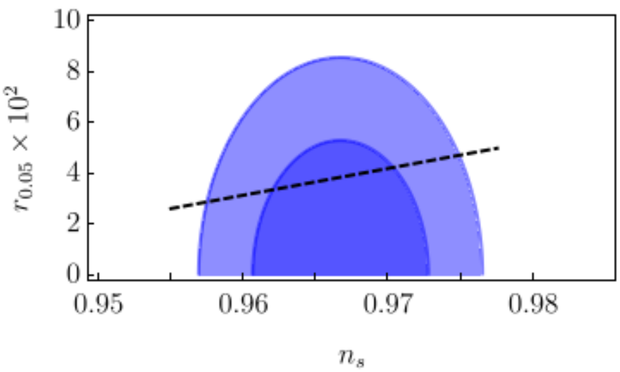

Planck 2016

$$\eta \simeq 6.1(\pm 0.04) \times 10^{-10}$$

CMB-S3 (3σ)

An observable within reach!

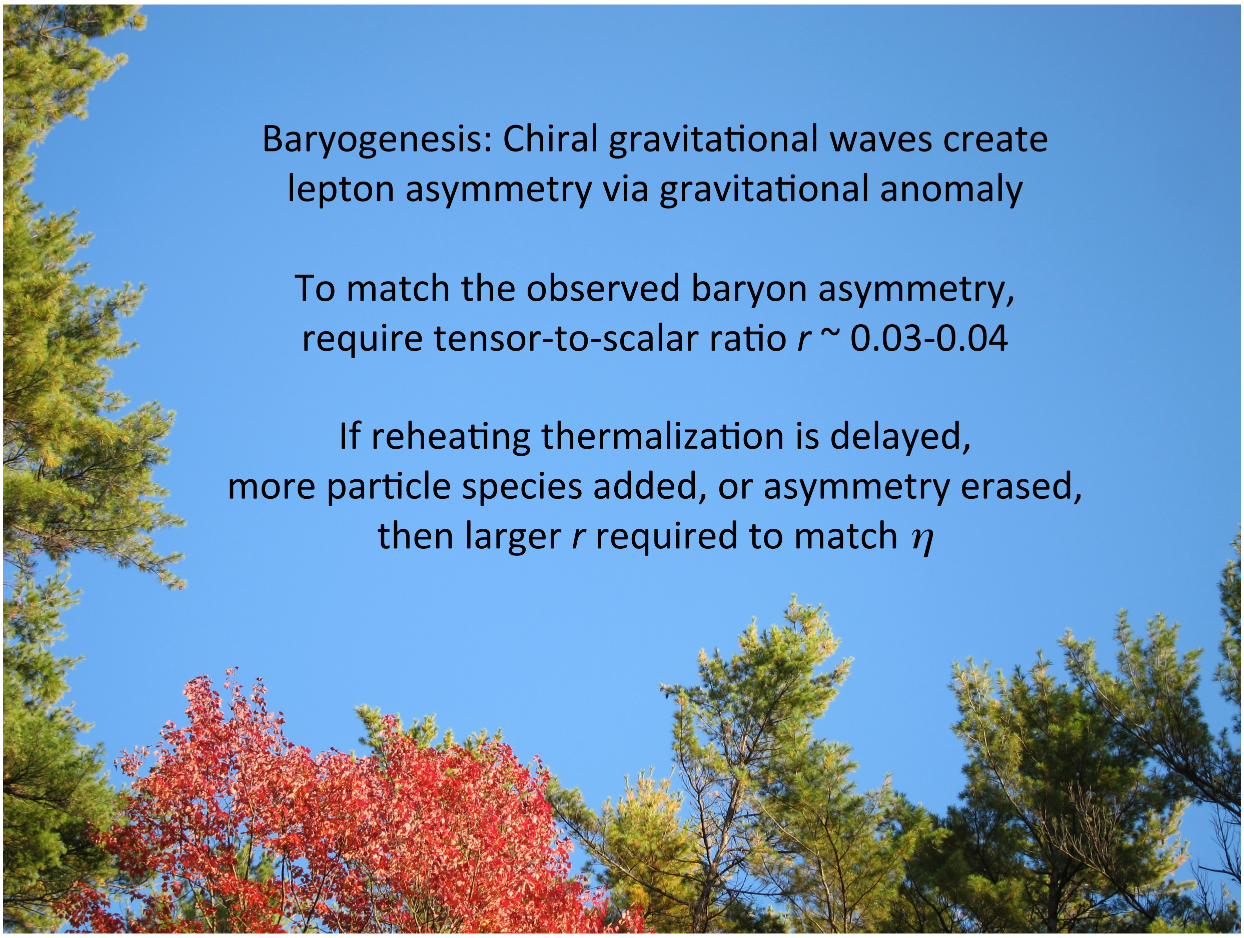

Use that Chiral, Blue-Tilted Spectrum

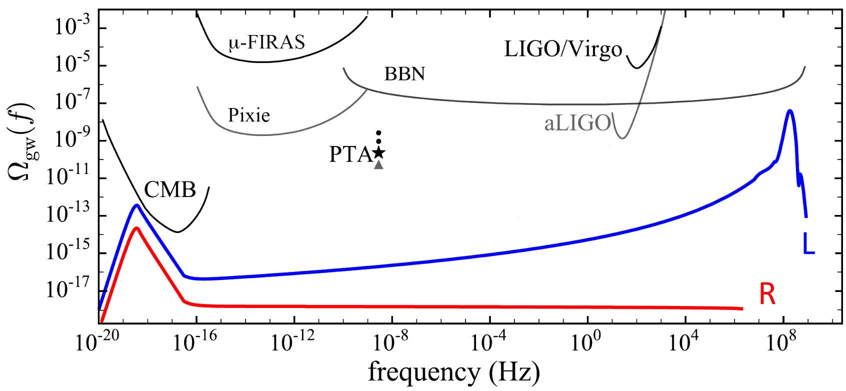

Lasky et al 2016
RC & Devulder 2017

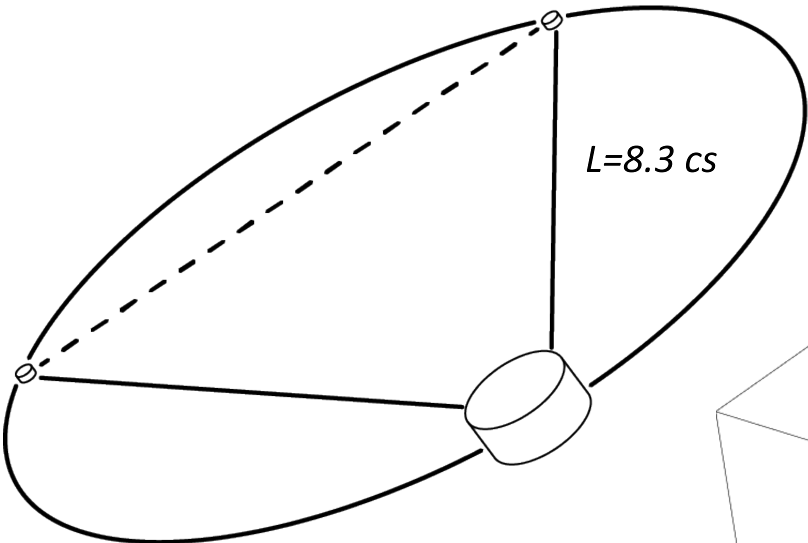

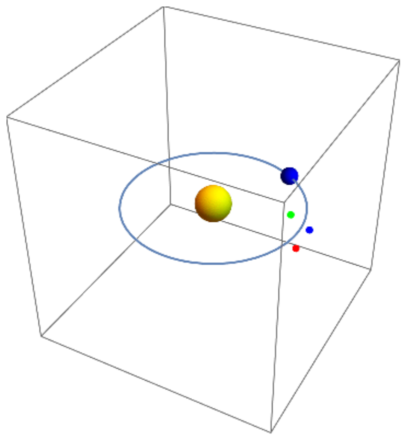

LISA:
Laser Interferometer Space Antenna

See sci.esa.int/lisa

Uncorrelated detectors help to see primordial gravitational waves.

Need two planes to distinguish V polarization.

Seto 2006
Seto & Taruya 2007
Crowder et al 2013
Kato & Soda 2015
Smith & RC 2016
Thorne et al 2017

BBO 2:
Big Bang Observer^2

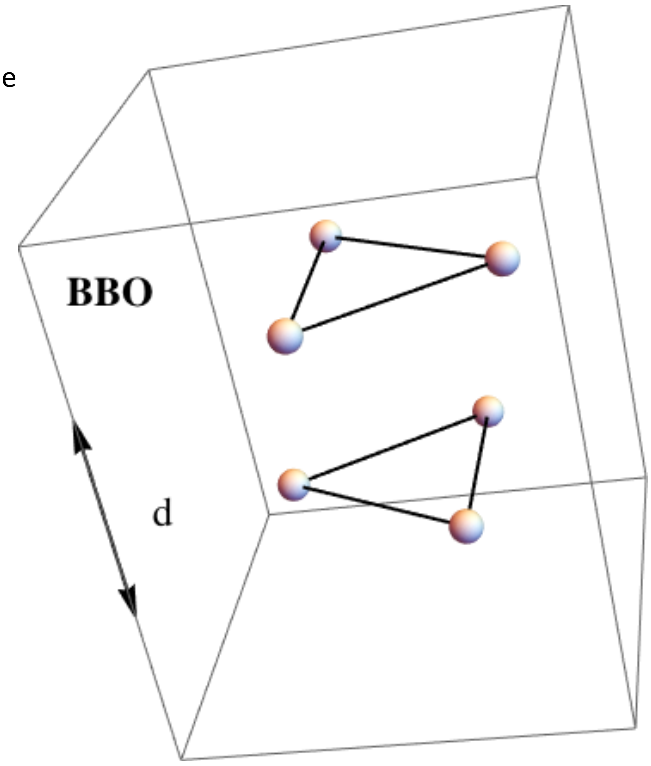

Chiral Gravitational Waves

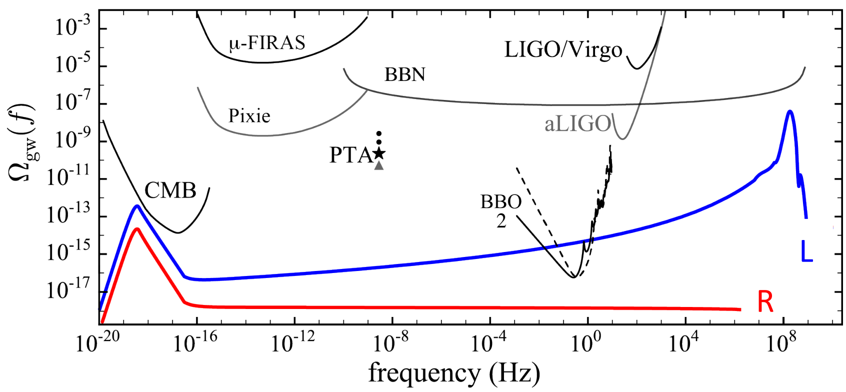

Lasky et al 2016
RC & Devulder 2017
In preparation: Smith & RC 2017

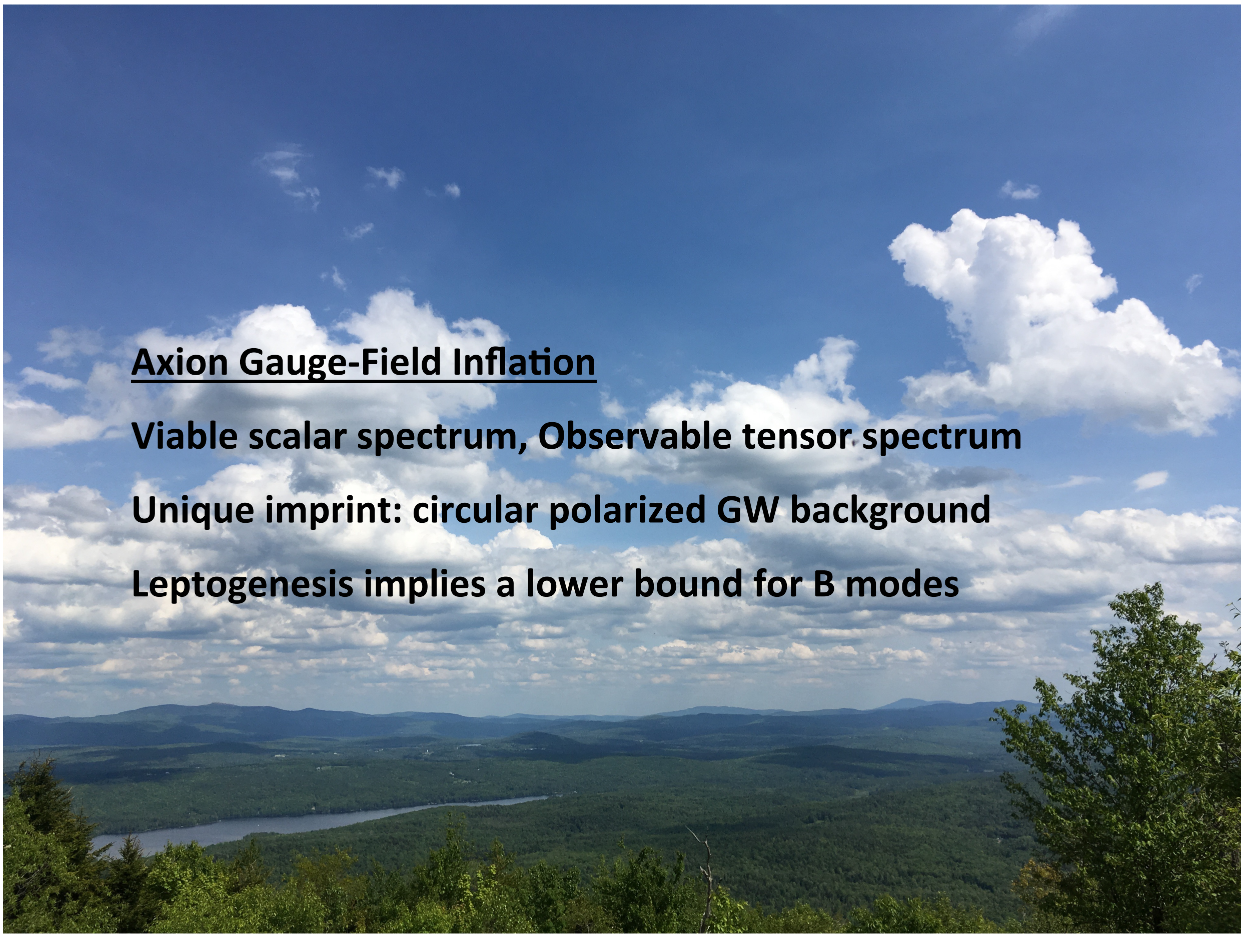
Axion Gauge-Field Inflation
Viable scalar spectrum, Observable tensor spectrum
Unique imprint: circular polarized GW background
Leptogenesis implies a lower bound for B modes

Session6a 11:15–12:30

[Chair Kei-ichi Maeda]

6a2. Seiga Sato (Waseda U.)
"Hybrid Higgs Inflation" (10+5)
[JGRG27 (2017) 113003]

Hybrid Higgs Inflation

† Seiga Sato

With †K.Maeda

†Waseda U.

17/11/30 JGRG27 @ Higashi Hiroshima, Kurara Hall

Introduction

the most of inflation models need a scalar field “inflaton” .

Standard Model

Scalar field＝Higgs field

Inflaton＝Higgs ?

Higgs inflation

$$L = \frac{M_p^2}{2}R - g^{\mu\nu}\frac{\partial_\mu h\,\partial_\nu h}{2} - V(h)$$

h : Higgs

$$V = \frac{\lambda}{4}(h^2 - v^2)^2$$

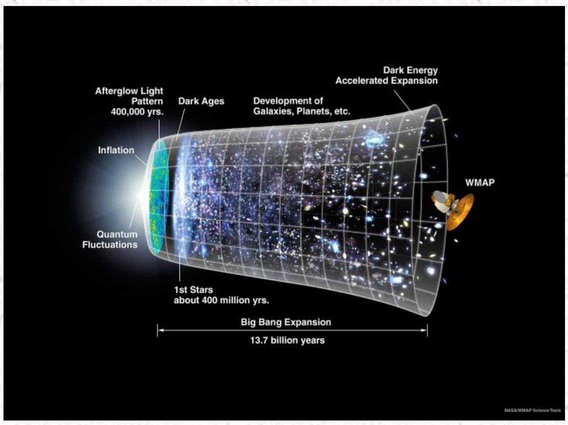

NASA(2006)

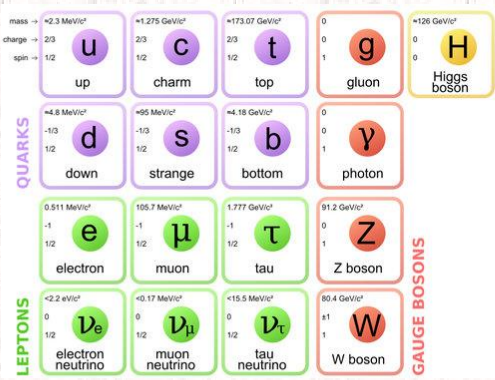

Wikimedia commons

Introduction

Problems of Higgs inflation

$\boxed{\lambda \simeq 10^{-13}}$

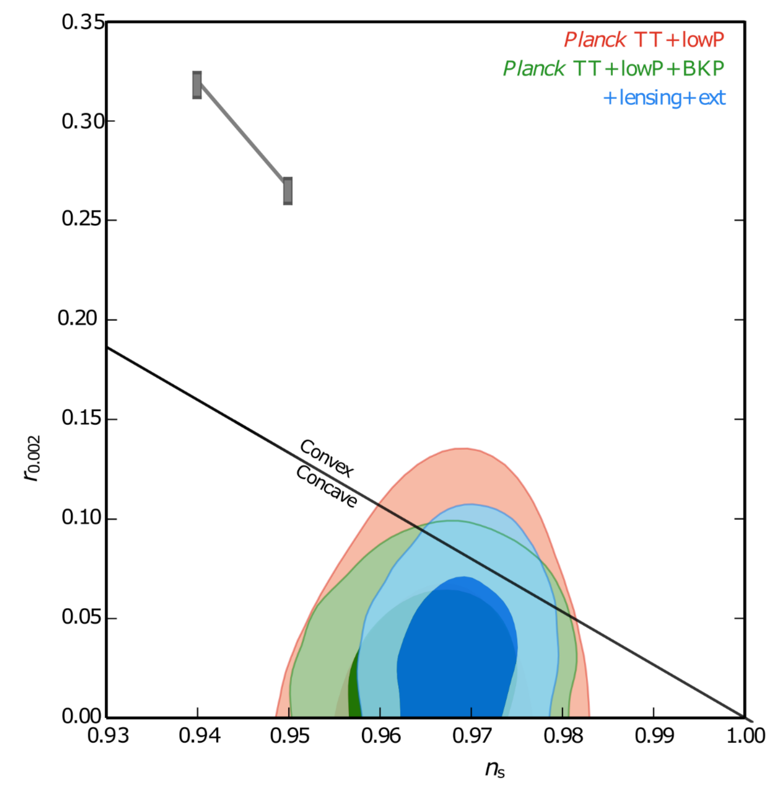

(Planck 2015 results)

Introduction

Higgs Inflation

- B.L.Spokoiny(1984)
- F.Bezrukov, D.Gorbunov &M.Shaposhnikov(2008)

$$S = \int dx^4 \sqrt{-g}\left[\left(\frac{M_p^2}{2} - \xi\frac{h^2}{2}\right)R - g^{\mu\nu}\frac{\partial_\mu h\,\partial_\nu h}{2} - V(h)\right]$$

Conformal transformation : $\bar{g}_{\mu\nu} \to g_{\mu\nu}$

$$g_{\mu\nu} \equiv \left(1 - \xi\frac{h^2}{M_p^2}\right)^{-1} \bar{g}_{\mu\nu}$$

K.Maeda&T.Futamase(1989)

$$S = \int dx^4 \sqrt{-\bar{g}}\left[\frac{M_p^2}{2}\bar{R} - \bar{g}^{\mu\nu}\frac{\partial_\mu \phi\,\partial_\nu \phi}{2} - U(\phi)\right]$$

$$\boxed{\frac{d\phi}{dh} \equiv \frac{1}{1 - \xi\frac{h^2}{M_p^2}}\sqrt{1 + (6\xi - 1)\xi\frac{h^2}{M_p^2}}}$$

Introduction

New Higgs Inflation

- C.Germani&A.Kehagias (2010)
- C.Germani, Y.Watanabe &N.Wintergerst(2014)

$$S = \int dx^4\sqrt{-g}\left[\frac{M_p^2}{2}R - \left(g^{\mu\nu} - \frac{G^{\mu\nu}}{M^2}\right)\frac{\partial_\mu h\,\partial_\nu h}{2} - V(h)\right]$$

Disformal transformation: $\bar{g}_{\mu\nu} \to g_{\mu\nu}$

$$g_{\mu\nu} \equiv \left(\bar{g}_{\mu\nu} + \frac{\partial_\mu h\,\partial_\nu h}{2M^2M_p^2}\right)$$

S.D.Vita&C.Germani(2016)

$$S = \int dx^4\sqrt{-\bar{g}}\left[\frac{M_p^2}{2}\bar{R} - \bar{g}^{\mu\nu}\frac{\partial_\mu\phi\,\partial_\nu\phi}{2} - U(\phi) + \left(\cancel{\text{higher derivative terms}}\right)\right]$$

$$\boxed{\frac{d\phi}{dh} \equiv \sqrt{1 + \frac{\lambda}{4M^2}\frac{h^4}{M_p^2}}}$$

slow-roll

How long is this valid?

Introduction

motivations

- when the observable quantities are estimated, Can the approximation be valid?

The cosmological perturbations are invariant under the disformal trans.

- M.Minamitsuji (2014)
- S.Tsujikawa (2015)
- Y.Watanabe, A.Naruko & M.Sasaki(2015)
- H.Motohashi, J.White(2015)

- Are there any other Higgs inflation models preferred by the CMB observations more ?

$$r \simeq \begin{cases} 10^{-5} & \text{(Higgs inflation)} \\ 0.1 & \text{(New Higgs inflation)} \end{cases}$$

Hybrid Higgs Inflation

R.Easther, K.Maeda, N.Musoke, S.S

$$S=\int dx^4\sqrt{-g}\left[\left(\frac{M_p^2}{2}-\xi\frac{h^2}{2}\right)R-\left(g^{\mu\nu}-\frac{G^{\mu\nu}}{M^2}\right)\frac{\partial_\mu h\,\partial_\nu h}{2}-V(h)\right]$$

$$V(h)=\frac{\lambda}{4}(h^2-v^2)^2\cong\frac{\lambda}{4}h^4 \qquad (\lambda\approx 0.1)$$

Disformal transformation: $g_{\mu\nu}\to\bar{g}_{\mu\nu}$

$$g_{\mu\nu}\equiv\left(1-\xi\frac{h^2}{M_p^2}\right)^{-1}\left(\bar{g}_{\mu\nu}+\frac{\partial_\mu h\,\partial_\nu h}{2M^2M_p^2}\right)$$

$$S=\int dx^4\sqrt{-g}\left[\frac{M_p^2}{2}\bar{R}-\bar{g}^{\mu\nu}\frac{\partial_\mu\phi\,\partial_\nu\phi}{2}-U(\phi)+\left(\cancel{\text{higher derivative terms}}\right)\right]$$

$$\boxed{\frac{d\phi}{dh}\equiv\frac{1}{1-\xi\frac{h^2}{M_p^2}}\sqrt{1+(6\xi-1)\xi\frac{h^2}{M_p^2}+\frac{\lambda}{4M^2}\frac{h^4}{M_p^2}}}$$

slow-roll

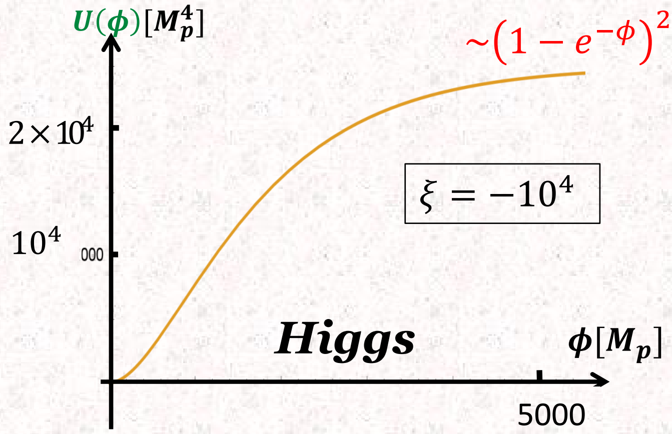

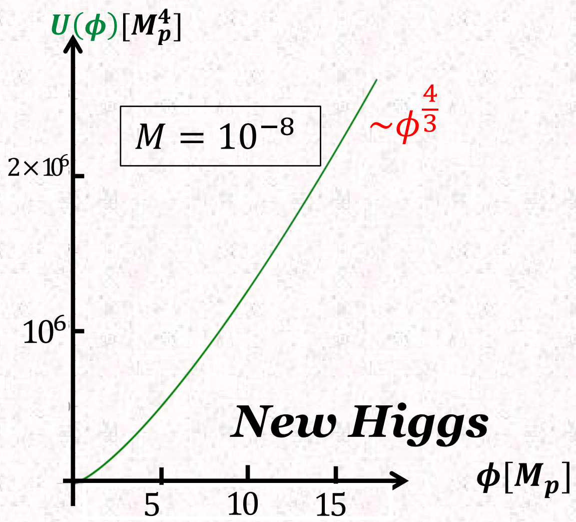

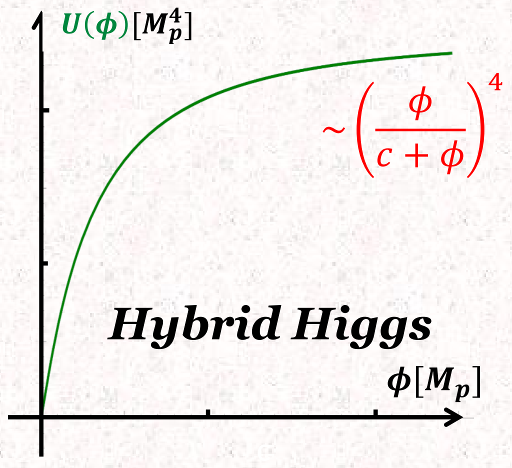

$M=10^{-8}$ $\qquad$ $\xi=-10^4$

Basic equations

$$
\begin{cases}
H^2 = \dfrac{1}{3(M_P^2 - \xi h^2)}\left[\left(1+\dfrac{9H^2}{M^2}\right)\dfrac{\dot{h}^2}{2} + 6\xi h\dot{h}H + V\right] \\[2ex]
\left(1+\dfrac{3H^2}{M^2}\right)\ddot{h} + 3H\left(1+\dfrac{3H^2+2\dot{H}}{M^2}\right)\dot{h} + 6\xi\left(\dot{H}+2H^2\right)h + \dfrac{dV}{dh} = 0 \\[2ex]
(3H^2+2\dot{H})(M_P^2-\xi h^2) + \left(1-\dfrac{3H^2}{M^2}\right)\dfrac{\dot{h}^2}{2} - V - \dfrac{d}{dt}\left[\dfrac{H\dot{h}^2}{M^2} + 2\xi h\dot{h}\right] - 2\xi H h^2 = 0
\end{cases}
$$

$$
\begin{cases}
\bar{H}^2 = \dfrac{1}{3M_P^2}\left[\dfrac{\phi'^2}{2} + U\right] \\[2ex]
\phi'' + 3\bar{H}\phi' + \dfrac{dU}{d\phi} = 0 \\[2ex]
3M_P^2(\bar{H}^2 + \bar{H}') = \dfrac{\phi'^2}{2} - U
\end{cases}
\qquad \boxed{{}' = \dfrac{d}{d\bar{t}}}
$$

Hybrid Higgs Inflation

Hubble parameter

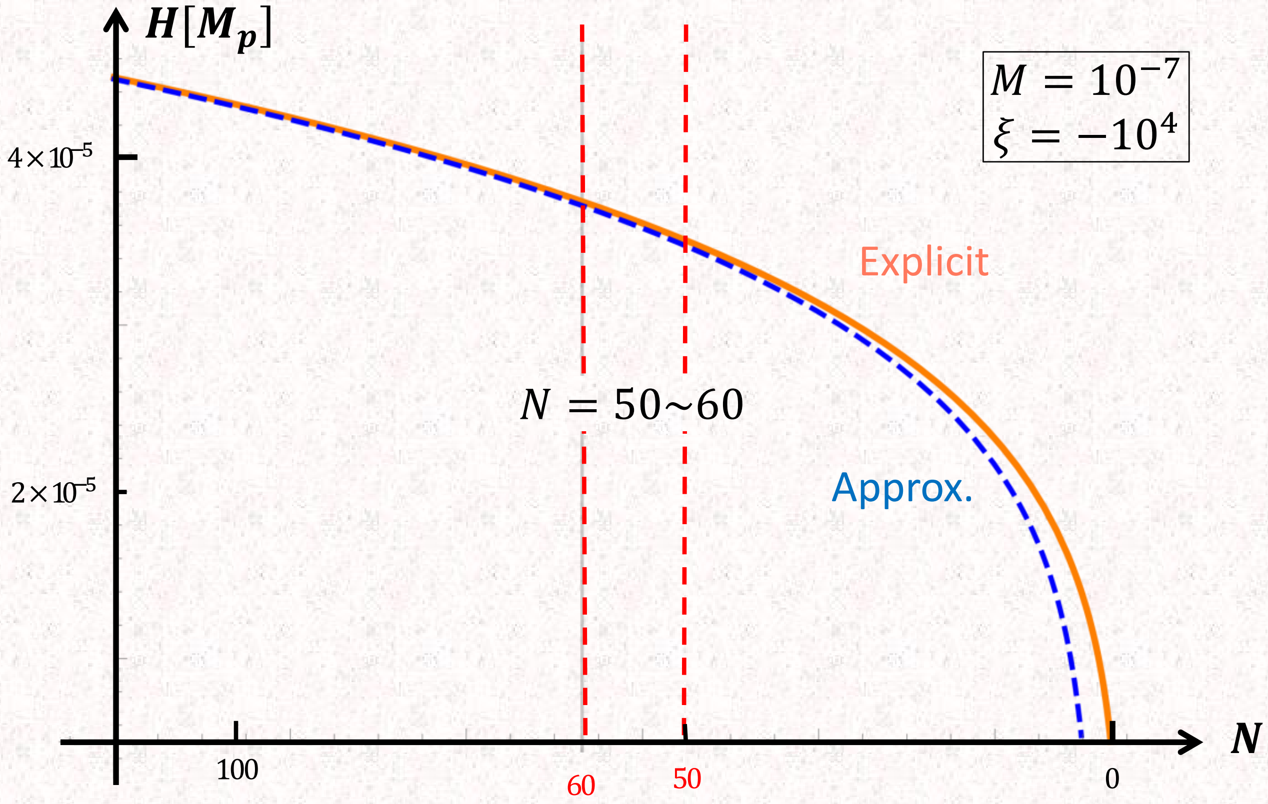

Hybrid Higgs Inflation

Phase diagram

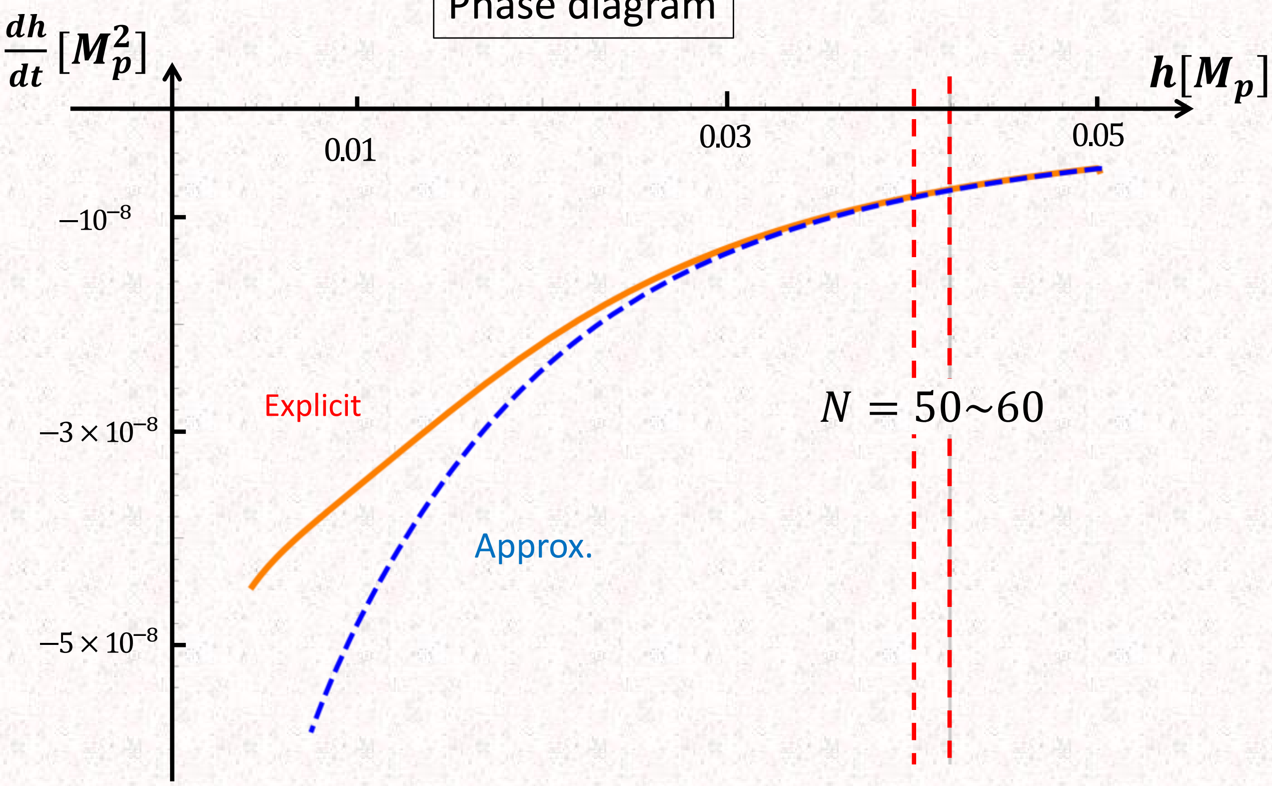

Hybrid Higgs Inflation

cosmological perturbations

slow-roll parameters

$$\epsilon = \frac{1}{2}\left(\frac{1}{U}\frac{dU}{d\phi}\right)^2 ,\eta = \frac{1}{U}\frac{d^2U}{d\phi^2}$$

Observavble quantities

$$\begin{cases} n_s \simeq 1 - 6\epsilon + 2\eta \,, r \equiv \dfrac{P_T}{P_\zeta} \simeq 16\epsilon \\ P_\zeta \simeq \dfrac{1}{24\pi^2 M_p^4}\dfrac{U}{\varepsilon} \approx 10^{-9} \end{cases}$$

Advantages of disformal truncation

Constraint on the relation between M and ξ

$$\begin{cases} P_\zeta \simeq \dfrac{1}{24\pi^2 M_p^4}\dfrac{U}{\varepsilon} = \dfrac{\lambda^2 h^{10} + 4\lambda M^2\xi(6\xi-1)h^8 + 4\lambda M^2 h^6}{3072\pi^2 M_p^4 (1-\xi h^2)^2} \approx 10^{-9} \\ N \simeq \dfrac{1}{M_p^2}\displaystyle\int_{\phi_{end}}^{\phi_N} \dfrac{U}{U'}\, d\phi \simeq \dfrac{1}{64 M_p^2 M^2 \xi^3}[\lambda\xi^2 h^4 \\ \qquad + (8M^2\xi^3(6\xi-1) + 2\lambda\xi)h^2 \\ \qquad + 2(\lambda + 24M^2\xi^3)\ln[1-\xi h^2]] \\ \qquad \approx 60 \end{cases}$$

cosmological perturbations

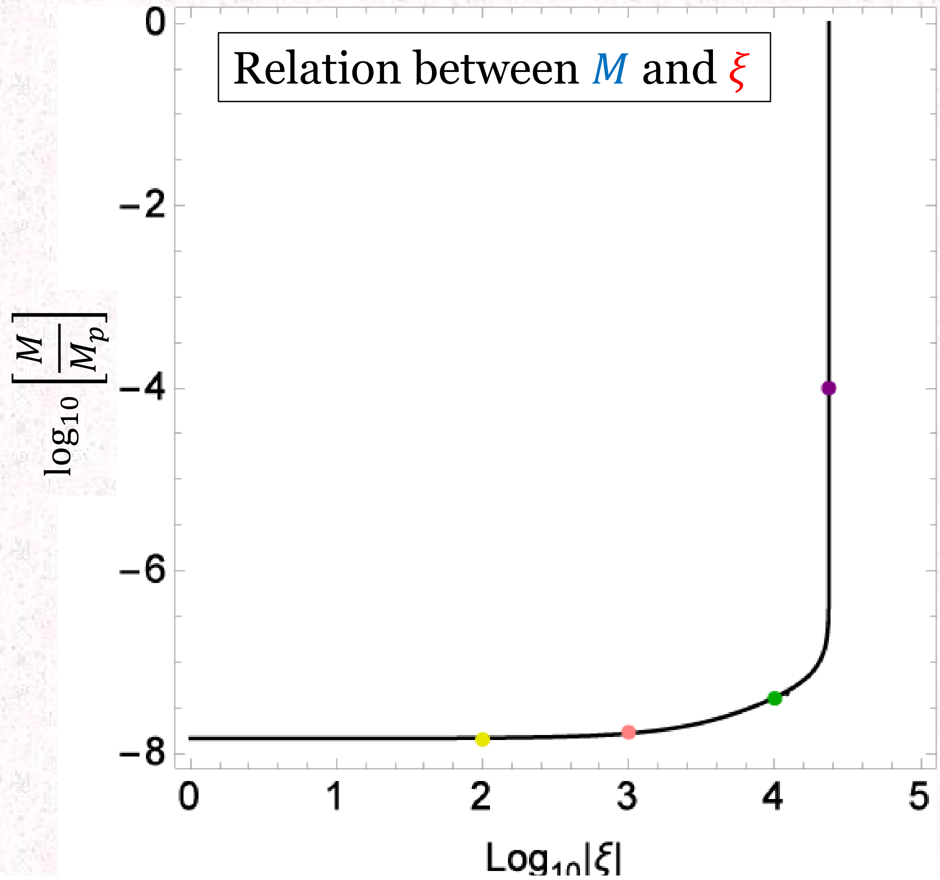

Hybrid Higgs Inflation

cosmological perturbations

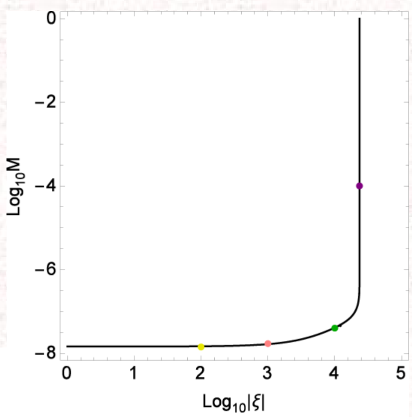

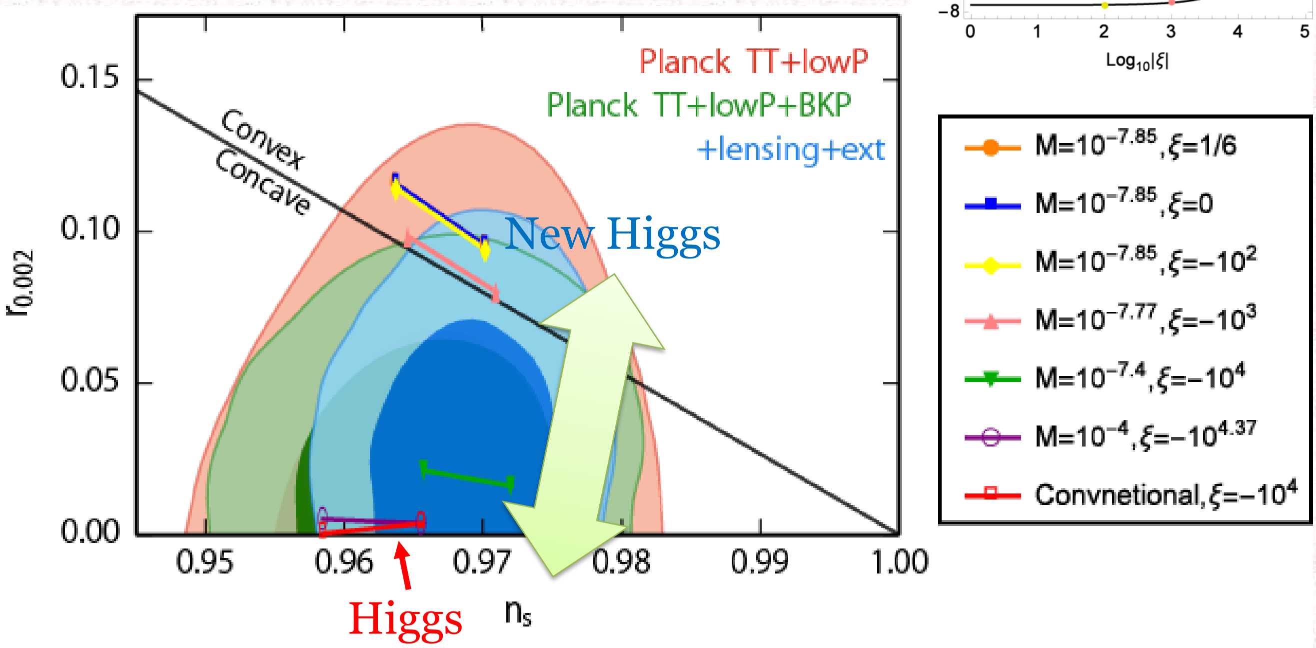

ADM decompositions

Hybrid Higgs inflation

$$S = \int dx^4 \sqrt{-g}\left[\left(\frac{M_p^2}{2} - \xi\frac{h^2}{2}\right)R - \left(g^{\mu\nu} - \frac{G^{\mu\nu}}{M^2}\right)\frac{\partial_\mu h\, \partial_\nu h}{2} - V(h)\right]$$

$$V(h) = \frac{\lambda}{4}(h^2 - v^2)^2 \cong \frac{\lambda}{4}h^4 \qquad (\lambda \approx 0.1)$$

ADM metric

$$ds^2 = -N^2dt^2 + \gamma_{ij}(dx^i + N^i dt)(dx^j + N^j dt)$$

$$\boxed{\begin{aligned} &N = 1 + \alpha, \quad \gamma_{ij} = a(t)e^{2\zeta}\left(\delta_{ij} + h_{ij} + \frac{1}{2}h_i{}^k h_{kj}\right) \\ &N_i = \partial_i \psi, \end{aligned}}$$

Scalar perturbations: α, ψ, ζ

Tensor perturbation: h_{ij} $\qquad \boxed{h_i{}^j{}_{,j} = 0 = h_i{}^i}$

ADM decompositions

K.Kamada, T.Kobayashi, T.Takahashi,M.Yamaguchi & J.Yokoyama(2012)

$$S_S^{(2)} = \int dx^4 M_P^2 a^3 \left[\underbrace{\left(3G + \frac{\Sigma G^2}{\Theta^2}\right)}_{G_S}\dot{\zeta}^2 - \frac{(\nabla_i\zeta)^2}{a^2}\underbrace{\left\{\frac{1}{a}\frac{d}{dt}\left(\frac{aG^2}{\Theta}\right) - F\right\}}_{F_S}\right]$$

$$F = 1 - \frac{\xi h^2}{M_P^2} + \frac{\dot{h}^2}{2NM^2M_P^2},$$

$$G = 1 - \frac{\xi h^2}{M_P^2} - \frac{\dot{h}^2}{2NM^2M_P^2},$$

$$\Theta \equiv H\left(1 - \frac{\xi h^2}{M_P^2} - \frac{3\dot{h}^2}{2NM^2M_P^2}\right) - \frac{\xi h\dot{h}}{M_P^2},$$

$$\Sigma \equiv -3H^2\left(1 - \frac{\xi h^2}{M_P^2}\right) + \left(9H^2 + \frac{M^2}{2}\right) \times \frac{\dot{h}^2}{NM^2M_P^2} - 6H\frac{\xi h\dot{h}}{M_P^2},$$

$$dy \equiv \frac{c_s}{a}dt$$

$$z \equiv \sqrt{2}a(F_S G_S)^{\frac{1}{4}}$$

$$u \equiv z\zeta$$ $\qquad$ Mukhanov-Sasaki variable

$$S_S^{(2)} = \int dy dx^3 M_P^2\left[\left(\frac{du}{dy}\right)^2 - (\nabla_i u)^2 - \frac{d^2 z}{dy^2}\frac{u^2}{z}\right]$$

ADM decompositions

$$\frac{d^2u}{dy^2} + \left(k^2 - \left(\nu_S^2 - \frac{1}{4}\right)\frac{1}{y^2}\right)u = 0$$

$$\nu_s \equiv \frac{3 - \epsilon_H + g}{2 - 2\epsilon_H - f + g}$$

$$f_S \equiv \frac{\dot{F}_S}{HF_S} \simeq const,$$

$$g_S \equiv \frac{\dot{G}_S}{HG_S} \simeq const,$$

$$\Rightarrow \quad u = \frac{\sqrt{\pi}}{2} e^{\frac{\pi}{2}i\left(\nu_S + \frac{1}{2}\right)} \sqrt{-y_S} H_{\nu_S}^{(1)}(-ky)$$

$H_\nu^{(1)}(x)$: $1st\ kind\ Hankel\ function$

Power spectrum

$$P_\zeta(k) \equiv \left(\frac{k^3}{2\pi^2}\right)|\zeta|^2 = \left(\frac{k^3}{2\pi^2}\right)\left|\frac{u}{z}\right|^2$$

$$= \frac{1}{2} 2^{2\nu_s - 3} \left|\frac{\Gamma(\nu_s)}{\Gamma(3/2)}\right|^2 \left(1 - \epsilon - \frac{f}{2} + \frac{g}{2}\right)^2 \frac{G_S^{1/2}}{F_S^{3/2}} \frac{H^2}{4\pi^2}$$

Spectrum index

$$1 - n_S = 2\nu_S - 3 \qquad r = \frac{P_T}{P_\zeta}$$

Horizon-cross

$k \sim -1/y$

ADM decompositions

$$\Delta r \equiv \frac{|r - r_{ADM}|}{r_{ADM}} \times 100$$

$$\Delta n_s \equiv \frac{|n_s - n_{s\,ADM}|}{n_{s\,ADM}} \times 100$$

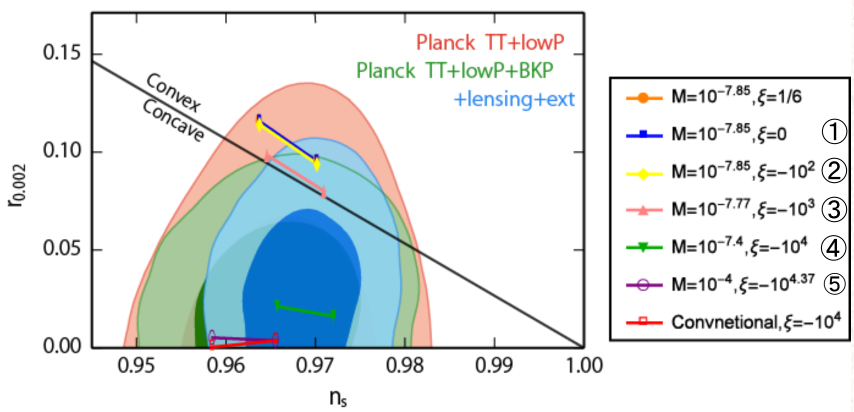

Parameter	$\Delta n_s[\%]$		$\Delta r[\%]$	
	N=60	N=50	N=60	N=50
①	5.8×10^{-2}	9.3×10^{-2}	3.4	4.2
②	7.5×10^{-2}	1.1×10^{-1}	3.6	4.5
③	7.6×10^{-2}	1.1×10^{-1}	3.6	4.6
④	1.2×10^{-1}	1.8×10^{-1}	5.1	6.5
⑤	3.6×10^{-1}	9.3×10^{-2}	3.5	4.4

$$\Delta n_s < 0.4\% \qquad \Delta r < 6.6\%$$

Summary & Discusions

- The disfomal truncation is very useful and valid during the inflation regime.

- "Hybrid Higgs inflation" is a good inflation model, which varies r without varying the n_s.

- The gravitational wave can be enhanced by the $G^{\mu\nu}\nabla_\mu h \nabla_\nu h$.

- Any other models to apply?

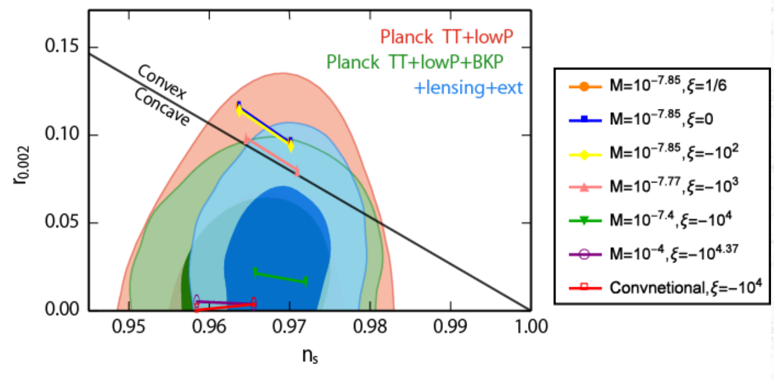

Thank you for listening

THE END

6a3. Kazuhiro Kogai (Nagoya U.)

"Exploring primordial anisotropic non-Gaussianity from galaxy alignment" (10+5)

[JGRG27 (2017) 113004]

JGRG27 6a3

Exploring Primordial Anisotropic Non-Gaussianity from Galaxy Alignment

November 30th, 2017

C-Lab Nagoya Univ.

M1 Kazuhiro Kogai

Collaborators

T. Matsubara (KEK)

A. J. Nishizawa, Y. Urakawa (Nagoya Univ.)

Angular Dependent Primordial Non-Gaussianity(NG)

Arkani-Hamed & Maldacena (15)

$$B_\phi(\mathbf{k}_1, \mathbf{k}_2, \mathbf{k}_3 = \mathbf{k}_L) = \sum_{\ell=0,2,\ldots} A_\ell \mathcal{P}_\ell(\hat{\mathbf{k}}_L \cdot \hat{\mathbf{k}}_S) \left(\frac{k_L}{k_S}\right)^\Delta P_\phi(k_L) P_\phi(k_S) \left[1 + \mathcal{O}\left(\left(\frac{k_L}{k_S}\right)^2\right)\right]$$

$\mathcal{P}_\ell$: Legendre Polynomial

Δ : Parameter related to the mass and the spin of a particle

$$\mathbf{k}_S = \mathbf{k}_1 - \frac{\mathbf{k}_L}{2}$$

Local-type

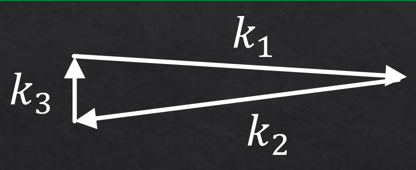

$$\mathbf{k}_1 + \mathbf{k}_2 + \mathbf{k}_3 = 0$$
$$k_3 = k_L \ll k_1, k_2$$

In String Theory

Inflaton ⟷ Higher spin particles ➡ Angular dependence $\boxed{\mathcal{P}_\ell(\hat{\mathbf{k}}_L \cdot \hat{\mathbf{k}}_S)}$

Interaction

Introduction

Intrinsic alignment

P.Catelan et al. (00), Hirata & Seljak (04)

Galaxy shape

$$\boxed{g_{ij} = [\mathrm{Tr}\ I_{kl}]^{-1}\left(I_{ij} - \frac{1}{3}\mathrm{Tr}\ I_{kl}\right)}$$

I_{ij} : Second moment tensor

Assumption

$$\boxed{g_{ij}(\boldsymbol{x}) = b_1^I K_{ij}(\boldsymbol{x}) + \frac{1}{2}b_2^I \delta(\boldsymbol{x}) K_{ij}(\boldsymbol{x}) + \frac{1}{2}b_t^I\left[K_{ik}K^k{}_j - \frac{1}{3}(K_{lm})^2\delta_{ij}\right](\boldsymbol{x})}$$

$K_{ij}(\boldsymbol{x}) = \left[\frac{\partial_i\partial_j}{\nabla} - \frac{1}{3}\delta_{ij}\right]\delta(\boldsymbol{x})$: Tidal field tensor $b_1^I,\ b_2^I,\ b_t^I$: Bias coefficients

Tidal effect picture

Gravitational field
Center of gravity

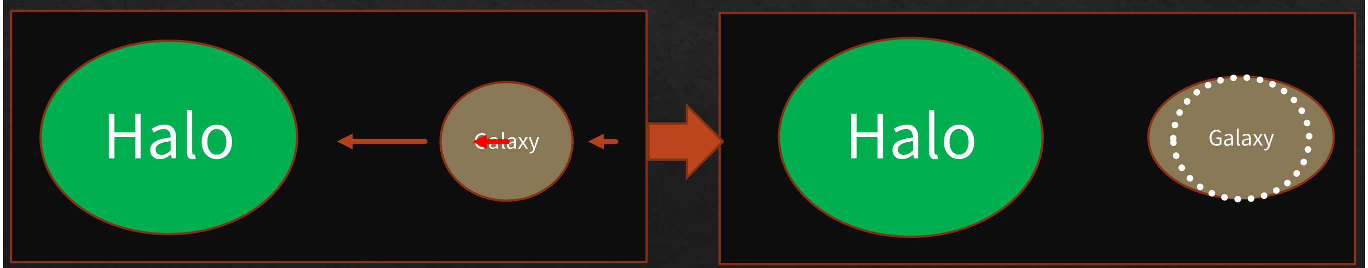

Introduction

How can we get the information of NG?

F.Schmidt et al. (15)

Galaxy shape

$$g_{ij}(\boldsymbol{x}) = b_1^I K_{ij}(\boldsymbol{x}) + \boxed{\frac{1}{2}b_2^I \delta(\boldsymbol{x}) K_{ij}(\boldsymbol{x}) + \frac{1}{2}b_t^I\left[K_{ik}K^k{}_j - \frac{1}{3}(K_{lm})^2\delta_{ij}\right](\boldsymbol{x})}$$

$K_{ij}(\boldsymbol{x}) = \left[\frac{\partial_i\partial_j}{\nabla} - \frac{1}{3}\delta_{ij}\right]\delta(\boldsymbol{x})$: Tidal field tensor

Galaxy shape autocorrelation

$$\langle g_{ij}(\boldsymbol{x}) g^{ij}(\boldsymbol{y})\rangle \sim b_1^{I2}\langle\delta(\boldsymbol{x})\delta(\boldsymbol{y})\rangle + b_2^I b_t^I \alpha \boxed{\langle\delta(\boldsymbol{x})\delta(\boldsymbol{y})\delta(\boldsymbol{y})\rangle}$$
$$+ b_2^I b_t^I \beta \boxed{\langle\delta(\boldsymbol{x})\delta(\boldsymbol{x})\delta(\boldsymbol{y})\rangle}$$

$$\delta(\boldsymbol{k}, z) = \frac{2}{3}\frac{k^2 T(k) D(z)}{\Omega_{m0} H_0^2}\phi(\boldsymbol{k})$$

$T(k)$: Transfer function, $D(z)$: Growth factor

$$\langle\phi(\mathbf{k}_1)\phi(\mathbf{k}_2)\phi(\mathbf{k}_3)\rangle = (2\pi)^3 B_\phi(\mathbf{k}_1, \mathbf{k}_2, \mathbf{k}_3)\delta_D(\mathbf{k}_1 + \mathbf{k}_2 + \mathbf{k}_3)$$

Introduction

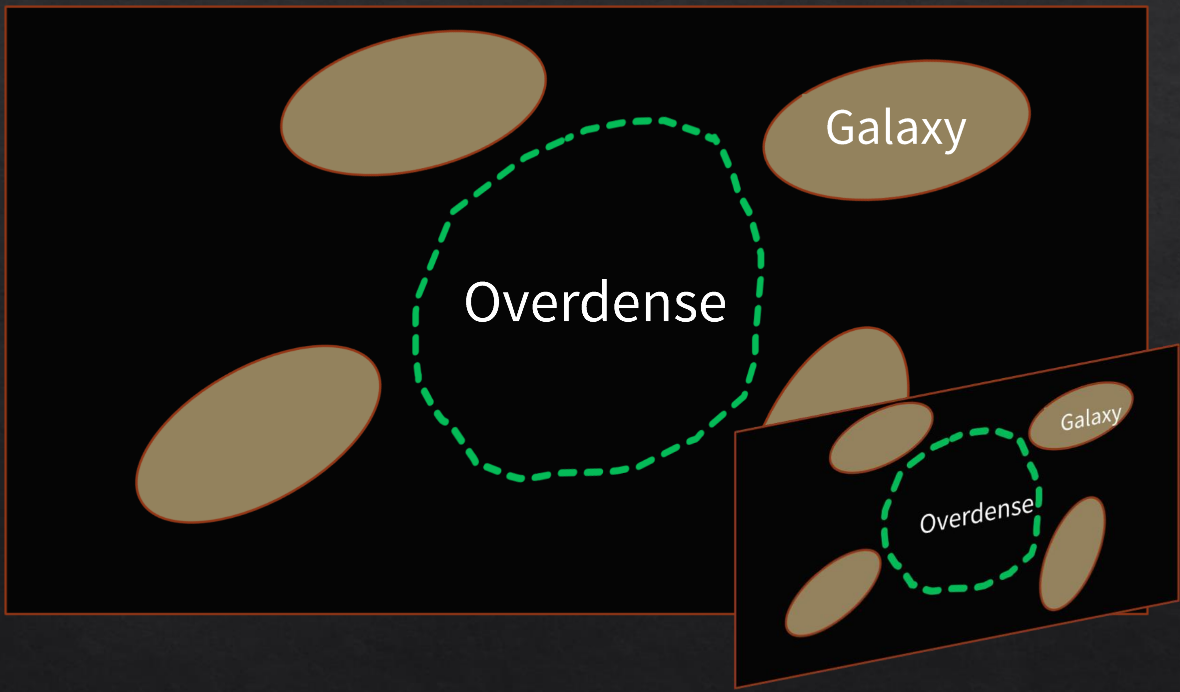

Introduction

Hirata & Seljak (04)
F.Schmidt et al. (15)

Galaxy shear
= Intrinsic shear + Weak lensing shear

Angular dependent primordial NG

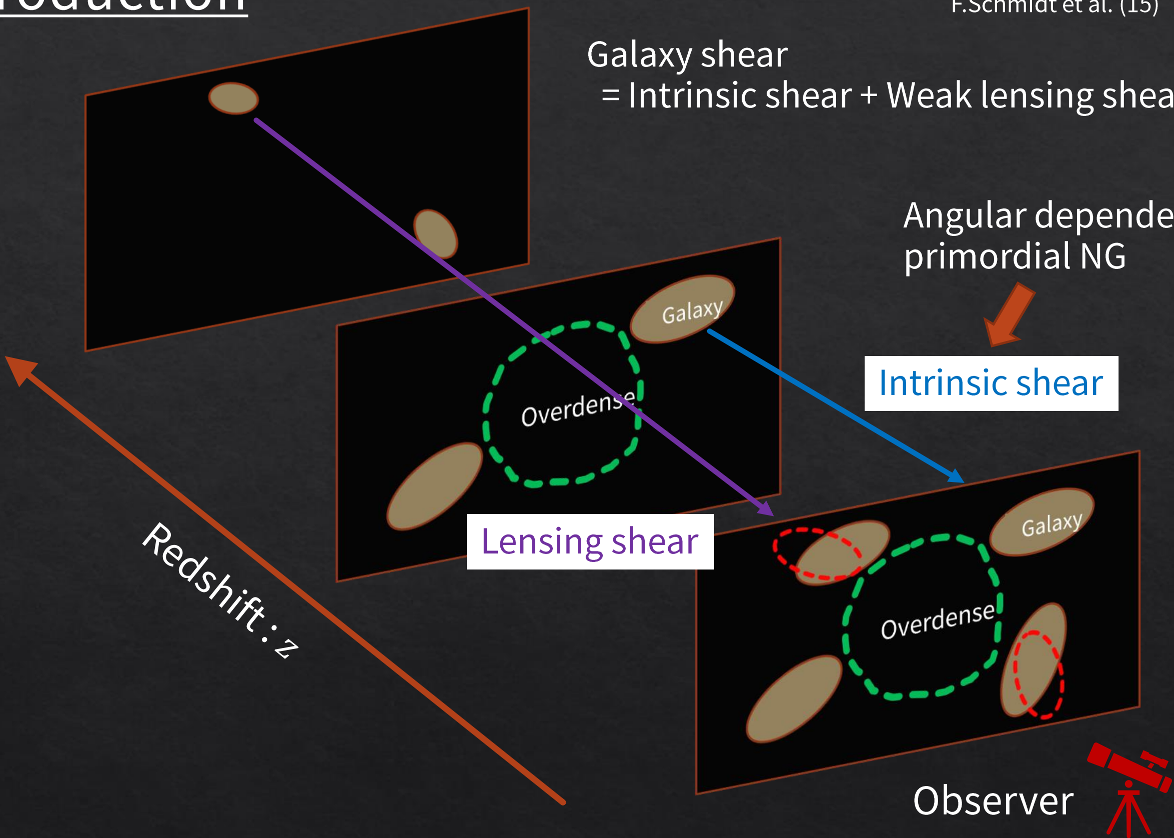

Motivation

Angular dependent primordial NG

F. Schmidt et al. (15)

NG from Massive Spin 2 (global isotropy)

$$B_\phi(\boldsymbol{k}_1,\,\boldsymbol{k}_2,\,\boldsymbol{k}_3=\boldsymbol{k}_L)\sim[A_0+A_2(\hat{\boldsymbol{k}}_L\cdot\hat{\boldsymbol{k}}_S)^2]P_\phi(k_L)P_\phi(k_S)$$

Can we distinguish by observation?

K.K. + (in progress)

NG from vector fields $\hat{\boldsymbol{p}}$ (Spin 1, No global isotropy)

$$B_\phi(\boldsymbol{k}_1,\,\boldsymbol{k}_2,\,\boldsymbol{k}_3=\boldsymbol{k}_L)\sim[A_0+\bar{A}_2(\boxed{\hat{\boldsymbol{p}}}\cdot\hat{\boldsymbol{k}}_S)^2]P_\phi(k_L)P_\phi(k_S)$$

Result

Shape auto correlation

3D Galaxy shape : g_{ij}

Projected galaxy shape : γ

Spherical harmonics expansion

$$\gamma(\hat{\boldsymbol{n}})=\sum_{lm}a^I_{lm}Y_{lm}(\hat{\boldsymbol{n}})$$

j_l : Spherical Bessel function

χ : Comoving distance

$C^{(s)}_{lm}$: Coefficient

$$a^I_{lm}\propto\int d^3k b_1\frac{j_l(k\chi)}{(k\chi)^2}Y_{l,m}(\hat{\boldsymbol{k}})+b_{NG}A_2\boxed{\sum_{s=-2}^{2}C^{(s)}_{lm}j_{l+s}(k\chi)Y_{l+s,m}}$$

Point ①

Non-Diagonal components

A given ell has the value from l-2 to l+2.

$\left\langle a^{I+G,E}_{l,(m=0)}a^{I+G,E*}_{l,(m=0)}\right\rangle$ K.K. + (in progress)

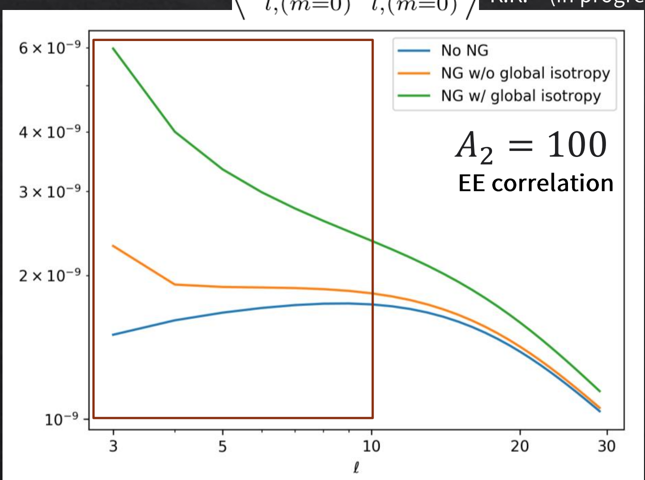

- In Large scale, (ℓ →small) their powers are enhanced by NG.

Result

$\left\langle a^{I,B}_{l,(m=l)} a^{I,B*}_{l,(m=l)} \right\rangle$ K.K. + (in progress)

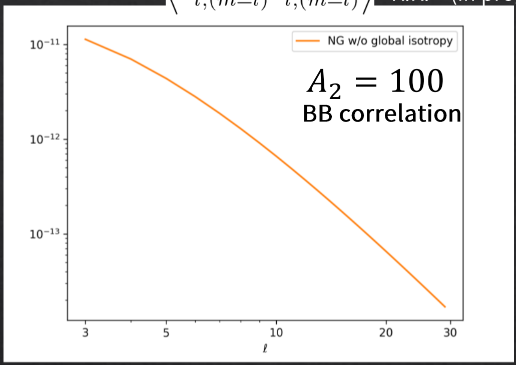

$\left\langle a^{I+G,E}_{l,(m=l)} a^{I,B*}_{l+1,(m=l)} \right\rangle$

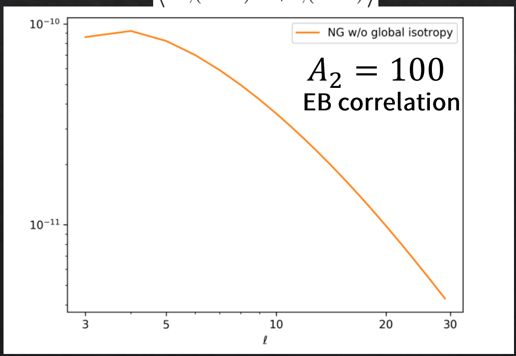

Angular dependent primordial NG

NG from vector fields $\hat{\boldsymbol{p}}$

$$B_\phi(\boldsymbol{k}_1,\, \boldsymbol{k}_2,\, \boldsymbol{k}_3 = \boldsymbol{k}_L) \sim [A_0 + \bar{A}_2(\boxed{\hat{\boldsymbol{p}}} \cdot \hat{\boldsymbol{k}}_S)^2] P_\phi(k_L) P_\phi(k_S)$$

Violation of global isotropy

Point ②

Generate B-mode

We neglected non-linear effects in weak lensing.

B-B is generated only from intrinsic alignment.

Summary

F. Schmidt et al. (15)

NG from Massive Spin 2 (global isotropy)

$$B_\phi(\boldsymbol{k}_1,\, \boldsymbol{k}_2,\, \boldsymbol{k}_3 = \boldsymbol{k}_L) \sim [A_0 + A_2(\hat{\boldsymbol{k}}_L \cdot \hat{\boldsymbol{k}}_S)^2] P_\phi(k_L) P_\phi(k_S)$$

Can we distinguish by observation?

K.K. + (in progress)

NG from vector fields $\hat{\boldsymbol{p}}$ (Spin 1, No global isotropy)

$$B_\phi(\boldsymbol{k}_1,\, \boldsymbol{k}_2,\, \boldsymbol{k}_3 = \boldsymbol{k}_L) \sim [A_0 + \bar{A}_2(\boxed{\hat{\boldsymbol{p}}} \cdot \hat{\boldsymbol{k}}_S)^2] P_\phi(k_L) P_\phi(k_S)$$

We can distinguish by observations from

Point ① • Angular Non-Diagonal components

Point ② • Generation of B-mode

6a4. Sakine Nishi (Rikkyo U.),
"Anisotropic inflation in Horndeski theory" (10+5)
[JGRG27 (2017) 113005]

Anisotropic Inflation in Horndeski theory

Sakine Nishi (Rikkyo University)

in collaboration with
Tsutomu Kobayashi (Rikkyo), Hiroaki W. H. Tahara (RESCEU),
and Jun'ichi Yokoyama (RESCEU)

JGRG27 @Hiroshima

Introduction

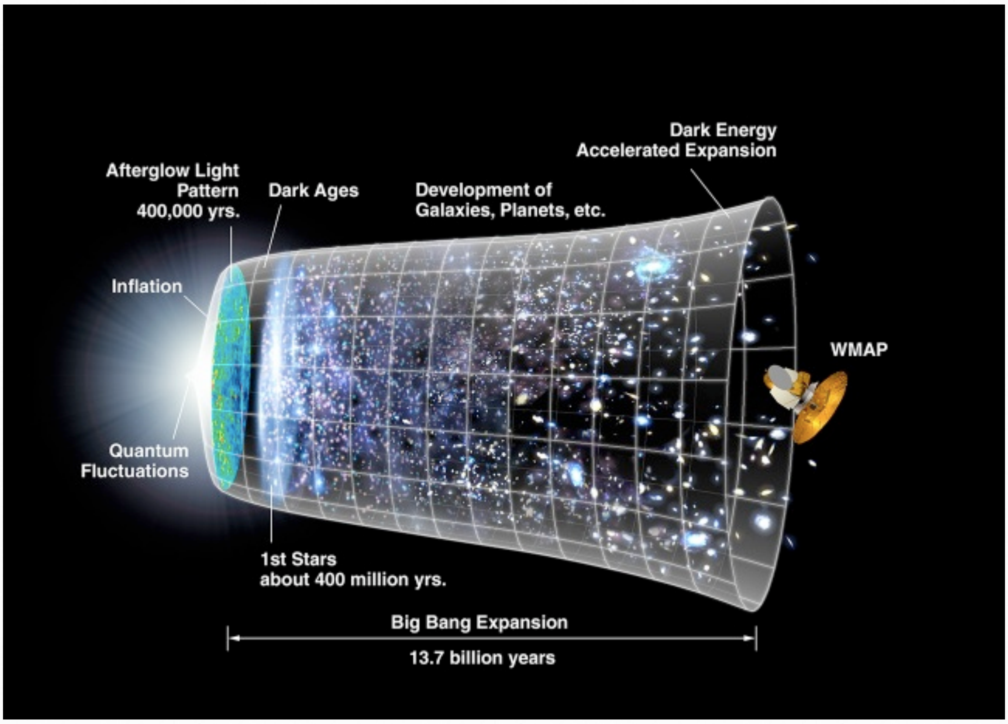

Introduction

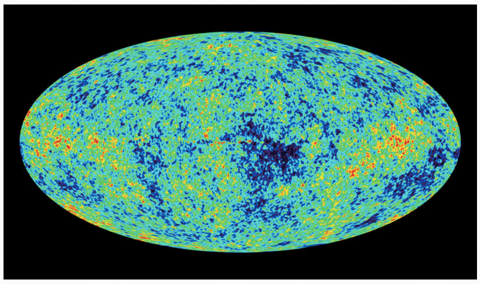

- Statistical isotropy

$$\mathcal{P}(\mathrm{k}) = \mathcal{P}(k)[1 + g_* \sin^2\theta]$$

$$-0.010 < g_* < 0.019$$ [Planck 2015]

- Anisotropic inflation $\rightarrow$ introduce vector field

ex.)

$$S = \int d^4x\sqrt{-g}\left[\frac{1}{2\kappa^2}R - \frac{1}{2}(\partial_\mu\phi)^2 - V(\phi) - \frac{1}{4}F_{\mu\nu}F^{\mu\nu} - \frac{1}{2}\left(m^2 - \frac{R}{6}\right)A_\mu A^\mu\right]$$

[Kannno, Kimura , Soda ,S.Yokoyama 2013]

Motivation

Anisotropic inflation $\rightarrow$ introduce vector field

Anisotropic inflation without vector field ?
(in the Horndeski theory)

Outline

- Introduction
- Action (Horndeski theory)
- Background
- Attractor
- Conclusions

Action

- Horndeski theory
  - the most general scalar-tensor theory which has up to 2nd derivative
  - The field eqs. have no 3rd and higher derivative terms

$$
\begin{aligned}
S_{\rm Hor} = \int \mathrm{d}^4x\sqrt{-g}\Big\{ & G_2(\phi, X) - G_3(\phi, X)\Box\phi + G_4(\phi, X)R \\
& + G_{4X}\left[(\Box\phi)^2 - (\nabla_\mu\nabla_\nu\phi)^2\right] + G_5(\phi, X)G^{\mu\nu}\nabla_\mu\nabla_\nu\phi \\
& - \frac{1}{6}G_{5X}\left[(\Box\phi)^3 - 3\Box\phi(\nabla_\mu\nabla_\nu\phi)^2 + 2(\nabla_\mu\nabla_\nu\phi)^3\right]\Big\}
\end{aligned}
$$

$$X := -g^{\mu\nu}\partial_\mu\phi\partial_\nu\phi/2$$

[G. W. Horndeski (1974)]
[C. Deffayet, Xian Gao, D. A. Steer, and G. Zahariade (2011)]
[T. Kobayashi, M. Yamaguchi and J. Yokoyama (2011)]

Action

- In ADM formalism

Horndeski condition

$$A_4 = -B_4 + 2XB_{4X},$$
$$A_5 = -\frac{1}{3}XB_{5X}.$$

$$
\begin{aligned}
L_2 &= A_2(t,N) \\
L_3 &= A_3(t,N)K \\
L_4 &= A_4(t,N)(K^2 - K_{ij}^2) + B_4(t,N)R^{(3)} \\
L_5 &= A_5(K^3 - 3KK_{ij}^2 + 2K_{ij}^3) \\
&\quad + B_5(t,N)K^{ij}\left(R_{ij} - \frac{1}{2}g_{ij}R^{(3)}\right)
\end{aligned}
$$

[J. Gleyzes, D. Langlois, F. Piazza, F. Vermizzi, 2014]

Background

- Introduce anitosropy (Bianchi type-I)

$$\mathrm{d}s^2 = -N^2\mathrm{d}t^2 + a^2\left[e^{-4\sigma_+}\mathrm{d}x^2 + e^{2\sigma_+ + 2\sqrt{3}\sigma_-}\mathrm{d}y^2 + e^{2\sigma_+ - 2\sqrt{3}\sigma_-}\mathrm{d}z^2\right]$$

- Action

$$
\begin{aligned}
L_2 &= A_2(t,N), \\
L_3 &= \frac{3a'}{aN}A_3(t,N), \\
L_4 &= \frac{6}{N^2}A_4(t,N)\left(\frac{a'^2}{a^2} - \sigma_-'^2 - \sigma_+'^2\right), \\
L_5 &= \frac{6}{a^3N^3}A_5(t,N)(a' - 2a\sigma_+')(a'^2 + 2aa'\sigma_+' + a^2(-3\sigma_-'^2 + \sigma_+'^2))
\end{aligned}
$$

Variation of

$a(t), N(t), \dot{\sigma}_\pm$

Background - Field equations

- background

$$\frac{\dot\sigma_\pm}{H} \ll 1$$

$$A_2 - 6A_4H^2 - 12A_5H^3 - \frac{1}{N}\frac{\mathrm{d}}{\mathrm{d}t}(A_3 + 4A_4H + 6A_5H^2)$$
$$-\frac{6}{N^2}A_4(\dot\sigma_-^2 + \dot\sigma_+^2) + \frac{18A_5a^2}{N^2}\left(\frac{\mathrm{d}}{\mathrm{d}t}\left(\dot\sigma_-^2 + \dot\sigma_+^2\right) + 3\dot\sigma_-^2 - \dot\sigma_+^2\right) = 0$$

$$(A_2N)' + 3(A_3N)'H + 6(A_4N^{-1})'\left(N^2H^2 - (\dot\sigma_-^2 + \dot\sigma_+^2)\right)$$
$$+6(A_5N^{-2})'(NH - 2\dot\sigma_+)(N^2H^2 - 2NH\dot\sigma_+ - 3\dot\sigma_-^2 + \dot\sigma_+^2) = 0$$

Background - Field equations

- anisotropy

$$\frac{\mathrm{d}}{\mathrm{d}t}\left[\frac{a^3}{N^2}\left\{(3A_5H + A_4)N\dot\sigma_- - 6A_5\dot\sigma_+\dot\sigma_-\right\}\right] = 0$$

$$\frac{\mathrm{d}}{\mathrm{d}t}\left[\frac{a^3}{N^2}\left\{(3A_5H + A_4)N\dot\sigma_+ + 3A_5\left(\dot\sigma_+^2 - \dot\sigma_-^2\right)\right\}\right] = 0$$

- fixed point $(a(t) \to \infty\ )$

$$\left(\frac{\dot\sigma_-}{b}, \frac{\dot\sigma_+}{b}\right) = (0,0), (0,1)\,, \left(\frac{\sqrt{3}}{2}, -\frac{1}{2}\right), \left(-\frac{\sqrt{3}}{2}, -\frac{1}{2}\right)$$

$$b = -\frac{N(3A_5H + A_4)}{3A_5}$$

Background - Attractor

↓ Isotropic inflation

$$\left(\frac{\dot{\sigma}_-}{b}, \frac{\dot{\sigma}_+}{b}\right) = (0,0), (0,1)\,, \left(\frac{\sqrt{3}}{2}, -\frac{1}{2}\right), \left(-\frac{\sqrt{3}}{2}, -\frac{1}{2}\right)$$

Background - Attractor

↓ Anisotropic inflation

$$\left(\frac{\dot{\sigma}_-}{b}, \frac{\dot{\sigma}_+}{b}\right) = (0,0), (0,1)\,, \left(\frac{\sqrt{3}}{2}, -\frac{1}{2}\right), \left(-\frac{\sqrt{3}}{2}, -\frac{1}{2}\right)$$

$$b = -\frac{N(3A_5H + A_4)}{3A_5}$$

- The solutions of anisotropic inflation needs A_5 term

Background

- ADM formalism [J. Gleyzes, D. Langlois, F. Piazza, F. Vermizzi, 2014]

$$
\begin{aligned}
L_2 &= A_2(t,N) \\
L_3 &= A_3(t,N)K \\
L_4 &= A_4(t,N)(K^2 - K_{ij}^2) + B_4(t,N)R^{(3)} \\
L_5 &= A_5(K^3 - 3KK_{ij}^2 + 2K_{ij}^3) \\
&\quad + B_5(t,N)K^{ij}\left(R_{ij} - \frac{1}{2}g_{ij}R^{(3)}\right)
\end{aligned}
$$

$$\boxed{\dot{\boldsymbol{\sigma}}_\pm \in K_{ij}}$$

Background

- conditions
  - small anisotropy

$$\frac{\dot{\sigma}_\pm}{H} \ll 1 \longrightarrow \dot{\sigma} \sim b = -\frac{N(3A_5H + A_4)}{3A_5} \ll 1$$

→ large

  - Background

$$(NA_2)' + 3A_3'H + \underline{\left(\frac{A_4}{N}\right)'(6H^2 - \sigma^2) + \left(\frac{A_5}{N^2}\right)'(6H^3 + 3H\sigma^2 + 2\sigma^3)}\Bigg|_{N=1} = 0$$

$$\left(\frac{A_4}{N}\right)'\Bigg|_{N=1} \gtrsim \left(\frac{A_5}{N^2}\right)'\Bigg|_{N=1}$$

Background

- ADM formalism [J. Gleyzes, D. Langlois, F. Piazza, F. Vermizzi, 2014]

$$
\begin{aligned}
L_2 &= A_2(t,N) \\
L_3 &= A_3(t,N)K \\
L_4 &= A_4(t,N)(K^2 - K_{ij}^2) + B_4(t,N)R^{(3)} \\
L_5 &= A_5(K^3 - 3KK_{ij}^2 + 2K_{ij}^3) \\
&\quad + B_5(t,N)K^{ij}\left(R_{ij} - \frac{1}{2}g_{ij}R^{(3)}\right)
\end{aligned}
$$

$\downarrow$ de-Sitter inflation

Attractor

$$\left(\frac{\dot\sigma_-}{b}, \frac{\dot\sigma_+}{b}\right) = (0,0), (0,1), \left(\frac{\sqrt{3}}{2}, -\frac{1}{2}\right), \left(-\frac{\sqrt{3}}{2}, -\frac{1}{2}\right)$$

- de-Sitter inflation +small anisotropy

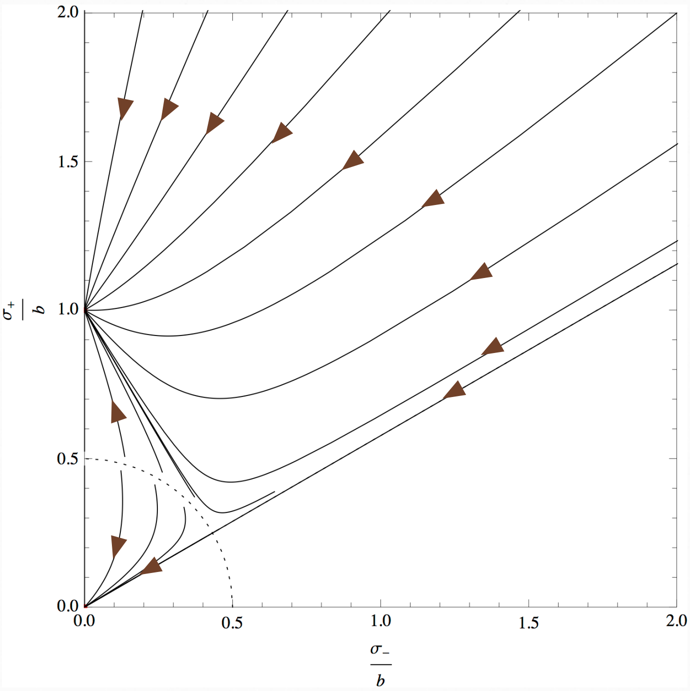

$$H = \text{const.}$$
$$N = \text{const.}$$

Attractor

$$\left(\frac{\dot{\sigma}_-}{b}, \frac{\dot{\sigma}_+}{b}\right) = (0,0), \boxed{(0,1)}, \left(\frac{\sqrt{3}}{2}, -\frac{1}{2}\right), \left(-\frac{\sqrt{3}}{2}, -\frac{1}{2}\right)$$

- de-Sitter inflation +small anisotropy

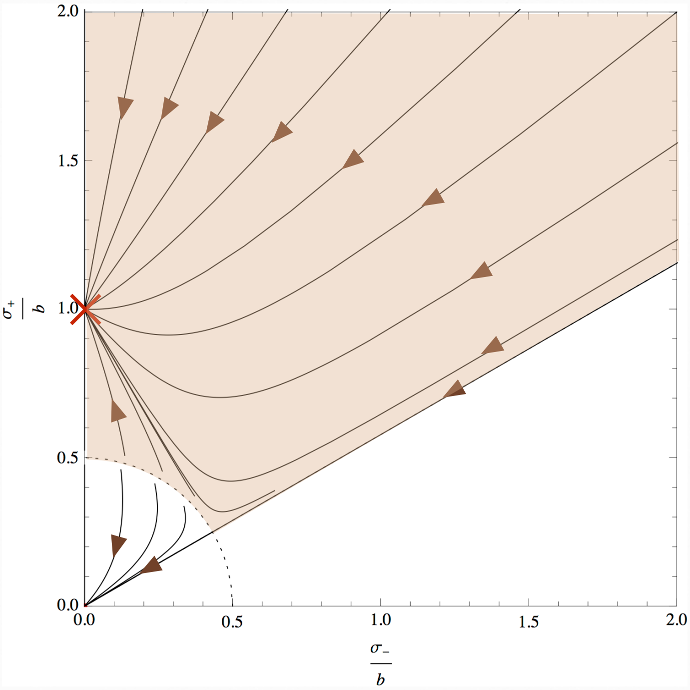

$$H = \text{const.}$$
$$N = \text{const.}$$

Attractor

$$\left(\frac{\dot{\sigma}_-}{b}, \frac{\dot{\sigma}_+}{b}\right) = \boxed{(0,0)}, (0,1), \left(\frac{\sqrt{3}}{2}, -\frac{1}{2}\right), \left(-\frac{\sqrt{3}}{2}, -\frac{1}{2}\right)$$

- de-Sitter inflation +small anisotropy

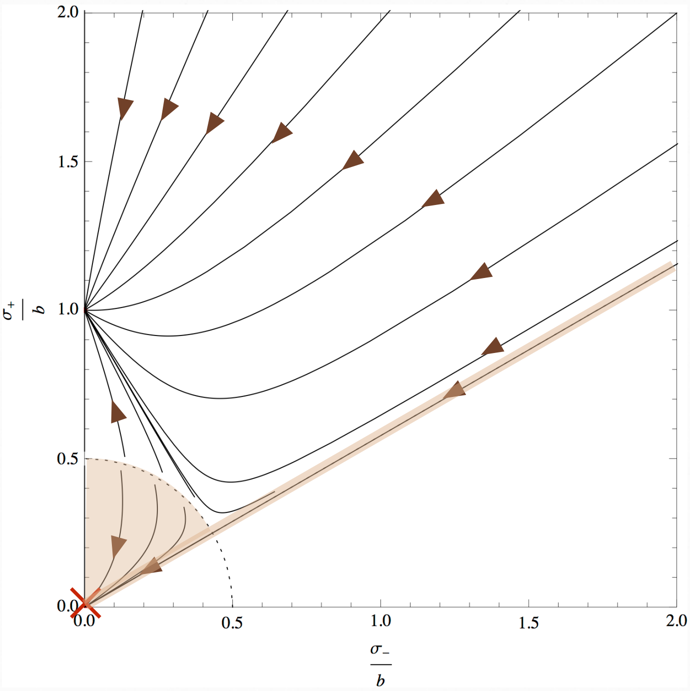

$$H = \text{const.}$$
$$N = \text{const.}$$

Conclusions

- Generalized model of Anisotropic inflation without vector field in Horndeski theory
- K_{ij}^3 term generates anisotropy
- Perturbations $\rightarrow$ Next talk

Session6b 11:15–12:30

[Chair: Akihiro Ishibashi]

6b1. Naritaka Oshita (RESCEU U. Tokyo),

“Probing atoms of spacetime with ringdown gravitational waves from a perturbed black hole”
(10+5)

[JGRG27 (2017) 113007]

Symmetry structure

$\phi_+(t,\boldsymbol{x}) \underset{\delta_+}{\rightarrow} \phi_+(t+\epsilon_+,\boldsymbol{x})$ and $\phi_-(t,\boldsymbol{x}) \underset{\delta_+}{\rightarrow} \phi_-(t,\boldsymbol{x})$,

$\phi_+(t,\boldsymbol{x}) \underset{\delta_-}{\rightarrow} \phi_+(t,\boldsymbol{x})$ and $\phi_-(t,\boldsymbol{x}) \underset{\delta_-}{\rightarrow} \phi_-(t+\epsilon_-,\boldsymbol{x})$

Coarse graining
Integrate out σ

$\phi_+(t,\boldsymbol{x}) \underset{\delta_R}{\rightarrow} \phi_+(t+\epsilon_R,\boldsymbol{x})$ and $\phi_-(t,\boldsymbol{x}) \underset{\delta_R}{\rightarrow} \phi_-(t+\epsilon_R,\boldsymbol{x})$

$\cancel{\phi_+(t,\boldsymbol{x}) \underset{\delta_A}{\rightarrow} \phi_+(t+\epsilon_A,\boldsymbol{x}) \text{ and } \phi_-(t,\boldsymbol{x}) \underset{\delta_A}{\rightarrow} \phi_-(t-\epsilon_A,\boldsymbol{x})}$ Broken by ϕ_+- ϕ_- mixing

EFT of NG boson with dissipative and stochastic effects based on symmetry structure

1. Construction of effective action

The effective action for NG boson $\pi_\pm$ takes the form

$$S_{eff}[\pi_+,\pi_-] = \int d^4x \Big[\underbrace{\left((\partial_\mu\pi_+)^2 - (\partial_\mu\pi_-)^2\right)}_{\text{Kinetic term}} + \underbrace{\beta(\dot\pi_+^2 - \dot\pi_-^2)}_{\text{Modification of sound speed}}$$
$$+ \underbrace{iA_i(\pi_+ - \pi_-)^2}_{\text{Scale-independent noise}} + \underbrace{iA_d\left(\partial_\mu(\pi_+ - \pi_-)\right)^2}_{\text{Scale-dependent noise}}$$
$$+ \underbrace{\gamma_i\pi_-\dot\pi_+}_{\text{Scale-independent dissipation}} + \underbrace{\gamma_d\partial_\mu\pi_-\partial^\mu\dot\pi_+}_{\text{Scale-dependent dissipation}} + O(\pi^3)\Big]$$

This action is constructed based on the following criterions

- Criterion 1: Symmetry structure

	δ_R	δ_A	
Blue	✓	✓	Operators in EFT of inflation (cf. [2])
Orange	✓		Effects of noise & dissipation ▲ Our new results

- Criterion 2: Microscopic unitary condition (cf. [3])

$S_{micro}(\phi_+ = \phi_-; \sigma_+ = \sigma_-) = 0 \implies S_{eff}[\pi_+ = \pi_-] = 0$

$\mathrm{Im}S_{eff}[\pi_+,\pi_-] \geq 0 \implies$ Noise is a dumping factor

2. KMS condition

At equilibrium, the action enjoys the KMS condition given by

$$S[\pi_+(t),\pi_-(t)] = S[\pi_+(-t),\pi_-(-t-i\beta)]$$
$$\rightarrow A_i = \frac{2\gamma_i}{\beta}, A_d = \frac{2\gamma_d}{\beta}$$

Note that the first relation coincide with Fluctuation-Dissipation theorem.

3. Dispersion relation of NG boson

Dispersion relation is determined by

$w^2 - c_s^2\boldsymbol{k}^2 + ic_s^2\gamma w = 0$,where $c_s^2 = \frac{1}{1+\beta}$ c_s: sound speed

$$\rightarrow w(\boldsymbol{k}) = -\frac{i}{2}c_s^2\gamma \pm \frac{i}{2}\sqrt{c_s^4\gamma^2 - 4c_s^2\boldsymbol{k}^2}$$

If $\gamma^2 \gg 4\boldsymbol{k}^2$

$$w(\boldsymbol{k}) \sim -\frac{i}{c_s^2\gamma}\boldsymbol{k}^2 \quad and \quad -ic_s^2\gamma + \frac{i}{c_s^2\gamma}\boldsymbol{k}^2,$$

this modes are diffusive modes. (cf. [4])

If $\gamma^2 \ll 4\boldsymbol{k}^2$, this mode is just a propagating mode, $w(\boldsymbol{k}) = \pm c_s|\boldsymbol{k}|$

Conclusion

- Dissipative and stochastic effects break one of the two time translation symmetries in Schwinger-Keldysh formalism.
- We incorporate dissipative and stochastic effects into the EFT framework based on such a symmetry structure.
- We have in mind generalizing this flat space results to de-Sitter space, in other words inflation.
- Constructing effective action in de-Sitter space is straightforward and identifying the KMS condition for de-Sitter space is in progress.

Reference

1. M. Hongo, S. Kim, T. Noumi and A. Ota, "Open system effective field theory for time translational symmetry breaking " In progress.
2. C. Cheung, P. Creminelli, A. L. Fitzpatrick, J. Kaplan and L. Senatore "The Effective Field Theory of Inflation" JHEP 0803 (2008) 014 arXiv:0709.0293 [hep-th].
3. M. Crossley, P. Glorioso and H. Liu, "Effective field theory of dissipative fluids," JHEP 1709 (2017) 095 arXiv:1511.03646 [hep-th].
4. Y. Minami and Y. Hidaka, "Spontaneous symmetry breaking and Nambu-Goldstone modes in dissipative systems," arXiv:1509.05042 [cond-mat.stat-mech].

6b3. Kunihito Uzawa (Kwansei Gakuin U.), "Supersymmetry breaking and singularity in dynamical brane backgrounds" (10+5) [JGRG27 (2017) 113009]

SUPERSYMMETRY BREAKING AND SINGULARITY IN DYNAMICAL BRANE BACKGROUNDS

Kunihito Uzawa
(Kwansei Gakuin Univ.)

Phys. Rev. D96 (2017) 084053
[arXiv:1705.01496 [hep-th]]

with Kengo Maeda

[1] Introduction

♦ Dynamical branes in string theory

- **brane collision**

  (Gibbons & Lu & Pope, Phys.Rev.Lett. 94 (2005) 131602)
  (Maeda & Minamitsuji & Ohta & Uzawa, Phys. Rev. D82 (2010)046007)
  (Uzawa, Phys.Rev. D90 (2014) 025024)

- **cosmic Big-Bang of our universe**

  (Chen, et al., Nucl.Phys. B732 (2006) 118-135)
  (Minamitsuji & Ohta & Uzawa, Phys. Rev. D82 (2010)086002))

- **black hole in expanding universe**

  (Maeda & Ohta & Uzawa, JHEP 0906 (2009) 051)
  (Maeda & Nozawa, Phys.Rev. D81 (2010) 044017)

- The cosmological scenario from the time dependent solution until the present have been much explored.
- However, the study of SUSY breaking in terms of dynamical solution is much less extensive.
- One motivation for the present work is to improve this situation.

✍ The dynamical D3-brane solution preserves ¼ SUSY in the conifold background.
(H. Kodama & K. Uzawa, JHEP 0507 061 (2005))

☆ Question

Do supersymmetries preserve in the dynamical M-brane background?

[3] Preserved supersymmetry (11d SUGRA)

The 11-dimensional action is invariant under local SUSY transformations :

$e^A{}_M$: graviton Ψ_M : gravitino,
A_{MNP} : 3-form gauge potential

$$\delta e^A{}_M = \bar{\varepsilon}\Gamma^A \Psi_M ,$$

$$\delta A_{MNP} = -3\,\bar{\varepsilon}\Gamma_{[MN}\Psi_{P]} ,$$

$$\begin{aligned} \delta\Psi_M &= D_M \varepsilon \\ &= \left[\nabla_M + \frac{1}{12\cdot 4!}\left(\Gamma_M F_{MNPQ}\Gamma^{MNPQ} - 12F_{MNPQ}\Gamma^{NPQ}\right)\right]\varepsilon \end{aligned}$$

★Supersymmetry in dynamical M2-brane

- **The only fermionic field is the gravitino Ψ_M, which vanishes classically.**

- **Supersymmetric configuration is a nontrivial solution to the Killing spinor equation :**

$$\delta\Psi_M = 0 ,$$

$$\Rightarrow \left[\nabla_M + \frac{1}{12\cdot 4!}\left(\Gamma_M F_{MNPQ}\Gamma^{MNPQ} - 12F_{MNPQ}\Gamma^{NPQ}\right)\right]\varepsilon = 0$$

☆ **Ansatz for fields**

- **11-dim metric**

(1+2)-dim worldvolume spacetime

$$ds^2 = g_{MN}dx^M dx^N = \boxed{h^{-2/3}(x,r)\eta_{\mu\nu}(\mathrm{X})dx^\mu dx^\nu}$$

$$+\boxed{h^{1/3}(x,r)\left(dr^2 + r^2 u_{ab}(\mathrm{Z})dz^a dz^a\right)}$$

8-dim transverse space to brane

- **4-form field strength & gravitino**

$$F_{r\mu\nu\rho} = \pm h^{-2}\partial_r h\, \varepsilon_{\mu\nu\rho}\,, \quad \Psi_M = 0$$

11-dimensional gamma matrices satisfying

$$\Gamma^M\Gamma^N + \Gamma^N\Gamma^M = 2g^{MN}\,,$$

$$\Gamma^\mu = h^{1/3}\gamma^\mu\,, \quad \Gamma^r = h^{-1/6}\,\gamma^r\,, \quad \Gamma^a = r^{-1}h^{-1/6}\,\gamma^a$$

and we define

$$\gamma_{(3)} = \gamma_0\,\gamma_1\,\gamma_2$$

☆ Killing spinor equation

$$\bar{\nabla}_\mu \varepsilon = \left[\partial_\mu + \boxed{\frac{1}{6}\partial_\nu \ln h \gamma^\nu{}_\mu} - \boxed{\frac{1}{6} h^{-3/2} \partial_r h \gamma^\mu \gamma^r \left(1 \pm \gamma_{(3)}\right)} \right] \varepsilon \,,$$

$$\bar{\nabla}_r \varepsilon = \left[\partial_r - \boxed{\frac{1}{12} h^{-1/2} \partial_\nu h \gamma^\nu \gamma^r} + \frac{1}{6} \chi h^{-1} \partial_r h \gamma_{(3)} \right] \varepsilon \,,$$

$$\bar{\nabla}_a \varepsilon = \left[{}^{\mathrm{Z}}\nabla_a - \boxed{\frac{r}{12} h^{-1/2} \partial_\nu h \gamma^\nu \gamma_a} - \boxed{\frac{r}{12} h^{-1} \partial_r h \gamma^r \gamma_a \left(1 \pm \gamma_{(3)}\right)} \right] \varepsilon$$

- If the function h(x, r) is included in the spinor $\varepsilon = h^{-1/6}\ \varepsilon_0$ (ε_0 : constant Killing spinor), we find …

- Solution for dynamical background

$$\partial_\mu h \gamma^\mu \varepsilon = 0 \,, \quad \left(1 \pm \gamma_{(3)}\right) \varepsilon = 0$$

- Integrability condition $[\nabla_M, \nabla_N]\ \varepsilon = 0$ gives

$$\eta^{\mu\nu} \partial_\mu h \partial_\nu h = 0 \,, \qquad \partial_\mu \partial_\nu h = 0$$

Dynamical M2-brane solution :

(1+2)-dim worldvolume spacetime

$$ds^2 = \boxed{\left(c_\mu x^\mu + c + \frac{M}{r^6}\right)^{-2/3} \eta_{\mu\nu}(\mathrm{X})dx^\mu dx^\nu}$$

$$+ \boxed{\left(c_\mu x^\mu + c + \frac{M}{r^6}\right)^{1/3} \left(dr^2 + r^2 d\Omega_{(7)}^2\right)}$$

8-dim transverse space to brane

$$F_{r\mu\nu\rho} = -\frac{6M}{r^7}\left(c_\mu x^\mu + c + \frac{M}{r^6}\right)^{-2} \varepsilon_{\mu\nu\rho}\,, \qquad \Psi_M = 0$$

Dynamical spacetime

(1) $M \neq 0$, $c_\mu c^\mu = 0$, $c_0 \neq 0$, $c_1 \neq 0$, $c_2{}^2 = c_0{}^2 - c_1{}^2$: ¼ SUSY

(2) $M = 0$ (or $r \to \infty$), $c_\mu c^\mu = 0$, $c_0 \neq 0$, $c_1 \neq 0$, $c_2{}^2 = c_0{}^2 - c_1{}^2$: ½ SUSY, plane wave

(3) $M \neq 0$, $c_0 \neq 0$, $c_1 = 0$, $c_2 = 0$: Non SUSY

(4) $c_\mu = 0$, $c = 0$: Static, Maximal SUSY

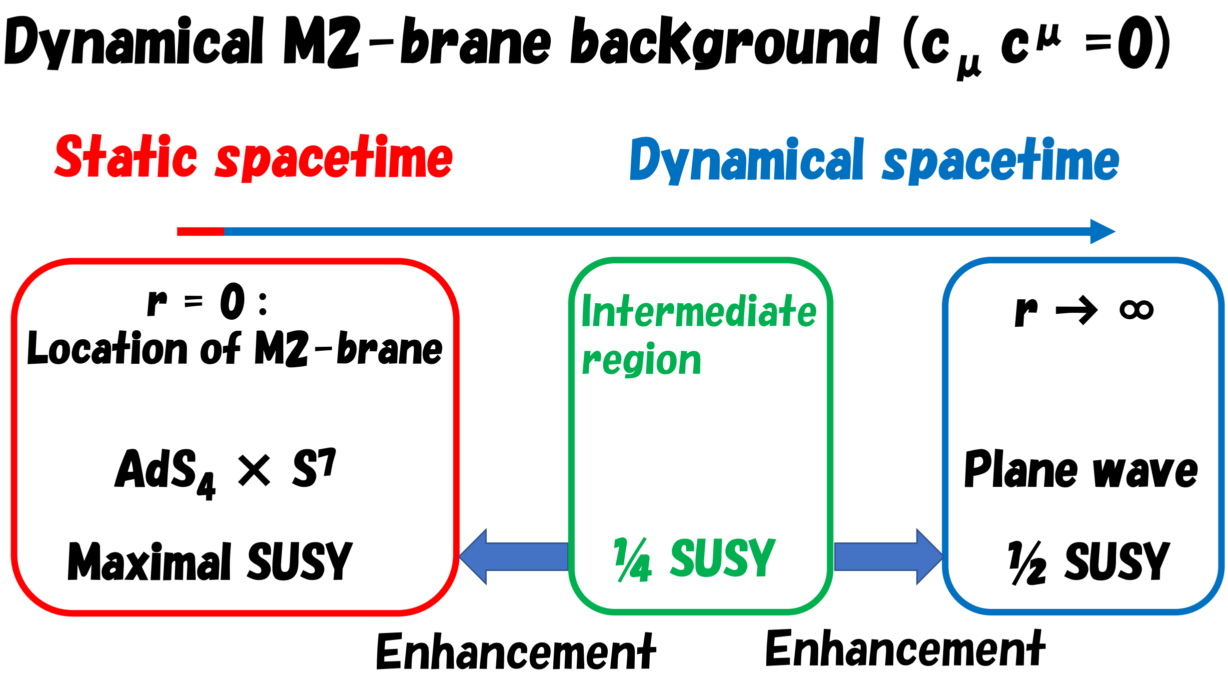

Dynamical M2-brane background ($c_\mu c^\mu = 0$)
Static spacetime
Dynamical spacetime
$r = 0$:
Location of M2-brane
$AdS_4 \times S^7$
Maximal SUSY
Intermediate region
¼ SUSY
$r \to \infty$
Plane wave
½ SUSY
Enhancement
Enhancement

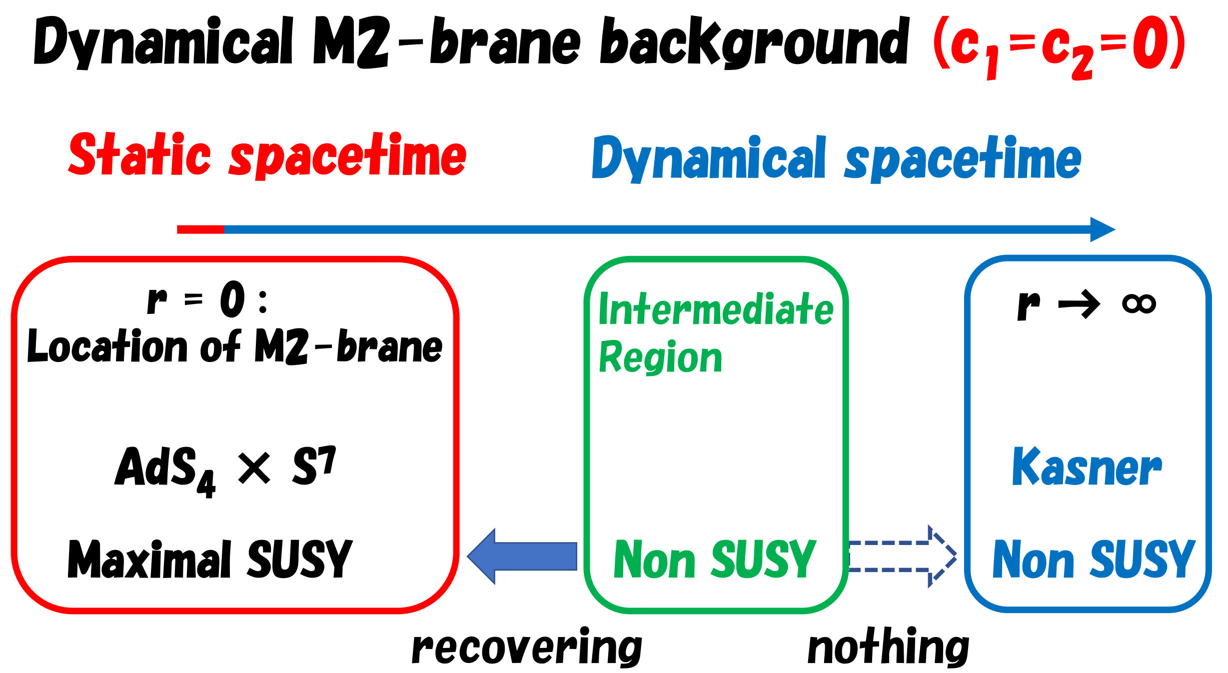

Dynamical M2-brane background ($c_1 = c_2 = 0$)
Static spacetime
Dynamical spacetime
$r = 0$:
Location of M2-brane
$AdS_4 \times S^7$
Maximal SUSY
Intermediate Region
Non SUSY
$r \to \infty$
Kasner
Non SUSY
recovering
nothing

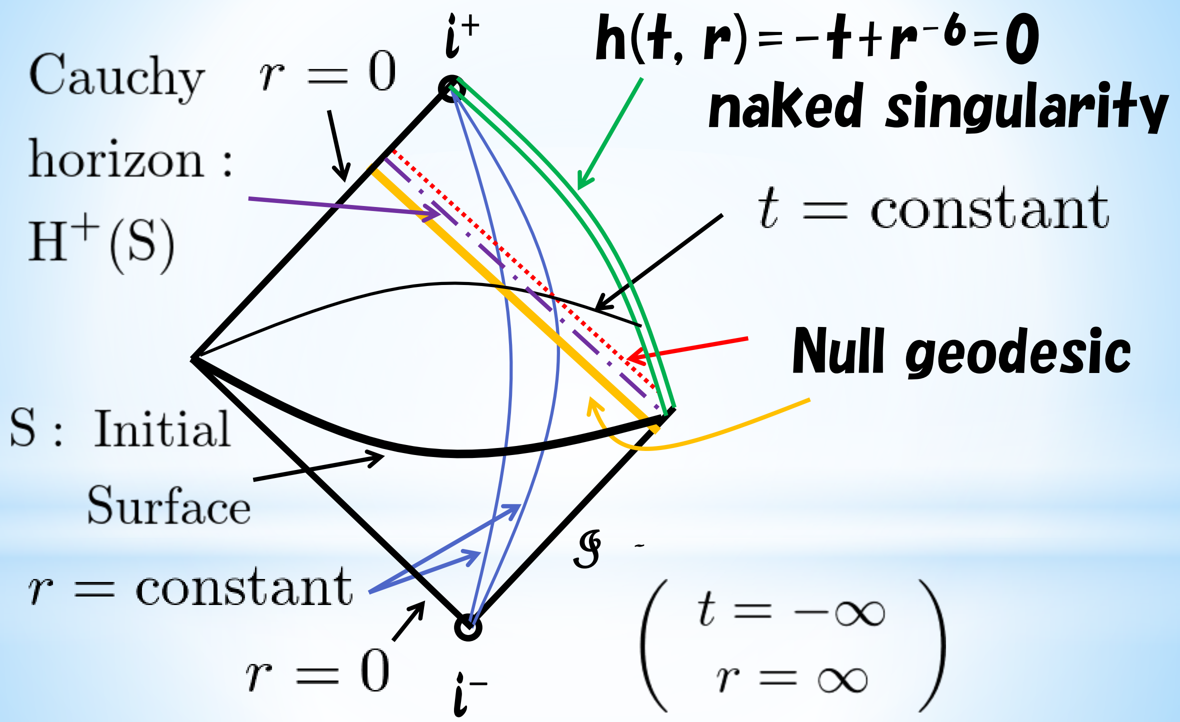

[4] SUSY breaking and enhancement of SUSY

(1) SUSY solution: $h = h(\tau, x^i, r)$, $\tau / \tau_0 = (ct)^{2/3}$

$$- \left(c\,t + c_i x^i + \frac{M}{r^6} \right)^{-\frac{2}{3}} dt^2 + \cdots$$

$$= - \left[1 + \left(\frac{\tau}{\tau_0} \right)^{-\frac{3}{2}} \left(c_i x^i + \frac{M}{r^6} \right) \right]^{-\frac{2}{3}} d\tau^2 + \cdots$$

(2) As time increases (for $c_i x^i \ll M/r^6$),

$$1 + \left(\frac{\tau}{\tau_0} \right)^{-\frac{3}{2}} \left(c_i x^i + \frac{M}{r^6} \right) \to 1 + \left(\frac{\tau}{\tau_0} \right)^{-\frac{3}{2}} \frac{M}{r^6}$$

(3) $h(\tau, x^i, r)$ (SUSY) $\to$ $h(\tau, r)$ (Non SUSY)

Time evolution (But toy model !!)

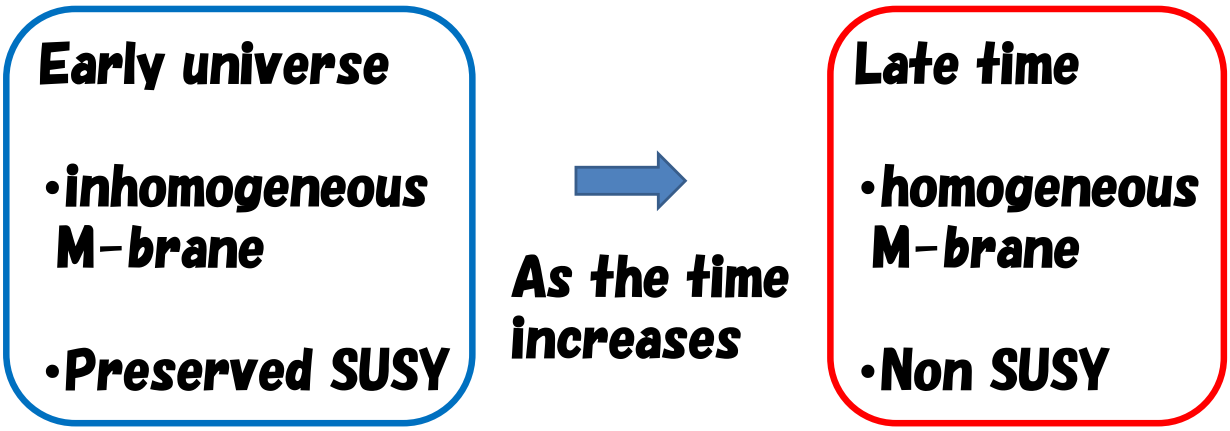

SUSY breaking

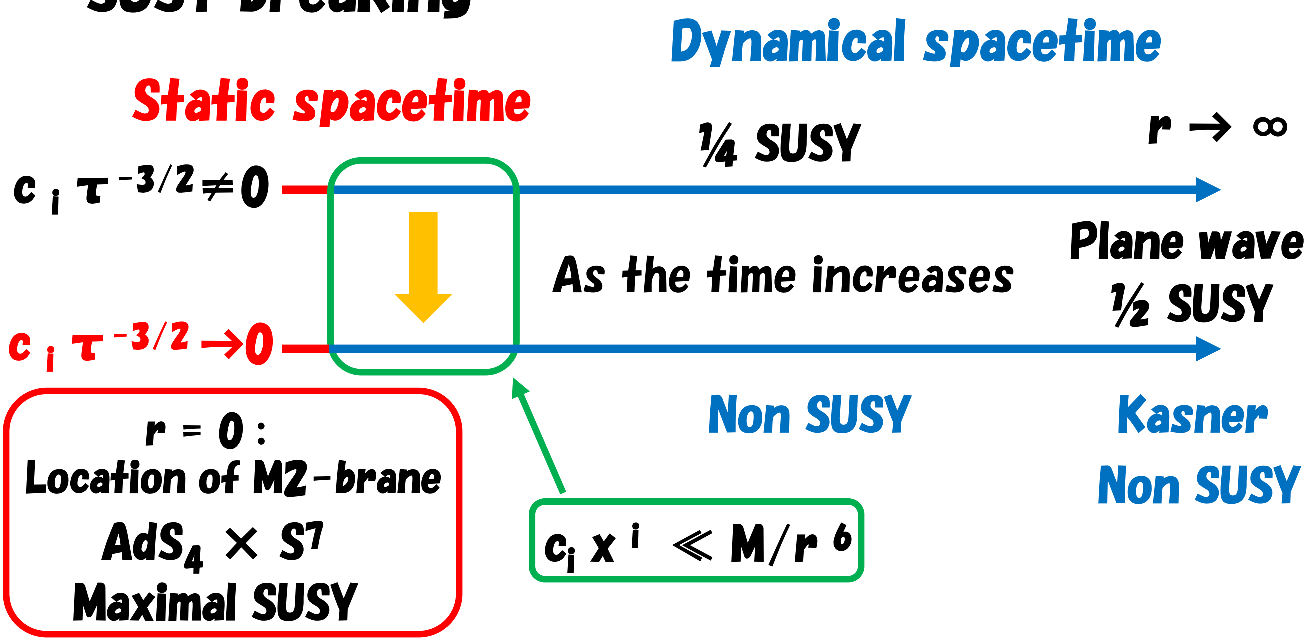

[3] Summary and comments

(1) The dynamical M2-brane background preserved the ¼ supersymmetry. For vanishing M2-brane charge, we also find ½ SUSY solution.

(2) The solutions of field equations cannot give a homogeneous expansion at constant r unless supersymmetries are completely broken.

(3) Although the solution itself is by no means realistic, its interesting behavior suggests a possibility that the Universe preserved originally SUSY and began to evolve toward a Universe without SUSY.

6b4. Umpei Miyamoto (Akita Prefectural U.), “Nonlinear perturbation of black branes at large D“ (10+5)

[JGRG27 (2017) 113010]

Non-linear perturbation of black branes at large D

Umpei Miyamoto
Akita Prefectural University

JHEP06(2017)033 [arXiv:1705.00486]

27th JGRG@Hiroshima 2017.11.30

Contents

Background

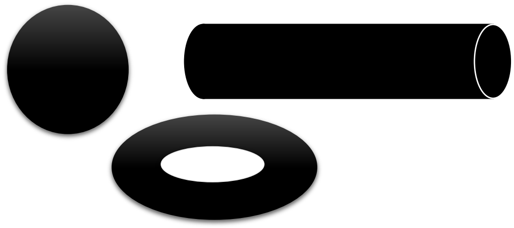

- Higher-dim. BHs
  - Instability & various phase structures (e.g. Gregory-Laflamme inst.)
  - Gauge/Gravity correspondence (e.g. AdS/CFT, AdS/CMP, Fluid/Gravity)

Holes cut out in Minkowski space

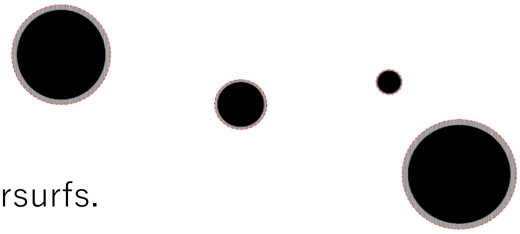

- Large-D approach (R. Emparan, R. Suzuki, K. Tanabe, and more)
  - 1/D expansion of GR
  - Horizons are Constant-Mean-Curvature hypersurfs.

http://www2.yukawa.kyoto-u.ac.jp/ws/2013/string13/Emparan.pdf

Preceding works：Black branes at large D

(Emparan-Suzuki-Tanabe PRL2015)

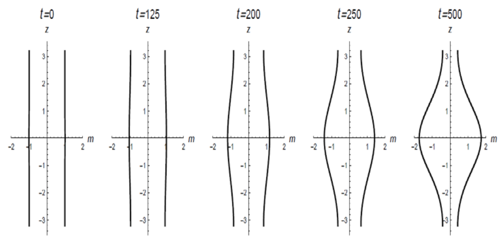

- Leading-order EOMs of BBs in 1/D (Asympt. flat & AdS)
  - 1+1 diffusion eqs. for m(t,z) and p(t,z)
  - GL-unstable BS converges to a non-uniform BS (Sorkin 2004)

- Related work (Herzog-Spillane-Yarom 2016)
  - Holographic dual of Riemann problem ➔Non-Equilibrium Steady States (NESSs)

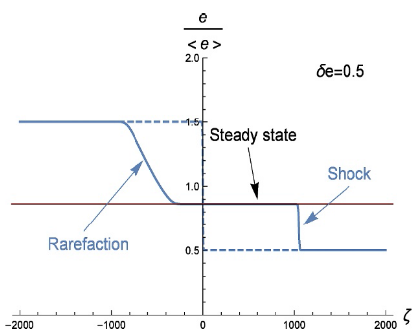

- Question: Can we say anything analytically using simplified EOMs?

My work : Non-linear pert. of large-D black branes (UM JHEP2017)

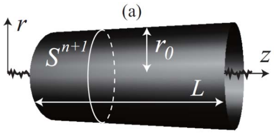

$$(\partial_t - \partial_z^2)m + \partial_z p = 0,$$
$$(\partial_t - \partial_z^2)p - \partial_z m = -\partial_z(\frac{p^2}{m}),$$

- Diffusion eqs. of m(t,z)and p(t,z)

$$m(t,z;\epsilon) = 1 + \sum_{\ell=1}^{\infty} m_\ell(t,z)\epsilon^\ell,$$

- Expand them around a uniform brane

$$p(t,z;\epsilon) = \sum_{\ell=1}^{\infty} p_\ell(t,z)\epsilon^\ell,$$

- Laplace & Fourier tr. wrt t and z, resp.
  - Solve algebraic eqs.
  - Inverse tr.
  - General solutions

$$\dot{m}_\ell - m_\ell'' + p_\ell' = 0,$$
$$\dot{p}_\ell - p_\ell'' - m_\ell' = \psi_\ell,$$

$$\psi_2 = -2p_1p_1',$$
$$\psi_3 = 2m_1p_1p_1' + m_1'p_1^2 - 2p_1p_2' - 2p_1'p_2.$$

General form of solutions at O(ε ^l)

$$\begin{pmatrix} m_\ell(t,z) \\ p_\ell(t,z) \end{pmatrix} = \sum_{\sigma=+,-} \boldsymbol{B}_\sigma \begin{pmatrix} \mathcal{F}^{-1}[e^{s_\sigma(k)t}\bar{m}_\ell(0,k)] \\ \mathcal{F}^{-1}[e^{s_\sigma(k)t}\bar{p}_\ell(0,k) + e^{s_\sigma(k)t} * \bar{\psi}_\ell(t,k)] \end{pmatrix}$$

$$\boldsymbol{B}_\sigma := \frac{1}{2}\begin{pmatrix} 1 & -\sigma i \\ \sigma i & 1 \end{pmatrix},$$
$$s_\sigma(k) := k(\sigma 1 - k).$$

I have obtained the soln. at every order as the linear combinations of inverse Fourier tr. of initial spectra m_l(0,k) & p_l(0,k).

Applicat'n to GL inst. $m_1(0,z) = \sum_{n=1}^{N} a_n \cos(k_n z + \varphi_n)$

- Superposit'n of sinusoidal waves as initial condition
  ➔Obtain solns. up to 2nd order

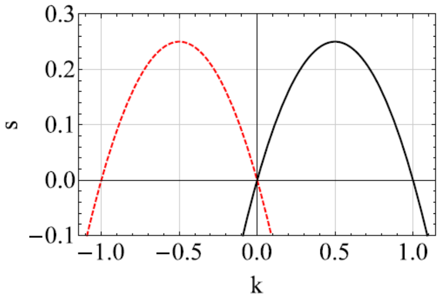

- A couple of GL-stable modes constitute a "beat"

- The beat grows if its size is greater than GL critical length

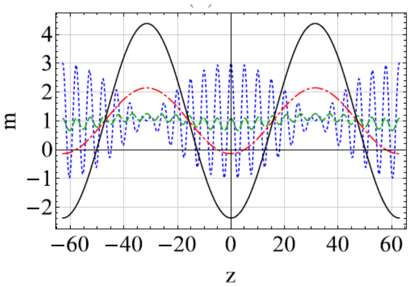

Applicat'n to Riemann problem

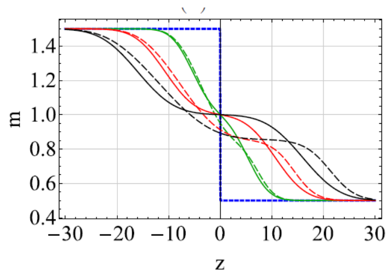

- Step-funct'n as m1(t=0,z)
  - 1st order soln. in terms of Gauss error fun.
  - Semi-analytic descript'n of NESS

$$m_1(t,z) = \frac{\alpha}{2}\left[\mathrm{erf}\left(\frac{t+z}{2\sqrt{t}}\right) - \mathrm{erf}\left(\frac{t-z}{2\sqrt{t}}\right)\right],$$

$$p_1(t,z) = -\frac{\alpha}{2}\left[\mathrm{erf}\left(\frac{t-z}{2\sqrt{t}}\right) + \mathrm{erf}\left(\frac{t+z}{2\sqrt{t}}\right)\right].$$

- Superposit'n of sinusoidal waves as m1(t=0,z)
  - Obtain solutions up to 2nd order
  - Reproduce details of NESS

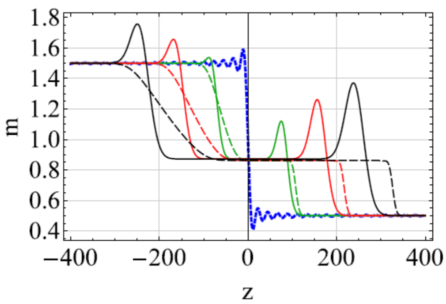

Conclusion

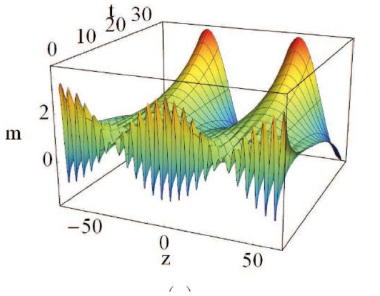

- Perturb BBs at large-D around the uniform soln. and obtain the general form of soln. at every order

- Write down the explicit form of solns. for several initial conditions.
  - Property of GL inst. in non-linear regime
  - Analytic description of NESS

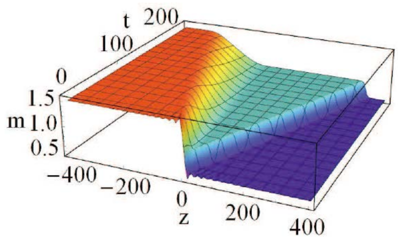

- Future prospects
  - 1/D corrections & BBs with charges
  - Application to turbulence (Rozali et al. 2017)

6b5. Gonalo Quinta (Superior Technical Institute, U. of Lisbon),

"Vacuum polarization around a charged black hole in 5 dimensions" (10+5)

[JGRG27 (2017) 113011]

Vacuum Polarization Around a Charged Black Hole in 5 Dimensions

Gonçalo M. Quinta
In collaboration with: Antonino Flachi, José P. S. Lemos

December 20, 2017

Instituto Superior Técnico - Multidisciplinary Center for Antrophysics (CENTRA)

Table of contents

Introduction

- To introduce quantum effects into the Einstein equation, one may take the semiclassical limit

$$G_{\mu\nu} = 8\pi \langle T_{\mu\nu} \rangle \, .$$

- However, it's a formidable task to compute the quantity $\langle T_{\mu\nu} \rangle$, even numerically. It's easier to compute the vacuum polaization $\langle \phi^2 \rangle$, which is related to $\langle T_{\mu\nu} \rangle$ and provides a good deal of information.

- Calculations are usually restricted to 4 dimensions. In this work, we will present a way to calculate this quantity around a charged black hole in 5 dimensions.

Vacuum polarization around a 5-dimensional black hole

Consider a massive non-minimally coupled quantum scalar field

$$\left(\Box - \mu^2 - \xi R\right) \phi(x) = 0 \, .$$

One may show that

$$\langle \phi^2(x) \rangle = \lim_{x' \to x} i\, G(x, x') = \lim_{x' \to x} G_E(x, x') \, ,$$

where the Green function $G(x, x')$ gives the probability amplitude for a particle to go from spacetime point x to x'. Using $\tau = -it$,

$$\left(\Box_E - \mu^2 - \xi R\right) G_E(x, x') = -\frac{\delta^{(5)}(x - x')}{\sqrt{g}} \, .$$

Vacuum polarization around a 5-dimensional black hole

The background geometry will be a 5-dimensional charged black hole

$$ds_E^2 = f(r)d\tau^2 + \frac{1}{f(r)}dr^2 + r^2 d\Omega_3^2, \quad f(r) = 1 - \frac{2m}{r^2} + \frac{q^2}{r^4}\,.$$

Expand the Green function in hyperspherical harmonics

$$G_E(x,x') = \frac{\kappa}{4\pi^3}\sum_{n=-\infty}^{\infty} e^{in\kappa\Delta\tau}\sum_{l=0}^{\infty}(l+1)C_l^{(1)}(\cos\gamma)G_{nl}(r,r')$$

($\kappa = 2\pi T$, $\Delta\tau = \tau' - \tau$, γ angular geodesic distance) and the differential equations becomes

$$\frac{d^2G_{nl}}{dr^2} + \left(\frac{3}{r} + \frac{f'}{2f}\right)\frac{dG_{nl}}{dr} - \left(\frac{n^2\kappa^2}{f^2} + \frac{l(l+2)}{fr^2} + \frac{m^2+\xi R}{f}\right)G_{nl} = -\frac{\delta(r-r')}{r^3 f}\,.$$

Vacuum Polarization around a 5-dimensional black hole

A WKB ansatz turns the mode Green function into

$$G_{nl}(r,r) = \frac{1}{2\,r^{N+1}\,W(r)}$$

and the homogeneous differential equation into

$$W^2 = \Phi + a_1\frac{W'}{W} + a_2\frac{W'^2}{W^2} + a_3\frac{W''}{W}$$

with

$$\Phi = l\,(l+2)\,\frac{f}{r^2} + n^2\kappa^2 + M^2(r)f\,,$$

$$a_1 = \frac{ff'}{2}, \quad a_2 = -\frac{3}{4}f^2, \quad a_3 = \frac{f^2}{2}\,,$$

The problem is reduced to calculating the WKB function $W(r)$.

Vacuum Polarization around a 5-dimensional black hole

Taking the partial concincidence limit $\mathbf{x} \to \mathbf{x}'$ with the WKB ansatz,

$$G_E(x, x') = \frac{\kappa}{8\pi^3 r^3} \sum_{n=-\infty}^{\infty} e^{in\kappa\Delta\tau} \sum_{l=0}^{\infty} \frac{(l+1)^2}{W(r)} .$$

We express the WKB solution iteratively as

$$\frac{1}{W} = \frac{1}{\Phi^{1/2}} \left(1 + \delta_1\Phi + \delta_2\Phi + \cdots\right) .$$

At first order

$$\delta_1\Phi = -\frac{a_1}{4}\frac{\Phi'}{\Phi^2} + \left(\frac{a_3 - a_2}{8}\right)\frac{\Phi'^2}{\Phi^3} - \frac{a_3}{4}\frac{\Phi''}{\Phi^2} .$$

Regularization of the l modes

$\langle\phi^2(x)\rangle$ has **two divergences**: a (non-physical) divergence in the angular modes l; and a (physical) divergence in the energy modes n.

First we deal with the l modes. The divergent terms come from the large l behavior, which can be written in the form

$$\mathcal{T}_l = \frac{\kappa}{8\pi^3 r^3} \sum_n e^{in\kappa\Delta\tau} \sum_l R_l(r) .$$

Subtracting and taking $\Delta\tau \to 0$, we get the regularized result in the angular modes

$$\langle\phi^2(x)\rangle = \frac{\kappa}{8\pi^3 r^3} \sum_{n=-\infty}^{\infty} \sum_{l=0}^{\infty} \left\{ \frac{(l+1)^2}{W(r)} - \mathcal{T}_l \right\} .$$

Regularization of the n modes

$$\langle\phi^2(x)\rangle \sim \sum_n \left(\# n^2 \log n + \# \log n + \# + \frac{\#}{n} + \frac{\#}{n^2} + \dots \right)$$

Divergent terms in the n modes correspond to loop divergences. The Schwinger-DeWitt expansion predicts that

$$\langle\phi^2(x)\rangle_{div} = \lim_{\Delta\tau\to 0} \frac{1}{16\pi^2\sqrt{f}} \left\{ \frac{\pi}{\Delta\tau} \left(\left(\frac{1}{6} - \xi \right) R - m^2 - \frac{f'}{4r} + \frac{f'^2}{16f} \right) + \frac{2}{f^2\Delta\tau^3} \right\}$$

We should compare the two results to see if they are the same. The renormalized vacuum polarization will then be

$$\langle\phi^2(x)\rangle_{ren} = \left[\langle\phi^2(x)\rangle_{WKB} - \langle\phi^2(x)\rangle_{div} \right] + \delta\langle\phi^2(x)\rangle$$

Regularization of the n modes

To check explicit cancellation, define

$$\langle\phi^2(x)\rangle = \frac{\kappa}{8\pi^3 r^3} \sum_{n=-\infty}^{\infty} \sum_{l=0}^{\infty} \left\{ \frac{(l+1)^2}{W(r)} - \mathcal{T}_l \right\} \equiv \sum_{n=1}^{\infty} \sum_{l=0}^{\infty} g(l) .$$

The Abel-Plana sum formula can be used to perform the l summation

$$\langle\phi^2(x)\rangle = \sum_{n=1}^{\infty} \left(\underbrace{\frac{g(0)}{2}}_{\mathcal{P}_1} + \underbrace{\int_0^\infty g(x) dx}_{\mathcal{P}_2} + \underbrace{i \int_0^\infty \frac{g(ix) - g(-ix)}{e^{2\pi x} - 1} dx}_{\mathcal{P}_3} \right) .$$

We will only need to consider WKB up to first order, i.e.

$$\frac{1}{W} = \frac{1 + \delta\Phi}{\sqrt{\Phi}} .$$

Regularization of the n modes

Evaluating each term separatly,

$$\mathrm{div}\left[\mathcal{P}_1\right] = \sum_{n=1}^{\infty} \frac{1}{2n\kappa}$$

$$\mathrm{div}\left[\mathcal{P}_2\right] = \sum_{n=1}^{\infty} \left\{ -\frac{1}{3n\kappa} + \frac{r^3}{8\sqrt{f}} \left[\frac{4n^2\kappa^2}{f} + \left(m^2 - [a_1] + \frac{f'}{r} - \frac{f'^2}{4f} + \frac{f''}{3} \right) \right] \left(1 + \ln\left(\frac{rn\kappa}{2\sqrt{f}} \right) \right) \right\}$$

$$\mathrm{div}\left[\mathcal{P}_3\right] = \sum_{n=1}^{\infty} \left(-\frac{1}{6n\kappa} \right)$$

leads to the total divergent piece

$$\mathrm{div}\left[\mathcal{P}_1 + \mathcal{P}_2 + \mathcal{P}_3\right] = \sum_{n=1}^{\infty} \left\{ \frac{r^3}{8\sqrt{f}} \left[\frac{4n^2\kappa^2}{f} + \left(m^2 - [a_1] + \frac{f'}{r} - \frac{f'^2}{4f} + \frac{f''}{3} \right) \right] \left(1 + \ln\left(\frac{rn\kappa}{2\sqrt{f}} \right) \right) \right\} .$$

This must be compared which the Schwinger-De Witt result.

Regularization of the n modes

The trick is to use the formulas

$$\sum_{n=1}^{\infty} \log\left(n\kappa\right) \cos(n\kappa\Delta\tau) = -\frac{\pi}{2\kappa}\frac{1}{\Delta\tau} + O(\Delta\tau)\,,$$

$$\sum_{n=1}^{\infty} n^2\kappa^2 \log\left(n\kappa\right) \cos(n\kappa\Delta\tau) = \frac{\pi}{2\kappa}\frac{1}{\Delta\tau^3} + O(\Delta\tau)\,,$$

in

$$\langle\phi^2(x)\rangle_{div} = \lim_{\Delta\tau\to 0} \frac{1}{16\pi^2\sqrt{f}} \left\{ \frac{\pi}{\Delta\tau} \left(\left(\frac{1}{6} - \xi \right) R - m^2 - \frac{f'}{4r} + \frac{f'^2}{16f} \right) + \frac{2}{f^2\Delta\tau^3} \right\} .$$

This will give **exactly** the same divergent terms, so we may subtract them to obtain a fully renormalized result.

Numerical Results

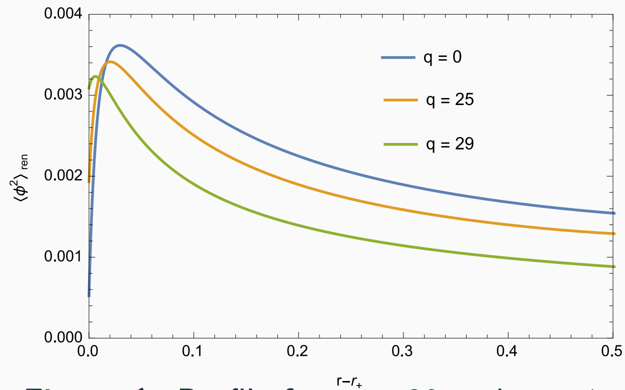

Figure 1: Profile for $m = 30$ and $\mu = 1$.

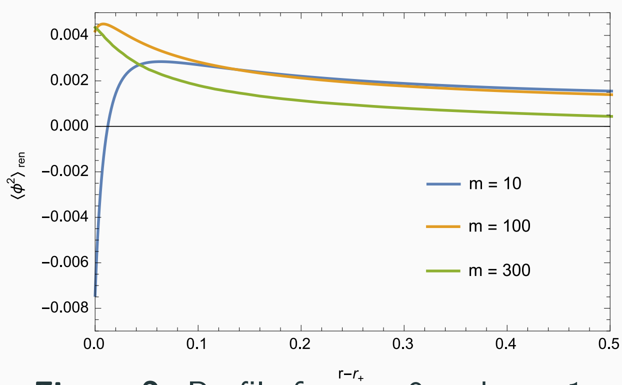

Figure 2: Profile for $q = 0$ and $\mu = 1$.

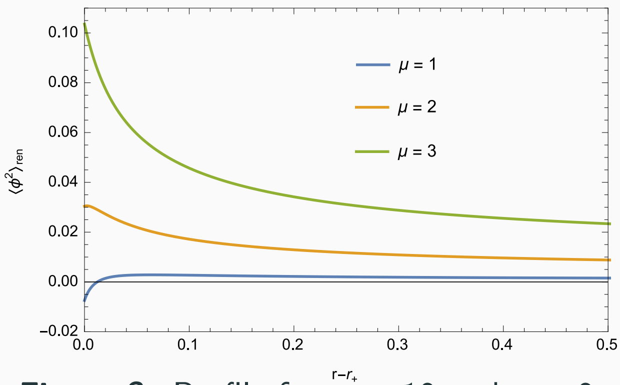

Figure 3: Profile for $m = 10$ and $q = 0$.

Summary

- Although widely studied for $D = 4$, the vacuum polarization in higher dimensional spacetimes doesn't usually get much attention due to the high complexity of the countertems involved in the regularization procedure.
- We fully studied the case of a 5-dimensional charged black hole, and obtained a renormalized quantity. The regularity of the result was explicitly proven by direct calculation of the counterterms.
- Although quantum calculations with higher dimensional black holes are increasing, there are still a lot of physical aspects to be understood.

Thank you for your attention!

聞いてくれてありがとう!

Session7a 14:00–15:45

[Chair: Jiro Soda]

7a1. Tomoya Kinugawa (ICRR U. of Tokyo), "Gravitational waves from remnants of first stars" (10+5)

[JGRG27 (2017) 113012]

Gravitational waves from remnants of first stars

Tomoya Kinugawa
(ICRR, University of Tokyo)

GW150914

PRL **116,** 061102 (2016) Selected for a Viewpoint in *Physics* PHYSICAL REVIEW LETTERS week ending 12 FEBRUARY 2016

Observation of Gravitational Waves from a Binary Black Hole Merger

B. P. Abbott *et al.**
(LIGO Scientific Collaboration and Virgo Collaboration)
(Received 21 January 2016; published 11 February 2016)

On September 14, 2015 at 09:50:45 UTC the two detectors of the Laser Interferometer Gravitational-Wave Observatory simultaneously observed a transient gravitational-wave signal. The signal sweeps upwards in frequency from 35 to 250 Hz with a peak gravitational-wave strain of 1.0×10^{-21}. It matches the waveform predicted by general relativity for the inspiral and merger of a pair of black holes and the ringdown of the resulting single black hole. The signal was observed with a matched-filter signal-to-noise ratio of 24 and a false alarm rate estimated to be less than 1 event per 203 000 years, equivalent to a significance greater than 5.1σ. The source lies at a luminosity distance of 410^{+160}_{-180} Mpc corresponding to a redshift $z = 0.09^{+0.03}_{-0.04}$. In the source frame, the initial black hole masses are $36^{+5}_{-4} M_\odot$ and $29^{+4}_{-4} M_\odot$, and the final black hole mass is $62^{+4}_{-4} M_\odot$, with $3.0^{+0.5}_{-0.5} M_\odot c^2$ radiated in gravitational waves. All uncertainties define 90% credible intervals. These observations demonstrate the existence of binary stellar-mass black hole systems. This is the first direct detection of gravitational waves and the first observation of a binary black hole merger.

- $36M_\odot + 29M_\odot$, circular orbit

GW150914,GW170104

- More than facor 2 larger mass of BH compared with that in X-ray binary
- Many theories exist such as
- 1) PopII BBH
- 2)PopIII BBH

Low metal field binaries

- 3) Primordial Binary BH(PBBH)
- 4) Three body origin from Globular Cluster
- 5) Fragmentation of very massive stars
- ……………………

Why field binaries?

- There are many massive close binaries

  Example

  Milky way young open clusters

  71 O stars fbinary=69+/-9% (P<3200days) Sana et al. 2012

  30 Doradus (Tarantula Nebula)

  362 O stars fbinary=51+/-4%(P<3200days) Sana et al. 2013

Why low metal?

- If the progenitor of BH is Pop I (=Solar metal stars)

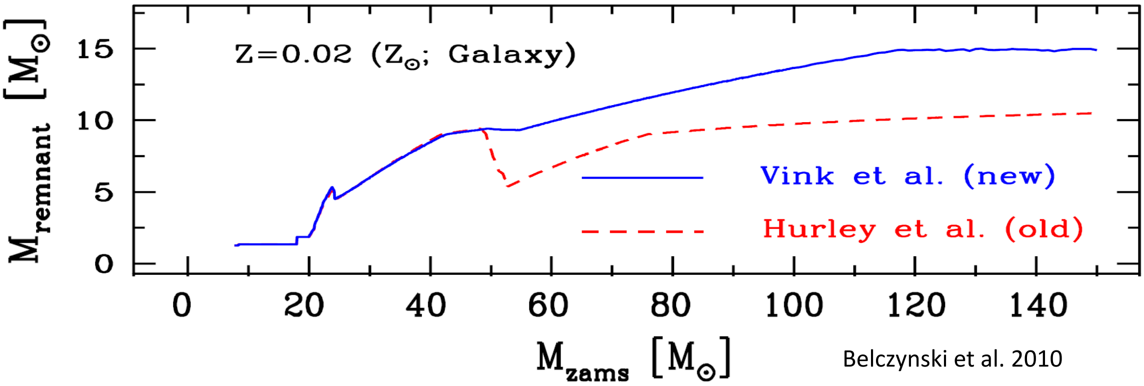

Belczynski et al. 2010

- The orbit become wide due to wind mass loss

Why low metal?

- If the progenitor is low metal,
- Pop II (Z<0.1Zsun)

  Typical mass is same as Pop I

  But, week wind mass loss

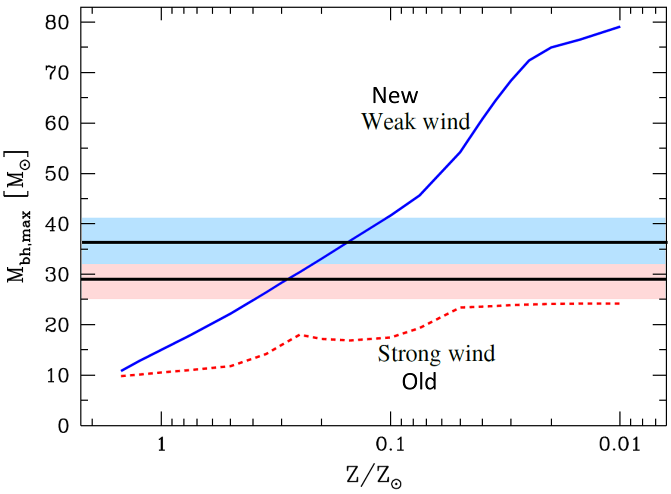

Minitial: 8Msun<M<150Msun

Single stellar evolution with 2 stellar wind models.

(Belczynski et al.2010, Abbot et al.2016)

- Pop III (No metal)

  Pop III stars are ***the first stars*** after the Big Bang.

  Typical mass is more massive than Pop I, II

  MpopIII~10-100Msun

  No wind mass loss due to no metal.

Total mass distribution of BH-BH which merge within the Hubble time

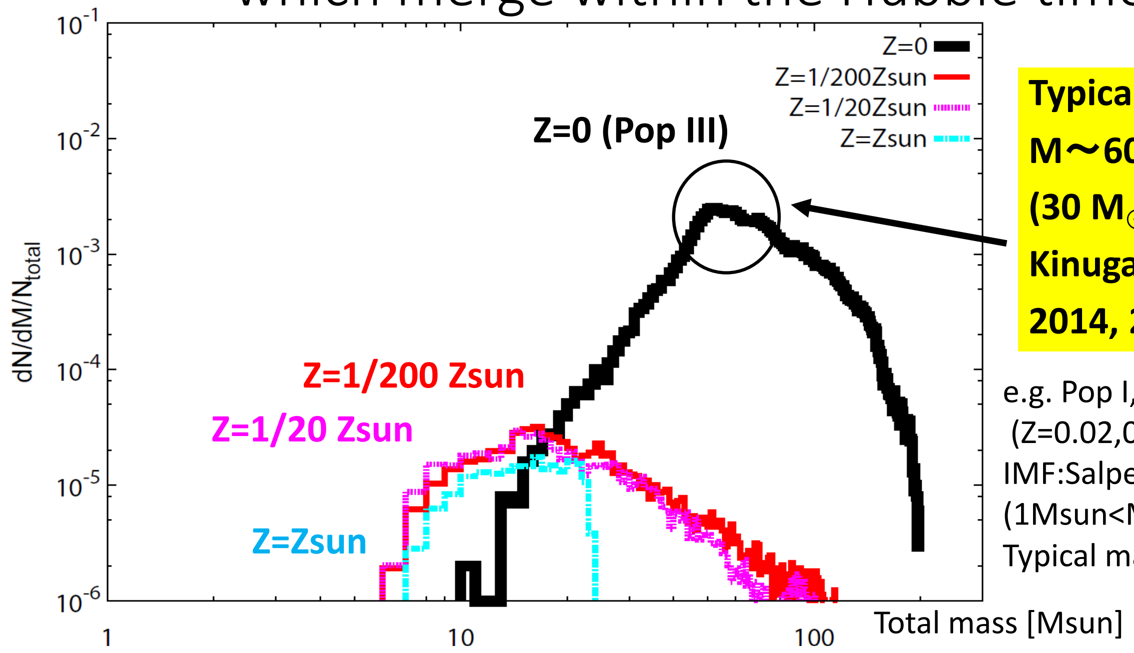

Typical total mass
$M \sim 60\ M_\odot$
$(30\ M_\odot + 30\ M_\odot)$
Kinugawa et al. 2014, 2016

e.g. Pop I, Pop II
(Z=0.02,0.001,0.0001)
IMF:Salpeter
(1Msun<M<140Msun)
Typical mass $\sim 10\ M_\odot$

What do determine the BH-BH mass?

- Steller wind mass loss
- Binary interactions

(Mass transfer, Common envelope)

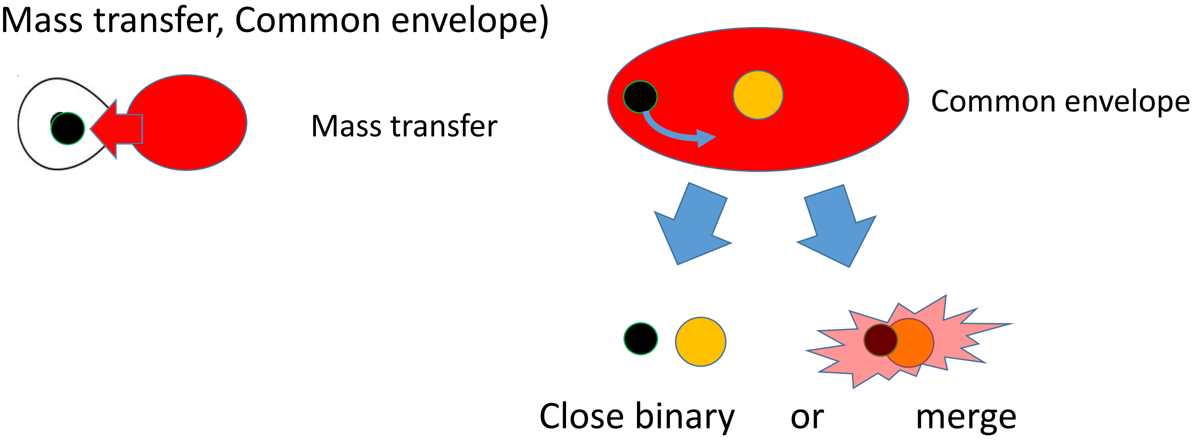

Why Pop III binaries become 30Msun BH-BH

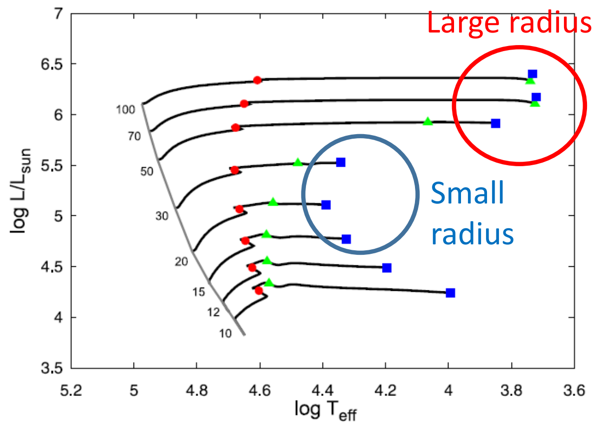

Figure 1. The Hertzsprung-Russell (HR) diagram for the Pop III stars of mass 10 $M_\odot \leqslant M \leqslant 100\ M_\odot$ using the data taken from Marigo et al. (2001). The number attached to each solid curve is the mass of each star in unit of $M_\odot$. The dashed line shows the ZAMS (Zero Age Main Sequence) stars. Red circles, green triangles and blue squares correspond to the beginning of He-burning, the end of the He-burning and the beginning of the C-burning, respectively.

- M>50Msun red giant

→Mass transfer is unstable
→common envelope
→1/3~1/2 of initial mass
(~25-30Msun)

- M<50Msun blue giant

→Mass transfer is stable
→mass loss is not so effective
→2/3~1 of initial mass (25-30Msun)

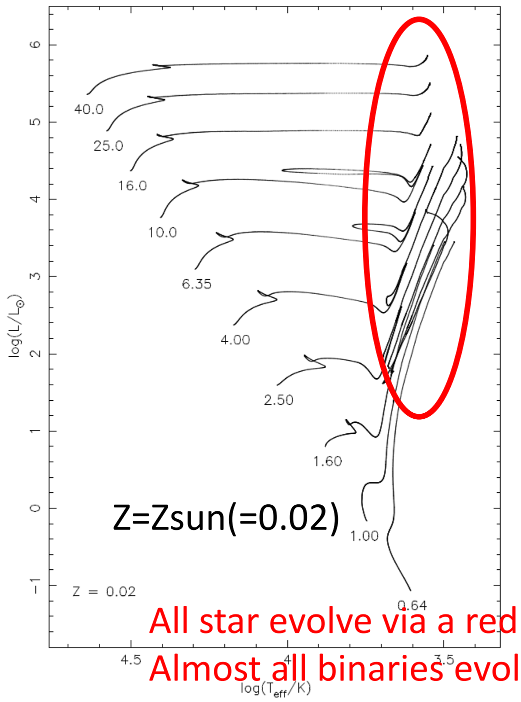

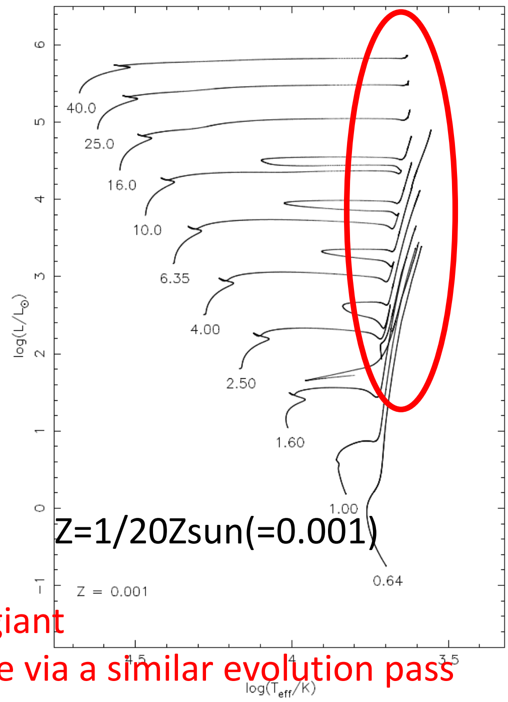

All star evolve via a red giant

Almost all binaries evolve via a similar evolution pass

Figure 1. Selected OVS evolution tracks for $Z = 0.02$, for masses 0.64, 1.0, 1.6, 2.5, 4.0, 6.35, 10, 16, 25 and 40 $M_\odot$.

Figure 2. Same as Fig. 1 for $Z = 0.001$. The 1.0 $M_\odot$ post He flash track has been omitted for clarity.

Total mass distribution of BBH which merge within the Hubble time

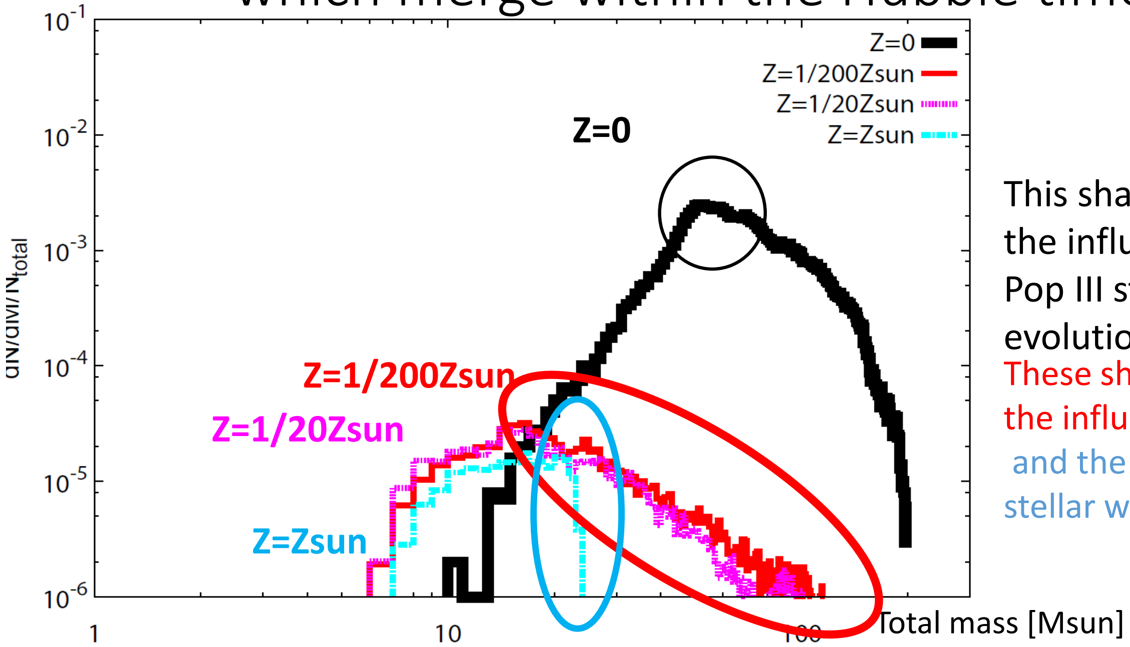

This shape reflects the influence of Pop III stellar evolution

These shapes have the influence of IMF and the influence of stellar wind mass loss

Pop III BBH remnants for gravitational wave

- Pop III stars were born and died at z~10
- The typical merger time of compact binaries ~$10^{8\text{-}10}$yr
- We might see Pop III BBH at the present day.

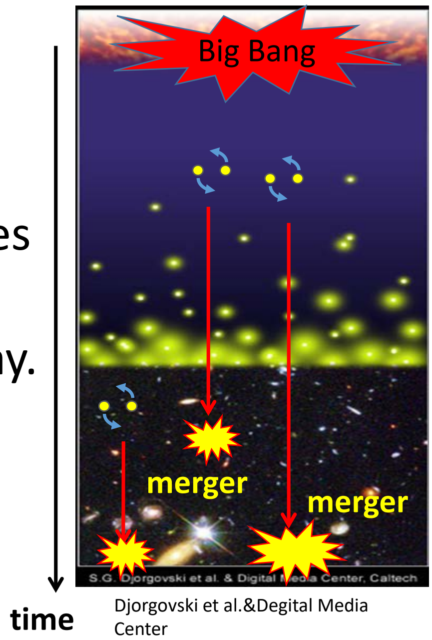

Djorgovski et al.&Degital Media Center

Pop III BBH?

ASTROPHYSICAL IMPLICATIONS OF THE BINARY BLACK-HOLE MERGER GW150914

ApJL Abbot. et al 2016

2014, Dominik et al. 2015).

On the extreme low-metallicity end, it has been proposed that BBH formation is also possible in the case of stellar binaries at zero metallicity (Population III [PopIII] stars; see Belczynski et al. 2004; Kinugawa et al. 2014). The predictions from these studies are even more uncertain, since we have no observational constraints on the properties of first-generation stellar binaries (e.g., mass function, mass ratios, orbital separations). However, if one assumes that the properties of PopIII massive binaries are not very different from binary populations in the local universe (admittedly a considerable extrapolation), then recently predicted BBH total masses agree astonishingly well with GW150914 and can have sufficiently long merger times to occur in the nearby universe (Kinugawa et al. 2014). This is in contrast to the predicted mass properties

Detection range of KAGRA and Adv. LIGO

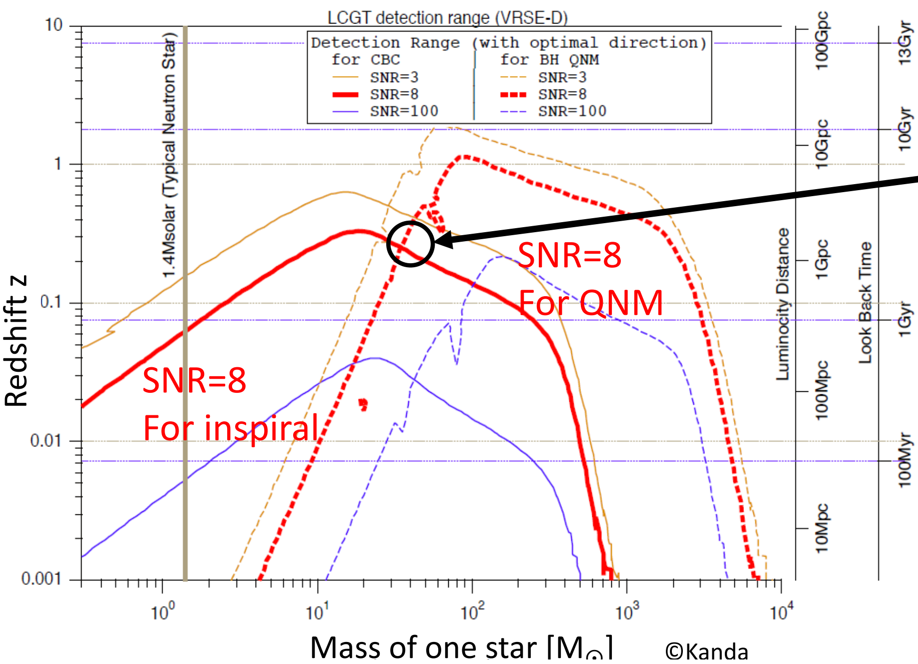

$M_{BH}\sim 30M_\odot$

SNR=8

Luminocity distance $\sim$1.5 Gpc

Redshift z$\sim$0.28

Detection rate of Pop III BH-BH

- **Detection rate of Pop III BBH (GW150914 like BBH) in our standard model**

$$\mathbf{R \sim 180} \left(\frac{SFR_{peak}}{10^{-2.5}}\right) \left(\frac{f_b/(1+f_b)}{0.33}\right) \; [\mathrm{yr}^{-1}] \; (S/N>8)$$

- Typical mass

$M \sim 30\, M_{\odot}$ →We can see the QNM of merged BBH

We might detect (or detected?) the Pop III BBH by GW

1. We might see BH QNM from Pop III BBH
   → We might check GR by Pop III BH QNM
2. The mass distribution might distinguish Pop III from Pop I, Pop II
   →The evidence of Pop III star

Cumulative BBH merger rate

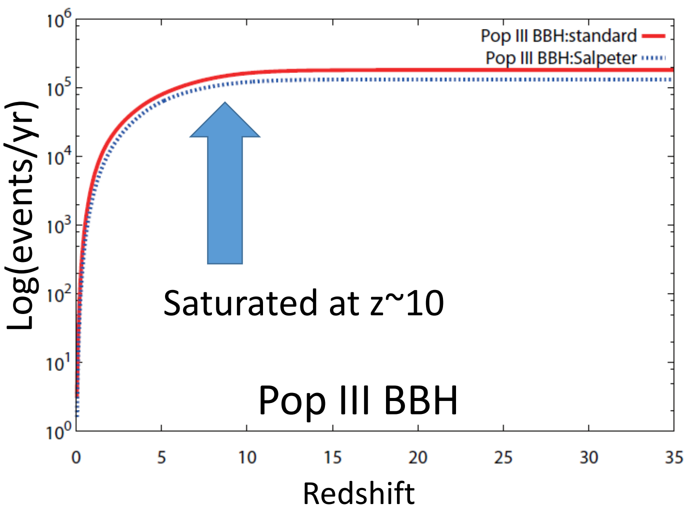

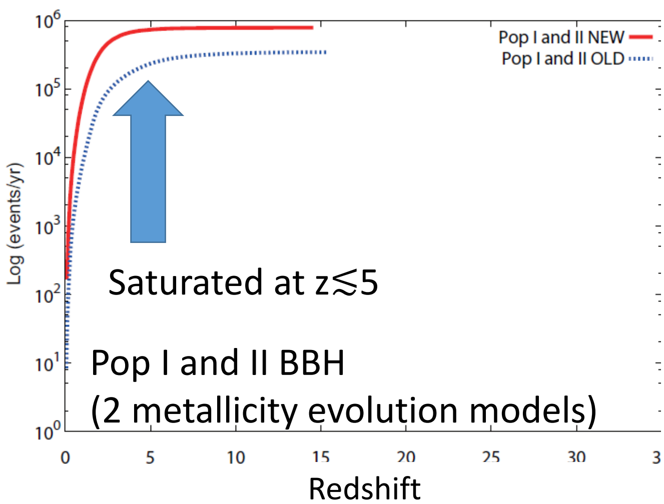

future plan of GW observer : pre-DECIGO and DECIGO

- DECIGO: Japanese space gravitational wave observatory project
- Pre-DECIGO: test version of DECIGO

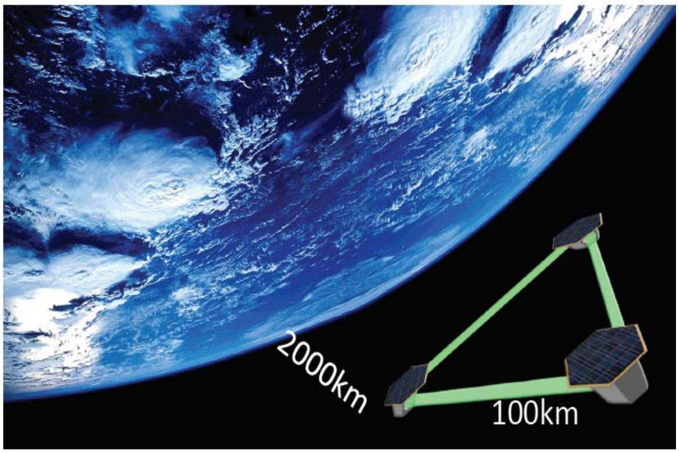

©Nakamura

- Pre-DECIGO : z~10 (30 Msun BH-BH)
  ~10^5 events/yr
- DECIGO can see Pop III BH-BHs when Pop III stars were born! (Nakamura, Ando, Kinugawa et al. 2016)

Summary

- Pop III binaries tend to become 30Msun+30Msun BH-BH
- **Pop III BBH detection rate of aLIGO in our standard model**

  $$R \sim 180 \left(\frac{SFR_{peak}}{10^{-2.5}}\right) \left(\frac{f_b/(1+f_b)}{0.33}\right) [\mathrm{yr}^{-1}] (S/N>8)$$

- The mass distribution or the redshift dependence might distinguish Pop III from Pop I,II.
- DECIGO can see Pop III BH-BH merger when they were born

7a2. Asuka Ito (Kobe U.),
“Primordial gravitational waves and early universes”
(10+5)
[JGRG27 (2017) 113013]

Primordial gravitational waves and early universes

Asuka Ito (Kobe Univ.)

with Jiro Soda (Kobe Univ.)

Ref: Phys.Lett.B771, [arXiv: 1607.0706]

Contents

Contents

1. **Observations of cosmological magnetic fields and magnetogenesis in the early universe**

   Inflation vs cyclic universe

2. Primordial gravitational waves from magnetic field production in a cyclic universe

3. Conclusion

Cosmological magnetic fields

Several observations imply there exist magnetic fields on galaxy and galaxy cluster scales

$$B_{galaxy} \sim 10^{-6} \text{ Gs} \quad , \quad B_{cluster} \sim 10^{-5} \text{ Gs}$$

In particular, Gamma ray burst observation infer existence of magnetic fields in void

$$B_{void} \gtrsim 10^{-16} \text{ Gs}$$

They imply that the seed of magnetic fields must be produced in the early universe

How can we produce?

Magnetogenesis

Ratra suggested a mechanism of magnetogenesis during inflation (1992)

$$\boxed{S = \int d^4x \sqrt{-g} \left[-\frac{1}{2}(\partial_\mu \phi)^2 - V(\phi) - \frac{1}{4} f(\phi) F_{\mu\nu} F^{\mu\nu} \right]}$$

This coupling prevent dilution of the gauge field due to expansion

$$f(\phi) = \left(\frac{a}{a_{end}} \right)^n$$ **(a: scale factor, n: positive constant)**

However, this mechanism suffers from the strong coupling problem during inflation, namely, $f(\phi) < 1$

On the other hand...

Magnetogenesis

In cyclic universe models, there is no strong coupling problem during the contracting phase

$$\boxed{S = \int d^4x \sqrt{-g} \left[-\frac{1}{2}(\partial_\mu \phi)^2 - V(\phi) - \frac{1}{4} f(\phi) F_{\mu\nu} F^{\mu\nu} \right]}$$

$$f(\phi) = \left(\frac{a}{a_{end}} \right)^n \longrightarrow f(\phi) > 1$$ **during contracting phase**

Magnetogenesis in $f(\phi)FF$

Inflation	**vs**	**cyclic universe**
difficult		**succesfull**
		(F. A. Memviela (2013))

ekpyrotic scenario

As a explicit cyclic universe model, we consider an ekpyrotic scenario.

In 4-dim, it is described by a scalar field rolling on an effective potential.

$$\boxed{S = \int d^4x\sqrt{-g}\left[-\frac{1}{2}(\partial_\mu \phi)^2 - V(\phi)\right]}$$

where ϕ **represents the size of a extra dimension.**

$\dot{\phi} > 0 \longrightarrow$ **expanding**

$\dot{\phi} < 0 \longrightarrow$ **contracting**

- **In the ekpyrotic scenario, quantum fluctuations are produced during a contracting phase**

PGWs in cyclic universe

Quantum fluctuations of GWs in the contracting phase is blue spectrum $P_h(k) \propto k^2$

This is common to other cyclic universe models!

➡ **We can not observe PGWs in cyclic universe models**

➡ **It is believed that detection of PGWs kills cyclic universe**

However, I will show that this is not true if magnetic field production occurs in cyclic universe!

Magnetogenesis in ekpyrotic

$$S = \int d^4x\sqrt{-g}\left[-\frac{1}{2}(\partial_\mu\phi)^2 - V(\phi)\right]$$

In the contracting phase for quantum fluctuations, the potential is given by

$$V(\phi) = V_0 e^{\lambda\frac{\phi}{M_{pl}}}$$

(V_0 and λ are negative constants)

We also consider a exponential type gauge kinetic function

$$S = \int d^4x\sqrt{-g}\left[-\frac{1}{2}(\partial_\mu\phi)^2 - V_0 e^{\lambda\frac{\phi}{M_{pl}}} - \frac{1}{4}e^{2\rho\frac{\phi}{M_{pl}}}F_{\mu\nu}F^{\mu\nu}\right]$$

expected from dimensional reduction

Magnetogenesis in ekpyrotic

$$S = \int d^4x\sqrt{-g}\left[-\frac{1}{2}(\partial_\mu\phi)^2 - V_0 e^{\lambda\frac{\phi}{M_{pl}}} - \frac{1}{4}e^{2\rho\frac{\phi}{M_{pl}}}F_{\mu\nu}F^{\mu\nu}\right]$$

We treat the electromagnetic field as a perturbation.
Then the background solution is given by

$$a(\tau) = a_{end}\left(\frac{-\tau}{\tau_{end}}\right)^{\frac{2}{\lambda^2-2}}, \quad \frac{\phi}{M_{pl}} = \phi_0 - \frac{2\lambda}{\lambda^2-2}\ln\left(\frac{-\tau}{M_{pl}}\right)$$

Solving the perturbative equation,
we get magnetic fields at the end of the contracting phase as

$$B_k(\tau) \propto k^{\frac{1}{2}\frac{\lambda^2-4\rho\lambda-2}{\lambda^2-2}} H_{end}^2$$

H_{end} : Hubble at the end of the contracting phase

Magnetogenesis in ekpyrotic

$$\boxed{B_k(\tau) \propto k^{\frac{1}{2}\frac{\lambda^2-4\rho\lambda-2}{\lambda^2-2}} H_{end}^2}$$

We assume scale invariant magnetic fields which might be favored by observations

$$\left(\frac{1}{2}\frac{\lambda^2-4\rho\lambda-2}{\lambda^2-2} = -\frac{3}{2}\right)$$

$$\boxed{B_k(\tau) = \frac{3\sqrt{2}}{8k^{3/2}}(\lambda^2-2)^2 H_{end}^2}$$

ex. $H_{end} \sim 10^{-5} M_{pl}, \ |\lambda| \sim 17$ $\longrightarrow$ 10^{-12} Gs **(at present)**

$\therefore$ **This mechanism could explain observed magnetic fields!**

Contents

1. Observations of cosmological magnetic fields and magnetogenesis in the early universe

   Inflation vs cyclic universe

2. **Primordial gravitational waves from magnetic field production in a cyclic universe**

3. Conclusion

PGWs from magnetic field production

$$\boxed{S_{EM} = \int d^4x\sqrt{-g}\left[-\frac{1}{4}e^{2\rho\frac{\phi}{M_{pl}}}F_{\mu\nu}F^{\mu\nu}\right]}$$

3d order perturbation

$$\left(\vec{B} = \frac{e^{\rho\frac{\phi}{M_{pl}}}}{a^2}\left(\nabla\times\vec{A}\right)\right)$$

$$\boxed{S_{GW} = \int d^4x\sqrt{-g}\left[\frac{1}{2}B_iB_jh^{ij}\right]}$$

B_i **: physical magnetic field**

h_{ij} **: gravitational wave**

Magnetic field production induces primordial gravitational waves through a following diagram

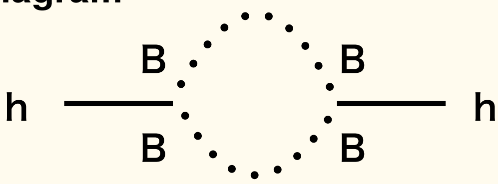

PGWs from magnetic field production

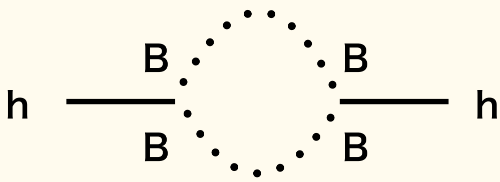

Using in-in formalism,
we can get the power spectrum of GW come from above diagram

$$\boxed{P_s(k) \simeq \frac{27}{16\pi^4}\lambda^8\left(\frac{H_{end}}{M_{pl}}\right)^4 \ln\left(\frac{k}{k_{in}}\right)}$$

nearly scale invariant (slightly blue)

To produce observed magnetic fields, we set

$$H_{end} \sim 10^{-5}M_{pl},\ \ |\lambda| \sim 17 \quad \rightarrow \quad \underline{P_s(k) \simeq 10^{-11}}$$

It is comparable to PGWs from inflation $P_{inf}(k) \simeq \left(\dfrac{H_{inf}}{\pi M_{pl}}\right)^2$

Conclusion

- As to the magnetic field production in $f(\phi)FF$ mechanism, cyclic universe is more favored than inflation

- Magnetic field production in cyclic universe models can induce abundant PGWs

  → Detection of PGWs can not kill cyclic universe

- To distinguish cyclic universe and inflation we need to see

  ex. (
  - spectrum of PGWs using various observations
  - non-gaussianity
  - if PGWs are quantum origin or not

  (• standard clock in non-gaussianity of scalar perturbation
  (X.Chen, M.H.Namjoo, Y.Wang (2016)))

7a3. Yi-Peng Wu (RESCEU U. of Tokyo), "Inflationary fluctuations with phase transitions" (10+5)

[JGRG27 (2017) 113014]

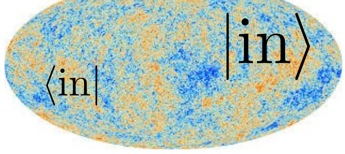

based on [1704.05026]

Yi-Peng Wu （呉　亦鵬）

RESearch Center for the Early Universe
The University of Tokyo

RESCEU 東京大学大学院理学系研究科附属ビッグバン宇宙国際研究センター Research Center for the Early Universe

in collaboration with
Jun'ichi Yokoyama (RESCEU),
Yi Wang & Siyi Zhou
(Hong Kong University of Science & Technology)

What is inflation all about?

$$a(t) \sim e^{Ht}$$

- The initial conditions of Big Bang cosmology.
- The generation of primordial density fluctuations.
- The small deviation from scale-invariant primordial power spectrum.

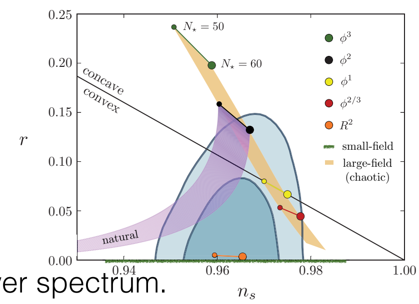

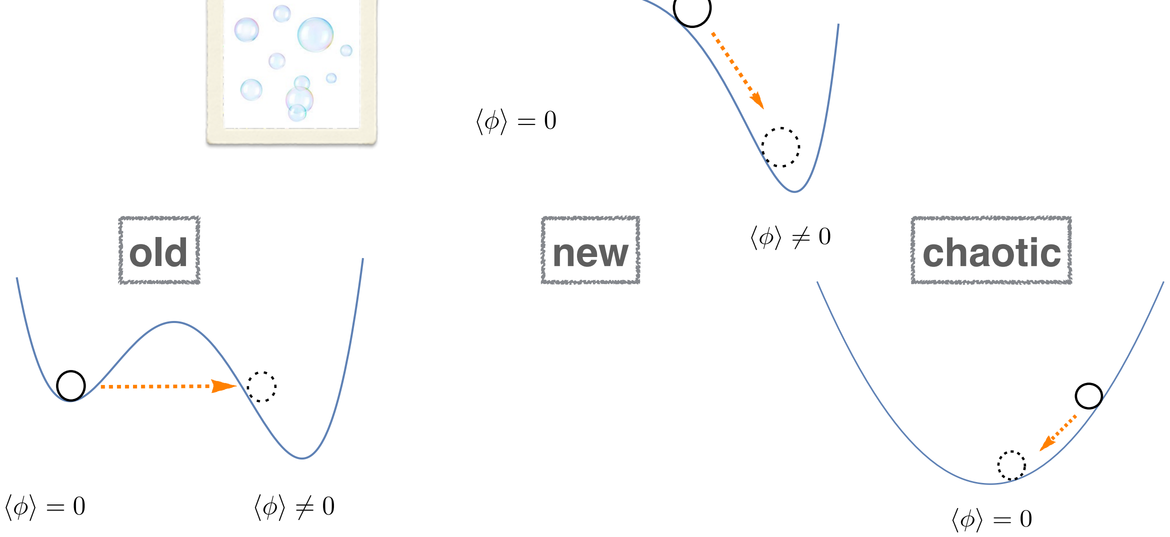

What is inflation all about?

➤ The transition of **vev** plays a fundamental role in all inflation scenarios.

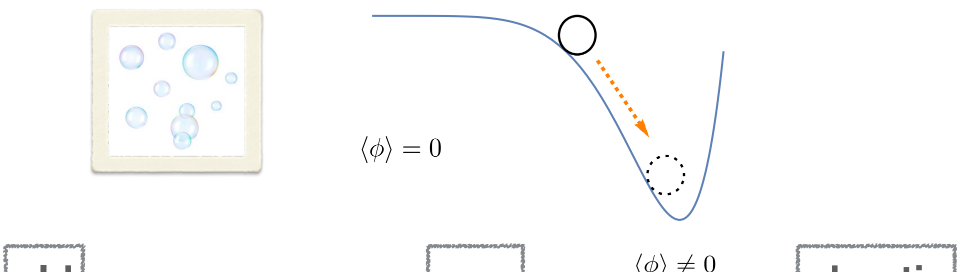

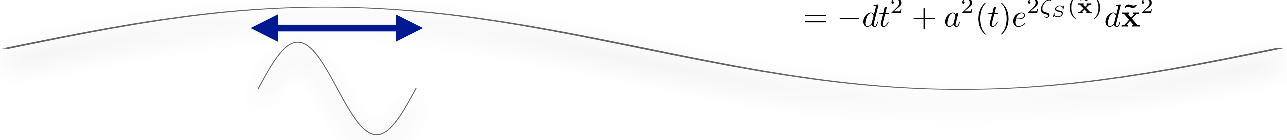

$$= -dt^2 + a^2(t)e^{2\zeta_S(\mathbf{x})}d\tilde{\mathbf{x}}^2$$

de Putter et al. [1610.00785]

The dilatation transformation
$$\langle\zeta(k_1)\zeta(k_2)\rangle_{\zeta_L} = e^{-(n_s-1)\zeta_L}\langle\zeta(\tilde{k}_1)\zeta(\tilde{k}_2)\rangle_0$$

The squeezed bispectrum
$$\lim_{k_3\to 0}\langle\zeta(k_1)\zeta(k_2)\zeta(k_3)\rangle = -(n_s-1)\langle\zeta(k_S)\zeta(k_S)\rangle\langle\zeta(k_L)\zeta(k_L)\rangle$$

- The curvature perturbation in single-clock inflation is conserved.
- The squeezed limit of bispectrum is suppressed by spacetime symmetry.

Cosmological collider

— probing signals of massive fields during inflation

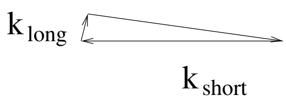

Assassi, Baumann & Green (2012)

Arkani-Hamed & Maldacena (2015)

The squeezed bispectrum

$$\frac{\langle\zeta\zeta\zeta\rangle}{\langle\zeta\zeta\rangle_{\text{short}}\langle\zeta\zeta\rangle_{\text{long}}} \sim \epsilon\sum_i w_i\left(\frac{k_{\text{long}}}{k_{\text{short}}}\right)^{\Delta_i}$$

k_{short}

Assassi, Baumann & Green (2012)

Arkani-Hamed & Maldacena (2015)

The squeezed bispectrum

$$\frac{\langle\zeta\zeta\zeta\rangle}{\langle\zeta\zeta\rangle_{\text{short}}\langle\zeta\zeta\rangle_{\text{long}}} \sim \epsilon \sum_i w_i \left(\frac{k_{\text{long}}}{k_{\text{short}}}\right)^{\Delta_i}$$

Example: spin-zero particles with masses m > 3H/2

$$\frac{\langle\zeta\zeta\zeta\rangle}{\langle\zeta\zeta\rangle_{\text{short}}\langle\zeta\zeta\rangle_{\text{long}}} \sim -\epsilon\, e^{-\pi\mu}|A(\mu)| \left[e^{i\delta(\mu)}\left(\frac{k_{\text{long}}}{k_{\text{short}}}\right)^{\Delta_+} + e^{-i\delta(\mu)}\left(\frac{k_{\text{long}}}{k_{\text{short}}}\right)^{\Delta_-}\right]$$

$$\Delta_\pm = \frac{3}{2} \pm i\mu\,, \qquad \mu = \sqrt{\frac{m^2}{H^2} - \frac{9}{4}}$$

See Bartolo et al. for higher spin particles [1709.05695]

Cosmological collider

— probing signals of massive fields during inflation

Steps towards new discovery: Chen, Wang & Xianyu (2016,2017a,b)

1. To work out the background signals during inflation.
2. ✔ To figure out how new particles enter the bispectrum.

$$\mathcal{L}_I \sim \frac{\mu}{R}\,\sigma\,(\partial\phi)^2$$

➤ Signals of massive fields in the primordial spectrum

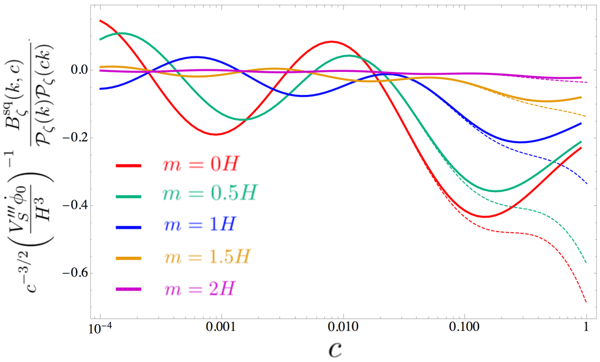

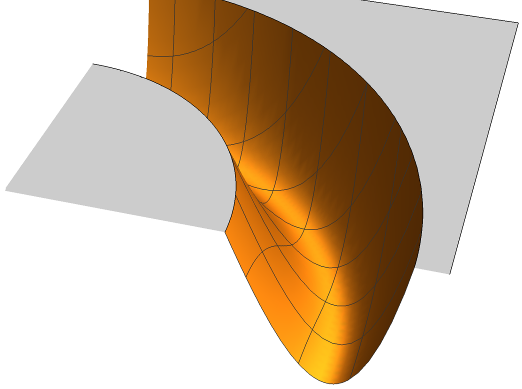

An, McAneny, Ridgway & Wise [1706.09971]

Example II. hybrid inflation(s)

$$\mathcal{L}_I \sim \frac{1}{2}\phi^2\sigma^2$$

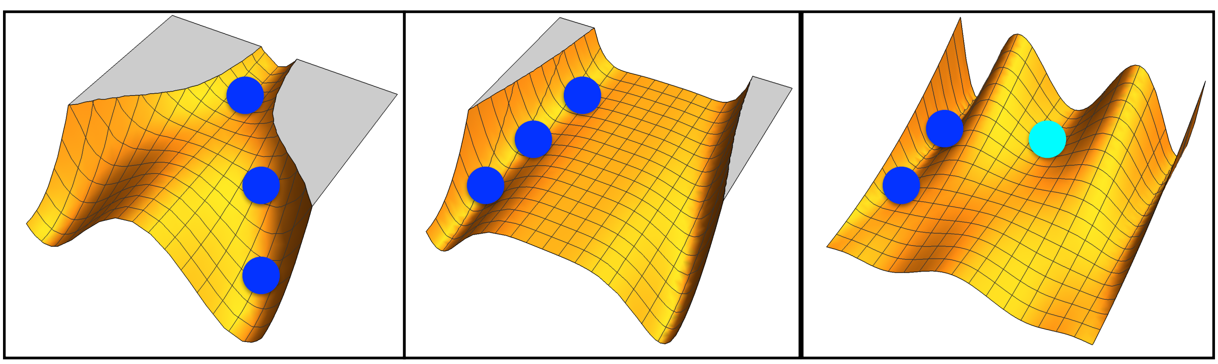

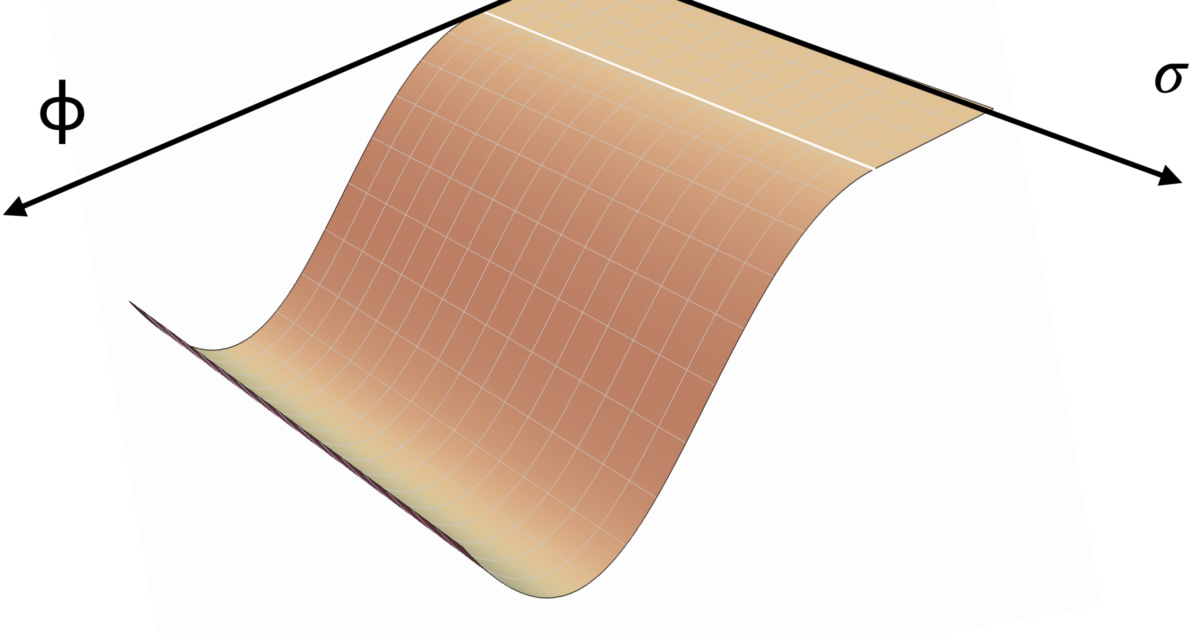

Loop corrections from massive fields

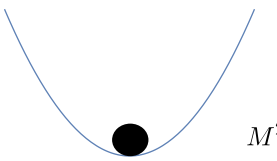

$$M^2 = \frac{1}{H^2}\frac{\partial^2 V(\sigma)}{\partial \sigma^2}$$

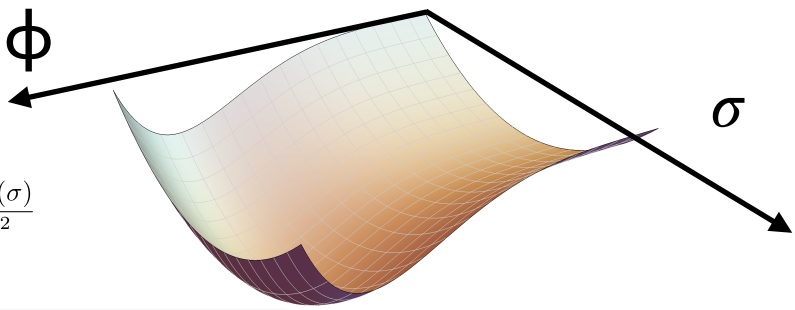

The massive wave function:

$$\sigma_k \to c_1(k) a^{L_+}\left[1+\mathcal{O}\left(\frac{k}{aH}\right)^2\right] + c_2(k) a^{L_-}\left[1+\mathcal{O}\left(\frac{k}{aH}\right)^2\right]$$

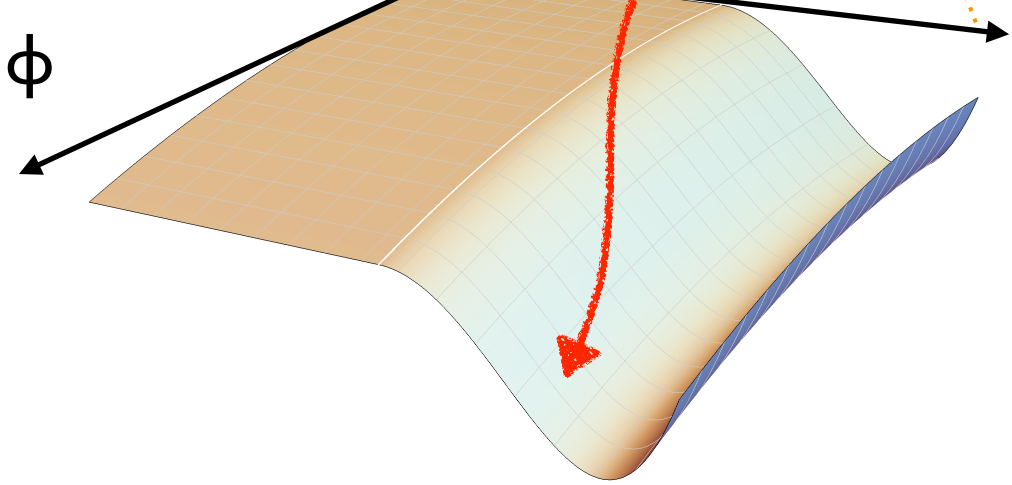

Loop corrections from tachyonic fields

$$M^2 = \frac{1}{H^2}\frac{\partial^2 V(\sigma)}{\partial \sigma^2}$$

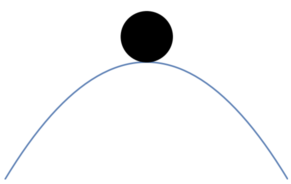

The massive wave function:

$$\sigma_k \to c_1(k) a^{L_+}\left[1 + \mathcal{O}\left(\frac{k}{aH}\right)^2\right] + c_2(k) a^{L_-}\left[1 + \mathcal{O}\left(\frac{k}{aH}\right)^2\right]$$

$$\text{where} \quad L_{\pm} = -\frac{3}{2} \pm \sqrt{\frac{9}{4} - M^2}$$

- Perturbative interactions (gravitational or derivative couplings)
- Standard initial states (the Bunch-Davies vacuum)

- **Effective field theory (equation-of-motion approach):**
  - Non-perturbative regime
  - Mixed initial vacuum states

Phase transition triggered by slow-rolling

Chen, Namjoo & Wang [1505.03955]

A modified potential:

$$V(\phi,\sigma) = V_{\mathrm{slow-roll}}(\phi) + V_0\left[1 - e^{-\sigma^2/\sigma_c^2}\right] + \frac{1}{2}m_0^2\sigma^2$$

$\sigma < \sigma_c$

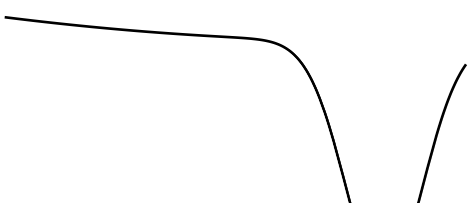

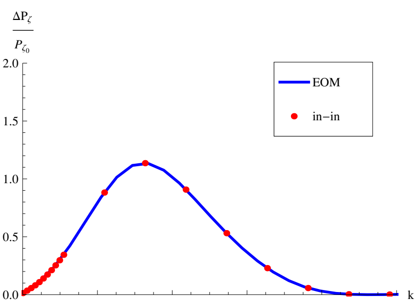

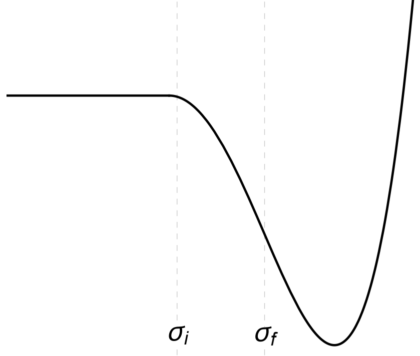

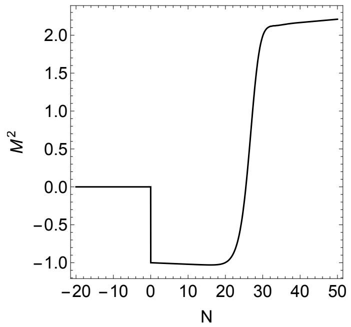

The critical value of classical evolution: $\sigma_i \geq 3H_i^3/(2\pi\lambda v^2)$

The duration of the growing phase:

$$\Delta N = N_f - N_i = \frac{3}{M^2}\ln\left(\frac{2\pi}{3\sqrt{3\lambda}}M^3\right) \qquad \text{classical}$$

$$\Delta N = \frac{3}{2M^2}\ln\left[\frac{M^6(2+4\pi^2/\lambda)}{27+2M^6}\right] \qquad \text{stochastic}$$

Phase transition triggered by quantum fluctuations

YPW & Yokoyama [1704.05026]

A step potential:

$$\begin{aligned} V_1(\sigma) =& \frac{\lambda}{4}v^4, && \sigma < 0, \\ =& \frac{\lambda}{4}(\sigma^2 - v^2)^2 && \sigma \geq 0, \end{aligned}$$

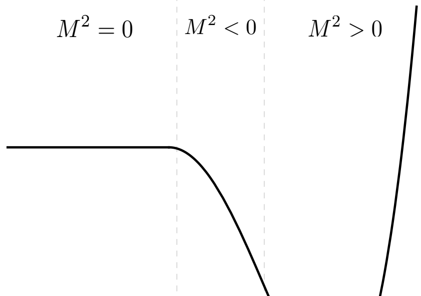

$$u_k'' + \left(k^2 - \frac{l^2 - 1/4}{\eta^2}\right)u_k = 0,$$

$$l = \begin{cases} 3/2, & \eta \leq \eta_i, \\ \sqrt{9/4 + M_-^2}, & \eta_i < \eta \leq \eta_f, \\ \sqrt{9/4 - M_+^2}, & \eta > \eta_f, \end{cases}$$

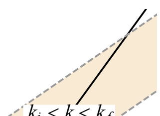

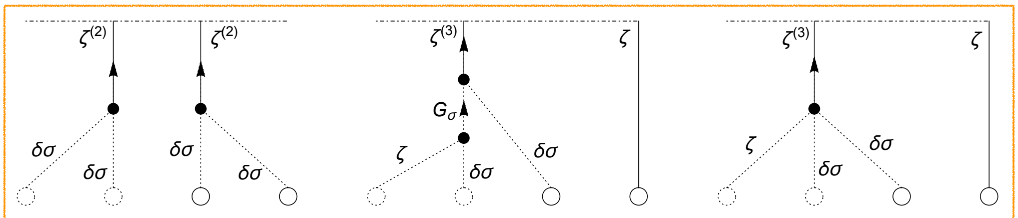

(a) CIM (b) CIS,1 (c) CIS,2

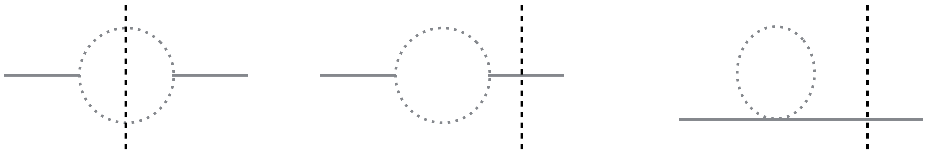

$$M^2 = 0$$

Senatore & Zaldarriaga [0912.2734]

One-loop channels:

$$\langle\zeta^2\rangle_{\rm CIM} = -\int^\eta d\eta_1 \int^\eta d\tilde\eta_1 \left\langle \left[H_I^{(3)}(\eta_1), \zeta(\eta)\right] \left(\left[H_I^{(3)}(\tilde\eta_1), \zeta(\eta)\right]\right)^\dagger \right\rangle,$$

$$\langle\zeta^2\rangle_{\rm CIS,1} = -2\,{\rm Re}\left[\int^\eta d\eta_2 \int_2^\eta d\eta_1 \left\langle \left[H_I^{(3)}(\eta_1), \left[H_I^{(3)}(\eta_2), \zeta(\eta)\right]\right] \zeta(\eta) \right\rangle\right],$$

$$\langle\zeta^2\rangle_{\rm CIS,2} = -2\,{\rm Im}\left[\int^\eta d\eta_1 \left\langle \left[H_I^{(4)}(\eta_1), \zeta(\eta)\right] \zeta(\eta) \right\rangle\right].$$

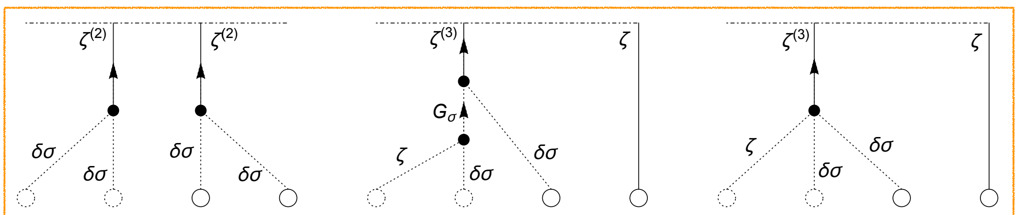

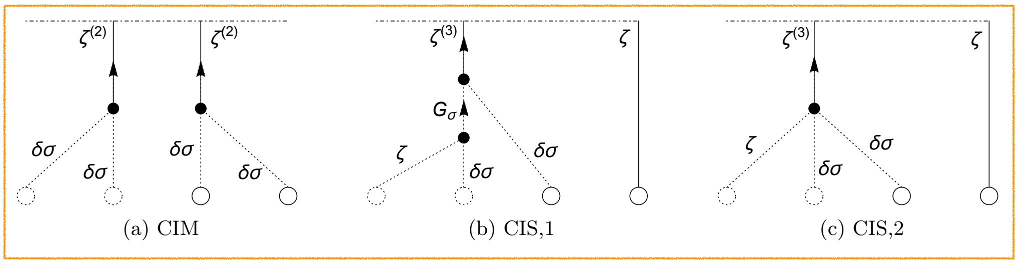

(a) CIM (b) CIS,1 (c) CIS,2

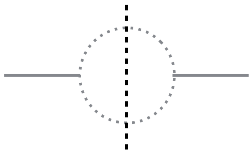

$$M^2 < 0$$

➤ The dominant decay channel changed!

Results of bilinear correlators

Loop corrections from phase transitions:

$$\langle \zeta^2 \rangle \sim \frac{H^2}{\epsilon M_p^2}\left[1 + c_* \frac{H^2}{\epsilon M_p^2}\epsilon^2 M^4 \Pi_\zeta(a) + \left(c_* \frac{H^2}{\epsilon M_p^2}\epsilon^2 M^4 \Pi_\zeta(a)\right)^2 + \dots\right]$$

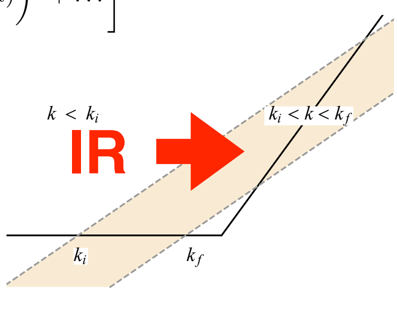

YPW & Yokoyama [1704.05026]

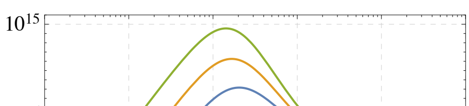

$$
\begin{aligned}
&\times \left[1 - \left(\frac{1+y^2-x^2}{2y}\right)^2\right]^2 |F_2(z) - F_2(z_i)|^2, \\
&= \frac{64\pi\kappa^4 H^4}{15k^3}\delta(\mathbf{k}+\mathbf{K})\boxed{\left(\frac{k}{k_i}\right)^3}\Pi_h(z), \qquad\qquad z = k\eta
\end{aligned}
$$

Conclusion: no important tensor-mode corrections from tachyonic phase transition

$$
F_n(z) \equiv \int \frac{d\tilde{z}}{2\tilde{z}^n}\Theta(z-\tilde{z})\left[e^{i(z-\tilde{z})}(1-iz)(\tilde{z}-i) + e^{i(\tilde{z}-z)}(1+iz)(i+\tilde{z})\right]\left(\frac{\tilde{z}}{z_i}\right)^{3-2l}
$$

$$
\begin{aligned}
\Pi_h(z) &\approx \frac{1}{9(5-2l)^2}, && \text{if} \quad \frac{3}{2} \le l < \frac{5}{2}, \\
&\approx \frac{1}{9}\ln^2\left(\frac{z_i}{z}\right), && \text{if} \quad l = \frac{5}{2}.
\end{aligned}
$$

Messages (for this moment)

- Loop corrections from spectator fields are never large, if they always stay in one stable vacuum during inflation.
- The transition of vacuum expectation values (**vev**s) of scalar fields play a fundamental role in all inflation scenarios.

7a4. Minxi He (RESCEU U. of Tokyo), "Higgs$-R^2$ Inflation" (10+5) [JGRG27 (2017) 113015]

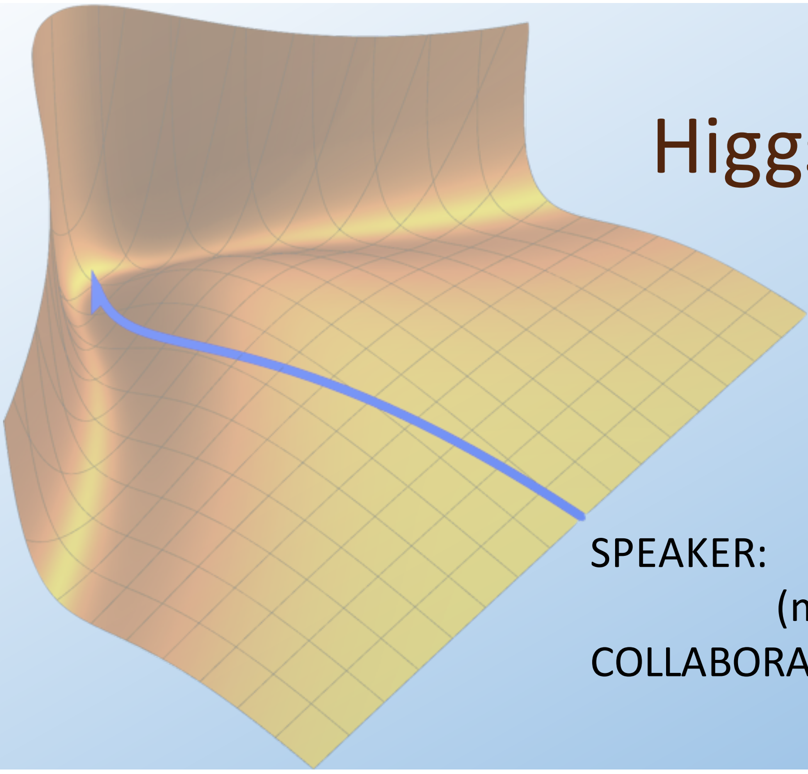

Higgs-R^2 Inflation

SPEAKER: Minxi He (RESCEU, UTOKYO)
(mean c her)
COLLABORATOR: Jun'ichi Yokoyama

OUTLINE

- MOTIVATION
- MODEL AND FORMALISM
- COMPARISON WITH EXPERIMENTS
- FUTURE WORK

MOTIVATION

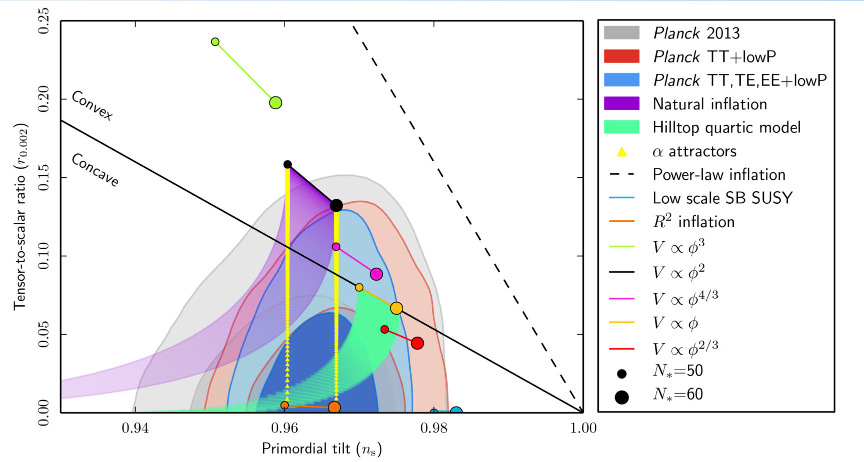

Fig. 12. Marginalized joint 68 % and 95 % CL regions for n_s and $r_{0.002}$ from *Planck* in combination with other data sets, compared to the theoretical predictions of selected inflationary models.

Planck Collaboration: arXiv:1502.02114[astro-ph.CO]

MODEL AND FORMALISM

R^2 inflation + Higgs inflation

A. A. Starobinsky, Phys. Lett. B 91, 99 (1980)

F. L. Bezrukov, M. E. Shaposhnikov, Phys.Lett.B659:703-706,2008

$$S = \int d^4x\sqrt{-\hat{g}}\left[\frac{M_p^2}{2}\hat{R} + \underline{\frac{M_p^2}{12M^2}}\hat{R}^2 + \underline{\frac{1}{2}\xi\chi^2}\hat{R} - \frac{1}{2}\hat{g}^{\mu\nu}\hat{\nabla}_\mu\chi\hat{\nabla}_\nu\chi - \underline{\frac{\lambda}{4}}\chi^4\right]$$

R^2 term Non-minimal coupling Higgs potential

$$F(\chi, R) \equiv \frac{M_p^2}{2}\hat{R} + \frac{1}{2}\xi\chi^2\hat{R} + \frac{M_p^2}{12M^2}\hat{R}^2 - \frac{\lambda}{4}\chi^4$$

Y. Ema, arXiv: 1701.07665[hep-ph]
Y-C. Wang, T. Wang, arXiv: 1701.06636v2[gr-qc]

MODEL AND FORMALISM

Define a new field $\sqrt{\frac{2}{3}}\frac{\psi}{M_p} \equiv \ln\left(\frac{2}{M_p^2}\left|\frac{\partial F}{\partial R}\right|\right)$ K. Maeda, Phys. Rev. D **39**, 3159

Conformal transformation from Jordan frame to Einstein frame $g_{\mu\nu}(x) = e^{\sqrt{\frac{2}{3}}\frac{\psi(x)}{M_p}}\hat{g}_{\mu\nu}(x)$

$$S = \int d^4x\sqrt{-g}\left[\frac{M_p^2}{2}R - \frac{1}{2}g^{\mu\nu}\nabla_\mu\psi\nabla_\nu\psi - \frac{1}{2}\underline{e^{-\sqrt{\frac{2}{3}}\frac{\psi}{M_p}}}g^{\mu\nu}\nabla_\mu\chi\nabla_\nu\chi - U(\psi,\chi)\right]$$

$$U(\psi,\chi) \equiv \frac{\lambda}{4}\chi^4 e^{-2\sqrt{\frac{2}{3}}\frac{\psi}{M_p}} + \frac{3}{4}M_p^2M^2e^{-2\sqrt{\frac{2}{3}}\frac{\psi}{M_p}}\left(e^{\sqrt{\frac{2}{3}}\frac{\psi}{M_p}} - 1 - \frac{1}{M_p^2}\xi\chi^2\right)^2$$

MODEL AND FORMALISM

An example

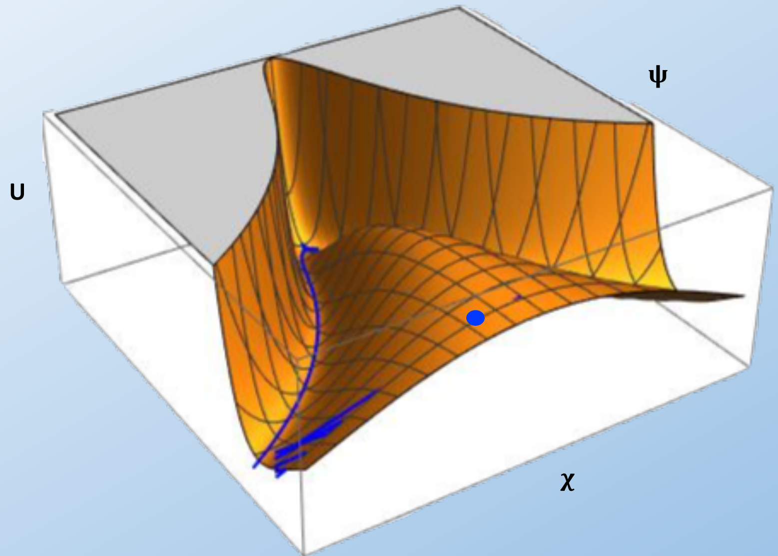

$\lambda = 0.01$
$\xi = 1000$
$M = 10^{-5}$

MODEL AND FORMALISM

An example

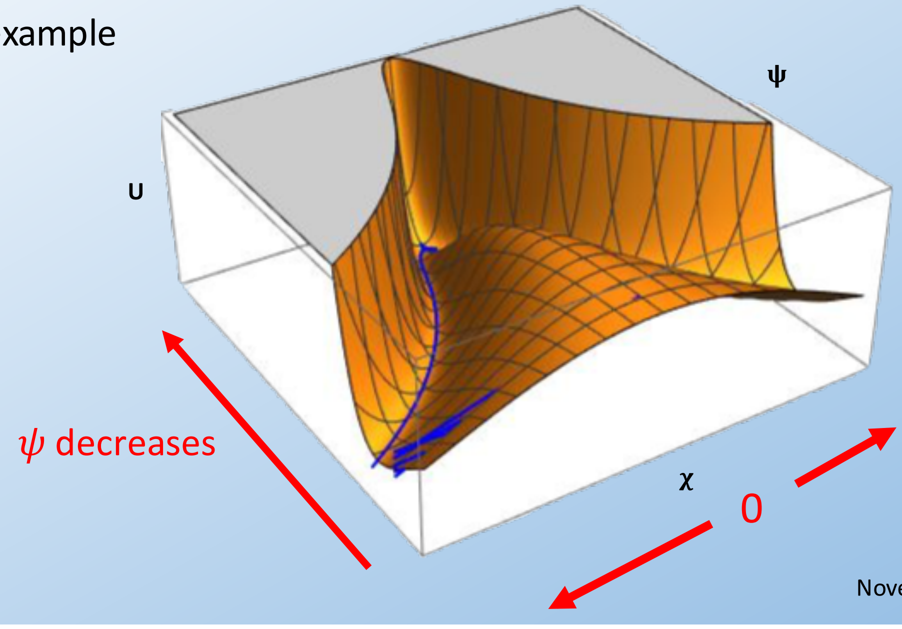

$\lambda = 0.01$
$\xi = 1000$
$M = 10^{-5}$

MODEL AND FORMALISM

An example

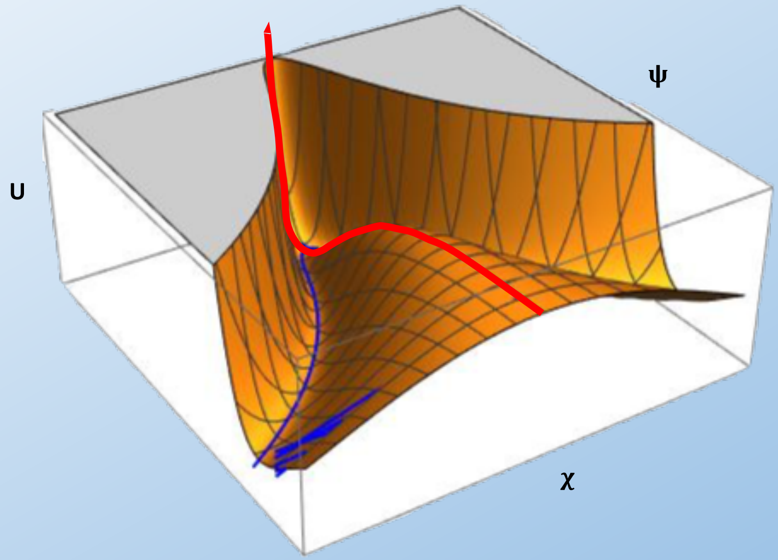

$\lambda = 0.01$
$\xi = 1000$
$M = 10^{-5}$

MODEL AND FORMALISM

$$U(\psi,\chi) \equiv \frac{\lambda}{4}\chi^4 \cancel{e^{-2\sqrt{\frac{2}{3}}\frac{\psi}{M_p}}} + \frac{3}{4}M_p^2 M^2 e^{-2\sqrt{\frac{2}{3}}\frac{\psi}{M_p}}\left(e^{\sqrt{\frac{2}{3}}\frac{\psi}{M_p}} - 1 - \cancel{\frac{1}{M_p^2}}\xi\chi^2\right)^2$$

MODEL AND FORMALISM

An example

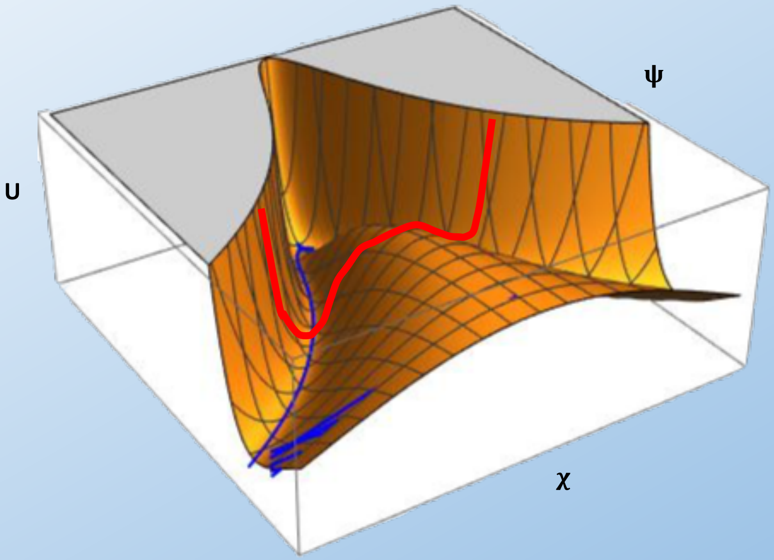

$$\lambda = 0.01$$
$$\xi = 1000$$
$$M = 10^{-5}$$

MODEL AND FORMALISM

$$U(\psi,\chi) \equiv \frac{\lambda}{4}\chi^4 e^{-2\sqrt{\frac{2}{3}}\cancel{\frac{\psi}{M_p}}} + \frac{3}{4}M_p^2 M^2 e^{-2\sqrt{\frac{2}{3}}\cancel{\frac{\psi}{M_p}}}\left(e^{\sqrt{\frac{2}{3}}\cancel{\frac{\psi}{M_p}}} - 1 - \frac{1}{M_p^2}\xi\chi^2\right)^2$$

MODEL AND FORMALISM

An example

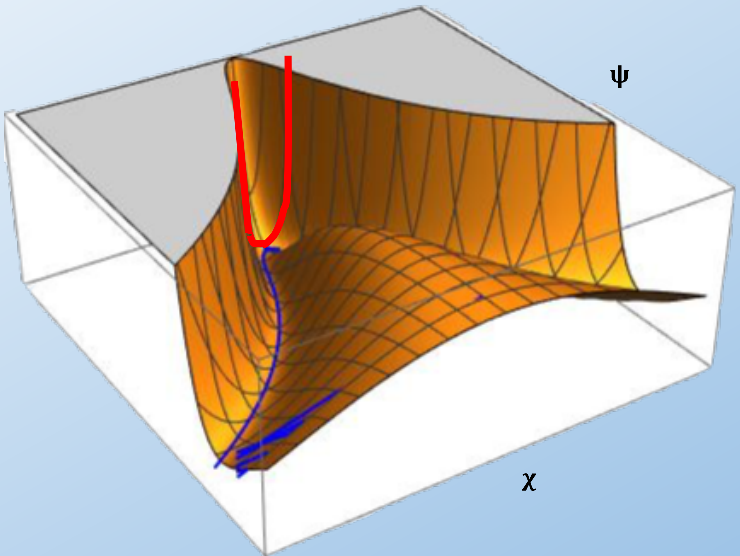

$$\lambda = 0.01$$
$$\xi = 1000$$
$$M = 10^{-5}$$

MODEL AND FORMALISM

$$U(\psi,\chi) \equiv \frac{\lambda}{4}\chi^4 e^{-2\sqrt{\frac{2}{3}}\frac{\psi}{M_p}} + \frac{3}{4}M_p^2 M^2 e^{-2\sqrt{\frac{2}{3}}\frac{\psi}{M_p}}\left(e^{\cancel{\sqrt{\frac{2}{3}}\frac{\psi}{M_p}}} \cancel{-1} - \frac{1}{M_p^2}\xi\chi^2\right)^2$$

MODEL AND FORMALISM

Pure Higgs

$$F(\chi,R) \equiv \frac{M_p^2}{2}\hat{R} + \frac{1}{2}\xi\chi^2\hat{R} + \cancel{\frac{M_p^2}{12M^2}}\hat{R}^2 - \frac{\lambda}{4}\chi^4$$

$$\sqrt{\frac{2}{3}}\frac{\psi}{M_p} \equiv \ln\left(\frac{2}{M_p^2}\left|\underline{\frac{\partial F}{\partial R}}\right|\right)$$

MODEL AND FORMALISM

An example

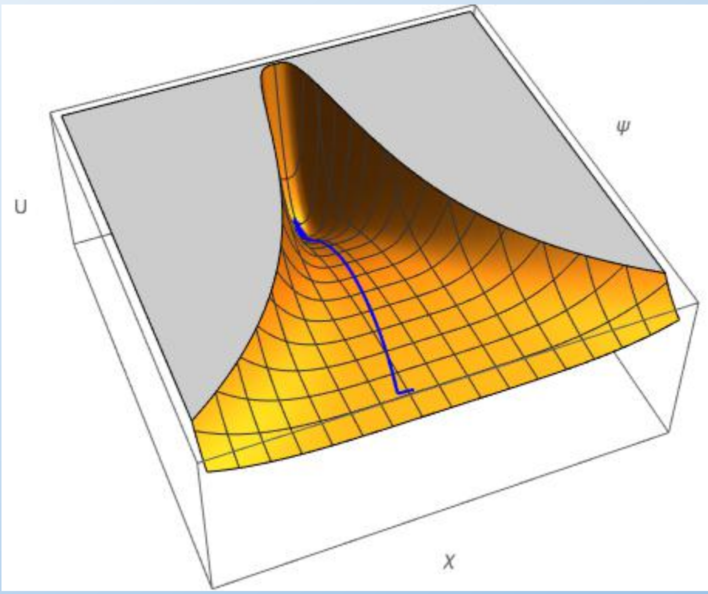

$\lambda = 0.01$
$\xi = 100$
$M = 10^{-5}$

MODEL AND FORMALISM

Rewrite the action in a more compactible form as

$$S = \int d^4x\sqrt{-g}[\frac{M_p^2}{2}R - \frac{1}{2}h_{ab}g^{\mu\nu}\partial_\mu\phi^a\partial_\nu\phi^b - U(\phi)]$$

$$where \quad a,b = 1,2, \quad \phi^1 = \psi, \quad \phi^2 = \chi$$

$$h_{11} = 1, \quad h_{22} = e^{-\sqrt{\frac{2}{3}}\frac{\psi}{M_p}}, \quad h_{12} = h_{21} = 0$$

We will set $M_p = 1$ below.

MODEL AND FORMALISM

Equations of motion for $\phi(\mathbf{x},t)=\phi_0(t)+\delta\phi(\mathbf{x},t)$

$$\frac{D\dot{\phi}_0^a}{dt}+3H\dot{\phi}_0^a+h^{ab}U_{,b}=0 \qquad where \quad \frac{D}{dt}\equiv\dot{\phi}_0^a\nabla_a$$

$$\frac{D^2\delta\phi^a_{\mathbf{k}}}{dt^2}+3H\frac{D\delta\phi^a_{\mathbf{k}}}{dt}-R^a{}_{bcd}\dot{\phi}_0^b\dot{\phi}_0^c\delta\phi^d_{\mathbf{k}}+\frac{k^2}{a^2}\delta\phi^a_{\mathbf{k}}+U^{;a}{}_{;b}\delta\phi^b_{\mathbf{k}}=\frac{1}{a^3}\frac{D}{dt}\left(\frac{a^3}{H}\dot{\phi}_0^a\dot{\phi}_0^b\right)h_{bc}\delta\phi^c_{\mathbf{k}}$$

M. Sasaki, E. Stewart, Prog.Theor.Phys.95:71-78,1996

- Geodesic equation of the field space within an expanding universe with potential $U(\psi,\chi)$
- Equations of geodesic deviation.

A. Achucarro et al, Phys.Rev.D84:043502,2011

MODEL AND FORMALISM

Equations of motion for $\phi(\mathbf{x},t)=\phi_0(t)+\delta\phi(\mathbf{x},t)$

$$\frac{D\dot{\phi}_0^a}{\underline{dt}}+3H\dot{\phi}_0^a+h^{ab}U_{,b}=0 \qquad where \quad \frac{D}{dt}\equiv\dot{\phi}_0^a\nabla_a$$

$$\frac{D^2\delta\phi^a_{\mathbf{k}}}{\underline{dt^2}}+3H\frac{D\delta\phi^a_{\mathbf{k}}}{dt}-\underline{R^a{}_{bcd}\dot{\phi}_0^b\dot{\phi}_0^c\delta\phi^d_{\mathbf{k}}}+\underline{\frac{k^2}{a^2}\delta\phi^a_{\mathbf{k}}}+U^{;a}{}_{;b}\delta\phi^b_{\mathbf{k}}=\frac{1}{a^3}\frac{D}{dt}\left(\frac{a^3}{H}\dot{\phi}_0^a\dot{\phi}_0^b\right)h_{bc}\delta\phi^c_{\mathbf{k}}$$

M. Sasaki, E. Stewart, Prog.Theor.Phys.95:71-78,1996

- Geodesic equation of the field space within an expanding universe with potential $U(\psi,\chi)$
- Equations of geodesic deviation. $\longrightarrow$
  - Not rolling in the local minimum
  - Not rolling along geodesics

A. Achucarro et al, Phys.Rev.D84:043502,2011

MODEL AND FORMALISM

- Mass hierarchy, slow-roll regime
- Decomposition into two directions, T^a and $-\dot{\theta}N^a \equiv D_t T^a$. (Also new slow-roll parameters.)

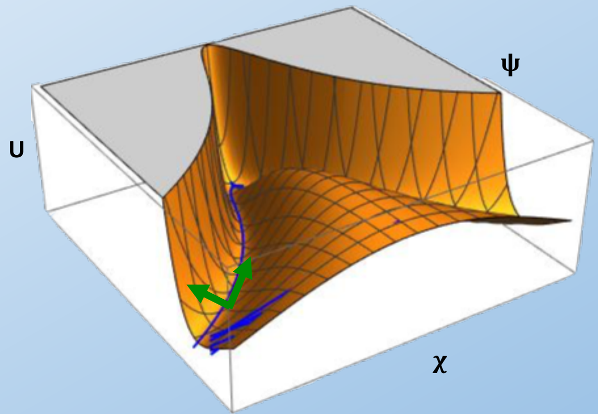

A. Achucarro et al, JCAP 1101:030,2011

MODEL AND FORMALISM

$$\mathcal{R} \propto T_a \delta\phi^a$$
$$\mathcal{F} \propto N_a \delta\phi^a$$

$$S_2 = \frac{1}{2}\int a^3 [\frac{\dot{\phi}_0^2}{H^2}\dot{\mathcal{R}}^2 - \frac{\dot{\phi}_0^2}{H^2}\frac{(\nabla\mathcal{R})^2}{a^2} + \dot{\mathcal{F}}^2 - \frac{(\nabla\mathcal{F})^2}{a^2} - \underline{M_{\rm eff}^2}\mathcal{F}^2 - 4\dot{\theta}\frac{\dot{\phi}_0^2}{H}\dot{\mathcal{R}}\mathcal{F}]$$

Effective mass including $\dot{\theta}$ & U_{NN} which is much larger than the H^2.

- Integrating out the high energy part
- Slow-roll regime where the heavy direction is determined by the light direction

$$S_{\rm eff} = \frac{1}{2}\int a^3 \frac{\dot{\phi}_0^2}{H^2}[\frac{\dot{\mathcal{R}}^2}{\underline{c_s^2(k)}} - \frac{k^2\mathcal{R}^2}{a^2}]$$

A. Achucarro et al, Phys. Rev. D 86, 121301(R) (2012)

MODEL AND FORMALISM

Mukhanov-Sasaki equation

$$v_k'' + (\underline{c_s^2} k^2 - \frac{z''}{z}) v_k = 0$$

Modified speed of sound but still close to 1 during slow-roll regime

$$c_s^{-2} = 1 + \frac{4\dot{\theta}^2}{\frac{k^2}{a^2} + U_{NN} + \epsilon H^2 R - \dot{\theta}^2}$$

Mode function

$$v_k = \frac{e^{-ic_s k\tau}}{\sqrt{2c_s k}}(1 - \frac{i}{c_s k\tau})$$

Power spectrum at large scale

$$\mathcal{P}_{\mathcal{R}}(k) \approx \frac{H^2}{4c_s k^3}\frac{1}{\epsilon}$$

ϵ has contribution from both fields

$$\epsilon \equiv -\frac{\dot{H}}{H^2} = \frac{\dot{\phi}_0^2}{2H^2}$$

MODEL AND FORMALISM

Scalar index

$$n_s - 1 = 2\underline{\eta_{||}} - 4\epsilon$$

Second slow-roll parameter in the tangent direction

Tensor-to-scalar ratio

$$r = 16\epsilon \underline{c_s}$$

Correction from speed of sound

COMPARISON WITH EXPERIMENTS

Fix $\lambda = 0.01$; (Then we have two free parameters, ξ and M.)
$\psi_0 = 5.7$; χ_0=0.01; $\psi_0' = 0$; $\chi_0' = 0$;
$c_s \approx 1$;
Requiring the amplitude of curvature perturbations to be 2×10^{-9}.

COMPARISON WITH EXPERIMENTS

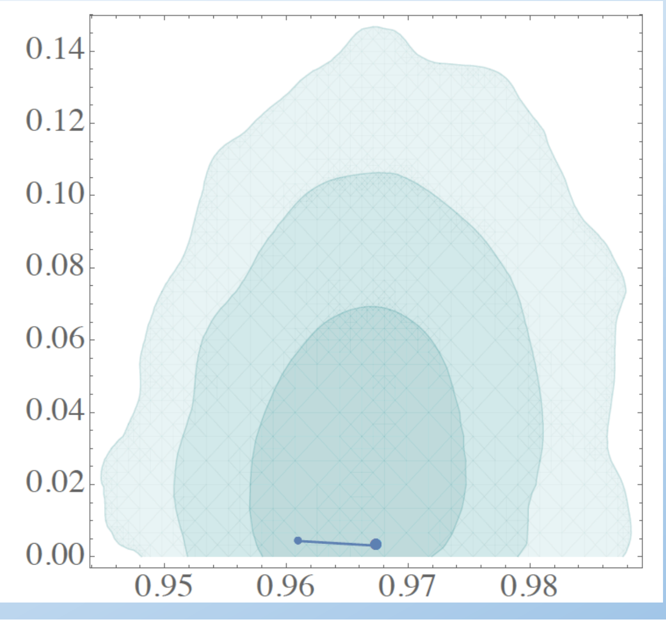

- Confined amplitude

COMPARISON WITH EXPERIMENTS

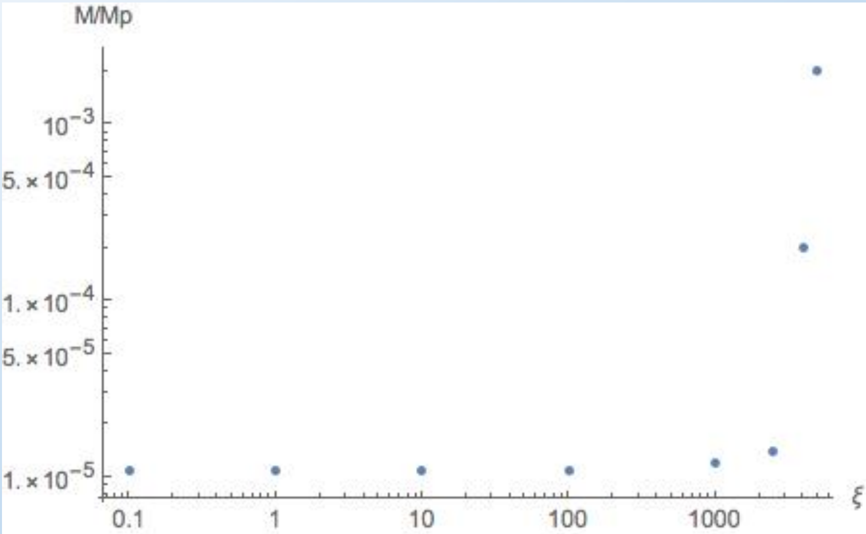

- Relation between the two paremeters given by confined amplitude

COMPARISON WITH EXPERIMENTS

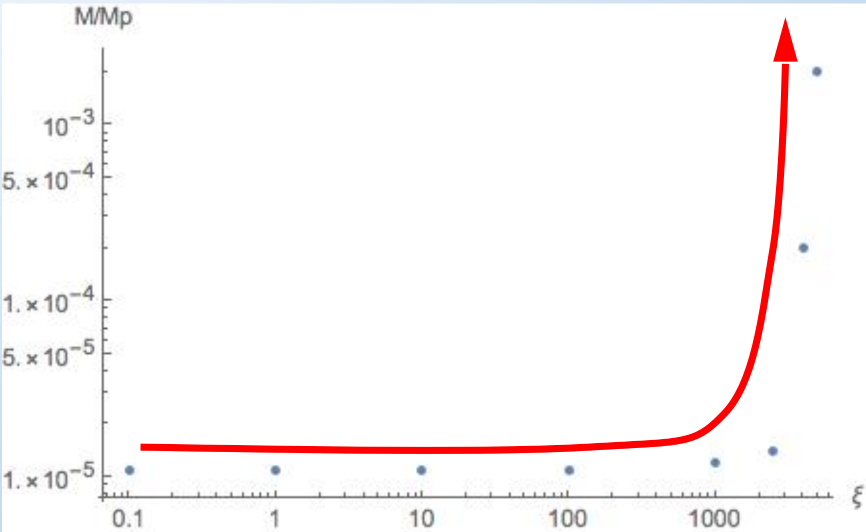

- Relation between the two paremeters given by confined amplitude

COMPARISON WITH EXPERIMENTS

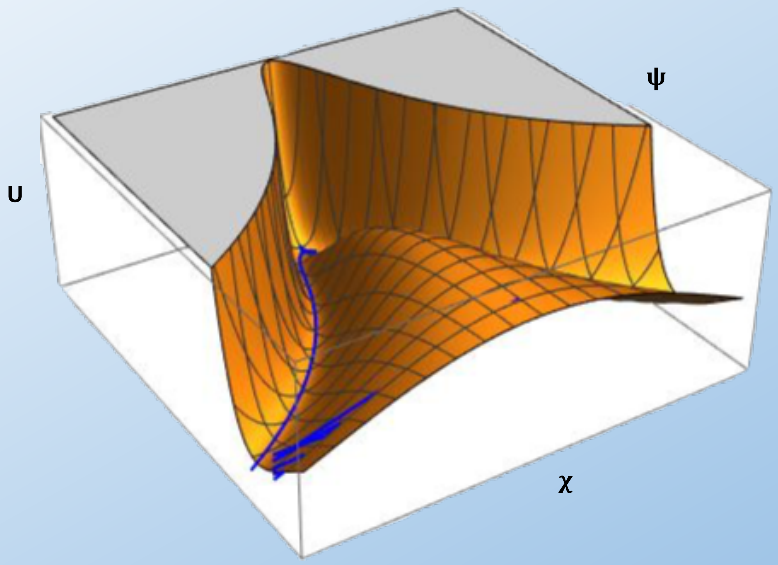

- ξ & effective mass of Higgs field & shape of potential

COMPARISON WITH EXPERIMENTS

- Large ψ suppresses terms with higher order of $e^{-\sqrt{\frac{2}{3}}\psi}$

Approximately $$H \propto U(\psi,\chi) \approx \frac{3}{4}M^2(\underline{1} - \underline{\xi\chi^2 e^{-\sqrt{\frac{2}{3}}\psi}})^2$$

- Constant term completely determined by M
- Determined by ξ and M

COMPARISON WITH EXPERIMENTS

e.g. $\xi = 1000$; $M = 10^{-5}$.

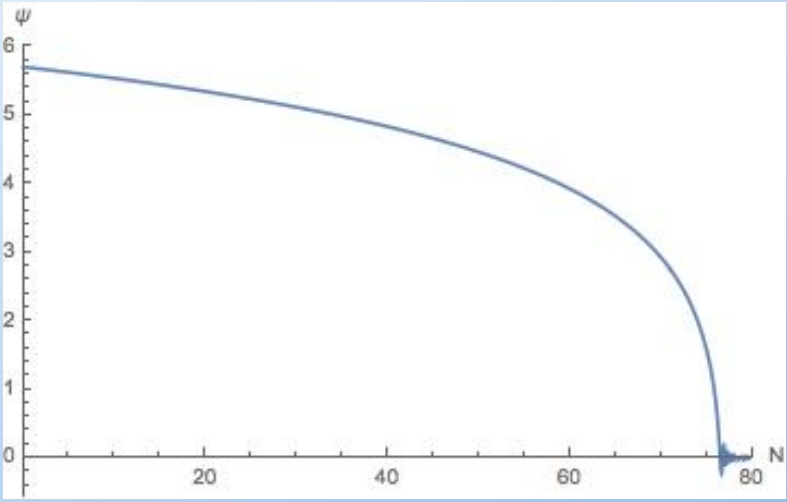

COMPARISON WITH EXPERIMENTS

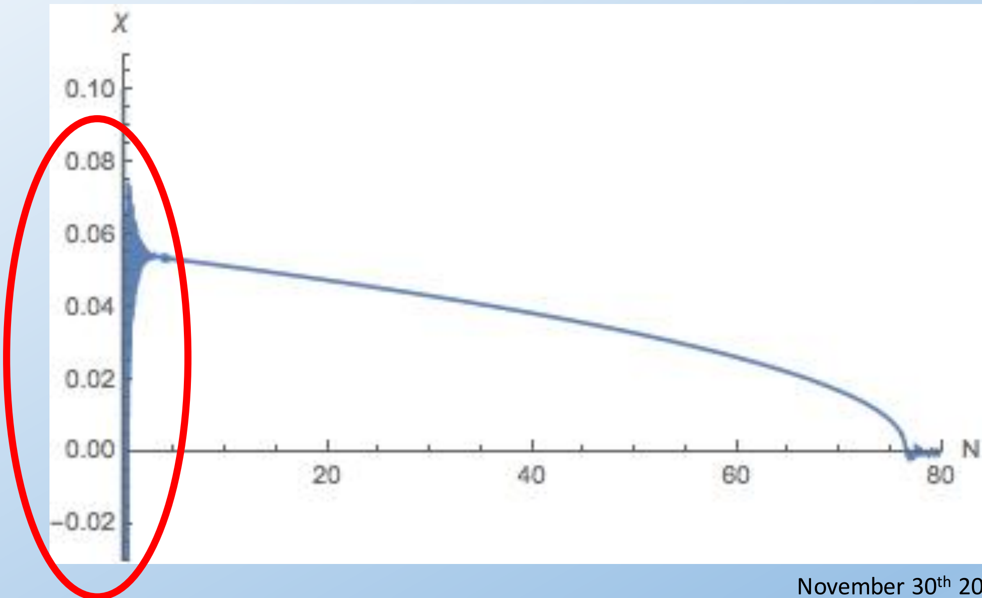

FUTURE WORK

- This work is on going. Mass hierarchy is considered here so that one of the fields dominates the inflation. The final goal is to consider the regime where both fields are of same importance to see whether there are more interesting features appear on power spectrum and bispectrum, isocurvature perturbations, etc.
- Find out different behaviors of the fields and predictions in different regions of parameter space, e.g. the correction from the speed of sound.
- Also it is worth considering the links with primordial black holes, reheating, etc.

November 30th 2017 @JGRG2017

Higgs-R^2 Inflation

THANK YOU FOR LISTENING!

SPEAKER: Minxi He (RESCEU, UTOKYO)
(mean c her)
COLLABORATOR: Jun'ichi Yokoyama

November 30th 2017 @JGRG2017

7a5. Kiyomi Hasegawa (Hirosaki U.),
"A possible solution to the Hubble (non-)constant problem" (10+5)
[JGRG27 (2017) 113016]

A possible solution to the "Hubble (non-)constant problem"

Kiyomi Hasegawa[(1)], Masumi Kasai[(1)] and Toshifumi Futamase[(2)]

(1) Hirosaki University (2) Kyoto Sangyo University

JGRG 27 (27 November - 1 December, 2017)

The "Hubble(non-)constant problem"

(originally stated by K. Tomita (2017))

The "Hubble(non-)constant problem"

(originally stated by K. Tomita (2017))

The Hubble constant is different in

the measurement of the CMB

and

the measurement of the SNe

The measurement of the CMB

$$H_0 = 67.8 \pm 0.9 \text{ km s}^{-1}\text{Mpc}^{-1}$$

P.A.R.Ade et al.(2016).

The measurement of the SNe

$$H_0 = 73.24 \pm 1.74 \text{ km s}^{-1}\text{Mpc}^{-1}$$

A. G. Riess et al.(2016).

The measurement of CMB

→**Global**

The measurement of SNe

→**Local**

For the Hubble parameter, there is about 10% discrepancy in

the global domain

and

the local domain

The "Hubble(non-)constant problem"

K. Tomita (2017)

Previous works for the
"Hubble (non-)constant problem"

Z. Berezhiani et al.(2015) .

decaying dark matter

K. Ichiki et al.(2016) .

local void model

K. Tomita (2017) .

second order perturbation

Our policy

We would like to show
the "Hubble (non-)constant problem"
can be solved within the general framework of

the linear perturbation theory of
the general relativistic
inhomogeneous universe

without assuming
unknown matters or specific toy models

Part1. Fundamentals

Part2. Linear perturbation

Part3. Spatial average

※ the light speed c=1

Part1. Fundamentals

matter: **The irrotational dust**

$$T^{\mu\nu} = \rho u^\mu u^\nu$$

ρ: **The density** of the matter

u^μ: 4-velocity of the matter

matter: **The irrotational dust**

$$T^{\mu\nu} = \rho u^{\mu} u^{\nu}$$

ρ: **The density** of the matter

u^{μ}: 4-velocity of the matter

coordinates:**synchronous comoving**

$$ds^2 = -dt^2 + {}^{(3)}g_{ij} dx^i dx^j$$

with $u^{\mu} = (1, 0, 0, 0)$

background

→**The Einstein-de Sitter universe**

(The following discussion is similarly established in the non-flat case.

flat with Λ case → P24)

background

→The Einstein-de Sitter universe

(The following discussion is similarly established in the non-flat case.
flat with Λ case → P24)

$$ds^2 = -dt^2 + a^2(t)\delta_{ij}dx^i dx^j$$

with $u^\mu = (1,0,0,0)$

background

→The Einstein-de Sitter universe

(The following discussion is similarly established in the non-flat case.
flat with Λ case → P24)

$$ds^2 = -dt^2 + a^2(t)\delta_{ij}dx^i dx^j$$

with $u^\mu = (1,0,0,0)$

$u_\mu T^{\mu\nu}{}_{;\nu} = 0$ gives

$$\dot{\rho}_b + 3\frac{\dot{a}}{a}\rho_b = 0$$

background

→The Einstein-de Sitter universe

(The following discussion is similarly established in the non-flat case.

flat with Λ case → P24)

$$ds^2 = -dt^2 + a^2(t)\delta_{ij}dx^i dx^j$$

with $u^\mu = (1,0,0,0)$

$u_\mu T^{\mu\nu}{}_{;\nu} = 0$ gives

$$\dot{\rho}_b + 3\frac{\dot{a}}{a}\rho_b = 0$$

$G_{00} = 8\pi G T_{00}$ gives the Friedmann equation

$$\left(\frac{\dot{a}}{a}\right)^2 = \frac{8\pi G}{3}\rho_b$$

background

→The Einstein-de Sitter universe

(The following discussion is similarly established in the non-flat case.

flat with Λ case → P24)

$$ds^2 = -dt^2 + a^2(t)\delta_{ij}dx^i dx^j$$

with $u^\mu = (1,0,0,0)$

$u_\mu T^{\mu\nu}{}_{;\nu} = 0$ gives

$$\dot{\rho}_b + 3\frac{\dot{a}}{a}\rho_b = 0$$

$G_{00} = 8\pi G T_{00}$ gives the Friedmann equation

$$\left(\frac{\dot{a}}{a}\right)^2 = \frac{8\pi G}{3}\rho_b$$

ρ_b : **background density**

Part2. Linear perturbation

$$g_{\mu\nu} = {}^{(b)}g_{\mu\nu} + h_{\mu\nu}$$

$$\rho = \rho_b(1+\delta)$$

${}^{(b)}g_{\mu\nu}$: the metric of the background

$h_{\mu\nu}$: the perturbation component of the metric

δ : the density fluctuation

$$g_{\mu\nu} = {}^{(b)}g_{\mu\nu} + h_{\mu\nu}$$

$$\gg$$

$$\rho = \rho_b(1 + \delta)$$

$$\gg$$

${}^{(b)}g_{\mu\nu}$: the metric of the background

$h_{\mu\nu}$: the perturbation component of the metric

δ : the density fluctuation

the perturbation quantities
are **smaller enough** than
the background quantities

$$g_{\mu\nu} = {}^{(b)}g_{\mu\nu} + h_{\mu\nu}$$

$$\rho = \rho_b(1 + \delta)$$

${}^{(b)}g_{\mu\nu}$: the metric of the background

$h_{\mu\nu}$: the perturbation component of the metric

δ : the density fluctuation

performing the gauge fix like

synchronous comoving,

we solve the Einstein equation in

the linear approximation

$$ds^2 = -dt^2 + a^2 \left(\delta_{ij} - \frac{4a}{3{H_0}^2}\phi_{,ij} - \frac{10}{3}\phi\delta_{ij} \right) dx^i dx^j$$

$$\text{with } u^\mu = (1, 0, 0, 0)$$

$$ds^2 = -dt^2 + a^2 \left(\delta_{ij} - \frac{4a}{3{H_0}^2}\phi_{,ij} - \frac{10}{3}\phi\delta_{ij} \right) dx^i dx^j$$

$$\text{with } u^\mu = (1, 0, 0, 0)$$

the Poisson equation

$$\Delta\phi = 4\pi G \rho_b a^2 \delta$$

$$ds^2 = -dt^2 + a^2 \left(\delta_{ij} - \frac{4a}{3{H_0}^2}\phi_{,ij} - \frac{10}{3}\phi\delta_{ij} \right) dx^i dx^j$$

with $u^\mu = (1, 0, 0, 0)$

the Poisson equation

$$\Delta\phi = 4\pi G \rho_b a^2 \delta$$

$$ds^2 = -dt^2 + a^2 \left(\delta_{ij} - \frac{4a}{3{H_0}^2}\phi_{,ij} - \frac{10}{3}\phi\delta_{ij} \right) dx^i dx^j$$

with $u^\mu = (1, 0, 0, 0)$

the Poisson equation

$$\Delta\phi = 4\pi G \rho_b a^2 \delta$$

$$ds^2 = -dt^2 + a^2 \left(\delta_{ij} - \frac{4a}{3{H_0}^2} \underline{\phi_{,ij}} - \frac{10}{3} \underline{\phi} \delta_{ij} \right) dx^i dx^j$$

with $u^\mu = (1, 0, 0, 0)$

the Poisson equation

$$\underline{\Delta\phi} = 4\pi G \rho_b a^2 \underline{\delta}$$

$$\phi = \phi(\vec{x})$$

$$\delta \propto a(t)$$

Part3.
Spatial average

what is

the

background density ρ_b

in the

realistic inhomogeneous

universe ?

the background

density

in the realistic

inhomogeneous universe is

the spatial average

density

the background density in the realistic inhomogeneous universe is

the spatial average density

to express this phrase with the formula...

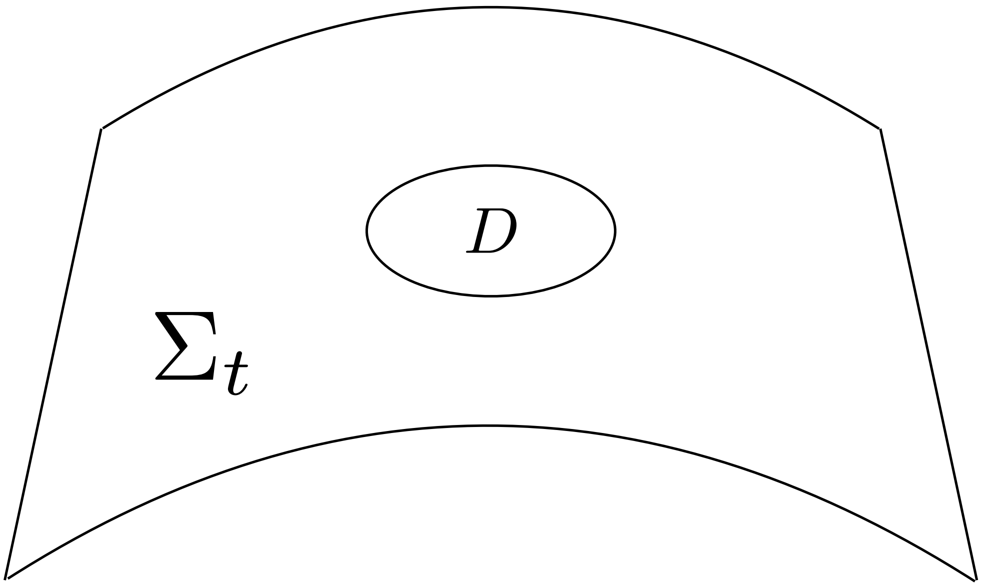

Σ_t: **constant time hypersurface**

D : **finite domain included in Σ_t**

we define the following quantities in the domain D

- **Volume**

$$V \equiv \int_D \sqrt{{}^{(3)}g}\, d^3x$$

$${}^{(3)}g = \det({}^{(3)}g_{ij})$$

we define the following quantities in the domain D

- **Volume**

$$V \equiv \int_D \sqrt{{}^{(3)}g}\, d^3x$$

- **Spatial avarage density**

$$\langle \rho \rangle_D \equiv \frac{1}{V} \int_D \rho \sqrt{{}^{(3)}g}\, d^3x$$

$${}^{(3)}g = \det({}^{(3)}g_{ij})$$

we define the following quantities in the domain D

- Volume

$$V \equiv \int_D \sqrt{{}^{(3)}g}\, d^3x$$

- Spatial avarage density

$$\langle \rho \rangle_D \equiv \frac{1}{V} \int_D \rho \sqrt{{}^{(3)}g}\, d^3x$$

- Volume expansion rate

$$3\frac{\dot{a}_D}{a_D} \equiv \frac{\dot{V}}{V}$$

a_D:scale factor of the domain D

$${}^{(3)}g = \det({}^{(3)}g_{ij})$$

the definition

of

the background density

$$\rho_b \equiv \lim_{D \to \Sigma_t} \langle \rho \rangle_D = \lim_{D \to \Sigma_t} \frac{1}{\int_D \sqrt{^{(3)}g}\, d^3x} \int_D \rho \sqrt{^{(3)}g}\, d^3x$$

M. Kasai (1993).

Σ_t: constant time hypersurface

D : finite domain included in Σ_t

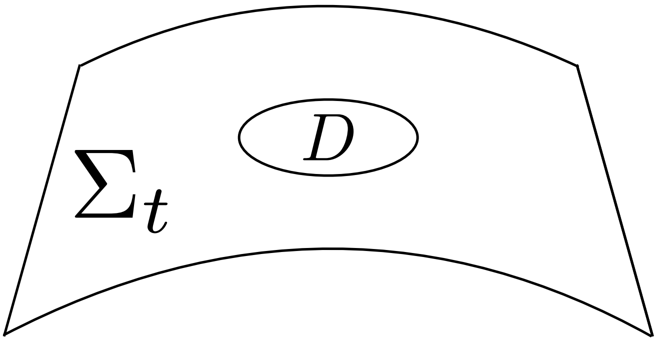

$$\rho_b \equiv \lim_{D \to \Sigma_t} \langle \rho \rangle_D = \lim_{D \to \Sigma_t} \frac{1}{\int_D \sqrt{^{(3)}g}\, d^3x} \int_D \rho \sqrt{^{(3)}g}\, d^3x$$

M. Kasai (1993).

Σ_t: constant time hypersurface

D : finite domain included in Σ_t

when $D \to \Sigma_t$,

$$\rho_b = \langle \rho \rangle_D$$

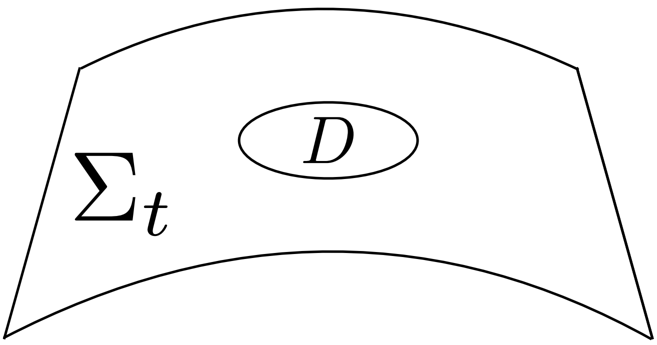

$$\rho_b \equiv \lim_{D \to \Sigma_t} \langle \rho \rangle_D$$
$$= \lim_{D \to \Sigma_t} \frac{1}{\int_D \sqrt{^{(3)}g}\, d^3x} \int_D \rho \sqrt{^{(3)}g}\, d^3x$$

M. Kasai (1993).

Σ_t: constant time hypersurface

D : finite domain included in Σ_t

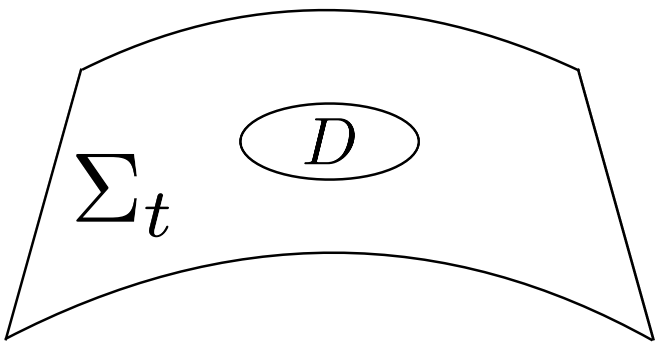

when $D \to \Sigma_t$,

$$\rho_b = \langle \rho \rangle_D$$

generally,

$$\rho_b \neq \langle \rho \rangle_D$$

background density | spatial average density

$$\rho_b \neq \langle \rho \rangle_D$$

By the way,
reviewing
Part.1,

the universe in which the volume expansion is driven by

the background density

$$\rho_b$$

the universe in which the volume expansion is driven by

the background density

$$\rho_b$$

$$\downarrow$$

the Einstein-de Sitter universe

the universe in which the volume expansion is driven by

the domain-dependent average density

$$\langle \rho \rangle_D$$

$$\downarrow$$

?

to answer this question ,

the spatial average

Einstein equation

$\langle u_\mu T^{\mu\nu}{}_{;\nu}\rangle_D = 0$ gives

$$\frac{d}{dt}\langle\rho\rangle_D + 3\frac{\dot{a}_D}{a_D}\langle\rho\rangle_D = 0 \quad \textbf{(exact)}$$

$\langle u_\mu T^{\mu\nu}{}_{;\nu}\rangle_D = 0$ gives

$$\frac{d}{dt}\langle\rho\rangle_D + 3\frac{\dot{a}_D}{a_D}\langle\rho\rangle_D = 0 \quad \textbf{(exact)}$$

$\langle G_{00}\rangle_D = 8\pi G\langle T_{00}\rangle_D$ gives the Friedmann equation

$$\left(\frac{\dot{a}_D}{a_D}\right)^2 + \frac{K_{\text{eff}}}{{a_D}^2} = \frac{8\pi G}{3}\langle\rho\rangle_D$$

where $\quad \langle\rho\rangle_D = \rho_b\left(1 + \langle\delta\rangle_D\right)$

$\langle u_\mu T^{\mu\nu}{}_{;\nu} \rangle_D = 0$ gives

$$\frac{d}{dt}\langle\rho\rangle_D + 3\frac{\dot{a}_D}{a_D}\langle\rho\rangle_D = 0 \quad \textbf{(exact)}$$

$\langle G_{00} \rangle_D = 8\pi G \langle T_{00} \rangle_D$ gives the Friedmann equation

$$\left(\frac{\dot{a}_D}{a_D}\right)^2 + \frac{K_{\rm eff}}{{a_D}^2} = \frac{8\pi G}{3}\langle\rho\rangle_D$$

$$\text{where} \quad \langle\rho\rangle_D = \rho_b\left(1 + \langle\delta\rangle_D\right)$$

$$K_{\rm eff} = \frac{10}{9}\langle\Delta\phi\rangle_D = \text{const.}$$

$\langle u_\mu T^{\mu\nu}{}_{;\nu} \rangle_D = 0$ gives

$$\frac{d}{dt}\langle\rho\rangle_D + 3\frac{\dot{a}_D}{a_D}\langle\rho\rangle_D = 0 \quad \textbf{(exact)}$$

$\langle G_{00} \rangle_D = 8\pi G \langle T_{00} \rangle_D$ gives the Friedmann equation

$$\left(\frac{\dot{a}_D}{a_D}\right)^2 + \frac{K_{\rm eff}}{{a_D}^2} = \frac{8\pi G}{3}\langle\rho\rangle_D$$

$$\text{where} \quad \langle\rho\rangle_D = \rho_b\left(1 + \langle\delta\rangle_D\right)$$

$$K_{\rm eff} = \frac{10}{9}\langle\Delta\phi\rangle_D = \text{const.}$$

domain D behaves as **the homogeneous and isotropic universe** **with the curvature** $K_{\rm eff}$

Finally,

Finally,

we consider

the

"Hubble (non-)constant problem"

with above discussion

we define

the Hubble parameter

of the domain D

Hubble parameter of the domain D

$$\tilde{H}_0 \equiv \left.\frac{\dot{a}_D}{a_D}\right|_{t_0}$$

Hubble parameter of the domain D

$$\tilde{H}_0 \equiv \frac{\dot{a}_D}{a_D}\bigg|_{t_0} \neq H_0 \equiv \frac{\dot{a}}{a}\bigg|_{t_0}$$

this is generally different from
the Hubble parameter
of the background H_0

in the
linear
approximation...

$$\tilde{H}_0 = H_0 \left(1 - \frac{1}{3} \langle \delta(t_0) \rangle_D \right)$$

$$\tilde{H}_0 = H_0 \left(1 - \frac{1}{3} \langle \delta(t_0) \rangle_D \right)$$

If $\langle \delta(t_0) \rangle_D = -0.3$,

$$\tilde{H}_0 = H_0 \left(1 - \frac{1}{3}\langle\delta(t_0)\rangle_D\right)$$

If $\langle\delta(t_0)\rangle_D = -0.3$ **,**

$$\tilde{H}_0 = 1.1H_0$$

$$\tilde{H}_0 = H_0 \left(1 - \frac{1}{3}\langle\delta(t_0)\rangle_D\right)$$

If $\langle\delta(t_0)\rangle_D = -0.3$ **,**

$$\tilde{H}_0 = 1.1H_0$$

the Hubble parameter value can

vary 10%

depending on

the scale of the domain

the “Hubble (non-)constant problem”
can be solved within the general framework of

the linear perturbation theory of
the general relativistic
inhomogeneous universe

without assuming
unknown matters or specific toy models

the end

Session7b 14:00–15:45

[Chair: Tetsuya Shiromizu]

7b1. Alex Vano-Vinuales (Cardiff U.), "Free hyperboloidal evolution in spherical symmetry" (10+5)

[JGRG27 (2017) 113018]

Free hyperboloidal evolution in spherical symmetry

Alex Vano-Vinuales

Cardiff University

JGRG27 - 30th November 2017

AVV, S. Husa & D. Hilditch, 2014, CQG 32 (2015) 175010, gr-qc/1412.3827.
AVV & S. Husa, gr-qc/1412.4801, gr-qc/1601.04079, gr-qc/1705.06298.

Reaching future lightlike infinity

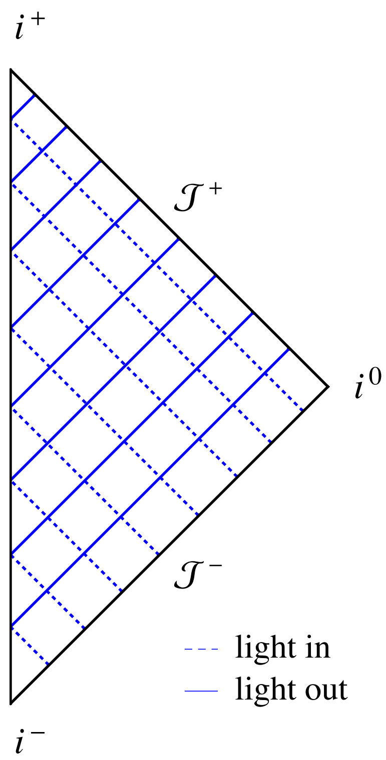

Gravitational waves are only well defined at future null infinity ($\mathscr{I}^+$), where observers of astrophysical events are located.

The study of global properties also benefits from including $\mathscr{I}^+$.

A possible approach: Penrose's conformal compactification of spacetime.
The physical metric $\tilde{g}_{\mu\nu}$ is rescaled

$$g_{\mu\nu} \equiv \Omega^2 \tilde{g}_{\mu\nu}, \qquad (1)$$

with $\Omega|_{\mathscr{I}^+} = 0$ to keep $g_{\mu\nu}$ finite there.

Spacetime slices

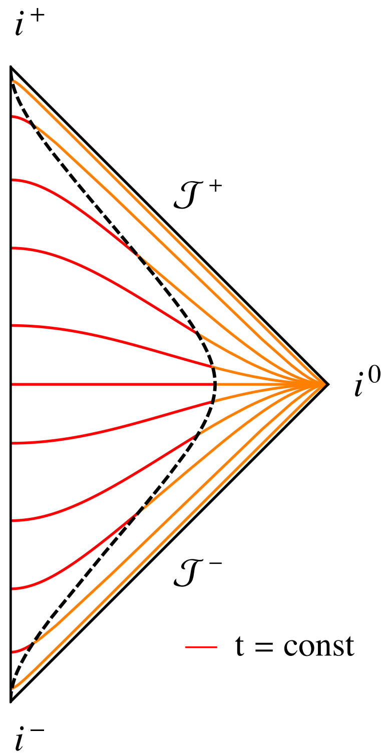

Standard slicing options for the initial value formulation of the Einstein equations, to solve them as an evolution in time:

- Standard Cauchy slices

Introduction Implementation Simulations Conclusions

Spacetime slices

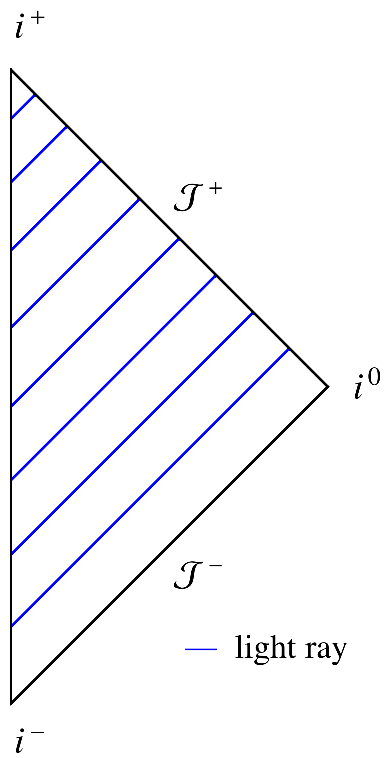

Standard slicing options for the initial value formulation of the Einstein equations, to solve them as an evolution in time:

- Standard Cauchy slices
- Null slices

3/ 14
Free hyperboloidal evolution in spherical symmetry Alex Vano-Vinuales

Spacetime slices

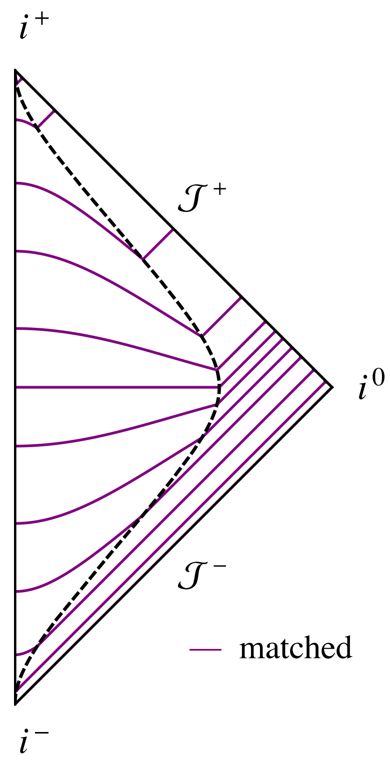

Standard slicing options for the initial value formulation of the Einstein equations, to solve them as an evolution in time:

- Standard Cauchy slices
- Null slices
- Cauchy-Characteristic matching / extraction

Spacetime slices

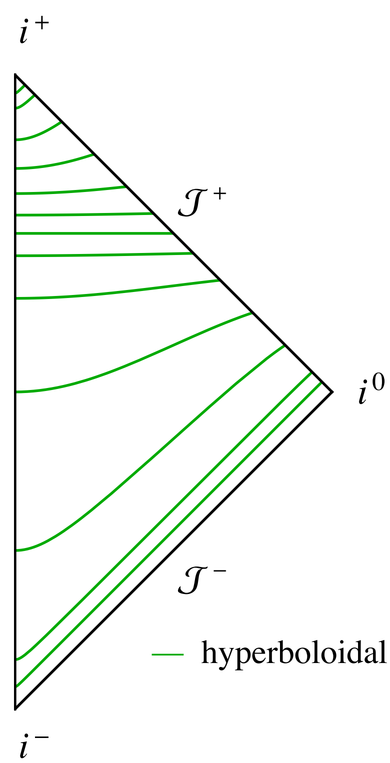

Standard slicing options for the initial value formulation of the Einstein equations, to solve them as an evolution in time:

- Standard Cauchy slices
- Null slices
- Cauchy-Characteristic matching / extraction
- Hyperboloidal slices

Advantages of the hyperboloidal approach:

- Extraction at $\mathscr{I}^+$, no approximations.
- Slices spacelike & smooth everywhere.
- More resolution for the central part.

Schwarzschild trumpet data

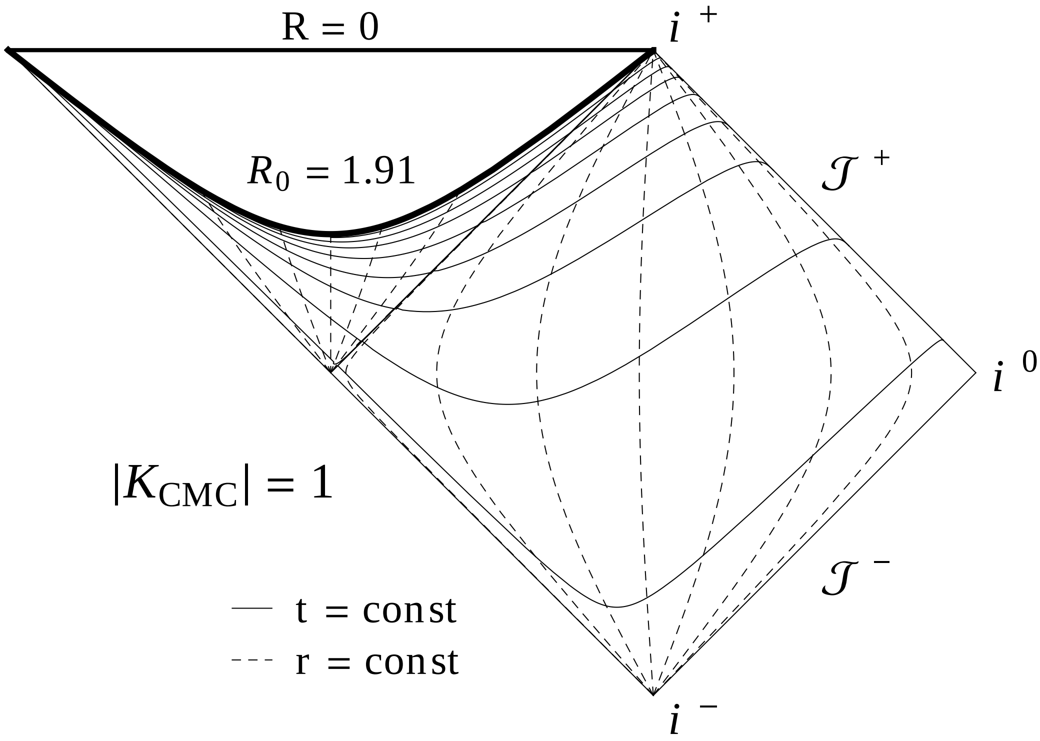

Brief history of the numerical hyperboloidal IVP

- Conformal Field Equations by Friedrich: generality maintained and regularity manifestly shown.
- Numerical implementations by Hübner (tested by Husa, continuum instabilities found) and by Frauendiener.
- Free evolution (generalized harmonic) and a fixed conformal factor by Zenginoğlu: Schwarzschild in spherical symmetry.
- Moncrief and Rinne's constrained axisymmetric code.
- Tetrad formalism by Bardeen, Sarbach and Buchman.
- Wave equation tests in dual foliation formalism by Hilditch.

Main difficulties of the numerical implementation:

- Extra formally divergent terms at $\mathscr{I}^+$ appear in the equations:

$$G_{\mu\nu} = 8\pi\, T_{\mu\nu} - \frac{2}{\Omega}\left(\nabla_\mu\nabla_\nu\Omega - g_{\mu\nu}\nabla^\gamma\nabla_\gamma\Omega\right) - \frac{3}{\Omega^2} g_{\mu\nu}(\nabla_\gamma\Omega)\nabla^\gamma\Omega. \quad (2)$$

- Non-trivial background ($\tilde{K} \neq 0$), unlike with Cauchy slices.

Basic approach

Formulation:

- Free evolution: BSSN, Z4
- Time-independent $\Omega = |K_{CMC}| \frac{r_{\mathscr{I}}^2 - r^2}{6 r_{\mathscr{I}}}$
- Spherical symmetry
- + Massless scalar field

Hyperboloidal initial data:

- Height function approach
- Compactified slice
- Minkowski spacetime
- Schwarzschild trumpet

perturbed by a scalar field.

Hyperbolic gauge conditions:

- Slicing (α): Bona-Massó
  $\dot{\alpha} = \beta^r \alpha' - f(\alpha)\,\alpha^2\,(K - K_0) + L_{\alpha 0}$
- Shift (β^a): Gamma-driver
  $\dot{\beta}^r = \beta^r \beta^{r\prime} + \lambda\,\Lambda^r - \eta\,\beta^r + L_{\beta r 0}$
- Preferred conformal gauge

with scri-fixing condition.

Numerical implementation:

- Method Of Lines
  - Finite differences
  - Runge-Kutta 4th order
- Kreiss-Oliger dissipation
- (Non-)staggered grid.

Numerical grid at $\mathscr{I}^+$

- Staggered grid:
  simpler implementation; values on $\mathscr{I}^+$ using extrapolation.

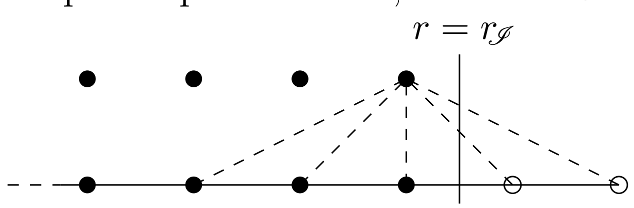

- Non-staggered grid:
  requires regularity conditions at $\mathscr{I}^+$ and calculating the limits of the divergent terms in the equations; quantities given on $\mathscr{I}^+$.

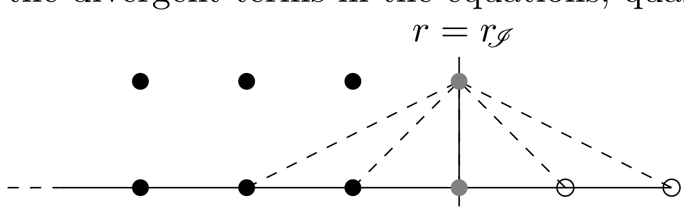

Scalar field - convergence at $\mathscr{I}^+$

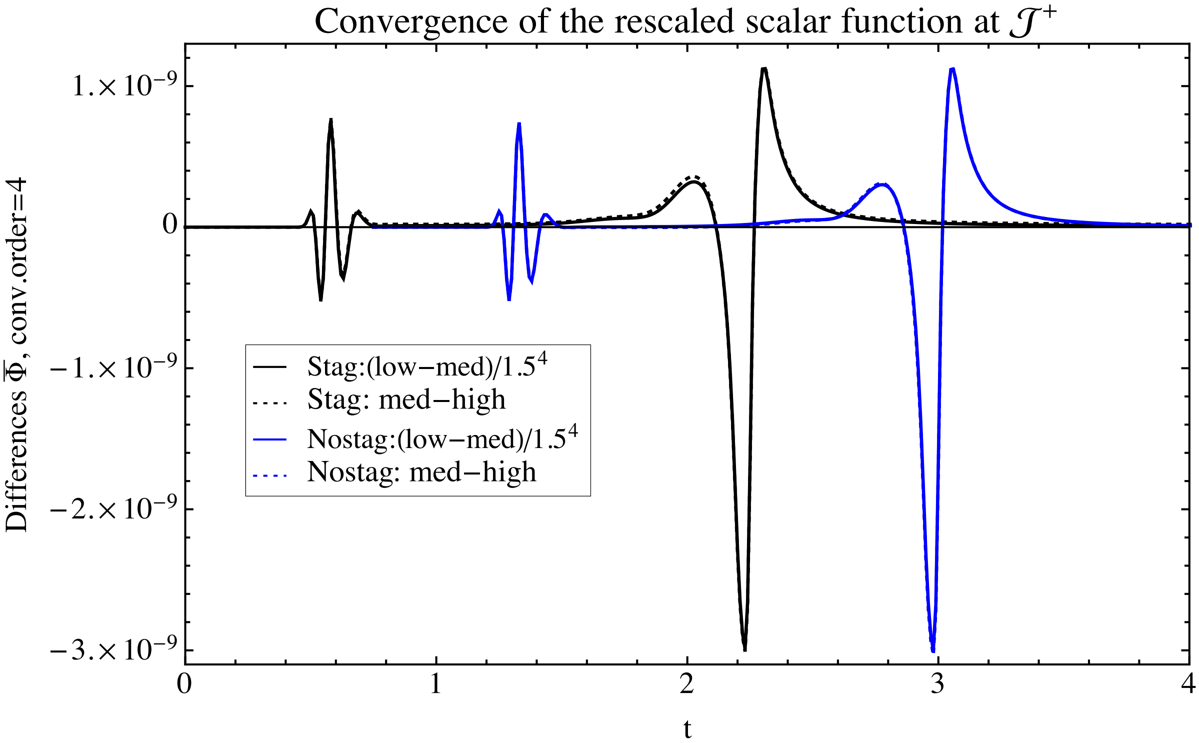

AVV and S. Husa, arXiv:1705.06298 [gr-qc]

Scalar field

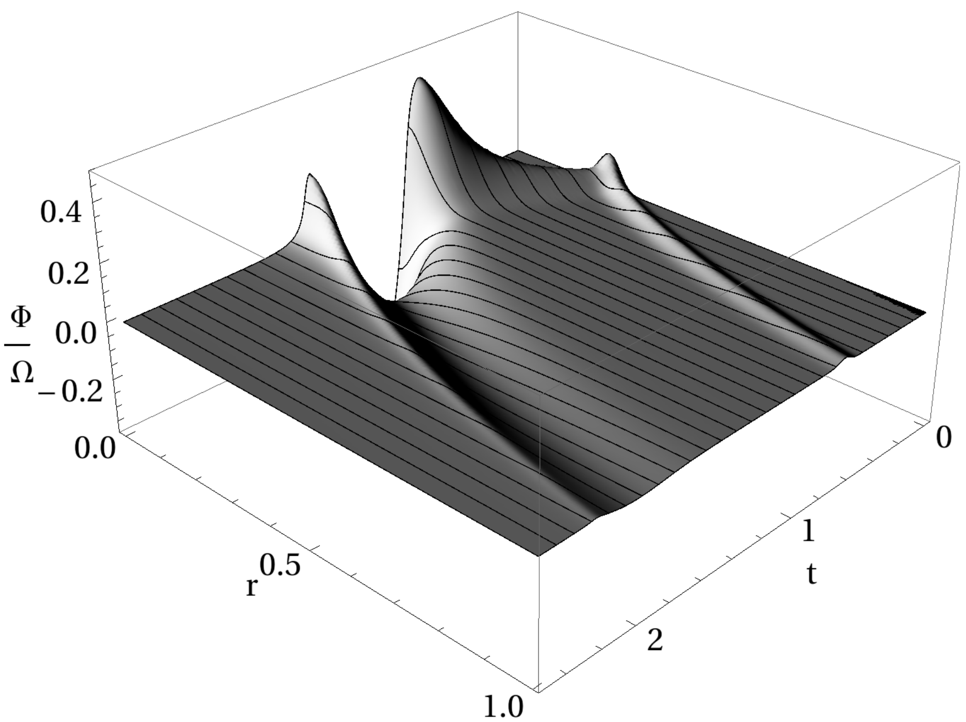

AVV, S. Husa and D. Hilditch, arXiv:1412.3827 [gr-qc]

Scalar field signal at $\mathscr{I}^+$

Rescaled scalar function at $\mathcal{J}^+$ for different gauge conditions

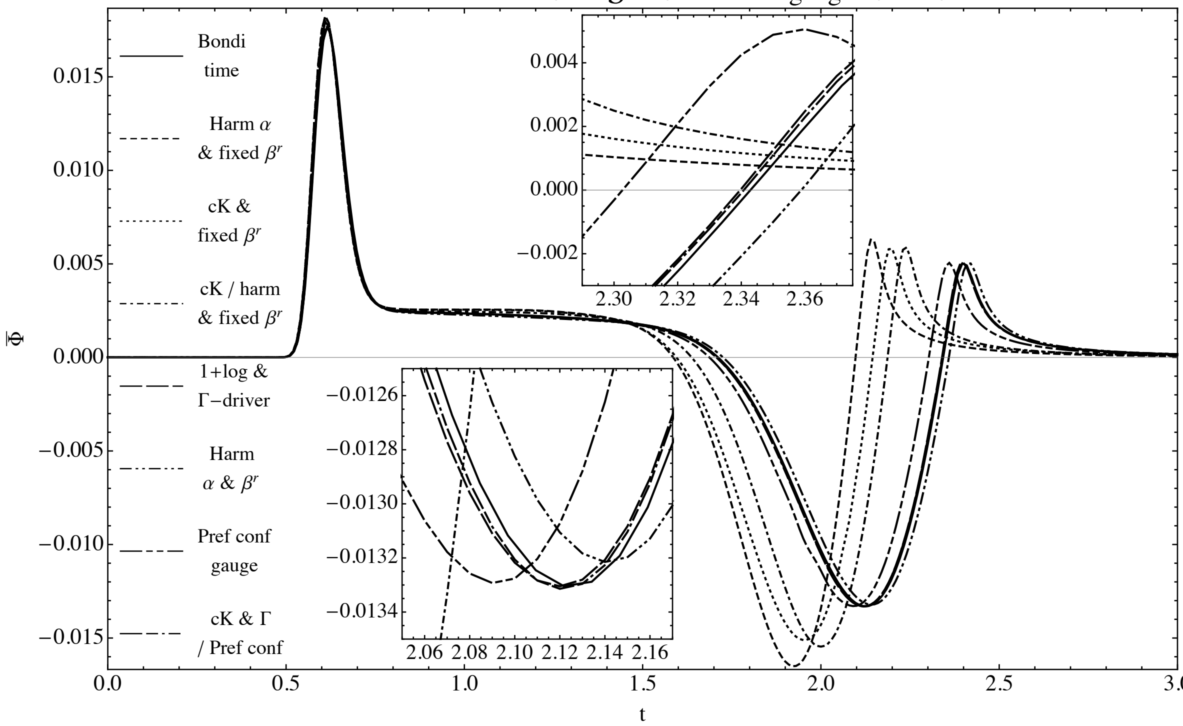

AVV and S. Husa, arXiv:1705.06298 [gr-qc]

Evolution: χ, $\tilde{K}$, α, β^r, Φ/Ω

Effect of slicing conditions $(\partial_t \alpha = \partial_r \alpha - f(\alpha)K + L_0,\ \partial_t \beta^r)$

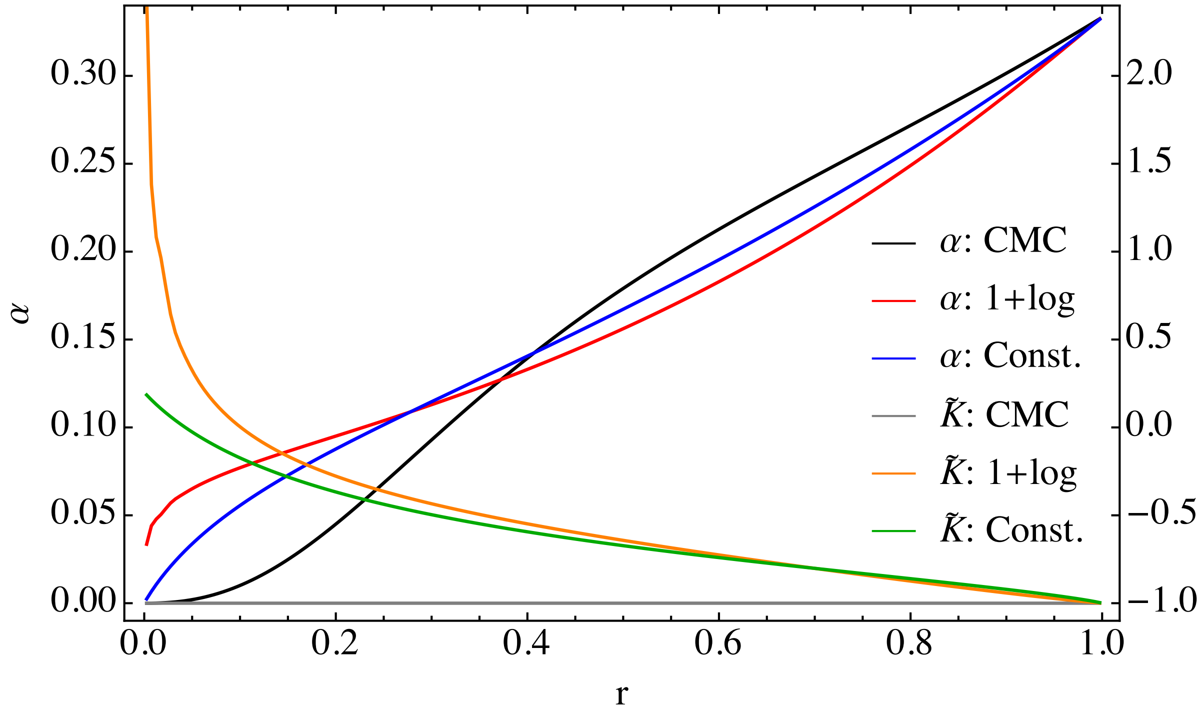

Stationary solution of the slicing condition (trumpet)

$$\partial_t \tilde{\alpha} = RHS(\tilde{r}, \tilde{\alpha}, \partial_{\tilde{r}}\tilde{\alpha}, \ldots) = 0. \tag{3}$$

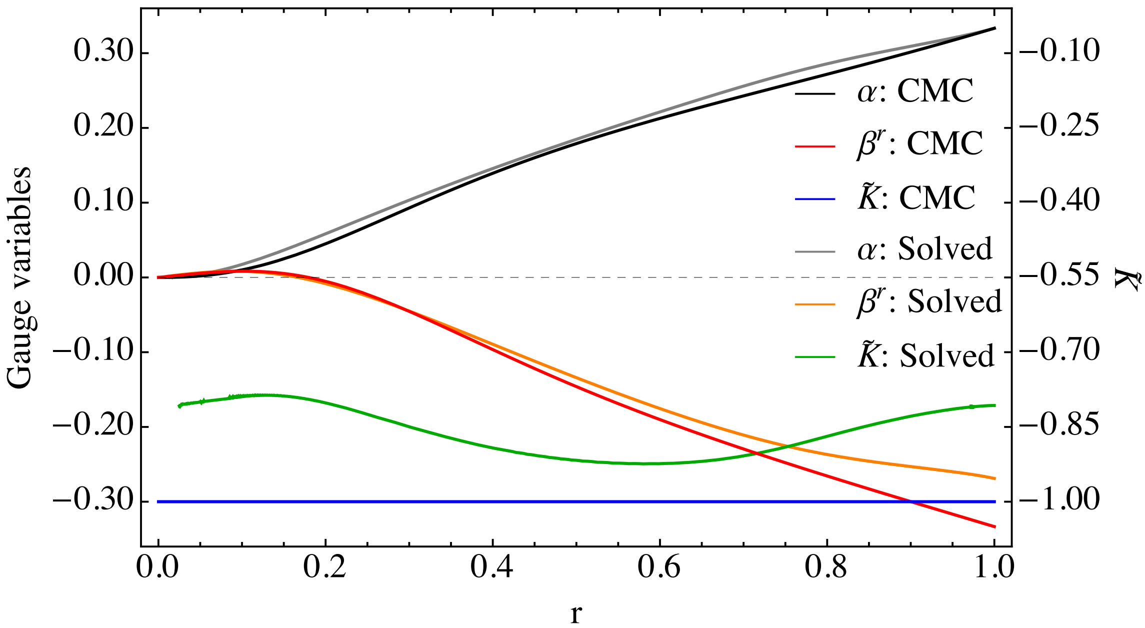

Summary

Hyperboloidal initial value problem:

- promising and efficient approach for numerical simulations,
- allows the study of global properties and extraction of signals.
- To our knowledge, this is the first stable free evolution with a standard formulation.

Getting ready for further work:

- Simulations in AdS ($\mathscr{I}^+$ is timelike $\rightarrow$ boundary conditions).
- 3-dimensional code and initial data $\rightarrow$ binary systems.

AVV, S. Husa & D. Hilditch, 2014, CQG 32 (2015) 175010, gr-qc/1412.3827.
AVV & S. Husa, gr-qc/1412.4801, gr-qc/1601.04079, gr-qc/1705.06298.

7b2. Takafumi Kokubu (KEK), "Example of Null junction conditions: Energy emission from a naked singularity" (10+5) [JGRG27 (2017) 113019]

JGRG27@ Hiroshima

Example of Null Junction Conditions: Energy Emission from a Naked Singularity

Takafumi Kokubu (KEK)
with
Sanjay Jhingan (Yamanashi-Gakuin U.)
Tomohiro Harada (Rikkyo U.)

in preparation.

Our Aim

- **Making a dynamical model to emit energy which is caused by an extremely high curvature region**

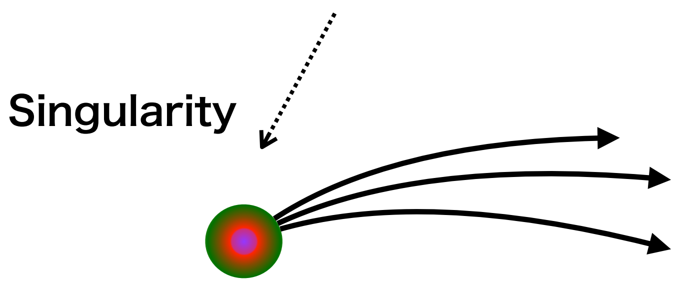

We want to see whether such model can be one of possible candidates describing high energy phenomena in Universe.

Relativistic jet, super nova, super-radiance, etc.

Introduction

- **Naked Singularities** are solutions to Einstein eq.

- over spinning Kerr solution $(a^2 > m^2, \theta = \pi/2)$
- over charged RN solution $(Q^2 > m^2)$
- negative mass Schw. solution $(m < 0)$

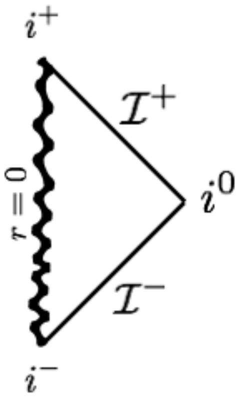

Introduction

- **The Cosmic-Censorship Hypothesis** Penrose(1969)

- naked singularity should not be formed by realistic initial data

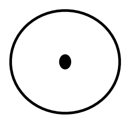

- **Counterexamples**

- singularity can be naked
- e.g. end states of collapsing matter

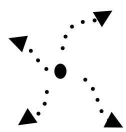

dust, massless scalar, perfect fluid

Eardley-Smarr(1979) Roberts(1989) Ori-Piran(1987)

Naked singularity is in actual existence ?

Naked Singularity formation from a gravitational collapse

Lemaitre-Tolman-Bondi（LTB）: Inhomogeneous dust collapse

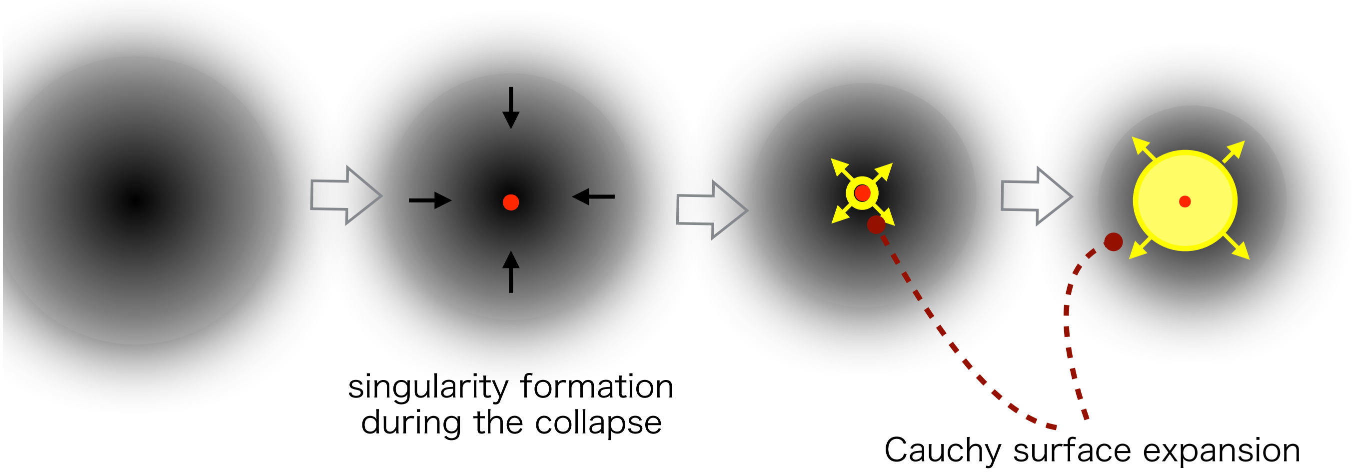

Matching

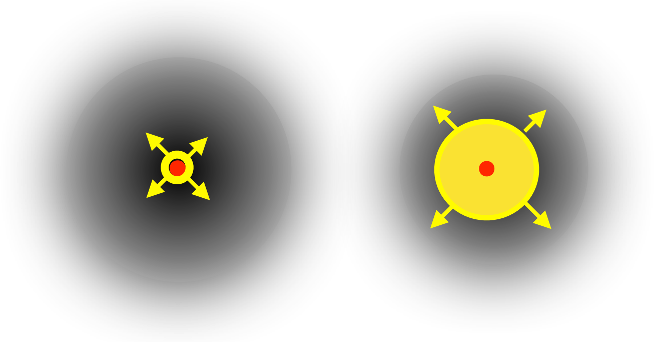

Outside: dust solution
Inside: Undetermined

Matching

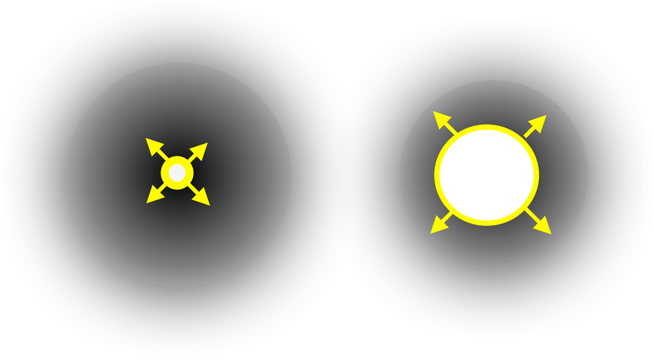

Outside: dust solution
Inside:

Matching

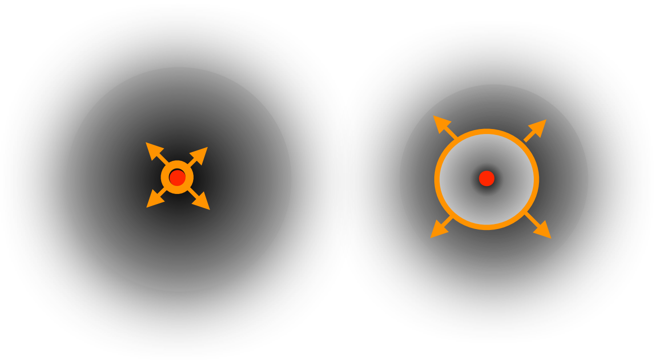

Outside: dust solution
Inside: dust solution with a singularity

Matching

As a result of matching..

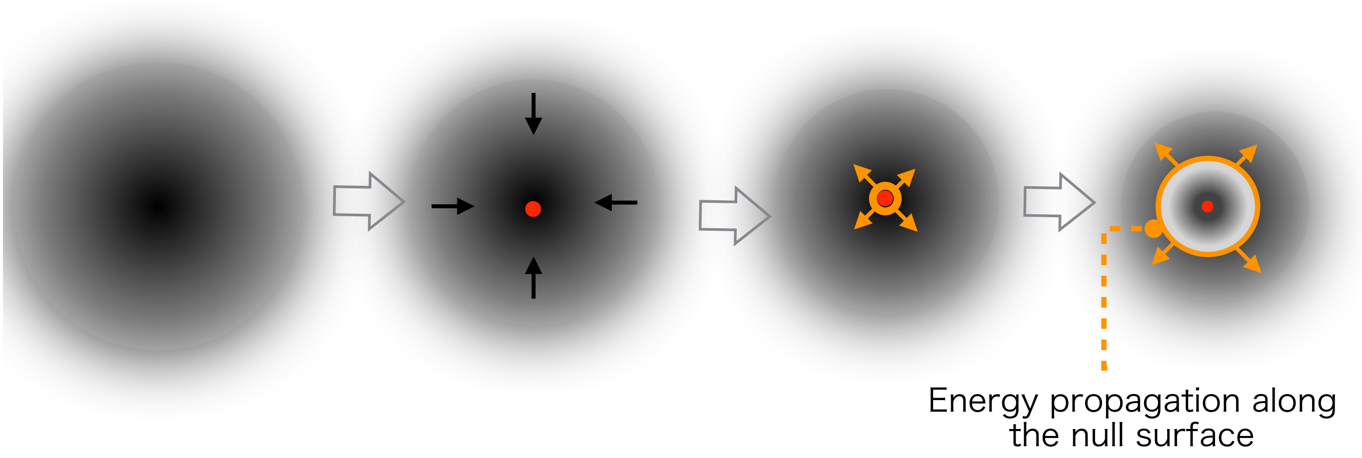

<u>**A dynamical energy emission model from the singularity**</u>

Model

Let's construct a particular model

$$ds_\pm^2 = A_\pm(t_\pm, r_\pm)dt_\pm^2 + B_\pm(t_\pm, r_\pm)dr_\pm^2 + C_\pm(t_\pm, r_\pm)(d\theta^2 + \sin^2 d\varphi^2)$$

(+) & (-): **self-similar** LTB

$$A_\pm = -1,\ B_\pm = (R'_\pm)^2,\ C_\pm = R_\pm^2.$$

$$R_\pm = r_\pm \left(1 - \frac{3\sqrt{2\kappa_\pm}}{2}\frac{t_\pm}{r_\pm}\right)^{2/3}$$

Dust: $\rho_\pm = \dfrac{\kappa_\pm}{4\pi R_\pm^2 R'_\pm}$

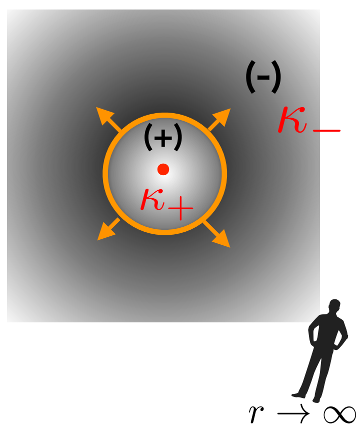

Shell's whole **energy**: $E_{\rm shell} := 4\pi R^2 T^{\alpha\beta} u_\alpha^- u_\beta^- \Big|_\Sigma$

which is proportional to the **luminosity** $L_{\rm shell} := 4\pi R^2 T_{\alpha\beta} u_-^\alpha n_-^\beta \Big|_\Sigma$

$$E_{\rm shell} \propto L_{\rm shell}$$

Luminosity

$$E_{\text{shell}} \propto R$$

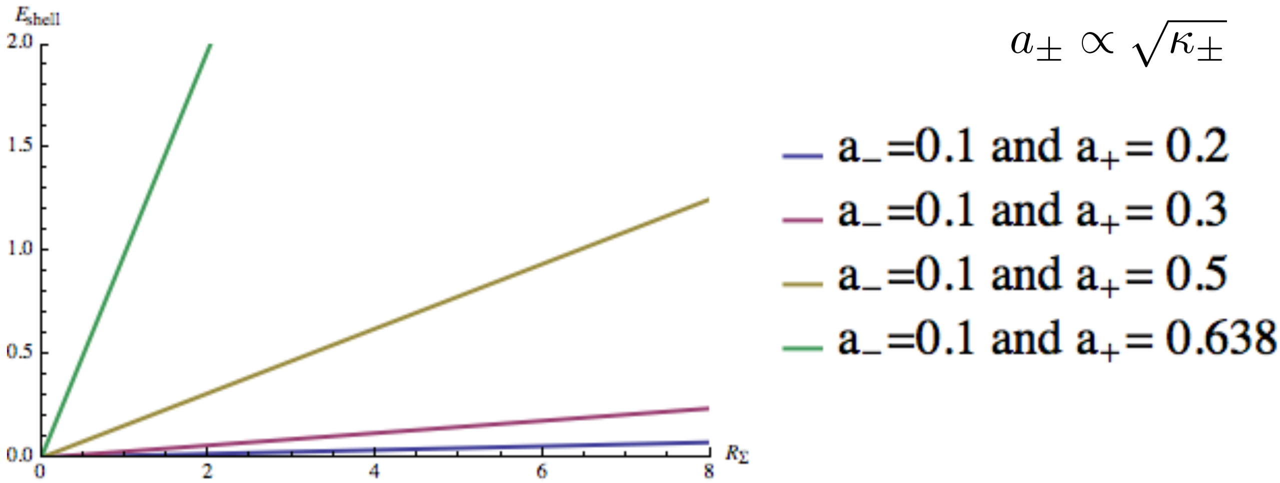

Interpretation of the result

- from the conservation law for null shell

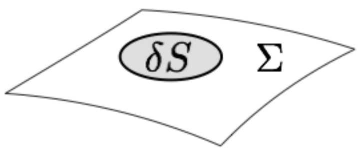

$$\underline{p\frac{\mathrm{d}}{\mathrm{d}\lambda}\delta S} + \underline{[T_{\alpha\beta}k^\alpha k^\beta]\delta S} = 0$$

the energy absorbed into the shell from its surrounding dust

the work done by the shell's expansion

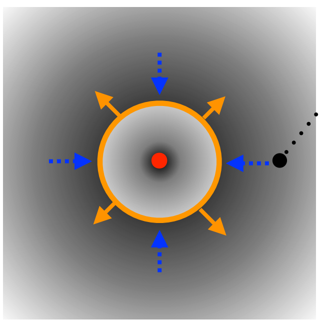

Energy supply to shell
➡ infinite dust (SS-LTB)
➡ luminosity divergence

To make it more realistic

Self-Similar sol.

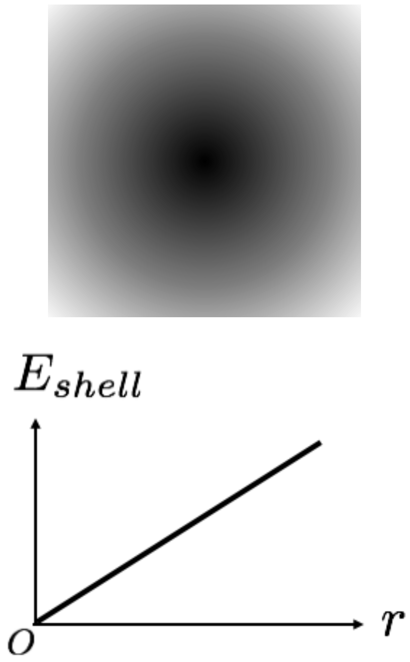

with cut-off

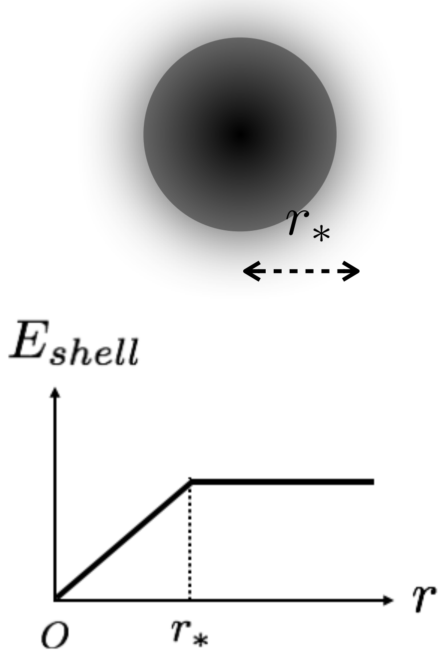

Summary

- We proposed a model for energy emission from a naked singular region in a self-similar dust spacetime by gluing two self-similar dust solutions at the CH.
- It is found that the energy increases in proportion to shell-radius. It is because of the self-similarity.
- The null shell expands in collapsing dust region while absorbing the energy of the surrounding dust.
- Self-similar sol. with an appropriate cut-off could make this sol. more realistic .

7b3. Shinpei Kobayashi (Tokyo Gakugei U.), "Fuzzy spacetime in noncommutative gravity" (10+5) [JGRG27 (2017) 113020]

Fuzzy Spacetime in Noncommutative Gravity

Shinpei Kobayashi (Tokyo Gakugei University)

in collaboration with Tsuguhiko Asakawa (Maebashi Inst. Tech.)

JGRG27 @ Kurara, Higashihiroshima
Nov.26 – Dec.1, 2017

Quantum geometry?

- string theory
  - string field theory, matrix models,...
- loop quantum gravity
- (causal) dynamical triangulation
- noncommutative geometry
  - κ-Minkowski space, twisted diffeomorphism,...
- anything universal?

Reduction of dimension

- implication of lower-dimensional gravity [Carlip, 2017]
  - string theory [Atick&Witten,1988, ...]
  - causal dynamical triangulation [Ambjorn+,2005, ...]
  - κ-Minkowski spacetime [Arzano & Kowalski-Glikman, 2017]

- minimal scale ⇄ "loose" relation exists

$$\Delta x \gtrsim \sqrt{\alpha'}, \quad \Delta x \Delta y \gtrsim \theta, \quad \Delta x \Delta y \Delta z \gtrsim \lambda, \cdots$$

cf. QM $\quad [x,\ p] = i\hbar \quad \rightleftarrows \quad \Delta x \Delta p \geq \dfrac{\hbar}{2}$

Spacetime coordinates and noncommutativity

- a realization: noncommutative coordinates

$$[x, y] = i\theta, \qquad \theta \quad \text{: noncommutative parameter}$$

- position (of a particle) → uncertain: $\Delta x \Delta y \gtrsim \theta$

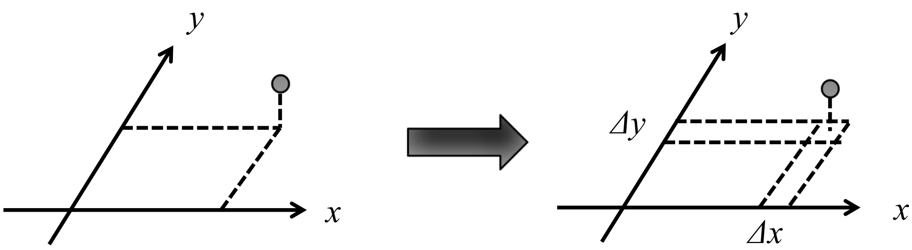

- spacetime coordinates are not completely independent

Round way: deformed product of functions

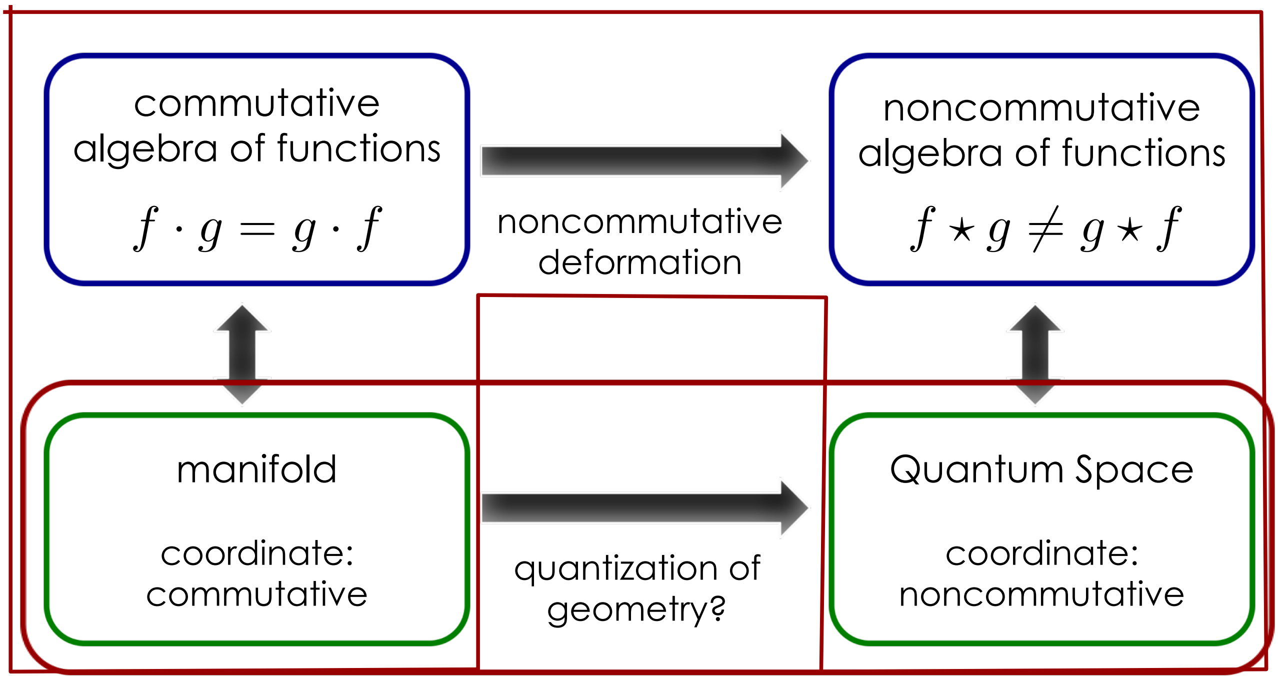

A realization of noncommutativity

- Noncommutativity between space coordinates

$$[x, y] = i\theta, \qquad \theta \;\; \text{: constant parameter}$$

$$\longrightarrow \; [z, \bar{z}] = 1 \qquad \left(z = \frac{x + iy}{\sqrt{2\theta}}, \;\; \bar{z} = \frac{x - iy}{\sqrt{2\theta}} \right)$$

- a realization: Wick-Voros product

$$(f \star g)(z, \bar{z}) = \exp\left(\frac{\partial}{\partial \bar{z}'} \frac{\partial}{\partial z''} \right) f(z', \bar{z}') g(z'', \bar{z}'') \Big|_{z' = z'' = z}$$

$$\Downarrow$$

$$[z, \bar{z}]_\star = z \star \bar{z} - \bar{z} \star z = 1 \qquad \text{cf.)} \quad [a, a^\dagger] = 1$$

Noncommutative product of functions

functions with ordinary product (commutative):

$$S = \int dt d^2x \left(\partial_z \phi \partial_{\bar{z}} \phi + \frac{m}{2} \phi^2 + \cdots \right)$$

$$\Downarrow$$

functions with noncommutative product:

$$S = \int dt d^2x \left(\partial_z \phi \star \partial_{\bar{z}} \phi + \frac{m}{2} \phi \star \phi + \cdots \right)$$

algebraic structure of functions is changed

Function ⇄ Operator

- working on function with noncommutative product: complicated

$\rightarrow$ switching to operator formalism (cf. wave function ⇄ matrix)

QM

$$[x, p] = i\hbar \qquad [a, a^\dagger] = 1$$

$$\hat{a} = \frac{\hat{x} + i\hat{p}}{\sqrt{2\hbar}} \qquad \hat{a}^\dagger = \frac{\hat{x} - i\hat{p}}{\sqrt{2\hbar}} \qquad \hat{N} = \hat{a}^\dagger \hat{a} = \frac{\hat{x}^2 + \hat{p}^2}{2\hbar}$$

number

$$\Rightarrow \quad \hat{N}\,|\,n\,\rangle = n\,|\,n\,\rangle \qquad \hat{O} = \sum_{n=0}^{\infty} O_n |n\rangle\langle n|$$

same structure

NCG

$$[x, y] = i\theta \qquad [z, z^\dagger] = 1$$

$$\hat{z} = \frac{\hat{x} + i\hat{y}}{\sqrt{2\theta}} \qquad \hat{z}^\dagger = \frac{\hat{x} - i\hat{y}}{\sqrt{2\theta}} \qquad \hat{N} = \hat{z}^\dagger \hat{z} = \frac{\hat{x}^2 + \hat{y}^2}{2\theta}$$

radius

Various fuzzy objects

- GMS soliton [Gopakumar+, 2000, Kraus&Larsen 2000, ...]
  fuzzy disc [Lizzi+, 2003]
  fuzzy annulus [SK and Asakawa, 2013]

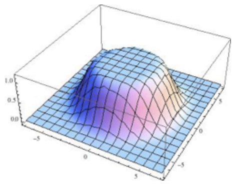

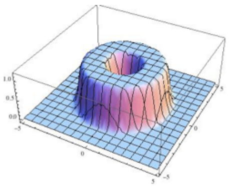

- angular NC soliton [SK&Asakawa, 2013]

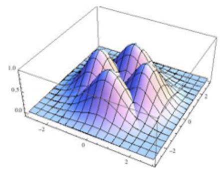

- cosmological solution [Asakawa&SK, 2010]

Toward BH in noncommutative gravity

- sample: (commutative)(1+1)-D gravity with matter

$$S = \frac{1}{16\pi G}\int d^2x\sqrt{-g}\left(\psi R + \Lambda + \frac{1}{2}(\nabla\psi)^2\right) + S_m$$

- BH solution [Mann+, 1991, 1999, Mureika-Nicolini, 2011]

$$ds^2 = -\alpha(x)dt^2 + \frac{1}{\alpha(x)}dx^2$$

"plane" symmetric

eom: $\alpha''(x) + 2\alpha'(x)\delta(x) + \Lambda = 4M\delta(x)$

solution: $\alpha(x) = -\frac{1}{2}\Lambda x^2 + 2M|x| - C$

Number operator = radius operator

N=4 case

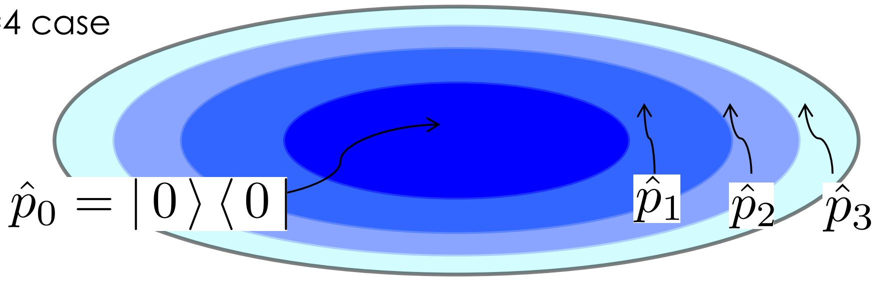

radius $\quad R \sim \sqrt{2N\theta} \quad \left(\because \hat{N} = \hat{a}^\dagger \hat{a} = \dfrac{\hat{x}^2 + \hat{y}^2}{2\theta} = \dfrac{\hat{R}^2}{2\theta} \right)$

total area $\quad 2\pi N\theta$, Each annulus has the area $2\pi\theta$

Noncommutative extension

- Euclidean 2D theory with $[\tau, x] = i\theta$
- space coordinate $\tau, x \;\rightarrow$ operator $\hat{\tau}, \hat{x}$
- ansatz: $\alpha = \alpha(x)$

$\uparrow$

linear along x

cf. (2+1)-D theory, circular symmetry
(eigenstates of the number operator)

- polar → Cartesian

Polar to Cartesian

- coherent state: translation in NC plane

$$
\begin{aligned}
|\zeta\rangle &= e^{\zeta \hat{z}^\dagger - \zeta^* \hat{z}}|0\rangle = e^{-|\zeta|^2/2} \sum_{n=0}^{\infty} \frac{\zeta^n}{\sqrt{n!}}|n\rangle \\
&= \hat{D}(\zeta)|0\rangle \quad \boxed{\text{displacement operator}}
\end{aligned}
$$

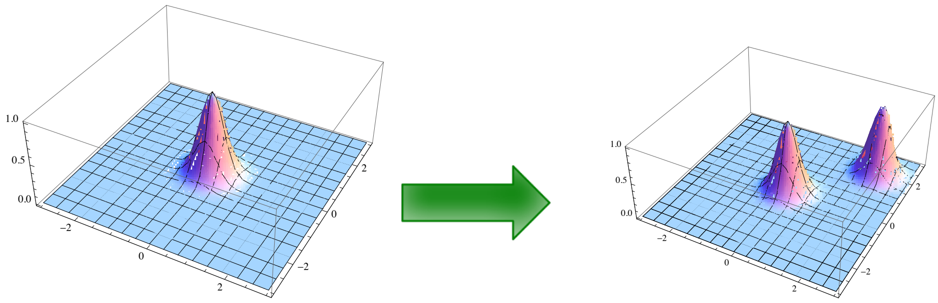

Polar to Cartesian

- squeezed state: realization of x-dependence

$$
\begin{aligned}
|\xi\rangle &= e^{\frac{1}{2}\xi^* \hat{z}^2 - \frac{1}{2}\xi \hat{z}^{\dagger 2}}|0\rangle \\
&= \hat{S}(\xi)|0\rangle \quad (\xi = A e^{i\varphi})
\end{aligned}
$$

$\varphi = 0$: squeezed in x-direction
$\varphi = \pi$: squeezed in τ-direction

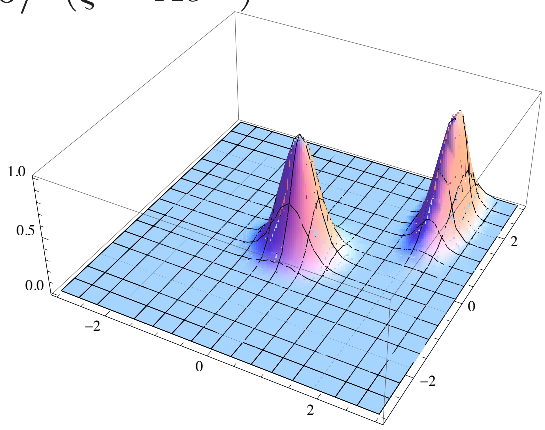

Composition of operator

- completeness: $\sum_{n=0}^{\infty} |n\rangle\langle n| = 1$
- translation of center (coherent state): $\frac{1}{\pi}\int d^2\zeta |\zeta, 0\rangle\langle\zeta, 0| = 1$
- x-dependence (squeezed state): $\frac{1}{\pi}\int d^2\zeta |\zeta, \xi, 0\rangle\langle\zeta, \xi, 0| = 1$

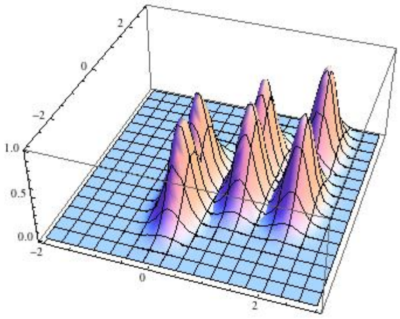

Operator EOM

- anzatz: $\hat{\alpha}(\hat{x}) = \int d^2\zeta \alpha(\zeta) |\zeta, \xi, 0\rangle\langle\zeta, \xi, 0|$
- eom: $\alpha''(x) + 2\alpha'(x)\delta(x) + \Lambda = 4M\delta(x)$
- derivative: $\frac{d}{dx} = \frac{1}{i\theta}[\tau, \cdot]$
- delta function (source): $\delta(x) \to |0, 0, \xi\rangle\langle 0, 0, \xi|_{\varphi=0}$

Summary

- spacetimes with noncommutative space(time) coordinate

  → some cosmological and BH solutions.

- Various eigenstates (number, coherent, squeezed,...) in QM

  → useful to reflect spacetime symmetry
  to apply to gravitational solutions

- (Though I did not talk about it today)
  All operators are related to D-brane

  → we can describe spacetime by D-brane more directly

- Experiment using Gaussian beam → analog gravity

7b4. Ren Tsuda (Ibaraki U.),
"Expanding Polyhedral Universe in Regge Calculus"
(10+5)
[JGRG27 (2017) 113021]

30 Novembar 2017

Expanding Polyhedral Universe in Regge Calculus

Prog. Theor. Exp. Phys. **2017**, 073E01
arXiv:1612.06536 [gr-qc]

Ren Tsuda (Ibaraki University)
In collaboration with
Takanori Fujiwara (Ibaraki University)

The 27th Workshop on General Relativity and Gravitation in Japan - JGRG27
27 November - 1 December, 2017 @Higashi Hiroshima Arts and Culture Hall, Kurara

Outline

1. Overview of Regge Calculus

2. Polyhedral Universe

3. Summary & Future Works

1. Overview of Regge Calculus

Polytopal decomposition

Regge Calculus $\cdots$ Lattice approach to Einstein's general relativity (T. Regge, *Nuovo Cimento* **19**, 1961)

Key idea $\cdots$ Polytopal decomposition

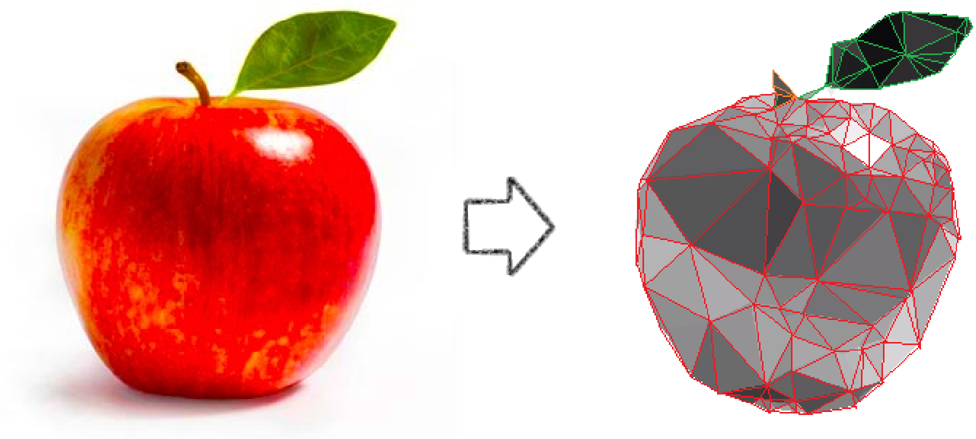

Smooth manifold $\Rightarrow$ Piecewise linear one

Regge calculus

An analog of the Einstein-Hilbert action is given by the **Regge action**

$$\frac{1}{16\pi}\int d^Dx\sqrt{-g}\,(R-2\Lambda) \to \frac{1}{8\pi}\left(\sum_{i\in\{\text{hinges}\}} A_i\varepsilon_i - \Lambda\sum_{i\in\{\text{blocks}\}} V_i\right)$$

A_i : Volume of a hinge; hinge is a $(D-2)$-dimensional face of the lattice, in simple words, hinge is a boundary of a boundary

ε_i : Deficit angle around the hinge A_i

V_i : Volume of a unit cell of the lattice

Metric is replaced by **lengths of edges** of PL manifold

$$g_{\mu\nu} \to l_i$$

Regge calculus describes the gravity as lattice geometry

2. Polyhedral Universe

Schläfli symbols

The foregoing investigations are mainly **restricted to regular polyhedra**.
There are only five types of the **regular polyhedra**
specified by the Schläfli symbols.

(P. A. Collins and R. M. Williams, *Phys. Rev.* **D 7**, 1973)

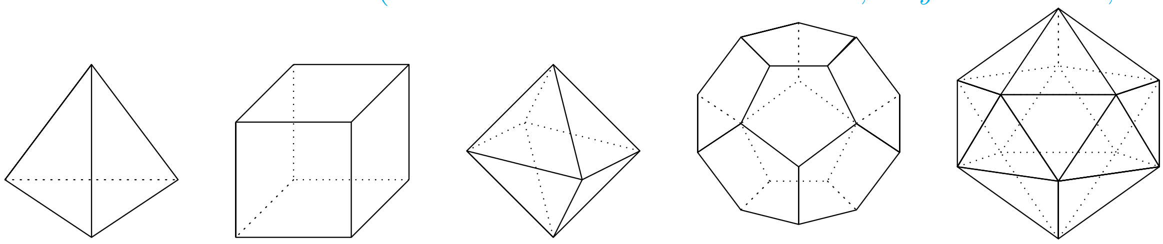

tetrahedron	cube	octahedron	dodecahedron	icosahedron
$\{3,3\}$	$\{4,3\}$	$\{3,4\}$	$\{5,3\}$	$\{3,5\}$

Schläfli Symbols for regular polyhedra $\{p,q\}$

$\cdots$ p: the number of the sides of a face

q: the number of the faces meeting at each vertex

Schläfli symbols

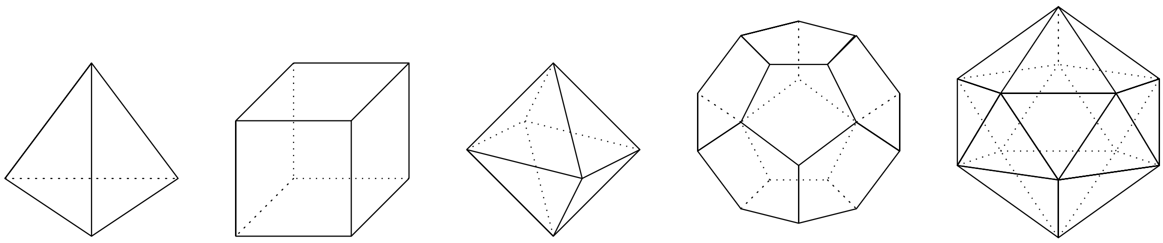

tetrahedron	cube	octahedron	dodecahedron	icosahedron
$\{3,3\}$	$\{4,3\}$	$\{3,4\}$	$\{5,3\}$	$\{3,5\}$

By using Schläfli symbols,
we can treat **all regular polyhedra in a unified way**
and give a **generic expression** for the equation

Expanding regular polyhedral universe

Space: 2-dim. surface of the polyhedron $\{p, q\}$

with edge length $l(t)$

Time: Continuum for simplification

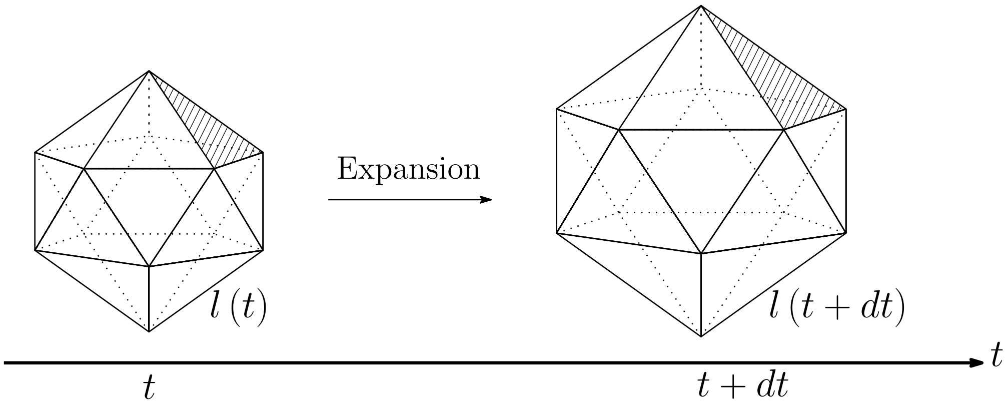

A expanding regular polyhedron

as a 3-dimensional universe

Regge equations for regular polyhedral models

Hamiltonian constraint

$$2\pi - q \arccos \frac{\dot{l}^2 - 4\cos\frac{2\pi}{p}}{4+\dot{l}^2} = \frac{q\Lambda}{2} \frac{l^2 \cos\frac{\pi}{p}}{\sqrt{4\sin^2\frac{\pi}{p} + \dot{l}^2}}$$

Evolution equation

$$\frac{\ddot{l}}{4+\dot{l}^2} = \frac{\Lambda}{4} l \left[1 - \frac{l\ddot{l}}{\left(\sin^2\frac{\pi}{p} + \dot{l}^2\right)} \right]$$

To compare with the continuum theory, we introduce a **circumradius** of the polyhedron as an analogue of the scale factor

$$a_{\mathrm{R}}(t) = \frac{\sin\frac{\pi}{q}}{2\sqrt{\sin^2\frac{\pi}{p} - \cos^2\frac{\pi}{q}}} l(t).$$

Behavior of the regular polyhedral models

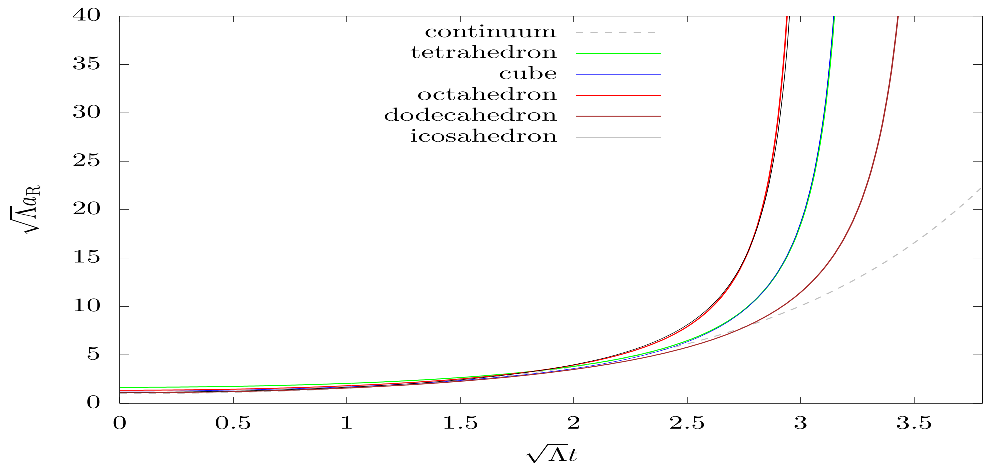

Sphere spends infinite time to expand to infinite size.

$\Updownarrow$

Polyhedron gets infinite size within finite time

Behavior of the regular polyhedral models

Expression of the time when polyhedral model gets infinite size

$$t_{p,q} = \int_0^{\frac{p-2}{p}\pi} d\theta \frac{2\pi - q(\theta - \sin\theta)}{2\sqrt{2q\Lambda(2\pi - q\theta)\sin\theta \sin\frac{(p-2)\pi + p\theta}{2p} \sin\frac{(p-2)\pi - p\theta}{2p}}}$$

In fact, in the era of $t \simeq t_{p,q}$, evolution equation is approximately given by

$$a_{\mathrm{R}} \simeq \frac{c_{p,q}}{\Lambda(t_{p,q} - t)}$$

where $c_{p,q}$ is defined by

$$c_{p,q} = \frac{2\pi}{q} \frac{\sec\frac{\pi}{p}\sin\frac{\pi}{q}}{\sqrt{\sin^2\frac{\pi}{p}\cos^2\frac{\pi}{q}}}$$

Up till now, we have considered regular polyhedron.

However, if we cease to stick to regular polyhedron, we can approximate a sphere more precisely.

One way to put this into practice is to introduce

"Geodesic domes".

Geodesic domes

Frequency ν $\cdots$ Degree of subdivision
each faces are subdivided into ν^2 small triangles

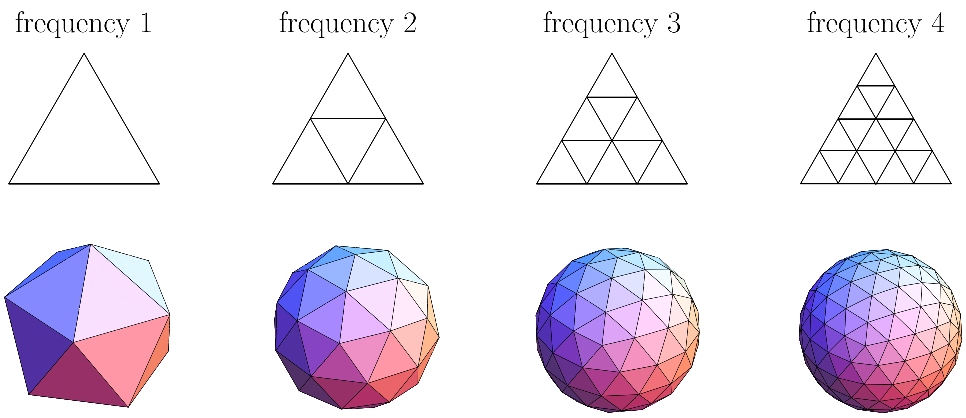

Geodesic domes are produced by the projection of tessellated icosahedron onto the circumshpere

Geodesic domes

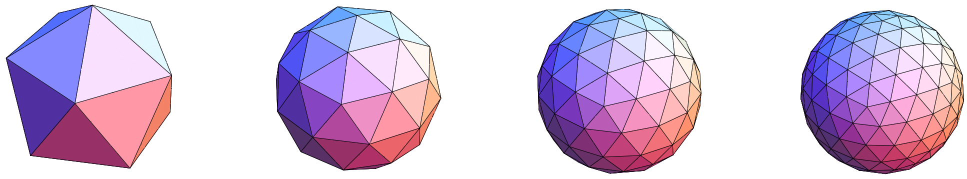

Better approximates a sphere than the regular polyhedra

However, **geodesic domes are not regular polyhedra**.
So, we **can not define the Schläfli symbols** for geodesic domes and need to introduce some **extra parameters to specify the shape** of them.

Geodesic dome universe

$\nu = 2$

$$\frac{1}{5}\varepsilon_1 + \frac{1}{2}\varepsilon_2 = \Lambda l^2 \left[\frac{\sin\xi \cos\frac{\xi}{2}}{\sqrt{4\cos^2\frac{\xi}{2} + \dot{l}^2}} + \frac{\sin^2\frac{\xi}{2}}{\sqrt{3 + 4\dot{l}^2 \sin^2\frac{\xi}{2}}} \right]$$

$$a_{\mathrm{gd}} = \frac{\sqrt{10 + 2\sqrt{5}}}{4} l$$

$$\xi = \text{const.}$$

$$\varepsilon_1 = 2\pi - 5\theta_{1,1} \quad , \quad \varepsilon_2 = 2\pi - 4\theta_{2,1} - 2\theta_{2,2}$$

$$\theta_{1,1} = \arccos\frac{4\cos\xi + \dot{l}^2}{4 + \dot{l}^2}$$

$$\theta_{2,1} = \arccos\frac{\left(2 + \dot{l}^2\right)\sin\frac{\xi}{2}}{\sqrt{\left(4 + \dot{l}^2\right)\left(1 + \dot{l}^2 \sin^2\frac{\xi}{2}\right)}}$$

$$\theta_{2,2} = \arccos\frac{1 + 2\dot{l}^2 \sin^2\frac{\xi}{2}}{2\left(1 + \dot{l}^2 \sin^2\frac{\xi}{2}\right)}$$

Geodesic dome universe

$\nu = 3$

$$\frac{1}{5}\varepsilon_1 + \varepsilon_2 + \frac{1}{3}\varepsilon_3 = \Lambda l^2 \left[\frac{\sin\xi \cos\frac{\xi}{2}}{\sqrt{4\cos^2\frac{\xi}{2} + l^2}} + \frac{2\sin^2\frac{\xi}{2}\cos^2\frac{\eta}{2}}{\sqrt{\sin^2\frac{\eta}{2} + l^2\sin^2\frac{\xi}{2}}} + \frac{\sin^2\frac{\xi}{2}\csc\frac{\eta}{2}\sin\zeta\cos\zeta}{\sqrt{4\sin^2\frac{\eta}{2}\cos^2\frac{\zeta}{2} + l^2\sin^2\frac{\xi}{2}}} \right]$$

$$a_{\mathrm{gd}} = \frac{\sqrt{10+2\sqrt{5}}}{4} l$$

$$\begin{aligned}
\xi &= \text{const.} \\
\eta &= \text{const.} \\
\zeta &= \text{const.} \\
\varepsilon_1 &= 2\pi - 5\theta_{1,1} \\
\varepsilon_2 &= 2\pi - 4\theta_{2,1} - 2\left(\theta_{2,1} + \theta_{2,2} + \theta_{2,3}\right) \\
\varepsilon_3 &= 3\left(\theta_{3,2} + \theta_{3,3}\right)
\end{aligned}$$

$$\theta_{1,1} = \arccos\frac{4\cos\xi + l^2}{4 + l^2} \quad , \quad \theta_{2,1} = \arccos\frac{\left(2+l^2\right)\sin\frac{\xi}{2}}{\sqrt{\left(4+l^2\right)\left(1 + l^2\sin^2\frac{\xi}{2}\right)}}$$

$$\theta_{2,2} = \arccos\frac{2\sin^2\frac{\eta}{2} + l^2\sin^2\frac{\xi}{2}}{\sqrt{\left(1 + l^2\sin^2\frac{\xi}{2}\right)\left(4\sin^2\frac{\eta}{2} + l^2\sin^2\frac{\xi}{2}\right)}}, \theta_{2,3} = \arccos\frac{\left(2\sin^2\frac{\eta}{2} + l^2\sin^2\frac{\xi}{2}\right)\sin\frac{\xi}{2}}{\sqrt{\left(4\sin^2\frac{\eta}{2} + l^2\sin^2\frac{\xi}{2}\right)\left(\sin^2\frac{\eta}{2} + l^2\sin^2\frac{\xi}{2}\sin^2\frac{\zeta}{2}\right)}}$$

$$\theta_{3,2} = \arccos\frac{4\cos\eta\sin^2\frac{\eta}{2} + l^2\sin^2\frac{\xi}{2}}{4\sin^2\frac{\eta}{2} + l^2\sin^2\frac{\xi}{2}} \quad , \quad \theta_{3,3} = \arccos\frac{4\cos\zeta\sin^2\frac{\eta}{2} + l^2\sin^2\frac{\xi}{2}}{4\sin^2\frac{\eta}{2} + l^2\sin^2\frac{\xi}{2}}$$

Geodesic dome universe

The number of the extra parameters is given by

$$\# = \begin{cases} \frac{(\nu+1)^2}{4} & : \ (\nu \text{ odd}) \\ \frac{\nu^2+2\nu}{4} & : \ (\nu \text{ even}) \end{cases}$$

- The higher the frequency, the more cumbersome equation becomes.
- In the limit $\nu \to \infty$, infinite number of extra parameters emerge.

To avoid the complexity of carrying out the Regge calculus for the geodesic dome,
we regard it as a "**pseudo-regular polyhedron**"

Pseudo-regular polyhedron

How about the Schläfli symbols $\{p,q\}$ for Pseudo-regular polydehdon ?

Since all the faces of the geodesic dome are triangles, we use $p=3$.
As for q, we employ the average number of faces meeting at a vertex.

So, we may define **"the fractional Schläfli symbols"**

$$\{p,q\} = \left\{3, \frac{30\nu^2}{5\nu^2+1}\right\}.$$

With this $\{p,q\}$, **we can use the equation for regular polyhedron** still hold true. It's quite simple and unified form for any frequency of pseudo-regular polyhedra.

Geodesic dome vs. Pseudo-regular polyhedron

a_{gd} : Geodesic Dome(———)

a_{R} : Pseudo-regular polyhedron(———)

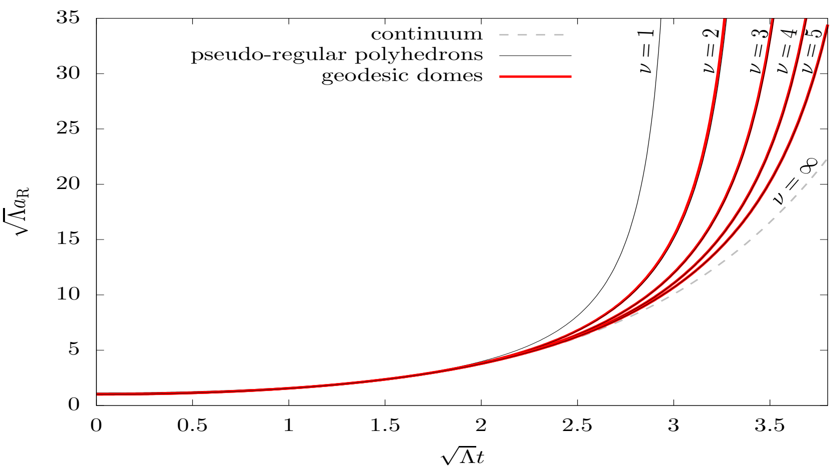

As you can see, the pseudo-regular polyhedra are quite close to the geodesic domes

Deviation $\left|\left(a_{\mathrm{R}} - a_{\mathrm{gd}}\right)/a_{\mathrm{gd}}\right|$

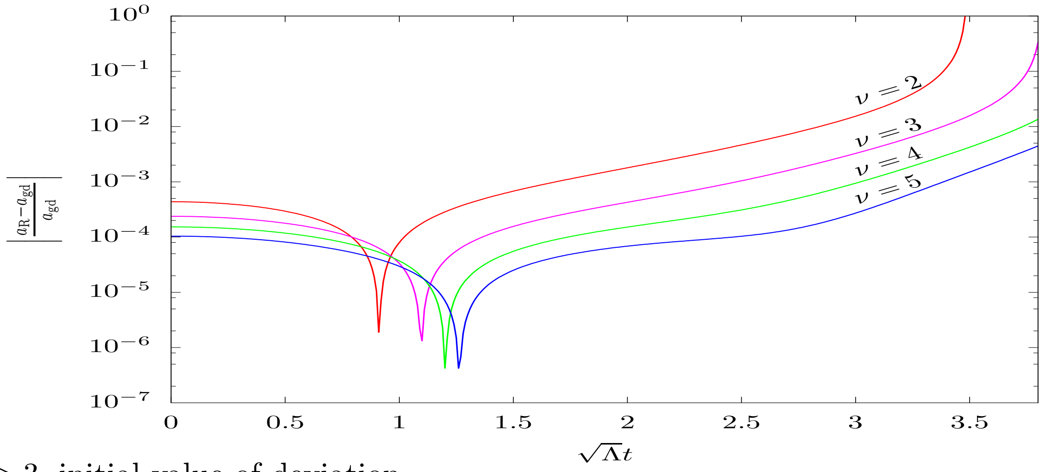

For $\nu \geq 3$, initial value of deviation

$$\left|\frac{a_{\mathrm{R}} - a_{\mathrm{gd}}}{a_{\mathrm{gd}}}\right| < 0.0013.$$

in spite of that **GD and PRP are essentially different** objects.

Infinite frequency limit

In contrast to the case of GD,
PRP can be evaluated in the limit $\nu \to \infty$.

Taking the limit $\nu \to \infty$,
Schläfli symbols

$$\{p, q\} = \left\{3, \frac{30\nu^2}{5\nu^2 + 1}\right\} \to \{3, 6\}$$

Initial value of the scale factor

$$a_{\mathrm{R}}(0) = 2\sqrt{\frac{\sqrt{3}\pi\left(\frac{2}{q} - \frac{1}{3}\right)}{\Lambda\left(3 - 4\cos^2\frac{\pi}{q}\right)}} \to \frac{1}{\sqrt{\Lambda}}$$

It coincides with the initial value of the 3-dimensional FLRW universe.

Infinite frequency limit

Taking the limit $\nu \to \infty$,

Time when PRP gets infinite size

$$t_{3,q} = \int_0^{\frac{1}{3}\pi} d\theta \frac{2\pi - q\left(\theta - \sin\theta\right)}{2\sqrt{2q\Lambda\left(2\pi - q\theta\right)\sin\theta \sin\frac{\pi+3\theta}{6}\sin\frac{\pi-3\theta}{6}}} \to \infty$$

Regge equation

$$\left\{ \begin{array}{rcl} \frac{\ddot{l}}{4+\dot{l}^2} & = & \frac{\Lambda}{4} l \left[1 - \frac{l\ddot{l}}{2\left(3+\dot{l}^2\right)}\right] \\ a_R\left(t\right) & = & \frac{l(t)}{\sqrt{3}} \tan\frac{\left(5\nu^2+1\right)\pi}{30\nu^2} \end{array} \right. \quad \Longrightarrow \quad \ddot{a}_{\mathrm{R}} = \Lambda a_{\mathrm{R}} \quad \text{(Friedmann eqs.)}$$

Exactly coincides with Friedmann equation.
So, **Regge calculus can recover General relativity** in the continuum limit.

3. Summary & Future Works

Summary

- We have investigated (2+1)-dim. polyhedral universe in Regge Calculus.

- By introducing the pseudo-regular polyhedral models,
  - behavior of the geodesic dome universes is approximated well.
  - the continuum solution can be reproduced in the infinite frequency limit.

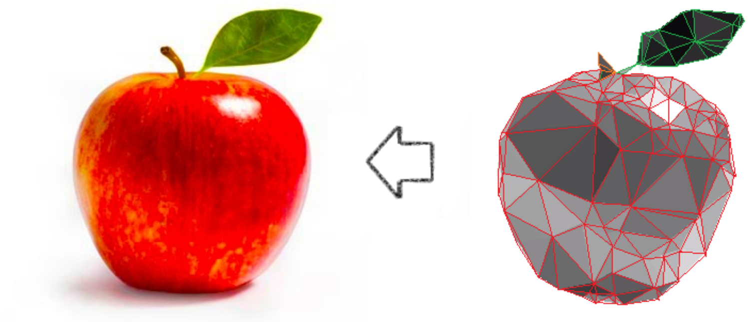

Future Works

We have considered vacuum closed compact universe in three dimensions.

- It is desired to extend our approach to four-dimensional polytopal universe.

- In three dimensions, investigating the non-compact hyperspherical universe with negative cosmological constant might be interesting.

- Inclusion of matter is also interesting.

This is all for my presentation.
Thank you for your kind attention.

Invited lecture 16:45–17:45

[Chair: Yuko Urakawa]

Masaki Shigemori (Queen Mary London, YITP),
“The Black-Hole Microstate Program” (50+10)
[JGRG27 (2017) 113024]

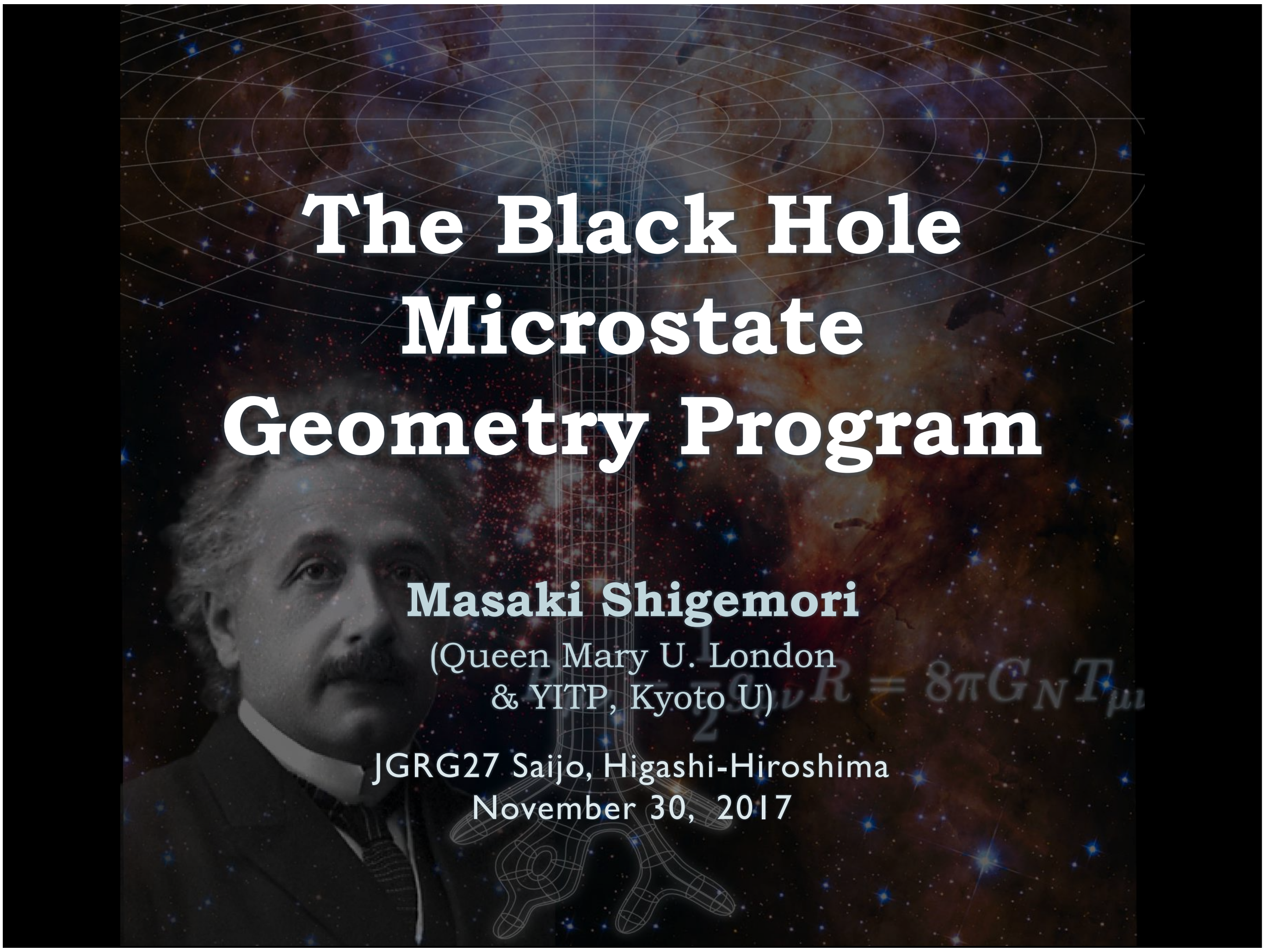

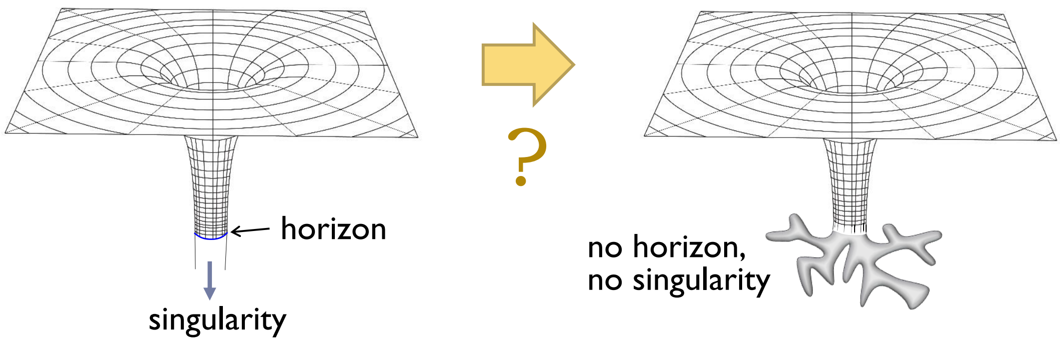

Can we replace the black hole
with a smooth, horizonless spacetime?

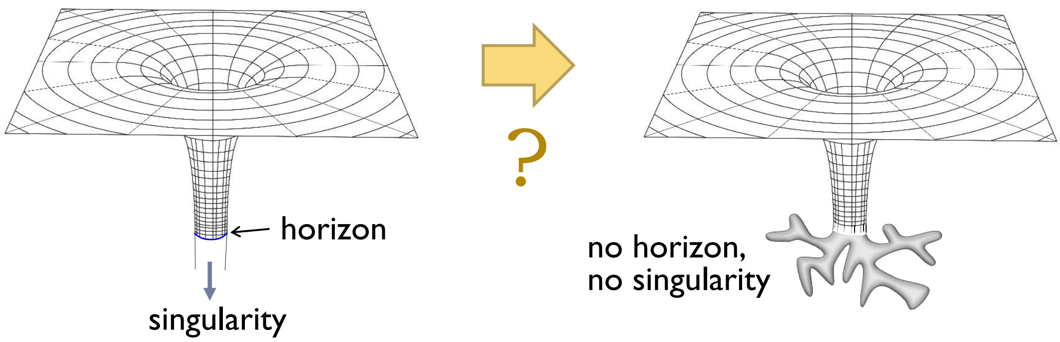

BH microstate geometry program:
Let's explicitly construct them!

- Uniqueness theorems?
- Why not collapse?
- Physical significance?

Plan

- Black hole microstates
- String theory and MGP
- Examples of microstate geometries
- Physical properties

Black Hole Microstates

Black holes

Most extreme situations in the universe

- Solution to Einstein equation
- Boundary of no return: horizon
- Ubiquitous in the universe
- Gravitational waves

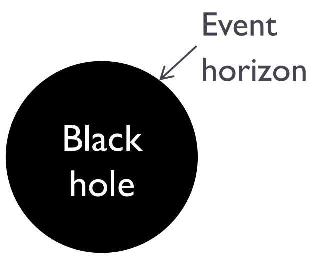

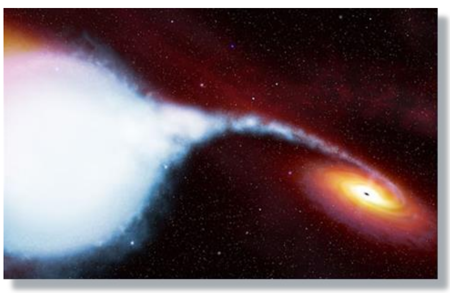

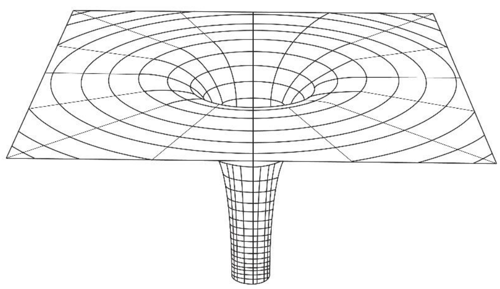

Two aspects of BH physics

Classical / macroscopic physics

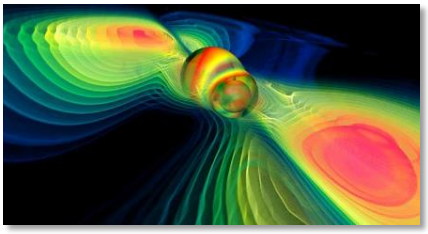

- Well understood
- No conceptual problem

Quantum / microscopic physics

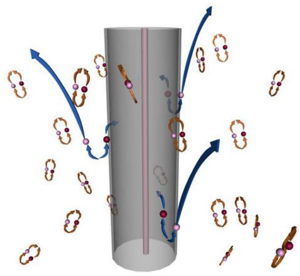

- Poorly understood
  - Hawking radiation, information paradox…
- Quantum gravity is needed

BHs have entropy

Can define BH entropy by

$$S_{\text{area}} \equiv \frac{A}{4G_N}$$

$\sim 10^{77}$ (solar mass)

10^{90} (Milky Way center)

→ BH is a thermodynamic object

Statistical mechanics

Thermodynamics is coarse-grained effective description of underlying microstates

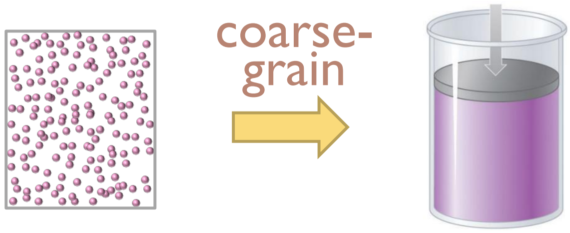

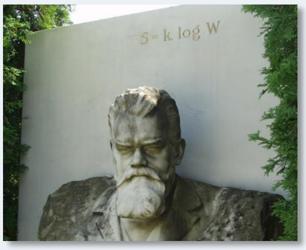

Boltzmann: entropy is (the log of) the number of microstates

$$S = \log N_{\text{micro}}$$

BH must represent a statistical mechanical ensemble of underlying microstates, and

$$S_{\text{area}} = \log N_{\text{micro}}$$

But where *are* these BH microstates?

- Uniqueness theorems
- Need quantum gravity?

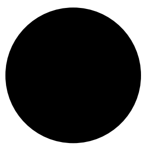

only one solution…?

Summary:

Where are black hole microstates?

String Theory & the Microstate Geometry Program

What is string theory?

Everything is made of the "string"!

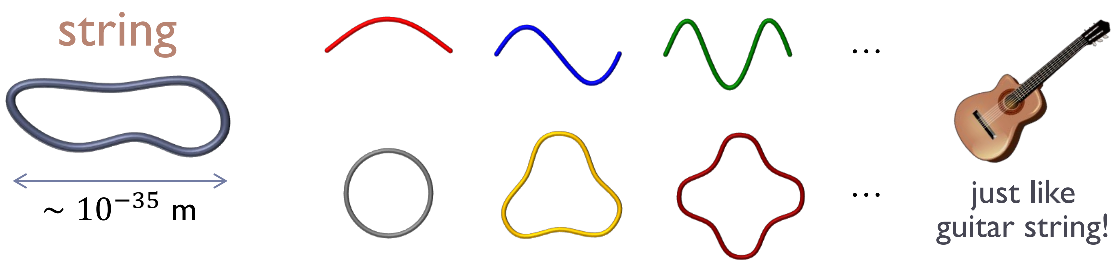

- Different vibration modes = different matter
- Consistent theory of quantum gravity
- Various predictions

Prediction 1: extra dimensions

- Spacetime is not 4 but 10-dimensional.
  Extra 6 dimensions are compactified.

What is compactification?

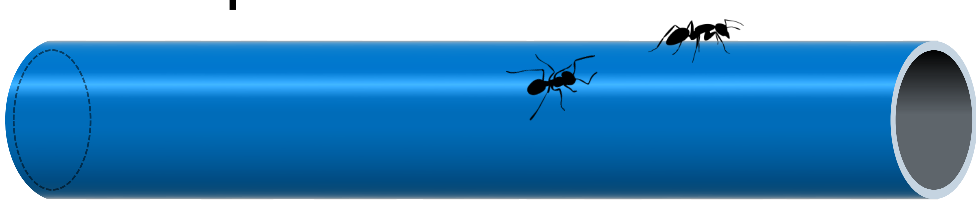

Tiny ants perceive a hose as a 2D object

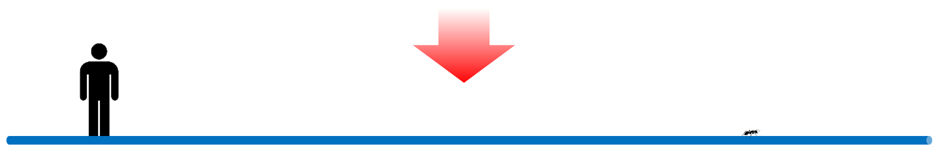

But it looks like a 1D object on a large scale

Likewise, 6 extra dimensions of our universe
may be compactified and thus invisible

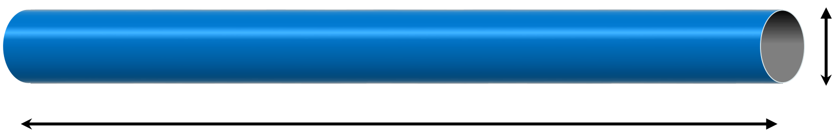

What are extra dimensions are good for?

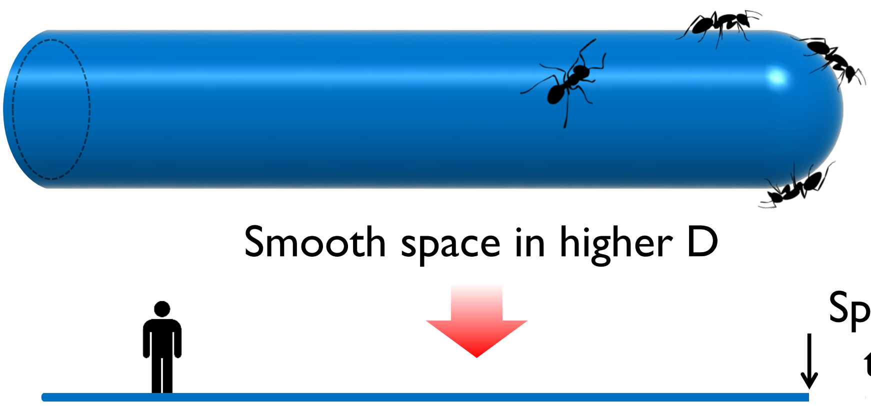

- Conversely, singular spacetimes in lower D are allowed in higher D!
- Room to store information about how a black hole was made, in higher dimensions.

Prediction 2: supersymmetry

Symmetry of snow flakes

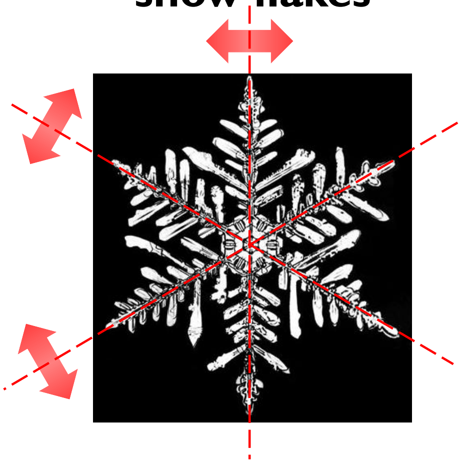

Supersymmetry

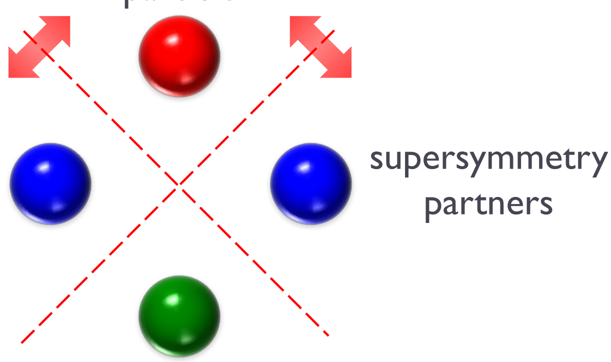

Particles have supersymmetry partners.

Gravity is extended to supergravity

Gravity $R_{\mu\nu} - \frac{1}{2} g_{\mu\nu} R = 8\pi G_{\rm N} T_{\mu\nu}$ Einstein equation

graviton

Supergravity "Super" Einstein equations

$$R_{\mu\nu} - \tfrac{1}{2} g_{\mu\nu} R = 8\pi G_{\rm N} T_{\mu\nu} + 2\big(g_{\mu\nu}\nabla^2\Phi - g_{\mu\nu}(\nabla\Phi)^2 - \nabla_\mu\nabla_\nu\Phi\big) + \cdots$$

$$R - \tfrac{1}{12} H_3^2 = 4(\nabla\Phi)^2 - 4\nabla^2\Phi$$

$$dH_3 = 0, \qquad \nabla_\alpha\big(e^{-2\Phi} H^{\alpha\mu\nu}\big) = \tfrac{1}{2} G_{\alpha\beta} G^{\alpha\beta\mu\nu} + \cdots$$

$$dG_2 = 0, \qquad \nabla_\alpha G^{\alpha\mu} = \tfrac{1}{3!} H_{\alpha\beta\gamma} G^{\mu\alpha\beta\gamma}$$

$$dG_4 = H_3 \wedge G_2, \qquad \nabla_\alpha G^{\alpha\mu\nu\rho} = \cdots$$

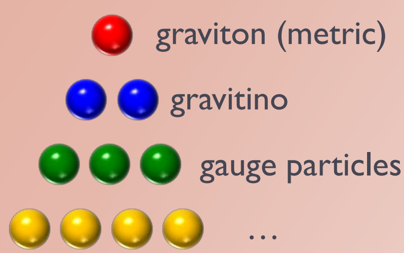

Richer physics.
More room to store information.

extra dimensions + supersymmetry

Higher-D supergravity

This theory allows for non-trivial solutions that have

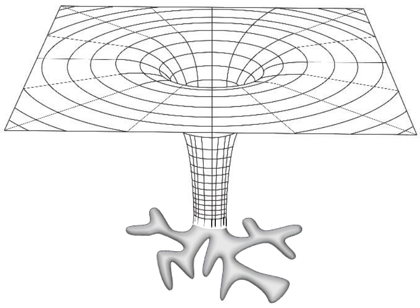

- No horizon
- No Singularity
- Same asymptotic charges as BH

"microstate geometries"

(No uniqueness theorem in higher D)

Microstate Geometry Program

How much portion of black hole entropy can be accounted for by smooth, horizonless solutions of classical gravity?

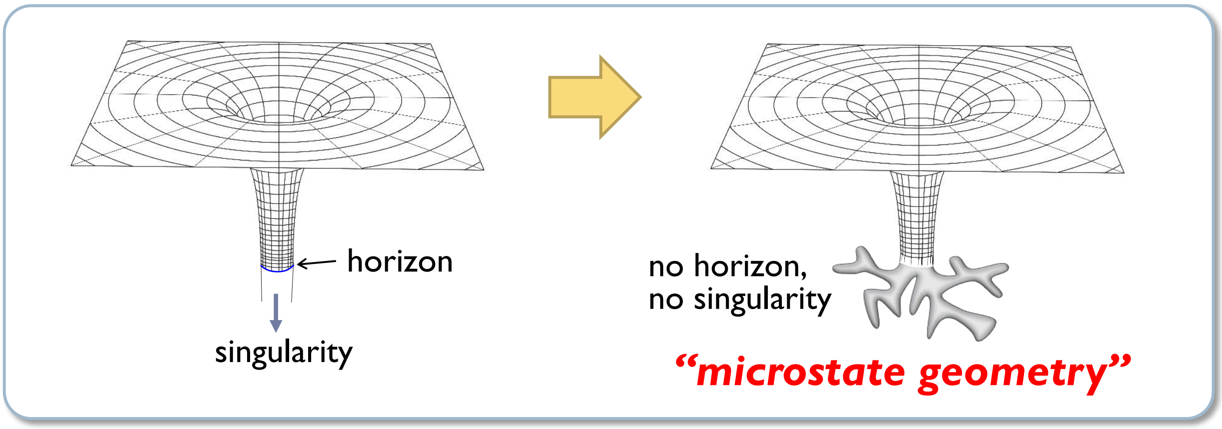

Let's explicitly construct them!

Caveats

- Mostly focused on microstates of supersymmetric BHs
  - Some non-supersymmetric examples
- No guarantee that all microstates are describable within supergravity
  - String theory contains more fields than supergravity
  - Cf. "Fuzzball" conjecture

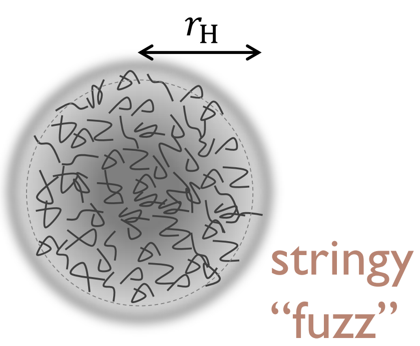

Examples of Microstate Geometries

Bubbling geometries

[Bena, Warner 2006]
[Berglund, Gimon, Levi 2006]

- Supersymmetric solution of 5D supergravity
- Compact S^1 is fibered over $\mathbb{R}^3$
- S^1 shrinks at points ("centers") on $\mathbb{R}^3$ → non-trivial S^2
- Microstate geometries for 5D (and 4D) BHs
- Fluxes support horizon-scale structure

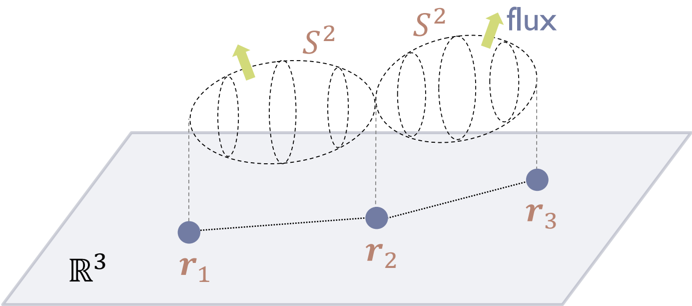

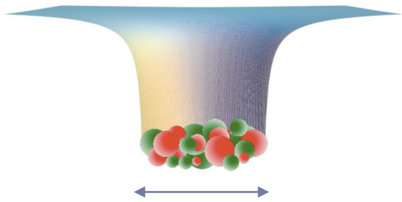

Scaling solution

[Denef] [Bena, Warner et al., 2006-07]

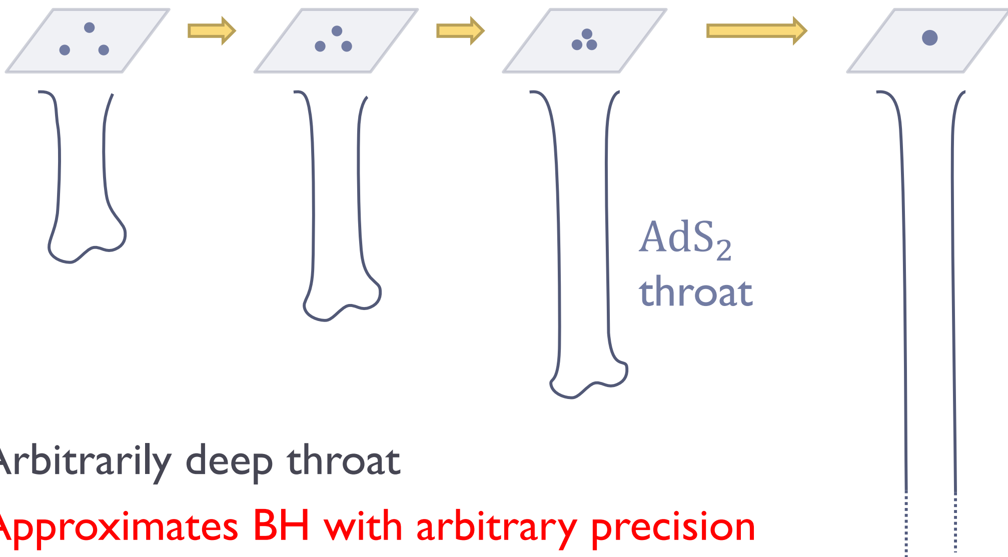

- Arbitrarily deep throat
- Approximates BH with arbitrary precision
- Quantum effects cut off the throat at finite depth

No solitons without topology (1)

- Komar mass/Smarr formula in 5D

[Gibbons-Warner '13]
[Haas '14]

$V^\mu = \frac{\partial}{\partial t}$: Killing

$$\Rightarrow \quad M \sim \int_{S^3} *_5\, dV \sim \int_{\Sigma^4} *_5\, (V^\mu R_{\mu\nu} dx^\nu)\,,$$

if there is no internal boundary.

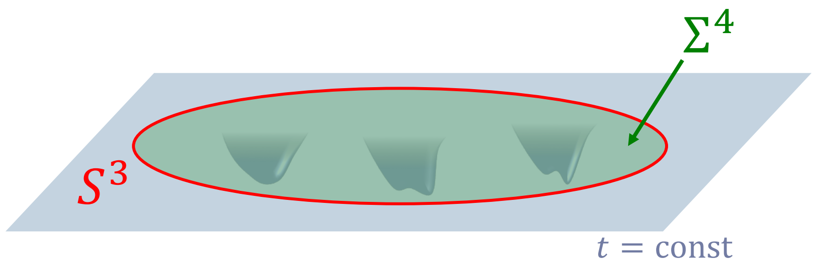

→

No solitons without topology (2)

EOMs / Bianchi:

$$dF^I = 0$$

$$dG_I = 0, \qquad G_I \equiv *_5\, Q_{IJ} F^J + C_{IJK} F^J \wedge A^K$$

$$R_{\mu\nu} = Q_{IJ} \partial_\mu X^I \partial_\nu X^J + Q_{IJ} F^I{}_{\mu\rho} F^J{}_\nu{}^\rho + Q^{IJ} G_{I\,\mu\rho\sigma} G_{J\,\nu}{}^{\rho\sigma} \qquad (*)$$

(ignoring numerical factors)

Assume time-independent config:

$$\mathcal{L}_V X^I = \mathcal{L}_V F^I = \mathcal{L}_V G_I = 0$$

$$\rightarrow d(\iota_V F^I) = d(\iota_V G_I) = 0 \qquad (\text{used } \mathcal{L}_V = d\iota_V + \iota_V d)$$

$$\rightarrow \iota_V F^I = \underbrace{f^I}_{\in H^1(\Sigma^4)} + (\text{exact}), \quad \iota_V G_I = \underbrace{g_I}_{\in H^2(\Sigma^4)} + (\text{exact}).$$

Now contract (*) with V^μ, and plug it into Smarr formula

No solitons without topology (3)

$$M \sim \int_{\Sigma^4} (f_I \wedge G^I + g^I \wedge F_I)$$

- M can be topologically supported by fluxes in the cohomology $H^*(\Sigma^4)$.
- No spatial topology → $M = 0$ → Spacetime is flat

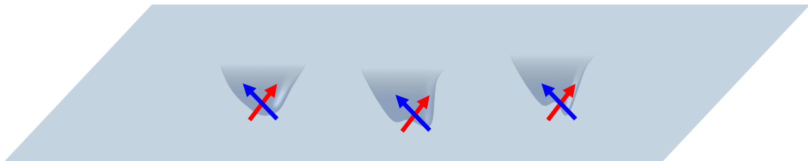

This is the mechanism for bubbling solutions

But they are not enough ☹

- Still too few to reproduce S_{area}

[de Boer, El-Showk, Messamah, Van de Bleeken 2008]
[Bena, Bobev, Ruef, Warner 2008]

- Parametrically more microstates needed!

$$S_{\text{geom}} \sim Q^{\frac{5}{4}} \quad \ll \quad S_{\text{area}} \sim Q^{\frac{3}{2}}$$

- More general solutions?

…Some hints from string theory. Go to 6D.

Superstratum

[Bena, Giusto, Martinet, Russo, MS, Turton, Warner 2015-17]

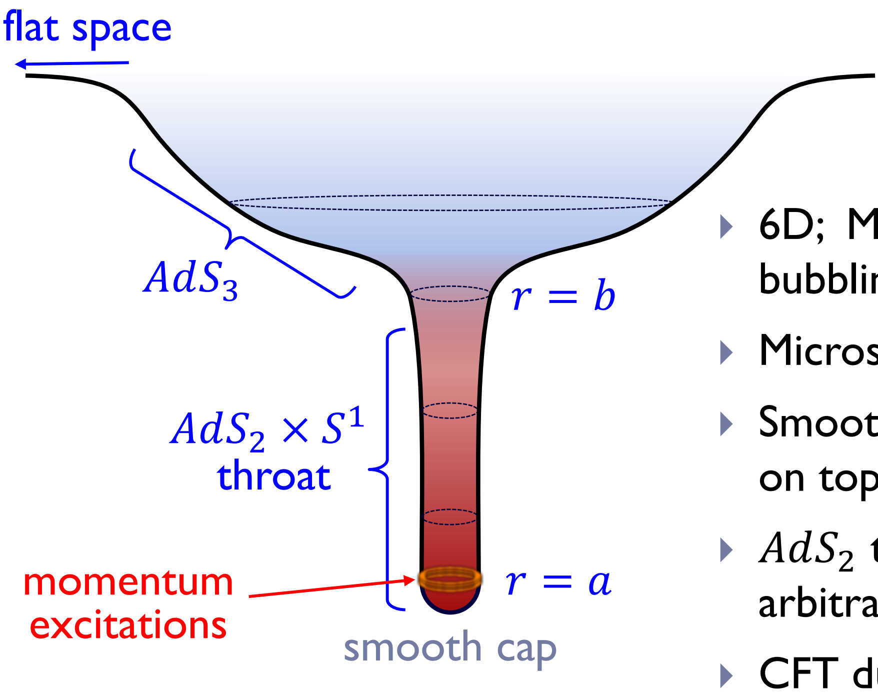

- 6D; More general than bubbling solution
- Microstates of 4,5,6D BH
- Smooth momentum waves on top of bubbling solution
- AdS_2 throat can be made arbitrarily deep
- CFT dual understood

Comments

Enough?

- No, still too few to reproduce BH entropy ☹
  – they are not typical states

But

- Basis for more general microstates
- Demonstrates that solution space of higher-D gravity is vast; need thorough exploration to understand grav physics
- They are completely new solutions anyway
  → interesting to study their properties

Physics of Microstate Geometries

Instability

[Eperon, Reall, Santos 2016]

Claim: Microstate geometries are non-linearly unstable, even though supersymmetric

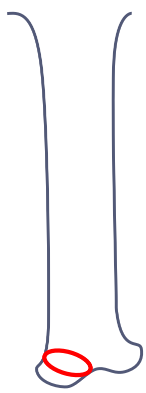

- Null geodesics on “evanescent ergosurface”
- Particles trapped near it will strongly backreact

⇩

- Adding small energy to microstate geometry makes system explore (vast) solution space
- Subsequent time evolution may or may not be describable within supergravity

Tidal force (1)

[Tyukov, Walker, Warner 2017]

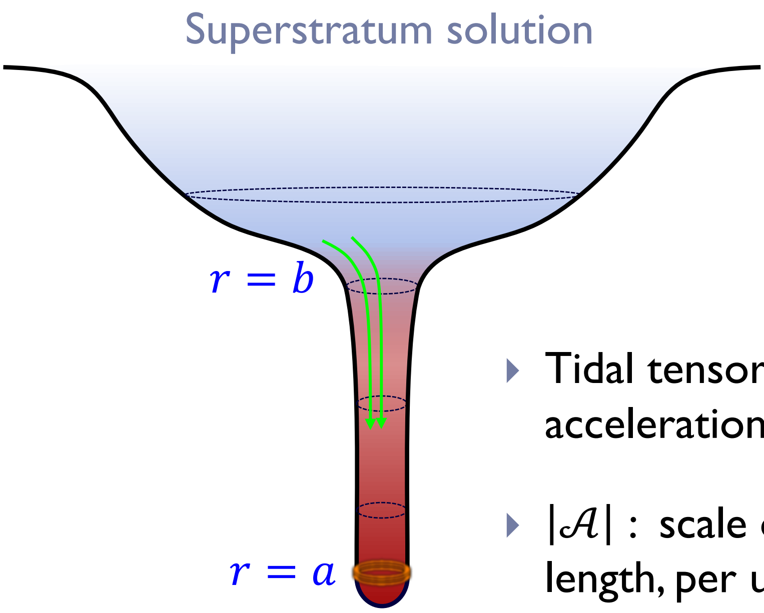

- Tidal tensor $\mathcal{A}^{\mu}{}_{\nu}$: relative acceleration of timelike geodesics
- $|\mathcal{A}|$: scale of tidal force per unit length, per unit mass

Tidal force (2)

[Tyukov, Walker, Warner 2017]

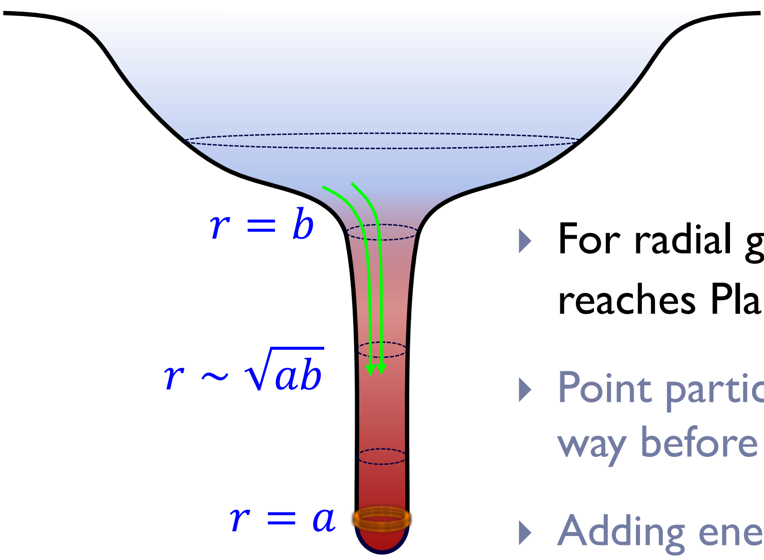

- For radial geodesics, tidal force reaches Planck scale at $r \sim \sqrt{ab}$
- Point particle gets ripped into strings way before reaching the bottom
- Adding energy will make system explore the space of microstates

Gravitational wave echoes (1)

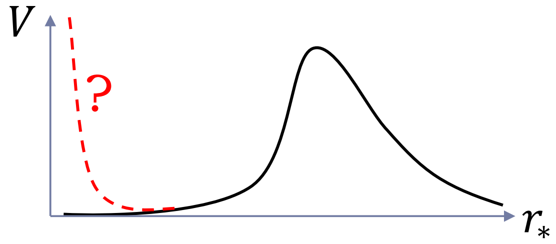

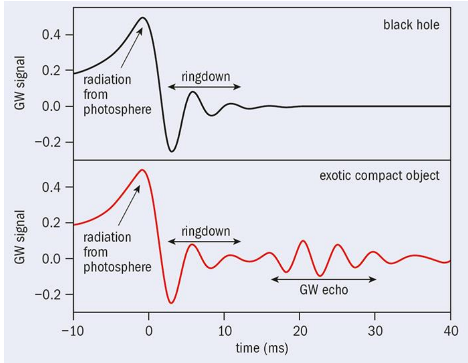

http://cerncourier.com/cws/article/cern/67457

- GW echoes allow us to probe the near-horizon structure of BHs

Gravitational wave echoes (2)

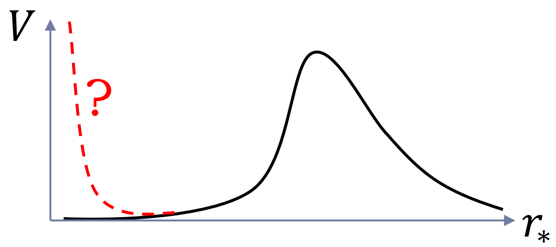

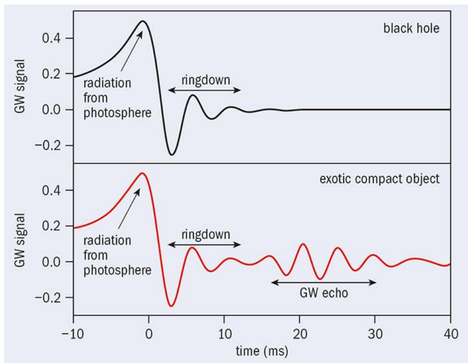

http://cerncourier.com/cws/article/cern/67457

- How do microstate geometries behave?
  - Infalling particle will become part of fuzzball
  - String theory is "soft" → no "hard" scattering back

⇨ Absorption; indistinguishable from GR BH?

Conclusions

Conclusions

- String theory leads us to consider higher-D gravity
  - BH microstate geometries
  - Vast solution space
  - Supports horizon-scale structure

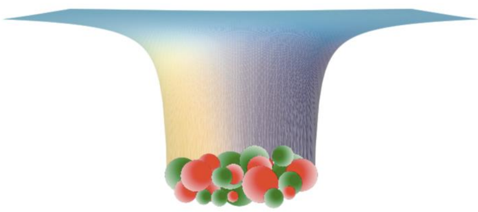

- Microstate geometry program
  - Many interesting solutions
  - Still too few to account for BH entropy
- A lot of interesting physics to explore! ☺

Friday Dec. 1st

Invited lecture 9:30–10:30

[Chair: Tsutomu Kobayashi]

Carlos Herdeiro (Aveiro Univ.),

"Kerr black holes with bosonic hair: theory and phenomenology" (50+10)

[JGRG27 (2017) 120101]

Kerr black holes with bosonic hair:

theory and phenomenology

C. Herdeiro
Departamento de Física da Universidade de Aveiro, Portugal

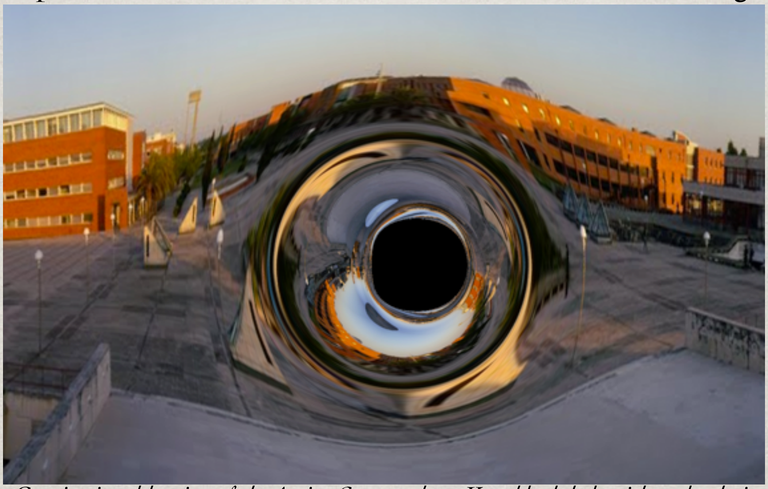

Gravitational lensing of the Aveiro Campus by a Kerr black hole with scalar hair

JGRG27 Meeting, Hiroshima, Japan
December 1st 2017

based on
PRL112(2014)221101
CQG32(2015)144001
PRL115(2015)211102
CQG33(2016)154001

with E. Radu (also P. Cunha)

Kerr black holes with bosonic hair:

theory and phenomenology

C. Herdeiro
Departamento de Física da Universidade de Aveiro, Portugal

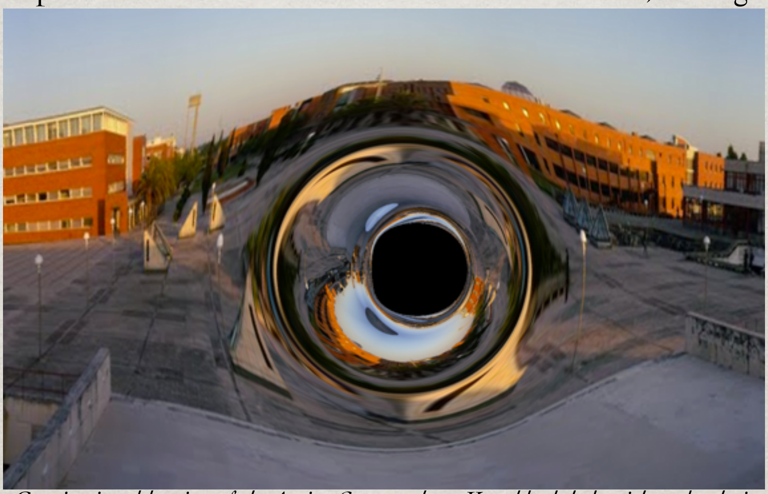

Gravitational lensing of the Aveiro Campus by a Kerr black hole with scalar hair

other references

IJMPD23(2014)1442014	PRD89(2014)12; 124018	PLB739(2014)1	PRD90(2014)10, 104024	PLB739(2014)302
IJMPD24(2015)1542014	PLB748(2015)30	PLB752(2016)291	PRD92(2015)084059	PRL116(2016)141101
PLB760 (2016) 279-287	PRD94 (2016)084045	JCAP1607(2016)049	PRD94(2016)044061	PLB761 (2016) 234
JCAP1610(2016)003	PRD94(2016)104023	CQG34(2017)165001	PRD95(2017)124025	JCAP1708(2017)014
PRD95(2017)104028	PRD95(2017)104035	PLB773(2017)129	1706.06597 (PRL in press)	JHEP1711(2017)037

with

C. Bambi, C. Benone, Y. Brihaye, R. Brito, A. Cardenas-Avendano, Z. Cao, V. Cardoso, L. C. Crispino, J. C. Degollado, J. F. M. Delgado, , V. Ferrari, J. A. Font, N. Franchini, E. Gourgoulhon, J. Grover, L. Gualtieri, J. Kunz, A. Maselli, P. J. Montero, Y. Ni, P. Pani, H. Rúnarsson, N. Sanchis-Gual, T. Shen, B. Subagyo, F. Vincent, A. Wittig, M. Zhou

Plan:

1) Motivation (Astrophysics, Cosmology, HEP)

2) Kerr black holes with scalar/Proca hair
  a) Basic theory
    i) Boson/Proca Stars
    ii) Scalar/Proca clouds around Kerr black holes
  b) Phenomenology
  c) Dynamics

3) Outlook

Motivation I
(astrophysics)

Over decades
strong observational evidence
has been gathered for
black holes.

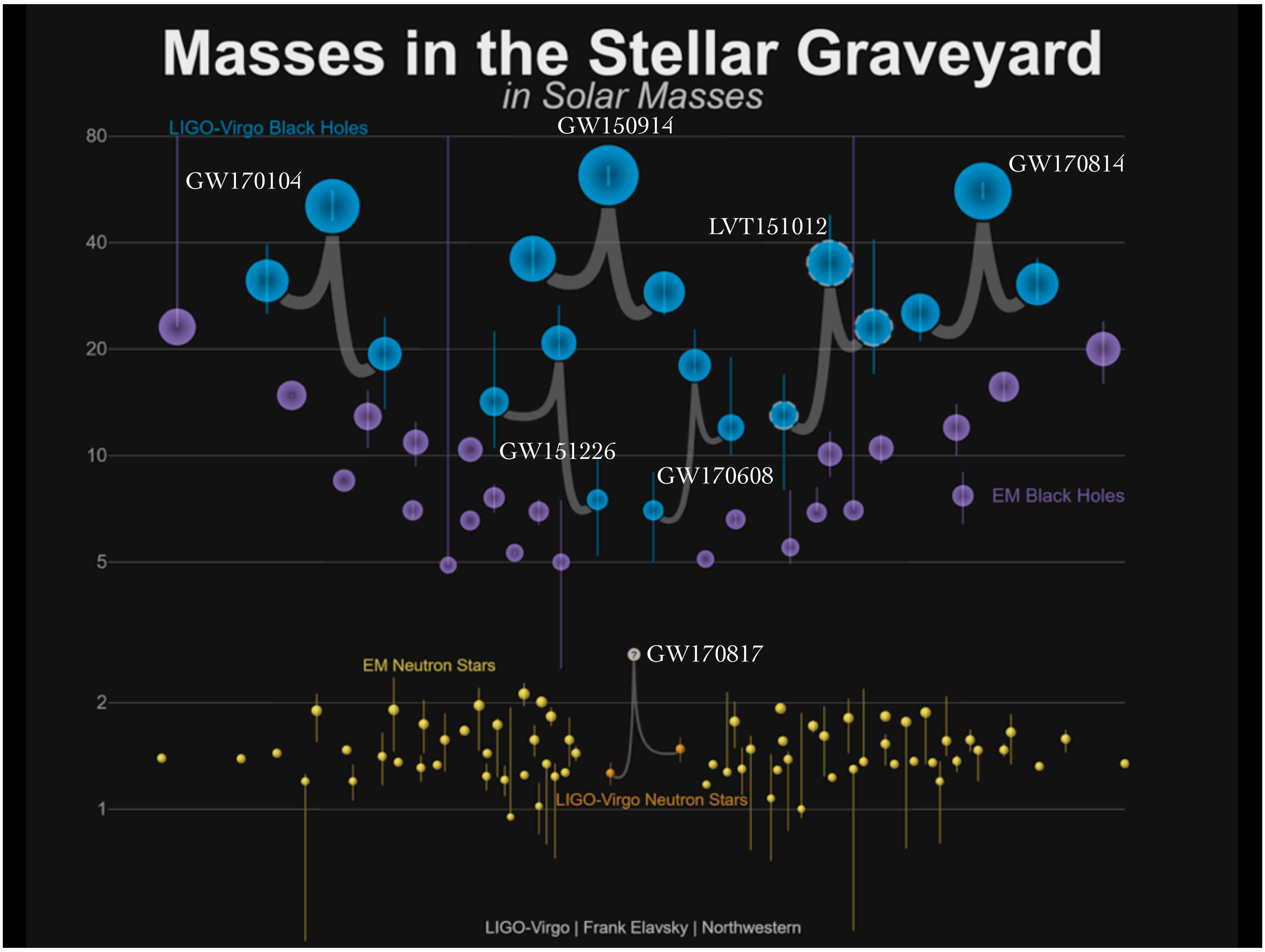

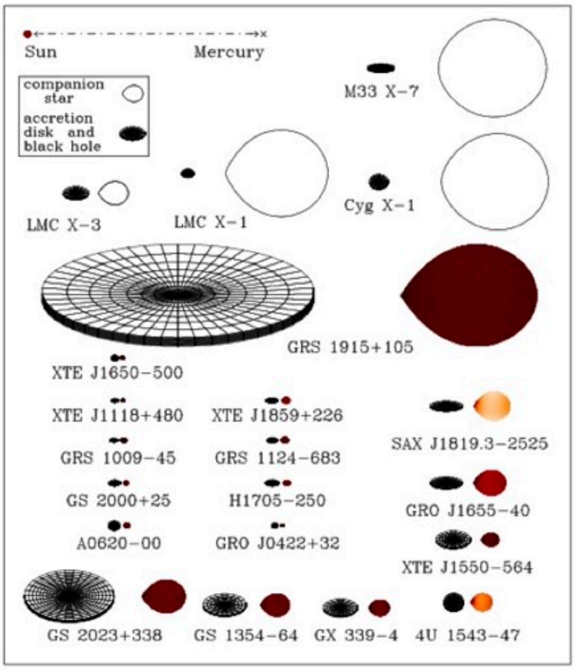

Figure 1.4 Sketches of 21 black hole binaries (see scale and legend in the upper-left corner). The tidally-distorted shapes of the companion stars are accurately rendered in Roche geometry. The black holes are located at the centers of the disks. A disk's tilt indicates the inclination angle i of the binary, where $i = 0$ corresponds to a system that is viewed face-on; e.g., $i = 21°$ for 4U 1543–47 (bottom right) and $i = 75°$ for M33 X–7 (top right). The size of a system is largely set by the orbital period, which ranges from 33.9 days for the giant system GRS 1915+105 to 0.2 days for tiny XTE J1118+480. Three systems hosting persistent X-ray sources — M33 X–7, LMC X–1 and Cyg X–1 — are located at the top. The other 18 systems are transient sources. (Figure courtesy of J. Orosz.)

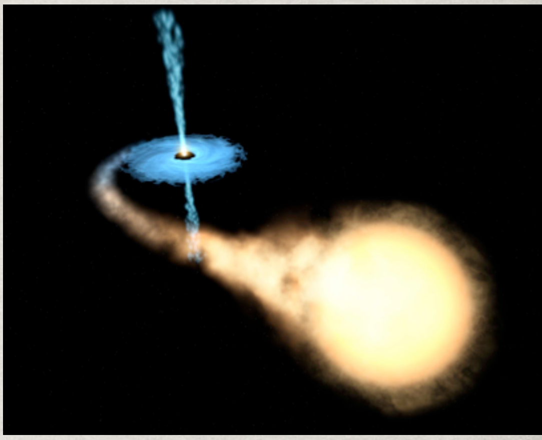

Artistic impression
of an accretion disk
around a stellar mass BH-star binary

Electromagnetic channel: X-ray band

Narayan and McClintock
1312.6698

Sketch of the electromagnetic spectrum of a black hole:

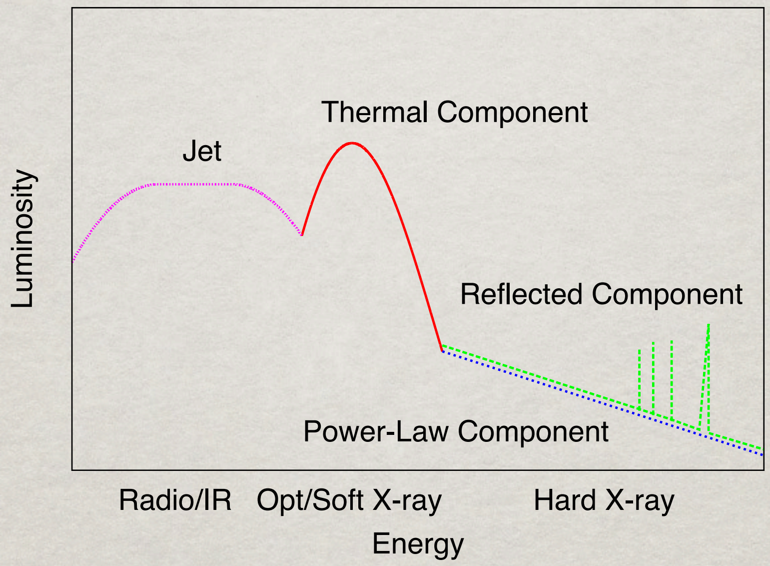

Two major techniques:
- continuum fitting method;
- reflexion spectrum (or iron line method);

From Bambi, Springer Book (2017)

The iron line method:

Propagation in strong gravity makes the **locally** Dirac delta-like line...

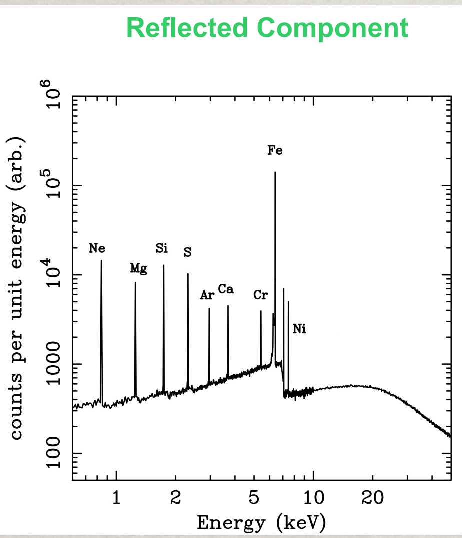

... broad and skew at the **observation** point...

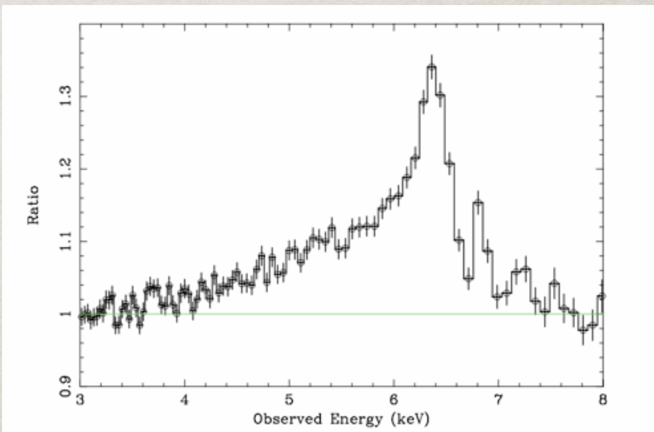

Guainazzi, Ap&SS320(2009)129

The next decades promise to
yield observational data of unprecedented
precision to test the true nature of these objects:
dawn of the precision black hole (astro)physics era

The next decades promise to
yield observational data of unprecedented
precision to test the true nature of these objects:
precision black hole (astro)physics era

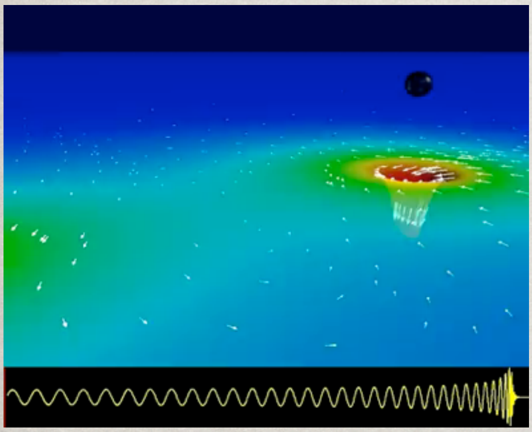

Many further detection are expected

Gravitational wave emission from a
black hole binary
Caltech-Cornell group;
Scheel et al. PRD79(2009)024003

EventHorizonTelescope

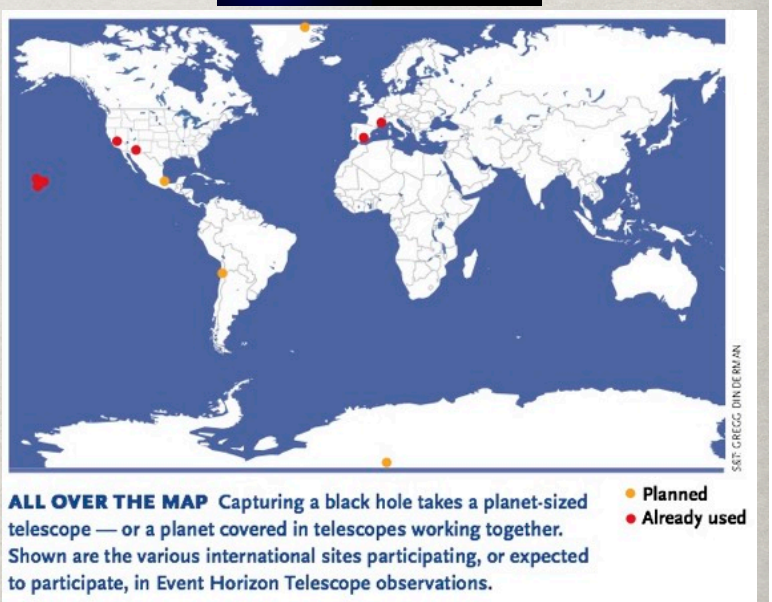

More accurate X-ray and interferometric data:

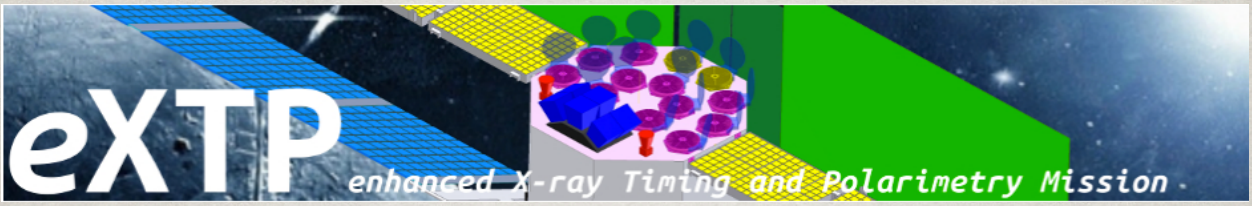

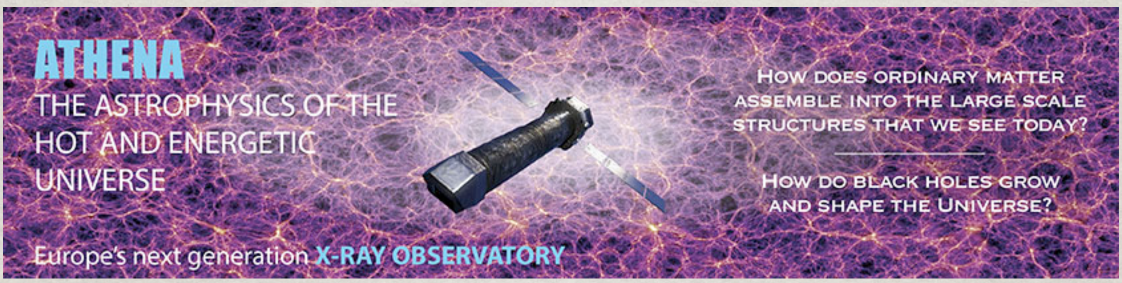

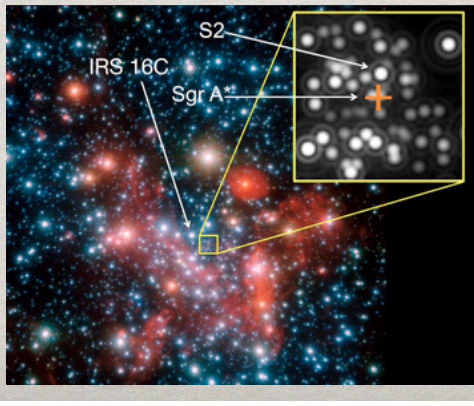

GRAVITY

It is therefore timely to study **alternatives**
to the General Relativity
Kerr black hole paradigm
and their phenomenology

I will present a novel class of such
alternative black hole models,
within GR

Reference example: Kerr black holes with scalar hair

Massive-complex-scalar-vacuum:

$$\mathcal{S} = \frac{1}{4\pi}\int d^4x\sqrt{-g}\left(\frac{R}{4} - \nabla_\alpha\Phi^*\nabla^\alpha\Phi - \mu^2|\Phi|^2\right)$$

$-V(|\Phi|) = -\lambda\Phi^4$

CH, Radu, Rúnarsson, PRD92(2015)084059

There are BH solutions:

- **within GR** (not alternative theories of gravity);
- with matter **obeying all energy conditions**;
- which can yield **distinct phenomenology**;

also
Kleihaus, Kunz and Yazadjiev
PLB744(2015)406

which are:

- asymptotically flat
- regular on and outside the horizon
- continuously connecting to the Kerr solution
- continuously connected to relativistic Bose-Einstein condensates (boson stars)
- with an independent scalar charge (primary hair)
- May form dynamically and be sufficiently long lived

Kerr Black Holes with scalar hair

CH and Radu, PRL112(2014)221101

Motivation II
(dark matter)

Ultra-light bosonic fields have been suggested as dark matter candidates ("fuzzy dark matter"); they gravitationally clump into boson stars // Bose-Einstein condensates

see e.g. recent discussion Hui, Ostriker, Tremaine, Witten, PRD95(2017)043541

Massive, complex, scalar field, minimally coupled to gravity (no self-interactions)

$$M_{\max} \simeq 1.315\frac{M_{Pl}^2}{\mu} = 1.315\times 10^{-19}M_\odot\left(\frac{\text{GeV}}{\mu}\right)$$

Introducing a quartic self-coupling

$$M_{\max} \overset{\lambda\gg1}{\simeq} 0.208\sqrt{\lambda}\frac{M_{Pl}^3}{\mu^2} = 0.208\sqrt{\lambda}M_\odot\left(\frac{\text{GeV}}{\mu}\right)^2$$

First observed by Colpi, Shapiro, Wasserman PRL57(1986)2485,
see e.g. for a discussion CH, Radu, Rúnarsson PRD92(2015)084059

Motivation III
(high energy physics)

In some HEP models it is natural to have bosonic particles with very low mass
(QCD axion, Axiverse Arvanitaki, Dimopoulos, Dubovsky, Kaloper and March-Russell PRD81(2010)123530)

These could have astrophysical impact
and **convert black holes into (new) particle detectors.**
Arvanitaki and Dubovsky, PRD83(2011)044026

Motivation III
(high energy physics)

In some HEP models it is natural to have bosonic particles with very low mass
(QCD axion, Axiverse Arvanitaki, Dimopoulos, Dubovsky, Kaloper and March-Russell PRD81(2010)123530)

These could have astrophysical impact
and **convert black holes into (new) particle detectors.**
Arvanitaki and Dubovsky, PRD83(2011)044026

The existence of a scalar field that triggers the superradiant instability of a "bald" BH can grow hair around the BH that saturates due to non-linear phenomena and forms a "hairy" BH

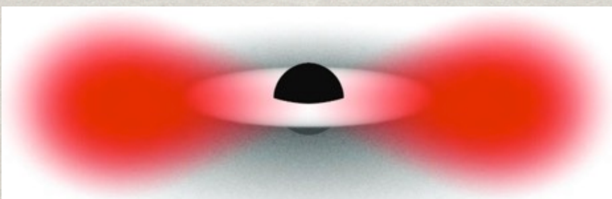

Brito, Cardoso, Pani Lect.Notes.Phys.906(2015)1

1) Kerr black holes with scalar/Proca hair

D=4, asymptotically flat, regular (on and outside the event horizon)

black hole (BH) solutions of Einstein's gravity

Vacuum:

$$\mathcal{S} = \frac{1}{16\pi}\int d^4x\sqrt{-g}R$$

Kerr Kerr 1963

Uniqueness Israel 1967; Carter 1970; Hawking 1972

No (independent-multipolar) hair

Electro-vacuum:

$$\mathcal{S} = \frac{1}{4\pi}\int d^4x\sqrt{-g}\left(\frac{R}{4}-\frac{1}{4}F_{\mu\nu}F^{\mu\nu}\right)$$

Kerr-Newman Newman et al. 1965

Uniqueness Israel 1968; Robinson 1975, 1977

No (independent-multipolar) hair

D=4, asymptotically flat, regular (on and outside the event horizon) **black hole (BH) solutions of Einstein's gravity**

Vacuum:

$$\mathcal{S} = \frac{1}{16\pi}\int d^4x\sqrt{-g}R$$

Kerr Kerr 1963

Uniqueness Israel 1967; Carter 1970; Hawking 1972

No (independent-multipolar) hair

Electro-vacuum:

$$\mathcal{S} = \frac{1}{4\pi}\int d^4x\sqrt{-g}\left(\frac{R}{4}-\frac{1}{4}F_{\mu\nu}F^{\mu\nu}\right)$$

Kerr-Newman Newman et al. 1965

Uniqueness Israel 1968; Robinson 1975, 1977

No (independent-multipolar) hair

Scalar-vacuum:

$$\mathcal{S} = \frac{1}{4\pi}\int d^4x\sqrt{-g}\left(\frac{R}{4}-\frac{1}{2}\nabla_\mu\Phi\nabla^\mu\Phi\right)$$

No BHs

No (scalar) hair Chase 1970

Many no-scalar-hair theorems:

(only scalars, D=4, asymptotically flat)

Theory Lagrangian density $\mathcal{L}$	No-hair theorem	Known scalar hairy BHs with regular geometry on and outside $\mathcal{H}$ (primary or secondary hair; regularity)
Scalar-vacuum $\frac{1}{4}R-\frac{1}{2}\nabla_\mu\Phi\nabla^\mu\Phi$	Chase[22]	
Massive-scalar-vacuum $\frac{1}{4}R-\frac{1}{2}\nabla_\mu\Phi\nabla^\mu\Phi-\frac{1}{2}\mu^2\Phi^2$	Bekenstein[11]	
Massive-complex-scalar-vacuum $\frac{1}{4}R-\nabla_\mu\Phi^*\nabla^\mu\Phi-\mu^2\Phi^*\Phi$	Pena– –Sudarsky[61]	Herdeiro–Radu[136,137] (primary, regular); generalizations:[159]
Conformal-scalar-vacuum $\frac{1}{4}R-\frac{1}{2}\nabla_\mu\Phi\nabla^\mu\Phi-\frac{1}{12}R\Phi^2$	Xanthopoulos– –Zannias[32] Zannias[33]	Bocharova–Bronnikov–Melnikov– –Bekenstein (BBMB)[16–18] (secondary, diverges at $\mathcal{H}$); generalizations:[87]
V-scalar-vacuum $\frac{1}{4}R-\frac{1}{2}\nabla_\mu\Phi\nabla^\mu\Phi-V(\Phi)$	Heusler[46,47,50] Bekenstein[26] Sudarsky[51]	Many, with non-positive definite potentials:[71–75,78–80] (typically secondary, regular)
P-scalar-vacuum $\frac{1}{4}R+P(\Phi,X)$	Graham– –Jha[62]	
Einstein-Skyrme $\frac{1}{4}R-\frac{1}{2}\nabla_\mu\Phi^a\nabla^\mu\Phi^a$ $-\kappa\lvert\nabla_{[\mu}\Phi^a\nabla_{\nu]}\Phi^b\rvert^2$		Droz–Heusler–Straumann[126] (primary but topological; regular); generalizations:[129,131]
Scalar-tensor theories $\varphi\hat{R}-\frac{\omega(\varphi)}{\varphi}\hat{\nabla}_\mu\varphi\hat{\nabla}^\mu\varphi-U(\varphi)$	Hawking[27] Saa[34,35] Sotiriou– –Faraoni[31]	
Horndeski/Galileon theories Full $\mathcal{L}$ in eq. (41)	Hui– –Nicolis[45]	Sotiriou-Zhou[43] (secondary; regular) Babichev–Charmousis[88,90] (secondary[88] or primary,[90] diverges at $\mathcal{H}^+$ or $\mathcal{H}^-$); generalizations:[91–93]

CH, Radu,
IJMPD 24(2015)1542014

Scalar case:

hairy BHs circumvent well known no-scalar-hair theorems

CH, Radu, IJMPD24(2015)1542014

due to:

1) harmonic time-dependence with a critical frequency

2) Rotation of the background

Two ingredients:

- Superradiant bound states of a massive scalar around Kerr

- Existence of a solitonic limit: (scalar) boson stars

Scalar -- Ingredient 1: Superradiance

$$\mathcal{S} = \frac{1}{4\pi}\int d^4x\sqrt{-g}\left(\frac{R}{4} - \nabla_\alpha\Phi^*\nabla^\alpha\Phi - \mu^2|\Phi|^2\right)$$

One solution is
Kerr solution + a vanishing scalar field

Consider linear scalar perturbations:
to first order it amounts to considering a test scalar field on Kerr.

Linear analysis: Klein-Gordon equation in Kerr

$$\Box\Phi = \mu^2\Phi \qquad\qquad \Phi = e^{-iwt}e^{im\varphi}S_{\ell m}(\theta)R_{\ell m}(r)$$

Radial Teukolsky equation: Teukolsky (1972); Brill et al. (1972)

$$\frac{d}{dr}\left(\Delta\frac{dR_{\ell m}}{dr}\right) = \left(a^2w^2 - 2maw + \mu^2r^2 + A_{\ell m} - \frac{K^2}{\Delta}\right)R_{\ell m}$$

$$\Delta \equiv r^2 - 2Mr + a^2$$

$$K \equiv (r^2 + a^2)w - am$$

Generically one obtains *quasi*-bound states:

$$\omega = \omega_R + i\omega_I$$

critical frequency

$$w_c = m\Omega_H$$

$$\omega = \omega_R + i\omega_I$$

critical frequency

$$w_c = m\Omega_H$$

$w_I < 0$ if $w_R > w_c$ decay

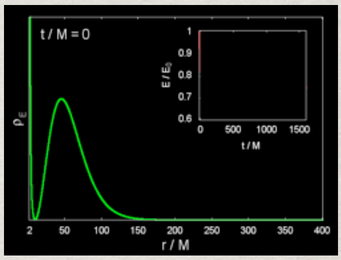

Degollado et. al., PRL 109 (2012) 081102

$w_I = 0$ if $w = w_c$ true bound states: *clouds*

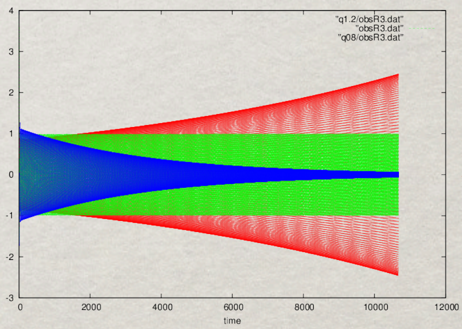

Degollado, CH, unpublished

$w_I > 0$ if $w_R < w_c$ grow

Press and Teukolsky Nature238(1972)211

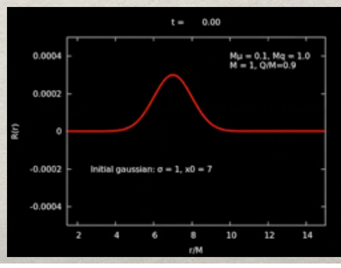

Degollado and CH PRD89(2014)063005

Klein-Gordon (linear) stationary clouds around Kerr:

Damour, Deruelle and Ruffini (1976); Zouros and Eardley (1979); Detweiler (1980); Hod 2012; (...); Yakov Shilapentokh-Rothman (2014)

Clouds for Kerr: discrete set labelled by (n,l,m) subject to one quantization condition which yields BH mass,spin.

Hod PRD86(2012)104026

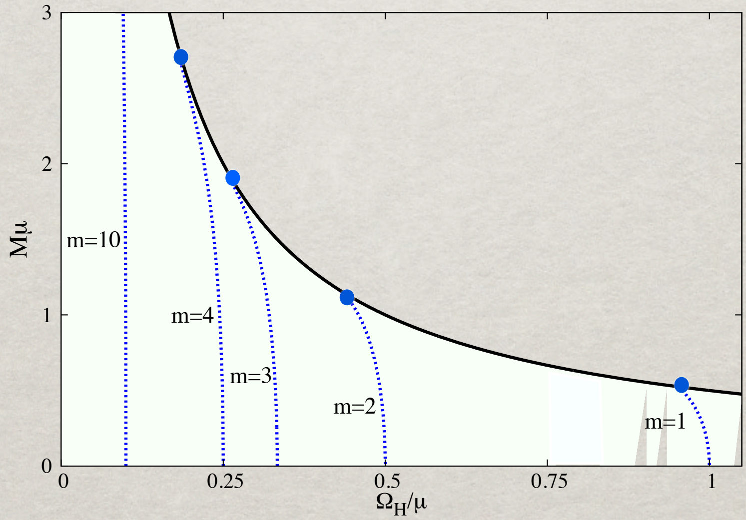

Clouds radial profile

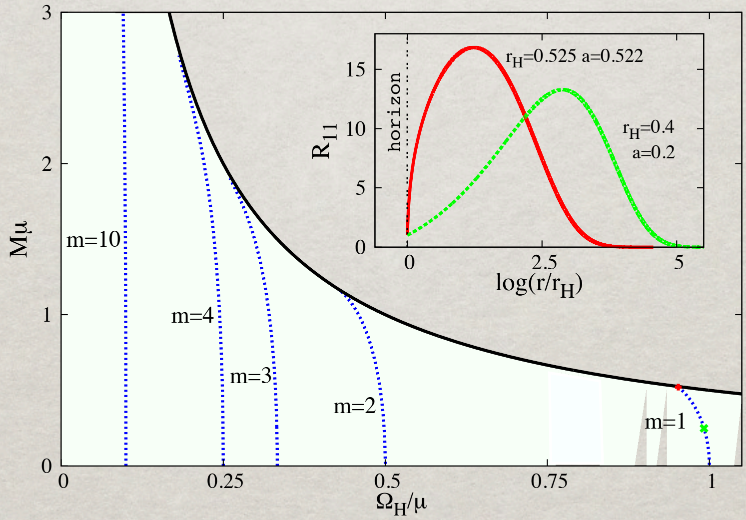

Variation of scalar clouds with quantum numbers: Benone, Crispino, CH and Radu, PRD90(2014)104024

Stability: stationary clouds

BH

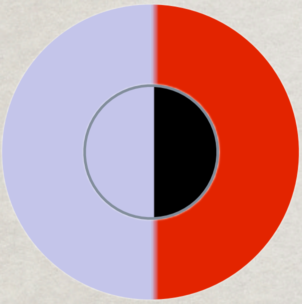

scalar mode

$\frac{w}{m} = \Omega_H$ is a rotation synchronization condition

Stability: stationary clouds

BH

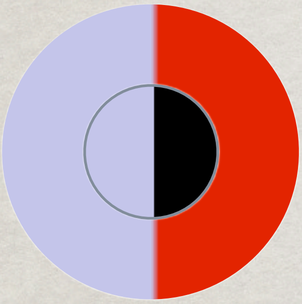

scalar mode

$\frac{w}{m} < \Omega_H$

Superradiant regime
black hole decreases angular velocity

Stability: stationary clouds

BH

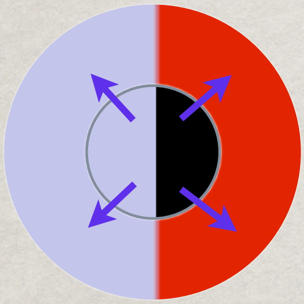

scalar mode

Transfer of rotational energy from BH to scalar cloud

$\frac{w}{m} < \Omega_H$ Superradiant regime
black hole decreases angular velocity

Stability: stationary clouds

BH

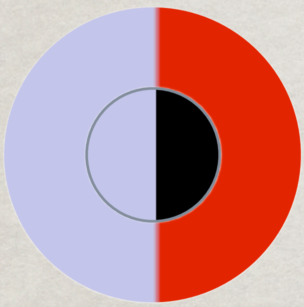

scalar mode

$\frac{w}{m} > \Omega_H$ decaying regime
black hole increases angular velocity

Stability: stationary clouds

BH

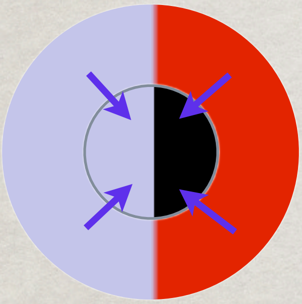

scalar mode

Transfer of rotational
energy from
scalar cloud to BH

$\frac{w}{m} < \Omega_H$

Superradiant regime
black hole decreases angular velocity

Stability: stationary clouds

BH

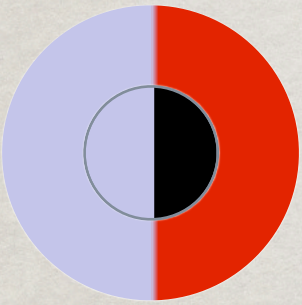

scalar mode

Suggests:
clouds as dynamical attractors
Synchronization locking (cf. tidal locking for earth-moon)

Benone, Crispino, CH and Radu, PRD90(2014)104024

Scalar -- Ingredient 2: Boson stars

Kaup, PR172(1968)1331; Ruffini and Bonazzola, PR187(1969)1767;
Reviews: Schunck and Mielke, CQG20(2003)R301
Liebling and Palenzuela, LivingRev.Rel.15(2012)6

$$\mathcal{S} = \frac{1}{4\pi}\int d^4x\sqrt{-g}\left(\frac{R}{4} - \nabla_\alpha \Phi^* \nabla^\alpha \Phi - \mu^2|\Phi|^2\right)$$

Rotating boson stars:

Yoshida, Eriguchi, PRD56(1997)762;
Schunck, Mielke, PLA 249(1998)389

$$ds^2 = -e^{2F_0(r,\theta)}dt^2 + e^{2F_1(r,\theta)}\left(dr^2 + r^2 d\theta^2\right) + e^{2F_2(r,\theta)}r^2\sin^2\theta\,(d\varphi - W(r,\theta)dt)^2$$

$$\Phi = \phi(r,\theta)e^{i(m\varphi - wt)}$$

Three input parameters: (w,m,n)

Solutions preserved by a single helicoidal Killing vector field:

$$\frac{\partial}{\partial t} + \frac{w}{m}\frac{\partial}{\partial\varphi}$$

Surfaces of constant scalar energy density

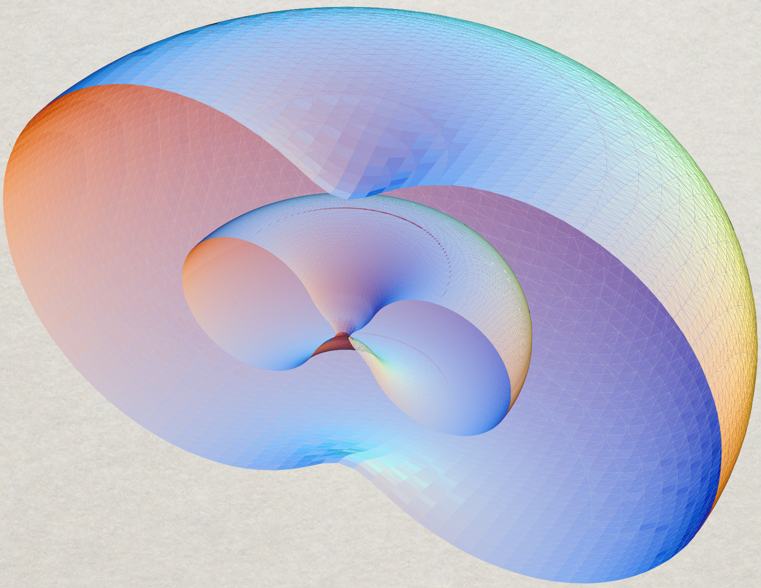

Boson stars phase space (nodeless):

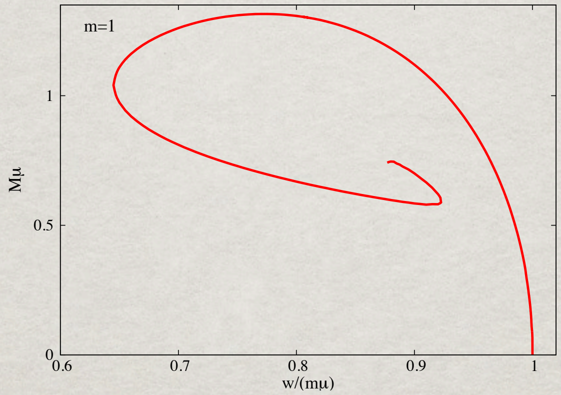

Conserved Noether charge: $$Q = \int_{\Sigma} dr d\theta d\varphi j^t \sqrt{-g}$$

For rotating boson stars: $$J = mQ$$

Convenient parameter: $$q \equiv \frac{mQ}{J}$$

Mixing the ingredients:

Using (scalar or vector) boson stars technology to compute
black holes surrounded by "heavy (scalar or vector) stationary clouds"

Einstein Klein-Gordon: non-linear setup

Ansatz:

$$ds^2 = -e^{2F_0(r,\theta)} N dt^2 + e^{2F_1(r,\theta)} \left(\frac{dr^2}{N} + r^2 d\theta^2\right) + e^{2F_2(r,\theta)} r^2 \sin^2\theta \, (d\varphi - W(r,\theta)dt)^2 \qquad N = 1 - \frac{r_H}{r}$$

$$\Phi = \phi(r,\theta) e^{i(m\varphi - wt)}$$

Asymptotically:

$$g_{tt} = -1 + \frac{2M}{r} + \ldots, \quad g_{\varphi t} = -\frac{2J}{r}\sin^2\theta + \ldots$$

$$\phi = f(\theta)\frac{e^{-\sqrt{\mu^2 - w^2}\, r}}{r} + \ldots$$

take: $w < \mu$

Near the horizon:

$$x \equiv \sqrt{r^2 - r_H^2}$$

$$F_i = F_i^{(0)}(\theta) + x^2 F_i^{(2)}(\theta) + \mathcal{O}(x^4)$$

$$W = \Omega_H + \mathcal{O}(x^2)$$

$$\phi = \phi_0(\theta) + \mathcal{O}(x^2)$$

take: $\Omega_H = \dfrac{w}{m}$

Four input parameters: m, w, r_H, n

Kerr black holes with scalar hair

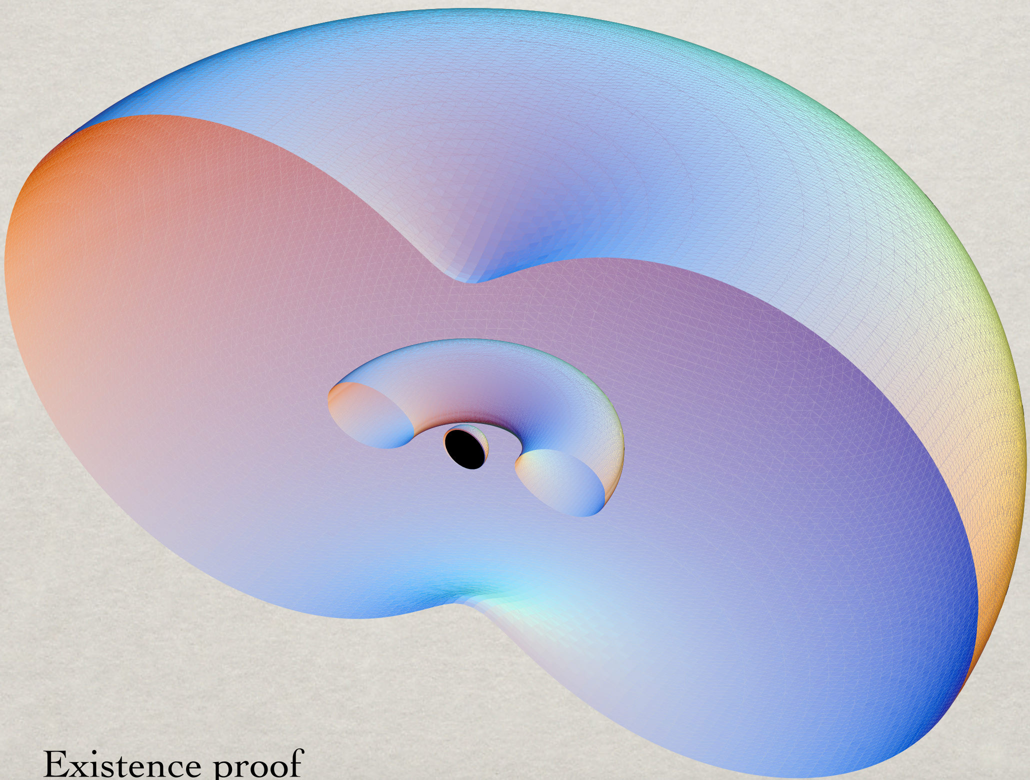

Existence proof

Chodosh and Shlapentokh-Rothman, CMP356(2017)1155

Hairy black holes phase space

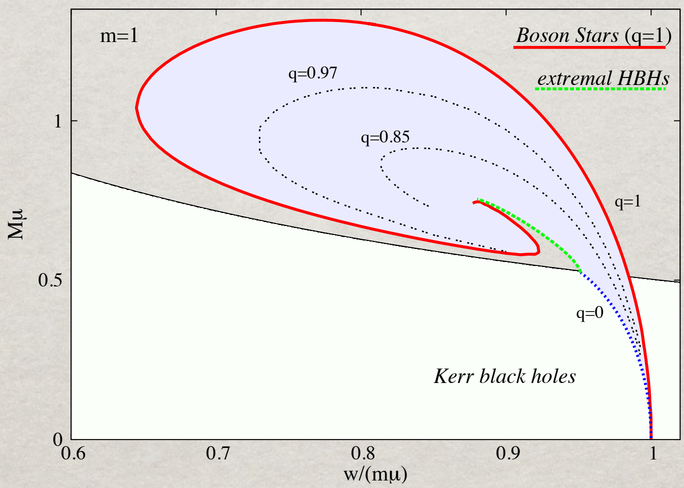

$$q \equiv \frac{mQ}{J}$$

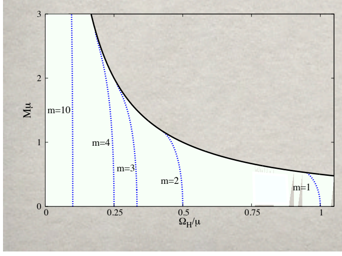

Family of solutions:
3 continuous parameters (M,J,q)
2 discrete parameters (m,n)

Same two ingredients exist for a *vector* field:

- Superradiant bound states of a massive *vector* around Kerr

(...)
Pani, Cardoso, Gualtieri, Berti, Ishibashi, PRL109(2012)131102; PRD86(2012)104017

- Existence of a solitonic limit: (*vector*) boson stars, a.k.a. *Proca stars*

Brito, Cardoso, CH, Radu, PLB752(2016)291

Can circumvent similar no-Proca-hair theorems

Bekenstein, PRD5(1972)1239; PRD5(1972)2403
CH, Radu, Rúnarsson, CQG33(2016)154001

Domain of existence:

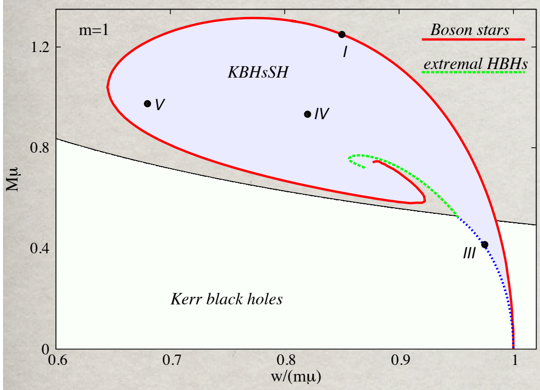

Scalar	w/μ	r_H/μ	μM_{ADM}	$\mu^2 J_{ADM}$	μM_H	$\mu^2 J_H$	$\mu M^{(\Psi)}$	$\mu^2 J^{(\Psi)}$
I - Scalar boson star	0.85	0	1.25	1.30	0	0	1.25	1.30
II - Vacuum Kerr	1.1112	0.0663	0.415	0.172	0.415	0.172	0	0
III - KBHSH	0.975	0.2	0.415	0.172	0.393	0.150	0.022	0.022
IV - KBHSH	0.82	0.1	0.933	0.739	0.234	0.114	0.699	0.625
V - KBHSH	0.68	0.04	0.975	0.850	0.018	0.002	0.957	0.848

Data avaliable online at:
http://gravitation.web.ua.pt

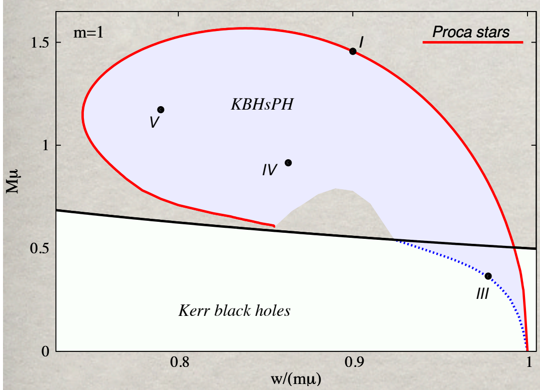

Vector	w/μ	r_H/μ	μM_{ADM}	$\mu^2 J_{ADM}$	μM_H	$\mu^2 J_H$	$\mu M^{(\mathcal{P})}$	$\mu^2 J^{(\mathcal{P})}$
I - Proca star	0.9	0	1.456	1.45	0	0	1.456	1.45
II - Vacuum Kerr	1.0432	0.1945	0.365	0.128	0.365	0.128	0	0
III - KBHPH	0.9775	0.2475	0.365	0.128	0.354	0.117	0.011	0.011
IV - KBHPH	0.863	0.09	0.915	0.732	0.164	0.070	0.751	0.662
V - KBHPH	0.79	0.06	1.173	1.079	0.035	0.006	1.138	1.073

2) Kerr black holes with scalar hair
iii) Phenomenology

There is a region of non uniqueness

(different solutions for same M,J); but degeneracy raised with q

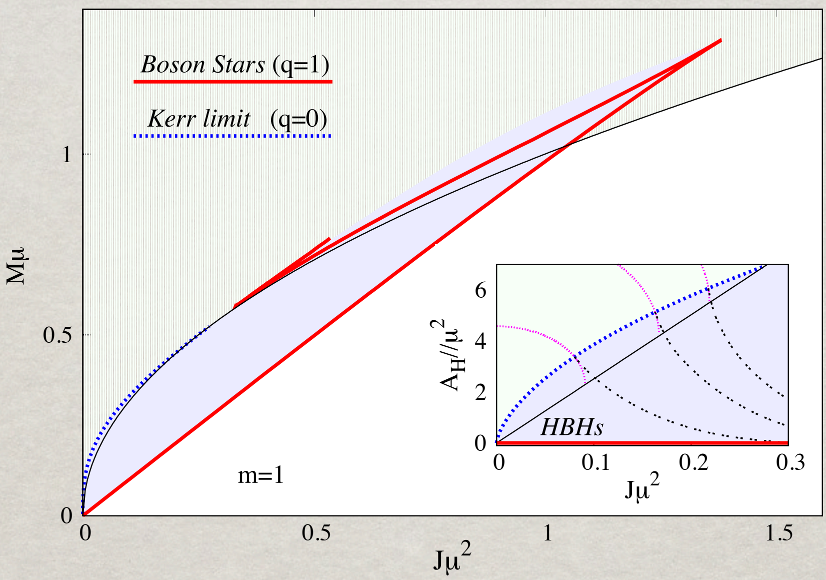

In this region, hairy black holes are entropically favoured

Can we distinguish by a local measurement degenerate configurations?

EventHorizonTelescope

Black hole shadows

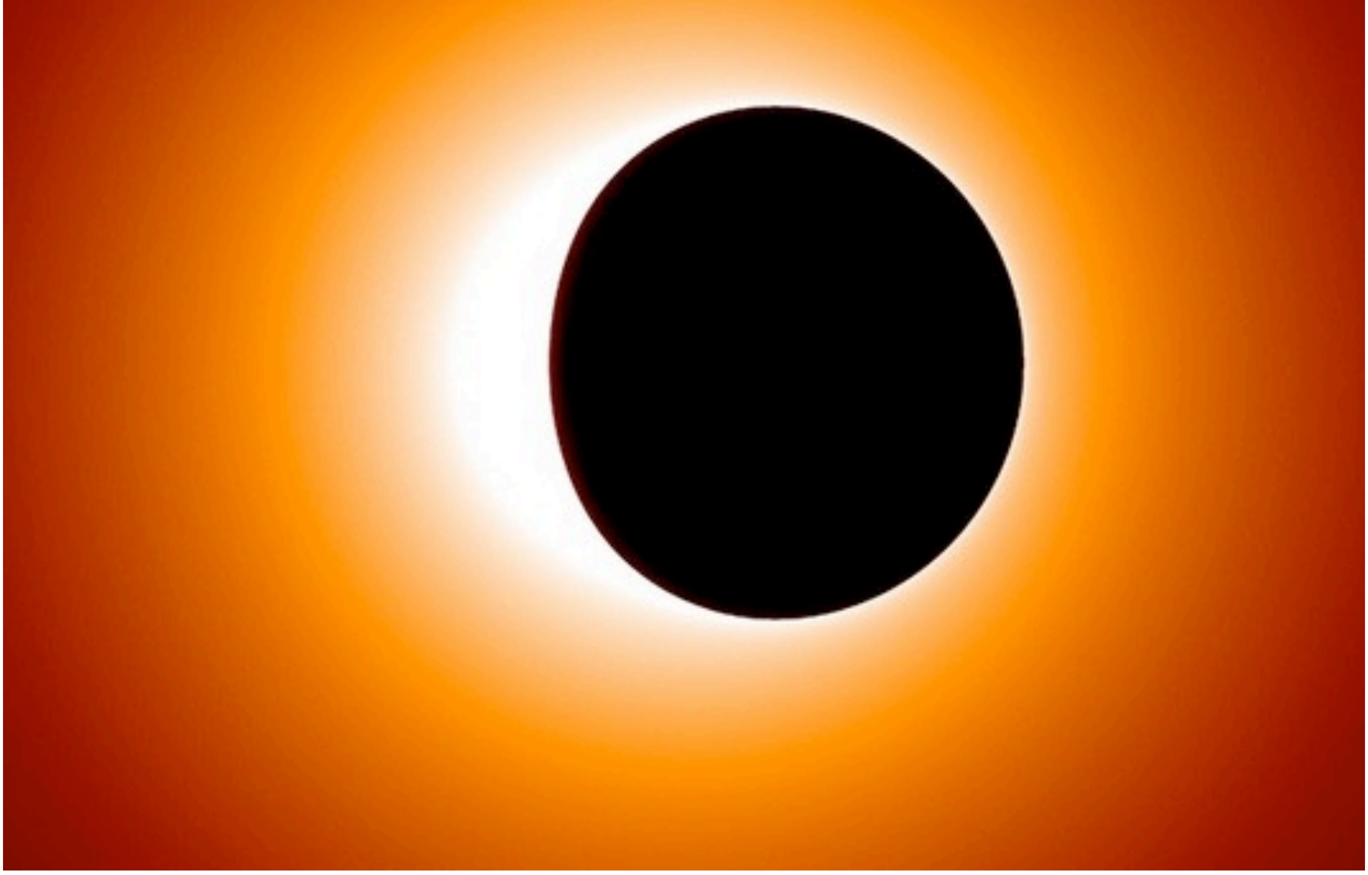

Shadow of a Kerr black hole:

(equatorial plane observation)

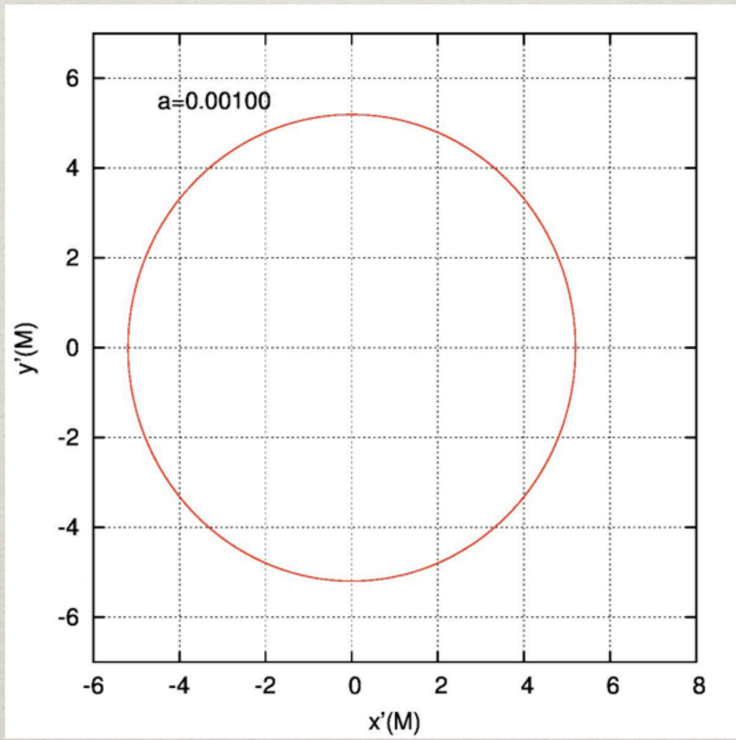

Cunha, M.Sc. Thesis

Technique: backwards ray-tracing

Cunha, M.Sc. Thesis

We have performed ray tracing to compute lensing and shadows.

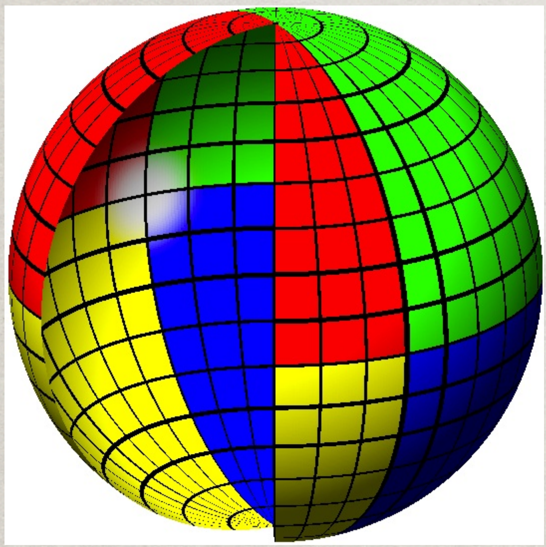

The full celestial sphere

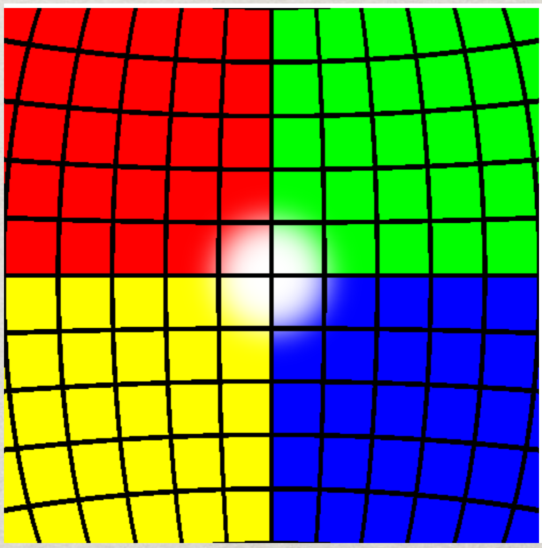

The “camera” opening angle

Following A. Bohn et al. CQG32(2015)065002

A Kerr-like hairy black hole

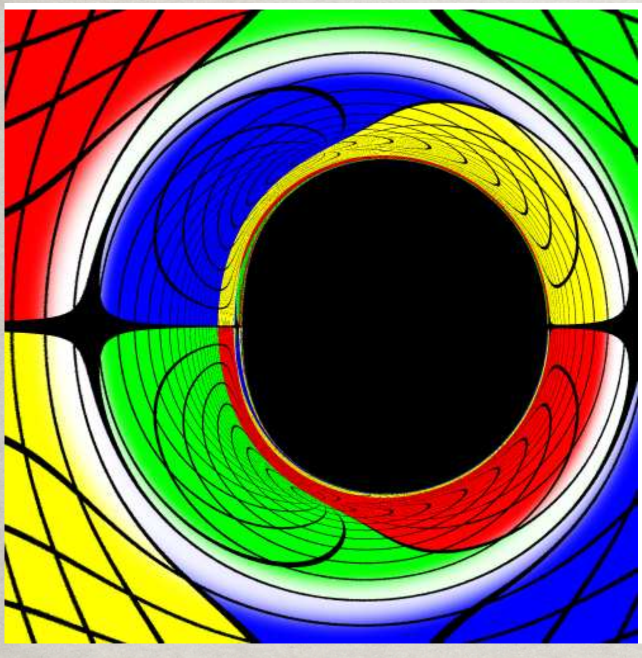

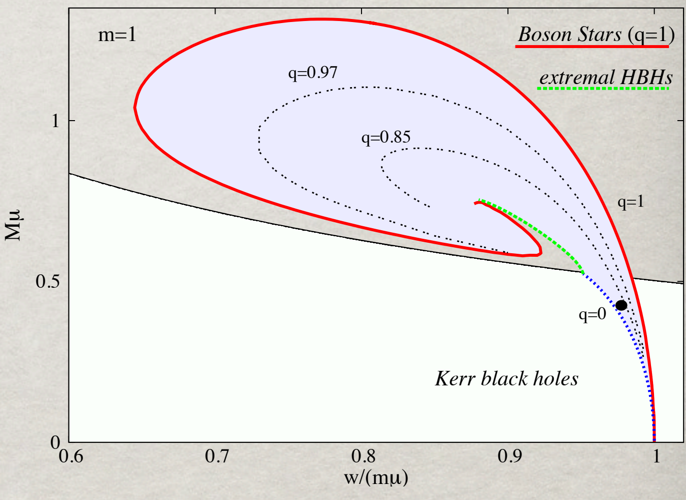

5% of mass;
13% of angular momentum
is stored in the scalar field

A Kerr-like Kerr BH with scalar hair

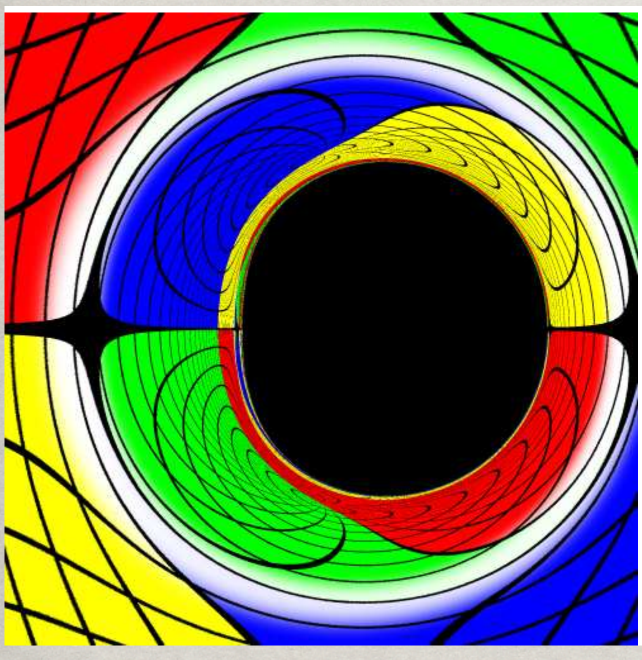

Kerr BH with scalar hair
M=0.393; J=0.15 (horizon)
M=0.022; J=0.022 (scalar field)

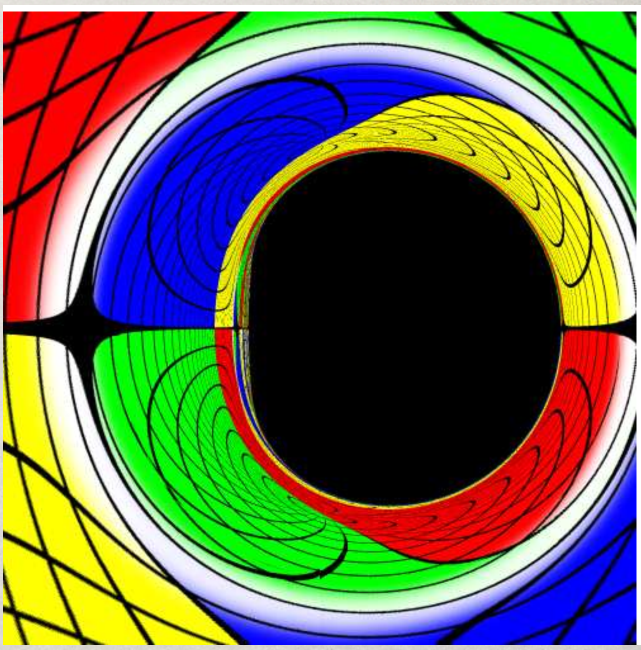

Vacuum Kerr BH
M=0.415; J=0.172

A non-Kerr-like hairy black hole

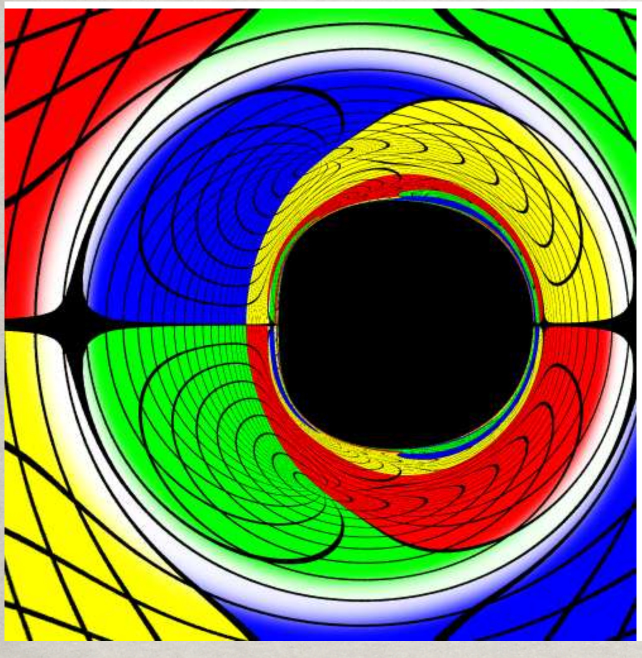

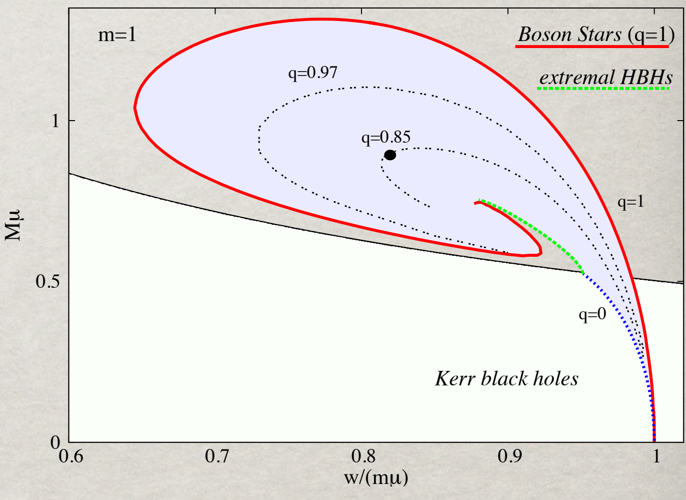

75% of mass;
85% of angular momentum
is stored in the scalar field

A non-Kerr-like hairy black hole

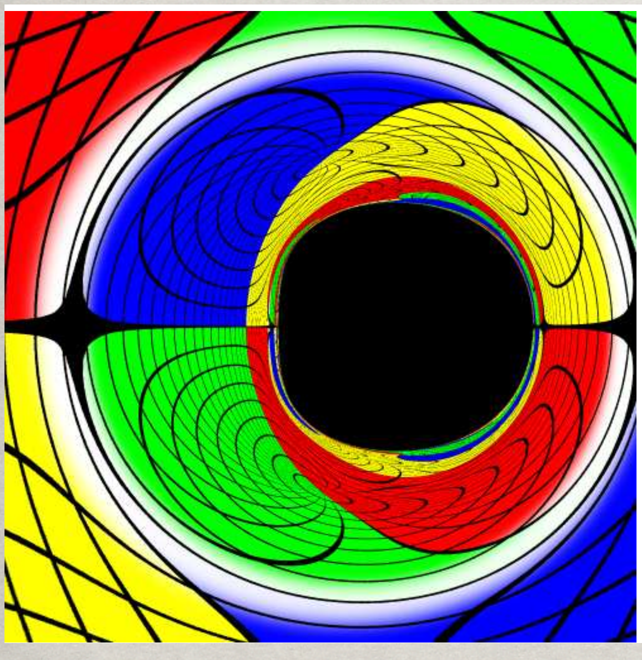

Kerr BH with scalar hair
M=0.234; J=0.114 (horizon)
M=0.699; J=0.625 (scalar field)

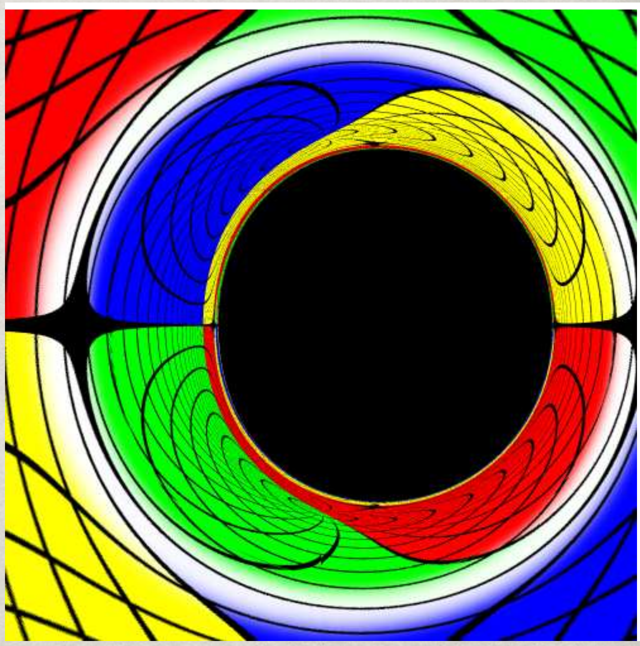

Vacuum Kerr BH
M=0.933; J=0.739

“Academic Setup”

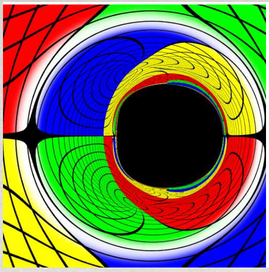

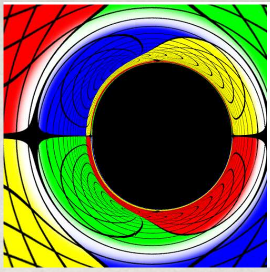

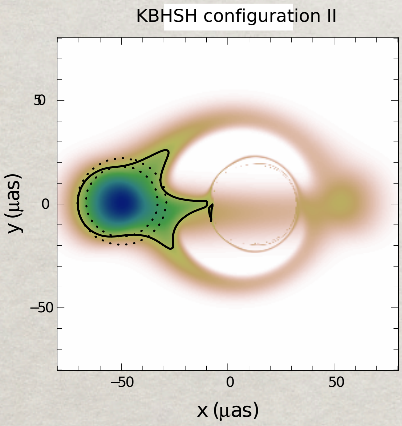

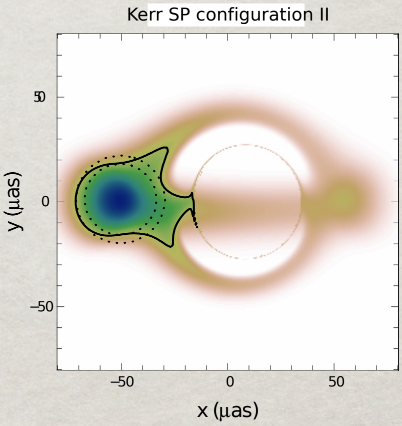

Differences remain in an astrophysically more realistic setup

Vincent, Gourgoulhon, CH, Radu, PRD94(2016)084045

Similar story for other observables such as the:

- iron Kα-line in the reflexion spectrum Ni, Zhou, Cardenas-Avendano, Bambi, CH, Radu, JCAP1610(2016)003
- QPOs Franchini, Pani, Maselli, Gualtieri, CH, Radu, Ferrari, PRD95(2017)124025

Iron Kα-line:

For our two solutions:

Annulus 1:	$r_{\rm in} = r_{\rm ISCO}$	$r_{\rm out} = r_{\rm ISCO} + 1$
Annulus 2:	$r_{\rm in} = r_{\rm ISCO} + 1$	$r_{\rm out} = r_{\rm ISCO} + 2$
Annulus 3:	$r_{\rm in} = r_{\rm ISCO} + 2$	$r_{\rm out} = r_{\rm ISCO} + 4$
Annulus 4:	$r_{\rm in} = r_{\rm ISCO} + 4$	$r_{\rm out} = r_{\rm ISCO} + 10$
Annulus 5:	$r_{\rm in} = r_{\rm ISCO} + 10$	$r_{\rm out} = r_{\rm ISCO} + 25$

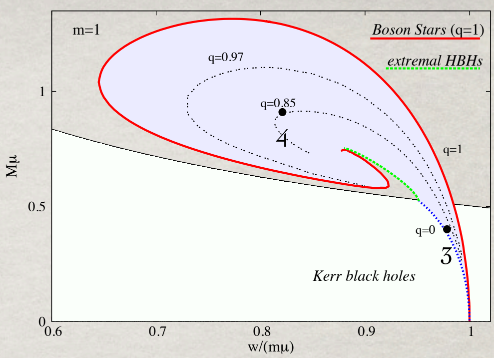

Config 3

5% of M; 13% of J in scalar field

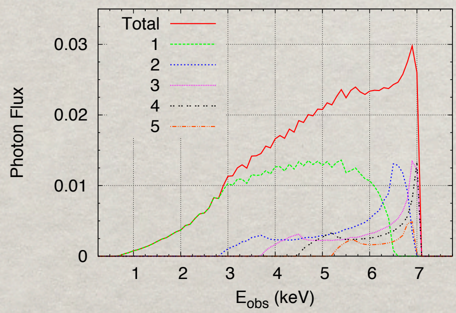

Config 4

75% of M; 85% of J in scalar field

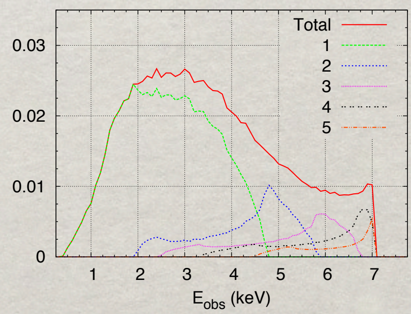

Ni, Zhou, Cardenas-Avendano, Bambi, CH, Radu, JCAP1610(2016)003

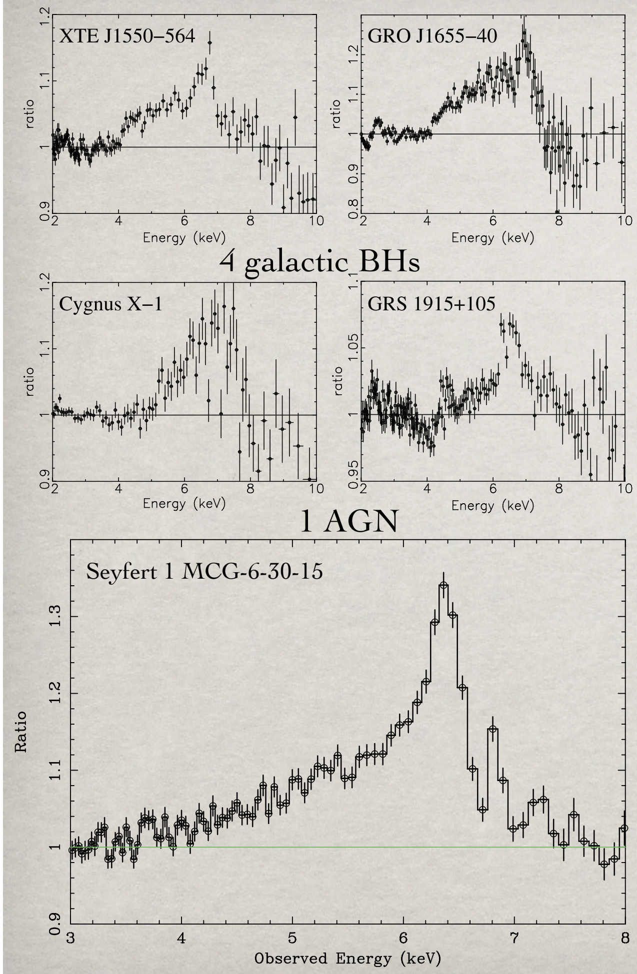

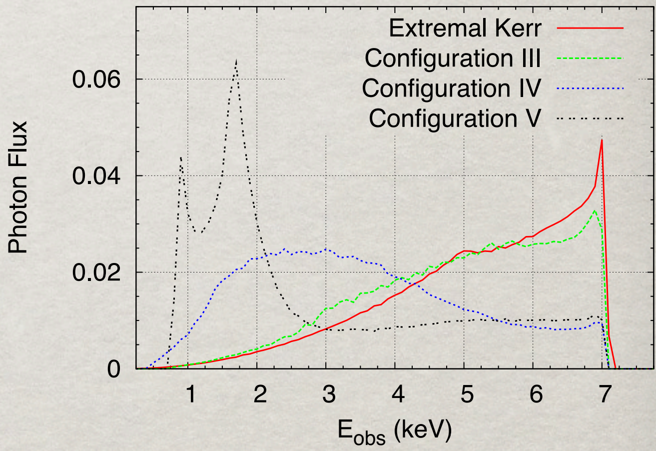

Guainazzi, Ap&SS320(2009)129

Dynamics:

1) Formation from Kerr

In the presence of these ultra-light fields, vacuum Kerr black holes are **unstable** (against superradiance).

What is the endpoint of this instability?

Recent dynamical evidence shows the process reaches an equilibrium state...

East and Pretorius, PRL119(2017)041101

Mass and angular momentum in "hair"

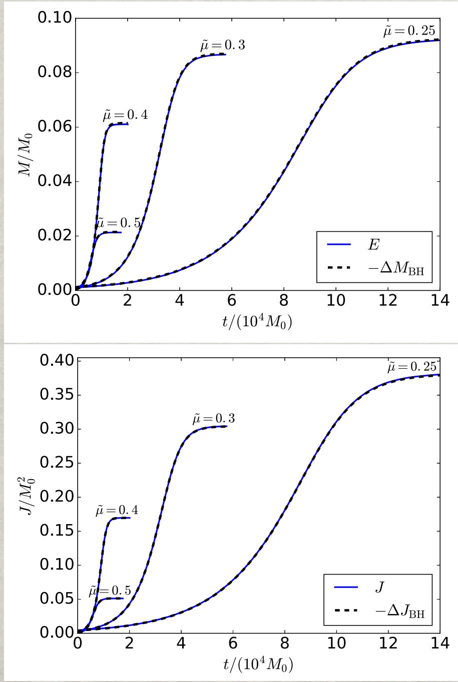

Black hole spin down and "synchronisation"

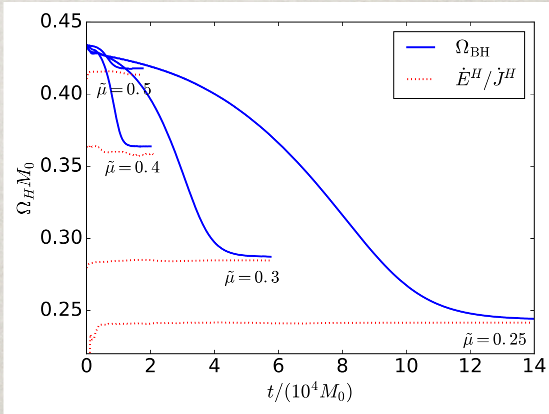

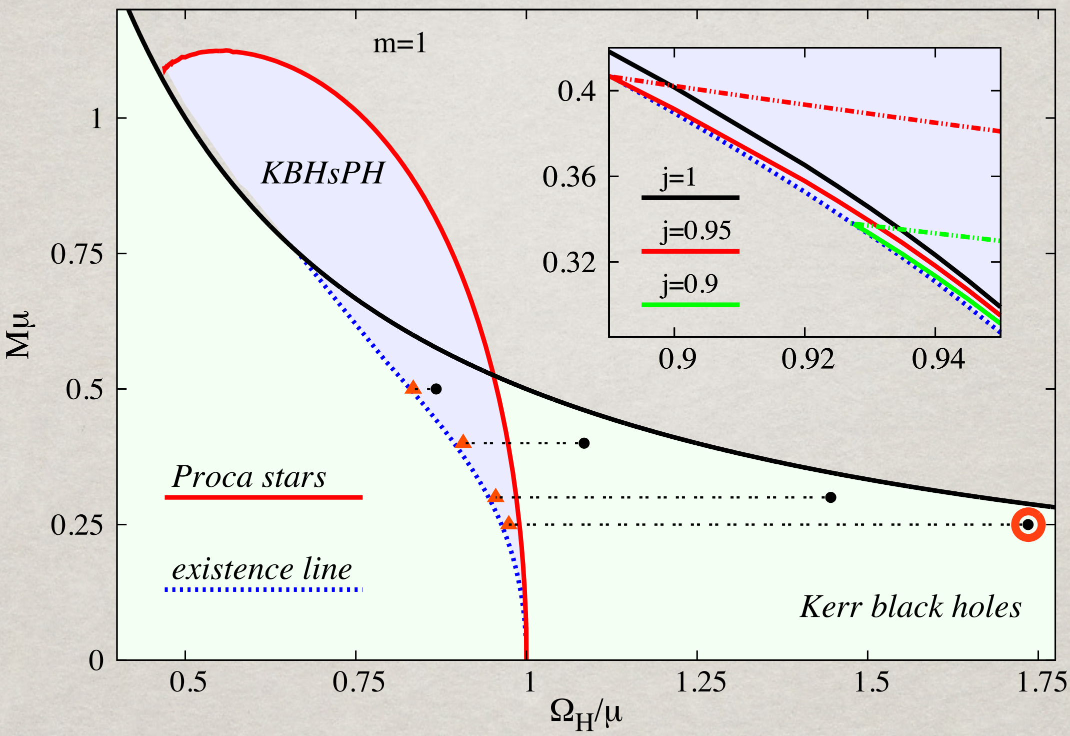

... which is a hairy black hole

CH, Radu, 1706:06597 (PRL in press)

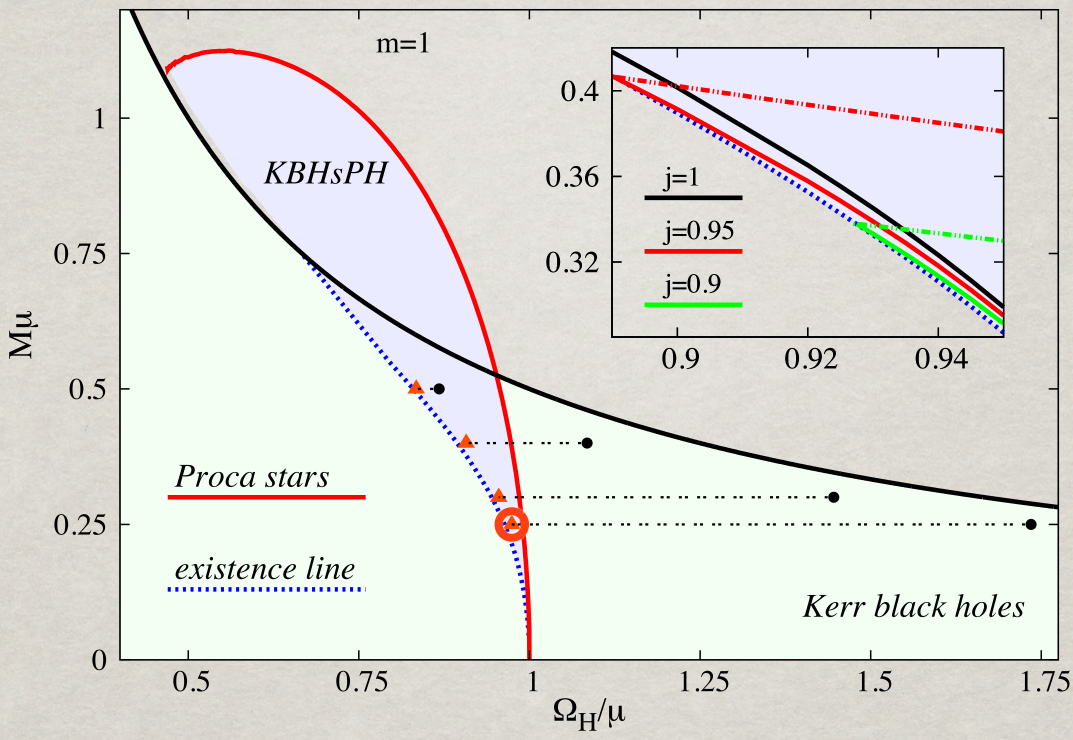

... which is a hairy black hole

CH, Radu, 1706:06597 (PRL in press)

Dolan, Physics10(2017)83

3) Outlook

Mechanism:
A (hairless) BH which is afflicted by the superradiant instability of a given field for which the energy-momentum tensor is time-independent, allows a hairy generalization with that field.

CH and Radu, PRL112(2014)221101;
CH and Radu, IJMPD23(2014)1442014

ありがとう

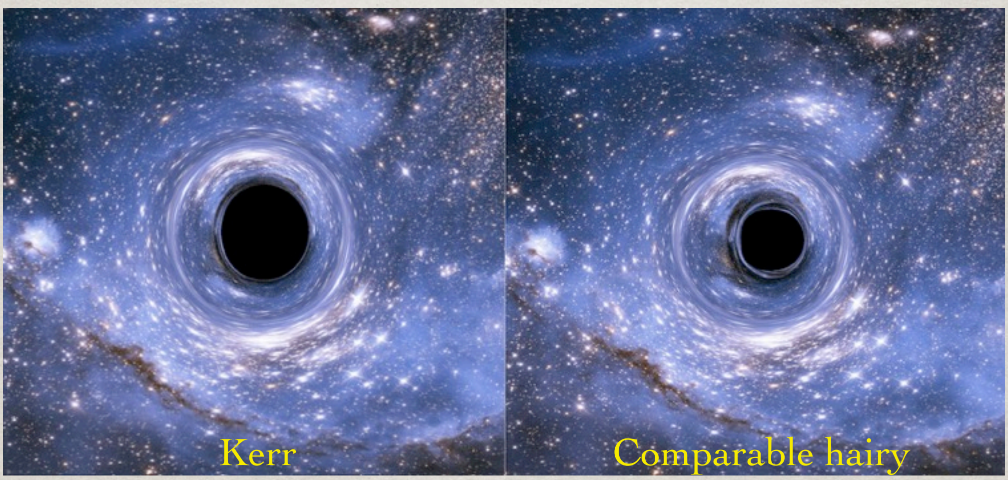

Image:
P. Cunha

Thank you for Your Attention!

Session9 10:45–11:45

[Chair: Hisaaki Shinkai)]

3. Kenji Tomita (YITP Kyoto U.),

"Cosmological models with the energy density of random fluctuations and the Hubble-constant problem" (10+5)

[JGRG27 (2017) 120104]

Cosmological models with the energy density of random fluctuations and the Hubble-constant problem

Kenji Tomita*

The second-order density perturbations corresponding to cosmological random fluctuations are considered and it is found that their super-horizon non-vanishing spatial average is useful to solve the serious problem on the cosmological tension between direct measured Hubble constants at present and those at the early stage.

*Prof. Emer. YITP, Kyoto Univ.

1. Hubble-constant problem

WMAP, Planck precise mesurements : 67.3 km /s/Mpc

direct measurements ([m,z] relation, etc) at present:

73.8 km/s/Mpc	Riess et al (2011)
78.7 km/s/Mpc	Suyu et al (2013)
74.3 km/s/Mpc	Freedman et al (2012)
	Freedman (2017)

The difference is about 10% and observationally serious.

For explanations of this gap between two kinds of Hubble constants, models of decaying dark matter, local void model, dark radiation, and so on have been proposed so far.

My standpoint is to consider a contribution of the energy density of random fluctuations to the dynamics of the universe, due to nonlinear perturbations.

2. Non-linear perturbation theories

a. General-relativistic theories

Linear theory : Lifshitz (1946, 1963)

Gauge-invariant linear theory: Bardeen (1986)

Second-order perturbation theories :

Tomita (1967 $(\Lambda=0)$, 2005 $(\Lambda\neq 0)$)

Russ et al, (1996) $(\Lambda=0)$

at the matter-dominant stage, and so on ....

b. Perturbations in Newtonian cosmology

Newtonian condition is L < 1/H , where

L is the linear length and H is the Hubble parameter .

The condition that L < 1/H holds always in the matter-dominant stage after the epoch of 1+ z = 1500 :

$$L_0 \ < \ L_{0\mathrm{m}} \ (\equiv \ 200\, h^{-1} / (15\,\Omega_M)^{1/2})$$

where L_0 is the present length, and $L_{0\mathrm{m}} = 110 \ h^{-1}$ for $\Omega_M = 0.22$

gives the horizon size at epoch 1+z = 1500.

3. Cosmological random fluctuations

Random fluctuations are caused by quantum fluctuation at the very early stage

Their density perturbations $\delta\rho/\rho$ are

observed as temperature perturbations (CMB) : $\delta T/T$

precise measurements of WMAP and Planck

spectrum (transfer function) : studied by BBKS

It is assumed that the spatial average of them as the first-order density perturbations vanishes ($<\delta_1\rho/\rho> = 0$) .

Then how is the mean energy density as the spatial average of second-order density perturbations $\delta_2\rho/\rho$?

Does it vanish or not ?

a. In the Newtonian case with $L_0 < L_{0\mathrm{m}}$

we have $<\delta_2\rho/\rho> = 0$

and $<\delta_n\rho/\rho> = 0$ also for n >2.

b. In the super-horizon case with $L_0 > L_{0\mathrm{m}}$
the linear length L of perturbations
is always larger than 1/H or cross it once .
-> Treatment of general-relativistic second-order
perturbations is necessary

In my recent first work (I), we used
the general-relativistic second-order perturbation theory
Tomita (2005) for $\Lambda \neq 0$ in the synchronous and comoving gauge
and obtained the spatial average $<\delta_2\rho/\rho>(\neq 0)$
in the form of an integral with respect to wave-number k .
The upper-limit of the wave-number k_max was specified as

$$L_{min} \equiv 2\pi/k_{max} = 102/h \ \mathrm{Mpc} \quad \mathrm{for} \quad \Omega_M = 0.22$$

where the minimum length is $L_{min} \simeq L_{0\mathrm{m}}$

Therefore $<\delta_2\rho/\rho>(\neq 0)$ comes from only the super-horizon fluctuations, and $<\delta_2\rho>$ is interpreted to be the average fluctuation energy densiy. By the way, $<\delta_2\rho/\rho> \sim <(\delta_1\rho/\rho)^2>$.

4. Energy density of random fluctuations and the Hubble-constant problem

In paper (I), we derived the second-order perturbations corresponding to not only density perturbations, but also metric perturbations. Using them, we derived the cosmologically renormalized quantities:

$$\rho_{rem} = \rho + <\delta_2\rho>, \qquad H_{rem} = [H^2 + <\delta_2(H^2)>]^{1/2}$$

$$(\Omega_\Lambda)_{rem} = \Omega_\Lambda [1 + <\delta_2\rho/\tilde{\rho}>]^{-1}, \qquad (\Omega_M)_{rem} = 1 - (\Omega_\Lambda)_{rem}$$

where $\tilde{\rho} = \rho + \lambda$, and $<\delta_2(H^2)>$ includes the second-order perturbation of the Hubble parameter H.

Here "renormalization" means only the transformation such as

$$\rho \rightarrow \rho_{rem}, \qquad H_{rem} \rightarrow H_{rem}, \qquad \Omega_\Lambda \rightarrow (\Omega_\Lambda)_{rem}$$

and so on. It is not related to any "dynamical renormalization process".

As a result, for the background model

$$\Omega_M = 0.22,\ \Omega_\Lambda = 1 - \Omega_M,\ H_0 = 67.3\,\mathrm{km\,s^{-1}\,Mpc^{-1}}$$

we obtain at present epoch

$$(\Omega_M)_{rem} = 0.305,\ (\Omega_\Lambda)_{rem} = 1 - (\Omega_M)_{rem},\ (H_0)_{rem} = 74.0\,\mathrm{km\,s^{-1}\,Mpc^{-1}}$$

consistent with present direct obs.

On the other hand, the models at the early stage (z >>1) have the values consistent with the background model.

: consistent with Planck obs.

-> This result may solve the Hubble-constant problem !

In my recent second paper (II), we expressed the fluctuation energy $\rho_f\ (\equiv \ <\delta_2 \rho>)$ as a function of ρ , and regarded it as one of the densities of the constituent pressureless matter. The total matter density is

$$\rho_T = \rho + \rho_f(\rho)$$

A new cosmological model with

$$ds^2 = g_{\mu\nu} dx^\mu dx^\nu = a^2(\eta)[-d\eta^2 + \delta_{ij}\, dx^i dx^j]$$

$$u^0 = 1/a,\quad u^i = 0$$

$$T^0_0 = -\rho_T,\quad T^0_i = 0,\quad T^i_j = 0$$

was introduced.

The present ratio of $\beta \equiv \rho_f(\rho)/\rho$ is 0.552

in the case of the background model parameter 0.22

Einstein eq.: $\rho_T\, a^2 = 3(a'/a)^2 - \Lambda a^2$

Energy-momentum conservation: $\rho_T\, a^3 = \rho_T(t_0)$

(a = 1 at the present epoch)

Background model, on the other hand, is expressed using the quantities $a^b,\ H^b,\ \rho^b$

Quantities in the new model and those in the background model are found to be related using the parameter $(\rho/\rho^b)_0$

In the case of $(\rho/\rho^b)_0 = 1.181$ for example, we obtain

$(\Omega_M, H)_0 = (0.341, 73.2)$: consistent with present direct obs.

corresponding to the background ones $(\Omega_M^b, H^b)_0 = (0.22, 67.3)$

At the early epoch with z >>1, we have $(\Omega_M^b, H^b) = (\Omega_M, H)$

: consistent with Planck obs.

This result also may explain the Hubble-constant problem.

$\boldsymbol{\beta} \equiv \rho_f/\rho, \quad 0 < \beta < \beta_0\ (= 0.551)$ $\quad\quad \boldsymbol{\alpha} \equiv H / H^b$

$u \equiv \rho/[3(H_0^b)^2], \quad 0 < 1/u < (0.22)^{-1}$ $\quad\quad (\rho/\rho^b)_0 = 1.181$

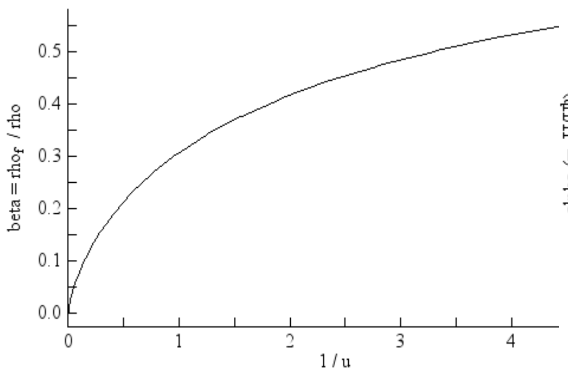

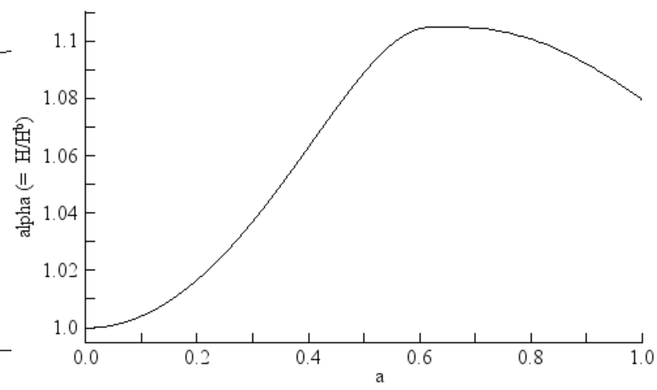

References

1. Hubble-constant problem
   G. Hinshaw et al., Astrophys. J. Suppl. **208**, 19 (2013)
   P.A.R. Ade et al., Asron. Astrophys. **571**, A16 (2014)
   P.A.R. Ade et al., Asron. Astrophys. **594**, A3 (2016)
   A.G. Riess et al. Astrophys. J. **730**, 2019 (2011)
   S.H. Suyu et al., Astrophys. J. **766**, 70 (2013)
   J.L. Bernal et al., JCAP **10**, 019 (2016)
   W.L. Freedman et al. , Astrophys. J. **758**, 24 (2012)
   W.L. Freedman, Nature Astron. **1**, 0169 (2017)
2. Non-linear perturbations
   (second-order perturbations)
   K. Tomita, Phys. Rev. **D71**, 083504 (2005)
   K. Tomita, Prog. Theor. Phys. **37**, 831 (1967)
   (Newtonian cosmology)
   N. Makino et al., Phys. Rev. **D46**, 585 (1992)
   F. Bernardeau et al., Phys. Rep. **367**, 1 (2002)
3. BBKS:
   J.M. Bardeen, J.R. Bond, N. Kaiser, and A.S. Szalay, Astrophys. J. **304**, 15 (1986)

My recent works

(I) K. Tomita, Prog. Theor. Exp. Phys. **2017**, 053E01 (2017);
arXiv: 1702.07821 [astro-ph.CO]

(II) K. Tomita, Prog. Theor. Exp. Phys. **2017**, 083E04 (2017);
arXiv: 1706.07655 [gr-qc]

(III) K. Tomita, arXiv: 1711.02775 [astro-ph.CO]

4. Marcus Werner (YITP Kyoto U.),
“Constructing predictive gravity theories” (10+5)
[JGRG27 (2017) 120105]

Constructing Predictive Gravity Theories

Marcus C. Werner, Kyoto University

Hiroshima University, 1 December 2017
JGRG27

Constructive gravity

Standard approach to modified gravity theories:

Stipulate some modification of the Einstein-Hilbert action.
$\rightarrow$ How to choose an action? Is the theory predictive?

However, a physical theory should be predictive:
$\rightarrow$ Well-posed Cauchy problem, time-orientability

New approach discussed here:

Derive gravity action such that the theory is predictive.
$\rightarrow$ 'Constructive gravity' program

Today: basic outline of the program, and recent results for the first derived, predictive gravity theory beyond GR.

Predictive kinematics

Consider a spacetime (M, G, F) endowed with some tensorial geometry field G and test matter field F, whose field equations yield a principal polynomial $P : T^*M \to \mathbb{R}$ (cf. null cone).

For causality, the Cauchy problem needs to be well-posed, requiring that P be hyperbolic.

For predictivity, time-orientability is also needed, such that the dual principal polynomial $P^\sharp : TM \to \mathbb{R}$ be hyperbolic as well.

Hence bihyperbolicity, i.e. the property that both P and $P^\sharp$ be hyperbolic, defines predictive spacetime kinematics in general.

From kinematics to dynamics

Geometrodynamical technique of the constructive gravity program: bihyperbolic kinematics $\Rightarrow$ gravitational dynamics.

[Cf. Hojman, Kuchař & Teitelboim (1976); Giesel, Schuller, Witte & Wohlfarth (2012); Schuller & Witte (2014)]

Basic idea:

- bihyperbolic spacetime structure $\Rightarrow$ generalized ADM split;
- lapse and shift define the hypersurface deformation algebra;
- canonical dynamics so that evolution $=$ deformation;
- supermomentum and superhamiltonian are derived;
- a PDE system for the gravity Lagrangian is obtained.

Deriving general relativity

One of those differential construction equations for the gravity Lagrangian $\mathcal{L}[G,K) = \sum_{k=0}^{\infty} C[G]_{A_1 \dots A_k} K^{A_1} \dots K^{A_k}$ reads thus,

$$0 = \frac{\partial C}{\partial \left(\frac{\partial^3 G^A}{\partial x^i \partial x^j \partial x^k} \right)} + \frac{\partial C_A}{\partial \left(\frac{\partial^2 G^B}{\partial x^{(i} \partial x^{j|}} \right)} M^{B|k)}.$$

Now suppose that $G = g$, a Lorentzian metric, then $M^{Ai} = 0$ and C can depend on at most second order derivatives of the metric.

The full analysis yields $C = -\frac{1}{2\kappa}\sqrt{-g}(R - 2\Lambda)$ with integration constants κ and Λ, i.e. GR! Cf. also Lovelock's theorem.

We will now apply this framework to seek predictive gravitational dynamics for a spacetime with non-metric G.

Area metric geometry

An area metric is a smooth 4th order tensor field G with symmetries such that, for any smooth vector fields X, Y, U, V,

$$G(X,Y,U,V) = G(U,V,X,Y),$$
$$G(X,Y,U,V) = -G(Y,X,U,V),$$
$$G(X,Y,U,V) = -G(X,Y,V,U).$$

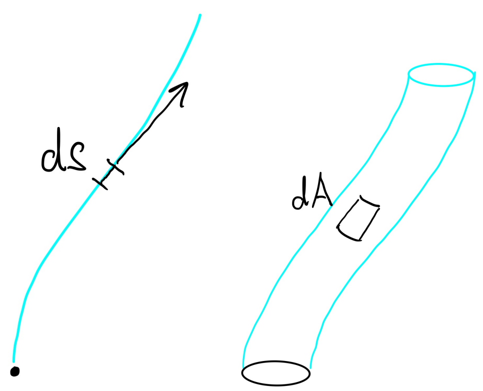

Are area metrics a useful differential geometry for string theory?
Note: the Nambu-Goto Lagrangian is $\propto \sqrt{-G_\eta(\dot{x}, x', \dot{x}, x')}$.

Area metric spacetime

Consider a generalized vacuum EM in an area metric spacetime,

$$L = -\frac{1}{8}\chi^{\mu\nu\rho\sigma}F_{\mu\nu}F_{\rho\sigma} \quad \text{with} \quad \chi^{\mu\nu\rho\sigma} = \omega_G G^{\mu\nu\rho\sigma},$$

where $\omega_G^{-1} = \frac{1}{4!}\epsilon_{\mu\nu\rho\sigma}G^{\mu\nu\rho\sigma}$. The null cone is quartic,

$$P(x,p) = P(x)^{\alpha\beta\gamma\delta}p_\alpha p_\beta p_\gamma p_\delta = 0,$$

with momentum p, and

$$P^{\alpha\beta\gamma\delta} \propto \epsilon_{\kappa\lambda\mu\nu}\epsilon_{\rho\sigma\tau\upsilon}G^{\kappa\lambda\rho(\alpha}G^{\beta|\mu\sigma|\gamma}G^{\delta)\nu\tau\upsilon},$$

which may or may not be bihyperbolic.

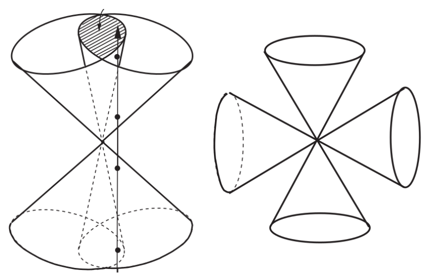

Perturbation about Minkowski

For small area metric perturbations about Minkowski spacetime,

$$G^{\mu\nu\rho\sigma} = \eta^{\mu\rho}\eta^{\nu\sigma} - \eta^{\mu\sigma}\eta^{\nu\rho} - \epsilon^{\mu\nu\rho\sigma} + H^{\mu\nu\rho\sigma}$$

with H small, then the principal polynomial tensor and its dual

$$P^{\mu\nu} = \eta^{\mu\nu} + H^{\mu\nu}, \quad P^\sharp_{\mu\nu} = \eta_{\mu\nu} - H_{\mu\nu},$$

where $H^{\mu\nu} = \frac{1}{2}H^{\alpha\mu\beta\nu}\eta_{\alpha\beta} - \frac{1}{4!}\epsilon_{\alpha\beta\gamma\delta}H^{\alpha\beta\gamma\delta}\eta^{\mu\nu}$.

Hence, light rays are governed by $P^\sharp$ and obey Lorentzian metric geometry. But what about the gravitational dynamics?

Area metric gravity theory

The gravitational dynamics for area metric kinematics can, so far, be derived perturbatively. For a point mass M, the solution is

$$
\begin{aligned}
G^{0a0b} &\equiv -\gamma^{ab} + H^{0a0b} = -\gamma^{ab} + (2A - \tfrac{1}{2}U + \tfrac{1}{2}V)\gamma^{ab}, \\
G^{0bcd} &\equiv \epsilon^{bcd} + H^{0bcd} = \epsilon^{bcd} + \left(\tfrac{3}{4}U - \tfrac{3}{4}V - A\right)\epsilon^{bcd}, \\
G^{abcd} &\equiv \gamma^{ac}\gamma^{bd} - \gamma^{ad}\gamma^{bc} + H^{abcd} = (1 + 2U - V)(\gamma^{ac}\gamma^{bd} - \gamma^{ad}\gamma^{bc}),
\end{aligned}
$$

with Euclidean metric γ^{ab}, Euclidean distance r of the unperturbed background, Levi-Civita symbol ϵ^{abc}, and scalar perturbations

$$
A = -\frac{M}{4\pi r}\left(\kappa - \lambda\eta e^{-\mu r}\right),\; U = -\frac{M}{4\pi r}\eta e^{-\mu r},\; V = \frac{M}{4\pi r}\left(\kappa - \tau\eta e^{-\mu r}\right),
$$

where $\eta, \kappa, \lambda, \mu, \tau$ are constants. [Alex, Möller & Schuller (2017), in prep.]

Modified Etherington

For this linearized area metric Schwarzschild solution, one can derive a modified Etherington distance duality relation,

$$
D_L = (1+z)^2 D_A\left(1 + \frac{3\kappa M}{8\pi}\left(\frac{e^{-\mu r_S}}{r_S} - \frac{e^{-\mu r_O}}{r_O}\right) + \mathcal{O}(M^2)\right),
$$

with Euclidean distances r_O, r_S between mass M and observer O, light source S, respectively. [Schuller & Werner, *Universe* **3**, 52 (2017), arXiv:1707.01261]

Of course, an area metric cosmological solution would be more interesting for comparison with the classic result. This is currently being pursued.

Conclusions

- The constructive gravity approach allows the derivation of gravitational dynamics from bihyperbolic kinematics.
- Predictive spacetime kinematics can be implemented mathematically with bihyperbolicity in general.
- Applying constructive gravity to area metric spacetimes, a linearized Schwarzschild-like solution has been constructed.
- Investigating light propagation on this background, we find a modified Etherington distance duality relation.
- This is observable, and the first astrophysical consequence of a derived, predictive gravity theory beyond GR.

American Mathematical Society MRC Conference

3-9 June 2018, Rhode Island, USA. Full NSF funding for participants.

See: www.ams.org/programs/research-communities/2018MRC-Gravity